EFFECTS OF FEEDSTOCKS AND INOCULUM SOURCES ON MIXED-ACID AND HYDROGEN FERMENTATIONS

A Dissertation

by

ANDREA KELLY FORREST

Submitted to the Office of Graduate Studies of
Texas A&M University
in partial fulfillment of the requirements for the degree of

DOCTOR OF PHILOSOPHY

December 2010

Major Subject: Chemical Engineering

Effects of Feedstocks and Inoculum Sources on Mixed-Acid and Hydrogen Fermentations

EFFECTS OF FEEDSTOCKS AND INOCULUM SOURCES ON MIXED-ACID AND HYDROGEN FERMENTATIONS

A Dissertation

by

ANDREA KELLY FORREST

Submitted to the Office of Graduate Studies of
Texas A&M University
in partial fulfillment of the requirements for the degree of

DOCTOR OF PHILOSOPHY

Approved by:

Chair of Committee,	Mark T. Holtzapple
Committee Members,	Charles J. Glover
	Mahmoud El-Halwagi
	Cady R. Engler
Head of Department,	Michael Pishko

December 2010

Major Subject: Chemical Engineering

ABSTRACT

Effects of Feedstocks and Inoculum Sources on Mixed-Acid and Hydrogen Fermentations.

(December 2010)

Andrea Kelly Forrest, B.S., Louisiana Tech University

Chair of Advisory Committee: Dr. Mark T. Holtzapple

With increasing energy demand, decreasing oil supply, and continuously accumulating waste in landfills, the interest in converting lignocellulosic biomass to liquid fuels has grown. The MixAlco™ process requires no exogenous enzymes, no sterility, can be adapted to any biodegradable feedstock, and converts lignocellulosic biomass into valuable chemicals and transportation fuels. This work focuses on the effects different feedstocks and inocula have on mixed-acid/hydrogen fermentations.

When volatile solids (VS) are digested, mixed-acid fermentations produce hydrogen gas as a secondary byproduct. Hydrogen is only produced when there is an excess of NADH within the cell and when the energy selectivity (γ) of the system has not been met. Continuous fermentations of paper produced 16.7 g carboxylic acid/L and 15.7 mL H_2/g VS digested. Continuous fermentations of pretreated bagasse produced 17.1 g carboxylic acid/L and 41.1 mL H_2/g VS digested. Both fermentations produced a fraction of the theoretical amount of hydrogen. The paper fermentation had a hydrogen percent yield of 6.9%, whereas the bagasse fermentation had a hydrogen percent yield of 22.6%. Hydrogen production was capped at this level because γ had been met for these systems.

The Bioscreening Project, a joint project between three departments, sought to improve the MixAlco™ process by finding natural cultures containing high biomass converters and high acid producers. A total of 505 inoculum samples were collected from 19 sites and screened using paper and yeast extract fermentations. The best converters were analyzed with Continuum Particle Distribution Modeling (CPDM). Nine inocula were run in paper and yeast extract countercurrent fermentations in which the overall performance varied less than 13%. Comparisons between six countercurrent train cultures showed an average culture similarity of 0.40 (Yue-Clayton similarity). With the dissimilar microbial cultures

and the very similar fermentation performance, the performance of the MixAlco™ process depends on fermentation conditions, not on the microorganisms.

Batch fermentations of office paper wastes, pineapple residue, *Aloe vera* rinds, wood molasses, sugar molasses, extracted algae, non-extracted algae, crude glycerol, obtained from the biodiesel process, and pretreated water hyacinths produced sufficient carboxylic acids and had sufficiently high conversions to be viable substrates for the MixAlco™ process.

ACKNOWLEDGEMENTS

I would like to thank my parents, Duane D. Forrest and D. Camille Forrest, and my siblings, Casey Forrest, Bryan Forrest, and Shannon Forrest-LeJeune, for all their support and guidance growing up. They always believed in me even when I did not. I also extend my thanks to my high school chemistry teacher, James Ruby, who lit the 'chemistry' flame that still burns today and to Kathy Doane who led my old Camp Fire Boys and Girls group and showed me the importance of understanding and preserving our environment in order to keep enjoying it.

I would like to thank Dr. Bill Elmore, my undergraduate advisor, at Louisiana Tech University, who continuously supported me and encouraged me to pursue my Ph.D. I also thank Jimmy and Annette Harvey, who helped me decide to return to school for my Ph.D even after working as a process engineer for several years.

My extreme gratitude goes to my academic advisor, Dr. Mark T. Holtzapple, for his support and guidance. It would have been impossible to complete this work without his inspiration and support. I extend my appreciation to my committee, Dr. Cady Engler, Dr. Charles Glover, and Dr. Mahmoud El-Halwagi, for their time reading this dissertation and their valuable comments. I would also like to thank Dr. John Dunkleman and Dr. Melinda Wales for all their support in running the lab and reviewing my papers. My thanks go to my group members, past and present, for all their support and encouragement. Special thanks to Rocio Sierra and Kristina Golub for continuous help in overcoming fermentation and laboratory problems. I thank Emily Hollister and Terry Gentry in the Department of Soil and Crop Sciences for all their help running DNA extractions and sequence comparisons. My appreciation goes to all the student workers who worked in our lab over the years. Without them, I would not have been able to collect all the data used in this dissertation.

I would also like to thank Towanna Arnold, Randy Marek, Louis Muniz, and the staff members in the Artie McFerrin Department of Chemical Engineering. They have provided tons of help throughout my time at Texas A&M University. Their support and encouragement will always be remembered.

TABLE OF CONTENTS

CHAPTER Page

CHAPTER Page

Page

LIST OF FIGURES

FIGURE Page

FIGURE Page

FIGURE Page

FIGURE Page

FIGURE Page

FIGURE Page

FIGURE Page

FIGURE Page

FIGURE Page

FIGURE Page

FIGURE Page

LIST OF TABLES

TABLE Page

TABLE Page

TABLE Page

TABLE Page

TABLE Page

TABLE Page

TABLE Page

CHAPTER I
INTRODUCTION

Increasing energy demand and decreasing oil supply necessitate the development of alternative energy sources (Parry and Darmstadter, 2003). Additionally, agricultural production generates millions of tons of waste that can lead to environmental problems (Holtzapple et al., 1999). Using agricultural residues as a sustainable source of energy is attractive because of their plentiful supply and relatively low cost. Further, their use averts disposal costs and minimizes environmental impacts.

Biomass is any organic matter originating from plants and includes agricultural wastes, forest residues, energy crops, and municipal solid waste. During photosynthesis, plants use solar energy to convert atmospheric carbon dioxide into sugars and lignocellulose. On combustion, the energy is released and carbon is converted back into carbon dioxide. This makes energy derived from biomass "carbon neutral," meaning that it releases the same amount of carbon dioxide that was captured by photosynthesis during its initial growth.

Lignocellulosic biomass is primarily composed of cellulose, hemicellulose, and lignin. Cellulose is the most abundant component of biomass, comprising between 35% and 50% of dry plant matter (Lynd et al., 1999). Cellulose is a monopolymer, composed of glucose with a molecular weight in excess of 50,000 g/mol, forming long fibers giving structural support. These fibers are buried in a matrix of structural polymers of hemicellulose (20 to 35 wt%) and lignin (5 to 35 wt%). Hemicellulose is a highly branched heteropolymer composed of both six-carbon and five-carbon sugars and acts as a linkage between cellulose and lignin. Lignin is a three-dimensional phenyl-propane polymer with phenylpropane units held together by ether and carbon-carbon bonds (Freudenberg and Neish, 1968). Lignin gives structural rigidity, prevents water loss, and acts as a chemical barrier to degradation.

This dissertation follows the style of *Bioresource Technology*.

The rate and extent of biomass utilization is often improved by pretreatment. The accessible surface area, cellulose crystallinity, and lignin content all affect biomass utilization (Mosier et al., 2005). Pretreatments can be mechanical, physical, chemical, or biological. Chemical treatments − such as various acids, alkalies, and alcohols − are simple and effective. Alkali chemicals (e.g., lime) are generally preferred because they are inexpensive and cause less cellulose degradation (Sierra et al., 2009).

The conversion of biomass into energy falls into two main categories: thermochemical and biochemical. Thermochemical conversion technologies include combustion, gasification, and pyrolysis. Combustion is the dominant conversion technology for biomass. For centuries, it has been the major source of energy for mankind, supplying heat for warmth and cooking. More recently, biomass combustion is used industrially to generate steam and electricity (Demirbas and Balat, 2006; Wu et al., 2004). Gasification converts solid fuels into combustible gases or syngas (CO and H_2). Gasification of a dry biomass is 40−50% more efficient than straight combustion, and generates electricity through a gas turbine (Dowaki et al., 2005; Dowaki et al., 2007). In the absence of oxygen, pyrolysis converts biomass at temperatures of 500 °C into liquid (bio-oil), gaseous, and solid (char) fractions (Adjaye et al., 1992; Miao and Wu, 2004). Although less developed than gasification, pyrolysis produces a burnable liquid fraction in addition to the gaseous product that can be used to fire engines and turbines (Blasi, 2008).

Biochemical conversion technologies include gaseous and liquid products. Gaseous biochemical conversion technologies produce flammable gases, primarily methane and hydrogen. Anaerobic digestion of wet biomass materials for methane has been demonstrated and applied commercially for various feedstocks, including domestic and industrial wastes and manure (Hansen et al., 2006; Nguyen et al., 2007). For a long time, several industries have used anaerobic digestion to process waste water with a high organic load. Conversion efficiencies in anaerobic digestion can reach as high as 35%, but highly depend on the type of feedstock (Alvarez and Lide, 2009; Demirel et al., 2010). Methane-rich gas can also be harvested from landfills, producing electricity and preventing hazardous methane buildup (DeJager and Blok, 1996; Han et al., 2010; Kumar et al., 2003; Nguyen et al., 2007; Qin et al., 2001).

Hydrogen gas has long been desired as a 'green' fuel because combustion produces only water with no carbon dioxide, hydrocarbons, or fine particulates. Additionally, hydrogen has a high energy yield of 122 kJ/g, which is 2.75 times greater than the combustion of fossil fuels (Benemann, 1996). Unfortunately, hydrogen has a low molecular weight and the difficulties of storing large quantities currently make hydrogen unfeasible as a standalone fuel. But, hydrogen can also be used to enrich other fuels (Chase et al., 2007; Jessop et al., 1995). The petrochemical industry uses hydrogenation to convert alkenes and aromatics into saturated alkanes and cycloalkanes. Hydrogenation can also be used to convert heavy oil residues into diesel and to convert coal into synthetic gasoline (Bergius, 1932). The Fischer-Tropsch process uses hydrogenation to convert carbon monoxide into a variety of hydrocarbons (Dry, 2002).

Hydrogen can be produced from steam reforming of hydrocarbons or electrolysis of water. Alternatively, it can be produced biologically using photosynthetic algae (Melis and Happe, 2001) or fermentative hydrogen-producing anaerobes (Nandi and Sengupta, 1998). Studies on fermentative hydrogen production have been conducted mostly using pure cultures, either natural or genetically modified (Asada et al., 2000; Evvyernie et al., 2001; Fabiano and Perego, 2002). However, hydrogen is a key intermediate from mixed cultures that anaerobically degrade liquid or solid waste into mixed acids (Lay et al., 1999; Mizuno et al., 2000; Sparling et al., 1997).

Liquid biochemical conversion technologies produce flammable liquids such as biodiesel, ethanol, and hydrocarbons. Biodiesel refers to fuel derived from vegetable oil or animal fat consisting of long-chain alkyl-esters (Demirbas, 2009). Biodiesel is made by reacting the triglycerides in extracted vegetable oils (e.g., soy, olive, peanut, and canola seed) or fat with an alcohol (e.g., methanol). The esters can then be used directly in any diesel engine for electricity generation or transportation. The average energy value of biodiesel is 37.3 MJ/L, which is 9% lower than standard petroleum-based diesel and can vary depending on the source of the feedstock oil (Ma and Hanna, 1999). Biodiesel has different solvent properties than petroleum diesel and is typically sold as blends (B5, B20) (Bozbas, 2008).

Biofuels can also be produced by anaerobic fermentation. To date, ethanol fermentation is the most widely used method (Hahn-Hagerdal et al., 2006). For recreational purposes, sugars of glucose, fructose, and sucrose have been fermented to ethanol for

millennia. More recently, ethanol has been produced for its energy value, used as a standalone fuel, or blended with gasoline. Large-scale ethanol production involves the conversion of not only the sugars contained within biomass, but also the starch and cellulose (Lin and Tanaka, 2006). The starches and celluloses must first be hydrolyzed to free sugars before ethanol-producing microorganisms can ferment them into ethanol. Until recently, the cost of the hydrolytic enzymes has made large-scale production of ethanol prohibitive. Several companies, with the help of funding from the US Department of Energy, are developing genetically engineered fungi to produce the cellulase and xylanase enzymes needed to hydrolyze biomass (Balat and Balat, 2009).

Anaerobic fermentation can also produce carboxylic acids, carbon dioxide, and hydrogen. These acid-producing fermentations are conducted by acidogens, microorganisms that are found in the rumen of animals, swamps, compost, and marine ecosystems. Inocula from different sources obtained similar products from biomass, but with different overall acid concentrations and conversions for the same retention times and volatile solids loading (Aiello-Mazzarri, 2002; Fu, 2007; Thanakoses, 2002). The major pathways of lignocellulose fermentation are shown in Figure 1-1. Cellulose and hemicelluloses are hydrolyzed to sugars, which can proceed through further reactions to produce acetate, propionate, butyrate, and hydrogen.

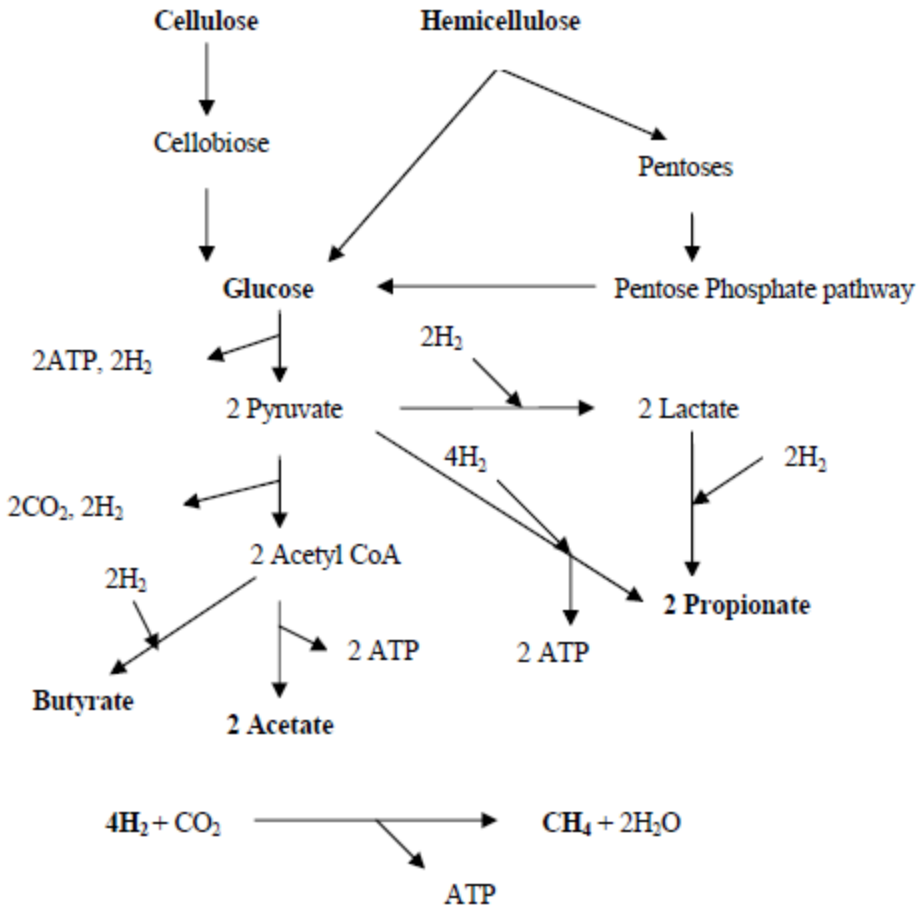

Figure 1-1. Major fermentation pathways (Prins, 1977).

The MixAlco™[1] process (Holtzapple et al., 1999; Holtzapple and Granda, 2009), developed by Dr. Mark Holtzapple, uses anaerobic fermentation to produce carboxylic acid salts (Figure 1-2). It is a flexible and cost-effective means of converting a variety of lignocellulosic feedstocks − including agricultural residues, municipal solid waste, and biosolids − into chemicals and liquid fuels. By employing a mixed culture of naturally occurring microorganisms to ferment the biomass into carboxylic salts, these carboxylic salts can be converted into a wide array of chemicals, including alcohols, jet fuel, and gasoline (Aiello-Mazzarri et al., 2006; Granda et al., 2009). The product spectrum from this process

[1] MixAlco is a registered trademark of Terrabon, Inc. Unless otherwise noted in this document, inclusion of such trademark in this document does not imply support or endorsement by Terrabon, Inc.

is temperature dependent and can be varied in response to market demand (Chan and Holtzapple, 2003). Additionally, this process has no sterility requirements, no enzyme addition, and can be adapted to any biodegradable feedstock (Agbogbo and Holtzapple, 2007).

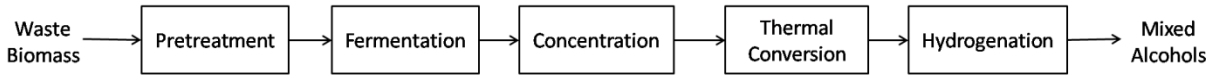

Figure 1-2. The MixAlco™ process.

Countercurrent fermentations are used to achieve high substrate conversion and product concentrations (Figure 1-3). In batch fermentations, conversion is limited because the accumulation of acids inhibits the fermentation. In countercurrent fermentations, the least reactive biomass contacts the lowest acid concentration. Fresh biomass is added to the fermentor with the highest acid concentration, while fresh water is added to the fermentor with the most digested biomass. Solid biomass and liquid product move in a countercurrent direction, reducing the inhibitory effect of accumulated acids.

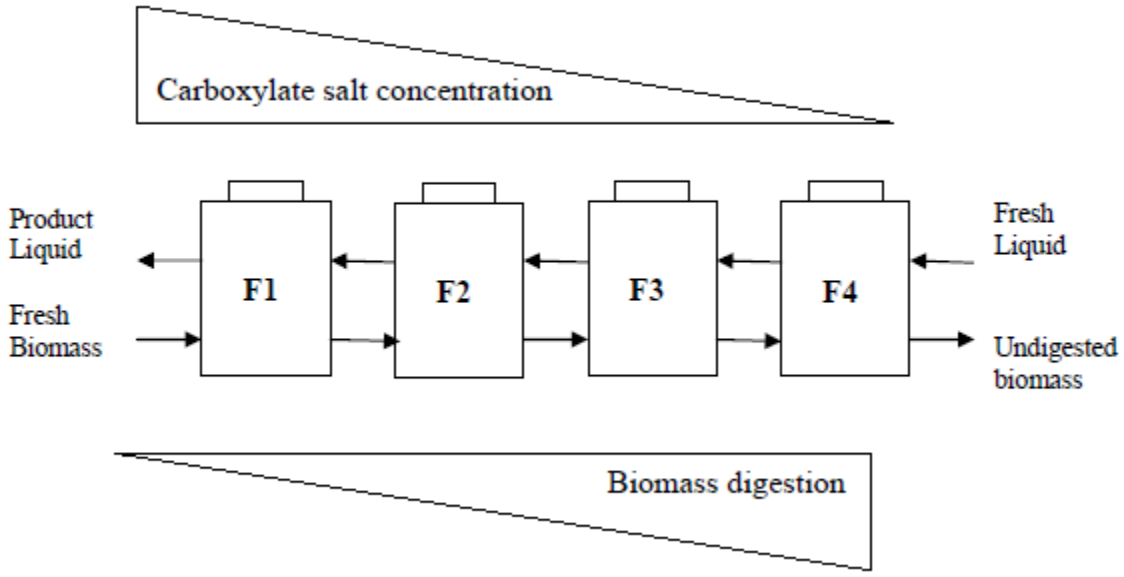

Figure 1-3. Four-stage countercurrent fermentation.

The MixAlco™ process is a desirable technology for converting lignocellulosic biomass to fuels and chemicals. It is well developed and starting commercial production. A MixAlco™ demonstration plant is currently operating in Bryan, TX. Although economic analysis of the MixAlco™ process shows that it is competitive with other lignocellulosic conversion technologies, more research is needed to make it competitive with traditional fossil fuels (Granda et al., 2009).

This main objectives of this research are (1) determine the theoretical and actual amount of hydrogen produced from mixed-acid fermentations, (2) process and screen multiple inocula sources and compare their fermentation profiles, and (3) ferment multiple substrates for their potential yield in the MixAlco™ process. The results obtained from this research will contribute to optimizing biomass conversion into chemicals and fuels. This dissertation is part of the research program developed by Dr. Holtzapple that has been performed at Texas A&M for the past 20 years.

CHAPTER II
MATERIALS AND METHODS

This chapter provides a guide to the general materials and methods used in this dissertation. First, biomass feedstocks and pretreatments are summarized. Then, the design of the different fermentors is discussed. Analytical techniques for gas and liquid product are also described.

2.1 Biomass feedstock

Several substrates were used as the carbon source for anaerobic fermentations in the dissertation: sugarcane bagasse, office paper wastes, wood molasses, sugar molasses, pineapple waste, glycerol, algae, *Aloe vera*, and water hyacinths. Chicken manure, yeast extract, and corn steep liquor were used as nutrient sources.

2.1.1 Sugarcane bagasse

Sugarcane bagasse is generated during the milling of sugarcane and is plentiful in tropical and subtropical regions. All bagasse used in this dissertation was obtained from the Lower Rio Grande Valley, the location of the Texas sugarcane industry. Air-lime pretreatment was used to enhance the digestibility of sugarcane bagasse (Section 2.2).

2.1.2 Office paper wastes

Many institutions generate huge volumes of waste paper, necessitating expensive disposal into limited landfill space. Using office paper waste as biomass feedstock not only reduces disposal costs but also earns revenue that would otherwise be lost. Office paper wastes were collected from the wastepaper bin in the graduate student computer lab and from the copier room (Department of Chemical Engineering, Texas A&M University, College Station, TX). The collected paper was shredded through a conventional paper shredder to achieve a homogeneous size. No additional treatments were necessary because the paper pulping and manufacturing process already treats the paper.

2.1.3 Wood molasses

Wood molasses is a group of products produced by direct hydrolysis of wood and is present in concentrated sulfite liquor. It is considered a byproduct because the primary reason to process wood is to produce pulp for paper products. The composition varies considerably depending on the species of wood and the commercial process. Wood molasses is generally high in sugars, especially pentoses, and in dissolved lignin. Most facilities burn off the organic sugar and lignin components to recover the sulfurous chemicals. It is used as a feed additive when the wood molasses production exceeds the recovery capacity of the individual facilities. Wood molasses used in this dissertation was provided by Temple Inland (Dipoll, TX).

2.1.4 Sugar molasses

Sugar molasses is the residual syrupy liquid from either sugarcane or sugar-beet processing. Once the initial juice is processed from the plant, it is boiled until the sucrose crystallizes. When the maximum amount of sucrose has been removed, the remaining thick liquid is sugar molasses. Although the majority of sucrose has been removed, it still contains high concentrations of both fructose and glucose along with vitamins, minerals, and salts. All sugar molasses used in this dissertation was obtained from the Lower Rio Grande Valley, the location of the Texas sugarcane industry.

2.1.5 Pineapple waste

Pineapple waste is generated from the residual pineapple plants after the pineapples are harvested. All pineapple waste used in this dissertation was obtained from Costa Rica. It was chipped in a wood chipper. Hot-lime pretreatment was used to enhance the digestibility of pineapple waste (Section 2.2).

2.1.6 Glycerol

Biodiesel is produced from the transesterification of triglycerides in fats and vegetable oils, resulting in glycerol as a byproduct. For every gallon of biodiesel produced, 1 pound of glycerol is produced. Unfortunately, this crude glycerol byproduct contains as much as 20% moisture and several catalytic and waste residues that make it difficult to use.

Vacuum distillation followed by carbon treatment can remove much of the impurities, but it is extremely energy intensive.

Three types of glycerol were used in this dissertation: (1) refined glycerol was obtained from Fisher Scientific (Cat # 3290-16); (2) crude glycerol, taken straight from the biodiesel process without any refining; and (3) distilled glycerol, which has not had any carbon treatment. The crude and distilled glycerol were obtained from Texas Molecular (Deer Park, TX).

2.1.7 Algae

The algae used in this research was from the *Chlamydomonas* genus, which has been grown as a potential alternative source of crude oil for the petroleum industry. Two varieties were examined in this research: (1) extracted algae, where 55% of the available oils had been extracted from the biomass, and (2) non-extracted algae. Both forms of algae were dried before fermentation and were supplied by Sapphire Energy.

2.1.8 *Aloe vera* rinds

Aloe vera is a succulent plant that grows in arid regions and is known for its medicinal properties. The juice extracted from the plant has a wide variety of uses, most notably the treatment of minor burns. Once the juice had been extracted, the resulting rinds are generally composted. For this dissertation, the *Aloe vera* rinds were obtained from Aloe Vera of America (Dallas, TX).

2.1.9 Water hyacinth

The water hyacinth is a free-floating aquatic plant native to South America (Simpson and Sanderson, 2002). It is an extremely vivacious grower that can double its population in less than two weeks, choking waterways and starving the water of oxygen thus killing fish. A single square meter of water surface area can hold as much as 50 wet kilograms of water hyacinths (Wolverton and McDonald, 1979). For this dissertation, the water hyacinths were obtained from a local pond in College Station, TX and air-dried for 6 weeks. Both hot-lime and air-lime pretreatments were used on the water hyacinths.

2.1.10 Chicken manure

Animal wastes such as chicken manure contain a large amount of proteins and minerals. Utilizing them for anaerobic fermentations provides an inexpensive nutrient source. Chicken manure was obtained from the Poultry Science Center (Texas A&M University, College Station, TX) and from Feathercrest Farms (Bryan, TX). Chicken manure was dried and stored for future use.

2.1.11 Yeast extract

Yeast extract is used as a common nutrient source in industrial fermentations. It is produced by salting and heating yeast cell cultures to lyse the cells, which produce more easily digested chemicals. Yeast extract was purchased from Fisher Scientific (Cat # AC61180-5000).

2.1.12 Corn steep liquor

Corn steep liquor is another common nutrient source in industrial fermentations. It is a byproduct of the corn wet milling process. Corn is milled to separate its chief components: starch, germ, fiber, and protein. Initially, corn is steeped in 120°F water for 20−36 hours. The corn then is separated and ground. To make corn steep liquor, the steepwater is concentrated to 45−50% solids and contains a significant fraction of the soluble components of corn, including high concentrations of proteins and sugars. The corn steep liquor used in this dissertation was obtained from Fisher Scientific (Cat # NC9576247).

For all substrates and nutrients, volatiles solids were determined (Appendix F). Dry matter content was determined by drying the sample overnight in a forced-draft oven at 105 °C via Standard Procedure No. 001 (NREL, 2004). Ash content was determined by heating the sample in a muffle furnace at 550 °C for at least 4 hours (NREL Standard Procedure No. 002).

2.2 Biomass pretreatment

Sugarcane bagasse, pineapple waste, and water hyacinths were chemically pretreated in this study. Two different pretreatment methods (hot-lime and air-lime) are described as follows:

2.2.1 Hot-lime-water treatment

Hot-lime-water treatment (Appendix A) was performed at 100 °C for 1 to 2 hours with loadings of 0.3 g $Ca(OH)_2$/g dry biomass. Distilled water was added to submerge the biomass in the treatment vessel. Additional water was added if the level boiled too low during the treatment. After the treatment, carbon dioxide was bubbled through the biomass slurry to neutralize the residual lime until the pH fell to 7.0. The resulting slurry was air dried for 5 days.

2.2.2 Air-lime treatment

Air-lime treatment (Appendix B) was performed at 50 °C for 4 to 8 weeks with loadings of 0.3 g $Ca(OH)_2$/g dry biomass. Distilled water was added to submerge the biomass in the treatment vessel. Additional water was added as necessary to maintain the water level for the duration of the treatment. Air was bubbled through the biomass slurry throughout the 4 to 8 weeks of pretreatment. After the pretreatment was complete, carbon dioxide was bubbled through the biomass slurry to neutralize the residual lime until the pH was 7.0. The resulting biomass was air dried for 5 days.

2.3 Fermentation materials and methods

2.3.1 Substrates

For anaerobic fermentations, the carbon sources were sugarcane bagasse, office paper wastes, wood molasses, sugar molasses, pineapple waste, glycerol, algae, *Aloe vera*, and water hyacinths. The nutrient sources were chicken manure, yeast extract, and corn steep liquor. For chicken manure fermentations, the preferred ratio is 80 wt% biomass/20 wt% chicken manure (Agbogbo, 2005; Aiello-Mazzarri, 2002).

2.3.2 Fermentation media

In this dissertation, both distilled and deoxygenated water were used in fermentations. Distilled water was obtained from the common supply line in the Brown Building. Deoxygenated water was prepared according to the method described in Appendix C. Deoxygenated water was prepared by boiling distilled water for 10 minutes after the water reached boiling. After cooling to room temperature, 0.275 g/L sodium sulfide and 0.275 g/L cysteine hydrochloride were added to eliminate possible residual oxygen in the anaerobic water.

2.3.3 Inoculum sources

Several inoculum sources were studied in this dissertation. Galveston inoculum was collected from the seashore of Galveston Island (Galveston, TX). The Galveston samples were taken from a 0.5-m-deep hole and stored in 1-L centrifuge bottles filled with deoxygenated water. All bioscreening samples (Table 2-1, Appendix M) were collected from the first 10-cm of soil and sealed in airtight plastic bags. In several fermentation screenings, a pure culture of *Clostridium thermocellum* was used as a comparison. *C. thermocellum* was obtained from ATCC (Cat # ATCC 27405) and grown on GS-2 medium (Appendix H) in Anaero Jars (Oxoid Cat # AG0025) in a Coy Chamber until ready for use.

Table 2-1. Bioscreening sampling sites.

Location	Date Sampled	Sample Labeling	# of Samples
La Sal del Rey, TX	6/23/2008	A	27
Galveston, TX	7/15/2009	B	1
Bryan, TX	7/15/2009	B	1
Bahamas	7/15/2009	B	1
Taiwan	7/22/2009	C	1
Gruella - Muleshoe, NM	10/10/2008	D	30
Enid, OK	10/14/2008	E	11
Brazoria, TX	10/26/2008	F	9
Roswell, NM-Carlsbad, TX	11/18/2008	G	53
San Francisco Bay, CA	2/13/2009	H	34
Big Bend National Park, TX	3/20/2009	J	23
Utah	5/1/2009	K, L	80
Savannah Area, GA	5/19/2009	M, N	63
Puerto Rico	6/5/2009	P	35
Florida	6/26/2009	Q	28
Santa Fe, NM	7/24/2009	R	20
Yellowstone	7/31/2009	S	48
Nevada	8/11/2009	T	17
Nevada-California	8/31/2009	U	24

2.3.4 Methanogen inhibitor

In the MixAlco™ process, methane is undesirable because it has a lower economic value then the acids. To achieve high carboxylic acid concentrations in the fermentations, methanogens should be inhibited. Iodoform (CHI_3) solution of 20 g iodoform/L ethanol was selected as the methanogen inhibitor in all fermentations. Because of light and air sensitivity, the solution was kept in wrapped bottles and capped immediately after use.

2.3.5 pH buffer

Ammonium bicarbonate (NH_4HCO_3) or calcium carbonate ($CaCO_3$) were used as pH buffers. A pH of 5.8 – 6.2 resulted from calcium carbonate buffer, wheras a pH of 6.9 – 7.1

results from ammonium bicarbonate buffer. In calcium carbonate buffered fermentations, urea was also added. No urea was required for ammonium bicarbonate buffered fermentations.

The pH was measured and monitored using an ORION portable full-featured pH/temperature meter (Model # 230A). The combination electrode with BNC connector allowed the pH meter to rapidly measure pH in the anaerobic fermentation system.

2.3.6 Temperature

Most anaerobic fermentations in this study were operated under thermophilic conditions (55 °C). Mesophilic conditions (40 °C) were used in Chapter X. The fermentation temperature was controlled by the incubator.

2.3.7 Fermentors

2.3.7.1 Initial screening fermentor

The initial site bioscreening fermentations were conducted in 250-mL polypropylene centrifuge bottles (61.8 × 127.7 mm, Nalgene brand NNI 3120-0250). No alterations were made to either the bottles or the caps. The bottles were placed vertically in a shaker table incubator running at 100 rpm.

2.3.7.2 Plastic fermentor

Plastic fermentors (Figures 2-1 and 2-2) were used in both batch and countercurrent fermentations. Fermentors were made from Beckman 1-L polypropylene centrifuge bottles (98 × 169 mm, Nalgene brand NNI 3120-1010). The bottle tops were sealed with a Size-11 rubber stopper with a hole drilled in the middle. A glass tube was inserted through the hole and capped with a rubber septum for gas release. Two 0.25-in-diameter stainless-steel tubes with welded ends were inserted into holes in the stopper.

Frequent gas venting was necessary to prevent fermentor breakage/explosions. The rubber septum was replaced once there was a visible hole from frequent gas venting.

The plastic fermentors were placed in a Wheaton Modular Cell Production Roller Apparatus (Figure 2-3) located in an incubator consisting of rollers and rotating horizontally at 2 rpm.

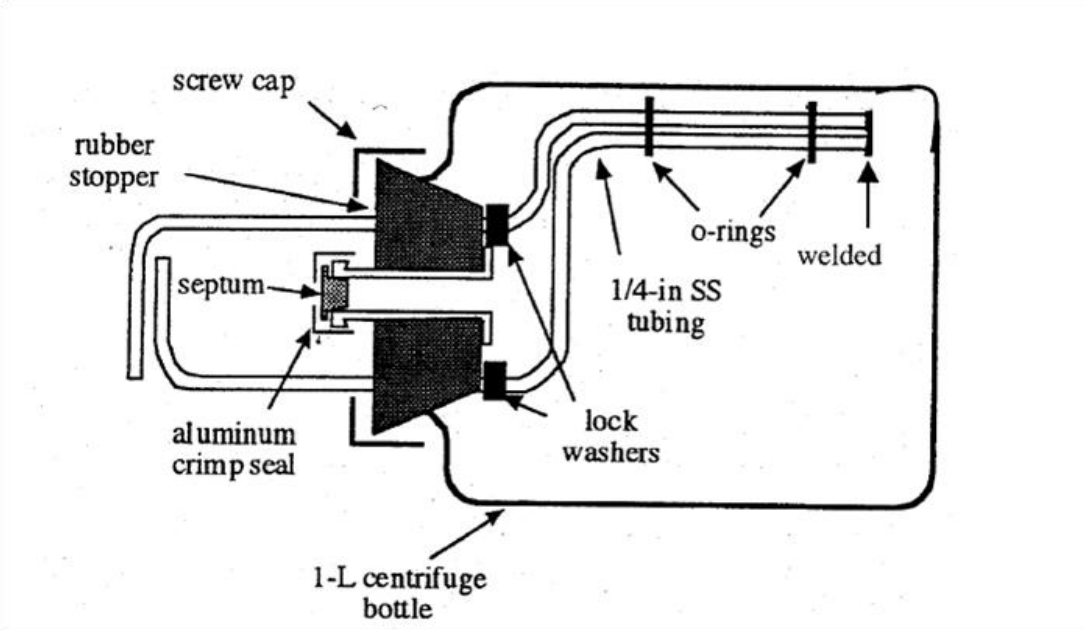

Figure 2-1. Design of the plastic fermentor.

Figure 2-2. Photograph of the plastic fermentor.

Figure 2-3. Photograph of the fermentation incubator.

2.3.7.3 Stainless-steel fermentor

Stainless-steel fermentors (SS) were used for all hydrogen fermentations. Each fermentor (Figures 2-4 and 2-5) consisted of a 6-in-long 4-in-diameter Sch-10 stainless steel pipe with a 1/8-in-thick stainless steel plate welded to each end. The top plate of the fermentor had a 2-in-diameter hole where a quick-connect fitting was welded (McMaster-Carr #4322K163). A 2-in gasket (McMaster-Carr #4509K15) and cap (McMaster-Carr #4322K222) were placed onto the fitting and held in place by a tightened clamp (McMaster-Carr #4322K153). A ¼-in quick-disconnect self-sealing valve was inserted into the cap for intermittent gas release (Swagelok # SS-QM2-B-400). A length of ¼-in stainless steel tubing is bent back on itself and inserted into the mouth of the fermentor to mix the contents. The vessels proved to be sealed tightly; no pressure loss was detected after 10 days with 150-psig H_2. The fermentors were placed on a Wheaton Modular Cell Production Roller Apparatus located in an incubator and rotated at 2 rpm.

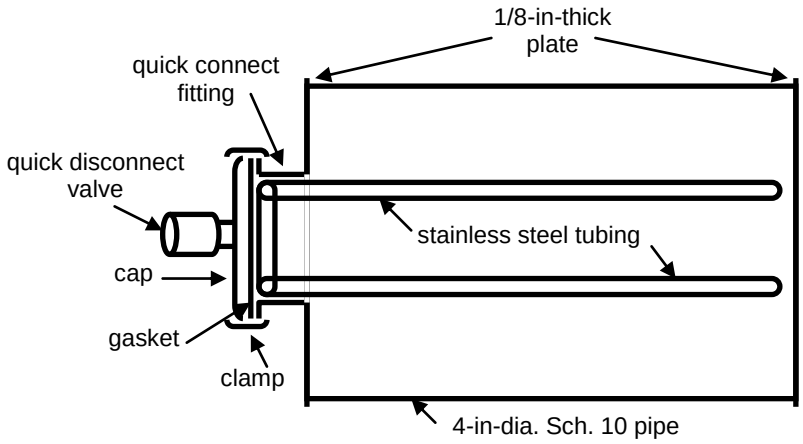

Figure 2-4. Design of the stainless-steel fermentor.

Figure 2-5. Photograph of the stainless-steel fermentor (clamp removed).

2.3.7.4 Continuously stirred tank reactor (CSTR)

The CSTR (Figure 2-6) was a 13.7-L fermentor from Schott Gerate with a motor-driven agitator and a gasket-sealed lid. Gas was vented through the lid. Hot water ran through a heating coil within the fermentor to maintain constant temperature. A pH probe was inserted through the lid for continuous pH control and monitoring.

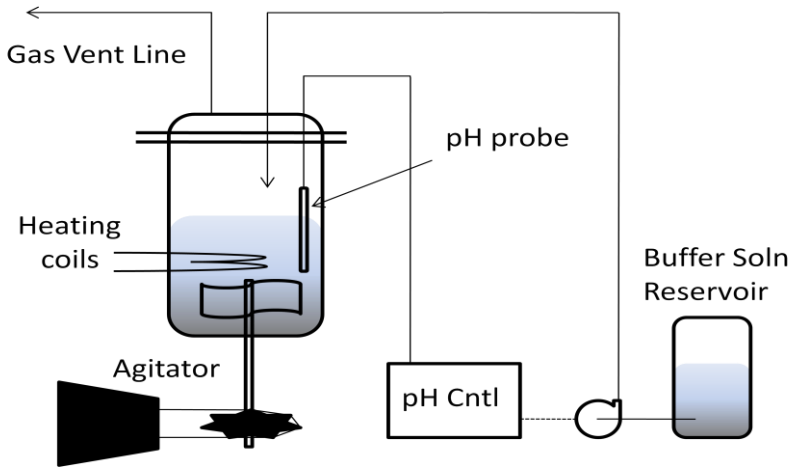

Figure 2-6. Design of the CSTR fermentor.

2.3.7.5 Packed-bed fermentor

The packed-bed fermentor (Figure 2-7) was made from 2-in- and 3-in-diameter PVC pipes and was glued together with 3-in PVC covers with 2-in holes. The outer jacket had a hot water inlet controlled to maintain the fermentor temperature. The packed column was filled with 15-mm Berl saddles. Gas was vented from the upper lid. The catch reservoir for the fermentor broth was made from 6-in PVC pipe sealed with 6-in caps. Broth was pumped out of the reservoir and through the packed column. A pH probe was inserted into the reservoir for continuous pH control and monitoring.

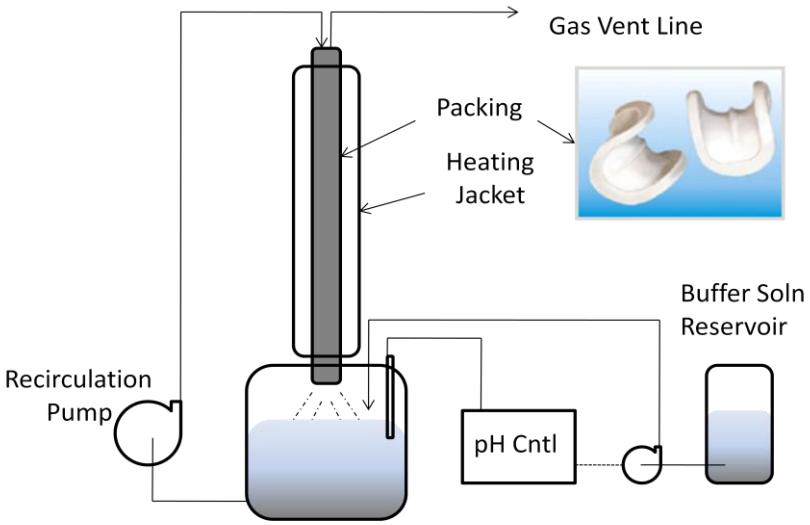

Figure 2-7. Design of the packed-bed fermentor.

2.3.8 Fermentation procedure

2.3.8.1 Batch experiments

During batch operation, no additional liquid or solids were added to the fermentation after the initial charge. Batch experiments were initiated by adding the desired substrates, nutrients, inoculum source, and pH buffer to the liquid medium. Batch fermentations were operated under thermophilic conditions (55 °C) or mesophilic conditions (40 °C).

2.3.8.2 CSTR experiments

CSTR fermentations were performed at 55 °C. Substrate (80 wt%) and chicken manure (20 wt%) were loaded into each fermentor at a total concentration of 100 g/L liquid. Continuous fermentation was initiated as batch cultures under anaerobic conditions. The experiments were conducted as batch fermentations until the culture was established (~10 d). The fermentor operated in a semi-continuous manner. Continuous operation was initiated with the transfer of slurry occurring every two days. The lid was removed, 500 mL of slurry was replaced with 500 mL of fresh slurry containing glycerol (48 g), chicken manure (12 g), and distilled water (462 mL), liquid samples were taken, and iodoform was added. The fermentor was then purged with nitrogen to maintain anaerobic conditions and the lid was replaced. The pH was monitored and continuously adjusted to 7.0 using 30 wt% ammonium bicarbonate buffer.

2.3.8.3 Packed-bed experiments

Packed-bed fermentations were performed at 55 °C. Substrate (80 wt%) and chicken manure (20 wt%) were loaded into each fermentor at a total concentration of 100 g/L liquid. Continuous fermentation was initiated as batch cultures under anaerobic conditions. The experiments were conducted as batch fermentations until the culture was established (~4 d). Slurry was continually recirculated through the packed-column throughout all fermentations. Continuous operation was initiated with the transfer of liquid in and out of the catch basin. Liquid samples were taken daily and iodoform was added. The pH was monitored and continuously adjusted to 7.0 using 30 wt% ammonium bicarbonate buffer.

2.3.8.4 Countercurrent experiments

In countercurrent operation, the liquid and solids flow in opposite directions in a four-fermentor train. Either plastic or SS fermentors were used. Countercurrent fermentations were initiated as batch fermentations until the culture was established (~10 days). The liquid and solid transfers were operated every two days. The liquid produced in one reactor was fed to the next reactor upstream, and the solids from a reactor were moved to the next reactor downstream as described in Figure 2-8. At each transfer, the fermentors were removed from the incubator and the produced gas was vented and measured. The fermentors were opened under nitrogen purging, capped with centrifuge bottle caps, and centrifuged for 25 min to separate the solids and the liquid. A sample of the liquid from Fermentor 1 (F1) was taken for carboxylic acid analysis and the rest was decanted for later VS analysis. Solids from Fermentor 4 (F4) were collected for VS analysis. Fresh biomass was added to F1 and fresh liquid was added to F4. A constant wet cake of predetermined weight was maintained in each fermentor to achieve steady-state conditions. Once the transfer was completed, the fermentors were purged with nitrogen, closed and placed back in the incubator. Steady-state conditions were evidenced when a consistent acid concentration was produced for at least 2 weeks in a row.

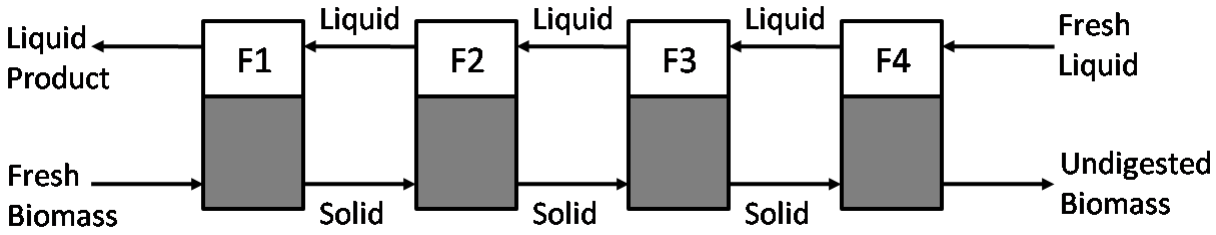

Figure 2-8. Flow diagram of a typical countercurrent fermentation.

2.4 Mass balance of fermentation system

Mass balances were performed in the countercurrent fermentations. Biomass is composed of volatile solids (VS) and ash. Most of the volatile solids are reactive whereas the ash is nonreactive. Figure 2-9 shows that a fermentation process digests the VS and produces gas and liquid products, with some solid components remaining.

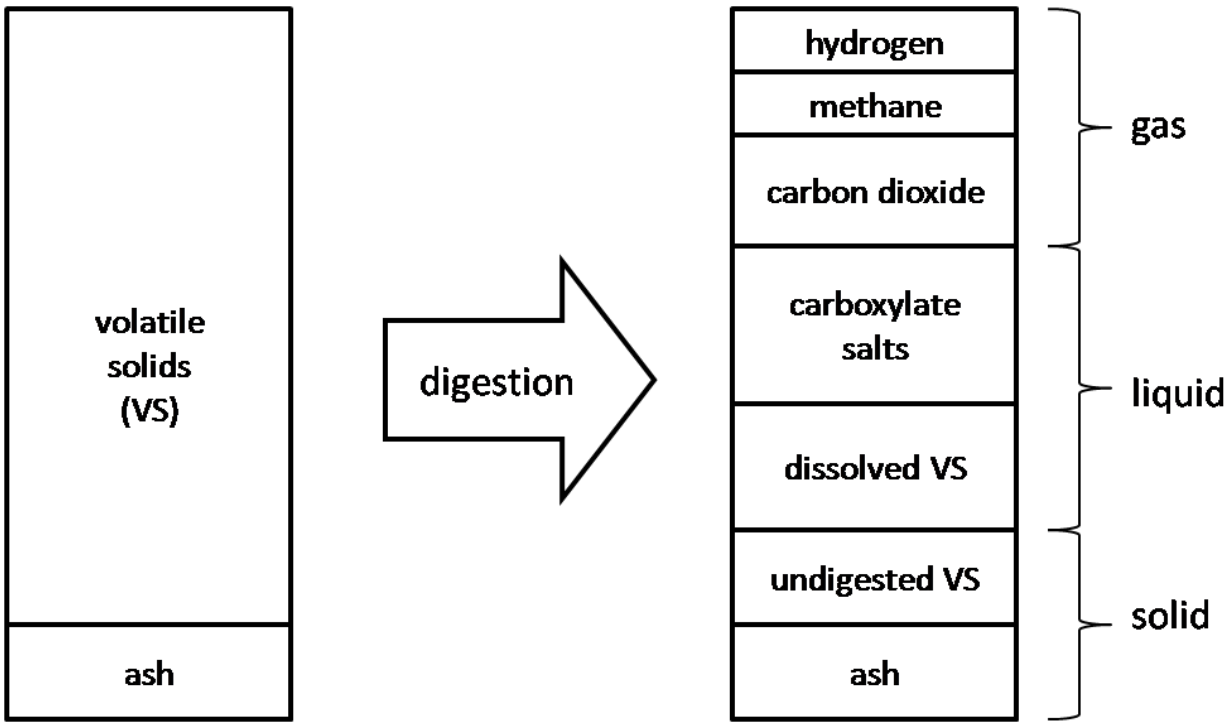

Figure 2-9. Biomass digestion.

A complete mass balance was performed on each countercurrent train over a steady-state period. The mass balance closure represents the difference between the mass entering and the mass exiting the system. In theory, the closure should be 100%. Deviations are due to unavoidable errors in the measurement process. The mass balance equations are defined as follows:

$$\text{VS in} = \text{VS out} \quad (2\text{-}1)$$

$$\text{VS in} = \text{Undigested VS} + \text{dissolved VS} + \text{carboxylic acids produced} + \text{biotic } CO_2 + CH_4 + H_2 \quad (2\text{-}2)$$

$$\text{Mass in} = \text{Mass out} \quad (2\text{-}3)$$

Biotic CO_2 is the carbon dioxide that is actually produced by the microorganisms during the course of the fermentation. The buffers used in the fermentation also release carbon dioxide when they neutralize the produced acids. The highly soluble ammonium bicarbonate buffer reacts immediately with any free acids, causing the release of carbon dioxide that is vented immediately during the transfer process and is not collected with the rest of the fermentation gases. But, the largely insoluble calcium carbonate reacts slowly

with the free acids, releasing carbon dioxide into the closed fermentor bottles while the fermentation progresses. For every two moles of carboxylic acid produced, one mole of *abiotic* CO_2 is released by the calcium carbonate buffer. For calcium carbonate buffered fermentations, the biotic CO_2 is calculated by subtracting the abiotic CO_2 from the total carbon dioxide measured in the fermentation.

Mass balance closure on the entire system was calculated over the steady-state period.

$$\text{Closure} = \frac{\text{Mass(out)}}{\text{Mass(in)}} \quad (2\text{-}4)$$

$$= \frac{\text{Undigested VS} + \text{Dissolved VS} + \text{Carboxylic Acids} + \text{CO}_2 + \text{CH}_4 + \text{H}_2}{\text{VS(in)}} \quad (2\text{-}5)$$

2.5 Definition of terms

2.5.1 Fermentation operating parameters

The operational parameters of the countercurrent fermentations are liquid residence time (LRT) and volatile solids loading rate (VSLR).

The LRT determines how long the liquid remains in the system and also affects the final product concentration. Long residence times allow high product concentrations whereas shorter residence times allow lower product concentrations (Holtzapple et al., 1999). LRT is calculated as

$$\text{Liquid residence time (LRT)} = \frac{\text{TLV}}{\text{Q}} \quad (2\text{-}6)$$

Q = flowrate of product liquid out of the fermentor set (L/d)

TLV = total liquid volume, calculated as:

$$\text{Total liquid volume (TLV)} = \sum_i (\overline{K_i} * w + \overline{F_i}) \quad (2\text{-}7)$$

$\overline{K_i}$ = average wet mass of solid cake in Fermentor *i* (g)

w = average liquid fraction of solid cake in Fermentor *i* (L liquid/g wet cake)

$\overline{F_i}$ = average volume of free liquid in Fermentor *i* (L)

The VSLR represents the rate at which the reactive biomass is added to the system, and is calculated by

$$\text{Volatile solids loading rate (VSLR)} = \frac{\text{VS fed/day}}{\text{TLV}} \quad (2\text{-}8)$$

A low VSLR increases the solid residence time, i.e., the length of time the solids remain in the system. Longer solid residence times increase digestion and improve product yields.

2.5.2 Fermentation performance parameters

The following terms were used to evaluate the fermentation performance in this dissertation:

$$\text{conversion} = \frac{\text{VS digested}}{\text{VS fed}} \quad (2\text{-}9)$$

$$\text{yield} = \frac{\text{total carboxylic acids produced}}{\text{VS fed}} \quad (2\text{-}10)$$

$$\text{total acid selectivity} = \frac{\text{total carboxylic acids produced}}{\text{VS digested}} \quad (2\text{-}11)$$

$$\text{total acid productivity} = \frac{\text{total carboxylic acids produced}}{\text{L liquid in all reactors} \times \text{time}} \quad (2\text{-}12)$$

2.6 Analytical methods

As mentioned in Section 2.4, gases (i.e., carbon dioxide, hydrogen, and methane) accumulate in the reactor during anaerobic fermentation. Frequent release and measurement avoids possible fermentor explosion.

2.6.1 Gas volume measurement

The volume of produced gas was measured by displacing water in a self-constructed inverted glass graduated cylinder apparatus (Figure 2-10) filled with 30 wt% $CaCl_2$ solution. Calcium chloride minimized microbial growth and reduced water evaporation. Also, $CaCl_2$ prevents CO_2 adsorption, because it had an acidic pH (5.6).

To ensure accurate measurement, the fermentors were cooled to room temperature before measuring the gas volume. The laboratory equipment allowed three gas volumes to be measured at the same time. A hypodermic needle was inserted into the fermentor septum and the released gases displaced the liquid in the cylinder until the pressure in the fermentor was equal to the pressure in the cylinder. The recorded length of water displacement was converted into produced gas volume (V) using the following equation: V (mL) = 21.2 × L (cm).

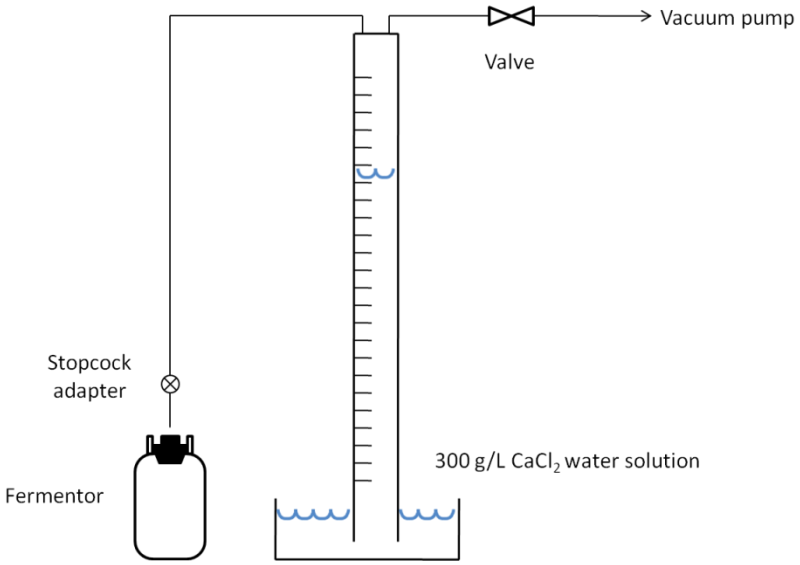

Figure 2-10. Diagram of the water displacement device used to measure gas volume produced from anaerobic fermentations.

2.6.2 Gas content measurement

A gas chromatograph (Agilent 6890 series, Agilent Technologies, Palo Alto, CA) equipped with a thermal conductivity detector (TCD) was used to determine the nitrogen, hydrogen, methane, and carbon dioxide composition of the fermentation gas. Gas samples were taken directly from the fermentor septum using a 5-mL syringe.

2.6.3 Carboxylic acids concentration in liquid samples

Each 3-mL sample taken from the fermentors was stored in the freezer at −20 °C for future analysis. They were thawed and thoroughly mixed before analysis.

Liquid samples were analyzed for total carboxylic acid concentration using an Agilent 6890 series chromatograph (Agilent Technologies, Palo Alto, CA) equipped with a flame ionization detector (FID) and a 7683 series injector. Liquid samples were mixed with 1.162 g/L of internal standard (4-methyl-*n*-valeric acid) and acidified with 3-M phosphoric acid. For calibration, a standard carboxylic acid mix (Matreya, LLC, Cat #1075) was injected prior to injecting the samples. Acid analysis was performed with a capillary column (J&W Scientific, model DD-FFAP). The oven temperature in the GC increased from 40 °C to 200 °C at 20 °C/min and was held an additional 1 min at 200 °C. More detail of sample preparation and analysis are described in Appendix E.

2.6.4 Volatile solid determination

During each transfer, liquid from F1 and solid from F4 were collected and stored at −20 °C for future analysis. The volatile solids (VS) content of both the liquid and solid samples were determined by first drying at 105 °C in an oven and then ashing at 575 °C in a furnace. The VS weight was calculated as the difference between the dry weight and the ash weight (Appendix F).

An additional calculation is needed for calcium carbonate buffered fermentations. In ammonium bicarbonate buffered fermentations, the ammonium salts of the carboxylic acids vaporize during the drying process and are not retained in the dry solids. But, in calcium carbonate buffered fermentations, the calcium salts are retained in the dry solids. These salts then react in the furnace during ashing, decomposing to calcium carbonate and degradation products. The actual VS remaining in the fermentor residue is calculated in Equation 2-13.

$$\text{Actual VS(g)} = \text{Measured VS(g)} - \text{Total Acids(g)} \times \text{VAF} \quad (2\text{-}13)$$

$$\text{Volatile Acid Factor(VAF)} = \sum(\text{Acid mass fraction}_i \times \text{Acid mass change}_i) \quad (2\text{-}14)$$

$$\text{Acid mass change} = \frac{\text{MW}_{\text{CaAcid}} - \text{MW}_{\text{CaCO3}}}{\text{MW}_{\text{CaAcid}}} \quad (2\text{-}15)$$

2.6.5 Structural carbohydrate and lignin analysis

A two-step acid hydrolysis was used to degrade biomass into forms that were more easily quantified. The biomass sample was taken through a primary 72% (w/w) sulfuric acid hydrolysis at 30 ºC for 1 h, followed by a secondary dilute acid (4%, w/w) hydrolysis at 121

ºC for 1 h. The resulting sugar monomers and acetyl content were analyzed using HPLC with Bio-Rad Aminex HPX-87P and HPX-87H columns, respectively. The acid-soluble lignin was measured by UV-Vis spectroscopy. The acid-insoluble lignin was determined using gravimetric analysis at 105 °C and 575 °C. The total lignin content was the summation of acid-insoluble lignin and acid-soluble lignin. This method is based on NREL standard procedure No. 002 (2004), with the detailed procedure given in Appendix G.

2.6.6 DNA extraction and microbial community identification

DNA extractions and microbial identifications were performed by Emily Hollister in the Soil and Crop Sciences Department. The composite samples from fermentations of interest were frozen and stored at −80 ºC until DNA extraction. Prior to extraction, the samples were thawed and centrifuged at 4000 × g for 10 min. DNA was extracted from the pellet materials using a PowerMax soil DNA extraction kit (Mo Bio Laboratories, Inc., Carlsbad, CA, USA), using a lysozyme-modified version of the manufacturer's protocol (Hollister et al., 2010). Briefly, 15 g aliquots (wet weight) of fermentation material and 15 mL of bead solution were added to each bead beating tube. After 5 min of bead beating, lysozyme was added (final concentration of 1 mg/mL), and samples were incubated at 37 ºC for 1 h. Following lysozyme treatment, solution "C1" was added and samples were incubated at 65 ºC for 30 min. The manufacturer's protocol was followed from this point onward. Following elution, DNA samples were concentrated and purified using illustra MicroSpin S-400 HR columns (GE Healthcare Bio-Sciences Corp, Piscataway, NJ, USA). DNA samples were quality checked according to US DOE Joint Genome Institute protocols and were submitted to the Joint Genome Institute for pyrotag sequencing of the V6 hypervariable region of the 16S rRNA gene.

Community DNA sequences were quality checked, and trimmed to a common length. Sequences were compared against the Greengenes NAST-aligned database (DeSantis et al., 2006) and used to assign identities down to the genus level for the entire sequence data set. Sequences of 97% similarity or higher to those within the database were considered identical. Those with less than 97% similarity were tentatively identified and considered closely related. Relative abundance of each identification was determined by the number of sequences of each type over the entire number of sequences.

2.7 Bioscreening steps

The Bioscreening Project is a joint project between three departments: the Soil and Crops Sciences Department, the Department of Plant Pathology and Microbiology, and the Department of Chemical Engineering. The purpose of the project was to find naturally occurring communities of microorganisms that were highly efficient at digesting biomass in the MixAlco™ process.

To do this, this study screened the fermentations in three main steps: (1) the initial screen, (2) the CPDM determination, and (3) the countercurrent fermentation.

The initial screen consisted of a batch fermentation in the 250-mL bottles of each sample taken from each site, incubated at 55 °C for 30 days. The Continuum Particle Distribution Modeling (CPDM) determination step determined the CPDM parameters for either the best sample from a particular site or of a sample that showed an interesting conversion. Step 3 ran countercurrent fermentations on samples that had produced CPDM 'maps' that showed higher conversions and acid concentrations that the base-line inocula of Galveston sand.

Fermentation material was sampled and stored at −80 °C throughout all three steps for later DNA extraction and identification.

2.8 CPDM method

The CPDM model was used to predict the countercurrent fermentation using data collected from batch fermentation. CPDM principles are detailed in Chapter VI. Five batch experiments were run simultaneously with different initial substrate concentrations of 20, 40, 70, 100, and 100+ g substrate/L liquid. The 100 and 100+ fermentors has the same initial substrate concentration, but the 100+ fermentor contained a medium with a mixture of carboxylate salts in a concentration of 20 g carboxylic acid/L liquid. The inoculum for the batch fermentors was taken from an adapted culture grown under the same type of substrates. Iodoform was added to inhibit methane production and liquid samples were taken every two days. The amount of measured carboxylic acid was converted to acetic acid equivalents (Aeq). The specific reaction rate as a function of acid concentration (Aeq) and substrate conversion (x) was expressed in Equation 2-16.

$$\hat{r}_{pred} = \frac{e(1-x)^f}{1+g(\phi \cdot \mathrm{Aeq})^h} \tag{2-16}$$

Nonlinear regression (SYSTAT SIGMAPLOT 12) was used to determine parameter *e, f, g,* and *h*. The $(1 - x)$ term in the numerator is the conversion penalty function described by South et al. (1995). The parameter ϕ represents the ratio of moles of acid to moles of acetic acid equivalents.

A self-coded MatLab program based on the CPDM model was used to predict the Aeq and conversion for the countercurrent fermentation at various solid loading rates (VSLR) and liquid residence times (LRT). Additionally, a "map" could be drawn to show the dependence of substrate conversion and product concentration for various VSLR and LRT. The experimental data collected from the countercurrent fermentations were used to validate the model prediction.

CHAPTER III
DETERMINATION OF HYDROGEN YIELD FROM BATCH AND COUNTERCURRENT FERMENTATIONS OF PAPER AND BAGASSE

The objectives of this chapter follow:

a) Examine the theoretical verse actual hydrogen yield from mixed-acid fermentations on both paper and bagasse.
b) Examine the Gibbs free energy of reaction at cellular conditions.
c) Develop a fermentor vessel that will contain hydrogen gas during both batch and continuous fermentations.
d) Determine the hydrogen production from batch fermentations of paper and bagasse.
e) Determine the hydrogen production from continuous countercurrent fermentations of paper and bagasse.

3.1 Introduction

Hydrogen has long been sought as the ultimate 'green' fuel (Veziroglu and Barbir, 1992). Hydrogen combustion produces only water with no CO, CO_2, hydrocarbons, or fine particulates. Its combustion also releases a large amount of energy (122 kJ/g) in comparison to typical fossil fuels (44 kJ/g). Difficult hydrogen storage and lack of infrastructure have made it unfeasible to use hydrogen as a fuel gas. Although hydrogen is the most abundant element, comprising roughly 75% of the universe, hydrogen in its elemental gaseous form is extremely rare on Earth. Rather hydrogen is found combined with other elements, such as oxygen to form water.

Hydrogen gas is costly to produce, with steam reformation and electrolysis being the two most common methods. Steam reforming is a well-established process and results in 95% of hydrogen production and use in the United States (FSEC, 2007). Steam reforming involves the reaction of a fossil fuel, typically natural gas, with steam over a nickel catalyst at temperatures in excess of 200 °C. This causes the natural gas to decompose into hydrogen and carbon monoxide. The carbon monoxide reacts further with the steam, creating carbon dioxide and additional hydrogen. This method of hydrogen production is costly, increasing

the unit energy cost by a factor of three. For example, with a natural gas cost of $6/MMBTU, steam reformed hydrogen cost would be $18/MMBTU (FSEC, 2007).

Hydrogen is also produced electrochemically. Passing a current between two platinum electrodes, hydrogen is evolved and collected at the cathode while oxygen is evolved and collected at the anode. Electrolysis hydrogen costs 5 times the amount of electricity used for its production. If electricity costs $0.07/kWh, then electrolysis hydrogen costs $39/MMBTU.

Alternatively, hydrogen can be produced biologically. It has been known for nearly 100 years that hydrogen can be both evolved or consumed by many forms of bacteria (Homann, 2003). Hydrogen can be produced using either photosynthetic algae (Melis and Happe, 2001) or fermentative hydrogen-producing anaerobes (Nandi and Sengupta, 1998). Studies on fermentative hydrogen production have been conducted mostly using pure cultures, either natural or genetically modified (Asada et al., 2000; Evvyernie et al., 2001; Fabiano and Perego, 2002). However, hydrogen is a key intermediate from mixed cultures that anaerobically degrade liquid or solid waste (Lay et al., 1999; Mizuno et al., 2000; Sparling et al., 1997).

It would be desirable to produce all 12 atoms of hydrogen from a glucose molecule, yielding 6 molecules of hydrogen gas. This is not actually possible. From a thermodynamic perspective, the most favorable products from the metabolism of 1 mol of glucose are 2 mol of acetate and 4 mol of H_2 (Eqn. 3-1).

$$C_6H_{12}O_6 + 2H_2O \rightarrow 2CH_3COOH + 2CO_2 + 4H_2 \quad (3\text{-}1)$$

However, in practice, such high-yielding H_2 fermentations are unknown. That is expected because such a reaction would not allow for cell growth, and would be eliminated by natural selection. This near-stoichiometric yield is only achievable under near equilibrium conditions, meaning very slow rates, and/or at very low partial pressures of H_2 (Woodward et al., 2000).

3.2. Energy metabolism

3.2.1 Hexose metabolism

Agricultural residues are composed of three main components: cellulose, hemicellulose, and lignin. Cellulose is a long-chain polymer of glucose with a molecular weight in excess of 50,000 g/mol and is the primary structural component of plant walls. Hemicellulose is a heteropolymer composed of both five-carbon sugars (xylose, arabinose) and six-carbon sugars (galactose, mannose). Hemicellulose acts as a linkage between cellulose and other components of plants, including lignin and pectin. Lignin is a cross-linked racemic macromolecule. It is hydrophobic and aromatic consisting of three phenylpropanoids: p-hydroxyphenyl, guaiacyl, and syringal (Freudenberg and Neish, 1968). Lignin acts as a chemical barrier, protecting the cellulose and hemicelluloses from degradation and digestion.

Although cellulose and hemicelluloses contain several types of sugars, the microbial pathways of digestion are distinguished by the number of carbons contained in the sugar substrates. This is made possible by the presence of several classes of isomerases, enzymes that catalyze the structural rearrangement of isomers. Pentose- and hexose-specific isomerases efficiently interconvert their target sugars (five and six carbons, respectively), facilitating entry into metabolic pathways for energy conversion. This splits the digestion sugars into two metabolic pathways: hexose digestion and pentose digestion.

3.2.1.1 Cellulose degradation

Cellulose is composed of individual glucose monomers linked together by a β(1-4) glycosidic bond (Fig. 3-1). Before the hexose can be metabolized and energy harvested, the long-chain macromolecules of cellulose must be decomposed. Cellulolysis, the degradation of cellulose, is catalyzed by glycosidic hydrolase family of enzymes, or cellulases, and results in the decomposition of cellulose into smaller polysaccharides, or cellodextrins (Demain et al., 2005). In some organisms, multiple cellulases are contained within a large membrane-bound enzyme complex called a cellulosome (Bayer et al., 1998).

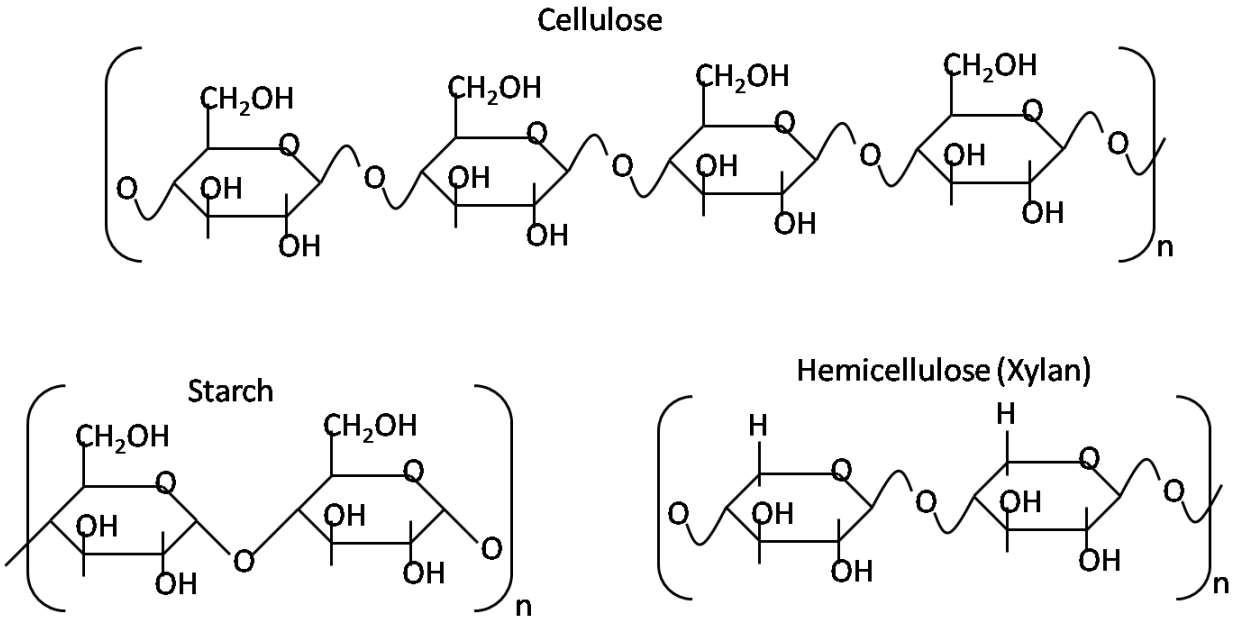

Figure 3-1. Chemical structure of three carbohydrates, cellulose, hemicelluloses (xylan), and starch. The structures show the β(1-4) glycosidic bonds of the cellulose and xylan and the α(1-4) bond of the starch.

The products of cellulase activity are cellodextrins, short-chain glucose polymers containing anywhere from two glucose monomers (cellobiose) to six glucose monomers (cellohexose). These cellodextrins pass through the cellular membrane via active transport, necessitating the consumption of ATP. ATP (adenosine triphosphate), a multifunctional intercellular compound, is utilized by all cells as their primary energy currency, using it to capture, transfer, and store the free energy needed to maintain the cell. The cellodextrins are then decomposed into individual units by either phosphorolytic or hydrolytic reactions.

Hydrolytic cleavage of cellodextrins is catalyzed by β-glucosidase enzymes and requires reaction with water (Eqn. 3-2). Phosphorolytic cleavage of cellodextrins is catalyzed by cellodextrin phosphorylase and requires neither ATP nor water, producing glucose-1-phosphate (G1P) (Eqn. 3-3) (Zhang and Lynd, 2004). G1P can then be converted to glucose-6-phosphate (G6P) by isomerases and used directly in the glycolysis pathway.

$$\mathrm{G}_n + (n-1)\mathrm{H_2O} \rightarrow n\mathrm{G} \tag{3-2}$$

$$\mathrm{G}_n + (n-1)\mathrm{PO_4^{3-}} + (n-1)\mathrm{H^+} \rightarrow (n-1)\mathrm{G1P} + \mathrm{G} \tag{3-3}$$

G_n is a cellodextrin chain of *n* monomers in length. PO_4^{3-} is inorganic phosphate, H^+ is hydrogen ions, G is glucose, and G1P is glucose-1-phosphate. Glucose-1-P is then easily converted into glucose-6-P to be used in glycolysis.

Hydrolytic cleavage is highly spontaneous at cellular conditions (ΔG = −530.18 kJ/mol at T = 55 °C, pH = 7.0, n = 4) wheras phosphorolytic cleavage is less spontaneous at cellular conditions (ΔG = −338.7 kJ/mol at T = 55 °C, pH = 7.0, n = 4). This illustrates the complexity of metabolic analysis based only on thermodynamics. Give the free energy difference between the two process, it would be anticipated that the hydrolytic pathway is preferred. Yet, several studies have demonstrated that the phosphorolytic pathway is preferred over the hydrolytic pathway (Lou et al., 1996; Lou et al., 1997; Mitchell, 1998; Strobel et al., 1995). In fact, Zhang and Lynd (2004) showed that 95% of all cellodextrin cleavage follows the phosphorolytic pathway in *Clostridium thermocellum*.

This seems counter-intuitive because it requires more energy to phosphorylate the cellodextrins then to hydrolyze them. Yet, this path results in a net increase in the total amount of ATP produced in the cell through glycolysis. Assuming cellotetraose (a cellodextrin of four glucose monomers), the ATP yield after glycolysis using the hydrolytic pathway would be eight ATP. Because the phosphorolytic pathway does not need ATP, only inorganic phosphate, the net yield of ATP from glycolysis would be 11 ATP.

3.2.1.2 Glycolysis

Within all organisms, both aerobic and anaerobic, glycolysis is the primary metabolic pathway, which converts glucose into pyruvate. The first step of glycolysis is mediated by the enzyme hexokinase, which has a broad substrate specificity, meaning it can utilize hexoses other than glucose. This, along with various isomerases and kinases, allows for the entry of a variety of six-carbon sugars (glucose, fructose, galactose, and mannose) into the glycolysis pathway. Unlike the one-step non-organic chemical balance shown in Eqn. 3-1, the breakdown of hexose takes several steps. For this study, the glycolysis pathway has been split into eight overall steps. Each mole of glucose forms 2 mol of pyruvate, 4 mol of the high-energy compound ATP (adenosine triphosphate), and 2 mol of NADH for each mol of glucose consumed (Table 3-1). Pyruvate is then used throughout the cell as a building block

for cellular structures, including the synthesis of carboxylic acids. Appendix T shows the detailed diagramed steps of glycolysis.

Table 3-1. Glycolysis pathway. Conversion of 1 mol of glucose to 2 mol of pyruvate.

Step	Reaction			
1	D-glucose + ATP	→	Glucose-6-P + ADP + H^+	(3-4)
2	Glucose-6-P	→	Fructose-6-P	(3-5)
3	Fructose-6-P + ATP	→	Fructose-1-6-P + ADP + H^+	(3-6)
4	Fructose-1-6-P	→	2 Glyceraldehyde-3-P	(3-7)
5	Glyceraldehyde-3-P + NAD^+ + P_i	→	1,3-Bisphosphoglycerate + NADH + H^+	(3-8)
6	1,3-Bisphosphoglycerate + ADP	→	2-Phosphoglycerate + ATP	(3-9)
7	2-Phosphoglycerate	→	Phosphoenolpyruvate + H_2O	(3-10)
8	Phosphoenolpyruvate + ADP + H^+	→	Pyruvate + ATP	(3-11)
Overall	Glucose + 2 ADP + 2 P_i + 2 NAD+	→	2 Pyruvate + 2 NADH + 2 H^+ + 2 ATP + 2 H_2O	(3-12)

P – Phosphate group, (PO_4^{2-})

P_i – Inorganic phosphate, (PO_4^{3-})

ATP – Adenosine triphosphate

ADP – Adenosine diphosphate

NAD^+, NADH – Nicotinamide adenine dinucleotide, reduced or oxidized

H^+ – Hydrogen ion

3.2.1.3 Carboxylic acid synthesis

When oxygen is available as the final electron acceptor, glycolysis is followed by the energy-harvesting pathways of cellular respiration: pyruvate oxidation, the TCA cycle (the citric acid cycle), and the respiratory chain. When oxygen is not available, fermentation is added to glycolysis for energy harvesting. Many different types of fermentation are performed by both prokaryotes and eukaryotes, and are typically distinguished by the pathway end-products. For example, lactic acid fermentation reduces pyruvate into lactate, wheras alcohol fermentation metabolizes pyruvate to ethyl alcohol. This study focuses on mixed-acid fermentation using a mixed culture of bacteria. The use of a mixed culture allows for the product profile to include not just acetic acid, but longer chain acids, such as propionic, butyric, valeric, caproic, and heptanoic.

As shown in Equation 3-13, converting pyruvate into acetate results in additional metabolic energy for the cell in the form of NADH and ATP.

$$\text{Pyruvate} + NAD^+ + \text{ADP} + \text{phosphate} \rightarrow \text{Acetate} + \text{NADH} + \text{ATP} + CO_2 \qquad (3\text{-}13)$$

As shown in Equation 3-14, converting pyruvate into propionate consumes energy in the form of NADH.

$$\text{Pyruvate} + 2\ \text{NADH} + 2\ H^+ \rightarrow \text{Propionate} + 2\ NAD^+ + H_2O \qquad (3\text{-}14)$$

All other higher molecular weight carboxylic acids are synthesized using acetate and propionate in their Co-enzyme A form as their basic building blocks. Carboxylic acid synthesis requires a large enzyme complex comprised of several separate proteins: acyl-carrier protein 1 (ACP1), acyl-carrier protein 2 (ACP2), and several other active sites that facilitate the linking of the building blocks and removal of oxygen.

The building of a fatty acid has three main parts: (1) initiation (Eqn. 3-15), (2) elongation (Eqn. 3-16), and (3) termination (Eqn. 3-17). Initiation begins when either an acetyl-CoA or a propionyl-CoA attach to the ACP1 site forming acetyl-ACP1 or propionyl-ACP1. CoA stands for Coenzyme A, a chemical prosthetic group that acts as a helper molecule in chemical reactions and as carrier molecules that can ‘taxi’ desirables around the

cell. Acetyl-CoA is a CoA with an acetate group attached and propionyl-CoA is a CoA with a propionate group attached.

Initiation (a)	$\text{Acetyl-CoA} + \text{ACP1} \rightarrow \text{Acetyl-ACP1} + \text{CoA}$	(3-15a)
Initiation (b)	$\text{Propionyl-CoA} + \text{ACP1} \rightarrow \text{Propionyl-ACP1} + \text{CoA}$	(3-15b)
Elongation	$\text{R}_n\text{-ACP1} + \text{Acetyl-ACP2} + 2\ \text{NADH} + 2\ \text{H}^+ \rightarrow \text{R}_{(n+2)}\text{-ACP1} + \text{H}_2\text{O}$	(3-16)
Termination	$\text{R-ACP1} + \text{H}_2\text{O} \rightarrow \text{R(carboxylate)} + \text{ACP1} + \text{H}^+$	(3-17)
Overall	$n\ \text{Acetate} + 2\times(n-1)\ \text{NADH} + 2\times(n-1)\ \text{H}^+ \rightarrow \text{Salt (length} = n\times 2) + (n-2)\ \text{H}_2\text{O} + 2\times(n-1)\ \text{NAD}^+$	(3-18)

Once ACP1 is filled, elongation begins. To begin, an acetyl-CoA reacts with CO_2 to form malonyl-CoA. Malonyl-CoA reacts with the ACP2 site to form acetyl-ACP2, thus releasing the adsorbed CO_2. The ACP2 site will only accept a malonyl-CoA, limiting fatty acid chain growth to multiples of two. The acetyl-ACP2 reacts with the group on ACP1, forming an acyl-ACP2 group. NADH is used to reduce and condense the double-bonded oxygen, releasing water. Once dehydrated, the acyl-ACP2 group is transferred to the ACP1 group and the cycle begins again.

Several factors affect the chain length of the growing fatty acid. The enzyme complex may release the acid after only one cycle, forming a butyrate or a valerate. Longer cycles of elongation result in fatty acids that may be used in fat storage or cell membrane synthesis, with anywhere from 18 to 22 carbons in the chain.

For the mixed-acid fermentations conducted during this research, the only carboxylate salts of interest vary from acetate (C2) to heptanoate (C7). Equations 3-19 through 3-24 show the overall reactions from glucose to each type of salt.

$$\text{Glucose} + 4\,[\text{ADP} + P_i] + 4\,NAD^+ \rightarrow 2\,\text{Acetate} + 4\,\text{ATP} + 4\,\text{NADH} + 2\,H^+ + 2\,CO_{2(aq)} + 2\,H_2O \quad (3\text{-}19)$$

$$\text{Glucose} + 2\,[\text{ADP} + P_i] + 2\,\text{NADH} + 2\,H^+ \rightarrow 2\,\text{Propionate} + 2\,\text{ATP} + 2\,NAD^+ + 4\,H_2O \quad (3\text{-}20)$$

$$\text{Glucose} + 3\,[\text{ADP} + P_i] \rightarrow \text{Butyrate} + 3\,\text{ATP} + 2\,CO_{2(aq)} + 3\,H_2O \quad (3\text{-}21)$$

$$\text{Glucose} + 3\,[\text{ADP} + P_i] + \text{NADH} + 2\,H^+ \rightarrow \text{Valerate} + 3\,\text{ATP} + NAD^+ + CO_{2(aq)} + 4\,H_2O \quad (3\text{-}22)$$

$$3/2\,\text{Glucose} + 6\,[\text{ADP} + P_i] + 2\,NAD^+ + H^+ \rightarrow \text{Caproate} + 6\,\text{ATP} + 2\,\text{NADH} + 3\,CO_{2(aq)} + 5\,H_2O \quad (3\text{-}23)$$

$$3/2\,\text{Glucose} + 5\,[\text{ADP} + P_i] + \text{NADH} + 3\,H^+ \rightarrow \text{Heptanoate} + 5\,\text{ATP} + NAD^+ + 2\,CO_{2(aq)} + 6\,H_2O \quad (3\text{-}24)$$

3.2.2 Pentose metabolism

Agricultural residues contain as much as 35 dry wt% hemicelluloses (Hespell and Whitehead, 1990). Unlike cellulose, which is composed only of chains of glucose, hemicellulose is a highly branched heteropolymer composed of a xylan-based backbone and a heterogeneous mixture of both five-carbon (xylose, arabinose) and six-carbon sugars (galactose, mannose) in the branches. Cellulosomes will degrade hemicelluloses to a lesser degree than they do cellulose, and a variety of xylanases with different specificities are required to degrade the xylan backbone (Fig. 3-2).

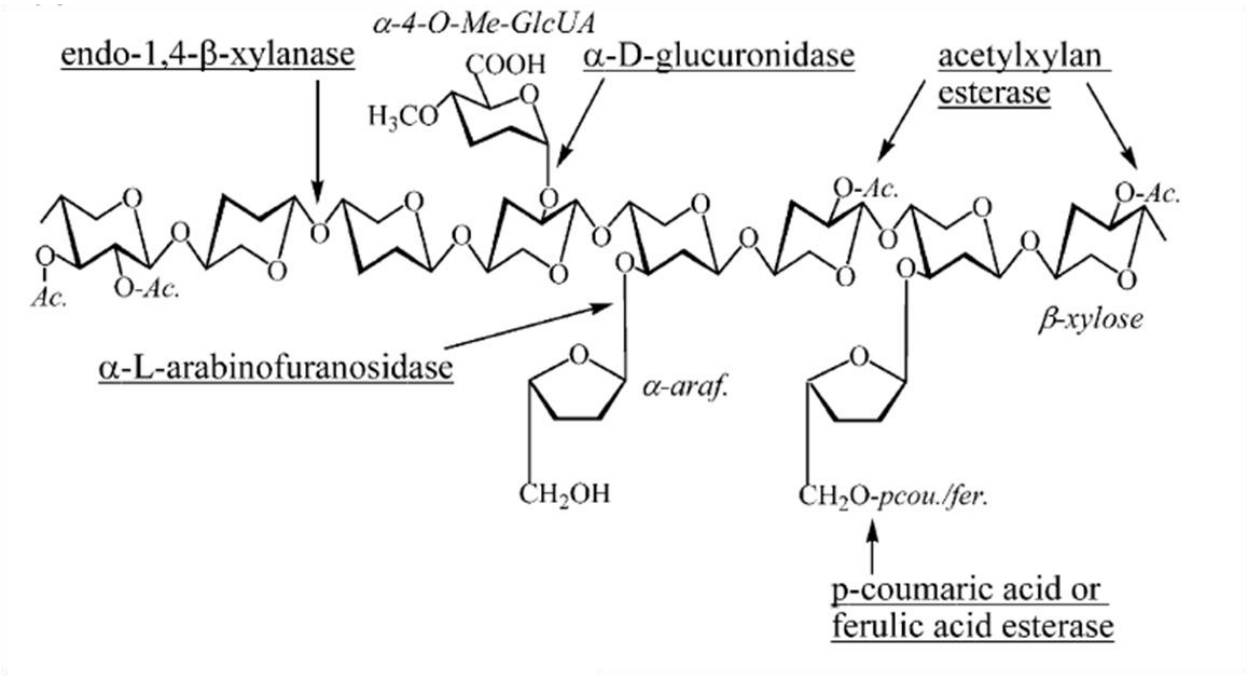

Figure 3-2. Structure of xylan and the sites of its attack by xylanolytic enzymes. The backbone of the substrate is composed of β(1,4)-linked xylose residues. *Ac*., Acetyl group; *α-araf*., α-arabinofuranose; *α-4-O-Me-GlcUA*, α-4-O-methylglucuronic acid; *pcou*., p-coumaric acid; *fer*., ferulic acid. Image adapted from Collins et al. (2005).

As with cellulases, xylanases decompose hemicellulose into short lengths of two to six xylose monomers, which can then be actively transported through the cell membrane. Although xylan-specific hydrolases and phosphorylases have been identified (Collins et al., 2005), to date there has been no research to determine whether microorganisms favor the phosphorolytic pathway as they do with glucans.

Once decomposed into their individual monomers, xylose enters the non-oxidative branch of the pentose phosphate pathway. The oxidative phase of the pathway is used to convert six-carbon sugars (e.g., glucose) into five-carbon sugars (e.g., ribose for DNA synthesis). The non-oxidative phase reverses the process to convert the five-carbon sugars into the six-carbon sugars necessary for the glycolysis pathway. During the non-oxidative phase, three xyloses are converted into 2 fructose-6-phosphates and 1 glyceraldehyde-3-phosphate that enter into the glycolysis pathway in Steps 3 and 5, respectively (Eqn. 3-25).

$$3\ \text{Xylose} + 3\ \text{ATP} \rightarrow 2\ \text{fructose-6-P} + \text{glyceraldehyde-3-P} + 3\ \text{ADP} \qquad (3\text{-}25)$$

Equations 3-26 through 3-31 show the overall reactions from xylose to each of the types of salts.

$$3\ \text{Xylose} + 10\ [\text{ADP} + \text{P}_\text{i}] + 10\ \text{NAD}^+ \rightarrow 5\ \text{Acetate} + 10\ \text{ATP} + 10\ \text{NADH} + 2\ \text{H}^+ + 5\ \text{CO}_{2(\text{aq})} + 5\ \text{H}_2\text{O} \quad (3\text{-}26)$$

$$3\ \text{Xylose} + 5\ [\text{ADP} + \text{P}_\text{i}] + 5\ \text{NADH} + 8\ \text{H}^+ \rightarrow 5\ \text{Propionate} + 5\ \text{ATP} + 5\ \text{NAD}^+ + 10\ \text{H}_2\text{O} \quad (3\text{-}27)$$

$$6\ \text{Xylose} + 15\ [\text{ADP} + \text{P}_\text{i}] + 6\ \text{H}^+ \rightarrow 5\ \text{Butyrate} + 15\ \text{ATP} + 10\ \text{CO}_{2(\text{aq})} + 15\ \text{H}_2\text{O} \quad (3\text{-}28)$$

$$6\ \text{Xylose} + 15\ [\text{ADP} + \text{P}_\text{i}] + 5\ \text{NADH} + 16\ \text{H}^+ \rightarrow 5\ \text{Valerate} + 15\ \text{ATP} + 5\ \text{NAD}^+ + 5\ \text{CO}_{2(\text{aq})} + 20\ \text{H}_2\text{O} \quad (3\text{-}29)$$

$$9\ \text{Xylose} + 30\ [\text{ADP} + \text{P}_\text{i}] + 10\ \text{NAD}^+ + 14\ \text{H}^+ \rightarrow 5\ \text{Caproate} + 30\ \text{ATP} + 10\ \text{NADH} + 15\ \text{CO}_{2(\text{aq})} + 25\ \text{H}_2\text{O} \quad (3\text{-}30)$$

$$9\ \text{Xylose} + 25\ [\text{ADP} + \text{P}_\text{i}] + 5\ \text{NADH} + 24\ \text{H}^+ \rightarrow 5\ \text{Heptanoate} + 25\ \text{ATP} + 5\ \text{NAD}^+ + 10\ \text{CO}_{2(\text{aq})} + 25\ \text{H}_2\text{O} \quad (3\text{-}31)$$

3.2.3 Hydrogen percent yield

A variety of microorganisms can use molecular hydrogen as an energy source. Biological hydrogen production depends on hydrogen-producing enzymes collectively known as hydrogenases. Hydrogenases catalyze the reversible oxidation of molecular hydrogen using NAD^+ (nicotinamide adenine dinucleotide). NAD^+ is a coenzyme found in all living cells, which is involved in reduction-oxidation reactions. It acts as an electron transporter shuttling electrons between reactions. NAD^+ is the oxidized form which reacts with hydrogen, accepting a hydride ion to generate NADH (the reduced form) and a free proton (H^+) (Eqn. 3-32). In this process, energy is transferred to the reduced product; the overall ΔG of the redox reaction is negative.

All metabolic pathways within the cell use nicotinamide adenine dinucleotide, in either its oxidized (NAD^+) or reduced (NADH) form. As described previously, glycolysis produces NADH, which is then used by other cellular pathways. Hydrogen gas is a

secondary byproduct of cellular metabolism and is released when there is excess NADH, thus regenerating NAD^+.

$$NADH + H^+ \leftrightarrow NAD^+ + H_2 \quad (3\text{-}32)$$

This reversible reaction is catalyzed by the enzyme class hydrogenase. The direction of the reactions is strongly influenced by both the partial pressure of hydrogen gas within the head space of the reactor and the ratio of NADH and NAD^+.

Lipid synthesis for fat storage and cell membranes consume significant quantities of the NADH (29.0 mol NADH/mol phospholipid average). Amino acid production for protein and enzyme synthesis consumes 1.83 mol NADH/mol amino acid (average).

Assuming that all NADH produced from each type of acid is regenerated to NAD^+ and H_2, then Equations 3-33 through 3-44 show the amount of hydrogen generated for each acid using hexose and pentose feedstocks.

1 hexose	→	2 acetate + 4 H_2	(3-33)
1 hexose	→	2 propionate – 2 H_2	(3-34)
1 hexose	→	1 butyrate + 0 H_2	(3-35)
1 hexose	→	1 valerate – 1 H_2	(3-36)
3/2 hexose	→	1 caproate + 2 H_2	(3-37)
3/2 hexose	→	1 heptanoate – 1 H_2	(3-38)
3/5 pentose	→	1 acetate + 2 H_2	(3-39)
3/5 pentose	→	1 propionate – 1 H_2	(3-40)
6/5 pentose	→	1 butyrate + 0 H_2	(3-41)
6/5 pentose	→	1 valerate – 1 H_2	(3-42)
9/5 pentose	→	1 caproate + 2 H_2	(3-43)
9/5 pentose	→	1 heptanoate – 1 H_2	(3-44)

Ideally, for energy production, every mol of sugar would convert into the desired acids and NADH. Further, the NADH would ultimately convert into NAD^+ and hydrogen. Instead, during the fermentation, there are multiple competing reactions that consume the sugars and NADH to make cellular components. This makes it difficult to calculate the maximum hydrogen yield.

The theoretical hydrogen gas production of the fermentation is affected by both the type of acid being produced and the type of sugar being digested. Theoretical hydrogen production can be determined by the mols of each type of sugar that are digested multiplied by the hydrogen selectivity weighted by mol fraction of each type of acid (Eqn. 3-45).

$$\text{Theoretical } H_2 \text{ prod. (mol)} = \sum_i \text{Sugar dig}_i\text{(mol)} \times \left[\sum_j (\sigma_j \times \chi_j)\right] \quad (3\text{-}45)$$

i = Types of sugar digested (i.e., hexose, pentose)
j = Types of acid (i.e., acetic, butyric)
σ_j = Hydrogen selectivity for Type j acid (mol H_2/mol sugar$_i$)
χ_j = Acid mol fraction (mol acid$_j$/mol total acid)

The percent yield of hydrogen is thereby calculated as the amount of actual hydrogen gas produced divided by the theoretical hydrogen (Eqn. 3-46).

$$\text{Percent yield (\%)} = \frac{\text{Actual } H_2 \text{ (mol)}}{\text{Theoretical } H_2 \text{ (mol)}} \times 100 \quad (3\text{-}46)$$

3.2.4 Gibbs free energy of reaction

In thermodynamics, both Gibbs free energy and Helmholtz free energy measure the "useful" work obtained from a system. Helmholtz free energy is used to measure changes in a closed system with constant temperature and volume while Gibbs free energy is used to measure changes in a system with constant temperature and pressure. Additionally, Gibbs free energy measures the chemical potential as a system approaches equilibrium. The systems studied in this chapter involve the chemical potential of several reactions attempting to reach equilibrium. Additionally, the overall system is at a pseudo-constant pressure as fermentor off-gases are vented every two days throughout the fermentations. Therefore,

Gibbs free energy is the thermodynamic parameter used to describe the reactions in this chaper.

Every cellular reaction involves energy changes, which are reported as Gibbs free energy. In living organisms, there is not just one chemical reaction. To live, cells must obtain energy from a fuel (e.g., hexose) and then use this energy to make complex chemicals (e.g., DNA and cell wall material) necessary for reproduction. The more energy the cell can realize from a reaction, the more energy it can use to live. The cell balances the reactions to obtain an optimal amount of energy from fuel. The cell will use all reactions possible to obtain energy, but the greater the energy from one reaction (i.e., the more negative the Gibbs free energy) the more the cell will favor it over another.

Microbial metabolism has two main processes: catabolism and anabolism (Stockar et al., 2006). Catabolic reactions decompose larger molecules to harvest energy that drives the anabolic reactions responsible for building macromolecules (e.g., DNA) for cell growth. Microorganisms use catabolic reactions to fuel the anabolic ones, resulting in a net Gibbs free energy that approaches zero (Henry et al., 2006).

$$\Delta G_T = \Delta G_C - \Delta G_A \tag{3-47}$$

$$\Delta G_T \cong 0 \tag{3-48}$$

ΔG_T is the total net Gibbs free energy expended by the microorganism, ΔG_C is the energy gained from the catabolic fueling reactions, and ΔG_A is the energy consumed from the anabolic growth reactions. Because ΔG_T is approximately zero, then ΔG_C is approximately equal to ΔG_A.

To understand how temperature and pH affect the microorganisms − and therefore the carboxylic acid and hydrogen production − one must understand Gibbs free energy. With any chemical reaction, energy is either absorbed into the formed molecular bonds or released from the broken bonds. A simple example is the combustion of wood. As wood burns, long complex chemicals within the wood decompose into smaller molecules thus, releasing energy as heat and light.

In short, Gibbs free energy measures the useful work or energy available from a system (Eqn. 3-49). During a reversible transformation, when a system changes from one

well-defined state to another well-defined final state, the Gibbs free energy equals the work exchanged by the system with its surroundings (Castellan, 1966). For chemical reactions, it is also the amount of chemical potential energy that is released or absorbed when a system moves from an initial state to equilibrium (Eqn. 3-50).

$$\Delta G = \Delta H - T\Delta S \quad (3\text{-}49)$$

$$\Delta G = \Delta G^{\circ} + RT\ln K_{eq} \quad (3\text{-}50)$$

ΔG is the Gibbs free energy, ΔG° is the Gibbs free energy at standard temperature and pressure, ΔH is the enthalpy, T is the temperature of the reaction, ΔS is the entropy, R is the ideal gas constant, and K_{eq} is the equilibrium constant at temperature T (in Kelvin). Standard conditions are 273 K, 1 atm, and pH = 0.

The standard Gibbs free energy of a reaction (ΔG_R°) is calculated by summing the standard Gibbs free energies of formation (Eqn. 3-51), where v is the stoichiometric number of Reactant i. v is positive for reactants on the right side of the equation and negative for reactants on the left side of the equation. The standard enthalpies of reaction (ΔH_R°) are calculated in the same way.

$$\Delta G_R^{\circ} = \sum v_i \, \Delta G_F^{\circ} \quad (3\text{-}51)$$

3.2.4.1 Temperature effects

At standard temperature and pressure, the equilibrium constant can be calculated from the standard Gibbs free energy of reaction ΔG_R° (Eqn. 3-52). As the temperature changes, both the Gibbs free energy and the equilibrium constant changes, making it difficult to calculate the Gibbs free energy at different temperatures. In 1884, Jacobus H. van't Hoff published *Études de Dynamique chimique* ("Studies in Chemical Dynamics") where he derived Equation 3-53 (the Van't Hoff equation) relating chemical equilibrium to temperature (Glasstone, 1949). Because enthalpy does not change significantly with temperature, the definite integral of this differential equation between temperatures T_1 and T_2 is given by Equation 3-43.

$$\Delta G^{\circ} = -RT\ln K_{eq} \tag{3-52}$$

$$\frac{d\ln K_{eq}}{dT} = \frac{\Delta H^{\circ}}{RT} \tag{3-53}$$

$$\ln\left(\frac{K_{eq2}}{K_{eq1}}\right) = \frac{\Delta H^{\circ}}{R}\left(\frac{1}{T_1} - \frac{1}{T_2}\right) \tag{3-54}$$

Inserting Equation 3-50 into 3-54 for each natural log term and rearranging yields Equation 3-55, which allows us to calculate the ΔG_R° for any temperature given the standard Gibbs free energy of reaction (ΔG_R°) and the standard enthalpy of reaction (ΔH_R°). T_1 is the standard temperature of 273 K.

$$\Delta G_R = \frac{T_2}{T_1} \times \left[\Delta G_R^{\circ} - \frac{(T_2 - T_1)}{T_2} \times \Delta H_R^{\circ}\right] \tag{3-55}$$

3.2.4.2 pH effects

pH is a measure of the concentration of hydrogen ions and quantifies the acidity or basicity of a solution. A pH of 7.0 is neutral. pH between 0.0 and 7.0 is considered acidic and pH between 7.0 and 14.0 is considered basic. The term pH was derived from the manner in which the hydrogen ion concentration is calculated − it is the negative logarithm of the hydrogen ion (H^+) concentration (Eqn. 3-56).

$$\mathrm{pH} = -\log[\mathrm{H}^+] \qquad \text{or} \qquad [\mathrm{H}^+] = 10^{-\mathrm{pH}} \tag{3-56}$$

Expanding the K_{eq} term of Equation 3-50 yields Equation 3-57.

$$\Delta G = \Delta G^{\circ} + RT\ln\frac{C^c D^d}{A^a B^b} \tag{3-57}$$

For the given reaction of NADH (Eqn. 3-32), Equation 3-57 becomes 3-58. Expanding the logarithm yields Equation 3-59.

$$\Delta G = \Delta G^{\circ} + RT\ln\frac{[\mathrm{NAD}]^1[\mathrm{H_2}]^1}{[\mathrm{NADH}]^1[\mathrm{H^+}]^1} \quad (3\text{-}58)$$

$$\Delta G = \Delta G^{\circ} + RT(\ln[\mathrm{NAD}] + \ln[\mathrm{H_2}] - \ln[\mathrm{NADH}] - \ln[\mathrm{H^+}]) \quad (3\text{-}59)$$

The previous Gibbs calculations (Eqns. 3-49 through 3-55) were made under the condition that the surrounding environment was not ionic. For this reason, a pH of 0 is used in the equations to represent NO pH activity rather than an extremely acidic solution. In actuality, the equilibrium term is affected by all hydrogen ions present (pH). As such, the pH term may be considered separate from the equilibrium term (Eqn. 3-60). K'_{eq} is the equilibrium constant K_{eq} without any pH effects. Substituting Equation 3-56 in for $\mathrm{H^+}$ and rearranging yields Equation 3-62, where *n* is the stoichiometric number for the hydrogen ions of the specific reaction and pH is the pH of the system.

$$\Delta G = \Delta G^{\circ} + RT\ln K'_{eq} + \text{pH term} \quad (3\text{-}60)$$

$$\text{pH term} = RT\ln[\mathrm{H^+}]^n \quad (3\text{-}61)$$

$$\text{pH term} = -nRT\ln[10] \times \text{pH} \quad (3\text{-}62)$$

Therefore, by combining Equations 3-55 and 3-62, the Gibbs free energy (kJ/mol) for any given temperature and pH can be calculated.

$$\Delta G_R = \frac{T_2}{T_1} \times \left[\Delta G_R^{\circ} - \frac{(T_2 - T_1)}{T_2} \times \Delta H_R^{\circ}\right] - nRT\ln[10] \times \text{pH} \quad (3\text{-}63)$$

Appendix I lists selected Gibbs free energies and enthalpies of formation and shows a sample calculation. Table 3-2 shows the Gibbs energies for each of the acids and hydrogen production at 25 and 55 °C and pH of 0 and 7. This table demonstrates how much cellular conditions affect acid and hydrogen production. For a given acid product, the microorganisms get a similar amount of energy from each type of sugar. Equation 3-32 (Reaction 13 in Table 3-2) has a negative Gibbs free energy at standard conditions and is thereby favorable. But, at cellular conditions (pH = 7) the Gibbs free energy becomes

positive. This reemphasizes that hydrogen will only be produced when there is an excess of NADH and the microorganism needs to balance its energy production.

Table 3-2. Gibbs free energies of reaction for selected cellular reactions of hexose and pentose.

	Substrate	Product	Hydrogen ions	ΔG_R°	ΔH_R°	ΔG_1	ΔG_2
Temperature (°C)				25	25	55	55
pH				0*	0*	0*	7
Rxn 1	Hexose	Acetate	2	−325.60	−538.21	−304.21	−392.15
Rxn 2	Hexose	Propionate	−2	−329.90	−226.75	−340.28	−252.34
Rxn 3	Hexose	Butyrate	0	−501.53	−566.14	−495.03	−495.03
Rxn 4	Hexose	Valerate	−2	−115.88	119.50	−139.57	−51.62
Rxn 5	Hexose	Caproate	−1	113.30	477.55	76.65	120.62
Rxn 6	Hexose	Heptanoate	−3	−23.25	351.57	−60.97	70.94
Rxn 7	Pentose	Acetate	2/3	−284.09	−454.39	−266.96	−296.27
Rxn 8	Pentose	Propionate	−8/3	−287.68	−194.84	−297.02	−179.76
Rxn 9	Pentose	Butyrate	−1/2	−430.70	−477.67	−425.98	−403.99
Rxn 10	Pentose	Valerate	−8/3	−220.54	−142.67	−228.37	−111.11
Rxn 11	Pentose	Caproate	−14/9	−172.23	−213.31	−168.10	−99.70
Rxn 12	Pentose	Heptanoate	−8/3	−42.18	33.07	−49.76	67.50
Rxn 13	NADH	Hydrogen	−1	−5.05	27.74	−8.35	35.62

*pH = 0 is used in the notation to represent no pH or ionic activity.

Similar to hydrogen production, both the type of sugar being digested and the type of acid being produced affect the Gibbs free energy. Because the products being released from the microorganism were produced to fuel other reactions, the total Gibbs free energy (kJ) released from catabolic reactions by the specific production of each type of acid and hydrogen can be calculated (Eqn. 3-64). The production of carbon dioxide is not included in the Gibbs calculation because it is a co-product of the acids and is covered by the acid portion of the calculation.

$$\Delta G_C(\text{kJ}) = \sum_j \text{Acid}_j(\text{mol}) \times \left[\sum_i \left(\chi_i \times \Delta G_{ji}\right)\right] + H_2(\text{mol}) \times \Delta G_{H2} \qquad (3\text{-}64)$$

Acid_j = carboxylic acid of Type *j* (mol)
χ_i = mol fraction of sugar of Type *i* (i.e., mol hexose/mol total sugars)
ΔG_{ji} = Gibbs free energy of reaction for Type *j* acid from Type *i* sugar

During fermentative metabolism, microorganisms produce acids to fuel the chemical reactions necessary for life and reproduction. Crabbendam et al. (1985) found that *Clostridium butyricum* needed a ΔG_A of 336 kJ/mol glucose (1.87 kJ/g glucose). Von Eysmondt et al. (1990) discovered the same ΔG_A for *Acetogenium kivui*. The amount of energy these microorganisms need depends on the temperature and substrate (Heijnen, 1994; Tijhuis et al., 1993).

For any given system of substrate, buffer, and incubation temperature, the microorganisms adjust the spectrum of products (ΔG_C), to match the needed ΔG_A. Therefore, we can define the energy selectivity (γ) of a system (Eqn. 3-65).

$$\gamma \equiv \frac{\Delta G_C}{\text{grams VS digested}} \tag{3-65}$$

This γ will be the same for any given system, whether during batch or continuous operation. In Equation 3-65, grams of volatile solids (VS) are used rather than mols because of the wide variety of substrates used in the MixAlco™ process. It would be too difficult to track each component individually to determine their individual energy selectivities. For *Klebsiella aerogenes*, Streekstra et al. (1987a; 1987b) found that the ΔG_C for each individual chemical (i.e., glucose, glycerol, mannitol) varied on a molar basis; however, on a mass basis, γ was the same.

3.3 Materials and methods

Both batch and four-stage countercurrent fermentations were used in this chapter. Each fermentation was started as a batch fermentation with 80 wt% substrate, 20 wt% dried chicken manure, and deoxygenated water. Office paper wastes and sugarcane bagasse were used as the substrates. Sugarcane bagasse was air-lime pretreated (Appendix B) for 4 weeks then air dried. Ammonium bicarbonate was added to buffer the pH to 7.0−7.4. The single-centrifuge procedure was used for all countercurrent trains. All fermentations were operated at 55 °C. Liquid and solids were sampled and transferred at 2-day intervals. The total liquid in the countercurrent train is the sum of the residual liquid in the wet solid cake and the

centrifuged liquid on top of the cake. It was determined by first centrifuging each fermentor in a train and separating the solid from the liquid.

Table 3-3 shows the fermentation configurations used in this chapter. The inoculum for the batch fermentations was fresh Galveston inoculum. The inoculum for the countercurrent fermentation of paper (PHC) was taken from the residual solid and liquid from the paper batch fermentation (PH). The inocula for the countercurrent fermentation of bagasse (BHC) was taken from the residual solid and liquid from the bagasse batch fermentation (BH).

Table 3-3. Experimental conditions for anaerobic hydrogen fermentations.

Configuration		Substrate	Batch/Continuous	Fermentation temperature (°C)	Iodoform* (mg/(L liq·day))
1	PH	Paper	Batch	55	3.0
2	BH	Bagasse	Batch	55	3.0
3	PHC	Paper	Continuous	55	3.0
4	BHC	Bagasse	Continuous	55	3.0

* Added as 20 g iodoform/L ethanol solution

3.4 Stainless steel vessel design

Previous anaerobic fermentations have been performed in plastic fermentors with rubber caps. The fermentors are robust and relatively inexpensive, easily used for sampling and transfers, and easily manufactured for replacement. Unfortunately, the low density of the plastic and the small cracks within the multi-use septums allows the small hydrogen molecule to leak, resulting in only trace amounts of hydrogen in any off-gas from the fermentations.

Of the materials easily obtainable by our laboratory, only glass and stainless steel are dense enough to contain hydrogen gas. Glass was not chosen for a fermentor material because it is easily broken, which would cause a safety hazard and loss of fermentation data. Stainless steel is much more robust, but significantly heavier. The stainless steel fermentor vessel of comparable size is 15 times heavier than its plastic counterpart.

Each fermentor (Fig. 3-3) consisted of a 6-in-long 4-in-diameter Sch-10 stainless steel pipe with a 1/8-in-thick stainless steel plate welded to each end. The top plate of the fermentor had a 2-in-diameter hole where a quick-connect fitting was welded. A 2-in gasket and cap were placed onto the fitting and held in place by a tightened clamp. A ¼-in quick connect self-sealing valve was inserted into the cap for intermittent gas release. A length of ¼-in stainless steel tubing is bent back on itself and inserted into the mouth of the fermentor to mix the contents. The vessels proved to seal tightly; no pressure loss was detected after 10 days with 150-psig H_2.

Figure 3-3. Photograph of the stainless-steel fermentor (clamp not shown).

3.5 Batch fermentations of paper and bagasse

Batch fermentations were conducted in triplicate with substrate (80 wt%) and chicken manure (20 wt%) in the SS fermentors at a concentration of 100 g dry biomass/L. The liquid volume in all fermentors was 400 mL. All fermentations were inoculated with a mixed culture of anaerobic microorganisms from a marine source (Galveston Island, TX). Ammonium bicarbonate was the only pH buffer used in this chapter. All batch fermentations were started at the same time and operated under identical conditions.

The pH in all batch fermentations was controlled near 7.0. If the measured pH fell below 7.0, ammonium bicarbonate was added to the fermentor until the pH reached the preset range (7.0−7.4). No additional ammonium bicarbonate was added if the pH was above 7.0. The production of carboxylic acids would lower the pH.

Nutrient and methane inhibitor concentrations influence culture growth and can effect fermentation performance. Chicken manure was the nutrient source and supplied all of the nutrients required for the microorganisms. Iodoform, a methane inhibitor, was added to reduce the effect of methanogenesis. Iodoform was added to each fermentator at a rate of 2.0 mg/(L liq·day).

The total carboxylic acid concentrations, conversion, selectivity, and yield were used to compare the different fermentation performance of the different pretreatment methods.

3.5.1 Effect of office paper on fermentation profile

The batch fermentation performance of 80 wt% office paper wastes/20 wt% chicken manure was conducted at 55 °C. The total carboxylic acid concentration, conversion, and selectivity of the fermentations were used to evaluate the performance. Figure 3-4 shows the total carboxylic acid concentration profile. Table 3-4 summarizes the fermentation results for anaerobic fermentation of office paper. Office paper achieved a total carboxylic acid concentration of 21.9 g/L and a conversion of 0.64 g VS digested/g VS fed. Office paper obtained a selectivity of 0.42 g acid/g VS digested and a productivity of 0.61 g acid/(L liq·day).

3.5.2 Effect of bagasse on fermentation profile

The batch fermentation performance of 80 wt% bagasse/20 wt% chicken manure was conducted at 55 °C. The total carboxylic acid concentration, conversion, and selectivity of the fermentations were used to evaluate the performance. Figure 3-4 shows the total carboxylic acid concentration profile. Table 3-4 summarizes the fermentation results for anaerobic fermentation of bagasse. Bagasse achieved a total carboxylic acid concentration of 21.1 g/L and a conversion of 0.64 g VS digested/g VS fed. Bagasse obtained a selectivity of 0.43 g acid/g VS digested and a productivity of 0.58 g acid/(L liq·day).

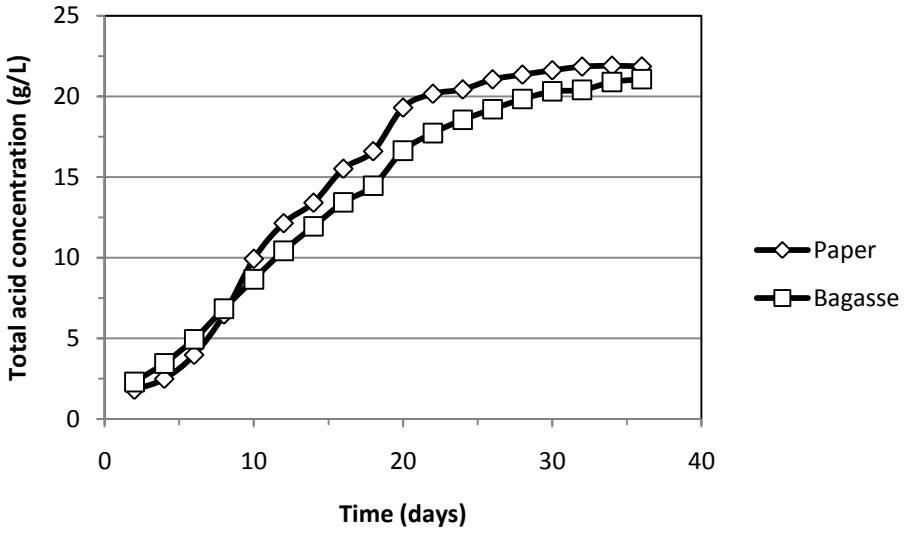

Figure 3-4. Comparison of the total acid concentration of 100 g/L of paper and air-lime treated bagasse (80% substrate/20% chicken manure) at 55 °C for hydrogen fermentations.

Table 3-4. Results for hydrogen fermentations, PH and BH, at 55 °C.

Fermentation	PH	BH
Substrate	Paper	Bagasse
Total carboxylic acid (g/L)	21.9 ± 4.41	21.1 ± 2.73
Acetic (wt%)	70.8 ± 7.27	83.4 ± 2.66
Propionic (wt%)	1.9 ± 0.50	1.5 ± 0.06
Butyric (wt%)	25.8 ± 7.46	14.2 ± 2.42
Valeric (wt%)	1.1 ± 0.55	0.95 ± 0.22
Caproic (wt%)	0.3 ± 0.26	0
Heptanoic (wt%)	0	0
Cumulative H_2 out (mL)	1114.9 ± 185.2	876.5 ± 48.7
H_2 selectivity (mL/g VS dig)	53.5 ± 3.79	44.6 ± 2.27
Conversion (g VS dig/g VS fed)	0.64 ± 0.11	0.64 ± 0.02
Selectivity (g acid/g VS dig)	0.42 ± 0.02	0.43 ± 0.04
Yield (g acid/g VS fed)	0.27 ± 0.05	0.27 ± 0.03
Productivity (g acid/(L liq·d))	0.61 ± 0.12	0.58 ± 0.07

Error is ± 1 standard deviation

3.5.3 Effect of substrate on hydrogen production

Figure 3-5 shows the cumulative hydrogen production for both paper and bagasse batch fermentations. Paper produced a total of 1115 mL of hydrogen with a hydrogen selectivity of 53.5 mL/g VS digested during the course of the fermentation whereas bagasse produced a total of 876 mL of hydrogen with a hydrogen selectivity of 44.6 mL/g VS digested. Table 3-5 shows the hydrogen production and the percent yield for both substrates. Paper produced 33.4% of the theoretical hydrogen yield (Eqn 3-46) whereas bagasse produced 25.0%.

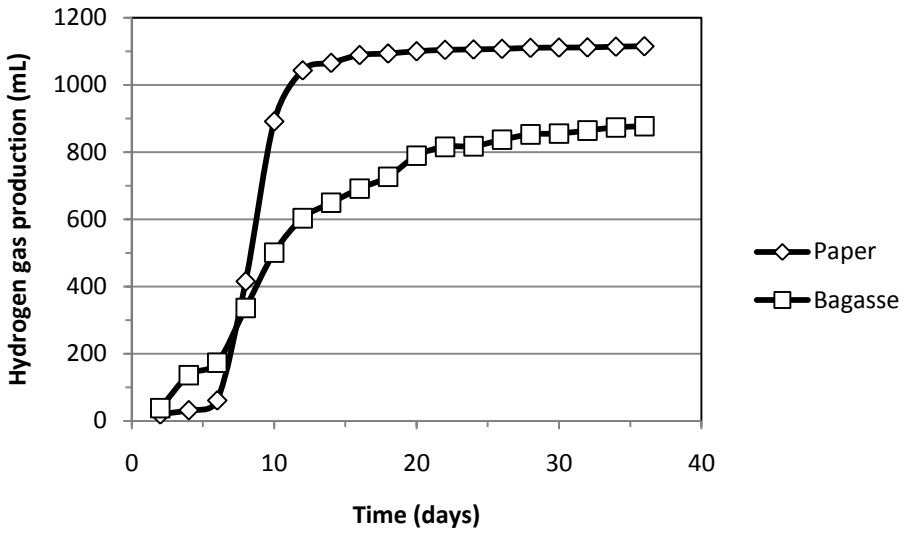

Figure 3-5. Cumulative hydrogen gas production for 100 g/L of paper and air-lime treated bagasse fermentations at 55 °C.

Table 3-5. Actual and theoretical hydrogen production and percent yield for PH and BH fermentations.

Fermentation	PH	BH
Substrate	Paper	Bagasse
VS in (g)	32.62	30.60
Hexose in (g)	22.53	13.99
Pentose in (g)	5.86	7.83
VS out (g)	11.75 ± 3.61	10.96 ± 0.69
Hexose out (g)	9.22 ± 1.62	4.69 ± 0.09
Pentose out (g)	1.56 ± 0.27	0.69 ± 0.01
Actual H_2 (mL)	1114.8 ± 185.2	876.5 ± 48.7
Actual H_2 (mol)	0.10 ± 0.02	0.08 ± 0.004
Theoretical H_2 (mol)	0.30 ± 0.05	0.32 ± 0.008
Percent Yield (Eqn. 3-46)	33.45 ± 0.51	24.97 ± 1.64

Error is ± 1 standard deviation

3.6 Countercurrent fermentations of paper and bagasse

3.6.1 Train PHC

Four batch fermentations were initiated by adding paper (36 g), yeast extract (4 g), calcium carbonate (6 g), urea (0.5 g), deoxygenated water (350 mL), PH inoculum (50 mL), and 120 L iodoform solution (20 g/L iodoform in ethanol). The PH inoculum was taken from the residual liquid and solid remaining for the batch paper fermentation. On each transfer, paper (9.6 g) and chicken manure (2.4 g) were added to F1. The transfer of solids and liquid was performed as in Appendix D. Fresh deoxygenated water (100 mL) was added to F4 on each transfer. The total acid concentration profile and acetate content profile are shown in Figures 3-6 and 3-7.

3.6.2 Train BHC

Four batch fermentations were initiated by adding paper (36 g), yeast extract (4 g), calcium carbonate (6 g), urea (0.5 g), deoxygenated water (350 mL), BH inoculum (50 mL), and 120 L iodoform solution (20 g/L iodoform in ethanol). The BH inoculum was taken from the residual liquid and solid remaining from the batch bagasse fermentation. On each transfer, pretreated bagasse (9.6 g) and chicken manure (2.4 g) were added to F1. The transfer of solids and liquid was performed as in Appendix D. Fresh deoxygenated water (100 mL) was added to F4 on each transfer. The total acid concentration profile and acetate content profile are shown in Figures 3-8 and 3-9.

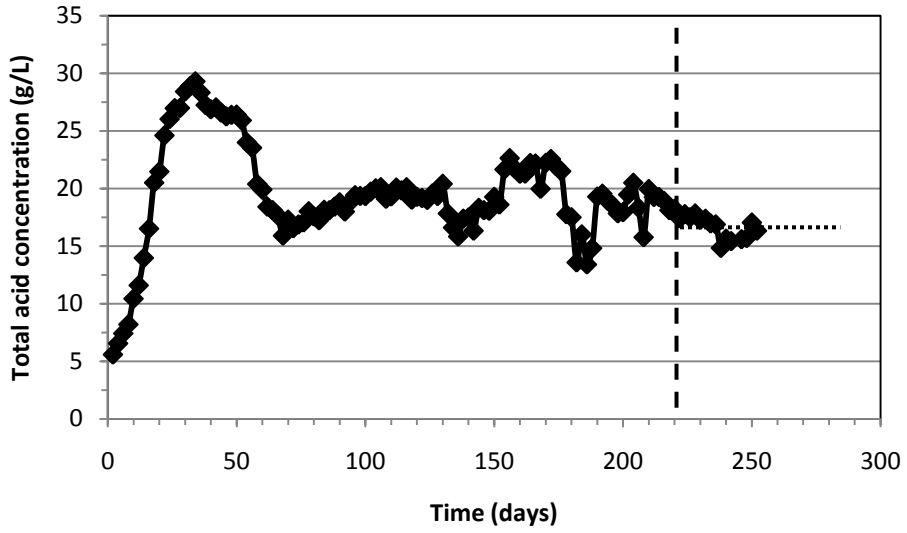

Figure 3-6. Total acid concentration for paper and chicken manure fermentation Train PHC. Dash line indicates steady state (16.9 g/L).

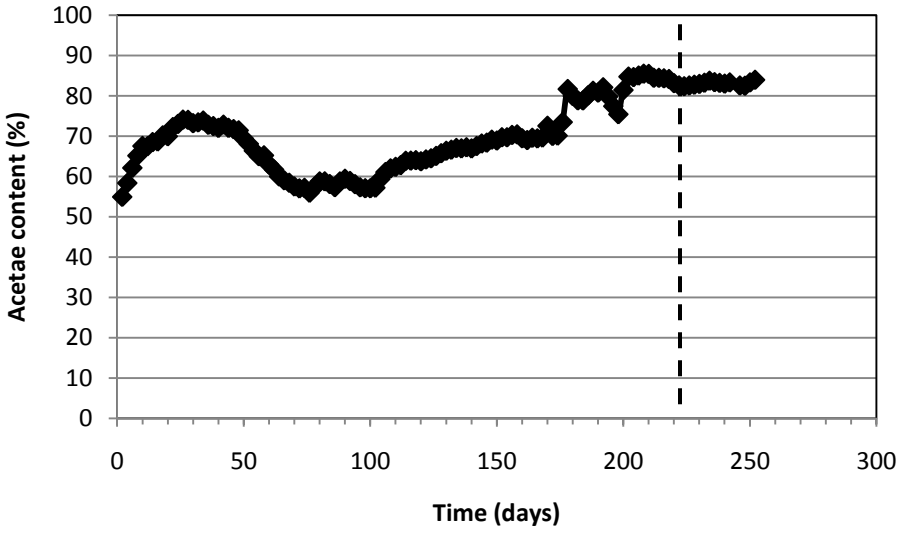

Figure 3-7. Acetate content for paper and chicken manure fermentation Train PHC.

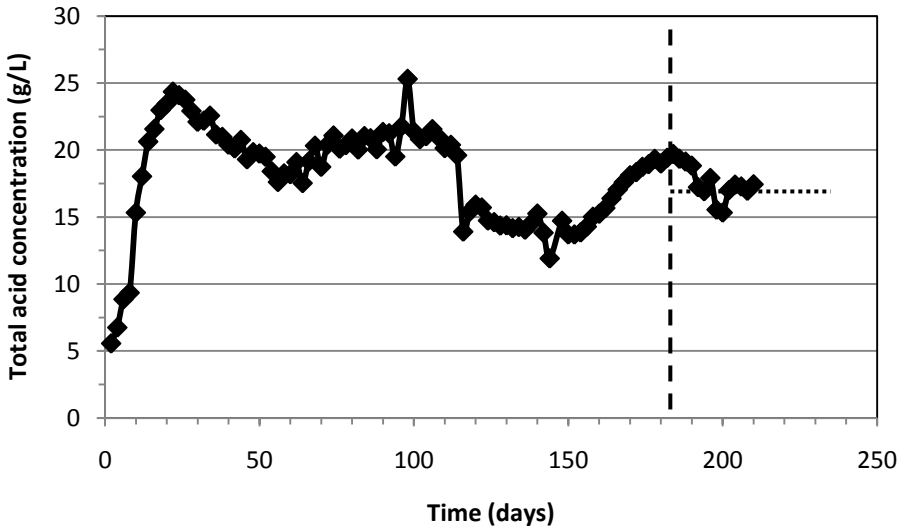

Figure 3-8. Total acid concentration for bagasse and chicken manure fermentation Train BHC. Dash line indicates steady state (17.1 g/L).

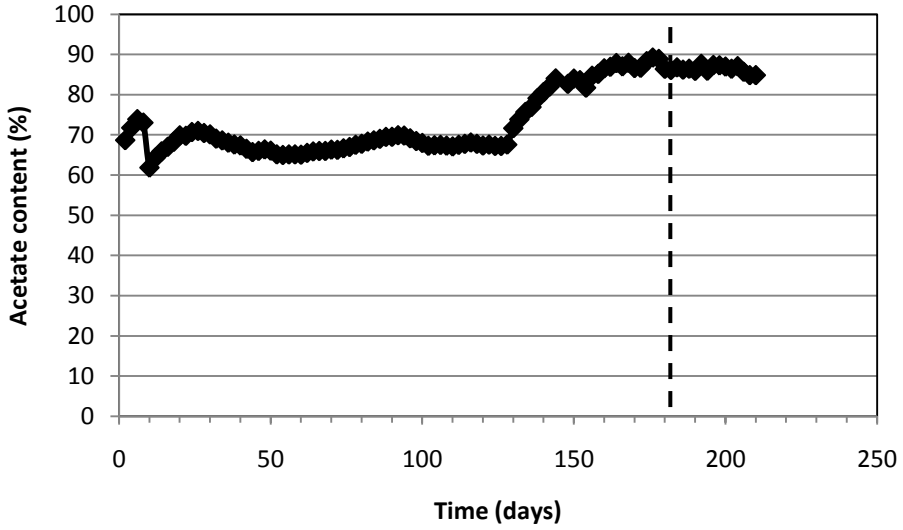

Figure 3-9. Acetate content for bagasse and chicken manure fermentation Train BHC.

3.6.3 Summary of countercurrent fermentations

Table 3-6 summarizes the operating conditions for the fermentation trains. Table 3-7 shows the results for these countercurrent fermentations. Figure 3-10 lists the mass balance closures for these fermentations.

The highest acid concentration occurred at a concentration of 17.1 g/L in Train BHC (LRT = 29.6 days and VSLR = 3.63 g VS/(L liq·day)). Fermentation Train PHC (LRT = 31.0 days and VSLR = 4.17 g VS/(L liq·day)) with an acid concentration of 16.7 g/L had the highest conversion (0.53 g VS digested/g VS fed) and productivity (1.01 g/(L liq·day)). The highest selectivity (0.39 g acid/g VS digested) was obtained from Train BHC. Train PHC produced an average hydrogen volume of 73.6 mL/transfer with a hydrogen selectivity of 15.7 mL/g VS digested. Train BHC produced an average volume of 176.0 mL/transfer of hydrogen each transfer with a hydrogen selectivity of 41.1 mL/g VS digested.

The gas head space within the fermentors contained nitrogen from purging during transfers, carbon dioxide, and hydrogen. The PHC fermentor bottles averaged 56.8% N_2, 38.6% CO_2, and 4.6% H_2. The BHC fermentor bottles averaged 57.9% N_2, 33.0% CO_2, and 9.1% H_2. On an industrial scale, nitrogen would not be used to purge the system. Instead, the fermentation systems would be maintained anaerobic and would contain only CO_2 and H_2. Removing the N_2, the hydrogen concentrations would be between 10 and 20% by volume.

Table 3-6. Operating parameters of hydrogen fermentations of paper and bagasse at 55 °C.

Fermentation Trains	PHC	BHC
LRT (day)	31.05	29.56
VSLR (g VS/(L·day))	4.17	3.63
VS feed at each transfer (g VS)	9.77	8.12
Solid feed at each transfer (g)	12.0	12.0
Substrate (g)	9.6	9.6
Chicken manure (g)	2.4	2.4
Liquid fed to F4 at each transfer (L)	0.10	0.10
Liquid volume in all four fermentors (L)	1.17	1.12
Temperature (°C)	55	
Frequency of transfer	Every two days	
F1 Retained weight (wet g)	1453	1453
F2-F4 Retained weight (wet g)	1465	1465
Iodoform addition rate (mg/L liquid fed to F4)	96	96
Urea addition rate (g urea/L liquid fed to F4)	20	20

Table 3-7. Fermentation results for hydrogen countercurrent fermentations using paper and bagasse.

Fermentation Trains	PHC	BHC
Total carboxylic acid concentration (g/L)	16.7 ± 1.51	17.1 ± 0.97
Acetic acid (wt%)	83.1 ± 0.67	86.3 ± 0.99
Propionic acid (wt %)	2.94 ± 0.22	2.83 ± 0.09
Butyric acid (wt %)	13.34 ± 0.81	10.63 ± 1.08
Valeric acid (wt %)	0.56 ± 0.05	0.00 ± 0.00
Caproic acid (wt %)	0.00 ± 0.00	0.00 ± 0.00
Heptanoic acid (wt %)	0.00 ± 0.00	0.03 ± 0.01
Hydrogen production (mL/transfer)	73.6 ± 16.47	176.0 ± 32.03
H_2 selectivity (mL/g VS dig)	15.7 ± 3.53	41.1 ± 7.48
Conversion (g VS digested/g VS fed)	0.57	0.53
Selectivity (g total acid/g VS digested)	0.37	0.39
Yield (g total acid/g VS fed)	0.18	0.17
Productivity (g total acid/(L liquid·day))	1.01	0.92
Mass balance closure (g VS out/g VS in)	0.986	1.021

Note: All errors are ± 1 standard deviation.

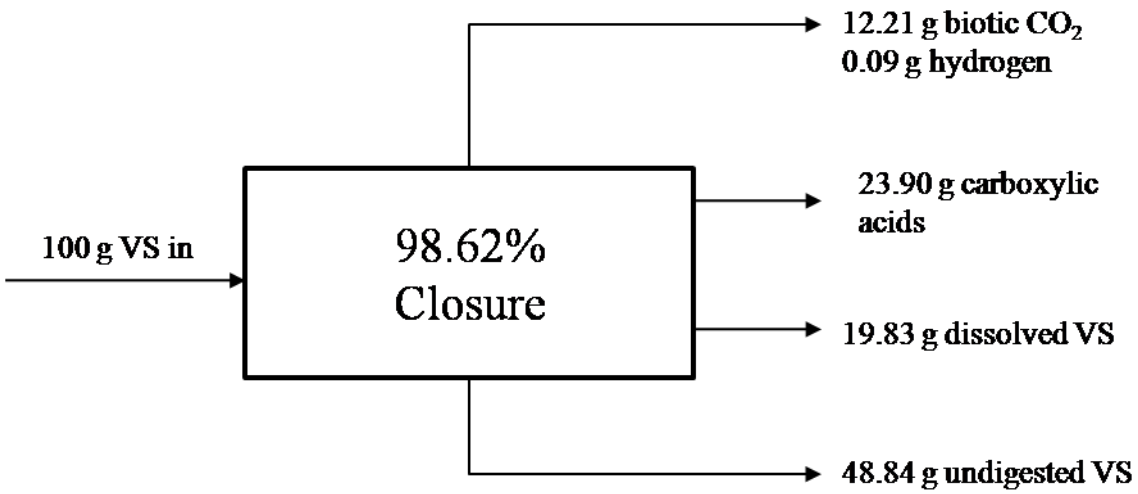

(a) For Fermentation PHC.

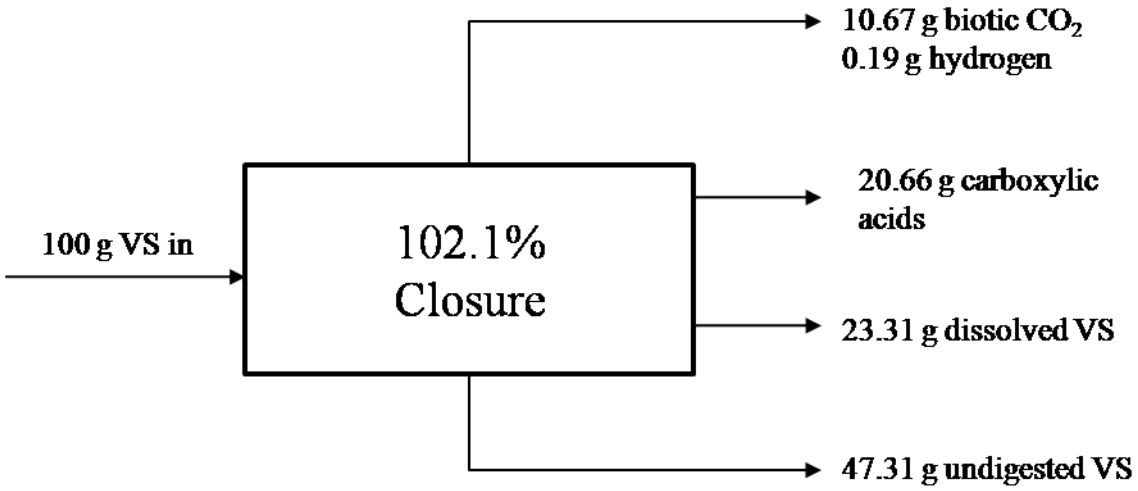

(b) For Fermentation BHC.

Figure 3-10. Mass balances for hydrogen fermentations PHC and BHC.

3.7 Hydrogen production

Paper produced an average of 15.7 mL H_2/g VS digested during each transfer of the countercurrent fermentation whereas bagasse produced an average of 41.1 mL H_2/g VS digested. Table 3-8 shows the hydrogen production and the percent yield for both substrates during countercurrent fermentations. Paper produced 6.93% of the theoretical hydrogen yield whereas the bagasse produced 22.61%.

Table 3-8. Percent yield of hydrogen fermentation Trains PHC and BHC.

Fermentation train	PHC	BHC
Substrate	Paper	Bagasse
VS in (g)	9.77	8.12
Hexose in (g)	6.76	4.20
Pentose in (g)	1.76	2.35
VS out (g)	3.53	3.84
Hexose out (g)	2.77	1.70
Pentose out (g)	0.48	0.44
Actual H_2 (mL)	73.6	176.0
Actual H_2 (mol)	0.00667	0.016
Theoretical H_2 (mol)	0.105	0.089
Percent Yield (Eqn. 3-46)	6.93	22.61

Table 3-9 shows the different percent yields (Eqn. 3-46) in both the batch and in the continuous fermentations. The bagasse BH batch (24.9%) and BHC continuous (22.6%) fermentations yielded similar amounts of hydrogen. But the hydrogen percent yield from the paper fermentations dropped significantly from the PH batch yield of 33.4% to the PHC continuous yield of 6.9%.

When shifting to continuous operation, it is unclear why the hydrogen production reduced in the paper fermentations, but not in the bagasse fermentations. The only significant change was that the percentage of acetic acid in the paper fermentations increased from 70% in the batch fermentation to 83% in the continuous fermentation. In contrast, the

acetic acid percentage stayed roughly constant in the bagasse fermentations: batch (83.4%) and continuous (86.3%). Considering Equations 3-33 through 3-44, the amount of hydrogen production should have increased in the paper fermentations with the increase in the acetic acid percentage. However, this was not observed.

These results emphasizes that hydrogen is a secondary byproduct, produced only when there is excess NADH. During the continuous fermentations, the paper fermentation used more NADH, perhaps for cell growth, leaving less to be regenerated into hydrogen.

Table 3-9. Comparison of hydrogen percent yield for paper and bagasse batch and continuous fermentations.

	PH	PHC	Change*	BH	BHC	Change*
Carboxylic acid concentration (g/L)	21.8	16.8		21.1	17.1	
Acetic acid (%)	70.84	83.06		83.38	86.33	
Conversion (g digested/g fed)	0.64	0.57		0.64	0.53	
Selectivity (g acid/g VS digested)	0.42	0.37		0.43	0.39	
Percent H_2 yield	33.45	6.93	−79.3	24.97	22.61	−9.45

* Change (%) = (Continuous value – Batch value)/Batch value × 100

3.8 Gibbs free energy and energy selectivity

Table 3-10 shows the energy selectivity (γ) for both the batch and continuous hydrogen fermentations of paper and bagasse. Compositional analysis was performed on both fresh feedstock and spent solids from both batch and continuous fermentations to determine the amounts of both hexose and pentose that were digested. Gibbs free energies of catabolism were determined by multiplying the actual moles of acid and H2 produced and the moles of sugar digested by the Gibbs free energies of reaction found in Table 3.2. Over the course of the fermentation, the paper batch fermentation (PH) produced an average of −46.7 kJ of energy whereas the bagasse batch fermentation (BH) produced −44.2 kJ. The PH fermentation had an energy selectivity of −2.11 kJ/g VS dig whereas the BH fermentation had an energy selectivity of −2.00 kJ/g VS dig. For the countercurrent fermentations, the paper PHC fermentation released an average ΔG_C of −9.25 kJ/transfer whereas the bagasse BHC fermentation released an average of −10.19 kJ/transfer. The PHC fermentation had a γ of −2.01 kJ/g VS dig and the BHC fermentation had −1.99 kJ/g VS dig.

Table 3-10. Energy selectivities for hydrogen batch and continuous fermentations.

Fermentation	PH	PHC	BH	BHC
Substrate	Paper	Paper	Bagasse	Bagasse
Mode	Batch	Continuous	Batch	Continuous
γ (kJ/g VS dig)	−2.11 ± 0.12	−2.01 ± 0.011	−2.00 ± 0.25	−1.99 ± 0.016

The similarity of γ between the batch and continuous fermentations highlights why hydrogen yields were so different between the paper batch and continuous fermentations, but the same for the bagasse batch and continuous fermentations. The microorganisms are balancing the amount of energy needed for anabolism (ΔG_A) with the amount of energy received from the catabolism (ΔG_C). At cellular conditions, hydrogen production reduces the ΔG_C. The microorganisms would only produce the amount of hydrogen that would result in a net ΔG_T of zero and no more (Figure 3-11).

Potentially, once the energy selectivity has been determined from the acid and hydrogen production of a specific system of substrate, buffer and incubation temperature, it could be used to predict the amount of hydrogen being produced in other fermentations of the same system.

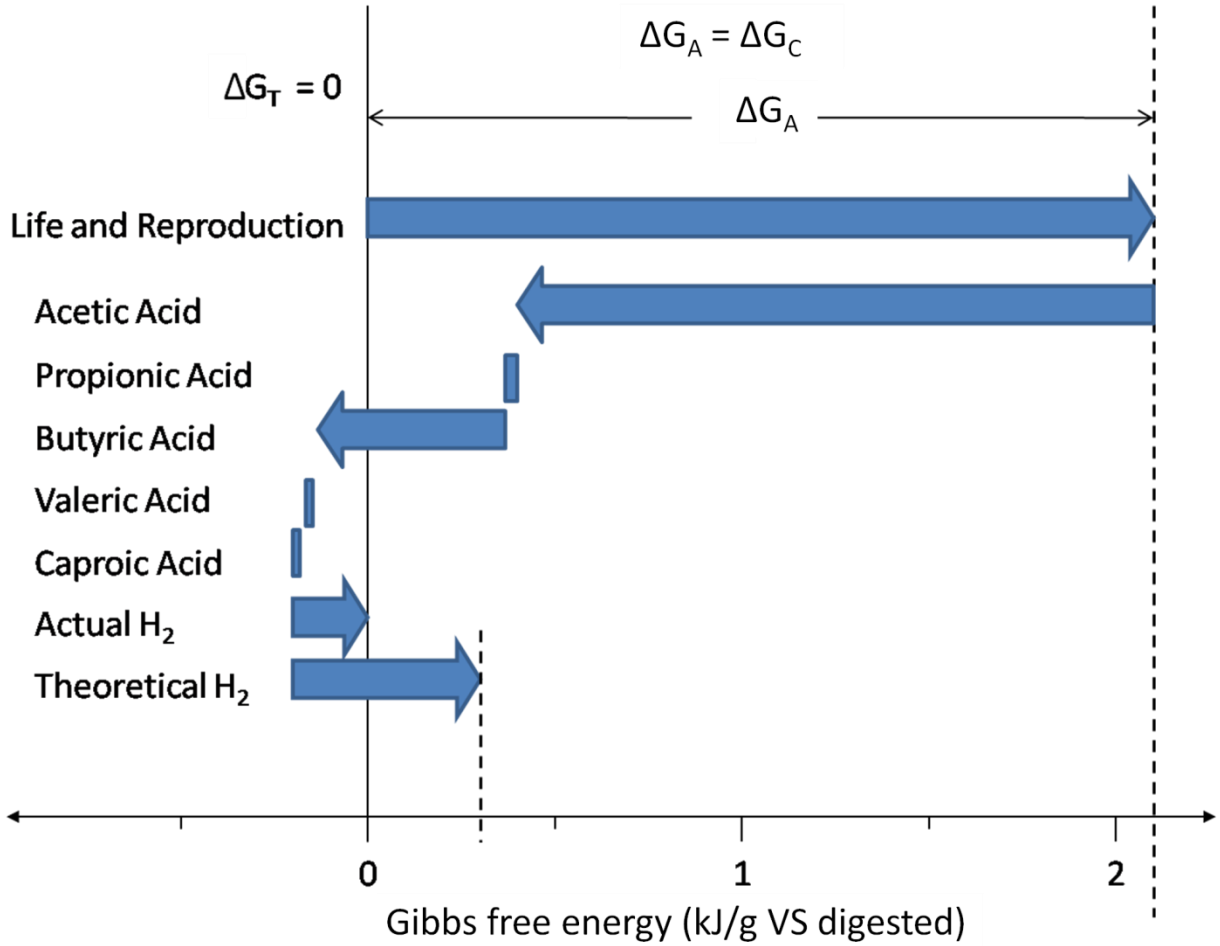

Figure 3-11. Gibbs energy balance for PH paper batch fermentation. ΔG_A is the Gibbs free energy necessary for anabolism and ΔG_C is the energy obtained from catabolic production of acids and hydrogen. ΔG_T is the net energy within the cell, which is zero. This shows that if the microorganism produced all the hydrogen it theoretically could, it would not have a net energy of zero.

3.9 Discussion

From the research in this chapter, the amount of hydrogen released from mixed-acid fermentations is determined not only by the types of sugar that are digested and the types of acid that are produced, but also by the energy selectivity of the microorganisms in the fermentation system. The microbes must balance the amount of energy they obtain from the digestion of sugars and the production of acids (ΔG_C) with the energy needed to live and reproduce (ΔG_A).

The maximum actual hydrogen yield achieved in this chapter was 53.5 mL H_2/g VS digested. The maximum theoretical hydrogen yield calculated, based on the results of this chapter, was 160.2 mL H_2/g VS digested. Based on current process economics for the MixAlco™ process (Granda et al., 2009), the maximum actual yield obtained would only supply 11% of the hydrogen needed for the downstream conversion of the carboxylic acids into mixed alcohols. Even the maximum theoretical yield would only supply 33% of the hydrogen needed for downstream processing.

There is enough potential hydrogen generated from the mixed-acid fermentation to justify the addition of gas separators into the industrial-scale fermentations, but additional sources of hydrogen will still be needed. Hydrogen could be obtained from the gasification of the spent fermentor solids or obtained from other sources, such as electrolysis of water or methane reforming.

3.10 Conclusions

The following conclusions can be made based on this chapter:

1) A stainless steel fermentor was constructed that successfully allowed the collection and quantification of hydrogen produced from both batch and continuous fermentations.
2) Batch fermentations of paper (PH) produced 21.8 g/L of carboxylic acid with a conversion of 0.64 g VS digested/g VS fed and a selectivity of 0.42 g acid/g VS digested. It produced 1115 mL of hydrogen with a hydrogen selectivity of 53.5 mL H_2/g VS digested and a percent yield of 33.4%. Batch fermentations of bagasse (BH) produced 21.07 g/L of carboxylic acid with a conversion of 0.64 g VS digested/g VS fed and a with a hydrogen selectivity of 44.6 mL H_2/g VS digested and a percent yield of 24.9%.
3) Continuous fermentations of paper (PHC) produced 16.7 g/L of carboxylic acids with a conversion of 0.53 g VS digested/g VS fed and a selectivity of 0.37 g acid/g VS digested. It produced 73.6 mL H_2/transfer with a hydrogen selectivity of 15.7 mL H_2/g VS digested and a percent yield of 6.93%. Continuous fermentations of bagasse (BHC) produced 17.1 g/L of carboxylic acids with a conversion of 0.53 g VS digested/g VS fed and a selectivity of 0.39 g acid/g VS digested. It produced 176 mL H_2/transfer with a hydrogen selectivity of 41.1 mL H_2/g VS digested and a percent yield of 22.61%.
4) Calculations of the Gibbs free energy of the catabolic reactions (ΔG_C) at cellular conditions determined the energy selectivities of each system. The paper fermentation system had an energy selectivity of -2.11 kJ/g VS dig and the bagasse fermentation system had an energy selectivity of -2.00 kJ/g VS dig.
5) Energy selectivities (γ) accurately determined why the paper fermentation produced less hydrogen during continuous operation than during batch operation.

CHAPTER IV
COMPARISON OF YEAST EXTRACT AND CORN STEEP LIQUOR AS SUBSTITUTE FOR CHICKEN MANURE

The objectives of this chapter follow:

a) Explain the bioscreening process and the steps of the experiment.
b) Evaluate yeast extract and corn steep liquor as nutrient sources for mixed-acid fermentations.
c) Determine the "best" ratio of nutrient to substrate for mixed-acid fermentations.
d) Determine the "best" nutrient to replace chicken manure for bioscreening fermentations.

4.1 Introduction

As energy demand increases and the availability of fossil fuels decreases, the need for alternative energy sources grows. Anaerobic fermentation of waste lignocellulosic biomass has the potential to meet this need (Chan and Holtzapple, 2003; Holtzapple et al., 1999). Over a billion tons of agricultural, municipal, and industrial wastes are generated annually in the United States that could potentially be used in biofuel production (Perlack et al., 2005). The MixAlco™ process is a flexible and cost-effective means to convert a variety of lignocellulosic feedstocks − including agricultural residues, municipal solid waste, and biosolids − into chemicals and liquid fuels. By employing a mixed culture of naturally occurring microorganisms to ferment the biomass into carboxylic salts, these carboxylic salts can be converted into a wide array of chemicals, including alcohols, jet fuel, and gasoline (Aiello-Mazzarri et al., 2006; Granda et al., 2009).

Employing a mixed culture is extremely well suited to a non-sterile, ever-changing environment with multiple feedstocks, offering advantages over a pure culture (Angenent et al., 2004; Das and Veziroglu, 2001). The mixed culture may establish a robust, synergistic community that grows faster than a pure culture. The mixed culture will also maintain itself better against microbial contamination (Rokem et al., 1980). The stability of the mixed culture system has been linked to increased diversity of the microbial community and to an

increased ability to adapt to changes in the environment of the system (Angenent et al., 2004).

Process development is based on natural and ecological selection or by varying the source of the natural inoculum (Kleerebezem and van Loosdrecht, 2007). To date, little research has been done to identify new communities for use in the MixAlco™ process; however, the few attempts to improve the community have greatly increased product yields. When a community isolated from a marine ecology (Galveston, TX) replaced the previous terrestrial community (College Station, TX), the acid yields doubled (Thanakoses, 2002). The natural saline environment of the marine ecology developed a community better suited to the salty environment of the MixAlco™ process.

Saline and thermal ecosystems are distributed globally and represent a wide range of ecosystem types, including salt lakes, hot springs, salt flats, thermal wells, and ancient salt deposits (Oren, 2002). The water, soil, and sediments of these environments harbor active and diverse communities that can survive non-standard and non-conventional environments (Caton et al., 2004; Humayoun et al., 2003; Ley et al., 2006; Mesbah et al., 2007). Microorganisms taken from these environments have been the subject of several studies that demonstrated their ability to anaerobically digest raw materials, reduce energy consumption, and improve the quality and purity of products (Antranikian et al., 2005; Nicholson and Fathepure, 2005).

The Bioscreening Project is a joint effort between three Texas A&M departments: the Department of Chemical Engineering, the Department of Plant Pathology and Microbiology, and the Department of Soil and Crop Sciences. This project seeks microorganisms that can degrade both cellulose and hemicelluloses for future use in the MixAlco™ process. Although sugarcane bagasse and other agricultural wastes have these materials in abundance, they also contain high amounts lignin that must be removed by pretreatments. Because this project spans a significant period of time, large quantities of a lignin-containing substrate would need to be pretreated at different times, resulting in variations in lignin and cellulose and hemicellulose content that could affect the results of any individual screen. On the other hand, office paper wastes have already been pretreated to exacting standards by the paper industry to achieve the desired thickness and finish of the end-product. Therefore, there

would be no variation in lignin content over a long time period by using this as the carbon source in the bioscreening fermentations.

The nutrient source used most often in the MixAlco™ process is dried chicken manure. Animal wastes such as chicken manure contain a large amount of proteins and minerals and provide an inexpensive easily available nutrient source. Unfortunately, chicken manure already contains many microorganisms that could overshadow and even overwhelm the microorganisms this project seeks to identify. Yeast extract (YE), obtained from the lysing of yeast cells, and corn steep liquor (CSL), obtained from the wet corn milling process, also contain large amounts of proteins and minerals and have the additional advantage of being sterile. Therefore, the objective of this chapter is to determine the amount of either yeast extract or corn steep liquor that provides enough nutrients to give a similar fermentation performance to fermentations using chicken manure.

4.2 Bioscreening process steps

Over 500 bacterial communities at over 20 different geological sites were selected and screened to find the highest performing inoculum for carboxylate platform fermentations. The bacterial communities were screened, ranked, and selected with a series of three sequential fermentation performance tests: an initial screen (Chapter V), the continuous particle distribution model (CPDM) (Chapter VI), and countercurrent fermentation trains (Chapter VII) (Figure 4-1). The communities that had the highest conversion from the 30-day initial batch screen and generated the best-performing maps from the 28-day batch CPDM fermentations were then run in four-fermentor countercurrent trains for over 4 months.

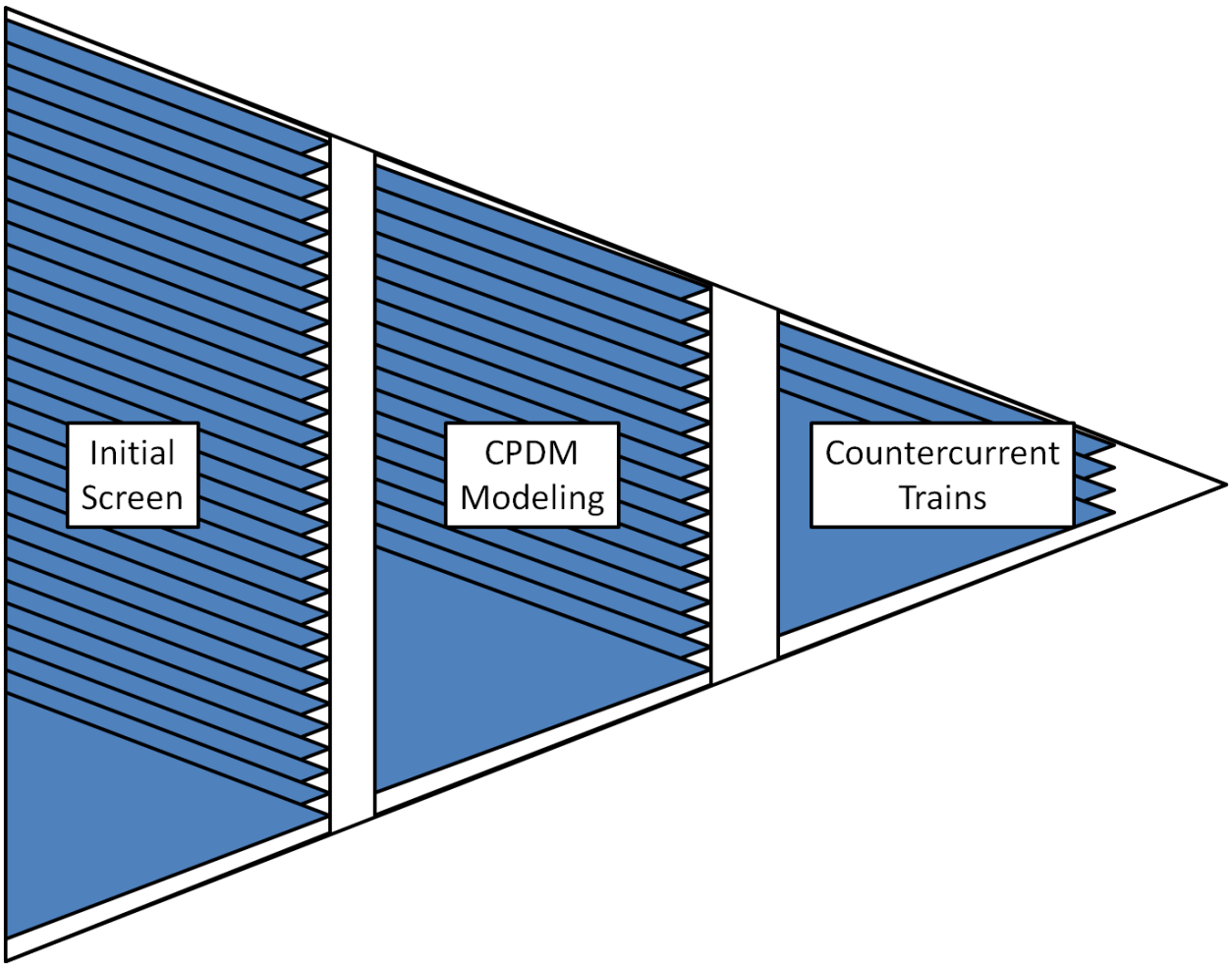

Figure 4-1. Overview of the bioscreening process.

4.3 Materials and methods

4.3.1 Selection of substrate

Office paper waste was selected as the carbon source for all bioscreening fermentations. Office paper wastes were collected from the wastepaper bin in the graduate student computer laboratory and from the copier room (Department of Chemical Engineering, Texas A&M University, College Station, TX). The collected paper was shredded through a conventional paper shredder to achieve a homogeneous size. No additional treatments were necessary because the paper pulping and manufacturing process already treats the paper.

4.3.2 Selection of nutrient source

For many years, both yeast extract and corn steep liquor have been used in ethanol fermentations. Several studies have shown that the preferred ratios of either nutrient are less than the 80 wt% substrate/20 wt% nutrient ratio that is favored for the MixAlco™ process, but they do not agree on the amount (Amartey and Jeffries, 1994; Bravo et al., 1995; Kayali et al., 2005; Lee et al., 2000). Also, they used pure cultures with single-sugar substrates that do not contain the complex components found in the MixAlco™ process. In this study, four ratios of both yeast extract and corn steep liquor were studied; 1, 5, 10, and 20 wt%, in comparison to the standard 20 wt% of chicken manure.

4.3.3 Batch fermentation

Batch fermentations were used in this chapter. All plastic fermentors were loaded with a 100 g/L total substrate/nutrient concentration. The batch fermentation procedures are detailed in Chapter II. Fresh Galveston Island inocula was used for all fermentations in this study. Ammonium bicarbonate was used as the only buffer. The incubation temperature was maintained at 55 °C. Table 4-1 lists the fermentation conditions used in this chapter. All fermentations were started at the same time and operated under identical conditions.

Table 4-1. Experimental condition matrix for anaerobic fermentations using different ratios of paper and nutrient.

Fermentation	Nutrient	Paper (g)	Nutrient (g)	Fermentation Temperature (°C)	Iodoform* (mg/(L liq·day))
YE01	Yeast Extract	39.6	0.4	55	2.0
YE05	Yeast Extract	38	2	55	2.0
YE10	Yeast Extract	36	4	55	2.0
YE20	Yeast Extract	32	8	55	2.0
CS01	Corn Steep Liquor	39.6	0.4	55	2.0
CS05	Corn Steep Liquor	38	2	55	2.0
CS10	Corn Steep Liquor	36	4	55	2.0
CS20	Corn Steep Liquor	32	8	55	2.0
R1	Chicken Manure	32	8	55	2.0

* Iodoform added as 20 g/L ethanol solution

4.3.4 Data analysis

The total carboxylic acid concentration, conversion, selectivity, and yield were used to compare the different fermentation performance of the different nutrient ratios. In general, higher acid concentration, higher conversion and higher selectivity are preferred.

4.4 Results and discussion

4.4.1 Effects of nutrient ratios

Anaerobic microorganisms produce a wide spectrum of carboxylic acids including acetic, propionic, butyric, and valeric. Maximizing the total acid concentration is a major consideration when comparing the nutrient ratios. The acetic acid percentage in the fermentation products is also of interest, because of its potential as a chemical product. Both the total acid concentration and the acetic acid percentage were monitored in this study to compare the nutrient ratios.

The different fermentation performances under each nutrient source are discussed in the following subsections.

4.4.1.1 Effect of yeast extract ratios on fermentations

In batch fermentation, the activities of four different ratios of yeast extract to paper were compared: 1, 5, 10, and 20 wt% of yeast extract to total substrate. The total carboxylic acid concentration, VS conversion, yield, and selectivity of the fermentation were compared to evaluate the different yeast extract ratios.

Figure 4-2 shows the total carboxylic acid profiles for the yeast extract ratios. The 10 wt% YE ratio seems to be the "best" of the four ratios. The highest acid concentration obtained for 10 wt% YE was 24.4 g/L. The acid production was based on the net acid accumulation during the fermentation. The total acids were 6.3, 20.8, and 16.7 g/L for the 1, 5, and 20 wt% ratios, respectively.

Table 4-2 summarizes the fermentation results for the yeast extract ratios. The fermentation using 10 wt% YE has a higher VS conversion (66.0%), and higher yield (0.27 g acids/g VS fed) than the other fermentations.

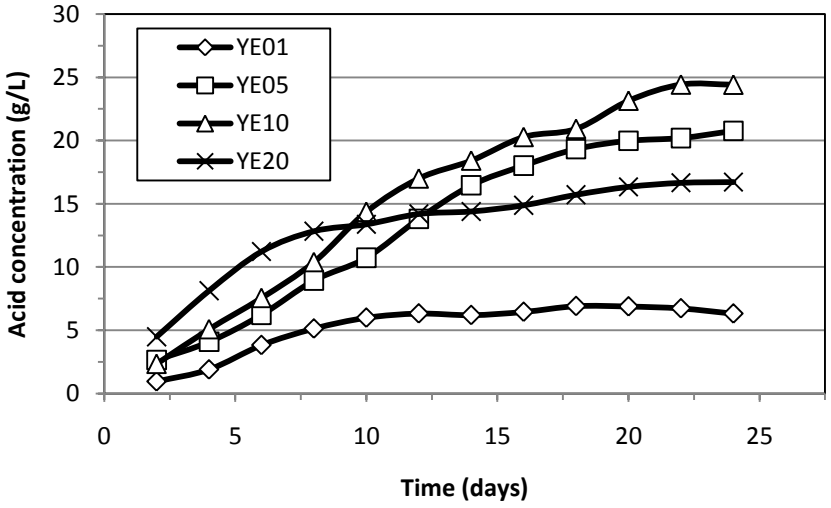

Figure 4-2. Comparison of the total acid concentrations for yeast extract nutrient ratios with paper substrate.

Table 4-2. Effects of yeast extract ratios on paper fermentations.

Fermentation	YE01	YE05	YE10	YE20
Total acid concentration (g/L)	6.32	20.76	24.41	16.72
Acetic (wt%)	93.79	77.40	72.93	61.98
Propionic (wt%)	0.00	2.54	3.35	6.33
Butyric (wt%)	5.12	18.40	21.26	25.38
Valeric (wt%)	1.10	1.67	2.46	6.31
Caproic (wt%)	0.00	0.00	0.00	0.00
Heptanoic (wt%)	0.00	0.00	0.00	0.00
Conversion (g VS digested/g VS fed)	0.44	0.55	0.66	0.43
Selectivity (g acid/g VS digested)	0.16	0.42	0.42	0.44
Yield (g acid/g VS fed)	0.07	0.23	0.27	0.19
Productivity (g acid/(L liq·day))	0.26	0.87	1.02	0.70

4.4.1.2 Effect of corn steep liquor ratios on fermentations

The batch fermentation activities of four different ratios of corn steep liquor to paper were compared. The ratios were 1, 5, 10, and 20 wt% of corn steep liquor (CSL) to total substrate. The total carboxylic acid concentration, VS conversion, yield, and selectivity of the fermentation were compared to evaluate the different corn steep liquor ratios.

Figure 4-3 shows the total carboxylic acid profiles for the corn steep liquor ratios. The 10 wt% corn steep liquor ratio seems to be the "best" of the four ratios of CSL. The highest acid concentration obtained for 10 wt% CSL was 20.6 g/L. The acid production was based on the net acid accumulation during the fermentation. The total acids were 11.7, 16.4, and 19.5 g/L for the 1, 5, and 20 wt% ratios, respectively.

Table 4-3 summarizes the fermentation results for the corn steep liquor ratios. The fermentation using 10 wt% CSL has a higher VS conversion (0.54 g VS digested/g VS fed), and higher yield (0.23 g acids/g VS fed) than the other fermentations.

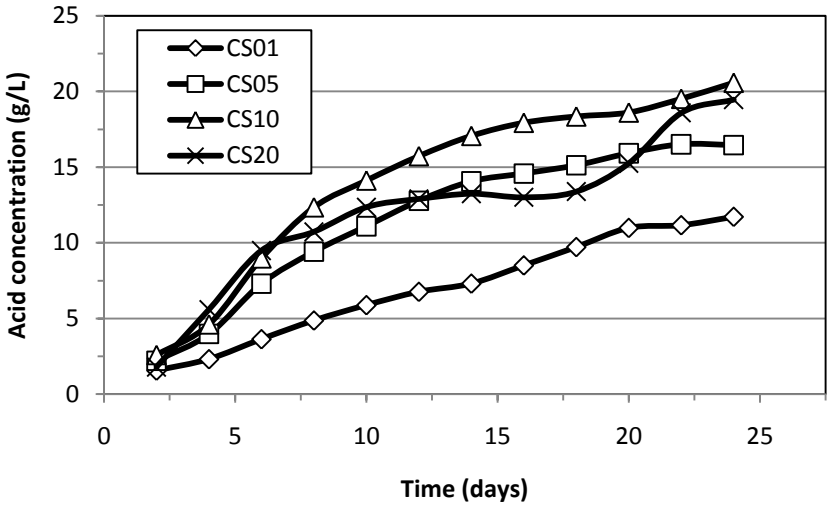

Figure 4-3. Comparison of the total acid concentrations for corn steep liquor nutrient ratios with paper substrate.

Table 4-3. Effects of corn steep liquor ratios on paper fermentations.

Fermentation	CS01	CS05	CS10	CS20
Total acid concentration (g/L)	11.72	16.45	20.58	19.47
Acetic (wt%)	80.35	79.08	70.98	72.68
Propionic (wt%)	1.56	1.45	3.32	2.93
Butyric (wt%)	18.09	18.57	25.23	23.46
Valeric (wt%)	0.00	0.90	0.47	0.93
Caproic (wt%)	0.00	0.00	0.00	0.00
Heptanoic (wt%)	0.00	0.00	0.00	0.00
Conversion (g VS digested/g VS fed)	0.39	0.50	0.54	0.52
Selectivity (g acid/g VS digested)	0.34	0.37	0.43	0.43
Yield (g acid/g VS fed)	0.13	0.18	0.23	0.22
Productivity (g acid/(L liq·day))	0.49	0.69	0.86	0.81

4.4.2 Comparison of nutrients yeast extract and corn steep liquor to chicken manure

Available nutrients are vital to microorganism growth. Without them, microorganism cannot perform the molecular reactions necessary for life. In this chapter, different ratios of both yeast extract and corn steep liquor were tested to find a sterile replacement for

inexpensive but non-sterile chicken manure as a nutrient source in the bioscreening experiments. Experimental data from Section 4.4.1 were analyzed against the fermentation performance of 20 wt% chicken manure in this section.

4.4.2.1 Effect on total acid concentration

Figure 4-4 shows the total acid concentration of the "best" ratio of both yeast extract and corn steep liquor against a 20 wt% mixture of chicken manure. An 80/20 wt% ratio of paper/chicken manure is the standard ratio for most MixAlco™ fermentations. A 10 wt% corn steep liquor ratio produced a total carboxylic acid profile nearly identical to the 20 wt% chicken manure whereas the 10 wt% yeast extract clearly produced more carboxylic acids.

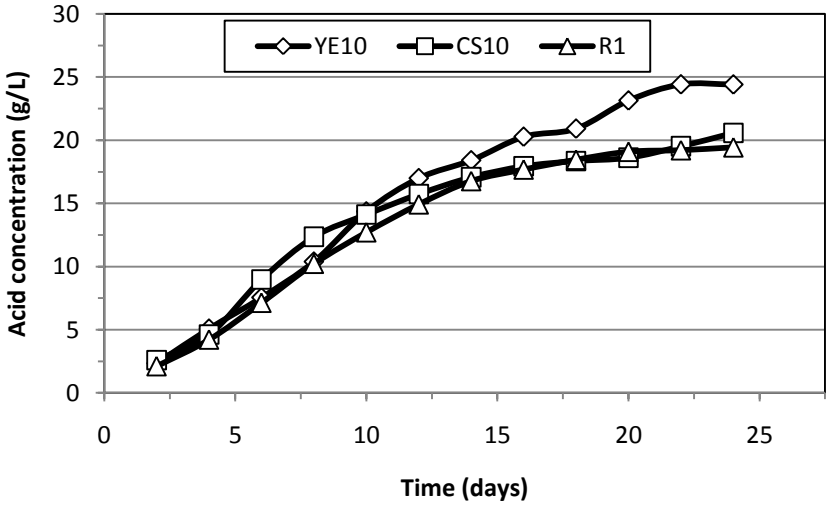

Figure 4-4. Comparison of the total acid concentrations for 10 wt% YE and 10 wt% CSL nutrient ratios with 20 wt% chicken manure with paper substrate fermentations. R1 is the fermentation with an 80/20 ratio of paper and chicken manure.

4.4.2.2 Effect on acetic acid percentage

Acetic acid (C2) is the major product in the fermentation broth. Figure 4-5 shows that both the 10 wt% YE and the 10 wt% CSL produced more acetic acid than the 20 wt% chicken manure. Both alternative nutrients achieved a final acetic acid percentage of nearly 75% whereas the chicken manure nutrient only achieved 65%.

4.4.2.3 Summary of fermentation performance

Table 4-4 summarizes the fermentation performance results for the "best" ratios of yeast extract and corn steep liquor and the chicken manure fermentations. The 10 wt% yeast extract fermentation had higher total acid concentration, acetic acid percentage, conversion, selectivity, and yield than the 10 wt% corn steep liquor fermentation. It also had a higher total acid concentration, acetic acid percentage, selectivity and yield than the chicken manure fermentation.

In summary, a 90 wt% paper/10 wt% yeast extract ratio is the best alternative to using chicken manure for the bioscreening experiments.

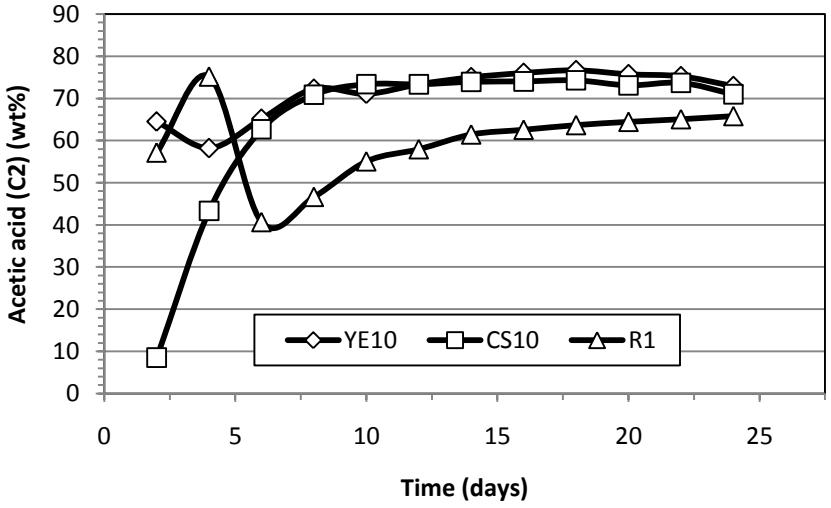

Figure 4-5. Comparison of acetic acid (C2) percentage for 10 wt% YE and 10 wt% CSL fermentations with a 20 wt% chicken manure fermentation (R1).

Table 4-4. Comparison of the "best" yeast extract (YE10) and corn steep liquor (CS10) fermentation with a chicken manure (R1) fermentation.

Fermentation	YE10	CS10	R1
Nutrient	YE	CSL	CM
Total acid concentration (g/L)	24.41	20.58	19.43
Acetic (wt%)	72.93	70.98	65.83
Propionic (wt%)	3.35	3.32	2.19
Butyric (wt%)	21.26	25.23	31.46
Valeric (wt%)	2.46	0.47	0.52
Caproic (wt%)	0.00	0.00	0.00
Heptanoic (wt%)	0.00	0.00	0.00
Conversion (g VS digested/g VS fed)	0.66	0.54	0.71
Selectivity (g acid/g VS digested)	0.42	0.43	0.32
Yield (g acid/g VS fed)	0.27	0.23	0.23
Productivity (g acid/(L liq·day))	1.02	0.86	0.81

4.5 Conclusions

The following conclusions can be made from this study:

1) Of all yeast extract ratios, a ratio of 90 wt% paper/10 wt% yeast extract produced the highest amount of carboxylic acids (24.4 g/L) and a conversion of 0.66 g VS digested/g VS fed.
2) Of all corn steep liquor ratios, a ratio of 90 wt% paper/10 wt% corn steep liquor produced the highest amount of carboxylic acids (20.6 g/L) and a conversion of 0.54 g VS digested/g VS fed.
3) In paper fermentations buffered with ammonium bicarbonate, both 10 wt% yeast extract and 10 wt% corn steep liquor produce more carboxylic acids than a 20 wt% ratio of chicken manure.
4) To replace chicken manure in the bioscreening fermentations, a ratio of 90 wt% paper and 10 wt% yeast extract is the best nutrient addition.

CHAPTER V
INITIAL SITE SCREENINGS FOR THE BIOSCREENING PROJECT

The objectives of this chapter follow:

a) Screen microorganism communities contained in soil samples taken from thermal and saline sites for biomass conversion and carboxylic acid production.
b) Determine the "best" community from each site based on conversion.
c) Select communities for further study that show promise in the MixAlco™ process.

5.1 Introduction

The MixAlco™ process is well-developed and is in the beginning stages of commercialization. The ultimate objective of the Bioscreening Project is to find microorganism communities, either naturally occurring, or a combination of naturally occurring microorganisms, that will quickly and efficiently convert biomass into carboxylic acids. This chapter focuses on the first step in the Bioscreening Project and compares different inoculum sources for anaerobic fermentation.

The performance of an anaerobic fermentation is influenced by various fermentation conditions, including pH, temperature, nutrient supply, and inoculums source. Selecting an inoculum source is perhaps the most important step in an anaerobic fermentation, because it provides the species of microorganisms for the fermentation process. Whether the microorganisms have the capability to convert the substrate into carboxylic acids and can adapt to the high saline environment of the MixAlco™ process will determine the final production and stability of the fermentation process.

In summary, this chapter covers the first step in the Bioscreening Project, the Initial Screen. Several locations at each site are screened for the "best" microorganism community based on the conversion of the substrate.

5.2 Site screening

5.2.1 Selection of sites

Previous research has shown that inocula taken from thermal and saline regions contains microorganisms better suited to the high salt content found in the MixAlco™ process. Aiello-Mazzari (2002), Chan and Holtzapple (2003), and Thanakoses (2002) all found that marine inoculum taken from Galveston, TX showed a better conversion of substrate and a higher production of acids than terrestrial inoculum taken from a local compost heap (College Station, TX). Compared to terrestrial inoculum, Thanakoses (2002) found that marine inoculum increased the total carboxylic acid concentration from 9.6 g/L to 16.2 g/L for 80% bagasse/20% chicken manure. Fu (2007) found that inoculum taken from the highly saline Great Salt Lake, UT produced 15.0 g/L of acids whereas the low saline inoculum from Galveston produced 13.0 g/L.

Sites screened in this chapter were selected based on high salt concentration and high temperature. Table 5-1 lists the sites sampled in this study. Site labels I and O were not used because, during manual labeling of sample tubes, it is very easy to confuse I and O for 1 and 0.

5.2.2 Sampling of sites

With the exception of site B, all sampling was conducted by members of Heather Wilkinson's group in the Department of Plant Pathology and Microbiology. Site B samples were collected by myself, or in the case of the Bahamas sample, donated to the laboratory. The pure culture of C. thermocellum was grown and provided by Terry Gentry's group in the Department of Soil and Crop Sciences. At each site, samples were taken along a transect that bisected the saline or thermal gradient of the site. A 3-in-wide core was taken from the first 10 inches of soil and sealed into an air-tight bag. Within the bag, each sample was homogenized to ensure an even distribution of the microorganism communities. The GPS coordinate of the sample was recorded. Figure 5-1 shows the GPS sampling of the transects at La Sal del Rey, TX. Appendix M has the GPS coordinates of all samples studied in this chapter.

Table 5-1. Sites sampled in Step 1 of the Bioscreening Project.

Site	Name	Total Samples
A	La Sal del Rey, TX	26
B	Galveston, TX Bryan, TX Bahamas *C. thermocellum*	4
C	Taiwan	1
D	Gruella-Muleshoe	30
E	Enid, OK	11
F	Brazoria, TX	9
G	Roswell-Carlsbad	53
H	San Francisco, CA	34
J	Big Bend, TX	22
K	Utah1	55
L	Utah2	25
M	Georgia1	41
N	Georgia2	22
P	Puerto Rico	35
Q	Florida	28
R	Santa Fe, NM	20
S	Yellowstone, WY	48
T	Nevada	17
U	Nevada-California	24

Figure 5-1. GPS coordinate tags of the three transects at La Sal del Rey, TX.

5.2.3 Fermentation

Once a site was sampled, all samples were transported back to the laboratory in the Jack E. Brown Building of Texas A&M University. As determined in Chapter IV, a ratio of 90 wt% paper and 10 wt% yeast extract was selected at the substrate for all bioscreening fermentations. Wet soil (2.5 g) from each sample was loaded into a 250-mL Nalgene bottle containing 9 g shredded office paper, 1 g yeast extract, 0.2 g urea, 2.2 g calcium carbonate, 3.2 g calcium acetate, 0.2 g calcium propionate, 0.5 g butyric acid, and 150 mL of distilled water. The calcium salts and butyric acid are added to the initial screen to mimic the 20 g/L carboxylic acid concentrations typically found in the MixAlco™ process. Each bottle was then capped and placed in a shaker incubator running at 100 rpm for 30 days. Iodoform (20 g/L ethanol soln) was added every two days to prevent methanogen growth. Initial and final acid concentrations were collected to determine the amount of acid produced during the

fermentation. Three control inocula were used for several of the sites: Galveston sand, a pure culture of *Clostridium thermocellum*, and a blank that had no inoculum.

5.2.4 Data analysis

The total carboxylic acid concentration, conversion, selectivity, and yield were used to compare the different inocula from each site. In this chapter, conversion was used as the primary determination for the overall performance of a sample. The inoculum with the highest conversion for the site was considered the "best" of the site. Spent fermentor solids was collected from all samples for DNA analysis and species identification.

5.3 Site results

5.3.1 Site A – La Sal del Rey, TX

Site A was the first site sampled as part of the project. A total of 26 samples were taken along three transects (T1, T2 and T3) at 20-meter intervals of the salt lake La Sal del Rey in southern Texas. Because Galveston, TX inocula had been used successfully in the past, it was used as a comparison in this project. As part of this project, the bacterial community at the end of the fermentation was to be cultured for the isolation of individual bacterial communities. Because the closing of the fermentation requires centrifugation, which might stress and damage the cells, bacterial samples were taken before the centrifugation step. Although it was assumed that these samples were homogeneous in comparison to the remaining material in the fermentor, analysis showed that they were not. Because of this, accurate conversion data could not be obtained for this site. The best selection for this site was determined by acid production alone.

Although the Galveston inoculum performed better than all the samples from this site, the best-performing bacterial community from for La Sal del Rey, TX was A23 found on Transect 3 (T3) at 195 feet along the transect. Table 5-2 shows the acid production for all samples of Site A.

Also, during future screenings, the bacterial isolation samples were not taken until after the centrifugation step to ensure accurate conversion data.

Table 5-2. Carboxylic acid results for Site A: La Sal del Rey, TX.

Sample ID	Inocula location	Change in acid conc. (g/L)	Sample ID	Inocula Location	Change in acid conc. (g/L)
A01	Galveston	12.91	A15	T2-195	6.84
A02	T1-0	11.77	A16	T2-260	6.75
A03	T1-65	9.85	A17	T2-325	6.82
A04	T1-130	10.18	A18	T2-390	11.27
A05	T1-195	11.34	A19	T2-455	9.25
A06	T1-260	9.55	A20	T3-0	11.39
A07	T1-325	11.63	A21	T3-65	5.14
A08	T1-390	10.28	A22	T3-130	9.70
A09	T1-455	11.71	A23	T3-195	12.79
A10	T1-520	7.63	A24	T3-260	9.45
A11	T1-595	9.85	A25	T3-325	11.98
A12	T2-0	4.13	A26	T3-390	9.17
A13	T2-65	7.01	A27	T3-455	11.57
A14	T2-130	8.17			

5.3.2 Site B – Bahamas and Terrestrial (Bryan, TX)

Site B compared inocula collected from San Salvador Island of the Bahamas and a terrestrial sample from Bryan, TX with the Galveston Inoculum. A pure culture of *Clostridium thermocellum* was also included. Because the Galveston sample is a mixed culture from a natural environment, there could be a significant variation in the microorganism communities from one inoculation to the next. There should not be such variation in inocula from a single pure culture.

Galveston and Terrestrial inocula produced nearly the same amount of acids, 4.3 g/L and 4.06 g/L respectively, but Galveston had a better conversion then the terrestrial microorganisms. With 5.18 g/L, Bahamas was the first culture to produce more acids than Galveston. The pure culture did not perform as well as the mixed cultures, but did show an appreciable amount of conversion at 0.32 g VS digested/g VS fed. Table 5-3 shows the results for Site B.

Table 5-3. Fermentation results for Site B.

Sample ID	B01	B02	B03	B04
Inocula type	Galveston	Terrestrial	Bahamas	Pure
Total acid concentration (g/L)	24.30	24.03	25.19	22.77
Change in acid conc. (g/L)	4.30	4.06	5.18	2.19
Conversion (g VS digested/g VS fed)	0.36	0.27	0.28	0.32

5.3.3 Site C – Taiwan

Site C came from a single inoculum sample obtained from the Green Sulphur Spring in the Beitou Valley of Taiwan. It produced 8.43 g/L of carboxylic acids and had a conversion of 0.35 g VS digested/g VS fed. Table 5-4 shows the results for Site C.

Table 5-4. Carboxylic acid and conversion results for Site C: Taiwan.

Sample ID	Change in acid conc. (g/L)	Conversion (g VS digested/g VS fed)
C01	8.43	0.35

5.3.4 Site D – Gruella, NM and Muleshoe, TX

For Site D, a total of 30 samples were collected from the marshes and lakes surrounding Gruella, NM and Muleshoe, TX. Samples were taken from Gruella, NM (GR), Paul's Lake's in Muleshoe, TX (MPL), White Lake in Muleshoe, TX (MWL), and Goose Lake in Muleshoe, TX (MGL). A Galveston inoculum sample was included with this run as a comparison. The top three performers, based on conversion were D18, D17 and D22 were all from Muleshoe, TX. They had conversions of 0.32, 0.30, and 0.30 g VS digested/g VS fed, respectfully. Table 5-5 shows the acid production and conversions from Site D.

Table 5-5. Carboxylic acid and conversion results for Site D.

Sample ID	Sample location	Change in acid conc. (g/L)	Conversion (g VS digested/g VS fed)	Sample ID	Sample location	Change in acid conc. (g/L)	Conversion (g VS digested/g VS fed)
D01	GR1	4.69	0.20	D17	MPL5	1.40	0.30
D02	GR2	0.09	0.22	D18	MPL6	1.82	0.32
D03	GR3	0.88	0.19	D19	MPL7	1.92	0.28
D04	GR4	4.62	0.27	D20	MPL8	1.00	0.20
D05	GR5	5.51	0.17	D21	MPL9	-0.31	0.24
D06	GR6	2.28	0.22	D22	MWL1	2.86	0.30
D07	GR7	3.43	0.22	D23	MWL2	2.06	0.14
D08	GR8	1.92	0.23	D24	MWL3	2.41	0.18
D09	GR9	3.37	0.24	D25	MWL4	1.68	0.21
D10	GR10	-1.27	0.21	D26	MGL1	3.96	0.18
D11	GR11	2.74	0.30	D27	MGL2	2.80	0.13
D12	GR12	2.64	0.23	D28	MGL3	2.16	0.13
D13	MPL1	3.64	0.21	D29	MGL4	2.53	0.23
D14	MPL2	2.38	0.22	D30	MGL5	2.43	0.17
D15	MPL3	2.11	0.22	D31	Galveston	5.88	0.19
D16	MPL4	2.73	0.29				

5.3.5 Site E – Enid, OK

Site E consisted of 11 samples collected from the Great Salt Plain near Enid, OK. The best-performing community (E08) had both the highest change in acid concentration (4.62 g/L) and the highest conversion (0.27 g VS digested/g VS fed). Table 5-6 shows the acid production and conversions for Site E.

Table 5-6. Carboxylic acid and conversion results for Site E: Enid, OK.

Sample ID	Change in acid conc. (g/L)	Conversion (g VS digested/g VS fed)
E01	4.32	0.23
E02	0.36	0.22
E03	2.21	0.19
E04	0.44	0.16
E05	2.05	0.25
E06	3.58	0.20
E07	4.25	0.23
E08	4.62	0.27
E09	2.34	0.21
E10	3.84	0.23
E11	1.54	0.17

5.3.6 Site F – Brazoria, TX

For Site F, a total of nine samples were collected from a salt marsh in the Brazoria National Wildlife Refuge near Brazoria, TX. F09 is the best performer from this site; the acid concentration changed by 4.83 g/L and the conversion was 0.40 g VS digested/g VS fed. Results are shown in Table 5-7.

Table 5-7. Carboxylic acid and conversion results for Site F: Brazoria, TX.

Sample ID	Change in acid conc. (g/L)	Conversion (g VS digested/g VS fed)
F01	3.44	0.34
F02	4.33	0.38
F03	3.14	0.29
F04	1.75	0.32
F05	1.15	0.36
F06	5.03	0.35
F07	0.44	0.28
F08	0.31	0.30
F09	4.83	0.40

5.3.7 Site G – Roswell and Carlsbad, NM

Site G consisted of 52 samples collected from the Roswell/Carlsbad area of New Mexico. Samples were taken from the Bitter Lake National Wildlife Refuge (BL) in Roswell, NM, Lazy Lagoon (LL), and Lea Lake in the Bottomless Lakes State Park in Roswell, NM and William Sink (WS), Laguna Tuston (LTU), Laguna Plata (LP), Laguna Tonto (LTO), Laguna Gatuna (LG), Laguna Quatro (LQ), Laguna Walden (LW), and Laguna Uno (LU) in the Carlsbad, NM branch of the Bureau of Land Management. As a comparison, a Galveston inoculum sample was included. The top three performers are G23, G13 and G08 with conversions of 0.38, 0.36, and 0.36 g VS digested/g VS fed (Table 5-8).

Table 5-8. Carboxylic acid and conversion results for Site G.

Sample ID	Sample location	Change in acid conc. (g/L)	Conversion (g VS digested/g VS fed)	Sample ID	Sample location	Change in acid conc. (g/L)	Conversion (g VS digested/g VS fed)
G01	BL1	3.33	0.19	G28	WS2	4.16	0.27
G02	BL2	2.30	0.17	G29	WS3	3.14	0.19
G03	BL3	4.92	0.18	G30	WS4	3.75	0.22
G04	BL4	2.86	0.17	G31	LTU1	4.02	0.14
G05	BL5	3.44	0.15	G32	LTU2	2.97	0.18
G06	Galveston	5.39	0.16	G33	LTU3	3.33	0.18
G07	BL7	4.87	0.33	G34	LTU4	4.70	0.29
G08	BL8	9.14	0.36	G35	LP1	2.71	0.18
G09	BL9	8.50	0.32	G36	LP2	4.29	0.18
G10	BL10	4.17	0.25	G37	LP3	3.34	0.12
G11	BL11	2.93	0.13	G38	LP4	4.31	0.12
G12	BL12	4.81	0.26	G39	LP5	2.71	0.19
G13	BL13	4.97	0.36	G40	LP6	3.13	0.14
G14	BL14	4.77	0.23	G41	LP7	5.33	0.10
G15	BL15	3.48	0.25	G42	LP8	4.79	0.17
G16	BL16	6.99	0.19	G43	LTO1	1.48	0.20
G17	BL17	2.18	0.26	G44	LTO2	2.36	0.09
G18	BL18	3.23	0.23	G45	LTO3	5.00	0.09
G19	BL19	3.85	0.35	G46	LTO4	7.13	0.34
G20	BL20	2.65	0.24	G47	LG1	2.70	0.34
G21	BL21	2.09	0.34	G48	LG2	5.00	0.21
G22	LL1	6.65	0.30	G49	LG3	3.37	0.28
G23	LL2	8.46	0.38	G50	LQ1	2.80	0.25
G24	LL3	6.61	0.34	G51	LQ2	3.30	0.21
G25	LL4	2.60	0.22	G52	LW	2.86	0.29
G26	Lea Lake	3.09	0.27	G53	LU	4.25	0.24
G27	WS1	3.07	0.21				

5.3.8 Site H – San Francisco, CA

For Site H, a total of 34 samples were collected from around the San Francisco Bay in California. As a comparison, a Galveston inoculum sample (Sample H35) was included. The top three performers are H01, H20 and H07 with conversions of 0.37, 0.35, and 0.29 g VS digested/g VS fed (Table 5-9).

Table 5-9. Carboxylic acid and conversion results for Site H: San Francisco, CA.

Sample ID	Change in acid conc. (g/L)	Conversion (g VS digested/g VS fed)	Sample ID	Change in acid conc. (g/L)	Conversion (g VS digested/g VS fed)
H01	0.71	0.37	H19	3.25	0.19
H02	0.85	0.27	H20	8.08	0.35
H03	0.55	0.27	H21	0.82	0.07
H04	1.62	0.17	H22	1.37	0.13
H05	2.17	0.10	H23	0.36	0.07
H06	0.78	0.11	H24	1.96	0.09
H07	2.06	0.29	H25	1.18	0.15
H08	2.01	0.19	H26	0.92	0.17
H09	0.79	0.14	H27	0.50	0.02
H10	0.90	0.17	H28	0.36	0.15
H11	0.87	0.23	H29	0.38	0.14
H12	0.62	0.12	H30	1.38	0.17
H13	1.19	0.17	H31	1.43	0.14
H14	1.09	0.13	H32	0.97	0.19
H15	0.45	0.14	H33	0.15	0.13
H16	1.52	0.15	H34	0.95	0.13
H17	1.29	0.06	H35	0.32	0.15
H18	0.74	0.12			

5.3.9 Site J – Big Bend, TX

For Site J, a total of 22 samples were collected from the Big Bend National Park, TX. As a comparison, both a Galveston inoculum sample (J23) and a pure culture of *C. thermocellum* (J24) were included. The top three performers, not including the Galveston sample, are J11, J04, and J19 with conversions of 0.38, 0.36, and 0.36 g VS digested/g VS fed (Table 5-10).

Table 5-10. Carboxylic acid and conversion results for Site J: Big Bend National Park, TX.

Sample ID	Change in acid conc. (g/L)	Conversion (g VS digested/g VS fed)	Sample ID	Change in acid conc. (g/L)	Conversion (g VS digested/g VS fed)
J01	0.82	0.31	J13	1.32	0.28
J02	0.00	0.30	J14	0.96	0.31
J03	0.93	0.31	J15	1.18	0.12
J04	1.30	0.36	J16	2.75	0.31
J05	1.92	0.32	J17	1.53	0.23
J06	3.30	0.28	J18	1.15	0.35
J07	1.64	0.26	J19	0.12	0.36
J08	1.54	0.30	J20	0.01	0.35
J09	0.78	0.30	J21	0.31	0.25
J10	2.55	0.29	J22	0.21	0.32
J11	1.78	0.38	J23	1.03	0.37
J12	2.01	0.27	J24	1.98	0.29

5.3.10 Site K – Utah 1

Site K consisted of the first 55 samples collected from Utah. Samples were taken from the Ogden Hot Springs (OHS), Wilson Health Springs (WHS), Fish Springs National Wildlife Refuge (FS), West Topas (WT), Abraham Hot Springs (AHS), and the Baker Hot Springs (BHS). As a comparison, a Galveston inoculum sample and a pure culture of *C. thermocellum* were included. The top three performers are K49, K37 and K51 with conversions of 0.33, 0.29, and 0.29 g VS digested/g VS fed (Table 5-11).

Table 5-11. Carboxylic acid and conversion results for Site K: Utah1.

Sample ID	Sample location	Change in acid conc. (g/L)	Conversion (g VS digested/g VS fed)	Sample ID	Sample location	Change in acid conc. (g/L)	Conversion (g VS digested/g VS fed)
K01	OHS1	0.27	0.08	K30	FS12	0.08	0.10
K02	OHS2	0.69	0.13	K31	FS13	0.55	0.17
K03	OHS3	1.81	0.12	K32	FS14	0.14	0.08
K04	OHS4	1.14	0.10	K33	FS15	0.28	0.15
K05	WHS1	0.81	0.09	K34	FS16	0.80	0.08
K06	WHS2	2.10	0.05	K35	FS17	0.21	0.16
K07	WHS3	0.54	0.12	K36	FS18	0.62	0.09
K08	WHS4	1.61	0.22	K37	FS19	1.06	0.29
K09	WHS5	1.41	0.18	K38	FS20	1.29	0.24
K10	WHS6	0.75	0.07	K39	WT	0.44	0.17
K11	WHS7	2.54	0.11	K40	AHS1	2.11	0.09
K12	WHS8	0.48	0.12	K41	AHS2	0.33	0.16
K13	WHS9	1.20	0.11	K42	AHS3	1.46	0.20
K14	WHS10	0.22	0.13	K43	AHS4	0.88	0.15
K15	WHS11	1.03	0.13	K44	AHS5	0.85	0.16
K16	WHS12	0.41	0.11	K45	BHS1	1.72	0.20
K17	WHS13	0.82	0.10	K46	BHS2	0.83	0.22
K18	WHS14	0.31	0.13	K47	BHS3	0.03	0.13
K19	FS1	0.85	0.15	K48	BHS4	0.88	0.04
K20	FS2	0.71	0.15	K49	BHS5	0.88	0.33
K21	FS3	0.29	0.10	K50	BHS6	0.86	0.10
K22	FS4	0.59	0.06	K51	BHS7	1.31	0.29
K23	FS5	0.63	0.12	K52	BHS8	0.91	0.06
K24	FS6	0.82	0.10	K53	BHS9	1.69	0.23
K25	FS7	1.02	0.10	K54	BHS10	0.41	0.15
K26	FS8	1.02	0.10	K55	BHS11	0.75	0.19
K27	FS9	0.85	0.02	K56	Galveston	0.28	0.08
K28	FS10	0.51	0.16	K57	Pure	0.96	0.05
K29	FS11	0.09	0.16				

5.3.11 Site L – Utah 2

Site L consisted of the last 25 samples collected from Utah. Samples were taken from the Utah Lake (UL), Antelope Island (AI), Great Salt Lake (GSL), Saratoga Hot Springs (SHS), Indian Hot Springs (IHS), Salt Creek Waterfowl Preserve (SCW), Knoll Spring (KS), Lincoln Beach (LB), Warm Springs (WS), and the Bear River Reserve (BBR). As a comparison, a Galveston inoculum sample and a pure culture of *C. thermocellum* were included. The top three performers are L10, L20 and L17 with conversions of 0.26, 0.24, and 0.22 g VS digested/g VS fed (Table 5-12).

Table 5-12. Carboxylic acid and conversion results for Site L: Utah 2.

Sample ID	Sample location	Change in acid conc. (g/L)	Conversion (g VS digested/g VS fed)	Sample ID	Sample location	Change in acid conc. (g/L)	Conversion (g VS digested/g VS fed)
L01	AI1	0.77	0.05	L15	Knoll1	0.56	0.11
L02	AI2	0.47	0.14	L16	LB1	0.71	0.18
L03	AI3	2.13	0.12	L17	UL1	0.60	0.22
L04	AI4	0.69	0.09	L18	UL2	0.95	0.03
L05	GSL1	0.90	0.10	L19	WS1	0.00	0.14
L06	GSL2	0.08	0.15	L20	WS2	1.26	0.24
L07	GSL3	0.96	0.07	L21	WS3	1.61	0.12
L08	SHS1	0.15	0.24	L22	WS4	0.81	0.12
L09	SHS2	0.47	0.16	L23	BRR1	0.85	0.20
L10	IHS1	0.80	0.26	L24	BRR2	0.37	0.19
L11	IHS2	0.11	0.09	L25	BRR3	0.87	0.11
L12	IHS3	1.52	0.15	L26	Galveston	0.95	0.21
L13	IHS4	0.70	0.18	L27	Pure	0.77	0.18
L14	SCW1	0.30	0.13				

5.3.12 Site M – Georgia 1

Site M consisted of the first 41 samples collected from Georgia. Samples were taken from the Savannah Wildlife Reserve (SWR), Cape Romain (CP), and Pinckney Island (PI). As a comparison, a Galveston inoculum sample and a pure culture of *C. thermocellum* were included. The top three performers are M24, M05 and M20 with conversions of 0.27, 0.25, and 0.24 g VS digested/g VS fed (Table 5-13).

Table 5-13. Carboxylic acid and conversion results for Site M: Georgia 1.

Sample ID	Sample location	Change in acid conc. (g/L)	Conversion (g VS digested/g VS fed)	Sample ID	Sample location	Change in acid conc. (g/L)	Conversion (g VS digested/g VS fed)
M01	SWR1	0.03	0.17	M23	CR21	0.27	0.18
M02	SWR2	0.35	0.23	M24	CR22	0.62	0.27
M03	CR1	0.83	0.03	M25	CR23	0.41	0.20
M04	CR2	1.50	0.09	M26	CR24	0.80	0.11
M05	CR3	0.11	0.25	M27	CR25	0.77	0.11
M06	CR4	0.91	0.07	M28	PI1	1.69	0.04
M07	CR5	1.91	0.15	M29	PI2	0.38	0.14
M08	CR6	0.67	0.16	M30	PI3	1.63	0.09
M09	CR7	0.55	0.04	M31	PI4	0.70	0.15
M10	CR8	1.52	0.12	M32	PI5	0.24	0.04
M11	CR9	0.64	0.23	M33	PI6	1.67	0.10
M12	CR10	0.43	0.16	M34	PI7	1.06	0.10
M13	CR11	0.38	0.22	M35	PI8	0.99	0.21
M14	CR12	1.13	0.13	M36	PI9	1.89	0.12
M15	CR13	2.37	0.08	M37	PI10	1.56	0.15
M16	CR14	0.24	0.14	M38	PI11	1.27	0.09
M17	CR15	0.80	0.11	M39	PI12	1.12	0.17
M18	CR16	3.16	0.09	M40	PI13	0.33	0.07
M19	CR17	0.06	0.18	M41	PI14	0.74	0.17
M20	CR18	2.15	0.24	M42	Galveston	0.91	0.09
M21	CR19	0.89	0.14	M43	Pure	1.76	0.14
M22	CR20	1.25	0.12				

5.3.13 Site N – Georgia 2

Site N consisted of the last 22 samples collected from Georgia. Samples were taken from the Savannah Wildlife Reserve (SWR), and Sapelo Island (SI). As a comparison, a Galveston inoculum sample and a pure culture of *C. thermocellum* were included. The top three performers, not including the Galveston or the pure culture, are N09, N20 and N18 with conversions of 0.20, 0.19, and 0.17 g VS digested/g VS fed (Table 5-14).

Table 5-14. Carboxylic acid and conversion results for Site N: Georgia 2.

Sample ID	Sample location	Change in acid conc. (g/L)	Conversion (g VS digested/g VS fed)	Sample ID	Sample location	Change in acid conc. (g/L)	Conversion (g VS digested/g VS fed)
N01	SI1	1.10	0.06	N13	SI13	1.57	0.14
N02	SI2	0.95	0.09	N14	SI14	1.27	0.11
N03	SI3	2.29	0.08	N15	SI15	0.62	0.01
N04	SI4	1.14	0.16	N16	SI16	1.88	0.10
N05	SI5	2.13	0.06	N17	SI17	2.41	0.11
N06	SI6	1.77	0.04	N18	SI18	0.25	0.17
N07	SI7	1.43	0.08	N19	SI19	0.12	0.17
N08	SI8	1.03	0.08	N20	SI20	0.83	0.19
N09	SI9	1.30	0.20	N21	SI21	4.89	0.12
N10	SI10	2.10	0.11	N22	SWR3	1.55	0.14
N11	SI11	3.06	0.17	N23	Galveston	1.23	0.29
N12	SI12	1.93	0.08	N24	Pure	0.19	0.21

5.3.14 Site P – Puerto Rico

For Site P, a total of 35 samples were collected from Puerto Rico. Samples were taken from Laguna Bouqueron National Wildlife Refuge (BWR), the Laguna Cartagena National Wildlife Refuge (CAR), the Cabo Rojo National Wildlife Refuge (CRR), and the Jabos Bay Research Reserve (JBR). As a comparison, both a Galveston inoculum sample and a pure culture of *C. thermocellum* were included. The top three performers, not including the Galveston sample, are P01, P03, and P06 with conversions of 0.28, 0.27, and 0.24 g VS digested/g VS fed (Table 5-15).

Table 5-15. Carboxylic acid and conversion results for Site P: Puerto Rico.

Sample ID	Sample location	Change in acid conc. (g/L)	Conversion (g VS digested/g VS fed)	Sample ID	Sample location	Change in acid conc. (g/L)	Conversion (g VS digested/g VS fed)
P01	BWR1	2.79	0.28	P20	CRR9	1.18	0.13
P02	BWR2	1.15	0.12	P21	CRR10	1.57	0.22
P03	BWR3	2.08	0.27	P22	JBR1	1.29	0.09
P04	BWR4	0.90	0.15	P23	JBR2	1.15	0.17
P05	BWR5	0.62	0.14	P24	JBR3	0.70	0.14
P06	BWR6	1.76	0.24	P25	JBR4	1.16	0.11
P07	BWR7	1.02	0.16	P26	JBR5	1.08	0.16
P08	CAR1	1.01	0.16	P27	JBR6	2.36	0.11
P09	CAR2	1.28	0.20	P28	JBR7	2.27	0.15
P10	CAR3	1.86	0.14	P29	JBR8	2.03	0.11
P11	CAR4	2.37	0.20	P30	JBR9	0.56	0.14
P12	CRR1	0.16	0.03	P31	JBR13	0.88	0.21
P13	CRR2	1.82	0.13	P32	JBR14	1.45	0.12
P14	CRR3	1.38	0.11	P33	JBR10	0.73	0.11
P15	CRR4	1.19	0.20	P34	JBR11	2.14	0.14
P16	CRR5	2.58	0.11	P35	JBR12	1.49	0.16
P17	CRR6	1.29	0.13	P36	Galveston	1.23	0.12
P18	CRR7	0.99	0.16	P37	Pure	0.27	0.19
P19	CRR8	0.71	0.11				

5.3.15 Site Q – Florida

For Site Q, a total of 28 samples were collected from several sites in Florida. Samples were taken from Caladesy Island SP (CIP), Honeymoon Island SP (HIP), Charlot Harbor SP (CHP), Rookery Bay Reserve (RBR), Collier-Seminole SP (CSP), and the Thousand Islands National Wildlife Reserce (TTI). As a comparison, both a Galveston inoculum sample and a pure culture of *C. thermocellum* were included. A blank fermentor with no inoculum was also run to determine how sterile the fermentation system was. The top three performers, not including the Galveston sample, are Q27, Q18, and Q26 with conversions of 0.18, 0.17, and 0.17 g VS digested/g VS fed (Table 5-16).

Table 5-16. Carboxylic acid and conversion results for Site Q: Florida.

Sample ID	Sample location	Change in acid conc. (g/L)	Conversion (g VS digested/g VS fed)	Sample ID	Sample location	Change in acid conc. (g/L)	Conversion (g VS digested/g VS fed)
Q01	CIP1	1.39	0.09	Q17	CHP6	0.41	0.15
Q02	CIP2	1.52	0.06	Q18	RBR1	1.53	0.17
Q03	CIP3	1.35	0.11	Q19	RBR2	1.48	0.11
Q04	CIP4	0.12	0.09	Q20	RBR3	2.20	0.09
Q05	CIP5	0.34	0.09	Q21	RBR4	1.57	0.05
Q06	CIP6	1.62	0.08	Q22	RBR5	1.02	0.13
Q07	CIP7	0.84	0.12	Q23	RBR6	0.46	0.15
Q08	HIP1	0.80	0.15	Q24	RBR7	1.03	0.12
Q09	HIP2	1.48	0.13	Q25	RBR8	1.96	0.13
Q10	HIP3	0.65	0.15	Q26	RBR9	1.47	0.17
Q11	HIP4	0.73	0.09	Q27	CSP1	0.64	0.18
Q12	CHP1	1.77	0.06	Q28	TTI1	0.69	0.09
Q13	CHP2	0.31	0.16	Q29	Galveston	1.19	0.13
Q14	CHP3	0.44	0.11	Q30	Pure	1.41	0.09
Q15	CHP4	1.44	0.16	Q31	Blank	0.24	0.08
Q16	CHP5	1.19	0.09				

5.3.16 Site R – Santa Fe, NM

For Site R, a total of 15 samples were collected from several sites in the Santa Fe National Park, NM. Samples were taken from the Jemez Spring Baths (JSB), the New Mexico Sulfur Springs (NSS), the Soda Lake Side (SLS), the San Antonio Cabin (SAC), and the Caribbean Lake Spring (CLS). Additionally, five stored soil samples were taken from three previous sites to determine if the storage method preserved the bacterial performance. As a comparison, both a Galveston inoculum sample, and a pure culture of *C. thermocellum* were included. A blank fermentor with no inoculum was also run to determine how sterile the fermentation system was. The top three performers are R01, R05, and R03 with conversions of 0.23, 0.20, and 0.14 g VS digested/g VS fed. Of the five stored samples, R17 and R18 performed similarly to the initial runs of L08 and Q08. But R16, R19 and R20 samples had lower conversions than the original runs. Results are shown in Table 5-17.

5.3.17 Site S – Yellowstone National Park

For Site S, a total of 48 samples were collected from several sites in the Yellowstone National Park, WY. Samples were taken from the Norris Gyser (NCYS), Sentinel Meadow (SMYS), Hydden Valley (HVYS), Wisky Flats (WFYS), Fireholl Drive (FDYS), and the Sulfatara Trail (STYS). As a comparison, both a Galveston inoculum sample, and a pure culture of *C. thermocellum* were included. A blank fermentor with no inoculum was also run to determine how sterile the fermentation system was. The top three performers are S48, S44, and S31 with conversions of 0.46, 0.41, and 0.16 g VS digested/g VS fed (Table 5-18).

Table 5-17. Carboxylic acid and conversion results for Site R: Santa Fe, NM.

Sample ID	Sample location	Change in acid conc. (g/L)	Conversion (g VS digested/g VS fed)	Sample ID	Sample location	Change in acid conc. (g/L)	Conversion (g VS digested/g VS fed)
R01	JSB1	1.83	0.23	R13	SLS1	0.08	0.15
R02	JSB2	0.46	0.12	R14	SAC1	0.05	0.17
R03	JSB3	0.32	0.14	R15	CLS1	0.07	0.11
R04	JSB4	2.08	0.14	R16	K51	0.12	0.09
R05	JSB5	0.12	0.20	R17	L08	0.12	0.05
R06	NSS1	1.03	0.07	R18	Q08	0.11	0.13
R07	NSS2	3.26	0.13	R19	K37	0.05	0.15
R08	NSS3	0.76	0.11	R20	K38	0.07	0.12
R09	NSS4	1.88	0.13	R21	Galveston	0.11	0.13
R10	NSS5	0.98	0.07	R22	Pure	0.07	0.17
R11	NSS6	2.37	0.07	R23	Blank	0.02	0.18
R12	NSS7	1.12	0.05				

Table 5-18. Carboxylic acid and conversion results for Site S: Yellowstone.

Sample ID	Sample location	Change in acid conc. (g/L)	Conversion (g VS digested/g VS fed)	Sample ID	Sample location	Change in acid conc. (g/L)	Conversion (g VS digested/g VS fed)
S01	NGYS1	0.92	0.03	S27	HVYS2	2.01	0.12
S02	NGYS2	1.07	0.03	S28	HVYS3	0.86	0.06
S03	NGYS3	2.10	0.16	S29	HVYS4	1.11	0.02
S04	NGYS4	1.20	0.05	S30	HVYS5	1.11	0.03
S05	NGYS5	0.82	0.10	S31	HVYS6	0.74	0.16
S06	NGYS6	0.28	0.11	S32	HVYS7	1.31	0.05
S07	NGYS7	1.02	0.14	S33	HVYS8	2.31	0.10
S08	NGYS8	0.53	0.11	S34	HVYS9	1.02	0.09
S09	NGYS9	0.86	0.07	S35	HVYS10	1.28	0.14
S10	NGYS10	1.08	0.08	S36	HVYS11	1.67	0.04
S11	NGYS11	1.95	0.05	S37	HVYS12	0.78	0.14
S12	NGYS12	0.74	0.05	S38	WFYS1	1.24	0.08
S13	NGYS13	0.05	0.04	S39	WFYS2	0.67	0.09
S14	NGYS14	2.69	0.10	S40	FDYS1	0.74	0.03
S15	NGYS15	1.49	0.04	S41	FHYS2	0.91	0.12
S16	NGYS16	1.25	0.04	S42	FHYS3	0.49	0.03
S17	NGYS17	1.74	0.11	S43	FHYS4	1.43	0.06
S18	NGYS18	1.42	0.05	S44	FHYS5	0.17	0.41
S19	NGYS19	0.52	0.04	S45	FHYS6	0.99	0.03
S20	SMYS1	1.80	0.14	S46	STYS1	1.27	0.07
S21	SMYS2	1.32	0.03	S47	STYS2	2.23	0.09
S22	SMYS3	0.70	0.08	S48	STYS3	1.61	0.46
S23	SMYS4	1.47	0.05	S49	Galveston	1.23	0.10
S24	SMYS5	0.65	0.06	S50	Pure	1.76	0.04
S25	SMYS6	0.57	0.07	S51	Blank	0.14	0.02
S26	HVYS1	1.03	0.07				

5.3.18 Site T – Nevada

For Site T, a total of 17 samples were collected from several sites in Nevada. Samples were taken from the Still Water Refuge (SWRN), the Great Boiling Spring (GBS), and Fly Ranch (FRN). As a comparison, both a Galveston inoculum sample, and a pure culture of *C. thermocellum* were included. A blank fermentor with no inoculum was also run to determine how sterile the fermentation system was. The top three performers are T02, T04, and T01 with conversions of 0.08, 0.07, and 0.07 g VS digested/g VS fed. Conversions were exceptionally low for this overall site when compared to the other sites. But because both controls (Galveston and pure culture) were also very low, these results are still representative of the site. Results are shown in Table 5-19.

Table 5-19. Carboxylic acid and conversion results for Site T: Nevada.

Sample ID	Sample location	Change in acid conc. (g/L)	Conversion (g VS digested/g VS fed)	Sample ID	Sample location	Change in acid conc. (g/L)	Conversion (g VS digested/g VS fed)
T01	SWRN1	0.75	0.07	T11	GBS8	0.07	0.03
T02	SWRN2	2.13	0.08	T12	GBS9	0.29	0.05
T03	SWRN3	1.34	0.02	T13	FRN1	1.34	0.06
T04	GBS1	1.80	0.07	T14	FRN2	1.16	0.06
T05	GBS2	1.37	0.05	T15	FRN3	1.18	0.03
T06	GBS3	1.43	0.05	T16	FRN4	1.19	0.06
T07	GBS4	0.85	0.05	T17	FRN5	1.61	0.05
T08	GBS5	0.32	0.04	T18	Galveston	1.36	0.04
T09	GBS6	1.29	0.06	T19	Pure	1.08	0.04
T10	GBS7	0.45	0.05	T20	Blank	1.19	0.04

5.3.19 Site U – Nevada-California.

For Site U, a total of 24 samples were collected from several sites in Nevada. Samples were taken from the California Buckeye Hot Spring (CBHS), the Mono Lake Navy Beach (MLNB), Mono Lake Island (MLIS), the Hot Creek at Mammoth (HCMA), and Owens Lake, California (OLCA). As a comparison, both a Galveston inoculum sample, and a pure culture of *C. thermocellum* were included. A blank fermentor with no inoculum was also run to determine how sterile the fermentation system was. The top three performers, not including the pure culture, are U22, U24, and U23 with conversions of 0.36, 0.31, and 0.25 g VS digested/g VS fed (Table 5-20).

Table 5-20. Carboxylic acid and conversion results for Site U: Nevada-California.

Sample ID	Sample location	Change in acid conc. (g/L)	Conversion (g VS digested/g VS fed)	Sample ID	Sample location	Change in acid conc. (g/L)	Conversion (g VS digested/g VS fed)
U01	CBHS1	0.03	0.12	U15	MLIS6	2.21	0.05
U02	CBHS2	0.80	0.10	U16	MLIS7	2.08	0.06
U03	CBHS3	2.40	0.11	U17	HCMA1	1.35	0.07
U04	CBHS4	1.18	0.06	U18	HCMA2	1.41	0.08
U05	MLNB1	1.15	0.08	U19	HCMA3	1.72	0.05
U06	MLNB2	1.27	0.10	U20	HCMA4	4.58	0.17
U07	MLNB3	1.26	0.16	U21	HCMA5	3.71	0.25
U08	MLNB4	0.36	0.10	U22	OLCA1	5.56	0.36
U09	MLNB5	0.29	0.06	U23	OLCA2	1.97	0.25
U10	MLIS1	0.93	0.13	U24	OLCA3	4.65	0.31
U11	MLIS2	1.55	0.14	U25	Galveston	2.37	0.18
U12	MLIS3	0.44	0.07	U26	Pure	2.21	0.31
U13	MLIS4	1.35	0.11	U27	Blank	3.69	0.18
U14	MLIS5	0.97	0.11				

5.4 Discussion

A total of 505 inoculum samples were analyzed in the initial screening step of the Bioscreening Project. From these, several samples will continue on into the next step (Chapter VI).

A wide range of conversions was observed across all the sites. Often, the changes in conversion matched changes in the local environment, i.e., moving from low salinity to high salinity, or moving from rich, moist earth to dry, crumbling sand. But, there were also several occasions where the conversion changed radically and suddenly. In Site G – Roswell/Carlsbad, NM, sample G45 had a low conversion of only 0.09 g VS digested/g VS fed whereas sample G46 had a conversion of 0.34 g VS digested/g VS fed. Both samples were taken only meters apart from Laguna Tonto. In Site K – Utah 1, sample K48 had a conversion of 0.04 g VS digested/g VS fed whereas sample K49 had a conversion of 0.33 g VS digested/g VS fed. In this case, both samples were taken only two meters apart along Baker Springs Rd with identical appearance in the surrounding soil.

Three sites, Site F – Brazoria, TX, Site G – Roswell/Carlsbad, NM, and Site J – Big Bend, TX had high conversions across the majority of the each site. The Department of Plant Pathology and Microbiology will examine the ecologies of these sites to determine why they have uniformly high conversions. Additionally, Site T – Nevada and Site Q – Florida had low conversions across the entire site. Site T had conversions below 0.09 g VS digested/g VS fed and all conversions at Site Q were below 0.19 g VS digested/g VS fed.

This illustrates the wide range of diversity in both bacterial density and identity found throughout the environment. These differences in conversions can be caused by changes in moisture content, temperature, and organic content. Additionally, not only can the pH of the local environment affect the bacterial community but also the specific types of salts and ions that are present. Additional research is being conducted on the soil composition of these sites by the Department of Soil and Crop Sciences to determine if there is a correlation between soil composition and microbial performance. Analysis of the ecology of Site A – La Sal del Rey, TX is available at Hollister et al. (2010).

5.5 Conclusions

The following conclusions can be made from this chapter:

1) A total of 505 inocula samples from 19 sites were screened during this step of the Bioscreening Project.
2) From each of their respective sites, A23, C01, D18, E08, F09, G23, H01, J11, K49, L10, M24, N09, P01, Q27, R01, S48, T02, and U22 had the best conversions from each of their respective sites. They show promise for the MixAlco™ process.
3) Additionally, F01, F02, F04, F05, F06, G07, G08, G13, G19, G21, G23, G24, G46, G47, H20, J04, J05, J18, J19, J20, J22, J23, and S44 also had high conversions above 0.32 g VS fed/g VS digested.
4) Several sites had both low and high performers. G45 had a conversion of 0.09 g VS fed/g VS digested and G46 had a conversion of 0.34 g VS fed/g VS digested. K48 had a conversion of 0.04 g VS fed/g VS digested whereas K49 was 0.33 g VS fed/g VS digested. S45 had a conversion of 0.03 g VS fed/g VS digested whereas S44 was 0.41 g VS fed/g VS digested. This is interesting because, in several cases, the high and low performers were collected only a meter or two from each other. This illustrates the wide range of diversity in both bacterial density and identity within a location can hold.
5) Of the sites across the United States that were screened, Site F – Brazoria, TX, Site G – Roswell/Carlsbad, NM, and Site J – Big Bend, TX had high conversions across the entire site. The Department of Plant Pathology and Microbiology under Dr. Heather Wilkinson will examine the ecologies of both sites to determine why they have uniformly high conversions.

CHAPTER VI
PRINCIPLES OF CPDM MODELING AND INOCULA SELECTION FOR BIOSCREENING

The objectives of this chapter follow:

a) Describe the Continuum Particle Distribution Model (CPDM).
b) Show the required batch experimental procedure used to obtain the model parameters for the CPDM prediction.
c) Describe the method used to predict the conversion and product concentration "map."
d) Determine the CPDM parameters for several inocula.
e) Predict the "better" inocula based on comparisons of the CPDM "maps."

6.1 Principles of CPDM methods

Countercurrent fermentations in the laboratory are time consuming. With the long residence times associated with these fermentation systems, it can take weeks, even months to reach steady state. The optimization of a single fermentation system could take years and would require thousands of man-hours. Each fermentation involves many complex reactions between the substrates, products, and the microorganisms. Traditional models of such systems are extremely difficult if not impossible. Continuum particle distribution modeling (CPDM) is an empirical approach that accurately models the complex reactions by generalizing the behavior of a specific reaction system (Loescher, 1996; Ross, 1998). The CPDM method has been used to successfully predict the product concentration and biomass conversion for several countercurrent fermentations (Agbogbo, 2005; Aiello-Mazzarri, 2002; Fu, 2007; Thanakoses, 2002).

The concept of a continuum particle (CP) is used in CPDM method to avoid the difficulties of tracking the varying geometry of individual discrete particles. A CP is defined as a collection of biomass particles that equal one gram volatile solids (VS) at time zero and is representative of the entire feedstock entering the fermentation (Ross, 1998). At time zero, all the CPs are the same. But, as the reactions occur, the conversion of each CP will not be identical. A distribution function is used to express the number of CPs in a given range of conversion shown in Equation 6-1.

$$S_0 = \int_0^1 \hat{n}\,(x)dx \tag{6-1}$$

S_0 = particle concentration (particles/L).

The total reaction rate (r) relates to the specific rate ($\hat{r}$) as a function of particle conversion and product concentration A (Eqn. 6-2). The specific rate $\hat{r}(x, A)$ contains information about the reacting system and the products and $\hat{n}(x)$ contains information about substrate concentrations and conversions.

$$r = \int_0^1 \hat{r}(x, A)\hat{n}(x)dx \tag{6-2}$$

For a batch reaction, all particles have the same conversion. Therefore, $\hat{n}(x) = 0$ everywhere except at x′.

$$n_0 = \int_0^1 \hat{n}(x)dx = \lim_{\varepsilon \to 0} \int_{x'-\varepsilon}^{x'+\varepsilon} \hat{n}(x)dx \tag{6-3}$$

The Dirac delta function can be used to represent the distribution function (Eqn. 6-4).

$$\hat{n}(x) = S_0\delta(x - x') \tag{6-4}$$

Substituting this into Equation 6-2 gives Equation 6-5.

$$r = \int_0^1 \hat{r}(x, A)\hat{n}(x)dx = \int_0^1 \hat{r}(x, A)S_0\delta(x - x')dx = \hat{r}(x', A)S_0 \tag{6-5}$$

The CPDM model relates the reaction rate with model parameters obtained from batch fermentations. The batch procedure is detailed in Section 6.3. With those model parameters, the CPDM method can determine optimal volatile solids loading rates (VSLR) and liquid residence times (LRT) rapidly (i.e., batch fermentation times of 28 days).

6.2 Batch experiments to obtain model parameters for CPDM method

To obtain CPDM parameters, the microorganisms are first adapted to the given system in the initial screen. The adapted microorganisms are then used to inoculate five batch fermentations containing different amounts of the initial substrate. The batch fermentation runs for 28 days to obtain the data needed for the modeling. The substrate concentrations used were 20, 40, 70, 100, and 100+ g substrate/L liquid. The 100 and 100+ fermentors had the same initial substrate concentration, but the 100+ fermentor contains medium with a mixture of carboxylate salts in a concentration of 20 g carboxylic acids/L liquid. Table 6-1 lists the components and distribution of the mixed carboxylic salts used in the 100+ batch fermentations.

Table 6-1. The carboxylate salts used in 100+ fermentations.

Formula	Weight ratio of acetate salts	Weight ratio of propionate salts	Weight ratio of butyrate salts
100+ g/L	80% Ca^{2+} salts	5% Ca^{2+} salts	15% Ca^{2+} salts

For the CPDM fermentations, the inoculum was taken from the residue from the initial screen, so that the microorganisms were already adapted to this type of substrate. Because of the small amount of material remaining at the end of the initial screen, the amount of inoculum was increased in an upculture batch fermentation containing the same substrate with the same 20 g carboxylic acid/L liquid as both the initial screen and the 100+ fermentors. The resulting broth from this upculture was used to inoculate the CPDM fermentors. The initial carboxylic acid concentration in the batch fermentors results from the acids contained in the inoculum. Calcium carbonate was used as the buffer in these fermentations. The pH, gas production, and gas composition were monitored during the fermentations. Iodoform (20 g/L ethanol soln) was added every other day to inhibit methane production. Liquid samples were taken from each fermentor and the amount of carboxylic acids was measured by gas chromatography (Chapter II).

Because a spectrum of acids are present, the concentration of each type of acid is converted into an acetic acid equivalent (Aeq). Aeq represents the amount of acetic acid that could have been produced in the fermentation if all the carboxylic acids produced were acetic

acid (Datta, 1981). The Aeq unit is based on the reducing power of the acids as presented in the following reducing-power-balanced disproportionate reactions (Loescher, 1996). Converting the acids into Aeq allows the CPDM modeling to account for them as one single parameter. Equations 6-6 through 6-10 are used to calculate the Aeq concentration.

Propionic acid:	7 HOAc	⟶	4 HOPr + 2 CO_2 + 2 H_2O	(6-6)
Butyric acid:	5 HOAc	⟶	2 HOBu + 2 CO_2 + 2 H_2O	(6-7)
Valeric acid:	13 HOAc	⟶	4 HOVa + 7 CO_2 + 6 H_2O	(6-8)
Caproic acid:	4 HOAc	⟶	HOCa + 2 CO_2 + 2 H_2O	(6-9)
Heptanoic acid:	19 HOAc	⟶	4 HOHe + 10 CO_2 + 10 H_2O	(6-10)

After the liquid samples were analyzed they were converted to Aeq by Equation 6-11.

Aeq = 60.05 (g/mol) × [acetic (mol/L) + 1.75 × propionic (mol/L) + 2.5 × butyric (mol/L) + 3.25 × valeric (mol/L) + 4.0 × caproic (mol/L) + 4.75 × heptanoic (mol/L)] (6-11)

For each batch fermentation, the Aeq and time data are fit to Equation 6-12 and *a*, *b* and *c* are determined by least squares regression, and *t* is the fermentation time in days.

$$\text{Aeq} = a + \frac{bt}{1 + ct} \tag{6-12}$$

Then the specific rate and conversion are determined by Equations 6-13 to 6-15.

$$\text{Rate} = \quad r = \frac{d(\text{Aeq})}{dt} = \frac{b}{(1 + ct)^2} \tag{6-13}$$

$$\text{Specific rate} = \quad \hat{r} = \frac{r}{So} \tag{6-14}$$

$$\text{Conversion} = \quad x(t) = \frac{\text{Aeq}(t) - \text{Aeq}(t = o)}{So \cdot \sigma} \tag{6-15}$$

So is the initial amount of substrate (g VS/L) and σ is the selectivity (g Aeq produced/g VS digested). Selectivity is assumed to be constant for the duration of the batch fermentations. Once Equations 6-13 to 6-15 have been determined, the data sets are fit to Equation 6-16 by nonlinear regression using computer software (Agbogbo, 2005; Aiello-Mazzarri, 2002).

$$r_{pred} = \frac{e(1-x)^f}{1+g(\phi \cdot \text{Aeq})^h} \tag{6-16}$$

where:

x = conversion of VS

e, f, g, and h = empirical constants

Φ = total grams acid/grams Aeq

Equation 6-16 is an empirical equation. South et al. (1995) described $(1-x)$ as the conversion penalty function. The term $(1-x)$ shows that, as the substrate is converted, the reaction rate decreases. The denominator term describes the inhibitory effect on the microorganisms by the product concentration, which decreases the reaction rate.

The values of Aeq, the specific reaction rate $\hat{r}$, and the conversion x are determined from the experimental data from the batch fermentations (Equations 6-11, 6-14, 6-15, respectively). In Equation 6-16, the parameter values of e, f, g, and h are fit by non-linear regression (*SYSSTAT SIGMAPLOT 12.0*).

Once the empirical constants (e, f, g and h) have been determined for a specific reaction system, Equation 6-16 may be used to model and optimize different reactor schemes that will use that system. The other required system parameters for CPDM method are selectivity, holdup (ratio of liquid to solid in wet solids), and moisture (ratio of liquid to solids in feed solids). Based on these parameters, the Matlab program for CPDM (Appendix J) can predict the Aeq concentration and conversion for countercurrent fermentations at various VSLRs and LRTs.

6.3 Conversion and product concentration "map"

The CPDM model can predict the final product concentration and substrate conversion based on a VSLR and LRT. With the results obtained for every computer run, a "map" can be drawn to show the dependence of the product concentration and substrate conversion on various VSLR and LRT. Also, the CPDM map can be used to compare the parameters of different microbial communities to use for a specific reaction scheme. The maps were obtained through a self-coded Matlab program (Appendices J and K).

6.4 Selection of bioscreening inocula for CPDM modeling

Although CPDM modeling is far less time-consuming then traditional laboratory-scale countercurrent fermentations, it is still time and labor intensive. With the sheer number of samples taken from numerous sites (509 in total), it would be impossible and undesirable to run CPDM modeling for every sample. To narrow the number of samples and select the best communities, a sample was chosen for CPDM modeling if it met one of the following two criteria: (1) obtained a conversion of 0.32 g VS digested/g VS fed or higher or (2) it was the best of the site. Table 6-2 shows the samples chosen for CPDM modeling in this chapter.

Table 6-2. Samples selected for CPDM modeling.

Site	Sample	Conversion >0.32	Best of Site	Site	Sample	Conversion >0.32	Best of Site
A	A23		√	H	H20	√	
B	B01	√	√	J	J04	√	
B	B02		√	J	J11	√	√
B	B03		√	J	J19	√	
B	B04	√	√	K	K49	√	√
C	C01	√	√	L	L10		√
D	D18	√	√	M	M24		√
E	E08		√	N	N09		√
F	F02	√		P	P01		√
F	F09	√	√	Q	Q10		√
G	G08	√		R	R08		√
G	G13	√		S	S44	√	
G	G23	√	√	S	S48	√	√
G	G46	√		T	T05		√
H	H01	√	√	U	U22		√

6.5 CPDM parameters and maps

6.5.1 Sample A23 from La Sal del Rey, TX (LSDR)

As mentioned in Section 6-3, batch experiments with 90 wt% paper /10 wt% yeast extract were performed to obtain model parameters for the CPDM method. The inocula for these fermentations were taken from the post reactor material of the initial screening then preserved in a 20% glycerol solution. Calcium carbonate was used to adjust the pH. Liquid samples from the fermentations were analyzed for carboxylic acids. Using Equation 6-11, the acids were converted to acetic acid equivalents (Aeq). The Aeq concentrations for the five A23 batch experiments are shown in Figure 6-1. The smooth lines are the predicted Aeq. Table 6-3 presents the fitted parameters *a*, *b*, and *c* for Equation 6-12.

Table 6-3. Values of the parameters *a*, *b*, and *c* fitted by least squares analysis for La Sal del Rey inocula A23.

Substrate Concentration (g/L)	*a* (g/L liquid)	*b* (g/(L liquid·d))	*c* (d^{-1})
20	1.91	1.50	0.150
40	1.91	1.30	0.120
70	1.97	2.00	0.110
100	2.08	1.80	0.100
100+	20.54	0.640	0.060

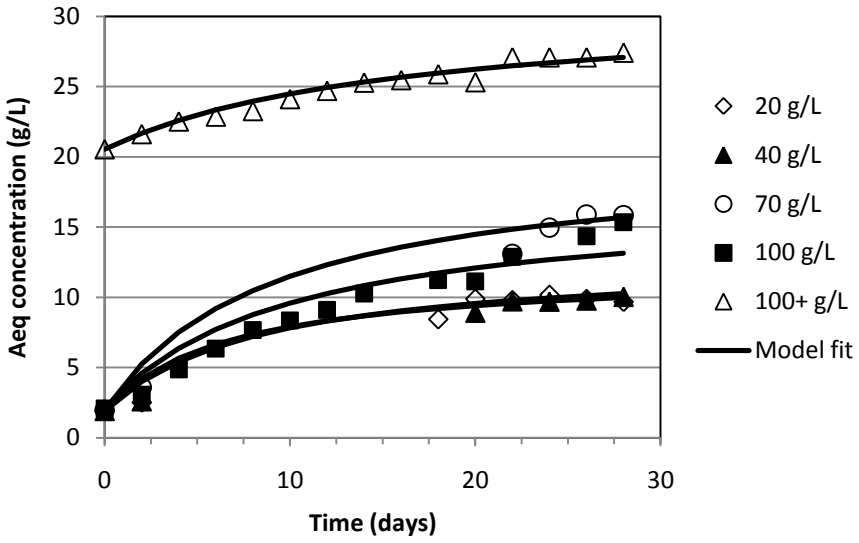

Figure 6-1. Aeq concentrations of A23 inoculated paper/yeast extract fermentation at 20, 40, 70, 100 and 100+ g substrate/L liquid with calcium carbonate.

The reaction rate and the specific reaction rate for the batch fermentations were calculated using Equations 6-13 and 6-14. Conversion was calculated with the experimental acetic acid equivalents using Equation 6-15. Parameters *e*, *f*, *g*, and *h* presented in the predicted rate equation (Equation 6-17) were calculated by nonlinear regression. Figure 6-2 compares the predicted specific rate with the experimental specific rate. The specific rate equation for La Sal del Rey inocula A23 follows:

$$\hat{r}_{pred} = \frac{0.044(1-x)^{1.00}}{1 + 0.033(\emptyset \cdot \text{Aeq})^{2.50}} \qquad (6\text{-}17)$$

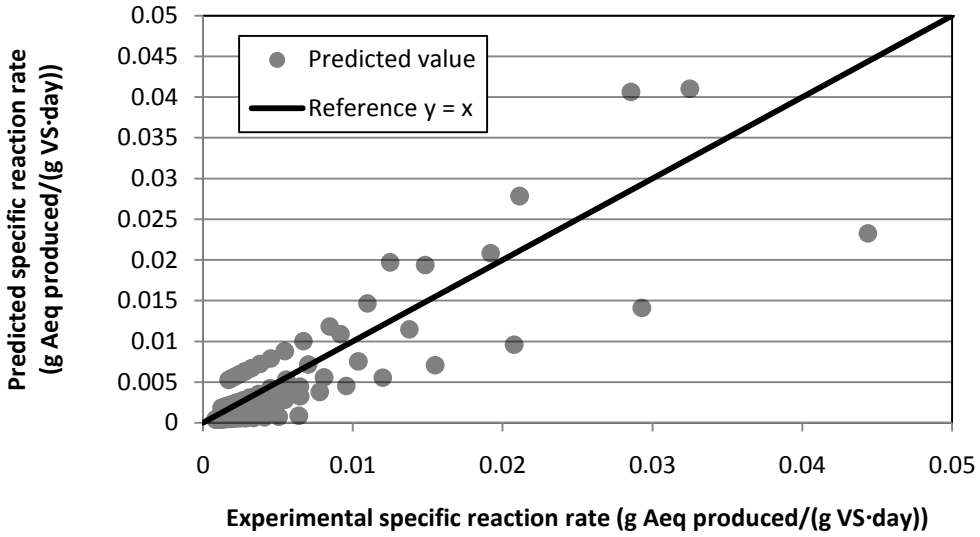

Figure 6-2. The experimental value and the CPDM prediction value for the specific reaction rate in five batch paper/yeast extract fermentation with A23 inocula.

Table 6-4. Parameter constant values in CPDM for La Sal del Rey inocula A23.

Parameter constant	Value
Holdup (g liquid/g VS cake)	2.0
Moisture (g liquid/ g solid feed)	0.06
Selectivity (g Aeq/g VS digested)	0.69
F1−F4 solid concentration (g VS/L)	169, 214, 214, 214
F1−F4 liquid volume (L)	0.48, 0.28, 0.28, 0.28
ϕ (g total acid/g Aeq)	0.77
e (g Aeq/(g VS·d))	0.044
f (dimensionless)	1.00
g (L/g total acid)$^{1/h}$	0.033
h (dimensionless)	2.50

Table 6-4 lists the system-specific variables required by the CPDM prediction. Figure 6-3 shows the CPDM "map" for La Sal del Rey inocula A23 in a 90 wt% paper/10 wt% yeast extract countercurrent fermentation with the single-centrifuge procedure at a fermentation solid concentration of 169 g VS/L liquid. The "map" predicts a total acid concentration of 14.09 g/L at LRT 30 day and VSLR of 12 g/(L·d), and a conversion of 0.15 g VS digested/g VS fed. At a VSLR of 4 g/(L·d) and LRT of 10 days, total acid concentration is 12.24 g/L and conversion is 0.56 g VS digested/g VS fed.

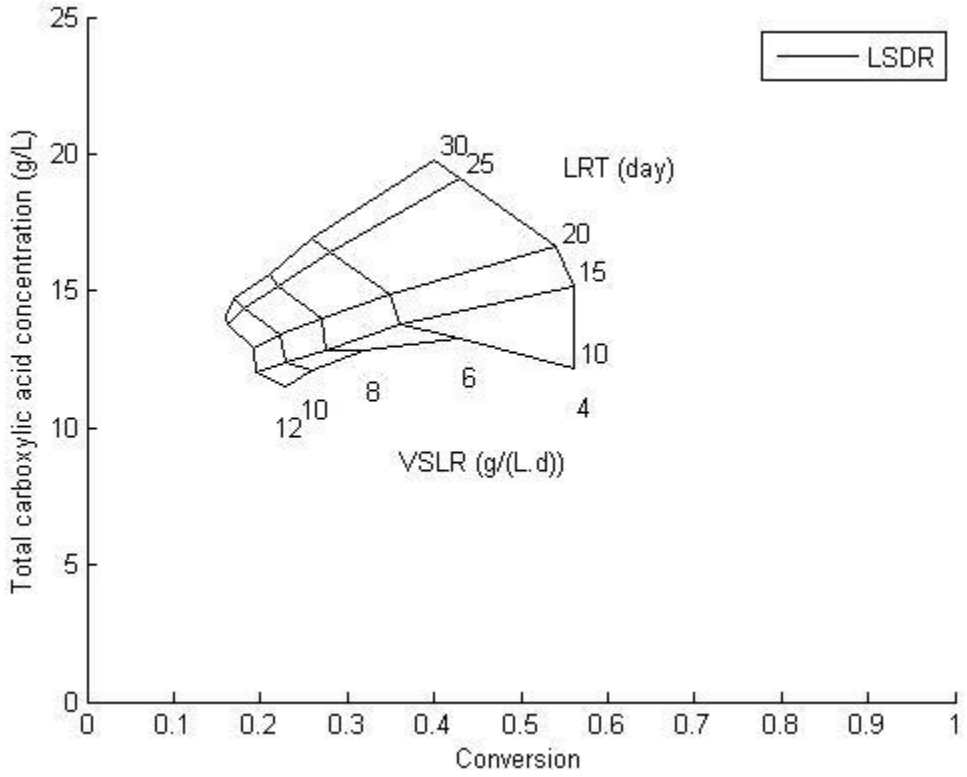

Figure 6-3. The CPDM "map" for 90 wt% paper/10 wt% yeast extract with A23 inocula.

6.5.2 Sample B01 from Galveston, TX

As mentioned in Section 6-3, batch experiments with 90 wt% paper /10 wt% yeast extract were performed to obtain model parameters for the CPDM method. The inocula for these fermentations were taken from the post reactor material of the initial screening then preserved in a 20% glycerol solution. Calcium carbonate was used to adjust the pH. Liquid samples from the fermentations were analyzed for carboxylic acids. Using Equation 6-11, the acids were converted to acetic acid equivalents (Aeq). Figure 6-4 shows the Aeq concentrations for the five B01 batch experiments. The smooth lines are the predicted Aeq. Table 6-5 presents the fitted parameters *a*, *b*, and *c* for Equation 6-12.

Table 6-5. Values of the parameters *a*, *b*, and *c* fitted by least squares analysis for Galveston inocula B01.

Substrate Concentration (g/L)	*a* (g/L liquid)	*b* (g/(L liquid·d))	*c* (d^{-1})
20	1.86	0.400	0.100
40	1.68	1.10	0.100
70	1.70	2.50	0.350
100	1.88	2.40	0.210
100+	21.48	2.70	0.500

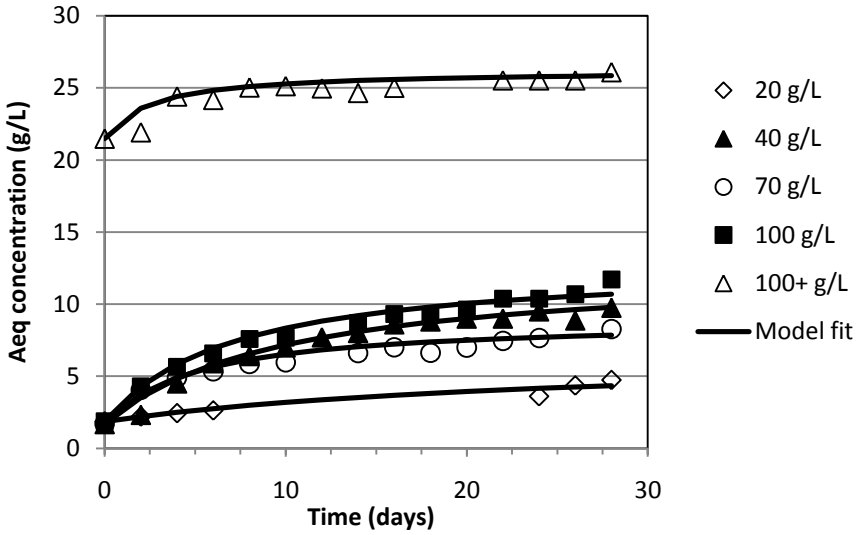

Figure 6-4. Aeq concentration for B01 inoculated paper/yeast extract fermentation at 20, 40, 70, 100, and 100+ g substrate/L liquid with calcium carbonate.

The reaction rate and the specific reaction rate for the batch fermentations were calculated using Equations 6-13 and 6-14. Conversion was calculated with the experimental acetic acid equivalents using Equation 6-15. Parameters *e*, *f*, *g*, and *h* presented in the predicted rate equation (Equation 6-18) were calculated by nonlinear regression. Figure 6-5 compares the predicted specific rate with the experimental specific rate. The specific rate equation for Galveston inocula B01 follows:

$$\hat{r}_{pred} = \frac{0.028(1-x)^{13.3}}{1 + 0.00200(\emptyset \cdot \text{Aeq})^{2.30}} \tag{6-18}$$

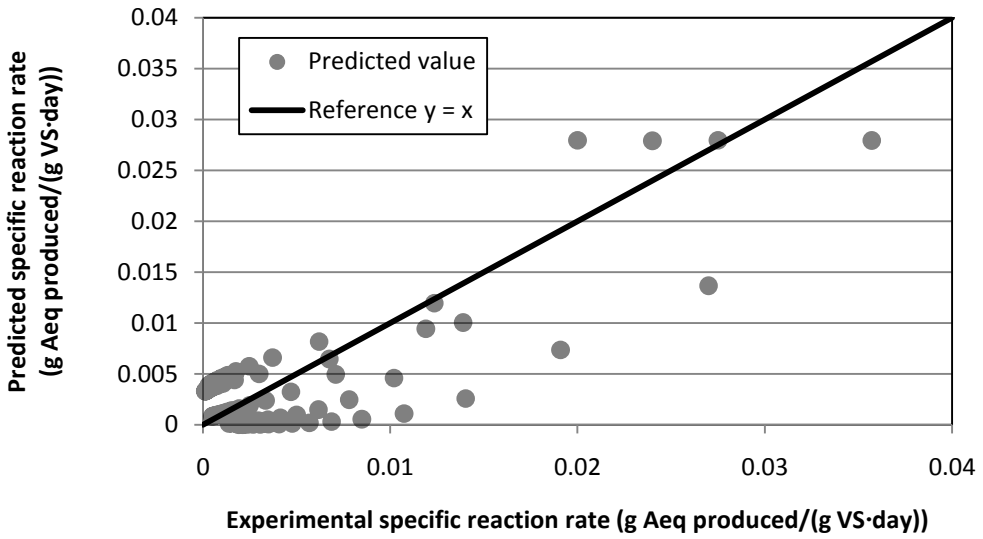

Figure 6-5. The experimental value and the CPDM prediction value for the specific reaction rate in five batch paper/yeast extract fermentation with B01 inocula.

Table 6-6. Parameter constant values in CPDM for Galveston inocula B01.

Parameter constant	Value
Holdup (g liquid/g VS cake)	2.0
Moisture (g liquid/ g solid feed)	0.06
Selectivity (g Aeq/g VS digested)	0.54
F1−F4 solid concentration (g VS/L)	169, 214, 214, 214
F1−F4 liquid volume (L)	0.48, 0.28, 0.28, 0.28
ϕ (g total acid/g Aeq)	0.63
e (g Aeq/(g VS·d))	0.028
f (dimensionless)	13.3
g (L/g total acid)$^{1/h}$	0.00200
h (dimensionless)	2.30

Table 6-6 lists the system-specific variables required by the CPDM prediction. Figure 6-6 shows the CPDM "map" for Galveston inocula B01 in a 90 wt% paper/10 wt% yeast extract countercurrent fermentation with the single-centrifuge procedure at a fermentation solid concentration of 169 g VS/L liquid. The "map" predicts a total acid concentration of 16.50 g/L at LRT 30 day and VSLR of 12 g/(L·d), and a conversion of 0.12 g VS digested/g VS fed. At a VSLR of 4 g/(L·d) and LRT of 10 days, total acid concentration is 10.94 g/L and conversion is 0.47 g VS digested/g VS fed.

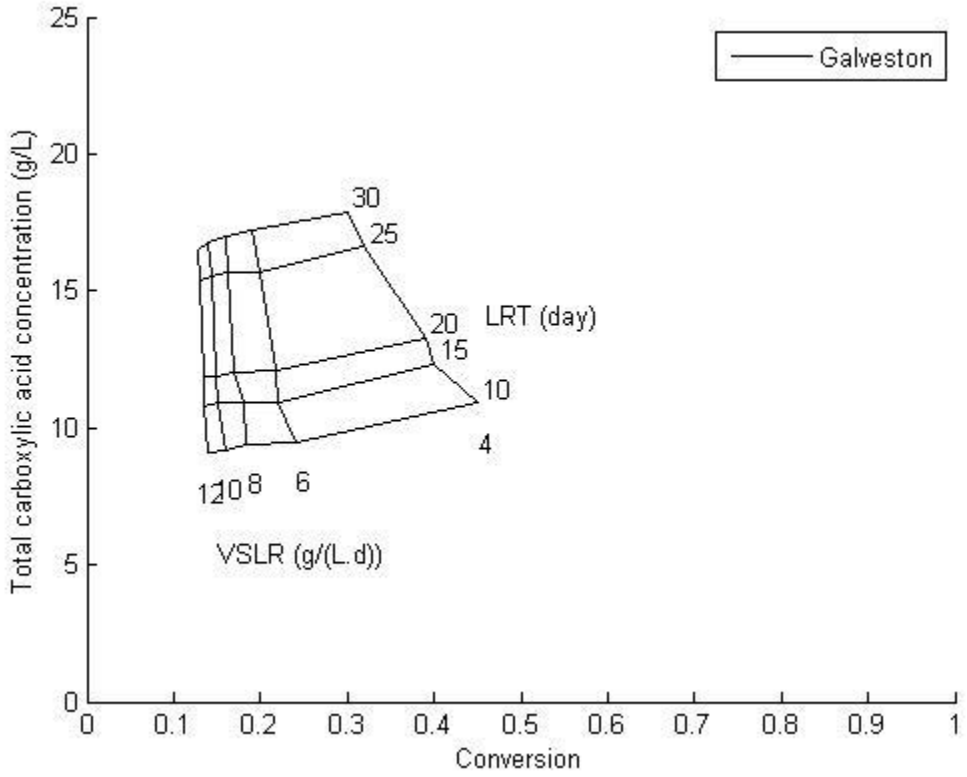

Figure 6-6. The CPDM "map" for 90 wt% paper/10 wt% yeast extract with B01 inocula.

6.5.3 Sample B02 from Bryan, TX (Terrestrial)

As mentioned in Section 6-3, batch experiments with 90 wt% paper /10 wt% yeast extract were done to obtain model parameters for the CPDM method. The inocula for these fermentations were taken from the post reactor material of the initial screening then preserved in a 20% glycerol solution. Calcium carbonate was used to adjust the pH. Liquid samples from the fermentations were analyzed for carboxylic acids. Using Equation 6-11, the acids were converted to acetic acid equivalents (Aeq). Figure 6-7 shows the Aeq concentrations for the five B02 batch experiments. The smooth lines are the predicted Aeq. Table 6-7 presents the fitted parameters *a*, *b*, and *c* for Equation 6-12.

Table 6-7. Values of the parameters *a*, *b*, and *c* fitted by least squares analysis for Terrestrial inocula B02.

Substrate Concentration (g/L)	*a* (g/L liquid)	*b* (g/(L liquid·d))	*c* (d^{-1})
20	1.64	0.600	0.300
40	1.29	0.900	0.070
70	1.32	1.80	0.100
100	1.60	1.90	0.170
100+	19.99	1.30	0.200

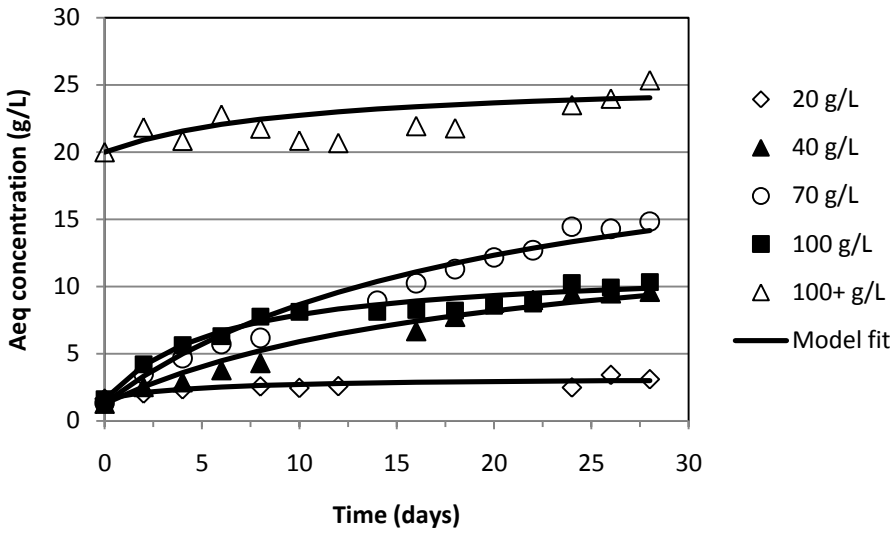

Figure 6-7. Aeq concentration for B02 inoculated paper/yeast extract fermentation at 20, 40, 70, 100 and 100+ g substrate/L liquid with calcium carbonate.

The reaction rate and the specific reaction rate for the batch fermentations were calculated using Equations 6-13 and 6-14. Conversion was calculated with the experimental acetic acid equivalents using Equation 6-15. Parameters *e*, *f*, *g*, and *h* presented in the predicted rate equation (Equation 6-19) were calculated by nonlinear regression. Figure 6-8 compares the predicted specific rate with the experimental specific rate. The specific rate equation for Terrestrial inocula B02 follows:

$$\hat{r}_{pred} = \frac{0.071(1-x)^{10.8}}{1 + 2.00(\emptyset \cdot \mathrm{Aeq})^{0.260}} \tag{6-19}$$

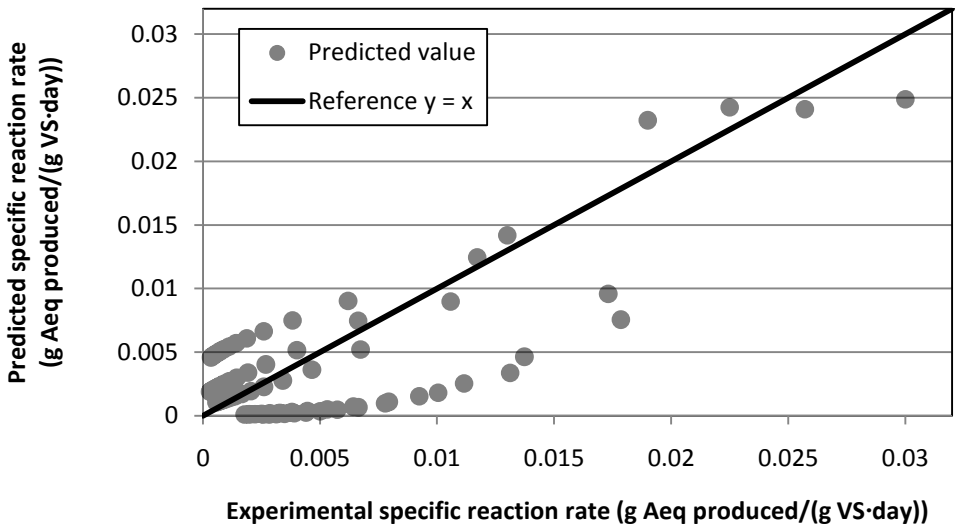

Figure 6-8. The experimental value and the CPDM prediction value for the specific reaction rate in five batch paper/yeast extract fermentation with B02 inocula.

Table 6-8. Parameter constant values in CPDM for Terrestrial inocula B02.

Parameter constant	Value
Holdup (g liquid/g VS cake)	2.0
Moisture (g liquid/ g solid feed)	0.06
Selectivity (g Aeq/g VS digested)	0.50
F1−F4 solid concentration (g VS/L)	169, 214, 214, 214
F1−F4 liquid volume (L)	0.48, 0.28, 0.28, 0.28
ϕ (g total acid/g Aeq)	0.65
e (g Aeq/(g VS·d))	0.071
f (dimensionless)	10.8
g (L/g total acid)$^{1/h}$	2.00
h (dimensionless)	0.260

Table 6-8 lists the system-specific variables required by the CPDM prediction. Figure 6-9 shows the CPDM "map" for Terrestrial inocula B02 in a 90 wt% paper/10 wt% yeast extract countercurrent fermentation with the single-centrifuge procedure at a fermentation solid concentration of 169 g VS/L liquid. The "map" predicts a total acid concentration of 15.13 g/L at LRT 30 day and VSLR of 12 g/(L·d), and a conversion of 0.14 g VS digested/g VS fed. At a VSLR of 4 g/(L·d) and LRT of 10 days, total acid concentration is 12.75 g/L and conversion is 0.46 g VS digested/g VS fed.

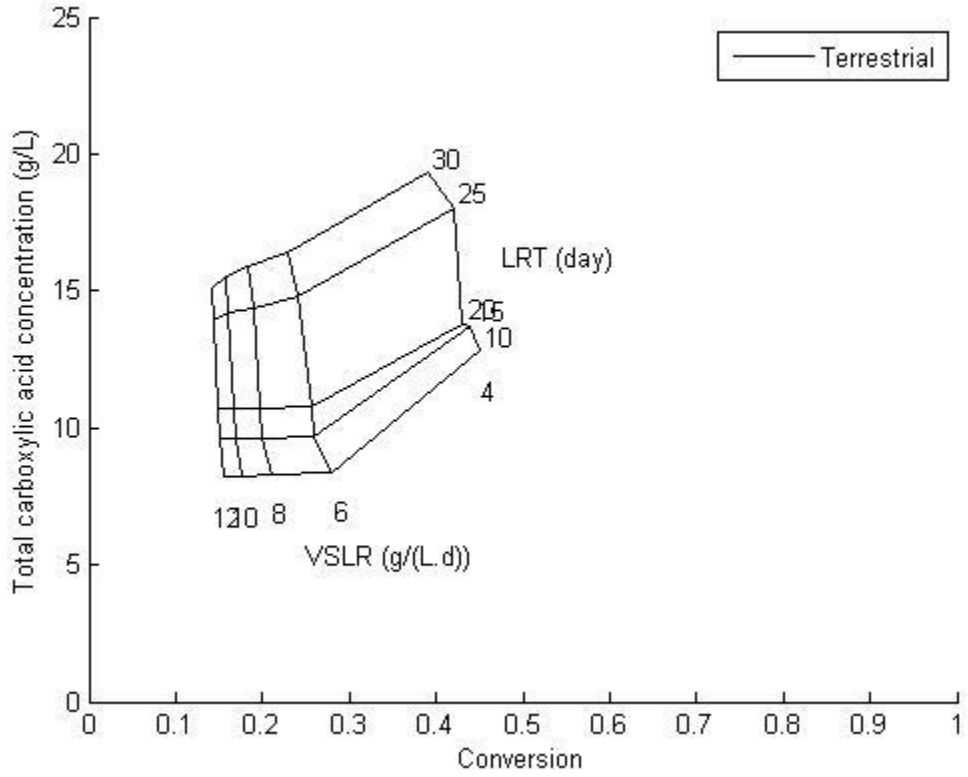

Figure 6-9. The CPDM "map" for 90 wt% paper/10 wt% yeast extract with B02 inocula.

6.5.4 Sample B03 from San Salvador Island of the Bahamas

As mentioned in Section 6-3, batch experiments with 90 wt% paper /10 wt% yeast extract were done to obtain model parameters for the CPDM method. The inocula for these fermentations were taken from the post reactor material of the initial screening then preserved in a 20% glycerol solution. Calcium carbonate was used to adjust the pH. Liquid samples from the fermentations were analyzed for carboxylic acids. Using Equation 6-11, the acids were converted to acetic acid equivalents (Aeq). Figure 6-10 shows the Aeq concentrations for the five B03 batch experiments. The smooth lines are the predicted Aeq. Table 6-9 presents the fitted parameters *a*, *b*, and *c* for Equation 6-12.

Table 6-9. Values of the parameters *a*, *b*, and *c* fitted by least squares analysis for Bahamas inocula B03.

Substrate Concentration (g/L)	*a* (g/L liquid)	*b* (g/(L liquid·d))	*c* (d^{-1})
20	1.75	2.00	0.600
40	1.50	0.720	0.120
70	1.24	1.34	0.130
100	2.03	0.660	0.0044
100+	18.59	0.313	0.014

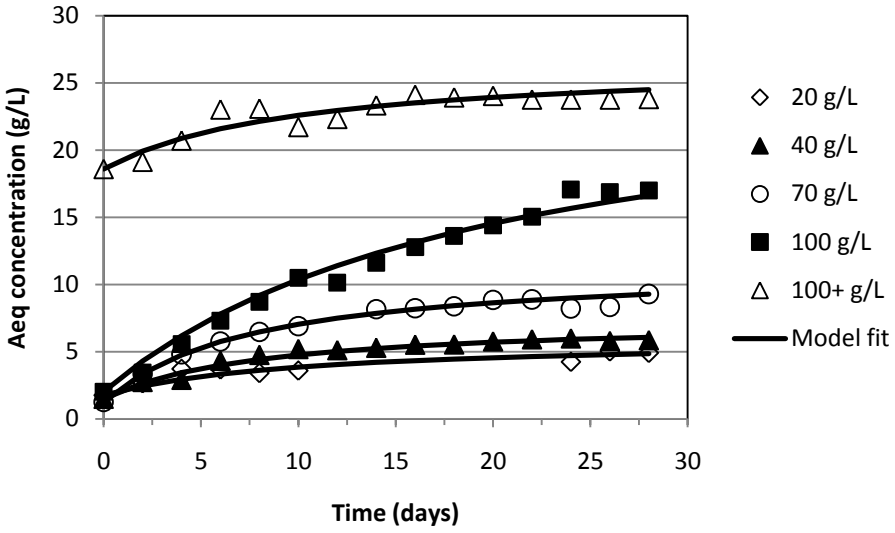

Figure 6-10. Aeq concentration for B03 inoculated paper/yeast extract fermentation at 20, 40, 70, 100, and 100+ g substrate/L liquid with calcium carbonate.

The reaction rate and the specific reaction rate for the batch fermentations were calculated using Equations 6-13 and 6-14. Conversion was calculated with the experimental acetic acid equivalents using Equation 6-15. Parameters *e*, *f*, *g*, and *h* presented in the predicted rate equation (Equation 6-20) were calculated by nonlinear regression. Figure 6-11 compares the predicted specific rate with the experimental specific rate. The specific rate equation for Bahamas inocula B03 follows:

$$\hat{r}_{pred} = \frac{0.046(1-x)^{6.80}}{1 + 0.250(\emptyset \cdot \mathrm{Aeq})^{1.40}} \tag{6-20}$$

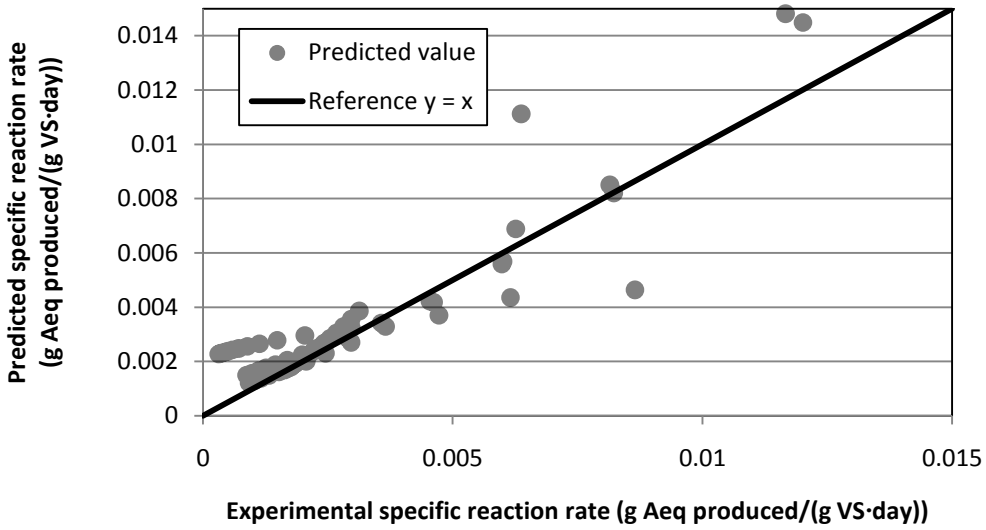

Figure 6-11. The experimental value and the CPDM prediction value for the specific reaction rate in five batch paper/yeast extract fermentation with B03 inocula.

Table 6-10. Parameter constant values in CPDM for Bahamas inocula B03.

Parameter constant	Value
Holdup (g liquid/g VS cake)	2.0
Moisture (g liquid/ g solid feed)	0.06
Selectivity (g Aeq/g VS digested)	0.58
F1−F4 solid concentration (g VS/L)	169, 214, 214, 214
F1−F4 liquid volume (L)	0.48, 0.28, 0.28, 0.28
ϕ (g total acid/g Aeq)	0.83
e (g Aeq/(g VS·d))	0.046
f (dimensionless)	6.80
g (L/g total acid)$^{1/h}$	0.250
h (dimensionless)	1.400

Table 6-10 lists the system-specific variables required by the CPDM prediction. Figure 6-12 shows the CPDM "map" for Bahamas inocula B03 in a 90 wt% paper/10 wt% yeast extract countercurrent fermentation with the single-centrifuge procedure at a fermentation solid concentration of 169 g VS/L liquid. The "map" predicts a total acid concentration of 12.47 g/L at LRT 30 day and VSLR of 12 g/(L·d), and a conversion of 0.14 g VS digested/g VS fed. At a VSLR of 4 g/(L·d) and LRT of 10 days, total acid concentration is 9.16 g/L and conversion is 0.47 g VS digested/g VS fed.

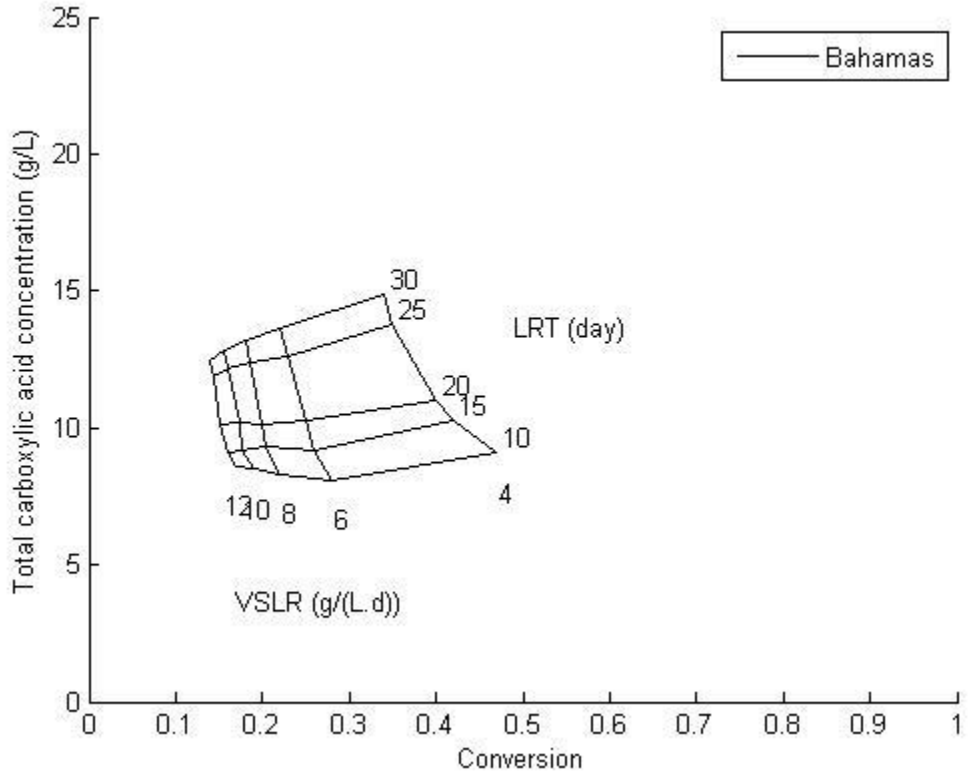

Figure 6-12. The CPDM "map" for 90 wt% paper/10 wt% yeast extract with B03 inocula.

6.5.5 Sample B04 of a pure culture of *Clostridium thermocellum*

As mentioned in Section 6-3, batch experiments with 90 wt% paper /10 wt% yeast extract were done to obtain model parameters for the CPDM method. The inocula for these fermentations were taken from the post reactor material of the initial screening then preserved in a 20% glycerol solution. Calcium carbonate was used to adjust the pH. Liquid samples from the fermentations were analyzed for carboxylic acids. Using Equation 6-11, the acids were converted to acetic acid equivalents (Aeq). Figure 6-13 shows the Aeq concentrations for the five B04 batch experiments. The smooth lines are the predicted Aeq. Table 6-11 presents the fitted parameters *a*, *b*, and *c* for Equation 6-12.

Table 6-11. Values of the parameters *a*, *b*, and *c* fitted by least squares analysis for Pure inocula B04.

Substrate Concentration (g/L)	*a* (g/L liquid)	*b* (g/(L liquid·d))	*c* (d^{-1})
20	0.120	0.140	0.080
40	0.120	0.630	0.150
70	0.140	0.740	0.066
100	0.190	1.90	0.070
100+	19.63	1.30	0.130

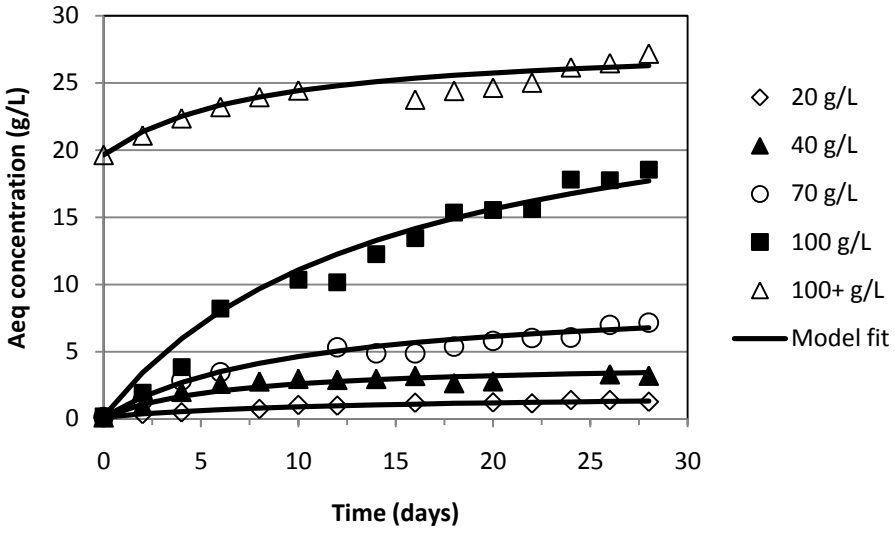

Figure 6-13. Aeq concentration for B04 inoculated paper/yeast extract fermentation at 20, 40, 70, 100, and 100+ g substrate/L liquid with calcium carbonate.

The reaction rate and the specific reaction rate for the batch fermentations were calculated using Equations 6-13 and 6-14. Conversion was calculated with the experimental acetic acid equivalents using Equation 6-15. Parameters *e*, *f*, *g*, and *h* presented in the predicted rate equation (Equation 6-21) were calculated by nonlinear regression. Figure 6-14 compares the predicted specific rate with the experimental specific rate. The specific rate equation for pure inocula B04 follows:

$$\hat{r}_{pred} = \frac{0.013(1-x)^{13.0}}{1 + 0.00400(\emptyset \cdot \text{Aeq})^{1.50}} \tag{6-21}$$

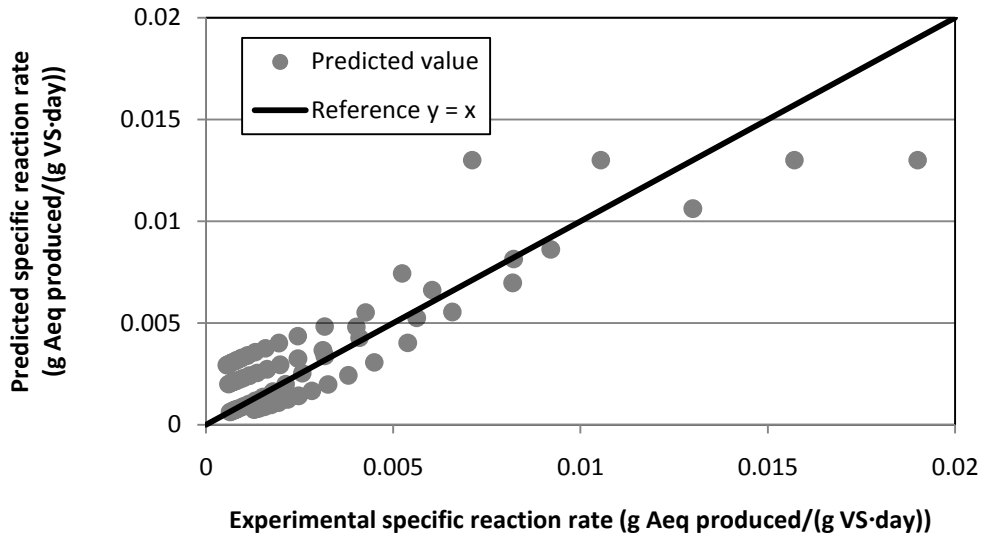

Figure 6-14. The experimental value and the CPDM prediction value for the specific reaction rate in five batch paper/yeast extract fermentation with B04 inocula.

Table 6-12. Parameter constant values in CPDM for pure *C. thermocellum* B04.

Parameter constant	Value
Holdup (g liquid/g VS cake)	2.0
Moisture (g liquid/ g solid feed)	0.06
Selectivity (g Aeq/g VS digested)	0.54
F1−F4 solid concentration (g VS/L)	169, 214, 214, 214
F1−F4 liquid volume (L)	0.48, 0.28, 0.28, 0.28
ϕ (g total acid/g Aeq)	0.80
e (g Aeq/(g VS·d))	0.013
f (dimensionless)	13.0
g (L/g total acid)$^{1/h}$	0.00400
h (dimensionless)	1.50

Table 6-12 lists the system-specific variables required by the CPDM prediction. Figure 6-15 shows the CPDM "map" for pure inocula B04 in a 90 wt% paper/10 wt% yeast extract countercurrent fermentation with the single-centrifuge procedure at a fermentation solid concentration of 169 g VS/L liquid. The "map" predicts a total acid concentration of 12.06 g/L at LRT 30 day and VSLR of 12 g/(L·d), and a conversion of 0.11 g VS digested/g VS fed. At a VSLR of 4 g/(L·d) and LRT of 10 days, total acid concentration is 9.84 g/L and conversion is 0.51 g VS digested/g VS fed.

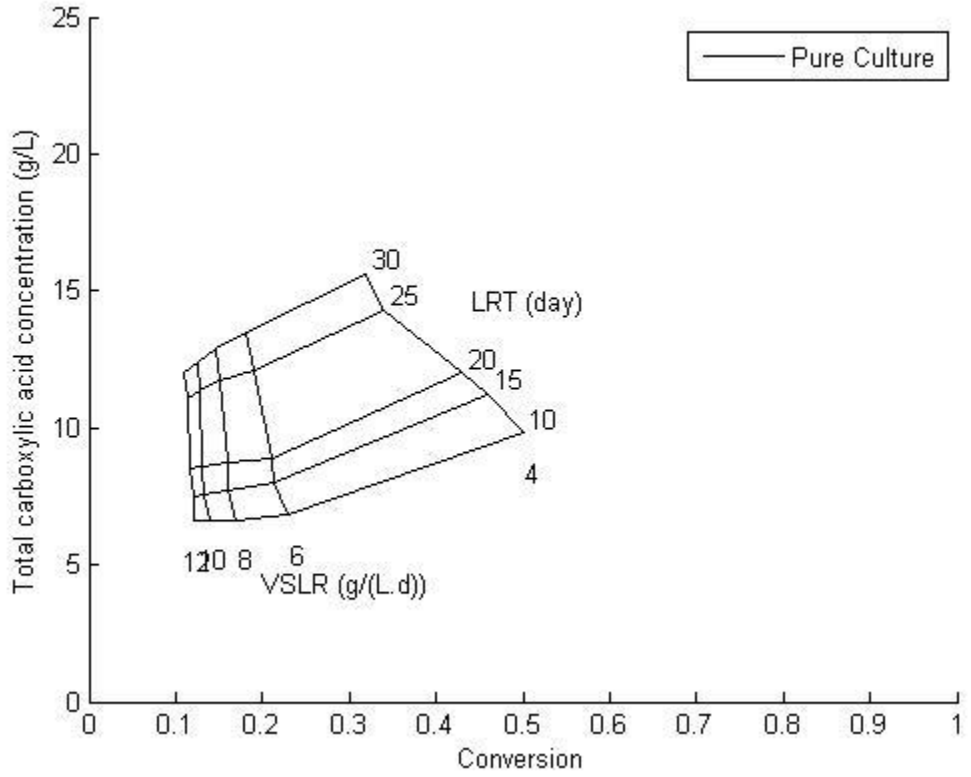

Figure 6-15. The CPDM "map" for 90 wt% paper/10 wt% yeast extract with B04 inocula.

6.5.6 Sample C01 from Taiwan

As mentioned in Section 6-3, batch experiments with 90 wt% paper /10 wt% yeast extract were done to obtain model parameters for the CPDM method. The inocula for these fermentations were taken from the post reactor material of the initial screening then preserved in a 20% glycerol solution. Calcium carbonate was used to adjust the pH. Liquid samples from the fermentations were analyzed for carboxylic acids. Using Equation 6-11, the acids were converted to acetic acid equivalents (Aeq). Figure 6-16 shows the Aeq concentrations for the five C01 batch experiments. The smooth lines are the predicted Aeq. Table 6-13 presents the fitted parameters *a*, *b*, and *c* for Equation 6-12.

Table 6-13. Values of the parameters *a*, *b*, and *c* fitted by least squares analysis for Taiwan inocula C01.

Substrate Concentration (g/L)	*a* (g/L liquid)	*b* (g/(L liquid·d))	*c* (d^{-1})
20	2.15	1.40	0.300
40	1.95	0.800	0.100
70	1.59	1.20	0.130
100	2.35	1.50	0.120
100+	21.19	1.40	0.150

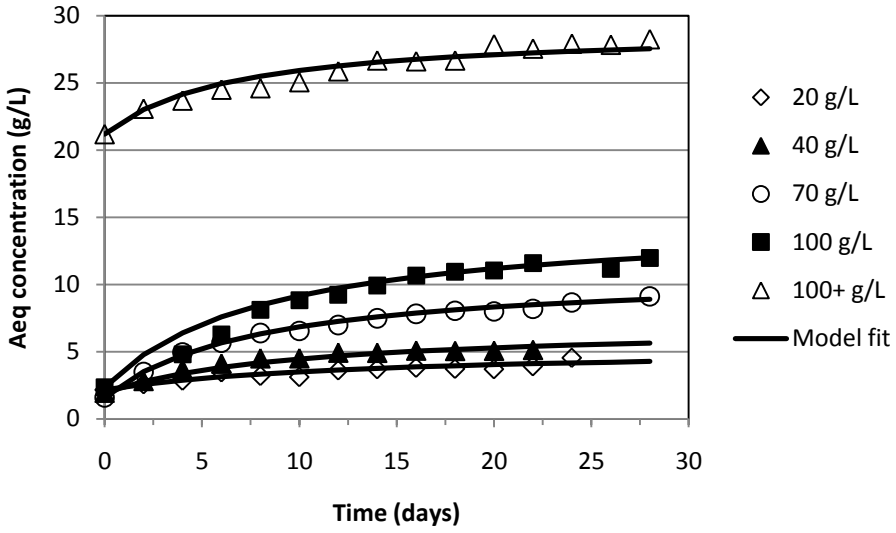

Figure 6-16. Aeq concentration for C01 inoculated paper/yeast extract fermentation at 20, 40, 70, 100, and 100+ g substrate/L liquid with calcium carbonate.

The reaction rate and the specific reaction rate for the batch fermentations were calculated using Equations 6-13 and 6-14. Conversion was calculated with the experimental acetic acid equivalents using Equation 6-15. Parameters *e*, *f*, *g*, and *h* presented in the predicted rate equation (Equation 6-22) were calculated by nonlinear regression. Figure 6-17 compares the predicted specific rate with the experimental specific rate. The specific rate equation for Taiwan inocula C01 follows:

$$\hat{r}_{pred} = \frac{0.032(1-x)^{8.10}}{1 + 0.0200(\emptyset \cdot \text{Aeq})^{1.50}} \tag{6-22}$$

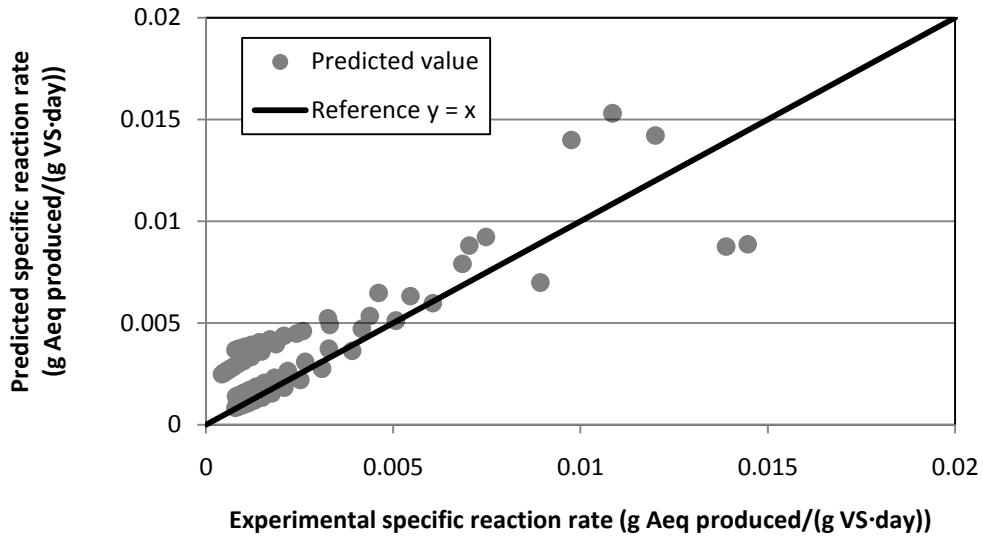

Figure 6-17. The experimental value and the CPDM prediction value for the specific reaction rate in five batch paper/yeast extract fermentation with C01 inocula.

Table 6-14. Parameter constant values in CPDM for Taiwan inocula C01.

Parameter constant	Value
Holdup (g liquid/g VS cake)	2.0
Moisture (g liquid/ g solid feed)	0.06
Selectivity (g Aeq/g VS digested)	0.45
F1−F4 solid concentration (g VS/L)	169, 214, 214, 214
F1−F4 liquid volume (L)	0.48, 0.28, 0.28, 0.28
ϕ (g total acid/g Aeq)	0.83
e (g Aeq/(g VS·d))	0.032
f (dimensionless)	8.10
g (L/g total acid)$^{1/h}$	0.0200
h (dimensionless)	1.50

Table 6-14 lists the system-specific variables required by the CPDM prediction. Figure 6-18 shows the CPDM "map" for Taiwan inocula C01 in a 90 wt% paper/10 wt% yeast extract countercurrent fermentation with the single-centrifuge procedure at a fermentation solid concentration of 169 g VS/L liquid. The "map" predicts a total acid concentration of 17.09 g/L at LRT 30 day and VSLR of 12 g/(L·d), and a conversion of 0.19 g VS digested/g VS fed. At a VSLR of 4 g/(L·d) and LRT of 10 days, total acid concentration is 10.33 g/L and conversion is 0.51 g VS digested/g VS fed.

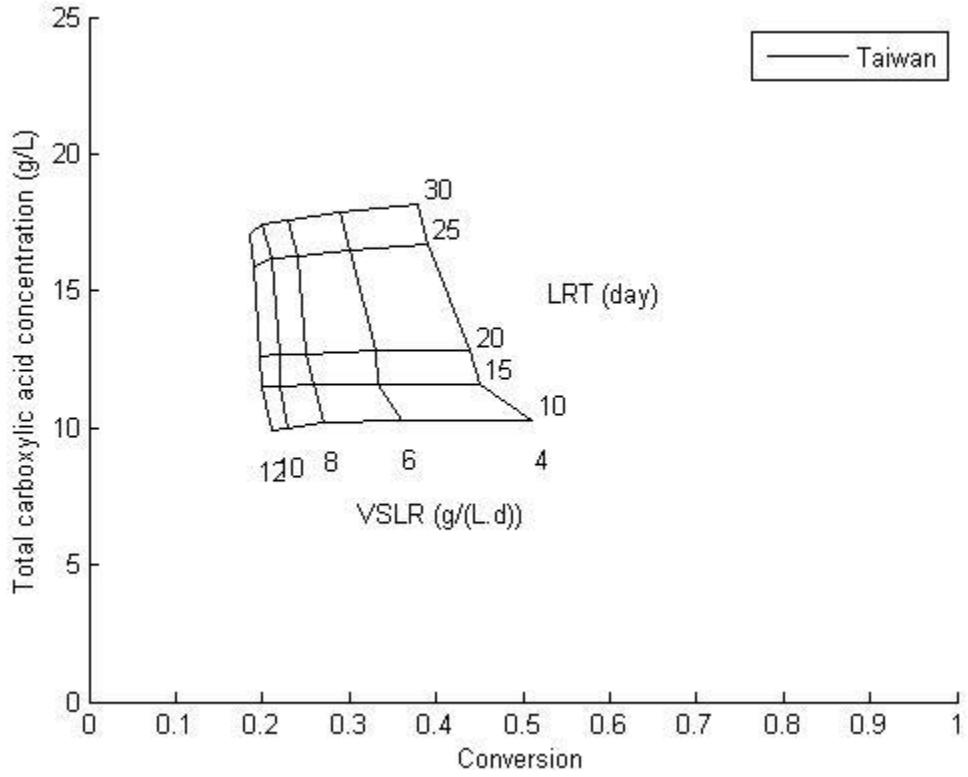

Figure 6-18. The CPDM "map" for 90 wt% paper/10 wt% yeast extract with C01 inocula.

6.5.7 Sample D18 from Site D – Gruella, NM and Muleshoe, TX

As mentioned in Section 6-3, batch experiments with 90 wt% paper /10 wt% yeast extract were done to obtain model parameters for the CPDM method. The inocula for these fermentations were taken from the post reactor material of the initial screening then preserved in a 20% glycerol solution. Calcium carbonate was used to adjust the pH. Liquid samples from the fermentations were analyzed for carboxylic acids. Using Equation 6-11, the acids were converted to acetic acid equivalents (Aeq). Figure 6-19 shows the Aeq concentrations for the five D18 batch experiments. The smooth lines are the predicted Aeq. Table 6-15 presents the fitted parameters *a*, *b*, and *c* for Equation 6-12.

Table 6-15. Values of the parameters *a*, *b*, and *c* fitted by least squares analysis for Site D inocula D18.

Substrate Concentration (g/L)	*a* (g/L liquid)	*b* (g/(L liquid·d))	*c* (d^{-1})
20	1.80	0.080	0.010
40	1.86	1.80	0.210
70	1.79	0.080	0.030
100	2.03	1.27	0.066
100+	20.64	0.580	0.150

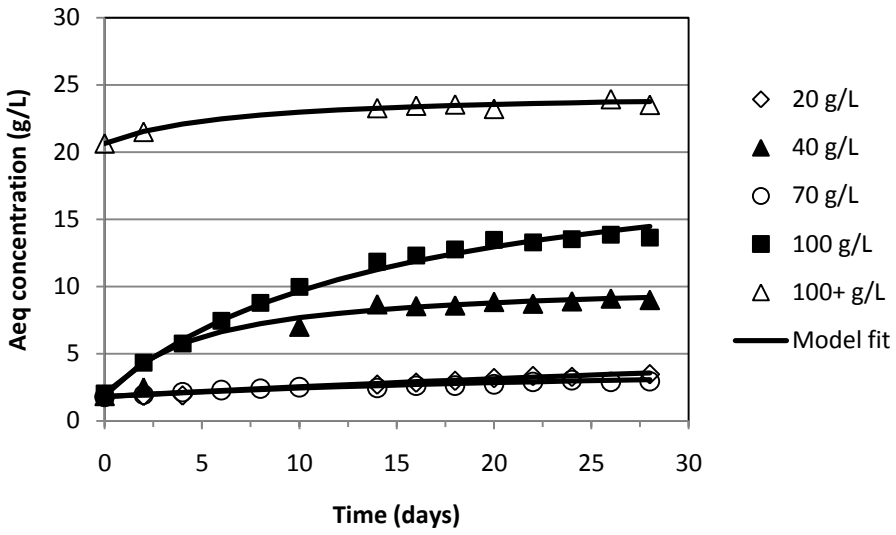

Figure 6-19. Aeq concentration for D18 inoculated paper/yeast extract fermentation at 20, 40, 70, 100, and 100+ g substrate/L liquid with calcium carbonate.

The reaction rate and the specific reaction rate for the batch fermentations were calculated using Equations 6-13 and 6-14. Conversion was calculated with the experimental acetic acid equivalents using Equation 6-15. Parameters *e*, *f*, *g*, and *h* presented in the predicted rate equation (Equation 6-23) were calculated by nonlinear regression. Figure 6-20 compares the predicted specific rate with the experimental specific rate. The specific rate equation for Site D inocula D18 follows:

$$\hat{r}_{pred} = \frac{0.055(1-x)^{1.03}}{1 + 1.89(\emptyset \cdot \text{Aeq})^{1.81}} \tag{6-23}$$

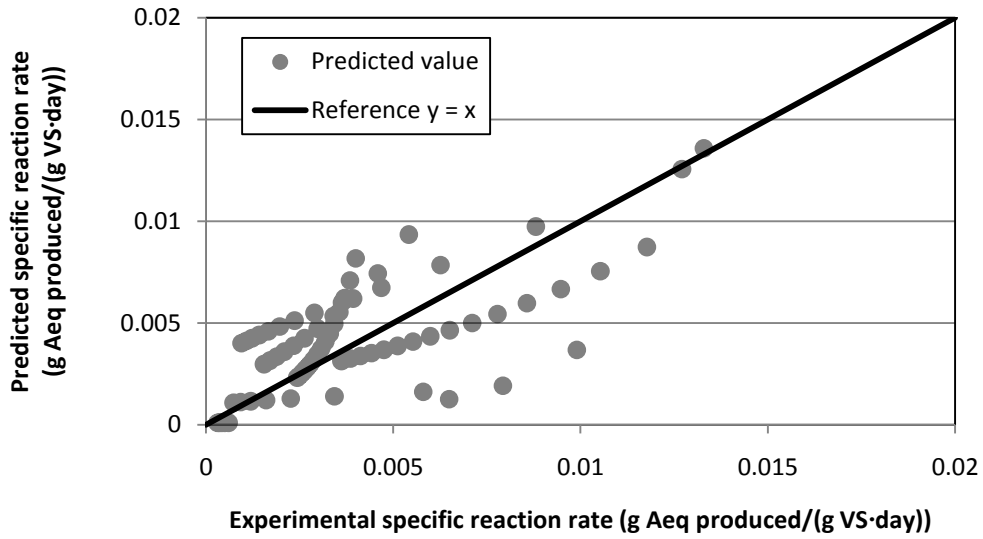

Figure 6-20. The experimental value and the CPDM prediction value for the specific reaction rate in five batch paper/yeast extract fermentation with D18 inocula.

Table 6-16. Parameter constant values in CPDM for Site D inocula D18.

Parameter constant	Value
Holdup (g liquid/g VS cake)	2.0
Moisture (g liquid/ g solid feed)	0.06
Selectivity (g Aeq/g VS digested)	0.33
F1−F4 solid concentration (g VS/L)	169, 214, 214, 214
F1−F4 liquid volume (L)	0.48, 0.28, 0.28, 0.28
ϕ (g total acid/g Aeq)	0.86
e (g Aeq/(g VS·d))	0.055
f (dimensionless)	1.03
g (L/g total acid)$^{1/h}$	1.89
h (dimensionless)	1.81

Table 6-16 lists the system-specific variables required by the CPDM prediction. Figure 6-21 shows the CPDM "map" for Site D inocula D18 in a 90 wt% paper/10 wt% yeast extract countercurrent fermentation with the single-centrifuge procedure at a fermentation solid concentration of 169 g VS/L liquid. The "map" predicts a total acid concentration of 6.01 g/L at LRT 30 day and VSLR of 12 g/(L·d), and a conversion of 0.14 g VS digested/g VS fed. At a VSLR of 4 g/(L·d) and LRT of 10 days, total acid concentration is 8.78 g/L and conversion is 0.44 g VS digested/g VS fed.

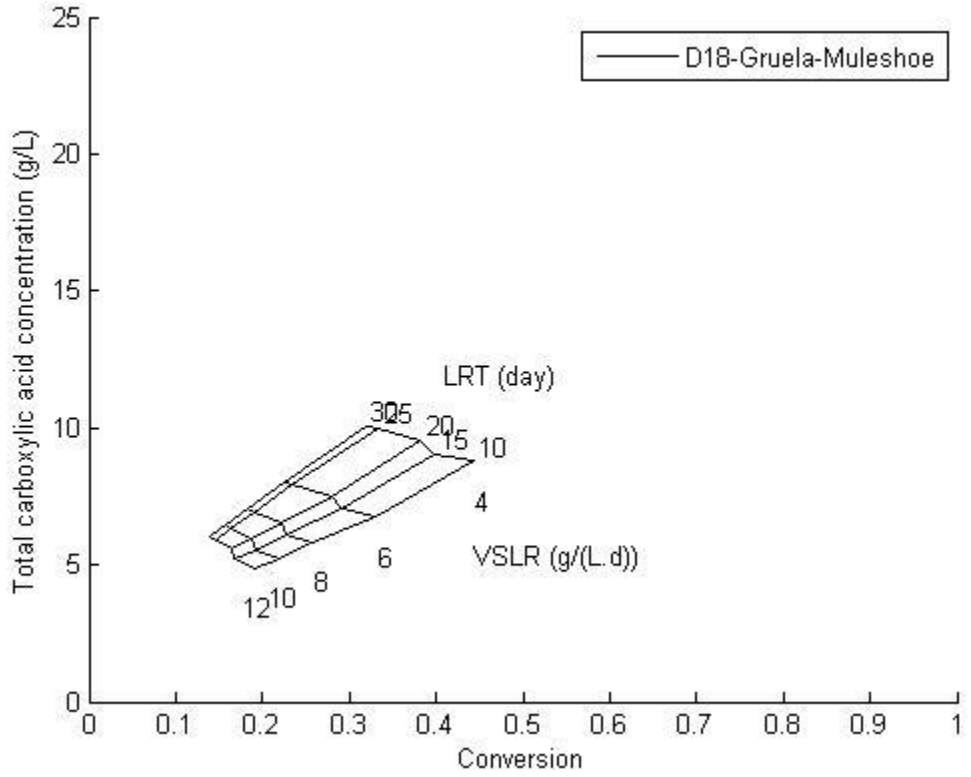

Figure 6-21. The CPDM "map" for 90 wt% paper/10 wt% yeast extract with D18 inocula.

6.5.8 Sample E08 from Site E – Enid, Oklahoma

As mentioned in Section 6-3, batch experiments with 90 wt% paper /10 wt% yeast extract were done to obtain model parameters for the CPDM method. The inocula for these fermentations were taken from the post reactor material of the initial screening then preserved in a 20% glycerol solution. Calcium carbonate was used to adjust the pH. Liquid samples from the fermentations were analyzed for carboxylic acids. Using Equation 6-11, the acids were converted to acetic acid equivalents (Aeq). Figure 6-22 shows the Aeq concentrations for the five E08 batch experiments. The smooth lines are the predicted Aeq. Table 6-17 presents the fitted parameters *a*, *b*, and *c* for Equation 6-12.

Table 6-17. Values of the parameters *a*, *b*, and *c* fitted by least squares analysis for Site E inocula E08.

Substrate Concentration (g/L)	*a* (g/L liquid)	*b* (g/(L liquid·d))	*c* (d^{-1})
20	2.00	0.092	0.055
40	1.92	0.250	0.100
70	2.07	1.10	0.100
100	2.10	1.37	0.100
100+	20.80	0.500	0.060

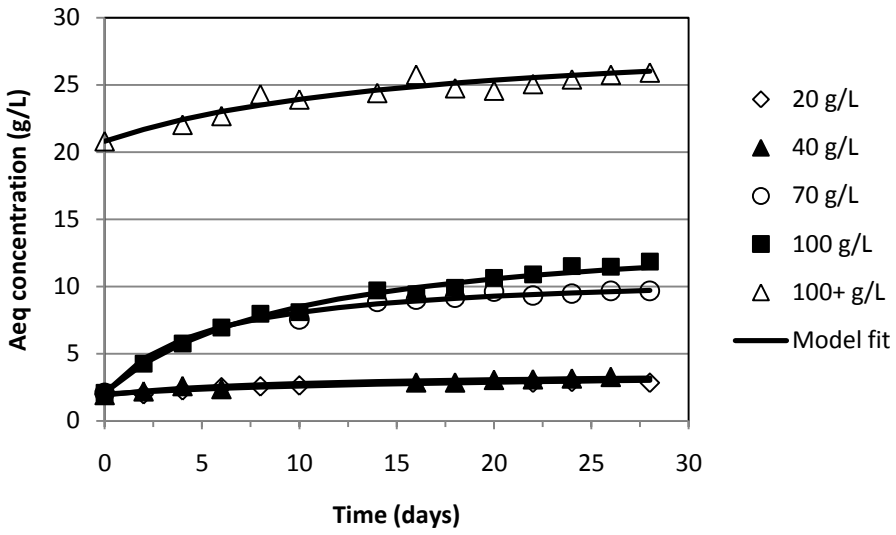

Figure 6-22. Aeq concentration for E08 inoculated paper/yeast extract fermentation at 20, 40, 70, 100, and 100+ g substrate/L liquid with calcium carbonate.

The reaction rate and the specific reaction rate for the batch fermentations were calculated using Equations 6-13 and 6-14. Conversion was calculated with the experimental acetic acid equivalents using Equation 6-15. Parameters *e*, *f*, *g*, and *h* presented in the predicted rate equation (Equation 6-24) were calculated by nonlinear regression. Figure 6-23 compares the predicted specific rate with the experimental specific rate. The specific rate equation for Site E inocula E08 follows:

$$\hat{r}_{pred} = \frac{0.0046(1-x)^{1.02}}{1 + 0.077(\emptyset \cdot \text{Aeq})^{0.970}} \tag{6-24}$$

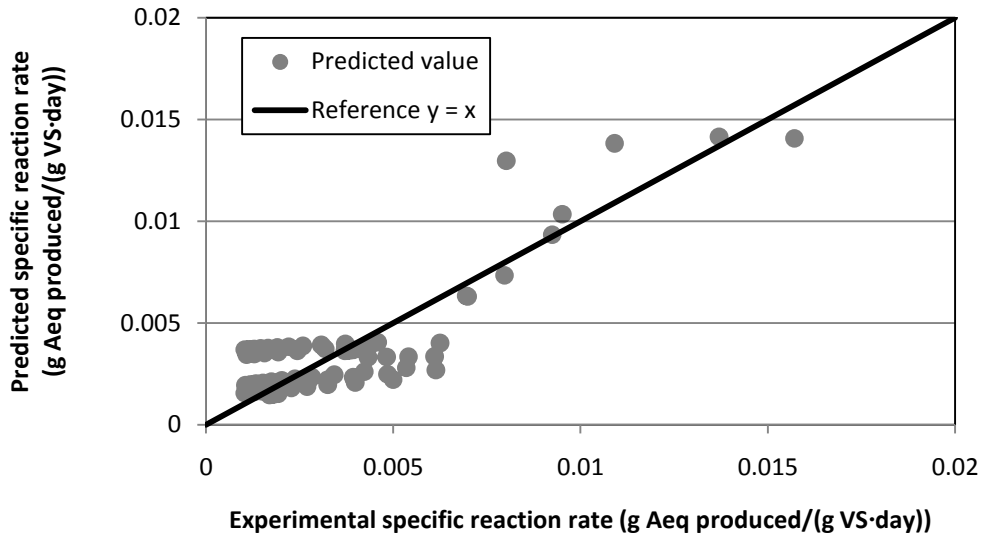

Figure 6-23. The experimental value and the CPDM prediction value for the specific reaction rate in five batch paper/yeast extract fermentation with E08 inocula.

Table 6-18. Parameter constant values in CPDM for Site E inocula E08.

Parameter constant	Value
Holdup (g liquid/g VS cake)	2.0
Moisture (g liquid/ g solid feed)	0.06
Selectivity (g Aeq/g VS digested)	0.49
F1−F4 solid concentration (g VS/L)	169, 214, 214, 214
F1−F4 liquid volume (L)	0.48, 0.28, 0.28, 0.28
ϕ (g total acid/g Aeq)	0.82
e (g Aeq/(g VS·d))	0.0046
f (dimensionless)	1.02
g (L/g total acid)$^{1/h}$	0.077
h (dimensionless)	0.970

Table 6-18 lists the system-specific variables required by the CPDM prediction. Figure 6-24 shows the CPDM "map" for Site E inocula E08 in a 90 wt% paper/10 wt% yeast extract countercurrent fermentation with the single-centrifuge procedure at a fermentation solid concentration of 169 g VS/L liquid. The "map" predicts a total acid concentration of 9.53 g/L at LRT 30 day and VSLR of 12 g/(L·d), and a conversion of 0.14 g VS digested/g VS fed. At a VSLR of 4 g/(L·d) and LRT of 10 days, total acid concentration is 13.19 g/L and conversion is 0.54 g VS digested/g VS fed.

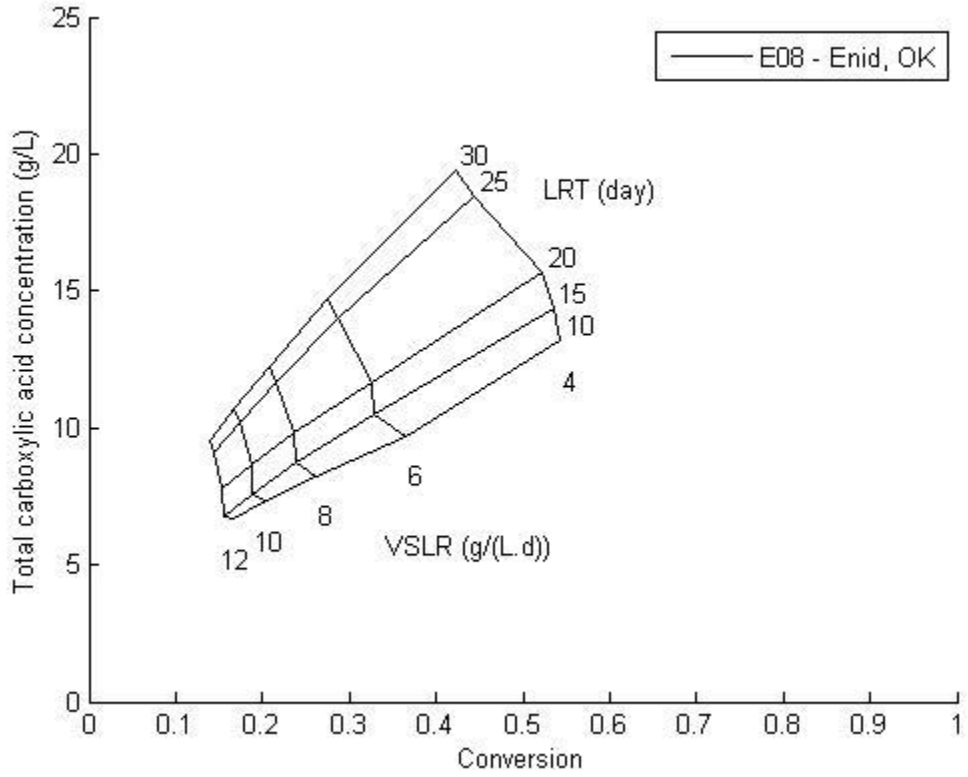

Figure 6-24. The CPDM "map" for 90 wt% paper/10 wt% yeast extract with E08 inocula.

6.5.9 Sample F02 from Site F – Brazoria, TX

As mentioned in Section 6-3, batch experiments with 90 wt% paper /10 wt% yeast extract were done to obtain model parameters for the CPDM method. The inocula for these fermentations were taken from the post reactor material of the initial screening then preserved in a 20% glycerol solution. Calcium carbonate was used to adjust the pH. Liquid samples from the fermentations were analyzed for carboxylic acids. Using Equation 6-11, the acids were converted to acetic acid equivalents (Aeq). Figure 6-25 shows the Aeq concentrations for the five F02 batch experiments. The smooth lines are the predicted Aeq. Table 6-19 presents the fitted parameters *a*, *b*, and *c* for Equation 6-12.

Table 6-19. Values of the parameters *a*, *b*, and *c* fitted by least squares analysis for Site F inocula F02.

Substrate Concentration (g/L)	*a* (g/L liquid)	*b* (g/(L liquid·d))	*c* (d^{-1})
20	2.06	0.054	0.0076
40	3.70	1.19	0.196
70	2.03	1.04	0.120
100	1.71	1.43	0.097
100+	23.10	0.215	0.0078

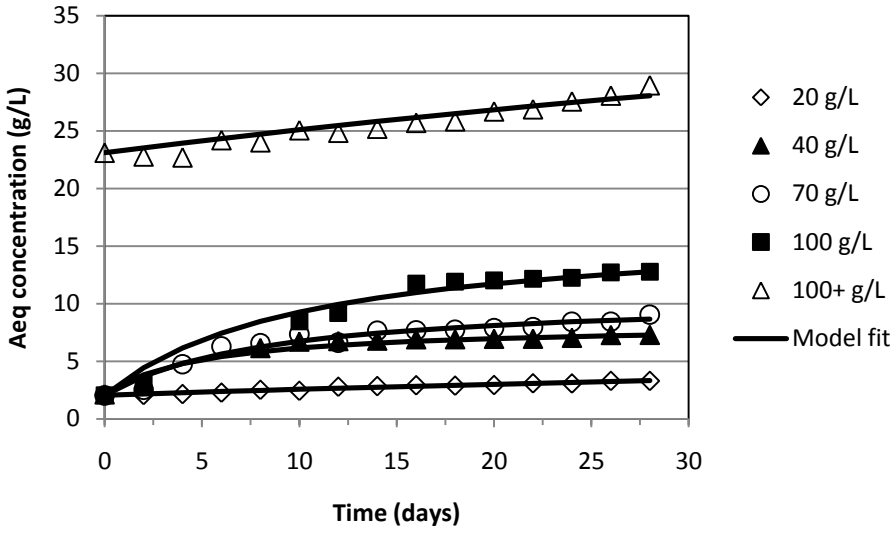

Figure 6-25. Aeq concentration for F02 inoculated paper/yeast extract fermentation at 20, 40, 70, 100, and 100+ g substrate/L liquid with calcium carbonate.

The reaction rate and the specific reaction rate for the batch fermentations were calculated using Equations 6-13 and 6-14. Conversion was calculated with the experimental acetic acid equivalents using Equation 6-15. Parameters *e*, *f*, *g*, and *h* presented in the predicted rate equation (Equation 6-25) were calculated by nonlinear regression. Figure 6-26 compares the predicted specific rate with the experimental specific rate. The specific rate equation for Site F inocula F02 follows:

$$\hat{r}_{pred} = \frac{0.0126(1-x)^{3.66}}{1 + 0.00100(\emptyset \cdot \text{Aeq})^{2.744}} \tag{6-25}$$

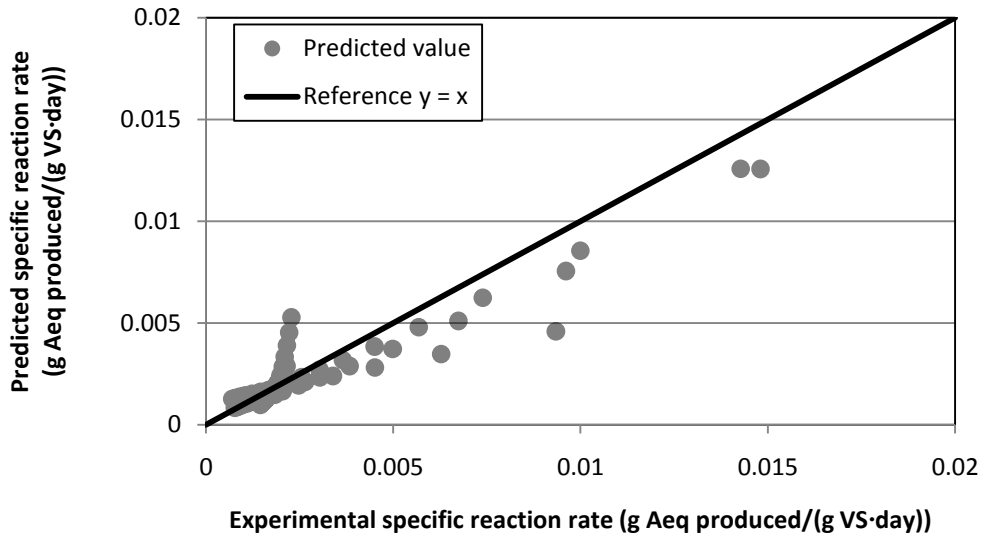

Figure 6-26. The experimental value and the CPDM prediction value for the specific reaction rate in five batch paper/yeast extract fermentation with F02 inocula.

Table 6-20. Parameter constant values in CPDM for Site F inocula F02.

Parameter constant	Value
Holdup (g liquid/g VS cake)	2.0
Moisture (g liquid/ g solid feed)	0.06
Selectivity (g Aeq/g VS digested)	0.45
F1−F4 solid concentration (g VS/L)	169, 214, 214, 214
F1−F4 liquid volume (L)	0.48, 0.28, 0.28, 0.28
ϕ (g total acid/g Aeq)	0.80
e (g Aeq/(g VS·d))	0.0126
f (dimensionless)	3.66
g (L/g total acid)$^{1/h}$	0.00100
h (dimensionless)	2.744

Table 6-20 lists the system-specific variables required by the CPDM prediction. Figure 6-27 shows the CPDM "map" for Site F inocula F02 in a 90 wt% paper/10 wt% yeast extract countercurrent fermentation with the single-centrifuge procedure at a fermentation solid concentration of 169 g VS/L liquid. The "map" predicts a total acid concentration of 12.52 g/L at LRT 30 day and VSLR of 12 g/(L·d), and a conversion of 0.28 g VS digested/g VS fed. At a VSLR of 4 g/(L·d) and LRT of 10 days, total acid concentration is 9.59 g/L and conversion is 0.50 g VS digested/g VS fed.

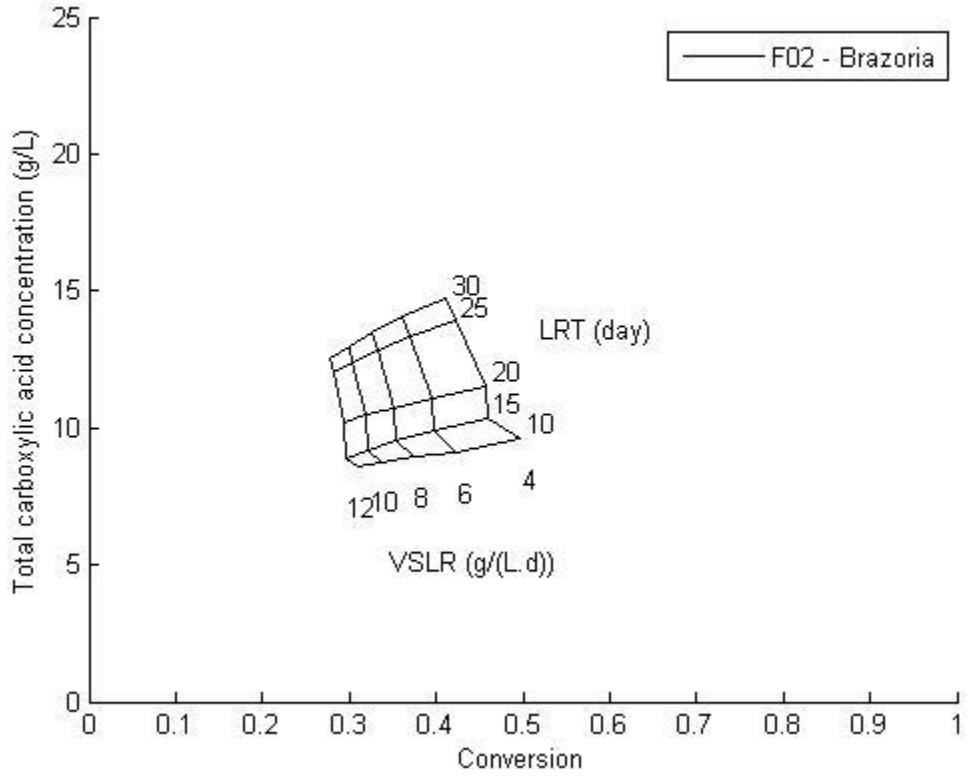

Figure 6-27. The CPDM "map" for 90 wt% paper/10 wt% yeast extract with F02 inocula.

6.5.10 Sample F09 from Site F – Brazoria, TX

As mentioned in Section 6-3, batch experiments with 90 wt% paper /10 wt% yeast extract were done to obtain model parameters for the CPDM method. The inocula for these fermentations were taken from the post reactor material of the initial screening then preserved in a 20% glycerol solution. Calcium carbonate was used to adjust the pH. Liquid samples from the fermentations were analyzed for carboxylic acids. Using Equation 6-11, the acids were converted to acetic acid equivalents (Aeq). Figure 6-28 shows the Aeq concentrations for the five F09 batch experiments. The smooth lines are the predicted Aeq. Table 6-21 presents the fitted parameters *a*, *b*, and *c* for Equation 6-12.

Table 6-21. Values of the parameters *a*, *b*, and *c* fitted by least squares analysis for Site F inocula F09.

Substrate Concentration (g/L)	*a* (g/L liquid)	*b* (g/(L liquid·d))	*c* (d^{-1})
20	1.56	0.160	0.100
40	1.91	0.130	0.040
70	1.87	1.20	0.150
100	1.22	1.50	0.100
100+	20.02	0.710	0.140

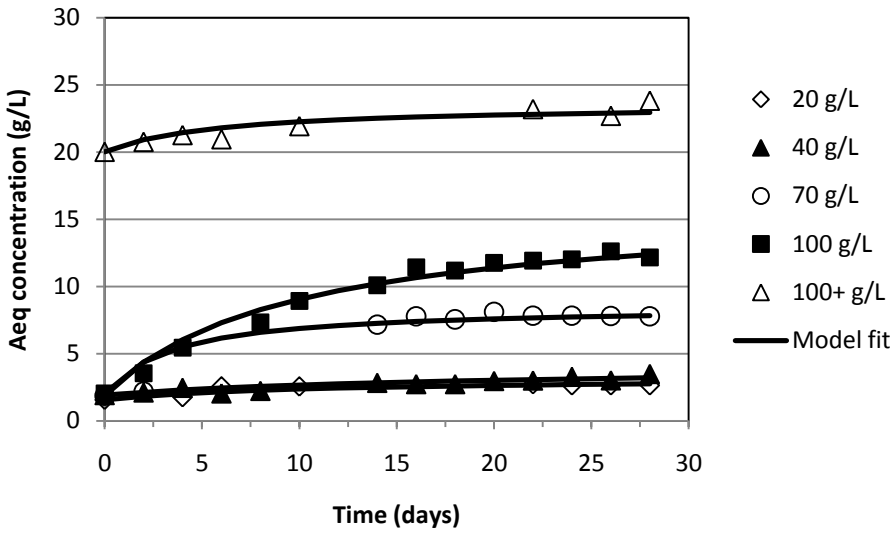

Figure 6-28. Aeq concentration for F09 inoculated paper/yeast extract fermentation at 20, 40, 70, 100, and 100+ g substrate/L liquid with calcium carbonate.

The reaction rate and the specific reaction rate for the batch fermentations were calculated using Equations 6-13 and 6-14. Conversion was calculated with the experimental acetic acid equivalents using Equation 6-15. Parameters *e*, *f*, *g*, and *h* presented in the predicted rate equation (Equation 6-26) were calculated by nonlinear regression. Figure 6-29 compares the predicted specific rate with the experimental specific rate. The specific rate equation for Site F inocula F09 follows:

$$\hat{r}_{pred} = \frac{0.00400(1-x)^{1.63}}{1 + 0.00100(\emptyset \cdot \text{Aeq})^{2.23}} \tag{6-26}$$

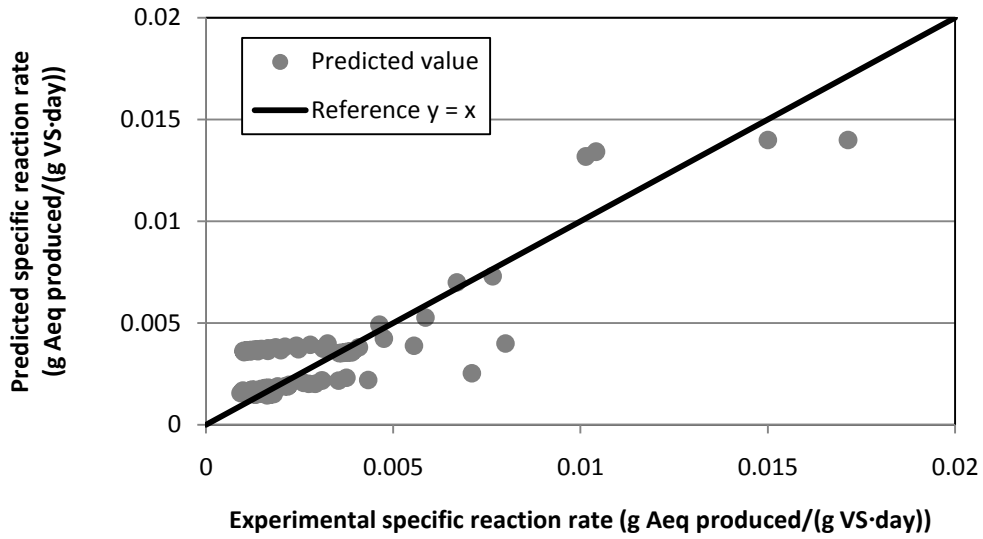

Figure 6-29. The experimental value and the CPDM prediction value for the specific reaction rate in five batch paper/yeast extract fermentation with F09 inocula.

Table 6-22. Parameter constant values in CPDM for Site F inocula F09.

Parameter constant	Value
Holdup (g liquid/g VS cake)	2.0
Moisture (g liquid/ g solid feed)	0.06
Selectivity (g Aeq/g VS digested)	0.45
F1−F4 solid concentration (g VS/L)	169, 214, 214, 214
F1−F4 liquid volume (L)	0.48, 0.28, 0.28, 0.28
ϕ (g total acid/g Aeq)	0.80
e (g Aeq/(g VS·d))	0.00400
f (dimensionless)	1.63
g (L/g total acid)$^{1/h}$	0.00100
h (dimensionless)	2.23

Table 6-22 lists the system-specific variables required by the CPDM prediction. Figure 6-30 shows the CPDM "map" for Site F inocula F09 in a 90 wt% paper/10 wt% yeast extract countercurrent fermentation with the single-centrifuge procedure at a fermentation solid concentration of 169 g VS/L liquid. The "map" predicts a total acid concentration of 10.57 g/L at LRT 30 day and VSLR of 12 g/(L·d), and a conversion of 0.16 g VS digested/g VS fed. At a VSLR of 4 g/(L·d) and LRT of 10 days, total acid concentration is 13.26 g/L and conversion is 0.60 g VS digested/g VS fed.

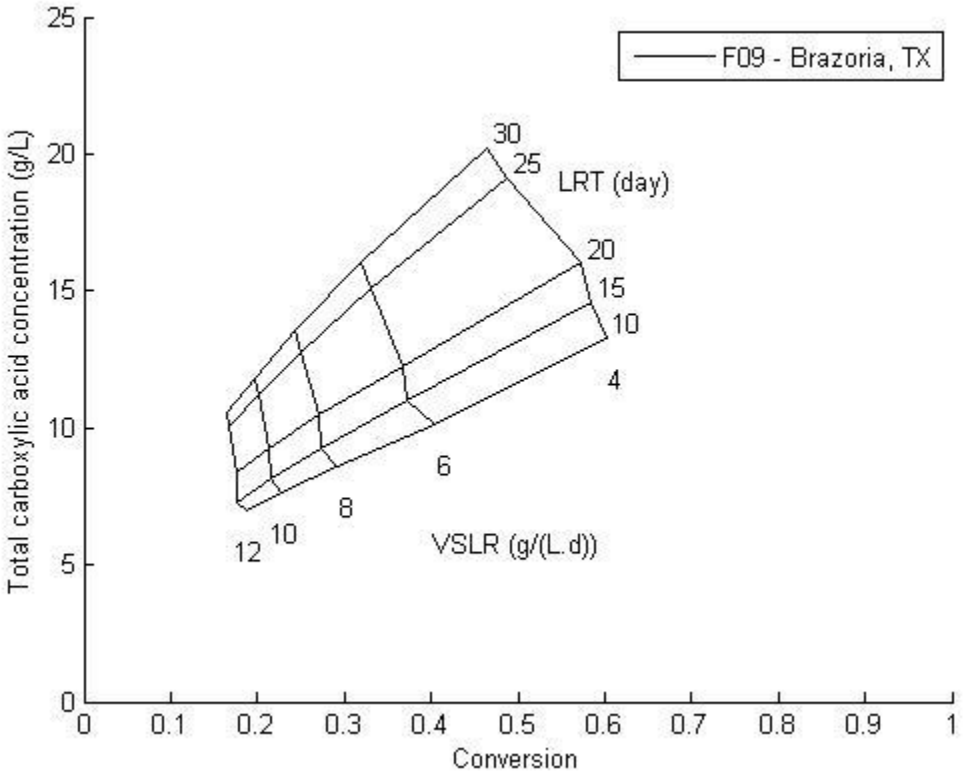

Figure 6-30. The CPDM "map" for 90 wt% paper/10 wt% yeast extract with F09 inocula.

6.5.11 Sample G08 from Site G – Roswell-Carlsbad, NM

As mentioned in Section 6-3, batch experiments with 90 wt% paper /10 wt% yeast extract were done to obtain model parameters for the CPDM method. The inocula for these fermentations were taken from the post reactor material of the initial screening then preserved in a 20% glycerol solution. Calcium carbonate was used to adjust the pH. Liquid samples from the fermentations were analyzed for carboxylic acids. Using Equation 6-11, the acids were converted to acetic acid equivalents (Aeq). Figure 6-31 shows the Aeq concentrations for the five G08 batch experiments. The smooth lines are the predicted Aeq. Table 6-23 presents the fitted parameters *a*, *b*, and *c* for Equation 6-12.

Table 6-23. Values of the parameters *a*, *b*, and *c* fitted by least squares analysis for Site G inocula G08.

Substrate Concentration (g/L)	*a* (g/L liquid)	*b* (g/(L liquid·d))	*c* (d^{-1})
20	1.88	0.729	0.146
40	1.90	0.652	0.080
70	2.12	2.64	0.194
100	1.51	2.59	0.099
100+	21.77	0.350	0.0093

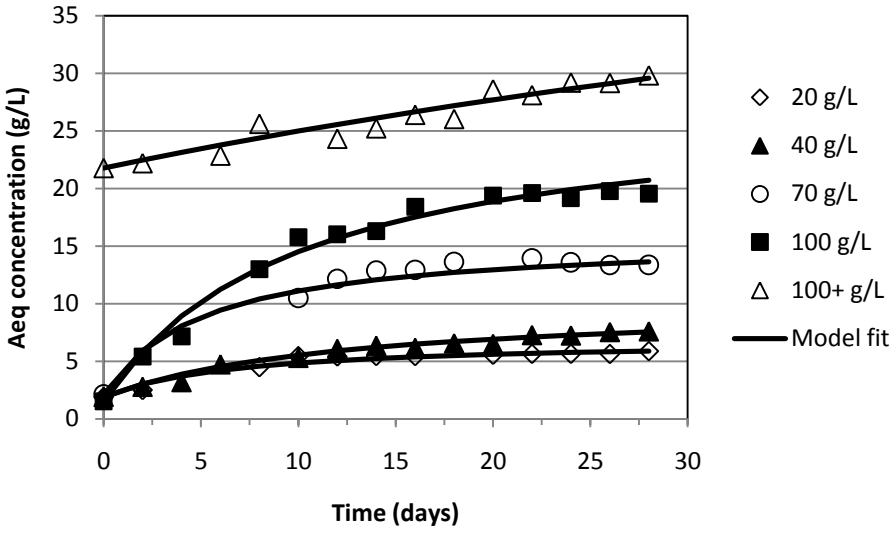

Figure 6-31. Aeq concentration for G08 inoculated paper/yeast extract fermentation at 20, 40, 70, 100, and 100+ g substrate/L liquid with calcium carbonate.

The reaction rate and the specific reaction rate for the batch fermentations were calculated using Equations 6-13 and 6-14. Conversion was calculated with the experimental acetic acid equivalents using Equation 6-15. Parameters *e*, *f*, *g*, and *h* presented in the predicted rate equation (Equation 6-27) were calculated by nonlinear regression. Figure 6-32 compares the predicted specific rate with the experimental specific rate. The specific rate equation for Site G inocula G08 follows:

$$\hat{r}_{pred} = \frac{0.0296(1-x)^{2.975}}{1 + 0.0137(\emptyset \cdot \text{Aeq})^{2.069}} \tag{6-27}$$

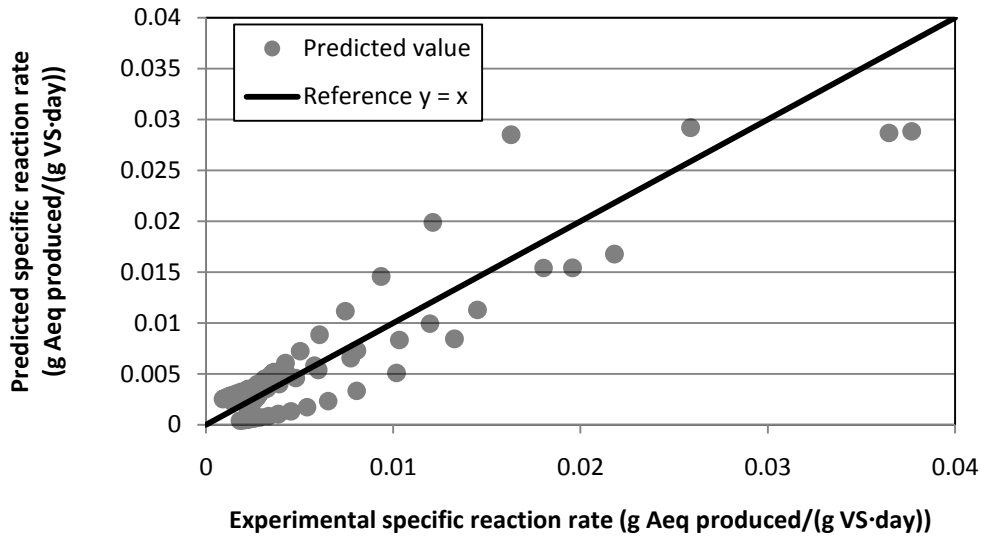

Figure 6-32. The experimental value and the CPDM prediction value for the specific reaction rate in five batch paper/yeast extract fermentation with G08 inocula.

Table 6-24. Parameter constant values in CPDM for Site G inocula G08.

Parameter constant	Value
Holdup (g liquid/g VS cake)	2.0
Moisture (g liquid/ g solid feed)	0.06
Selectivity (g Aeq/g VS digested)	0.37
F1−F4 solid concentration (g VS/L)	169, 214, 214, 214
F1−F4 liquid volume (L)	0.48, 0.28, 0.28, 0.28
ϕ (g total acid/g Aeq)	0.76
e (g Aeq/(g VS·d))	0.0296
f (dimensionless)	2.975
g (L/g total acid)$^{1/h}$	0.0137
h (dimensionless)	2.069

Table 6-24 lists the system-specific variables required by the CPDM prediction. Figure 6-33 shows the CPDM "map" for Site G inocula G08 in a 90 wt% paper/10 wt% yeast extract countercurrent fermentation with the single-centrifuge procedure at a fermentation solid concentration of 169 g VS/L liquid. The "map" predicts a total acid concentration of 17.43 g/L at LRT 30 day and VSLR of 12 g/(L·d), and a conversion of 0.28 g VS digested/g VS fed. At a VSLR of 4 g/(L·d) and LRT of 10 days, total acid concentration is 10.97 g/L and conversion is 0.57 g VS digested/g VS fed.

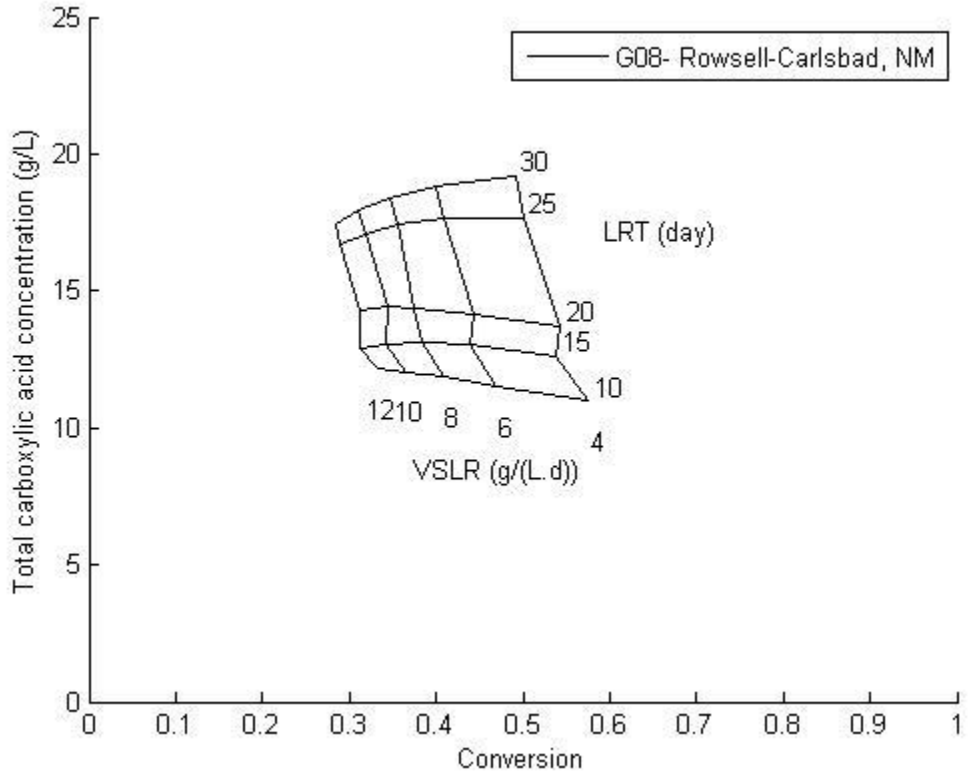

Figure 6-33. The CPDM "map" for 90 wt% paper/10 wt% yeast extract with G08 inocula.

6.5.12 Sample G13 from Site G – Roswell-Carlsbad, NM

As mentioned in Section 6-3, batch experiments with 90 wt% paper /10 wt% yeast extract were done to obtain model parameters for the CPDM method. The inocula for these fermentations were taken from the post reactor material of the initial screening then preserved in a 20% glycerol solution. Calcium carbonate was used to adjust the pH. Liquid samples from the fermentations were analyzed for carboxylic acids. Using Equation 6-11, the acids were converted to acetic acid equivalents (Aeq). Figure 6-34 shows the Aeq concentrations for the five G13 batch experiments. The smooth lines are the predicted Aeq. Table 6-25 presents the fitted parameters *a*, *b*, and *c* for Equation 6-12.

Table 6-25. Values of the parameters *a*, *b*, and *c* fitted by least squares analysis for Site G inocula G13.

Substrate Concentration (g/L)	*a* (g/L liquid)	*b* (g/(L liquid·d))	*c* (d^{-1})
20	1.60	0.200	0.042
40	1.72	0.330	0.100
70	1.81	0.180	0.050
100	1.87	1.20	0.100
100+	20.61	0.240	0.040

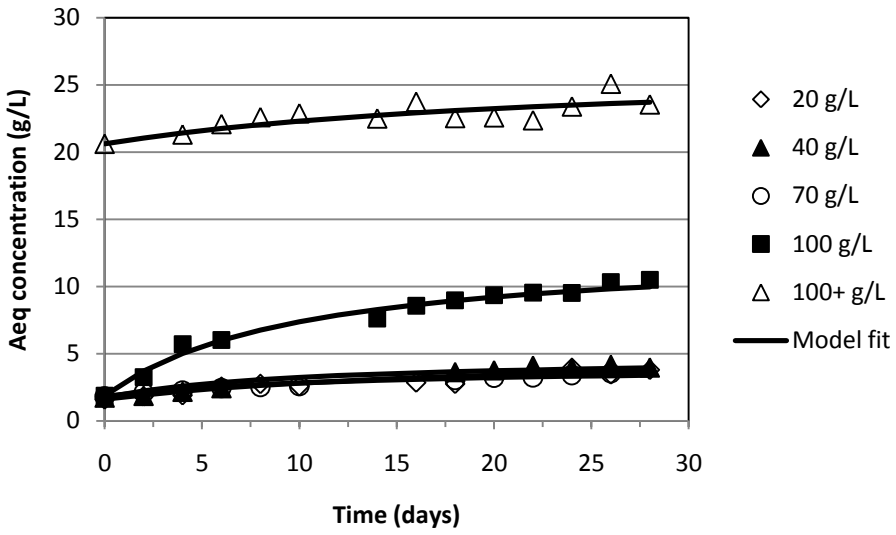

Figure 6-34. Aeq concentration for G13 inoculated paper/yeast extract fermentation at 20, 40, 70, 100, and 100+ g substrate/L liquid with calcium carbonate.

The reaction rate and the specific reaction rate for the batch fermentations were calculated using Equations 6-13 and 6-14. Conversion was calculated with the experimental acetic acid equivalents using Equation 6-15. Parameters *e*, *f*, *g*, and *h* presented in the predicted rate equation (Equation 6-28) were calculated by nonlinear regression. Figure 6-35 compares the predicted specific rate with the experimental specific rate. The specific rate equation for Site G inocula G13 follows:

$$\hat{r}_{pred} = \frac{0.0077(1-x)^{6.97}}{1 + 0.0028(\emptyset \cdot \text{Aeq})^{2.37}} \tag{6-28}$$

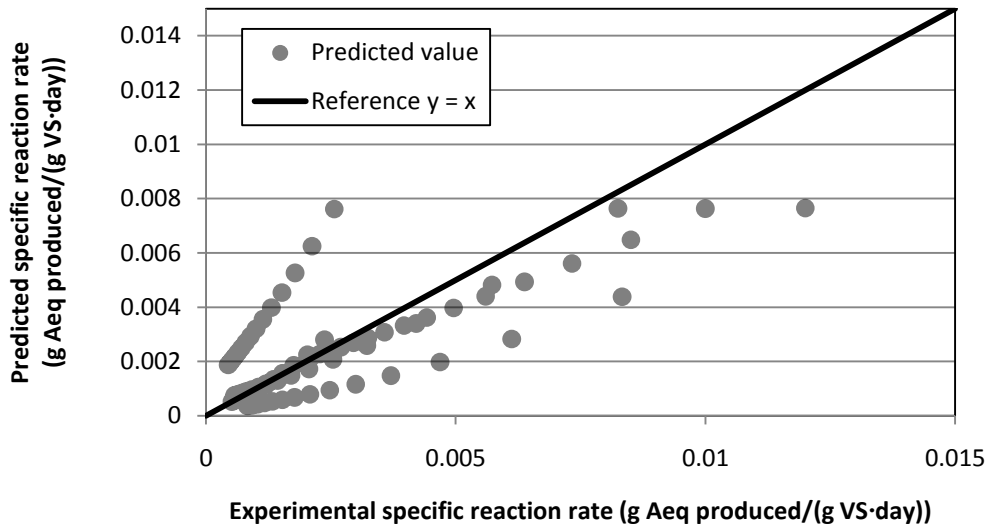

Figure 6-35. The experimental value and the CPDM prediction value for the specific reaction rate in five batch paper/yeast extract fermentation with G13 inocula.

Table 6-26. Parameter constant values in CPDM for Site G inocula G13.

Parameter constant	Value
Holdup (g liquid/g VS cake)	2.0
Moisture (g liquid/ g solid feed)	0.06
Selectivity (g Aeq/g VS digested)	0.33
F1−F4 solid concentration (g VS/L)	169, 214, 214, 214
F1−F4 liquid volume (L)	0.48, 0.28, 0.28, 0.28
ϕ (g total acid/g Aeq)	0.87
e (g Aeq/(g VS·d))	0.0077
f (dimensionless)	6.97
g (L/g total acid)$^{1/h}$	0.0028
h (dimensionless)	2.37

Table 6-26 lists the system-specific variables required by the CPDM prediction. Figure 6-36 shows the CPDM "map" for Site G inocula G13 in a 90 wt% paper/10 wt% yeast extract countercurrent fermentation with the single-centrifuge procedure at a fermentation solid concentration of 169 g VS/L liquid. The "map" predicts a total acid concentration of 8.77 g/L at LRT 30 day and VSLR of 12 g/(L·d), and a conversion of 0.16 g VS digested/g VS fed. At a VSLR of 4 g/(L·d) and LRT of 10 days, total acid concentration is 7.12 g/L and conversion is 0.37 g VS digested/g VS fed.

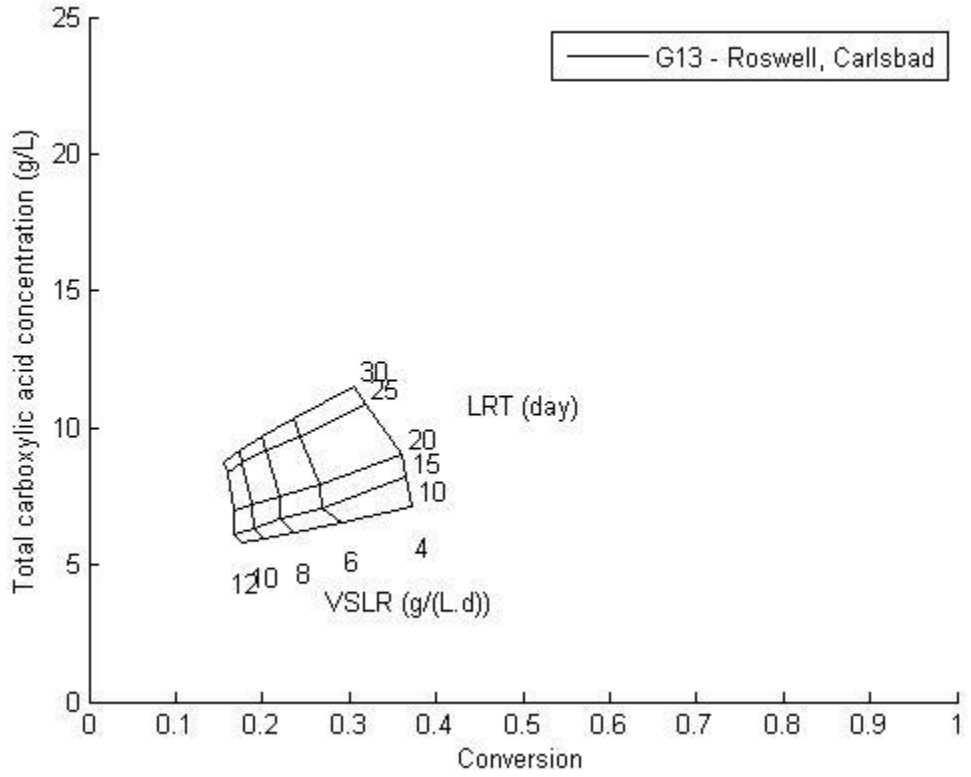

Figure 6-36. The CPDM "map" for 90 wt% paper/10 wt% yeast extract with G13 inocula.

6.5.13 Sample G23 from Site G – Roswell-Carlsbad, NM

As mentioned in Section 6-3, batch experiments with 90 wt% paper /10 wt% yeast extract were done to obtain model parameters for the CPDM method. The inocula for these fermentations were taken from the post reactor material of the initial screening then preserved in a 20% glycerol solution. Calcium carbonate was used to adjust the pH. Liquid samples from the fermentations were analyzed for carboxylic acids. Using Equation 6-11, the acids were converted to acetic acid equivalents (Aeq). Figure 6-37 shows the Aeq concentrations for the five G23 batch experiments. The smooth lines are the predicted Aeq. Table 6-27 presents the fitted parameters *a*, *b*, and *c* for Equation 6-12.

Table 6-27. Values of the parameters *a*, *b*, and *c* fitted by least squares analysis for Site G inocula G23.

Substrate Concentration (g/L)	*a* (g/L liquid)	*b* (g/(L liquid·d))	*c* (d^{-1})
20	1.53	0.160	0.050
40	2.24	0.670	0.100
70	2.33	1.02	0.060
100	4.33	6.90	0.500
100+	20.97	0.150	0.010

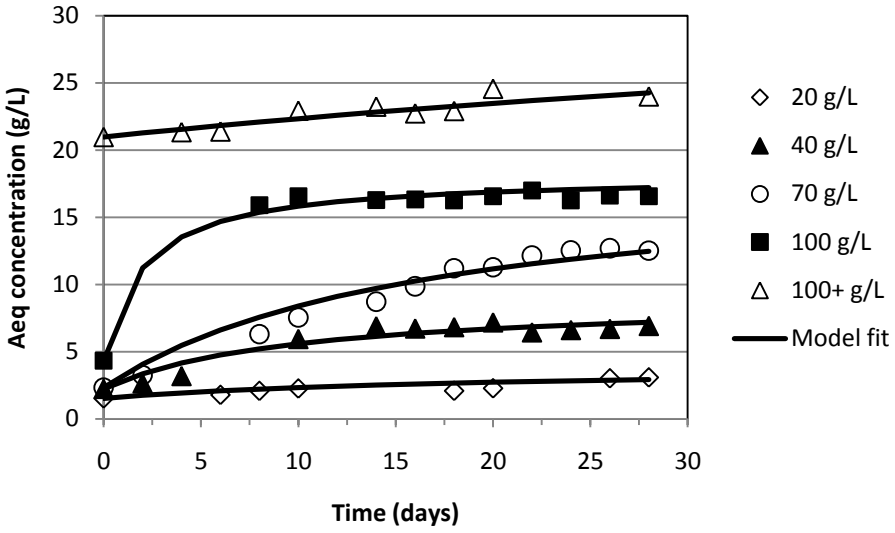

Figure 6-37. Aeq concentration for G23 inoculated paper/yeast extract fermentation at 20, 40, 70, 100, and 100+ g substrate/L liquid with calcium carbonate.

The reaction rate and the specific reaction rate for the batch fermentations were calculated using Equations 6-13 and 6-14. Conversion was calculated with the experimental acetic acid equivalents using Equation 6-15. Parameters *e*, *f*, *g*, and *h* presented in the predicted rate equation (Equation 6-29) were calculated by nonlinear regression. Figure 6-38 compares the predicted specific rate with the experimental specific rate. The specific rate equation for Site G inocula G23 follows:

$$\hat{r}_{pred} = \frac{0.025(1-x)^{23.5}}{1 + 0.00100(\emptyset \cdot \text{Aeq})^{3.05}} \tag{6-29}$$

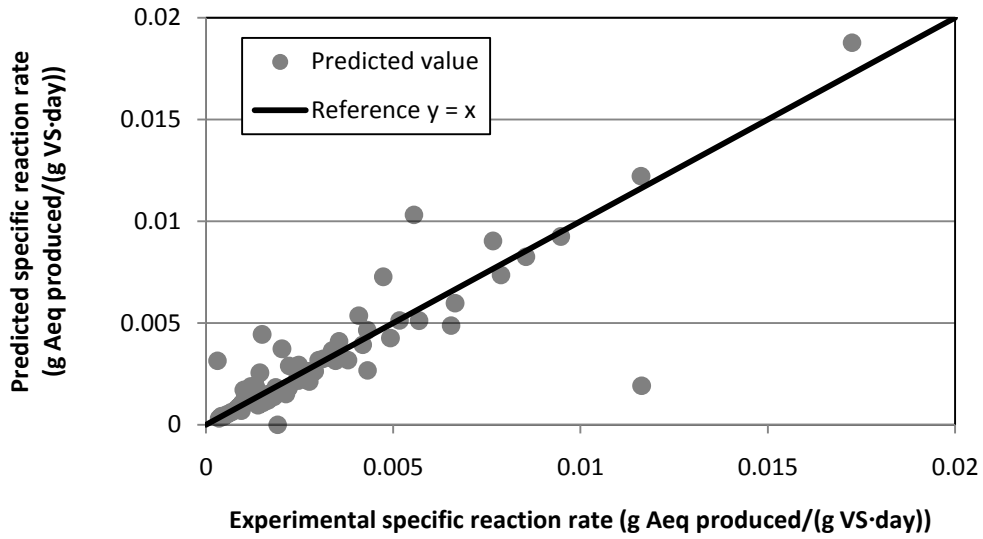

Figure 6-38. The experimental value and the CPDM prediction value for the specific reaction rate in five batch paper/yeast extract fermentation with G23 inocula.

Table 6-28. Parameter constant values in CPDM for Site G inocula G23.

Parameter constant	Value
Holdup (g liquid/g VS cake)	2.0
Moisture (g liquid/ g solid feed)	0.06
Selectivity (g Aeq/g VS digested)	0.35
F1−F4 solid concentration (g VS/L)	169, 214, 214, 214
F1−F4 liquid volume (L)	0.48, 0.28, 0.28, 0.28
ϕ (g total acid/g Aeq)	0.79
e (g Aeq/(g VS·d))	0.025
f (dimensionless)	23.5
g (L/g total acid)$^{1/h}$	0.00100
h (dimensionless)	3.05

Table 6-28 lists the system-specific variables required by the CPDM prediction. Figure 6-39 shows the CPDM "map" for Site G inocula G23 in a 90 wt% paper/10 wt% yeast extract countercurrent fermentation with the single-centrifuge procedure at a fermentation solid concentration of 169 g VS/L liquid. The "map" predicts a total acid concentration of 9.98 g/L at LRT 30 day and VSLR of 12 g/(L·d), and a conversion of 0.10 g VS digested/g VS fed. At a VSLR of 4 g/(L·d) and LRT of 10 days, total acid concentration is 9.30 g/L and conversion is 0.43 g VS digested/g VS fed.

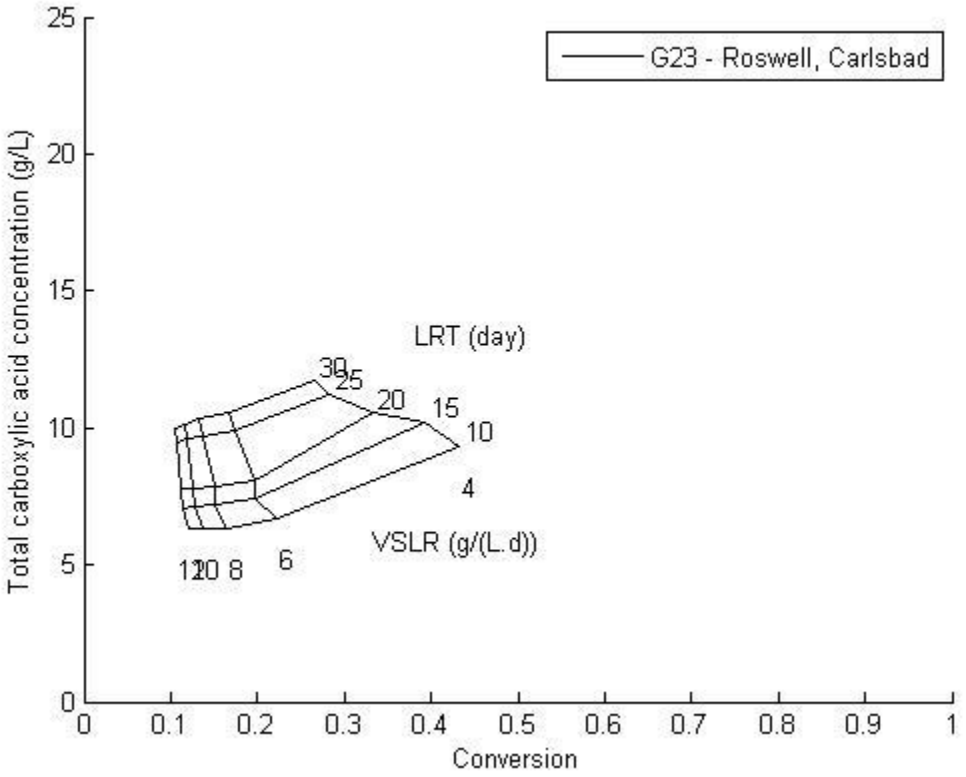

Figure 6-39. The CPDM "map" for 90 wt% paper/10 wt% yeast extract with G23 inocula.

6.5.14 Sample G46 from Site G – Roswell-Carlsbad, NM

As mentioned in Section 6-3, batch experiments with 90 wt% paper /10 wt% yeast extract were done to obtain model parameters for the CPDM method. The inocula for these fermentations were taken from the post reactor material of the initial screening then preserved in a 20% glycerol solution. Calcium carbonate was used to adjust the pH. Liquid samples from the fermentations were analyzed for carboxylic acids. Using Equation 6-11, the acids were converted to acetic acid equivalents (Aeq). Figure 6-40 shows the Aeq concentrations for the five G46 batch experiments. The smooth lines are the predicted Aeq. Table 6-29 presents the fitted parameters *a*, *b*, and *c* for Equation 6-12.

Table 6-29. Values of the parameters *a*, *b*, and *c* fitted by least squares analysis for Site G inocula G46.

Substrate Concentration (g/L)	*a* (g/L liquid)	*b* (g/(L liquid·d))	*c* (d^{-1})
20	2.01	0.130	0.100
40	2.01	1.00	0.200
70	2.28	4.20	0.400
100	2.34	1.90	0.200
100+	17.81	0.450	0.100

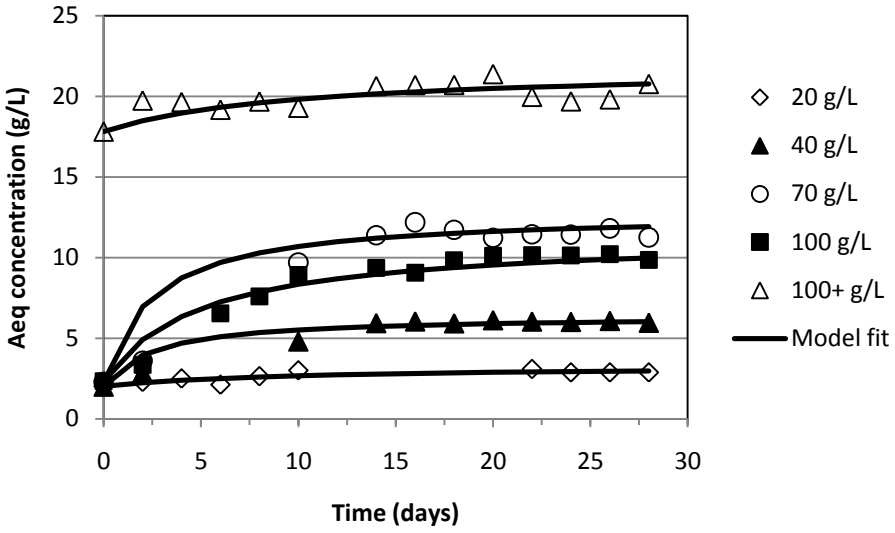

Figure 6-40. Aeq concentration for G46 inoculated paper/yeast extract fermentation at 20, 40, 70, 100, and 100+ g substrate/L liquid with calcium carbonate.

The reaction rate and the specific reaction rate for the batch fermentations were calculated using Equations 6-13 and 6-14. Conversion was calculated with the experimental acetic acid equivalents using Equation 6-15. Parameters *e*, *f*, *g*, and *h* presented in the predicted rate equation (Equation 6-30) were calculated by nonlinear regression. Figure 6-41 compares the predicted specific rate with the experimental specific rate. The specific rate equation for Site G inocula G46 follows:

$$\hat{r}_{pred} = \frac{0.027(1-x)^{5.56}}{1 + 0.00100(\emptyset \cdot \text{Aeq})^{3.36}} \tag{6-30}$$

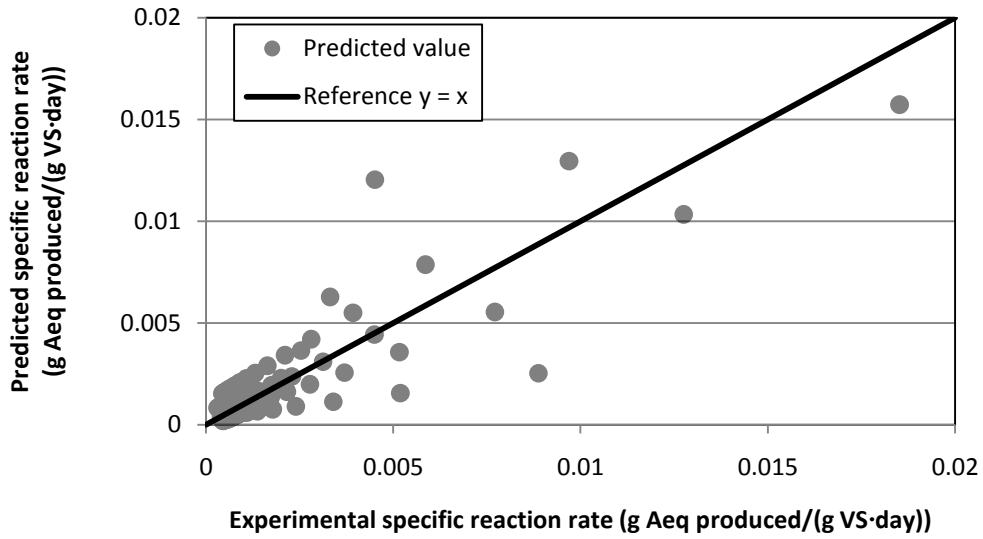

Figure 6-41. The experimental value and the CPDM prediction value for the specific reaction rate in five batch paper/yeast extract fermentation with G46 inocula.

Table 6-30. Parameter constant values in CPDM for Site G inocula G46.

Parameter constant	Value
Holdup (g liquid/g VS cake)	2.0
Moisture (g liquid/ g solid feed)	0.06
Selectivity (g Aeq/g VS digested)	0.21
F1−F4 solid concentration (g VS/L)	169, 214, 214, 214
F1−F4 liquid volume (L)	0.48, 0.28, 0.28, 0.28
ϕ (g total acid/g Aeq)	0.79
e (g Aeq/(g VS·d))	0.027
f (dimensionless)	5.56
g (L/g total acid)$^{1/h}$	0.00100
h (dimensionless)	3.36

Table 6-30 lists the system-specific variables required by the CPDM prediction. Figure 6-42 shows the CPDM "map" for Site G inocula G46 in a 90 wt% paper/10 wt% yeast extract countercurrent fermentation with the single-centrifuge procedure at a fermentation solid concentration of 169 g VS/L liquid. The "map" predicts a total acid concentration of 11.77 g/L at LRT 30 day and VSLR of 12 g/(L·d), and a conversion of 0.28 g VS digested/g VS fed. At a VSLR of 4 g/(L·d) and LRT of 10 days, total acid concentration is 9.39 g/L and conversion is 0.59 g VS digested/g VS fed.

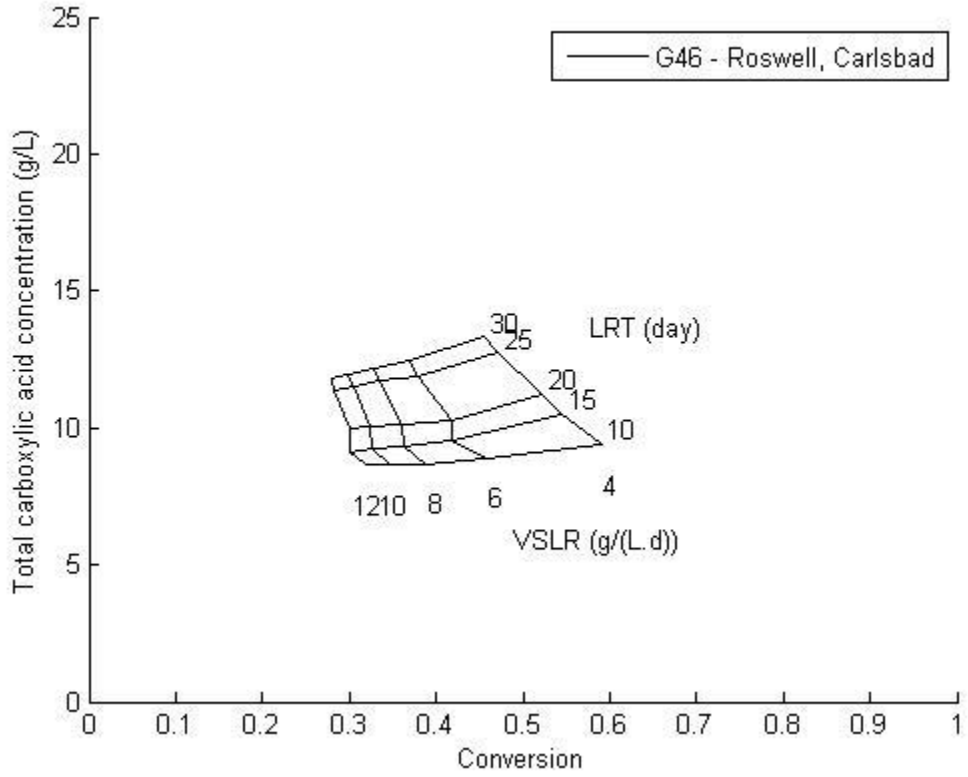

Figure 6-42. The CPDM "map" for 90 wt% paper/10 wt% yeast extract with G46 inocula.

6.5.15 Sample H01 from Site H – San Francisco, CA

As mentioned in Section 6-3, batch experiments with 90 wt% paper /10 wt% yeast extract were done to obtain model parameters for the CPDM method. The inocula for these fermentations were taken from the post reactor material of the initial screening then preserved in a 20% glycerol solution. Calcium carbonate was used to adjust the pH. Liquid samples from the fermentations were analyzed for carboxylic acids. Using Equation 6-11, the acids were converted to acetic acid equivalents (Aeq). Figure 6-43 shows the Aeq concentrations for the five H01 batch experiments. The smooth lines are the predicted Aeq. Table 6-31 presents the fitted parameters *a*, *b*, and *c* for Equation 6-12.

Table 6-31. Values of the parameters *a*, *b*, and *c* fitted by least squares analysis for Site H inocula H01.

Substrate Concentration (g/L)	*a* (g/L liquid)	*b* (g/(L liquid·d))	*c* (d^{-1})
20	2.219	0.250	0.100
40	0.877	1.45	0.200
70	2.32	1.73	0.100
100	2.29	0.840	0.010
100+	21.24	0.502	0.066

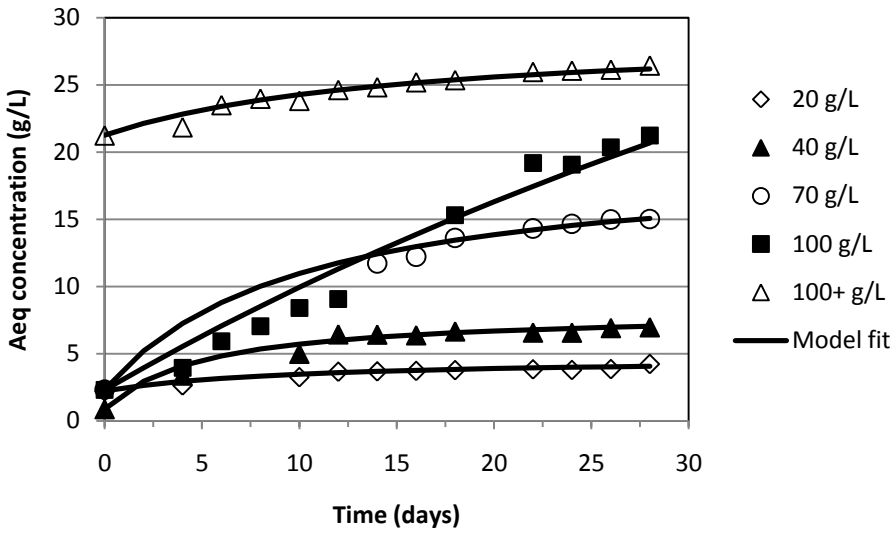

Figure 6-43. Aeq concentration for H01 inoculated paper/yeast extract fermentation at 20, 40, 70, 100, and 100+ g substrate/L liquid with calcium carbonate.

The reaction rate and the specific reaction rate for the batch fermentations were calculated using Equations 6-13 and 6-14. Conversion was calculated with the experimental acetic acid equivalents using Equation 6-15. Parameters *e*, *f*, *g*, and *h* presented in the predicted rate equation (Equation 6-31) were calculated by nonlinear regression. Figure 6-44 compares the predicted specific rate with the experimental specific rate. The specific rate equation for Site H inocula H01 follows:

$$\hat{r}_{pred} = \frac{0.018(1-x)^{3.32}}{1 + 0.00100(\emptyset \cdot \text{Aeq})^{2.77}} \tag{6-31}$$

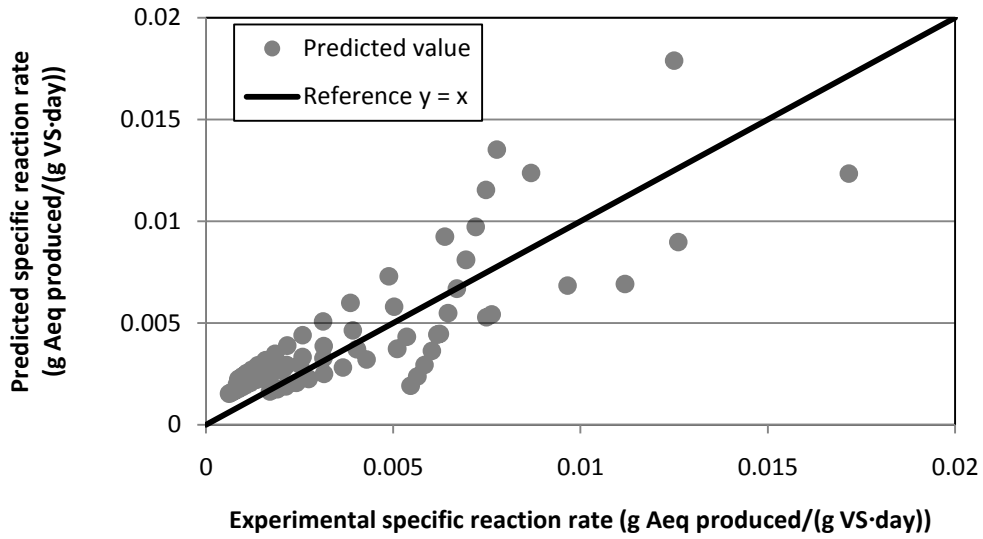

Figure 6-44. The experimental value and the CPDM prediction value for the specific reaction rate in five batch paper/yeast extract fermentation with H01 inocula.

Table 6-32. Parameter constant values in CPDM for Site H inocula H01.

Parameter constant	Value
Holdup (g liquid/g VS cake)	2.0
Moisture (g liquid/ g solid feed)	0.06
Selectivity (g Aeq/g VS digested)	0.32
F1−F4 solid concentration (g VS/L)	169, 214, 214, 214
F1−F4 liquid volume (L)	0.48, 0.28, 0.28, 0.28
ϕ (g total acid/g Aeq)	0.75
e (g Aeq/(g VS·d))	0.018
f (dimensionless)	3.32
g (L/g total acid)$^{1/h}$	0.00100
h (dimensionless)	2.77

Table 6-32 lists the system-specific variables required by the CPDM prediction. Figure 6-45 shows the CPDM "map" for Site H inocula H01 in a 90 wt% paper/10 wt% yeast extract countercurrent fermentation with the single-centrifuge procedure at a fermentation solid concentration of 169 g VS/L liquid. The "map" predicts a total acid concentration of 16.14 g/L at LRT 30 day and VSLR of 12 g/(L·d), and a conversion of 0.28 g VS digested/g VS fed. At a VSLR of 4 g/(L·d) and LRT of 10 days, total acid concentration is 11.02 g/L and conversion is 0.53 g VS digested/g VS fed.

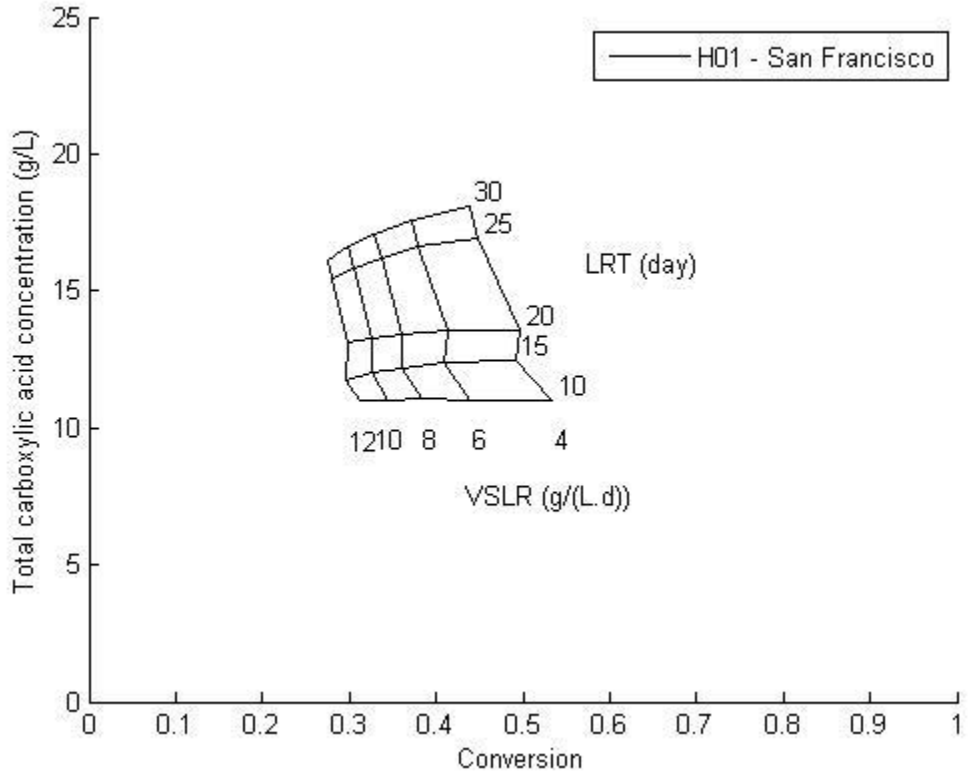

Figure 6-45. The CPDM "map" for 90 wt% paper/10 wt% yeast extract with H01 inocula.

6.5.16 Sample H20 from Site H – San Francisco, CA

As mentioned in Section 6-3, batch experiments with 90 wt% paper /10 wt% yeast extract were done to obtain model parameters for the CPDM method. The inocula for these fermentations were taken from the post reactor material of the initial screening then preserved in a 20% glycerol solution. Calcium carbonate was used to adjust the pH. Liquid samples from the fermentations were analyzed for carboxylic acids. Using Equation 6-11, the acids were converted to acetic acid equivalents (Aeq). Figure 6-46 shows the Aeq concentrations for the five H20 batch experiments. The smooth lines are the predicted Aeq. Table 6-33 presents the fitted parameters *a*, *b*, and *c* for Equation 6-12.

Table 6-33. Values of the parameters *a*, *b*, and *c* fitted by least squares analysis for Site H inocula H20.

Substrate Concentration (g/L)	*a* (g/L liquid)	*b* (g/(L liquid·d))	*c* (d^{-1})
20	1.818	0.145	0.010
40	1.938	0.635	0.013
70	1.743	1.71	0.070
100	2.05	1.28	0.013
100+	16.48	0.442	0.010

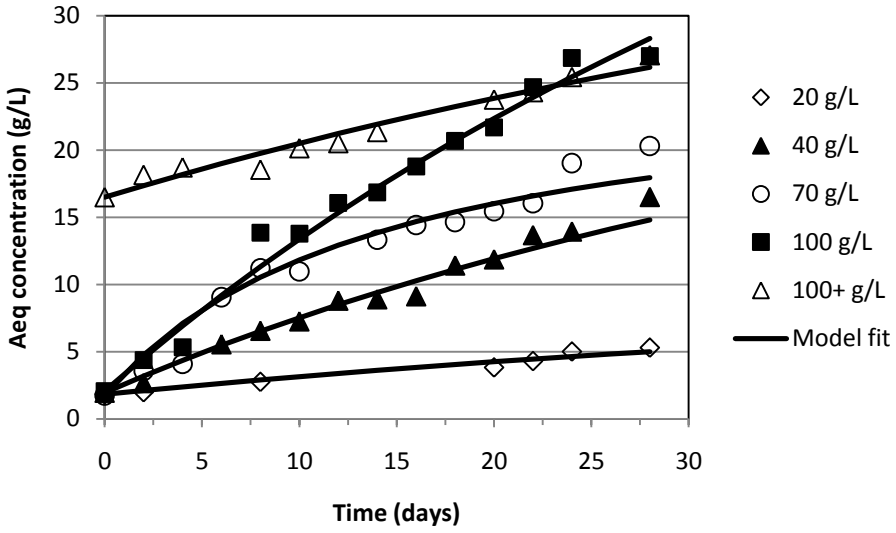

Figure 6-46. Aeq concentration for H20 inoculated paper/yeast extract fermentation at 20, 40, 70, 100, and 100+ g substrate/L liquid with calcium carbonate.

The reaction rate and the specific reaction rate for the batch fermentations were calculated using Equations 6-13 and 6-14. Conversion was calculated with the experimental acetic acid equivalents using Equation 6-15. Parameters *e*, *f*, *g*, and *h* presented in the predicted rate equation (Equation 6-32) were calculated by nonlinear regression. Figure 6-47 compares the predicted specific rate with the experimental specific rate. The specific rate equation for Site H inocula H20 follows:

$$\hat{r}_{pred} = \frac{0.014(1-x)^{1.00}}{1 + 0.00100(\emptyset \cdot \text{Aeq})^{2.525}} \tag{6-32}$$

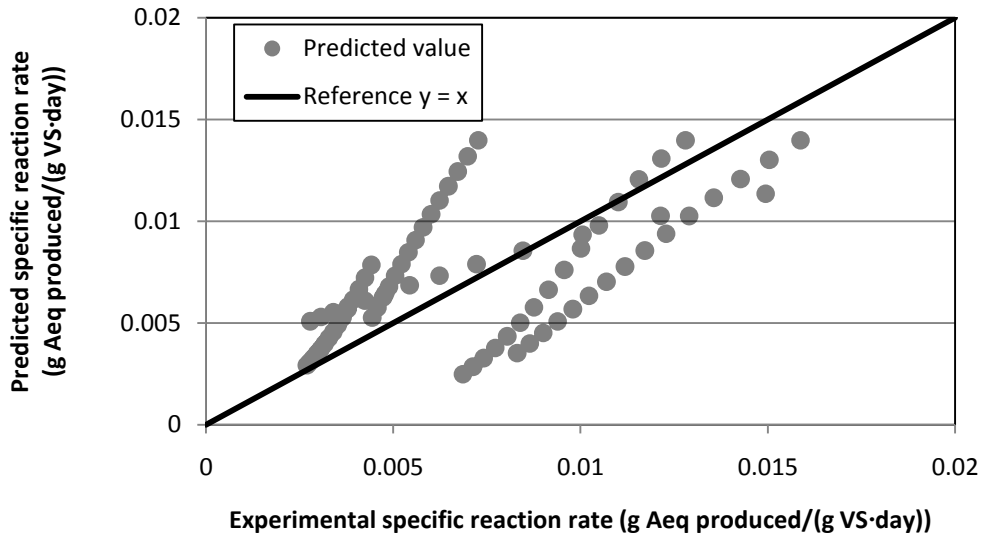

Figure 6-47. The experimental value and the CPDM prediction value for the specific reaction rate in five batch paper/yeast extract fermentation with H20 inocula.

Table 6-34. Parameter constant values in CPDM for Site H inocula H20.

Parameter constant	Value
Holdup (g liquid/g VS cake)	2.0
Moisture (g liquid/ g solid feed)	0.06
Selectivity (g Aeq/g VS digested)	0.42
F1−F4 solid concentration (g VS/L)	169, 214, 214, 214
F1−F4 liquid volume (L)	0.48, 0.28, 0.28, 0.28
ϕ (g total acid/g Aeq)	0.71
e (g Aeq/(g VS·d))	0.014
f (dimensionless)	1.00
g (L/g total acid)$^{1/h}$	0.00100
h (dimensionless)	2.525

Table 6-34 lists the system-specific variables required by the CPDM prediction. Figure 6-48 shows the CPDM "map" for Site H inocula H20 in a 90 wt% paper/10 wt% yeast extract countercurrent fermentation with the single-centrifuge procedure at a fermentation solid concentration of 169 g VS/L liquid. The "map" predicts a total acid concentration of 20.39 g/L at LRT 30 day and VSLR of 12 g/(L·d), and a conversion of 0.29 g VS digested/g VS fed. At a VSLR of 4 g/(L·d) and LRT of 10 days, total acid concentration is 16.34 g/L and conversion is 0.53 g VS digested/g VS fed.

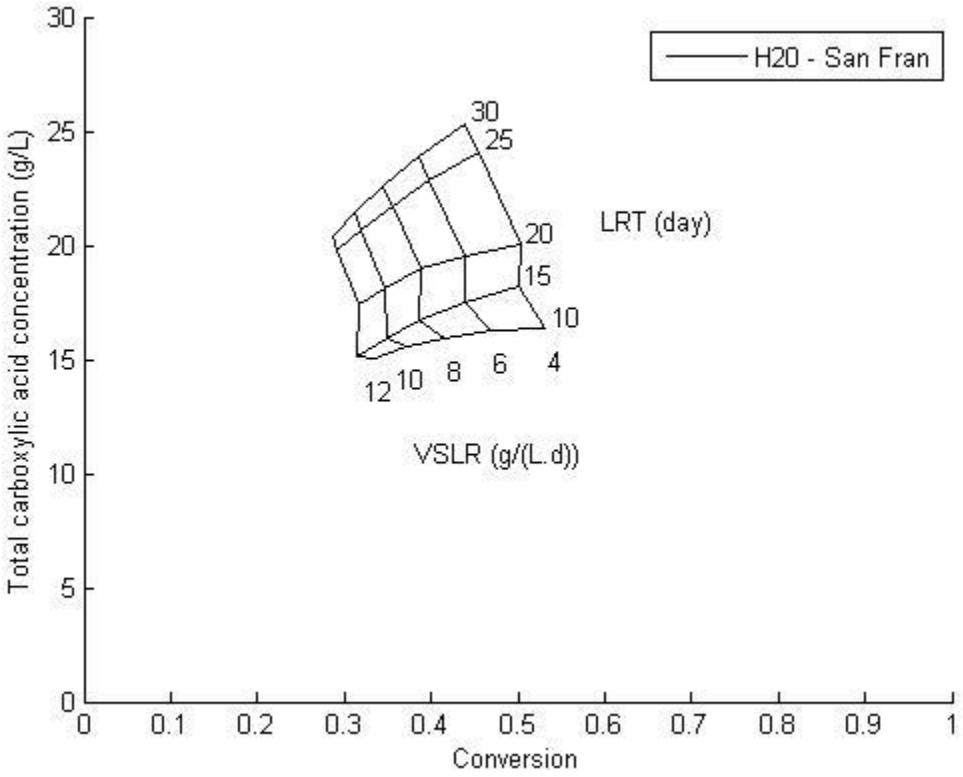

Figure 6-48. The CPDM "map" for 90 wt% paper/10 wt% yeast extract with H20 inocula.

6.5.17 Sample J04 from Site J – Big Bend National Forest, TX

As mentioned in Section 6-3, batch experiments with 90 wt% paper /10 wt% yeast extract were done to obtain model parameters for the CPDM method. The inocula for these fermentations were taken from the post reactor material of the initial screening then preserved in a 20% glycerol solution. Calcium carbonate was used to adjust the pH. Liquid samples from the fermentations were analyzed for carboxylic acids. Using Equation 6-11, the acids were converted to acetic acid equivalents (Aeq). Figure 6-49 shows the Aeq concentrations for the five J04 batch experiments. The smooth lines are the predicted Aeq. Table 6-35 presents the fitted parameters *a*, *b*, and *c* for Equation 6-12.

Table 6-35. Values of the parameters *a*, *b*, and *c* fitted by least squares analysis for Site J inocula J04.

Substrate Concentration (g/L)	*a* (g/L liquid)	*b* (g/(L liquid·d))	*c* (d^{-1})
20	1.64	0.169	0.010
40	1.94	0.720	0.100
70	1.88	0.810	0.050
100	2.14	0.700	0.030
100+	19.47	0.507	0.030

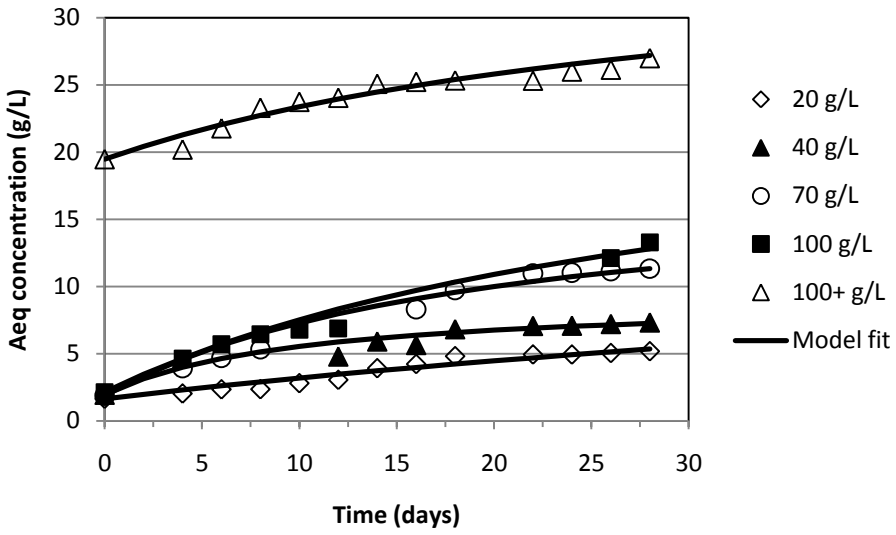

Figure 6-49. Aeq concentration for J04 inoculated paper/yeast extract fermentation at 20, 40, 70, 100, and 100+ g substrate/L liquid with calcium carbonate.

The reaction rate and the specific reaction rate for the batch fermentations were calculated using Equations 6-13 and 6-14. Conversion was calculated with the experimental acetic acid equivalents using Equation 6-15. Parameters *e*, *f*, *g*, and *h* presented in the predicted rate equation (Equation 6-33) were calculated by nonlinear regression. Figure 6-50 compares the predicted specific rate with the experimental specific rate. The specific rate equation for Site J inocula J04 follows:

$$\hat{r}_{pred} = \frac{0.016(1-x)^{1.05}}{1 + 0.344(\emptyset \cdot \text{Aeq})^{0.980}} \tag{6-33}$$

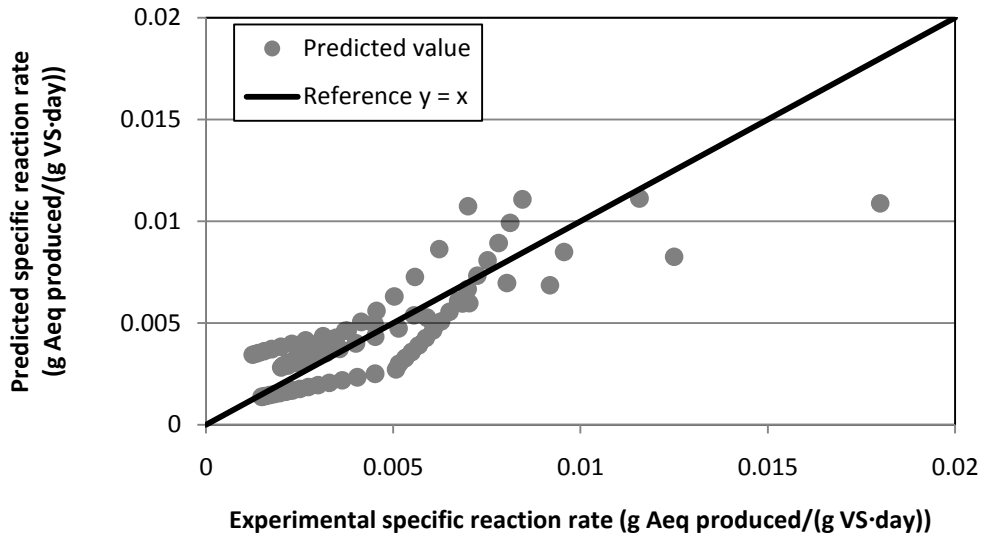

Figure 6-50. The experimental value and the CPDM prediction value for the specific reaction rate in five batch paper/yeast extract fermentation with J04 inocula.

Table 6-36. Parameter constant values in CPDM for Site J inocula J04.

Parameter constant	Value
Holdup (g liquid/g VS cake)	2.0
Moisture (g liquid/ g solid feed)	0.06
Selectivity (g Aeq/g VS digested)	0.33
F1−F4 solid concentration (g VS/L)	169, 214, 214, 214
F1−F4 liquid volume (L)	0.48, 0.28, 0.28, 0.28
ϕ (g total acid/g Aeq)	0.72
e (g Aeq/(g VS·d))	0.016
f (dimensionless)	1.05
g (L/g total acid)$^{1/h}$	0.334
h (dimensionless)	0.980

Table 6-36 lists the system-specific variables required by the CPDM prediction. Figure 6-51 shows the CPDM "map" for Site J inocula J04 in a 90 wt% paper/10 wt% yeast extract countercurrent fermentation with the single-centrifuge procedure at a fermentation solid concentration of 169 g VS/L liquid. The "map" predicts a total acid concentration of 12.08 g/L at LRT 30 day and VSLR of 12 g/(L·d), and a conversion of 0.24 g VS digested/g VS fed. At a VSLR of 4 g/(L·d) and LRT of 10 days, total acid concentration is 12.36 g/L and conversion is 0.56 g VS digested/g VS fed.

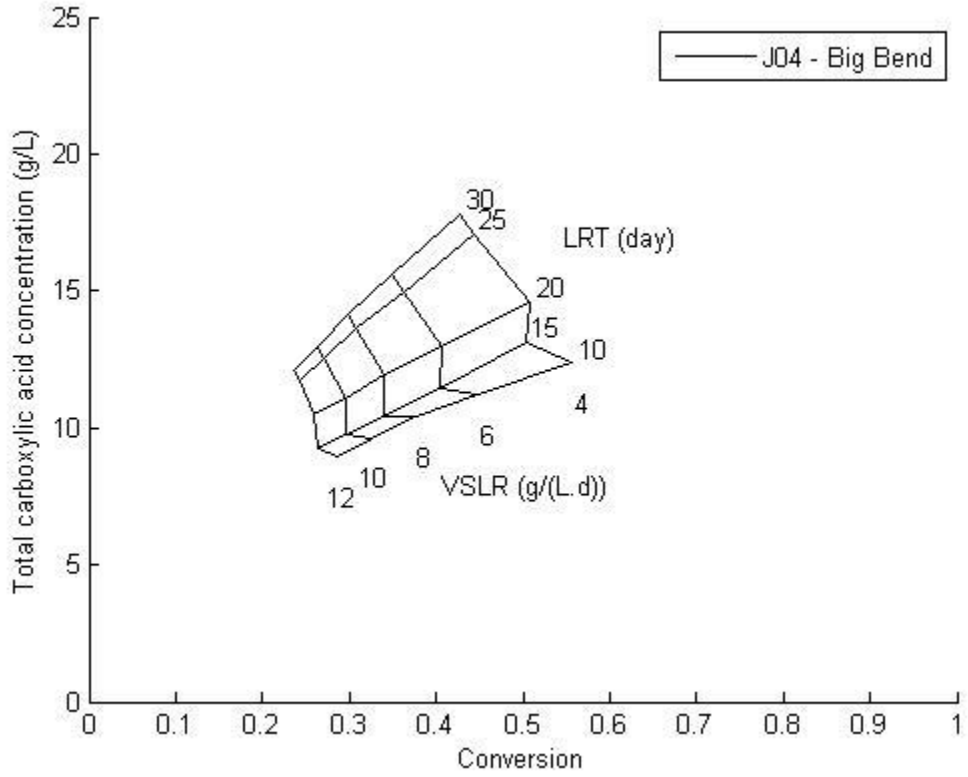

Figure 6-51. The CPDM "map" for 90 wt% paper/10 wt% yeast extract with J04 inocula.

6.5.18 Sample J11 from Site J – Big Bend National Forest, TX

As mentioned in Section 6-3, batch experiments with 90 wt% paper /10 wt% yeast extract were done to obtain model parameters for the CPDM method. The inocula for these fermentations were taken from the post reactor material of the initial screening then preserved in a 20% glycerol solution. Calcium carbonate was used to adjust the pH. Liquid samples from the fermentations were analyzed for carboxylic acids. Using Equation 6-11, the acids were converted to acetic acid equivalents (Aeq). Figure 6-52 shows the Aeq concentrations for the five J11 batch experiments. The smooth lines are the predicted Aeq. Table 6-37 presents the fitted parameters *a*, *b*, and *c* for Equation 6-12.

Table 6-37. Values of the parameters *a*, *b*, and *c* fitted by least squares analysis for Site J inocula J11.

Substrate Concentration (g/L)	*a* (g/L liquid)	*b* (g/(L liquid·d))	*c* (d^{-1})
20	1.87	0.036	0.010
40	2.13	0.456	0.096
70	2.07	0.780	0.050
100	2.11	1.271	0.030
100+	20.63	0.888	0.084

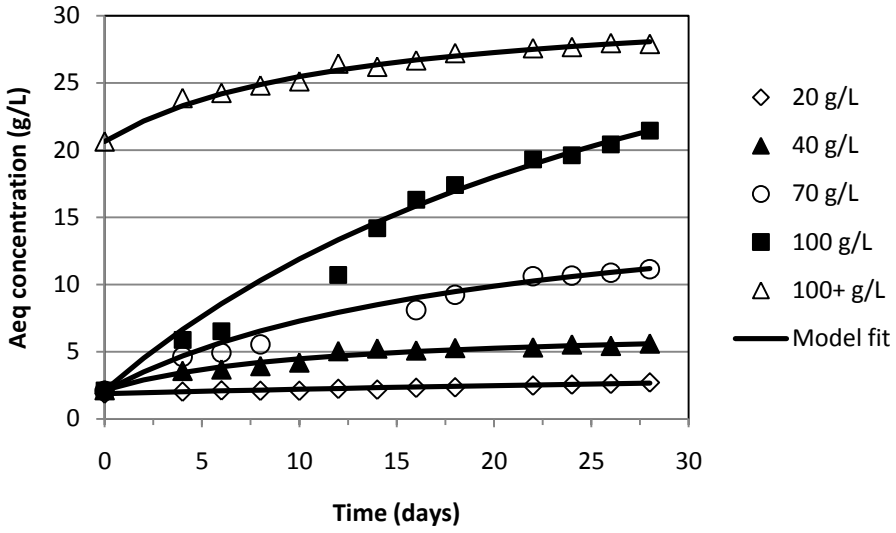

Figure 6-52. Aeq concentration for J11 inoculated paper/yeast extract fermentation at 20, 40, 70, 100, and 100+ g substrate/L liquid with calcium carbonate.

The reaction rate and the specific reaction rate for the batch fermentations were calculated using Equations 6-13 and 6-14. Conversion was calculated with the experimental acetic acid equivalents using Equation 6-15. Parameters *e*, *f*, *g*, and *h* presented in the predicted rate equation (Equation 6-34) were calculated by nonlinear regression. Figure 6-53 compares the predicted specific rate with the experimental specific rate. The specific rate equation for Site J inocula J11 follows:

$$\hat{r}_{pred} = \frac{0.0079(1-x)^{3.144}}{1 + 0.00100(\emptyset \cdot \text{Aeq})^{1.943}} \tag{6-34}$$

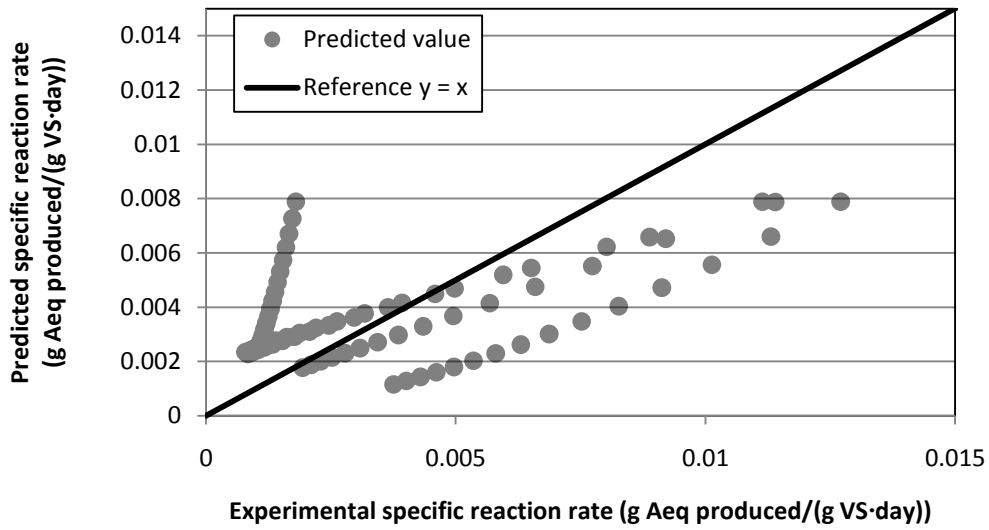

Figure 6-53. The experimental value and the CPDM prediction value for the specific reaction rate in five batch paper/yeast extract fermentation with J11 inocula.

Table 6-38. Parameter constant values in CPDM for Site J inocula J11.

Parameter constant	Value
Holdup (g liquid/g VS cake)	2.0
Moisture (g liquid/ g solid feed)	0.06
Selectivity (g Aeq/g VS digested)	0.30
F1−F4 solid concentration (g VS/L)	169, 214, 214, 214
F1−F4 liquid volume (L)	0.48, 0.28, 0.28, 0.28
ϕ (g total acid/g Aeq)	0.73
e (g Aeq/(g VS·d))	0.0079
f (dimensionless)	3.144
g (L/g total acid)$^{1/h}$	0.00100
h (dimensionless)	1.943

Table 6-38 lists the system-specific variables required by the CPDM prediction. Figure 6-54 shows the CPDM "map" for Site J inocula J11 in a 90 wt% paper/10 wt% yeast extract countercurrent fermentation with the single-centrifuge procedure at a fermentation solid concentration of 169 g VS/L liquid. The "map" predicts a total acid concentration of 12.62 g/L at LRT 30 day and VSLR of 12 g/(L·d), and a conversion of 0.23 g VS digested/g VS fed. At a VSLR of 4 g/(L·d) and LRT of 10 days, total acid concentration is 9.91 g/L and conversion is 0.47 g VS digested/g VS fed.

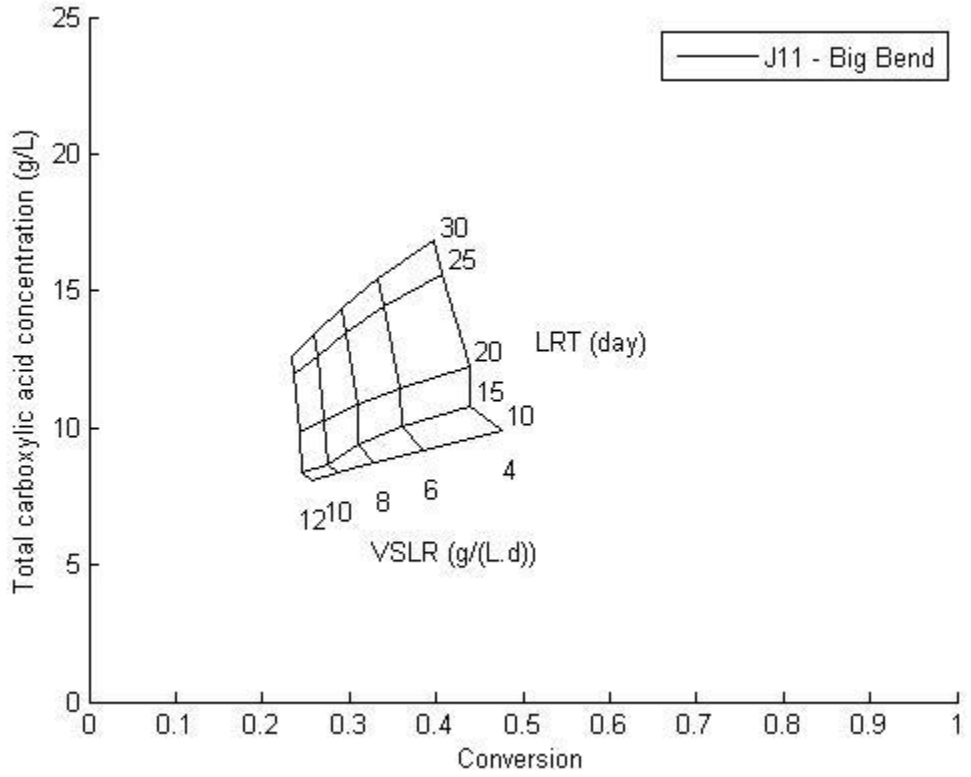

Figure 6-54. The CPDM "map" for 90 wt% paper/10 wt% yeast extract with J11 inocula.

6.5.19 Sample J19 from Site J – Big Bend National Forest, TX

As mentioned in Section 6-3, batch experiments with 90 wt% paper /10 wt% yeast extract were done to obtain model parameters for the CPDM method. The inocula for these fermentations were taken from the post reactor material of the initial screening then preserved in a 20% glycerol solution. Calcium carbonate was used to adjust the pH. Liquid samples from the fermentations were analyzed for carboxylic acids. Using Equation 6-11, the acids were converted to acetic acid equivalents (Aeq). Figure 6-55 shows the Aeq concentrations for the five J19 batch experiments. The smooth lines are the predicted Aeq. Table 6-39 presents the fitted parameters *a*, *b*, and *c* for Equation 6-12.

Table 6-39. Values of the parameters *a*, *b*, and *c* fitted by least squares analysis for Site J inocula J19.

Substrate Concentration (g/L)	*a* (g/L liquid)	*b* (g/(L liquid·d))	*c* (d^{-1})
20	1.78	0.099	0.010
40	1.87	0.756	0.100
70	1.85	2.96	0.200
100	1.83	0.879	0.037
100+	19.75	2.92	0.390

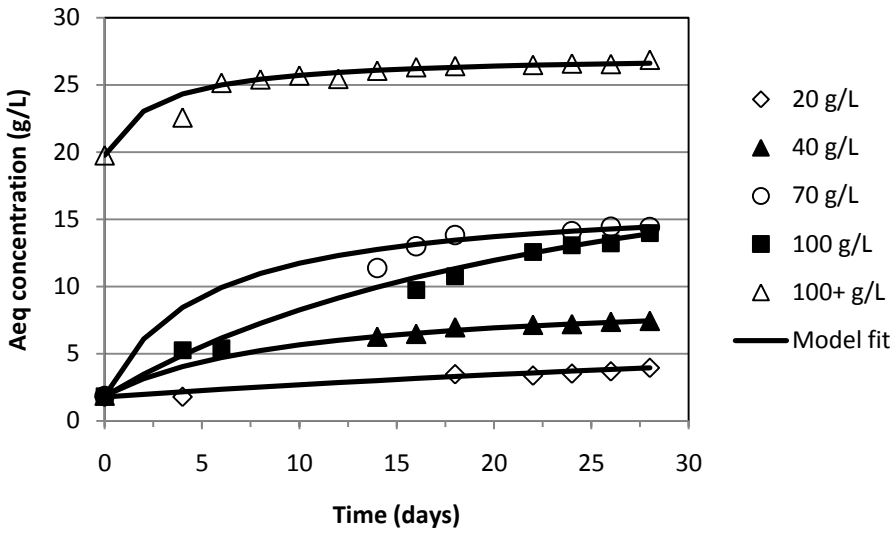

Figure 6-55. Aeq concentration for J19 inoculated paper/yeast extract fermentation at 20, 40, 70, 100, and 100+ g substrate/L liquid with calcium carbonate.

The reaction rate and the specific reaction rate for the batch fermentations were calculated using Equations 6-13 and 6-14. Conversion was calculated with the experimental acetic acid equivalents using Equation 6-15. Parameters *e*, *f*, *g*, and *h* presented in the predicted rate equation (Equation 6-35) were calculated by nonlinear regression. Figure 6-56 compares the predicted specific rate with the experimental specific rate. The specific rate equation for Site J inocula J19 follows:

$$\hat{r}_{pred} = \frac{0.016(1-x)^{5.03}}{1 + 0.00100(\emptyset \cdot \text{Aeq})^{2.28}} \tag{6-35}$$

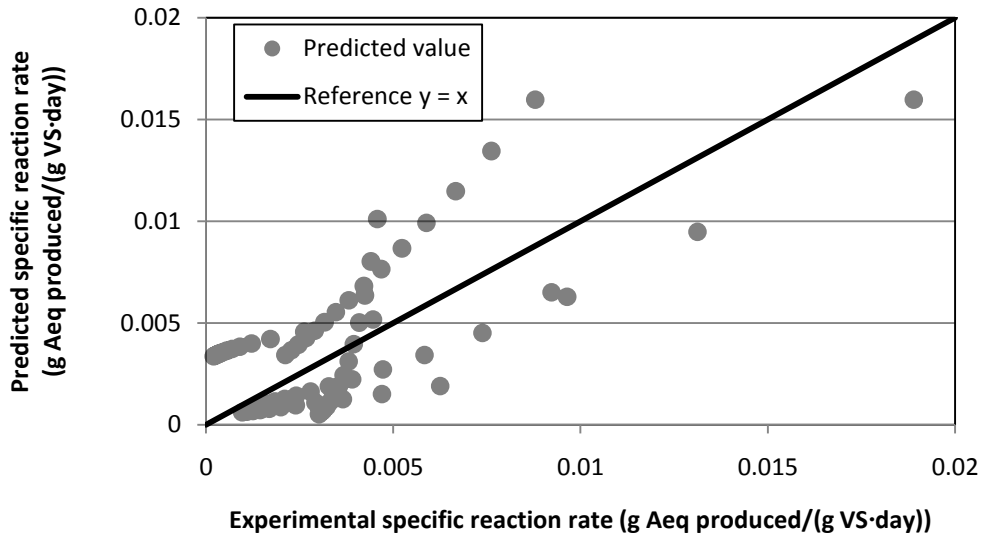

Figure 6-56. The experimental value and the CPDM prediction value for the specific reaction rate in five batch paper/yeast extract fermentation with J19 inocula.

Table 6-40. Parameter constant values in CPDM for Site J inocula J19.

Parameter constant	Value
Holdup (g liquid/g VS cake)	2.0
Moisture (g liquid/ g solid feed)	0.06
Selectivity (g Aeq/g VS digested)	0.36
F1−F4 solid concentration (g VS/L)	169, 214, 214, 214
F1−F4 liquid volume (L)	0.48, 0.28, 0.28, 0.28
ϕ (g total acid/g Aeq)	0.69
e (g Aeq/(g VS·d))	0.016
f (dimensionless)	5.03
g (L/g total acid)$^{1/h}$	0.00100
h (dimensionless)	2.28

Table 6-40 lists the system-specific variables required by the CPDM prediction. Figure 6-57 shows the CPDM "map" for Site J inocula J19 in a 90 wt% paper/10 wt% yeast extract countercurrent fermentation with the single-centrifuge procedure at a fermentation solid concentration of 169 g VS/L liquid. The "map" predicts a total acid concentration of 16.07 g/L at LRT 30 day and VSLR of 12 g/(L·d), and a conversion of 0.22 g VS digested/g VS fed. At a VSLR of 4 g/(L·d) and LRT of 10 days, total acid concentration is 10.09 g/L and conversion is 0.42 g VS digested/g VS fed.

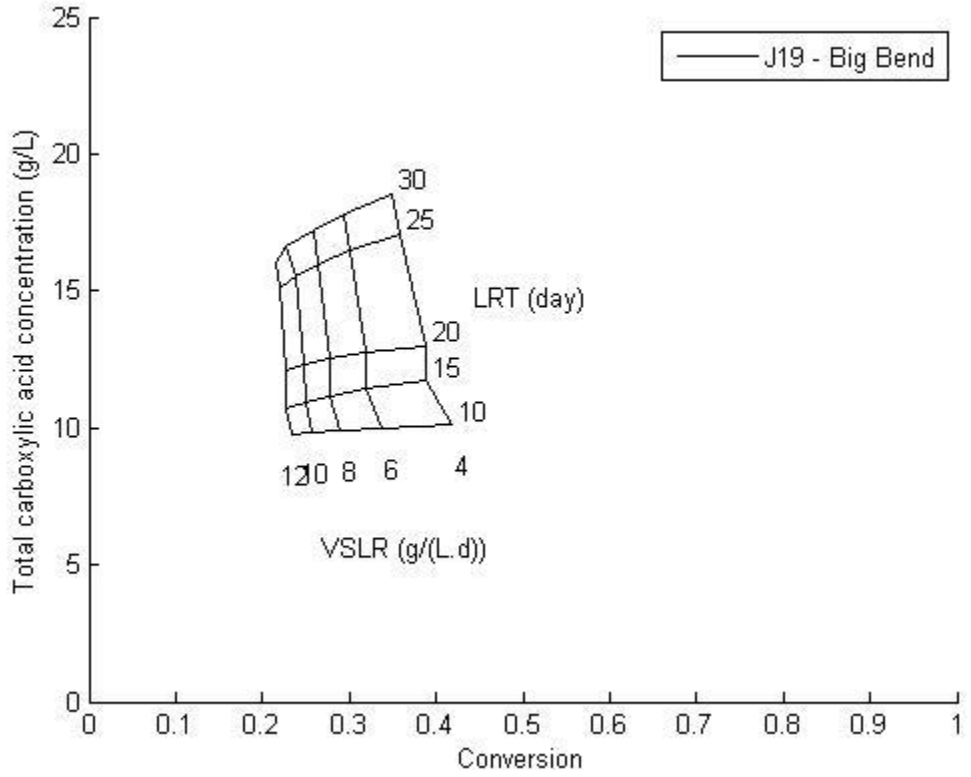

Figure 6-57. The CPDM "map" for 90 wt% paper/10 wt% yeast extract with J19 inocula.

6.5.20 Sample K49 from Site K – Utah1

As mentioned in Section 6-3, batch experiments with 90 wt% paper /10 wt% yeast extract were done to obtain model parameters for the CPDM method. The inocula for these fermentations were taken from the post reactor material of the initial screening then preserved in a 20% glycerol solution. Calcium carbonate was used to adjust the pH. Liquid samples from the fermentations were analyzed for carboxylic acids. Using Equation 6-11, the acids were converted to acetic acid equivalents (Aeq). Figure 6-58 shows the Aeq concentrations for the five K49 batch experiments. The smooth lines are the predicted Aeq. Table 6-41 presents the fitted parameters *a*, *b*, and *c* for Equation 6-12.

Table 6-41. Values of the parameters *a*, *b*, and *c* fitted by least squares analysis for Site K inocula K49.

Substrate Concentration (g/L)	*a* (g/L liquid)	*b* (g/(L liquid·d))	*c* (d^{-1})
20	1.93	0.28	0.020
40	2.03	2.16	0.020
70	2.06	5.55	0.020
100	2.14	1.38	0.030
100+	20.52	0.76	0.050

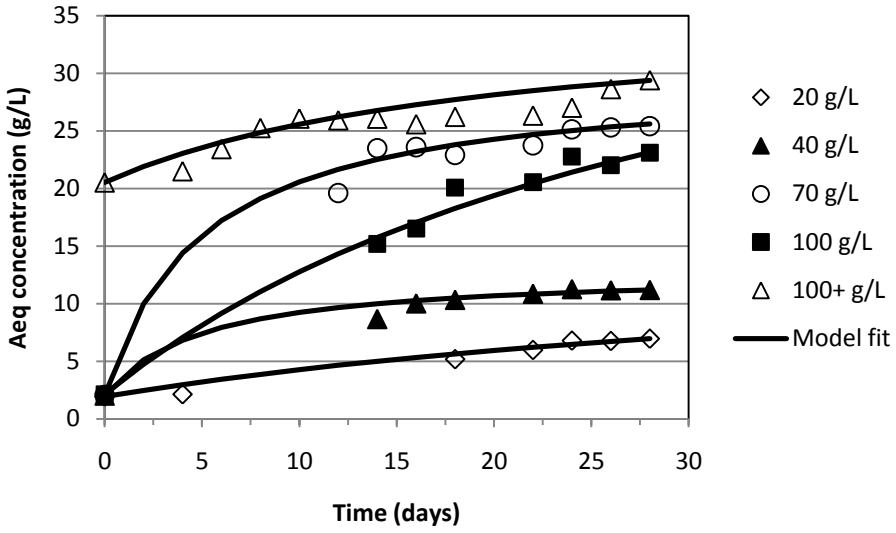

Figure 6-58. Aeq concentration for K49 inoculated paper/yeast extract fermentation at 20, 40, 70, 100, and 100+ g substrate/L liquid with calcium carbonate.

The reaction rate and the specific reaction rate for the batch fermentations were calculated using Equations 6-13 and 6-14. Conversion was calculated with the experimental acetic acid equivalents using Equation 6-15. Parameters *e*, *f*, *g*, and *h* presented in the predicted rate equation (Equation 6-36) were calculated by nonlinear regression. Figure 6-59 compares the predicted specific rate with the experimental specific rate. The specific rate equation for Site K inocula K49 follows:

$$\hat{r}_{pred} = \frac{0.057(1-x)^{1.442}}{1 + 0.473(\emptyset \cdot \text{Aeq})^{1.00}} \tag{6-36}$$

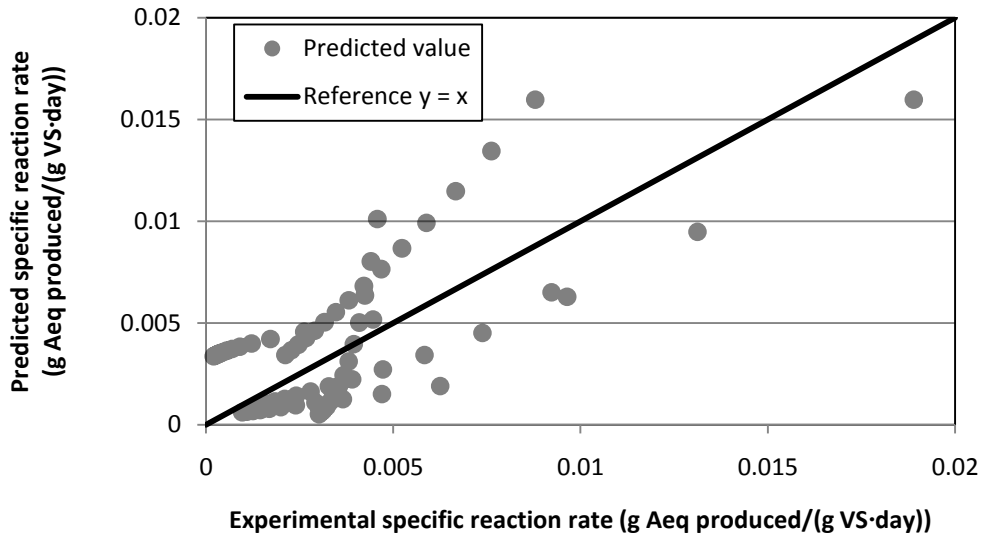

Figure 6-59. The experimental value and the CPDM prediction value for the specific reaction rate in five batch paper/yeast extract fermentation with K49 inocula.

Table 6-42. Parameter constant values in CPDM for Site K inocula K49.

Parameter constant	Value
Holdup (g liquid/g VS cake)	2.0
Moisture (g liquid/ g solid feed)	0.06
Selectivity (g Aeq/g VS digested)	0.44
F1−F4 solid concentration (g VS/L)	169, 214, 214, 214
F1−F4 liquid volume (L)	0.48, 0.28, 0.28, 0.28
ϕ (g total acid/g Aeq)	0.68
e (g Aeq/(g VS·d))	0.057
f (dimensionless)	1.442
g (L/g total acid)$^{1/h}$	0.473
h (dimensionless)	1.00

Table 6-42 lists the system-specific variables required by the CPDM prediction. Figure 6-60 shows the CPDM "map" for Site K inocula K49 in a 90 wt% paper/10 wt% yeast extract countercurrent fermentation with the single-centrifuge procedure at a fermentation solid concentration of 169 g VS/L liquid. The "map" predicts a total acid concentration of 20.24 g/L at LRT 30 day and VSLR of 12 g/(L·d), and a conversion of 0.28 g VS digested/g VS fed. At a VSLR of 4 g/(L·d) and LRT of 10 days, total acid concentration is 15.21 g/L and conversion is 0.52 g VS digested/g VS fed.

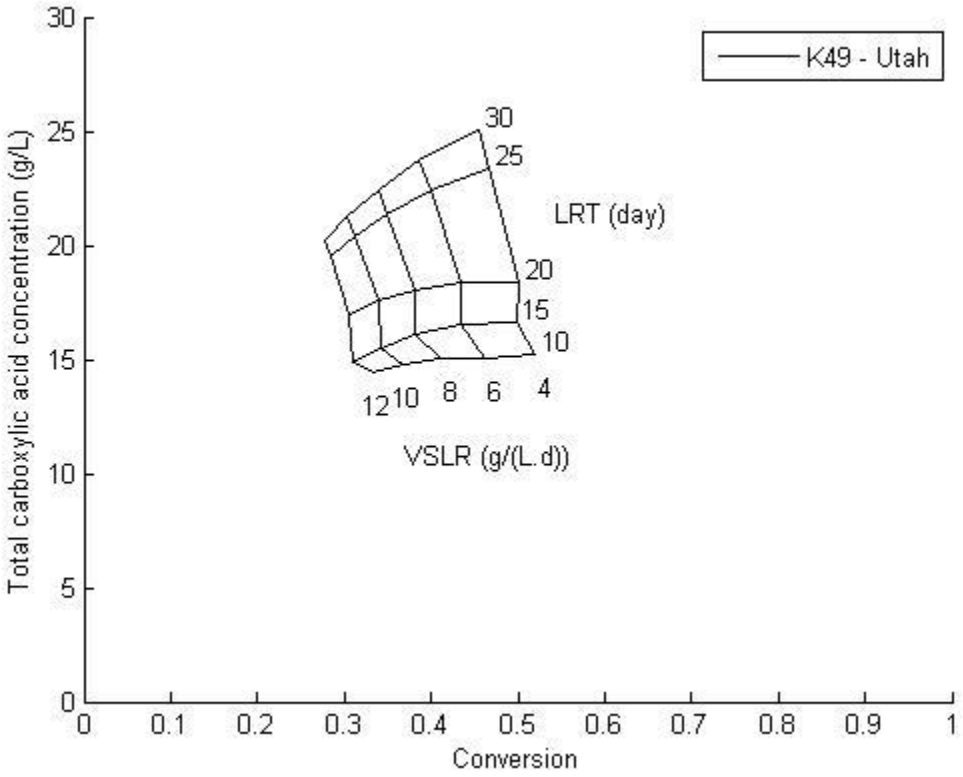

Figure 6-60. The CPDM "map" for 90 wt% paper/10 wt% yeast extract with K49 inocula.

6.5.21 Sample L10 from Site L – Utah2

As mentioned in Section 6-3, batch experiments with 90 wt% paper /10 wt% yeast extract were done to obtain model parameters for the CPDM method. The inocula for these fermentations were taken from the post reactor material of the initial screening then preserved in a 20% glycerol solution. Calcium carbonate was used to adjust the pH. Liquid samples from the fermentations were analyzed for carboxylic acids. Using Equation 6-11, the acids were converted to acetic acid equivalents (Aeq). Figure 6-61 shows the Aeq concentrations for the five L10 batch experiments. The smooth lines are the predicted Aeq. Table 6-43 presents the fitted parameters *a*, *b*, and *c* for Equation 6-12.

Table 6-43. Values of the parameters *a*, *b*, and *c* fitted by least squares analysis for Site L inocula L10.

Substrate Concentration (g/L)	*a* (g/L liquid)	*b* (g/(L liquid·d))	*c* (d^{-1})
20	0.98	0.405	0.116
40	1.93	1.29	0.010
70	1.11	3.32	0.217
100	2.31	1.903	0.099
100+	17.50	0.274	0.010

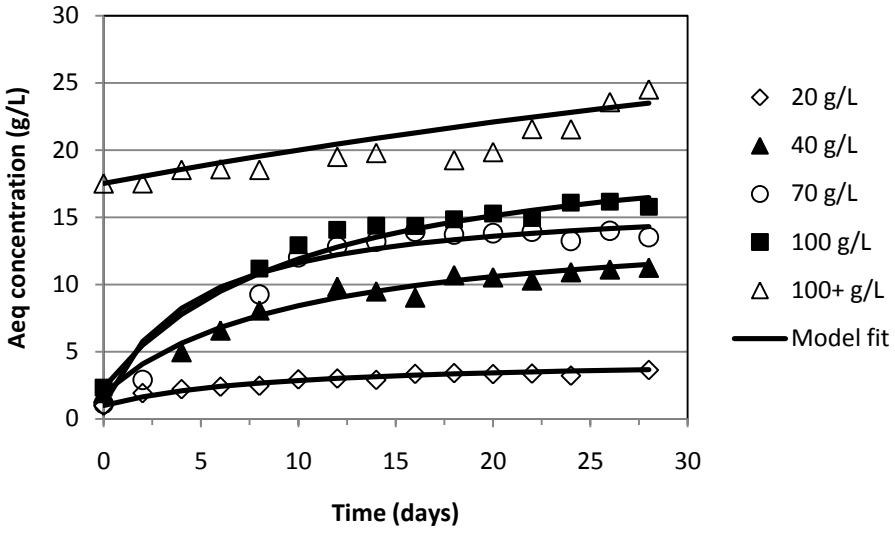

Figure 6-61. Aeq concentration for L10 inoculated paper/yeast extract fermentation at 20, 40, 70, 100, and 100+ g substrate/L liquid with calcium carbonate.

The reaction rate and the specific reaction rate for the batch fermentations were calculated using Equations 6-13 and 6-14. Conversion was calculated with the experimental acetic acid equivalents using Equation 6-15. Parameters *e*, *f*, *g*, and *h* presented in the predicted rate equation (Equation 6-37) were calculated by nonlinear regression. Figure 6-62 compares the predicted specific rate with the experimental specific rate. The specific rate equation for Site L inocula L10 follows:

$$\hat{r}_{pred} = \frac{0.0289(1-x)^{3.979}}{1 + 0.00100(\emptyset \cdot \text{Aeq})^{3.14}} \tag{6-37}$$

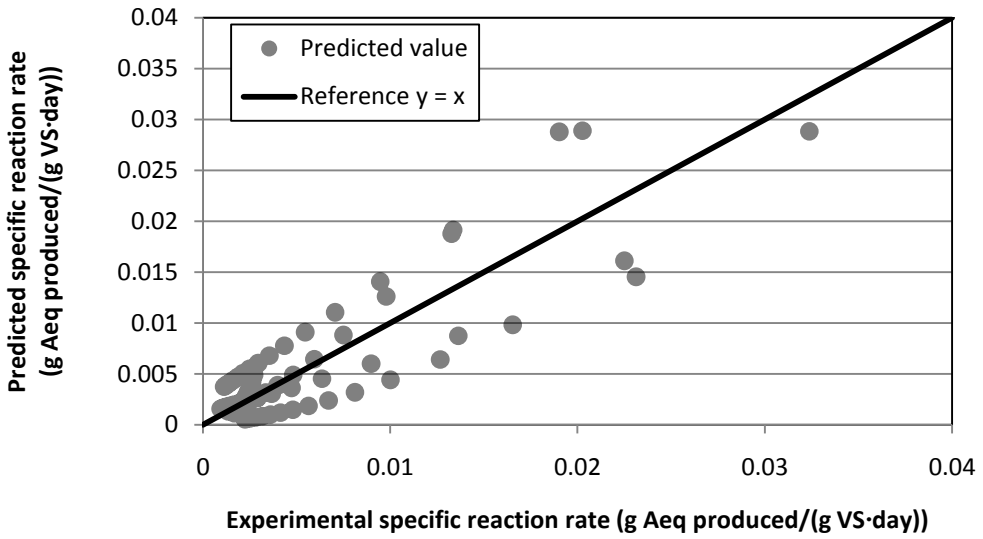

Figure 6-62. The experimental value and the CPDM prediction value for the specific reaction rate in five batch paper/yeast extract fermentation with L10 inocula.

Table 6-44. Parameter constant values in CPDM for Site L inocula L10.

Parameter constant	Value
Holdup (g liquid/g VS cake)	2.0
Moisture (g liquid/ g solid feed)	0.06
Selectivity (g Aeq/g VS digested)	0.39
F1−F4 solid concentration (g VS/L)	169, 214, 214, 214
F1−F4 liquid volume (L)	0.48, 0.28, 0.28, 0.28
ϕ (g total acid/g Aeq)	0.75
e (g Aeq/(g VS·d))	0.0289
f (dimensionless)	3.979
g (L/g total acid)$^{1/h}$	0.00100
h (dimensionless)	3.14

Table 6-44 lists the system-specific variables required by the CPDM prediction. Figure 6-63 shows the CPDM "map" for Site L inocula L10 in a 90 wt% paper/10 wt% yeast extract countercurrent fermentation with the single-centrifuge procedure at a fermentation solid concentration of 169 g VS/L liquid. The "map" predicts a total acid concentration of 16.45 g/L at LRT 30 day and VSLR of 12 g/(L·d), and a conversion of 0.25 g VS digested/g VS fed. At a VSLR of 4 g/(L·d) and LRT of 10 days, total acid concentration is 10.98 g/L and conversion is 0.52 g VS digested/g VS fed.

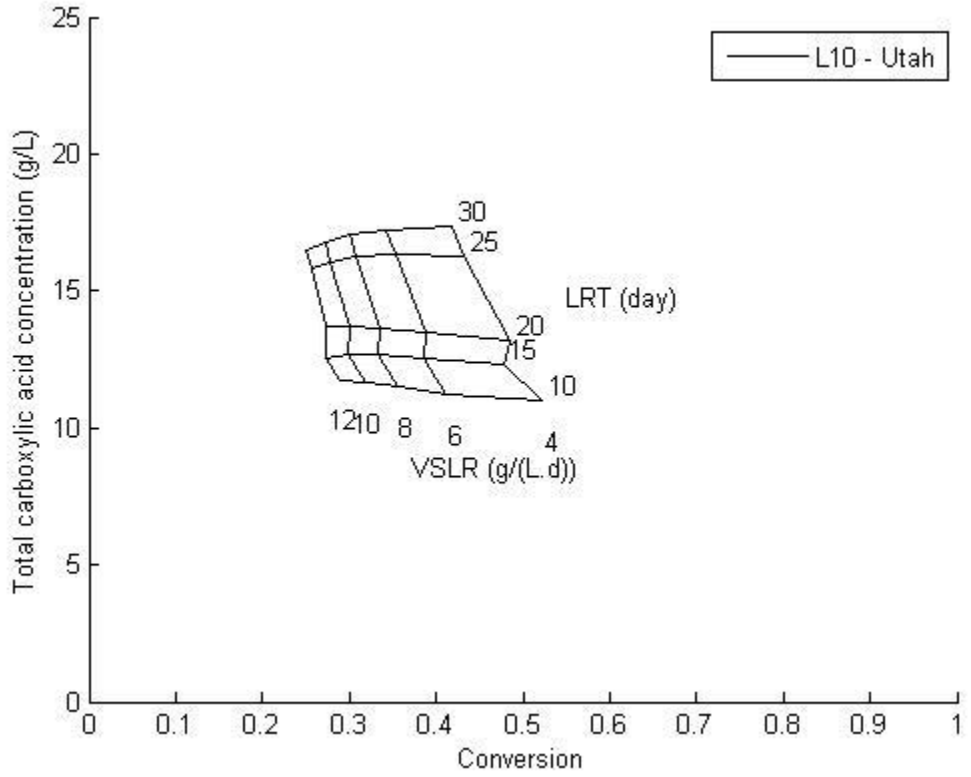

Figure 6-63. The CPDM "map" for 90 wt% paper/10 wt% yeast extract with L10 inocula.

6.5.22 Sample M24 from Site M – Georgia1

As mentioned in Section 6-3, batch experiments with 90 wt% paper /10 wt% yeast extract were done to obtain model parameters for the CPDM method. The inocula for these fermentations were taken from the post reactor material of the initial screening then preserved in a 20% glycerol solution. Calcium carbonate was used to adjust the pH. Liquid samples from the fermentations were analyzed for carboxylic acids. Using Equation 6-11, the acids were converted to acetic acid equivalents (Aeq). Figure 6-64 shows the Aeq concentrations for the five M24 batch experiments. The smooth lines are the predicted Aeq. Table 6-45 presents the fitted parameters *a*, *b*, and *c* for Equation 6-12.

Table 6-45. Values of the parameters *a*, *b*, and *c* fitted by least squares analysis for Site M inocula M24.

Substrate Concentration (g/L)	*a* (g/L liquid)	*b* (g/(L liquid·d))	*c* (d^{-1})
20	2.08	0.327	0.105
40	2.13	0.284	0.019
70	2.14	3.17	0.228
100	2.23	2.23	0.118
100+	20.62	0.996	0.078

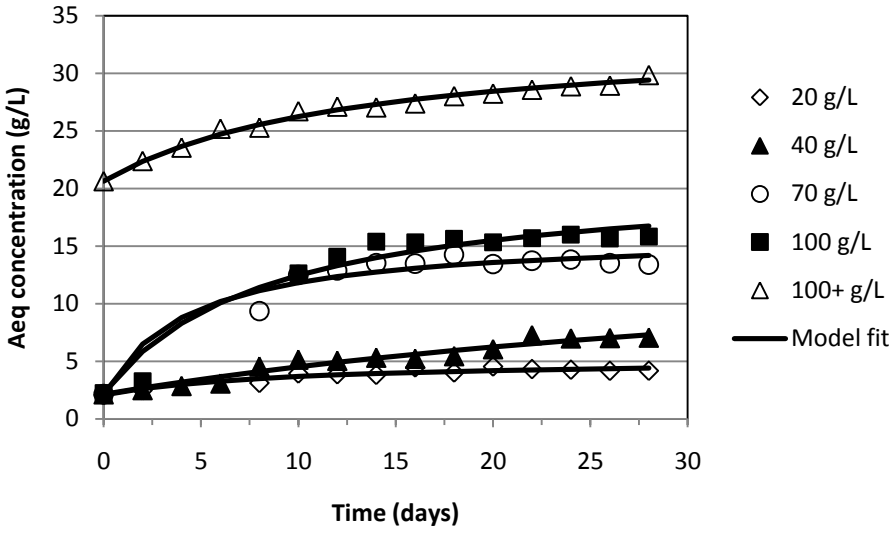

Figure 6-64. Aeq concentration for M24 inoculated paper/yeast extract fermentation at 20, 40, 70, 100, and 100+ g substrate/L liquid with calcium carbonate.

The reaction rate and the specific reaction rate for the batch fermentations were calculated using Equations 6-13 and 6-14. Conversion was calculated with the experimental acetic acid equivalents using Equation 6-15. Parameters *e*, *f*, *g*, and *h* presented in the predicted rate equation (Equation 6-38) were calculated by nonlinear regression. Figure 6-65 compares the predicted specific rate with the experimental specific rate. The specific rate equation for Site M inocula M24 follows:

$$\hat{r}_{pred} = \frac{0.0200(1-x)^{4.652}}{1 + 0.00100(\emptyset \cdot \text{Aeq})^{2.962}} \tag{6-38}$$

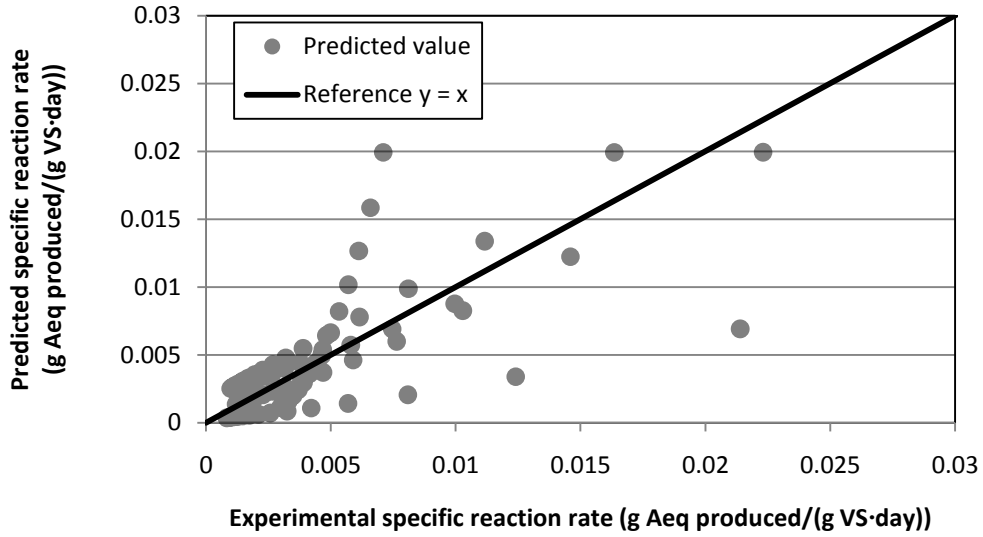

Figure 6-65. The experimental value and the CPDM prediction value for the specific reaction rate in five batch paper/yeast extract fermentation with M24 inocula.

Table 6-46. Parameter constant values in CPDM for Site M inocula M24.

Parameter constant	Value
Holdup (g liquid/g VS cake)	2.0
Moisture (g liquid/ g solid feed)	0.06
Selectivity (g Aeq/g VS digested)	0.41
F1−F4 solid concentration (g VS/L)	169, 214, 214, 214
F1−F4 liquid volume (L)	0.48, 0.28, 0.28, 0.28
ϕ (g total acid/g Aeq)	0.77
e (g Aeq/(g VS·d))	0.0200
f (dimensionless)	4.652
g (L/g total acid)$^{1/h}$	0.00100
h (dimensionless)	2.692

Table 6-46 lists the system-specific variables required by the CPDM prediction. Figure 6-66 shows the CPDM "map" for Site M inocula M24 in a 90 wt% paper/10 wt% yeast extract countercurrent fermentation with the single-centrifuge procedure at a fermentation solid concentration of 169 g VS/L liquid. The "map" predicts a total acid concentration of 16.57 g/L at LRT 30 day and VSLR of 12 g/(L·d), and a conversion of 0.22 g VS digested/g VS fed. At a VSLR of 4 g/(L·d) and LRT of 10 days, total acid concentration is 10.92 g/L and conversion is 0.50 g VS digested/g VS fed.

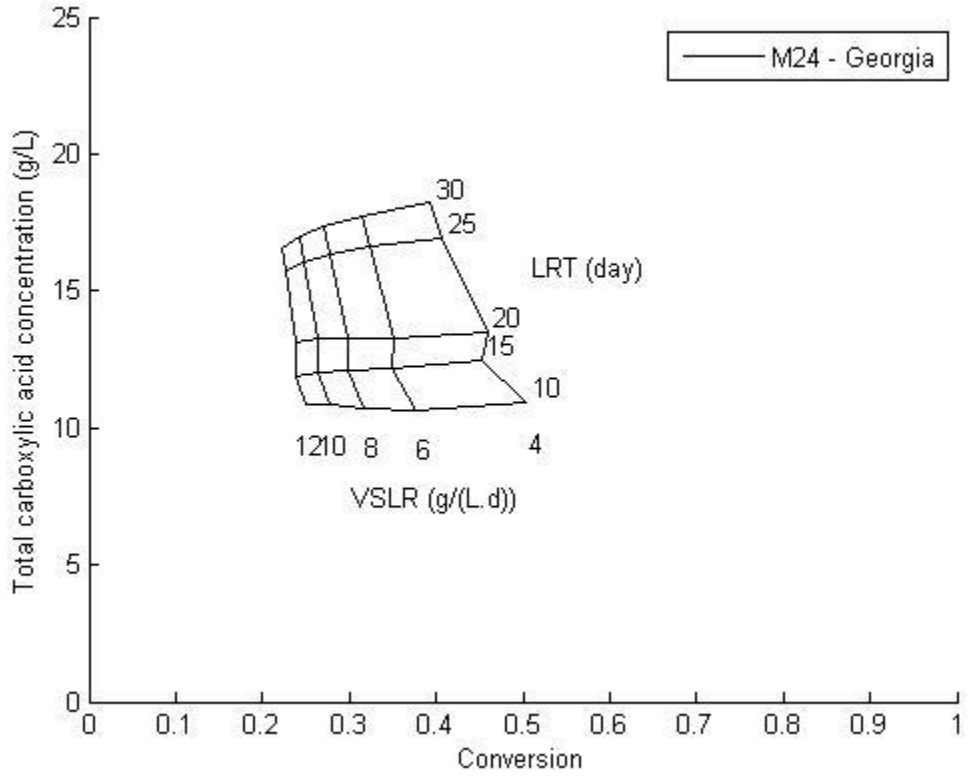

Figure 6-66. The CPDM "map" for 90 wt% paper/10 wt% yeast extract with M24 inocula.

6.5.23 Sample N09 from Site N – Georgia2

As mentioned in Section 6-3, batch experiments with 90 wt% paper /10 wt% yeast extract were done to obtain model parameters for the CPDM method. The inocula for these fermentations were taken from the post reactor material of the initial screening then preserved in a 20% glycerol solution. Calcium carbonate was used to adjust the pH. Liquid samples from the fermentations were analyzed for carboxylic acids. Using Equation 6-11, the acids were converted to acetic acid equivalents (Aeq). Figure 6-67 shows the Aeq concentrations for the five N09 batch experiments. The smooth lines are the predicted Aeq. Table 6-47 presents the fitted parameters *a*, *b*, and *c* for Equation 6-12.

Table 6-47. Values of the parameters *a*, *b*, and *c* fitted by least squares analysis for Site N inocula N09.

Substrate Concentration (g/L)	*a* (g/L liquid)	*b* (g/(L liquid·d))	*c* (d^{-1})
20	1.85	0.125	0.010
40	1.30	0.525	0.030
70	1.63	0.279	0.010
100	1.92	0.693	0.099
100+	15.52	0.368	0.020

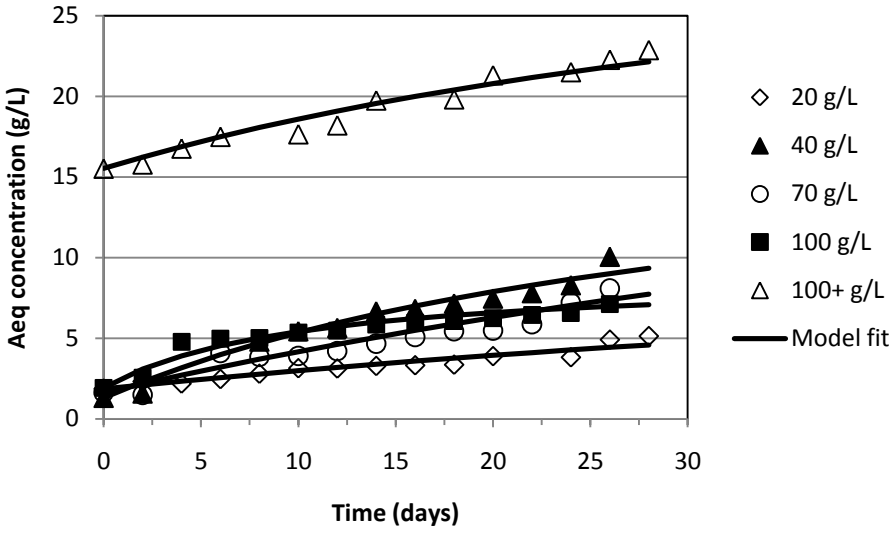

Figure 6-67. Aeq concentration for N09 inoculated paper/yeast extract fermentation at 20, 40, 70, 100, and 100+ g substrate/L liquid with calcium carbonate.

The reaction rate and the specific reaction rate for the batch fermentations were calculated using Equations 6-13 and 6-14. Conversion was calculated with the experimental acetic acid equivalents using Equation 6-15. Parameters *e*, *f*, *g*, and *h* presented in the predicted rate equation (Equation 6-39) were calculated by nonlinear regression. Figure 6-68 compares the predicted specific rate with the experimental specific rate. The specific rate equation for Site N inocula N09 follows:

$$\hat{r}_{pred} = \frac{0.0093(1-x)^{1.00}}{1 + 0.225(\emptyset \cdot \text{Aeq})^{0.950}} \tag{6-39}$$

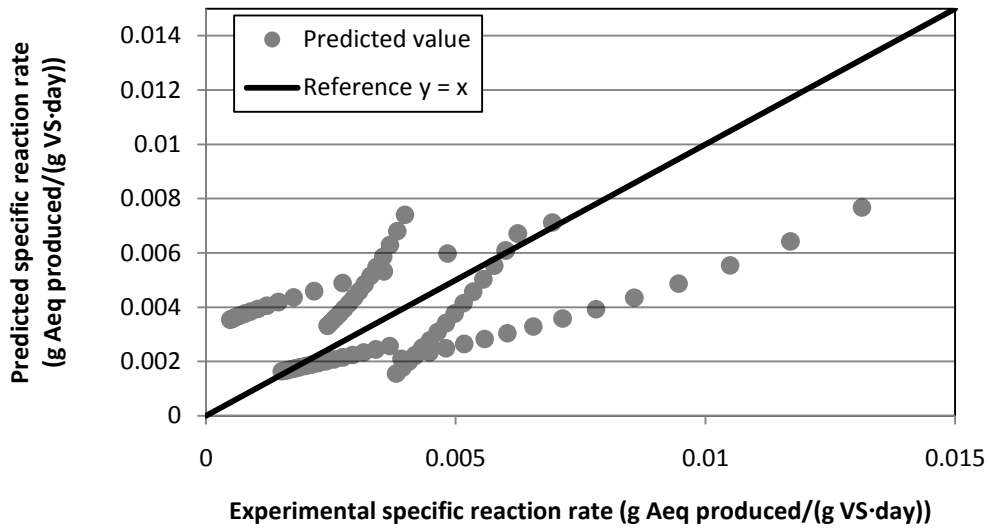

Figure 6-68. The experimental value and the CPDM prediction value for the specific reaction rate in five batch paper/yeast extract fermentation with N09 inocula.

Table 6-48. Parameter constant values in CPDM for Site N inocula N09.

Parameter constant	Value
Holdup (g liquid/g VS cake)	2.0
Moisture (g liquid/ g solid feed)	0.06
Selectivity (g Aeq/g VS digested)	0.32
F1−F4 solid concentration (g VS/L)	169, 214, 214, 214
F1−F4 liquid volume (L)	0.48, 0.28, 0.28, 0.28
ϕ (g total acid/g Aeq)	0.79
e (g Aeq/(g VS·d))	0.0093
f (dimensionless)	1.00
g (L/g total acid)$^{1/h}$	0.225
h (dimensionless)	0.950

Table 6-48 lists the system-specific variables required by the CPDM prediction. Figure 6-69 shows the CPDM "map" for Site N inocula N09 in a 90 wt% paper/10 wt% yeast extract countercurrent fermentation with the single-centrifuge procedure at a fermentation solid concentration of 169 g VS/L liquid. The "map" predicts a total acid concentration of 10.41 g/L at LRT 30 day and VSLR of 12 g/(L·d), and a conversion of 0.22 g VS digested/g VS fed. At a VSLR of 4 g/(L·d) and LRT of 10 days, total acid concentration is 12.08 g/L and conversion is 0.56 g VS digested/g VS fed.

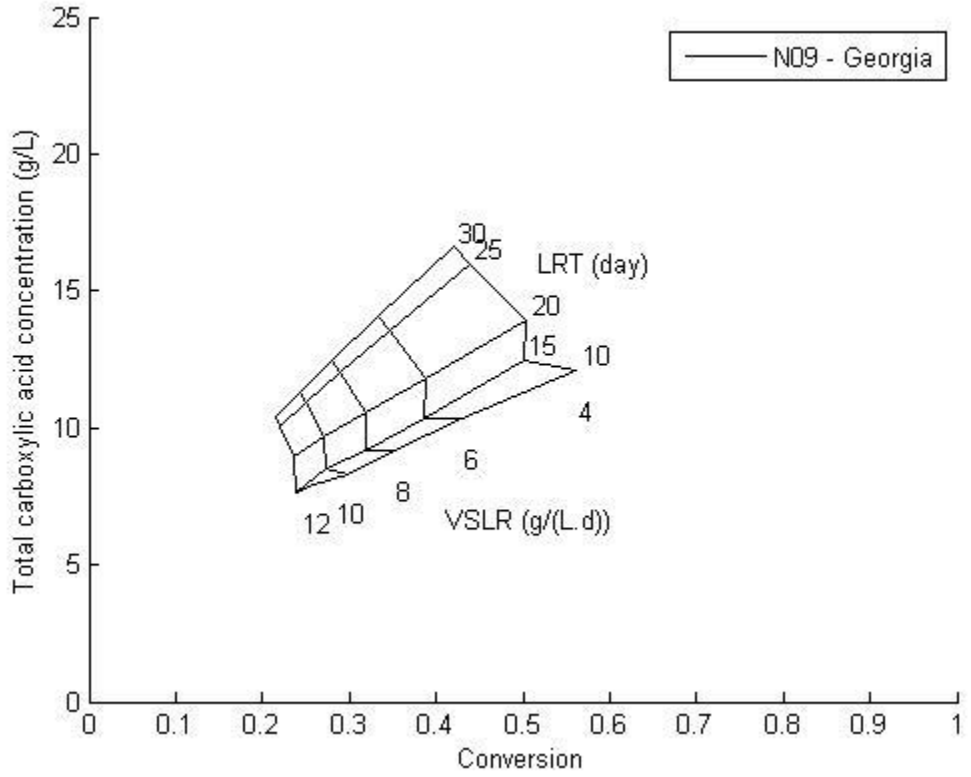

Figure 6-69. The CPDM "map" for 90 wt% paper/10 wt% yeast extract with N09 inocula.

6.5.24 Sample P01 from Site P – Puerto Rico

As mentioned in Section 6-3, batch experiments with 90 wt% paper /10 wt% yeast extract were done to obtain model parameters for the CPDM method. The inocula for these fermentations were taken from the post reactor material of the initial screening then preserved in a 20% glycerol solution. Calcium carbonate was used to adjust the pH. Liquid samples from the fermentations were analyzed for carboxylic acids. Using Equation 6-11, the acids were converted to acetic acid equivalents (Aeq). Figure 6-70 shows the Aeq concentrations for the five P01 batch experiments. The smooth lines are the predicted Aeq. Table 6-49 presents the fitted parameters *a*, *b*, and *c* for Equation 6-12.

Table 6-49. Values of the parameters *a*, *b*, and *c* fitted by least squares analysis for Site P inocula P01.

Substrate Concentration (g/L)	*a* (g/L liquid)	*b* (g/(L liquid·d))	*c* (d^{-1})
20	1.45	0.115	0.010
40	2.11	0.114	0.014
70	1.93	0.590	0.030
100	1.77	0.701	0.010
100+	18.04	0.278	0.008

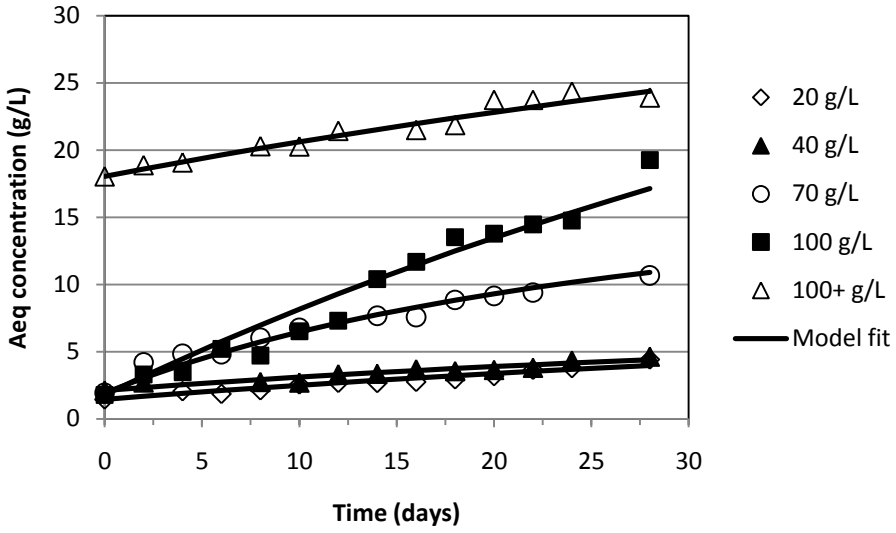

Figure 6-70. Aeq concentration for P01 inoculated paper/yeast extract fermentation at 20, 40, 70, 100, and 100+ g substrate/L liquid with calcium carbonate.

The reaction rate and the specific reaction rate for the batch fermentations were calculated using Equations 6-13 and 6-14. Conversion was calculated with the experimental acetic acid equivalents using Equation 6-15. Parameters *e*, *f*, *g*, and *h* presented in the predicted rate equation (Equation 6-40) were calculated by nonlinear regression. Figure 6-71 compares the predicted specific rate with the experimental specific rate. The specific rate equation for Site P inocula P01 follows:

$$\hat{r}_{pred} = \frac{0.0063(1-x)^{1.00}}{1 + 0.00100(\emptyset \cdot \text{Aeq})^{2.605}} \tag{6-40}$$

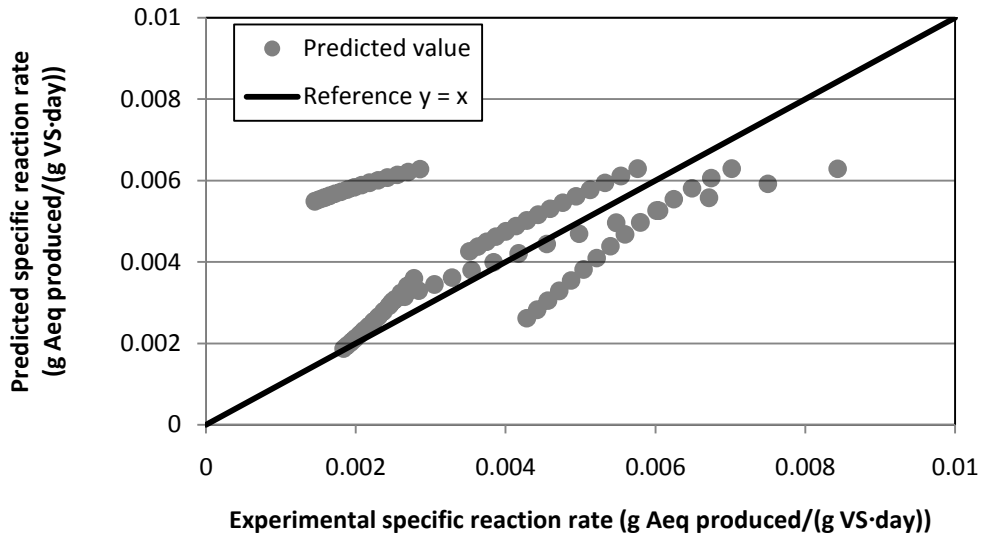

Figure 6-71. The experimental value and the CPDM prediction value for the specific reaction rate in five batch paper/yeast extract fermentation with P01 inocula.

Table 6-50. Parameter constant values in CPDM for Site P inocula P01.

Parameter constant	Value
Holdup (g liquid/g VS cake)	2.0
Moisture (g liquid/ g solid feed)	0.06
Selectivity (g Aeq/g VS digested)	0.39
F1−F4 solid concentration (g VS/L)	169, 214, 214, 214
F1−F4 liquid volume (L)	0.48, 0.28, 0.28, 0.28
ϕ (g total acid/g Aeq)	0.71
e (g Aeq/(g VS·d))	0.0063
f (dimensionless)	1.00
g (L/g total acid)$^{1/h}$	0.00100
h (dimensionless)	2.605

Table 6-50 lists the system-specific variables required by the CPDM prediction. Figure 6-72 shows the CPDM "map" for Site P inocula P01 in a 90 wt% paper/10 wt% yeast extract countercurrent fermentation with the single-centrifuge procedure at a fermentation solid concentration of 169 g VS/L liquid. The "map" predicts a total acid concentration of 12.75 g/L at LRT 30 day and VSLR of 12 g/(L·d), and a conversion of 0.21 g VS digested/g VS fed. At a VSLR of 4 g/(L·d) and LRT of 10 days, total acid concentration is 12.53 g/L and conversion is 0.47 g VS digested/g VS fed.

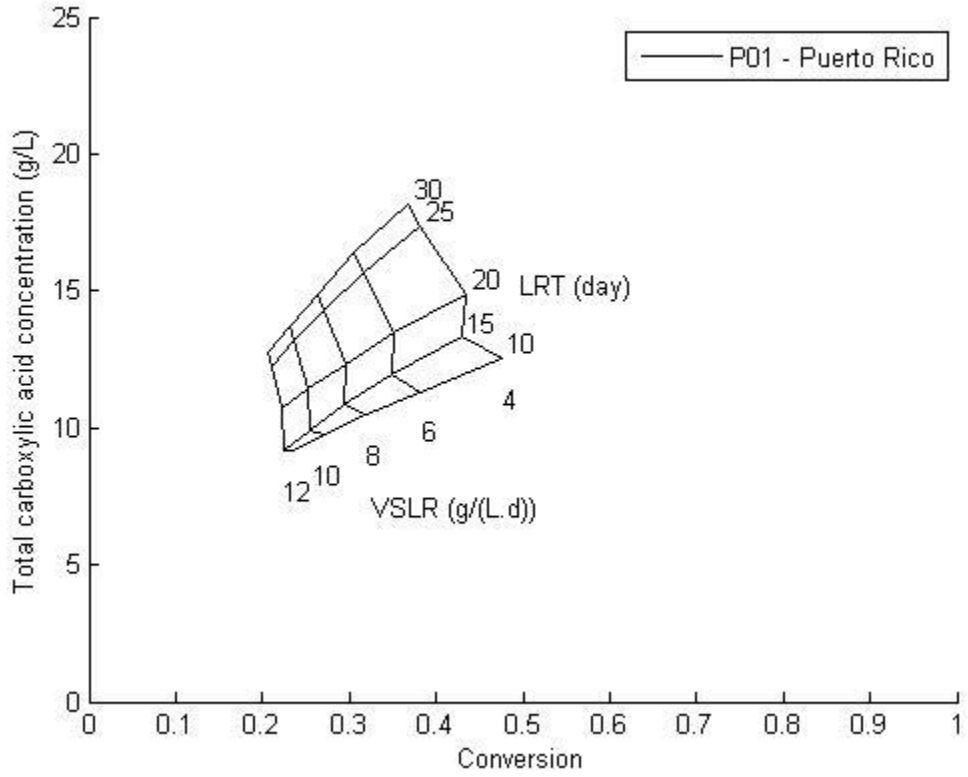

Figure 6-72. The CPDM "map" for 90 wt% paper/10 wt% yeast extract with P01 inocula.

6.5.25 Sample Q10 from Site Q – Florida

As mentioned in Section 6-3, batch experiments with 90 wt% paper /10 wt% yeast extract were done to obtain model parameters for the CPDM method. The inocula for these fermentations were taken from the post reactor material of the initial screening then preserved in a 20% glycerol solution. Calcium carbonate was used to adjust the pH. Liquid samples from the fermentations were analyzed for carboxylic acids. Using Equation 6-11, the acids were converted to acetic acid equivalents (Aeq). Figure 6-73 shows the Aeq concentrations for the five Q10 batch experiments. The smooth lines are the predicted Aeq. Table 6-51 presents the fitted parameters *a*, *b*, and *c* for Equation 6-12.

Table 6-51. Values of the parameters *a*, *b*, and *c* fitted by least squares analysis for Site Q inocula Q10.

Substrate Concentration (g/L)	*a* (g/L liquid)	*b* (g/(L liquid·d))	*c* (d^{-1})
20	1.76	0.087	0.030
40	2.50	0.209	0.026
70	2.65	0.215	0.003
100	2.77	0.580	0.020
100+	18.97	0.356	0.010

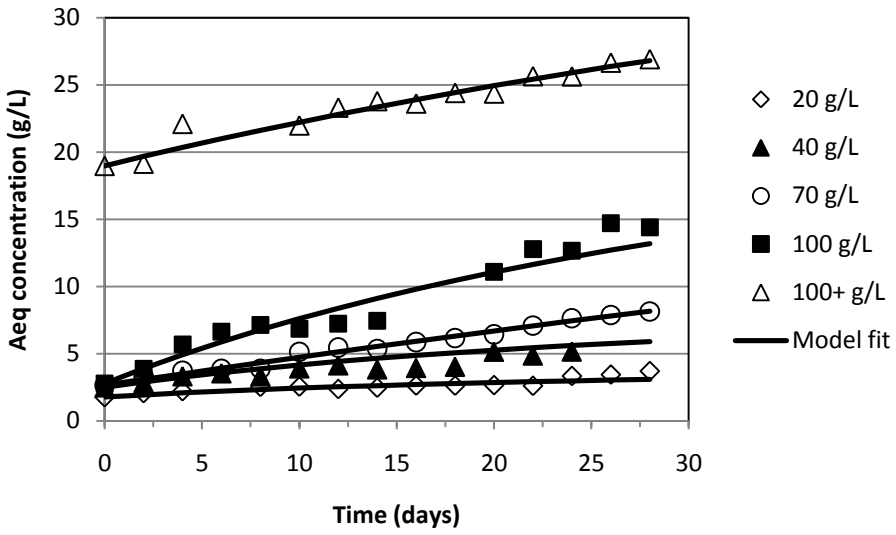

Figure 6-73. Aeq concentration for Q10 inoculated paper/yeast extract fermentation at 20, 40, 70, 100, and 100+ g substrate/L liquid with calcium carbonate.

The reaction rate and the specific reaction rate for the batch fermentations were calculated using Equations 6-13 and 6-14. Conversion was calculated with the experimental acetic acid equivalents using Equation 6-15. Parameters *e*, *f*, *g*, and *h* presented in the predicted rate equation (Equation 6-41) were calculated by nonlinear regression. Figure 6-74 compares the predicted specific rate with the experimental specific rate. The specific rate equation for Site Q inocula Q10 follows:

$$\hat{r}_{pred} = \frac{0.0044(1-x)^{1.986}}{1 + 0.00100(\emptyset \cdot \text{Aeq})^{1.895}} \tag{6-41}$$

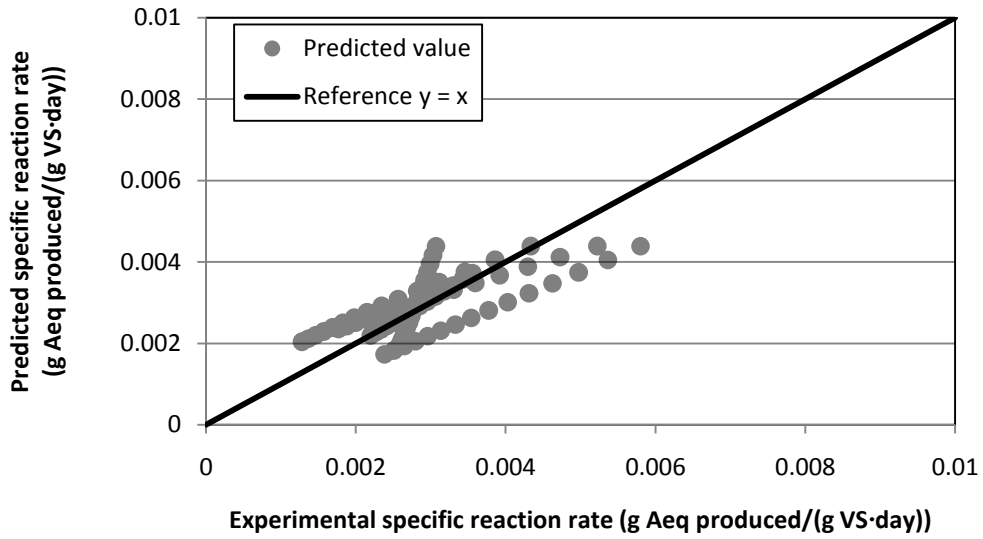

Figure 6-74. The experimental value and the CPDM prediction value for the specific reaction rate in five batch paper/yeast extract fermentation with Q10 inocula.

Table 6-52. Parameter constant values in CPDM for Site Q inocula Q10.

Parameter constant	Value
Holdup (g liquid/g VS cake)	2.0
Moisture (g liquid/ g solid feed)	0.06
Selectivity (g Aeq/g VS digested)	0.30
F1−F4 solid concentration (g VS/L)	169, 214, 214, 214
F1−F4 liquid volume (L)	0.48, 0.28, 0.28, 0.28
ϕ (g total acid/g Aeq)	0.75
e (g Aeq/(g VS·d))	0.0044
f (dimensionless)	1.986
g (L/g total acid)$^{1/h}$	0.00100
h (dimensionless)	1.895

Table 6-52 lists the system-specific variables required by the CPDM prediction. Figure 6-75 shows the CPDM "map" for Site Q inocula Q10 in a 90 wt% paper/10 wt% yeast extract countercurrent fermentation with the single-centrifuge procedure at a fermentation solid concentration of 169 g VS/L liquid. The "map" predicts a total acid concentration of 10.08 g/L at LRT 30 day and VSLR of 12 g/(L·d), and a conversion of 0.21 g VS digested/g VS fed. At a VSLR of 4 g/(L·d) and LRT of 10 days, total acid concentration is 10.74 g/L and conversion is 0.54 g VS digested/g VS fed.

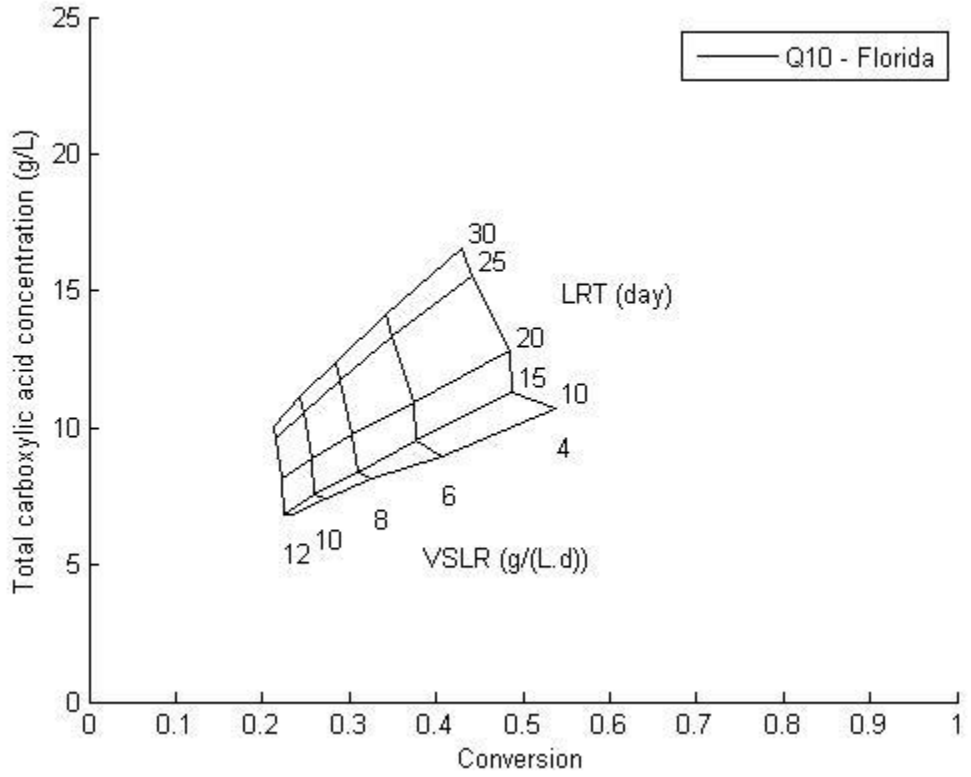

Figure 6-75. The CPDM "map" for 90 wt% paper/10 wt% yeast extract with Q10 inocula.

6.5.26 Sample R08 from Site R – Santa Fe, NM

As mentioned in Section 6-3, batch experiments with 90 wt% paper /10 wt% yeast extract were done to obtain model parameters for the CPDM method. The inocula for these fermentations were taken from the post reactor material of the initial screening then preserved in a 20% glycerol solution. Calcium carbonate was used to adjust the pH. Liquid samples from the fermentations were analyzed for carboxylic acids. Using Equation 6-11, the acids were converted to acetic acid equivalents (Aeq). Figure 6-76 shows the Aeq concentrations for the five R08 batch experiments. The smooth lines are the predicted Aeq. Table 6-53 presents the fitted parameters *a*, *b*, and *c* for Equation 6-12.

Table 6-53. Values of the parameters *a*, *b*, and *c* fitted by least squares analysis for Site R inocula R08.

Substrate Concentration (g/L)	*a* (g/L liquid)	*b* (g/(L liquid·d))	*c* (d^{-1})
20	1.67	0.082	0.036
40	2.27	0.146	0.002
70	2.45	0.448	0.060
100	2.51	0.723	0.044
100+	20.09	0.289	0.018

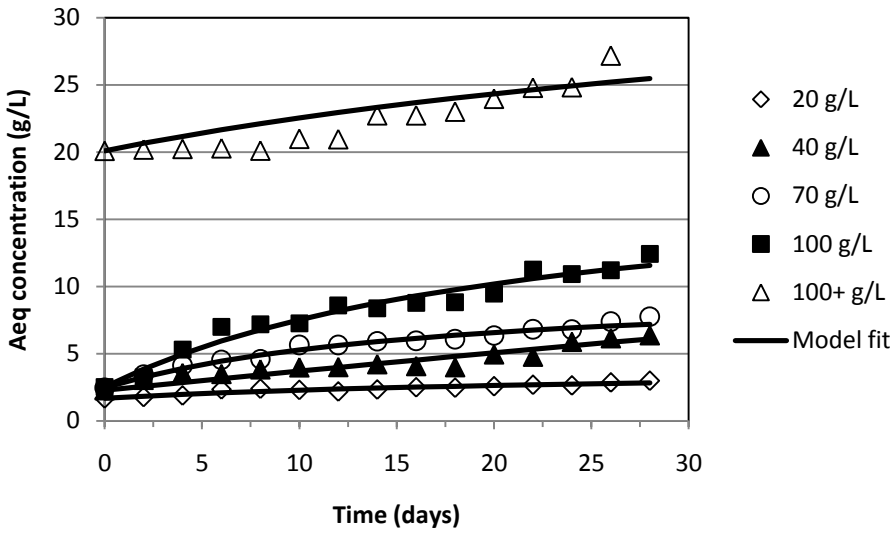

Figure 6-76. Aeq concentration for R08 inoculated paper/yeast extract fermentation at 20, 40, 70, 100, and 100+ g substrate/L liquid with calcium carbonate.

The reaction rate and the specific reaction rate for the batch fermentations were calculated using Equations 6-13 and 6-14. Conversion was calculated with the experimental acetic acid equivalents using Equation 6-15. Parameters *e*, *f*, *g*, and *h* presented in the predicted rate equation (Equation 6-42) were calculated by nonlinear regression. Figure 6-77 compares the predicted specific rate with the experimental specific rate. The specific rate equation for Site R inocula R08 follows:

$$\hat{r}_{pred} = \frac{0.0051(1-x)^{2.682}}{1 + 0.00100(\emptyset \cdot \text{Aeq})^{2.442}} \tag{6-42}$$

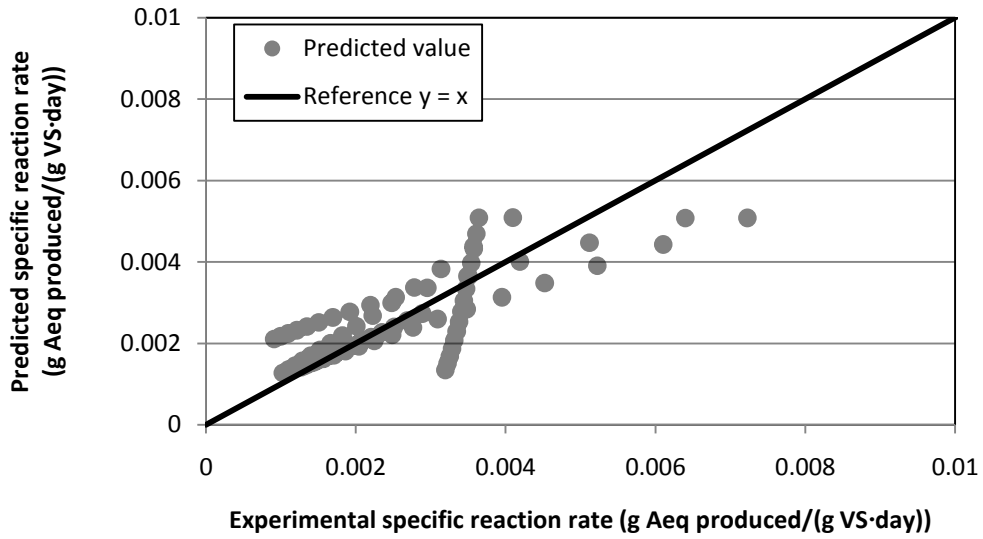

Figure 6-77. The experimental value and the CPDM prediction value for the specific reaction rate in five batch paper/yeast extract fermentation with R08 inocula.

Table 6-54. Parameter constant values in CPDM for Site R inocula R08.

Parameter constant	Value
Holdup (g liquid/g VS cake)	2.0
Moisture (g liquid/ g solid feed)	0.06
Selectivity (g Aeq/g VS digested)	0.27
F1−F4 solid concentration (g VS/L)	169, 214, 214, 214
F1−F4 liquid volume (L)	0.48, 0.28, 0.28, 0.28
ϕ (g total acid/g Aeq)	0.76
e (g Aeq/(g VS·d))	0.0051
f (dimensionless)	2.682
g (L/g total acid)$^{1/h}$	0.00100
h (dimensionless)	2.442

Table 6-54 lists the system-specific variables required by the CPDM prediction. Figure 6-78 shows the CPDM "map" for Site R inocula R08 in a 90 wt% paper/10 wt% yeast extract countercurrent fermentation with the single-centrifuge procedure at a fermentation solid concentration of 169 g VS/L liquid. The "map" predicts a total acid concentration of 9.92 g/L at LRT 30 day and VSLR of 12 g/(L·d), and a conversion of 0.23 g VS digested/g VS fed. At a VSLR of 4 g/(L·d) and LRT of 10 days, total acid concentration is 10.42 g/L and conversion is 0.56 g VS digested/g VS fed.

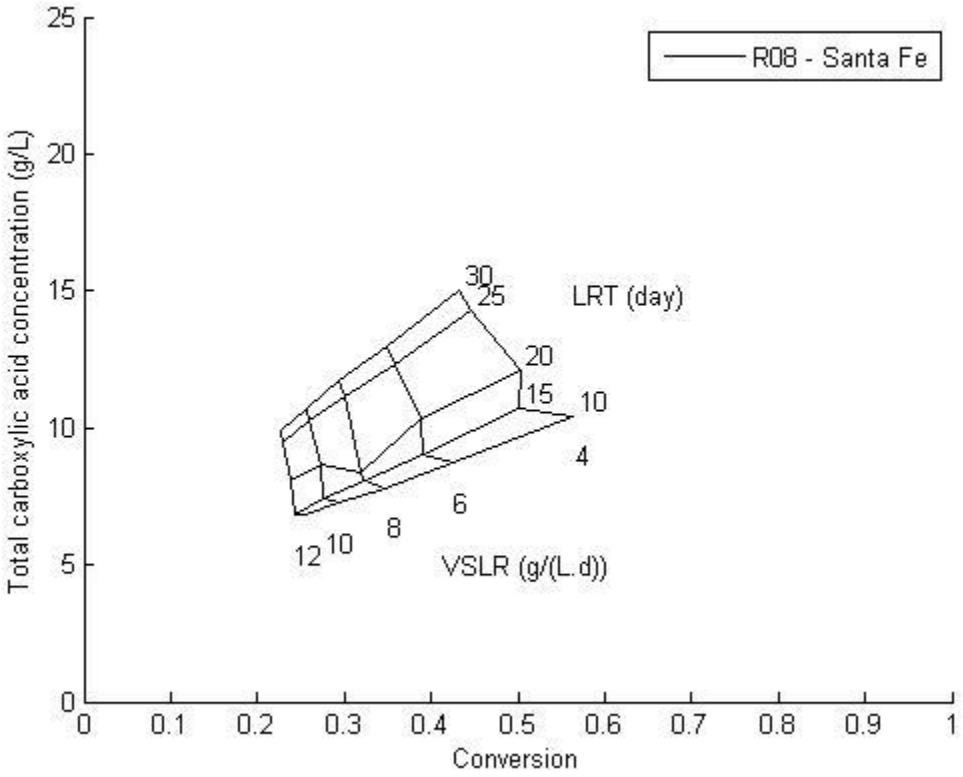

Figure 6-78. The CPDM "map" for 90 wt% paper/10 wt% yeast extract with R08 inocula.

6.5.27 Sample S44 from Site S – Yellowstone National Park

As mentioned in Section 6-3, batch experiments with 90 wt% paper /10 wt% yeast extract were done to obtain model parameters for the CPDM method. The inocula for these fermentations were taken from the post reactor material of the initial screening then preserved in a 20% glycerol solution. Calcium carbonate was used to adjust the pH. Liquid samples from the fermentations were analyzed for carboxylic acids. Using Equation 6-11, the acids were converted to acetic acid equivalents (Aeq). Figure 6-79 shows the Aeq concentrations for the five S44 batch experiments. The smooth lines are the predicted Aeq. Table 6-55 presents the fitted parameters *a*, *b*, and *c* for Equation 6-12.

Table 6-55. Values of the parameters *a*, *b*, and *c* fitted by least squares analysis for Site S inocula S44.

Substrate Concentration (g/L)	*a* (g/L liquid)	*b* (g/(L liquid·d))	*c* (d^{-1})
20	1.35	0.109	0.0095
40	1.59	0.325	0.043
70	1.94	0.968	0.010
100	1.39	0.573	0.033
100+	14.03	0.716	0.024

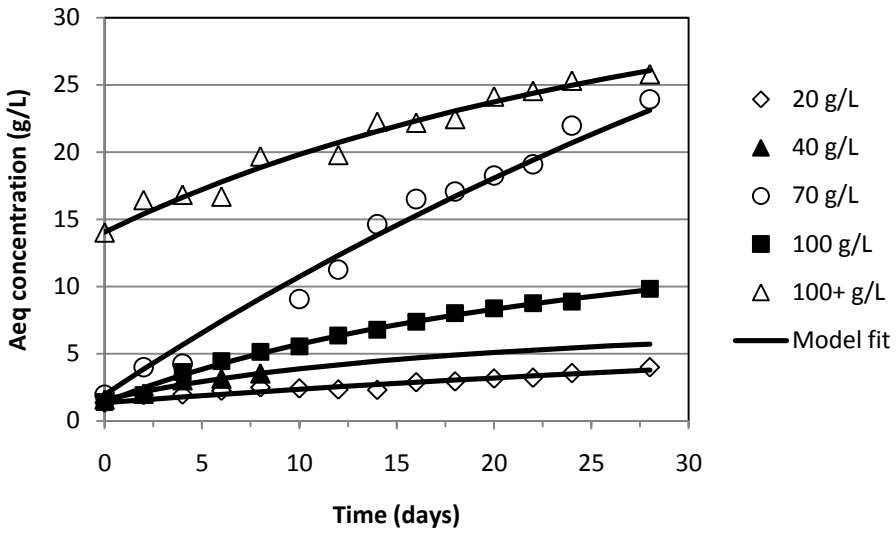

Figure 6-79. Aeq concentration for S44 inoculated paper/yeast extract fermentation at 20, 40, 70, 100, and 100+ g substrate/L liquid with calcium carbonate.

The reaction rate and the specific reaction rate for the batch fermentations were calculated using Equations 6-13 and 6-14. Conversion was calculated with the experimental acetic acid equivalents using Equation 6-15. Parameters *e*, *f*, *g*, and *h* presented in the predicted rate equation (Equation 6-43) were calculated by nonlinear regression. Figure 6-80 compares the predicted specific rate with the experimental specific rate. The specific rate equation for Site S inocula S44 follows:

$$\hat{r}_{pred} = \frac{0.0067(1-x)^{1.727}}{1 + 0.00100(\emptyset \cdot \text{Aeq})^{1.917}} \tag{6-43}$$

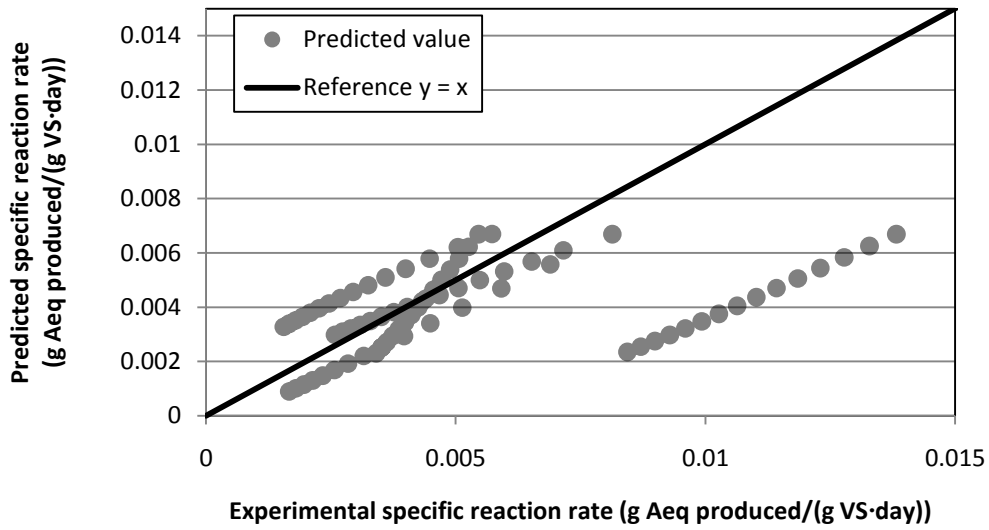

Figure 6-80. The experimental value and the CPDM prediction value for the specific reaction rate in five batch paper/yeast extract fermentation with S44 inocula.

Table 6-56. Parameter constant values in CPDM for Site S inocula S44.

Parameter constant	Value
Holdup (g liquid/g VS cake)	2.0
Moisture (g liquid/ g solid feed)	0.06
Selectivity (g Aeq/g VS digested)	0.38
F1−F4 solid concentration (g VS/L)	169, 214, 214, 214
F1−F4 liquid volume (L)	0.48, 0.28, 0.28, 0.28
ϕ (g total acid/g Aeq)	0.75
e (g Aeq/(g VS·d))	0.0067
f (dimensionless)	1.727
g (L/g total acid)$^{1/h}$	0.00100
h (dimensionless)	1.917

Table 6-56 lists the system-specific variables required by the CPDM prediction. Figure 6-81 shows the CPDM "map" for Site S inocula S44 in a 90 wt% paper/10 wt% yeast extract countercurrent fermentation with the single-centrifuge procedure at a fermentation solid concentration of 169 g VS/L liquid. The "map" predicts a total acid concentration of 14.57 g/L at LRT 30 day and VSLR of 12 g/(L·d), and a conversion of 0.24 g VS digested/g VS fed. At a VSLR of 4 g/(L·d) and LRT of 10 days, total acid concentration is 12.44 g/L and conversion is 0.57 g VS digested/g VS fed.

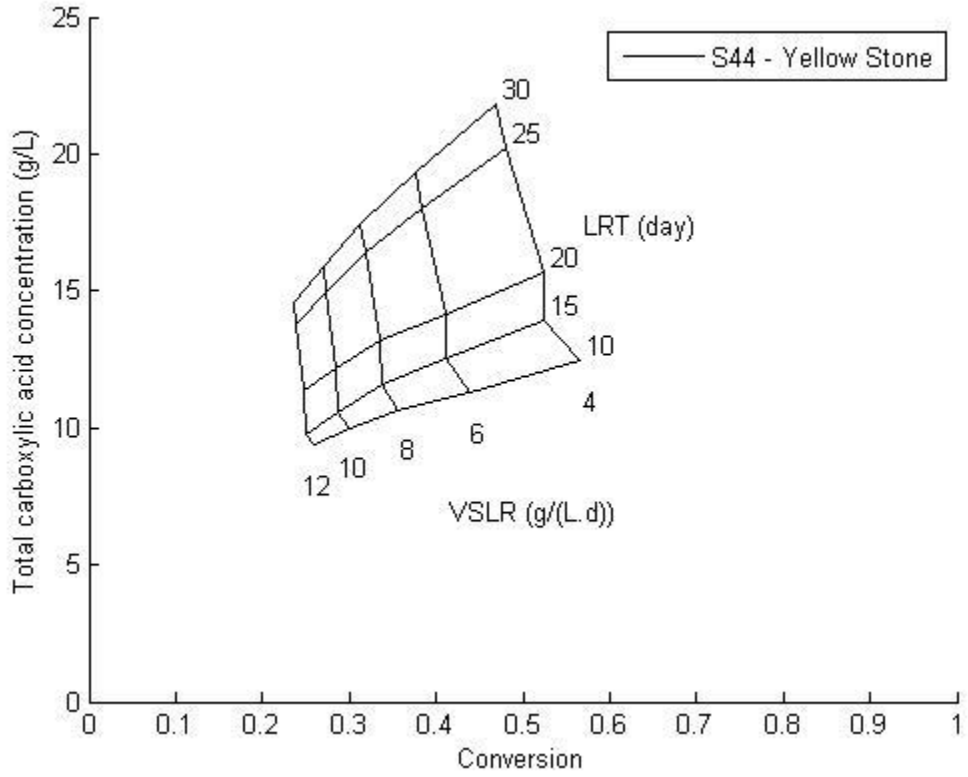

Figure 6-81. The CPDM "map" for 90 wt% paper/10 wt% yeast extract with S44 inocula.

6.5.28 Sample S48 from Site S – Yellowstone National Park

As mentioned in Section 6-3, batch experiments with 90 wt% paper /10 wt% yeast extract were done to obtain model parameters for the CPDM method. The inocula for these fermentations were taken from the post reactor material of the initial screening then preserved in a 20% glycerol solution. Calcium carbonate was used to adjust the pH. Liquid samples from the fermentations were analyzed for carboxylic acids. Using Equation 6-11, the acids were converted to acetic acid equivalents (Aeq). Figure 6-82 shows the Aeq concentrations for the five S48 batch experiments. The smooth lines are the predicted Aeq. Table 6-57 presents the fitted parameters *a*, *b*, and *c* for Equation 6-12.

Table 6-57. Values of the parameters *a*, *b*, and *c* fitted by least squares analysis for Site S inocula S48.

Substrate Concentration (g/L)	*a* (g/L liquid)	*b* (g/(L liquid·d))	*c* (d^{-1})
20	1.59	0.063	0.007
40	2.31	0.243	0.010
70	1.85	0.413	0.003
100	1.64	0.425	0.012
100+	14.63	0.449	0.010

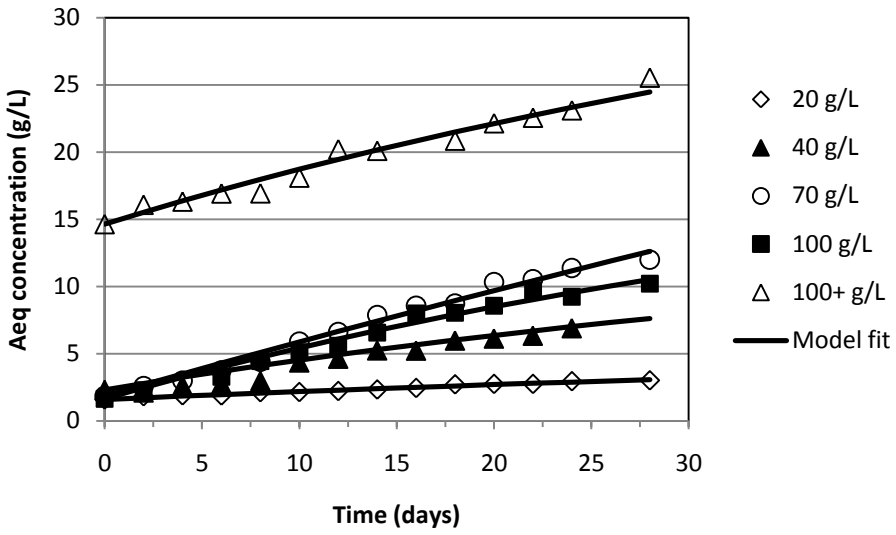

Figure 6-82. Aeq concentration for S48 inoculated paper/yeast extract fermentation at 20, 40, 70, 100, and 100+ g substrate/L liquid with calcium carbonate.

The reaction rate and the specific reaction rate for the batch fermentations were calculated using Equations 6-13 and 6-14. Conversion was calculated with the experimental acetic acid equivalents using Equation 6-15. Parameters *e*, *f*, *g*, and *h* presented in the predicted rate equation (Equation 6-44) were calculated by nonlinear regression. Figure 6-83 compares the predicted specific rate with the experimental specific rate. The specific rate equation for Site S inocula S48 follows:

$$\hat{r}_{pred} = \frac{0.0048(1-x)^{1.00}}{1 + 0.00100(\emptyset \cdot \text{Aeq})^{1.759}} \tag{6-44}$$

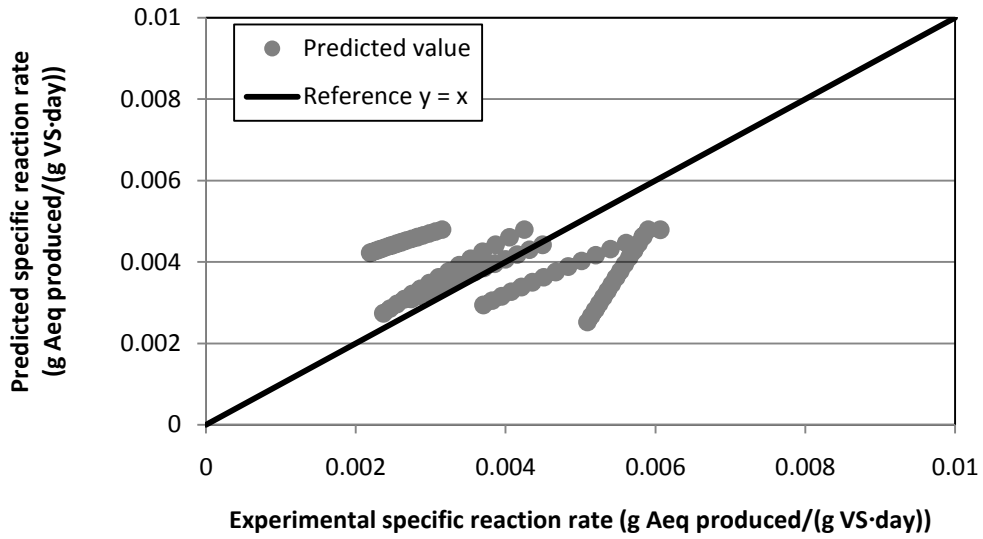

Figure 6-83. The experimental value and the CPDM prediction value for the specific reaction rate in five batch paper/yeast extract fermentation with S48 inocula.

Table 6-58. Parameter constant values in CPDM for Site S inocula S48.

Parameter constant	Value
Holdup (g liquid/g VS cake)	2.0
Moisture (g liquid/ g solid feed)	0.06
Selectivity (g Aeq/g VS digested)	0.40
F1−F4 solid concentration (g VS/L)	169, 214, 214, 214
F1−F4 liquid volume (L)	0.48, 0.28, 0.28, 0.28
ϕ (g total acid/g Aeq)	0.73
e (g Aeq/(g VS·d))	0.0048
f (dimensionless)	1.00
g (L/g total acid)$^{1/h}$	0.00100
h (dimensionless)	1.759

Table 6-58 lists the system-specific variables required by the CPDM prediction. Figure 6-84 shows the CPDM "map" for Site S inocula S48 in a 90 wt% paper/10 wt% yeast extract countercurrent fermentation with the single-centrifuge procedure at a fermentation solid concentration of 169 g VS/L liquid. The "map" predicts a total acid concentration of 11.47 g/L at LRT 30 day and VSLR of 12 g/(L·d), and a conversion of 0.18 g VS digested/g VS fed. At a VSLR of 4 g/(L·d) and LRT of 10 days, total acid concentration is 11.70 g/L and conversion is 0.44 g VS digested/g VS fed.

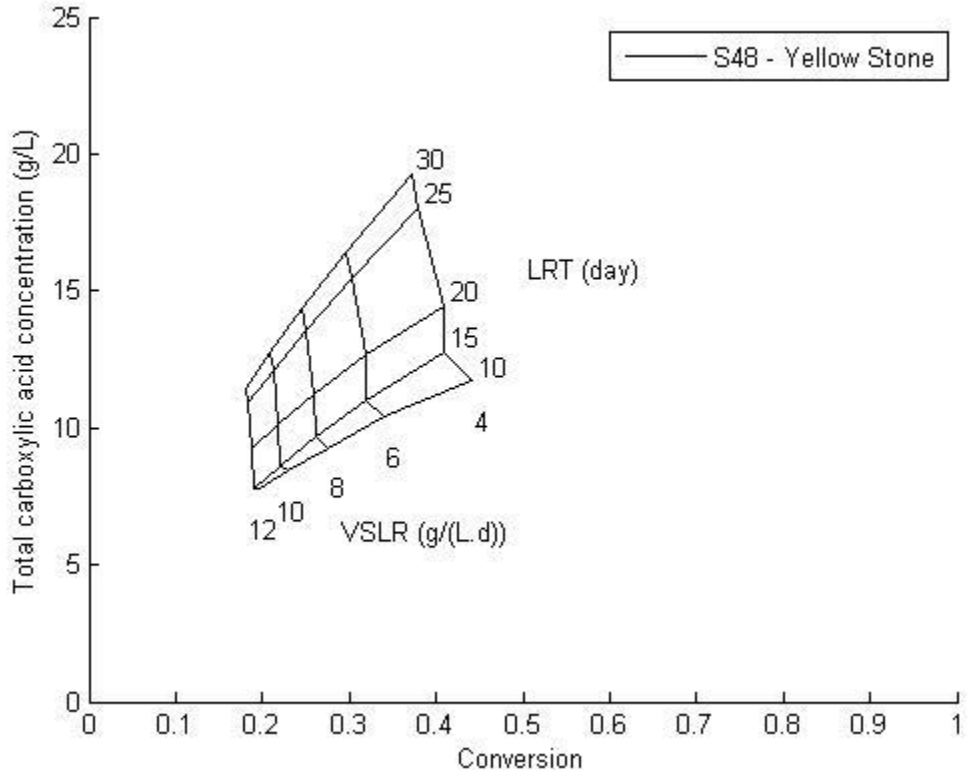

Figure 6-84. The CPDM "map" for 90 wt% paper/10 wt% yeast extract with S48 inocula.

6.5.29 Sample T05 from Site T – Nevada

As mentioned in Section 6-3, batch experiments with 90 wt% paper /10 wt% yeast extract were done to obtain model parameters for the CPDM method. The inocula for these fermentations were taken from the post reactor material of the initial screening then preserved in a 20% glycerol solution. Calcium carbonate was used to adjust the pH. Liquid samples from the fermentations were analyzed for carboxylic acids. Using Equation 6-11, the acids were converted to acetic acid equivalents (Aeq). Figure 6-85 shows the Aeq concentrations for the five T05 batch experiments. The smooth lines are the predicted Aeq. Table 6-59 presents the fitted parameters *a*, *b*, and *c* for Equation 6-12.

Table 6-59. Values of the parameters *a*, *b*, and *c* fitted by least squares analysis for Site T inocula T05.

Substrate Concentration (g/L)	*a* (g/L liquid)	*b* (g/(L liquid·d))	*c* (d^{-1})
20	0.64	0.016	0.010
40	0.91	1.207	0.064
70	1.01	1.528	0.125
100	1.19	1.136	0.088
100+	13.57	0.769	0.044

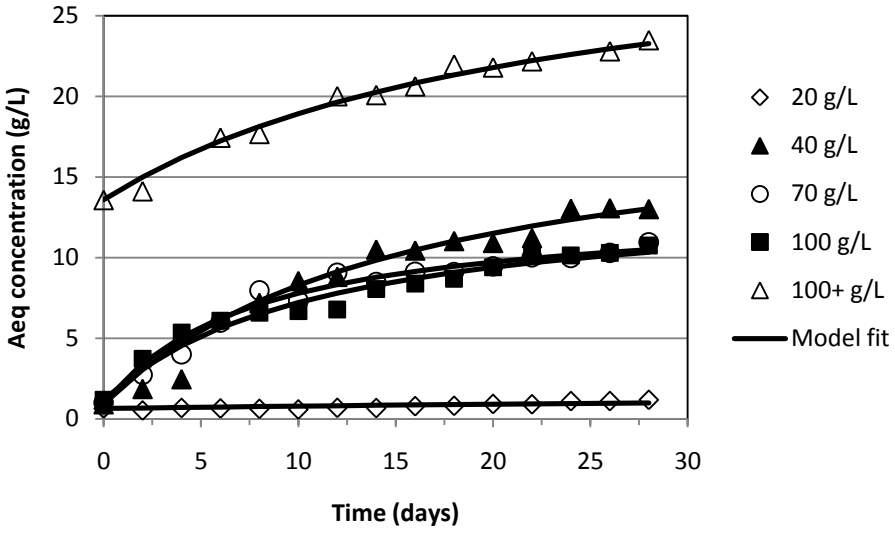

Figure 6-85. Aeq concentration for T05 inoculated paper/yeast extract fermentation at 20, 40, 70, 100, and 100+ g substrate/L liquid with calcium carbonate.

The reaction rate and the specific reaction rate for the batch fermentations were calculated using Equations 6-13 and 6-14. Conversion was calculated with the experimental acetic acid equivalents using Equation 6-15. Parameters *e*, *f*, *g*, and *h* presented in the predicted rate equation (Equation 6-45) were calculated by nonlinear regression. Figure 6-86 compares the predicted specific rate with the experimental specific rate. The specific rate equation for Site T inocula T05 follows:

$$\hat{r}_{pred} = \frac{0.0073(1-x)^{1.00}}{1 + 0.00100(\emptyset \cdot \text{Aeq})^{2.274}} \tag{6-45}$$

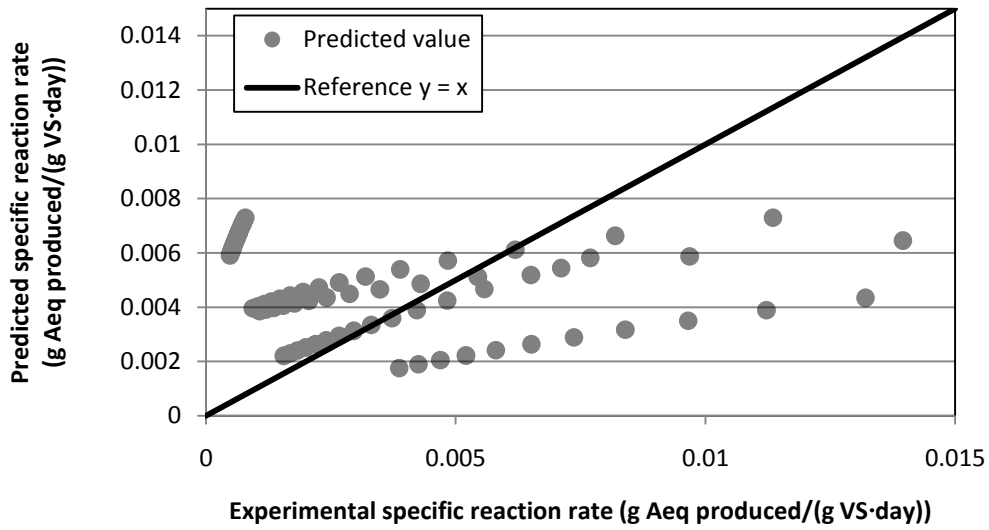

Figure 6-86. The experimental value and the CPDM prediction value for the specific reaction rate in five batch paper/yeast extract fermentation with T05 inocula.

Table 6-60. Parameter constant values in CPDM for Site T inocula T05.

Parameter constant	Value
Holdup (g liquid/g VS cake)	2.0
Moisture (g liquid/ g solid feed)	0.06
Selectivity (g Aeq/g VS digested)	0.25
F1−F4 solid concentration (g VS/L)	169, 214, 214, 214
F1−F4 liquid volume (L)	0.48, 0.28, 0.28, 0.28
ϕ (g total acid/g Aeq)	0.78
e (g Aeq/(g VS·d))	0.0073
f (dimensionless)	1.00
g (L/g total acid)$^{1/h}$	0.00100
h (dimensionless)	2.274

Table 6-60 lists the system-specific variables required by the CPDM prediction. Figure 6-87 shows the CPDM "map" for Site T inocula T05 in a 90 wt% paper/10 wt% yeast extract countercurrent fermentation with the single-centrifuge procedure at a fermentation solid concentration of 169 g VS/L liquid. The "map" predicts a total acid concentration of 15.04 g/L at LRT 30 day and VSLR of 12 g/(L·d), and a conversion of 0.35 g VS digested/g VS fed. At a VSLR of 4 g/(L·d) and LRT of 10 days, total acid concentration is 13.28 g/L and conversion is 0.66 g VS digested/g VS fed.

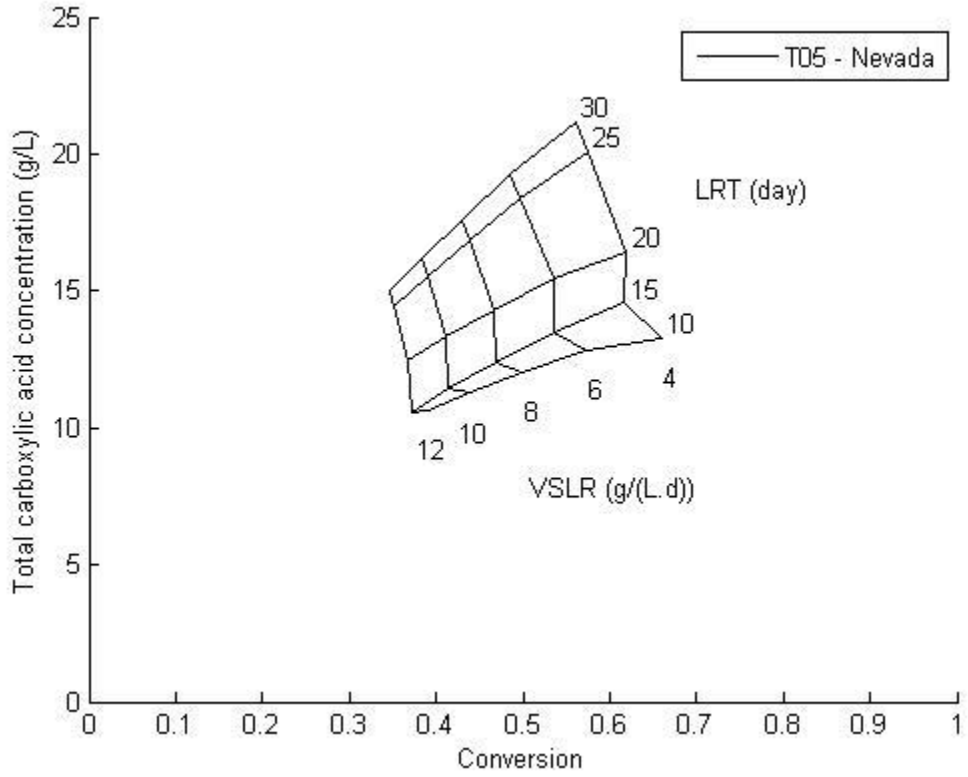

Figure 6-87. The CPDM "map" for 90 wt% paper/10 wt% yeast extract with T05 inocula.

6.5.30 Sample U22 from Site U – Nevada – California

As mentioned in Section 6-3, batch experiments with 90 wt% paper /10 wt% yeast extract were done to obtain model parameters for the CPDM method. The inocula for these fermentations were taken from the post reactor material of the initial screening then preserved in a 20% glycerol solution. Calcium carbonate was used to adjust the pH. Liquid samples from the fermentations were analyzed for carboxylic acids. Using Equation 6-11, the acids were converted to acetic acid equivalents (Aeq). Figure 6-88 shows the Aeq concentrations for the five U22 batch experiments. The smooth lines are the predicted Aeq. Table 6-61 presents the fitted parameters *a*, *b*, and *c* for Equation 6-12.

Table 6-61. Values of the parameters *a*, *b*, and *c* fitted by least squares analysis for Site U inocula U22.

Substrate Concentration (g/L)	*a* (g/L liquid)	*b* (g/(L liquid·d))	*c* (d^{-1})
20	1.57	0.176	0.015
40	1.75	0.296	0.010
70	2.26	0.519	0.031
100	1.71	1.18	0.096
100+	14.50	0.350	0.015

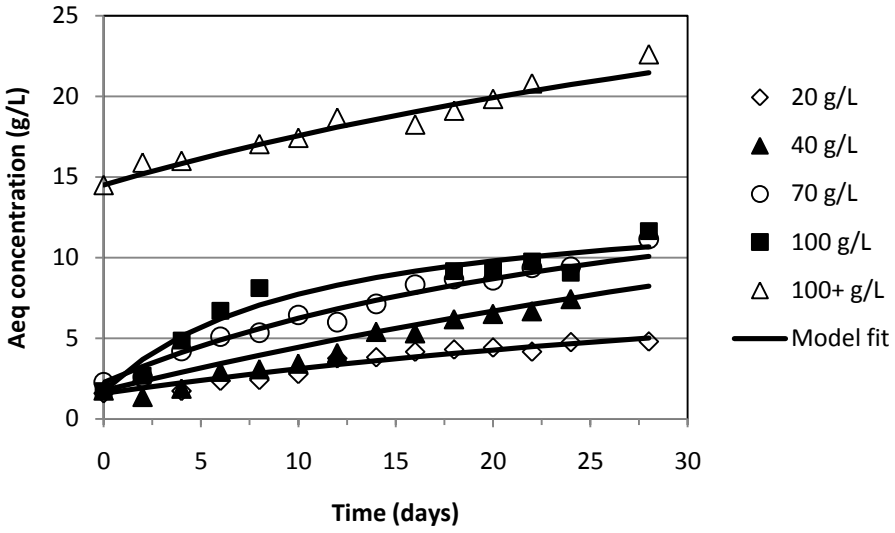

Figure 6-88. Aeq concentration for U22 inoculated paper/yeast extract fermentation at 20, 40, 70, 100, and 100+ g substrate/L liquid with calcium carbonate.

The reaction rate and the specific reaction rate for the batch fermentations were calculated using Equations 6-13 and 6-14. Conversion was calculated with the experimental acetic acid equivalents using Equation 6-15. Parameters *e*, *f*, *g*, and *h* presented in the predicted rate equation (Equation 6-46) were calculated by nonlinear regression. Figure 6-89 compares the predicted specific rate with the experimental specific rate. The specific rate equation for Site U inocula U22 follows:

$$\hat{r}_{pred} = \frac{0.0114(1-x)^{1.00}}{1 + 0.185(\emptyset \cdot \text{Aeq})^{1.086}} \tag{6-46}$$

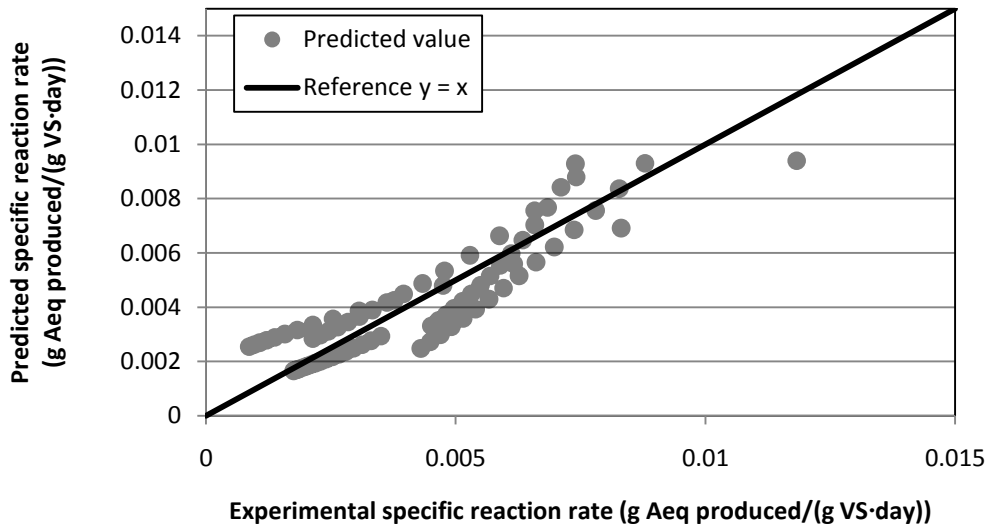

Figure 6-89. The experimental value and the CPDM prediction value for the specific reaction rate in five batch paper/yeast extract fermentation with U22 inocula.

Table 6-62. Parameter constant values in CPDM for Site U inocula U22.

Parameter constant	Value
Holdup (g liquid/g VS cake)	2.0
Moisture (g liquid/ g solid feed)	0.06
Selectivity (g Aeq/g VS digested)	0.31
F1−F4 solid concentration (g VS/L)	169, 214, 214, 214
F1−F4 liquid volume (L)	0.48, 0.28, 0.28, 0.28
ϕ (g total acid/g Aeq)	0.73
e (g Aeq/(g VS·d))	0.0114
f (dimensionless)	1.00
g (L/g total acid)$^{1/h}$	0.185
h (dimensionless)	1.086

Table 6-62 lists the system-specific variables required by the CPDM prediction. Figure 6-90 shows the CPDM "map" for Site U inocula U22 in a 90 wt% paper/10 wt% yeast extract countercurrent fermentation with the single-centrifuge procedure at a fermentation solid concentration of 169 g VS/L liquid. The "map" predicts a total acid concentration of 11.04 g/L at LRT 30 day and VSLR of 12 g/(L·d), and a conversion of 0.22 g VS digested/g VS fed. At a VSLR of 4 g/(L·d) and LRT of 10 days, total acid concentration is 11.33 g/L and conversion is 0.48 g VS digested/g VS fed.

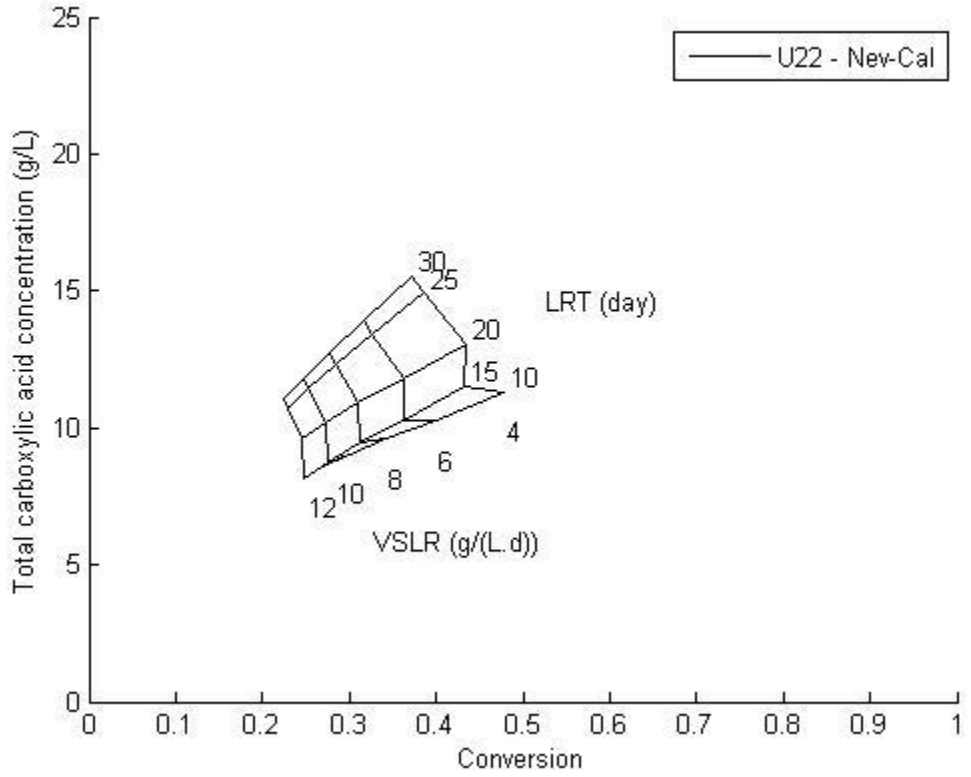

Figure 6-90. The CPDM "map" for 90 wt% paper/10 wt% yeast extract with U22 inocula.

6.6 Comparison of different inocula to Galveston inocula

Previous research in the Holtzapple laboratory (Chan and Holtzapple, 2003; Fu, 2007; Thanakoses, 2002) has shown that inoculum taken from the marine environment of Galveston Island, TX contains microorganisms that produce high conversions and high concentrations of carboxylic acids. By comparing the CPDM "maps," it is possible to determine whether inocula studied in this chapter are better at producing acids and converting biomass than the Galveston inoculum (B01). All maps were produced using the same fermentation system of 90 wt% paper, 10 wt% yeast extract buffer with calcium carbonate. Only the inocula were different.

Figure 6-91 shows an example of a comparison map, in this case Site A sample A23 was compared with Galveston sample B01. Additional maps are located in Appendix L. Table 6-63 shows the percent change of each inoculum source over Galveston.

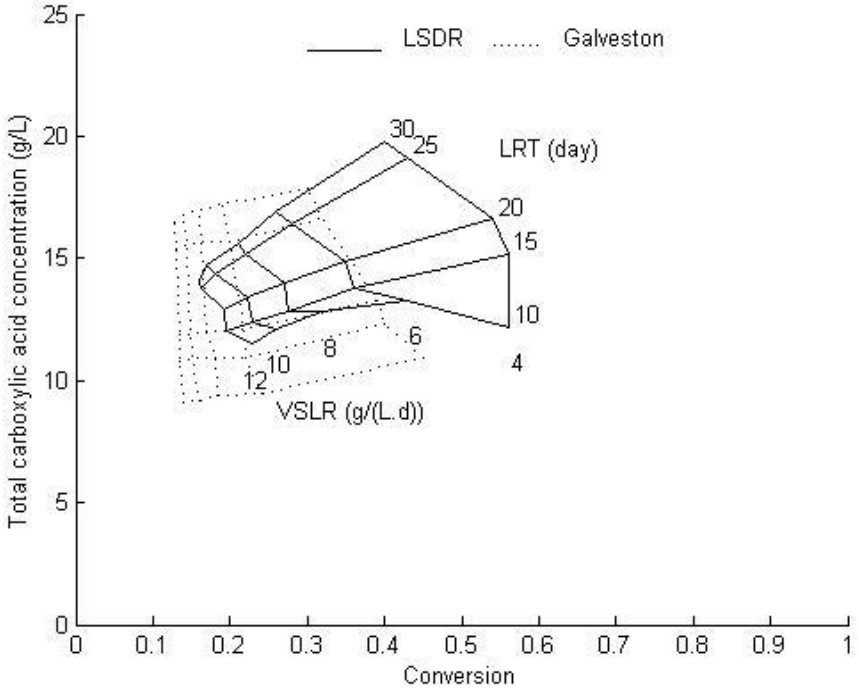

Figure 6-91. Comparison of CPDM "map" for 90 wt% paper/10 wt% yeast extract with La Sal del Rey (A23) inocula and Galveston (B01) inocula.

Table 6-63. CPDM "map" results for all inocula tested in comparison to Galveston (B01).

Inocula	Total acid concentration** (g/L)	Percent change from B01*	Conversion*** (g VS dig/g VS fed)	Percent change from B01*
A23	19.83	10.38	0.561	25.85
B01 (Gal)	17.96	N/A	0.446	N/A
B02	19.28	7.32	0.456	2.28
B03	14.90	−17.04	0.468	4.98
B04	15.62	−13.04	0.507	13.71
C01	18.24	1.51	0.511	14.66
D18	10.05	−44.04	0.444	−0.54
E08	19.40	7.98	0.543	21.82
F02	14.70	−18.15	0.497	11.35
F09	20.24	12.67	0.602	35.07
G08	19.17	6.71	0.576	29.04
G13	11.52	−35.86	0.372	−16.68
G23	11.70	−34.88	0.433	−2.95
G46	13.31	−25.89	0.591	32.49
H01	18.08	0.65	0.534	19.81
H20	25.32	40.96	0.532	19.30
J04	17.84	−0.71	0.557	25.00
J11	16.82	−6.37	0.475	6.61
J19	18.55	3.25	0.419	−6.07
K49	25.08	39.59	0.520	16.70
L10	17.36	−3.37	0.523	17.20
M24	18.21	1.38	0.504	12.94
N09	16.60	−7.59	0.563	26.13
P01	18.16	1.11	0.475	6.44
Q10	16.54	−7.91	0.538	20.63
R08	15.05	−16.20	0.564	26.46
S44	21.83	21.50	0.567	27.03
S48	19.26	7.21	0.442	−0.87
T05	21.17	17.87	0.659	47.76
U22	15.51	−13.66	0.479	7.43

* Percent change calculated as (Site – B01)/B01 × 100.
** at VSLR = 4 g VS/(L liq·d), LRT = 30 d
*** at VSLR = 4 g VS/(L liq·d), LRT = 10 d

Inocula A23, E08, F09, G08, H20, K49, S44, and T05 are better at converting biomass and producing carboxylic acids than Galveston (B01) inocula, showing a significant increase in both acid production and substrate conversion. Inocula K49 and H20 both show an increase of 40% in acid production (39.6 and 40.9%, respectively) and a greater than 15% in conversion (16.7 and 19.3%, respectively). Inocula F09 and G08 show a nearly 30% increase in conversion (35.1 and 29.0%, respectively) and T05 shows an increase of 47% in conversion over Galveston. Inocula B02, C01, H01, J04, M24, P01, Q10, R08 and S48 show no or only slight improvement over Galveston (B01) inocula, whereas inocula B03, B04, D18, F02, G13, G23, G46, J11, J19, L10, N09, and U22 perform worse than Galveston (B01) and do not show promise for future use in industrial-scale fermentations.

During this CPDM step, several inoculum showed a different performance than they did in the initial screening step. Sample A23, while the best of Site A, was worse than Galveston in the initial screen but showed better performance during CPDM. Sample S48 was a significantly better converter than Galveston during the initial screen but showed little difference during the CPDM step. Samples D18, G13, G23, G46, J11, L10, M24, P01, and U22 all performed better than Galveston during the Initial Screen but either showed no improvement during CPDM or performed worse than Galveston. The most likely cause for this change in performance is the storage between the two fermentation steps. All samples were stored at −20 C in 20% glycerol after the initial screen and before the CPDM. While freezing bacteria in the presence of glycerol has been shown to preserve the bacteria, there are thermophilic microorganisms that still do not survive this preservation method. The sudden drop in performance between the two steps, particularly sample S48 which is from a thermal spring in Yellowstone, was most likely caused by the freezing killing off the majority of the high converting microorganisms.

While this is disappointing for microbiologists who are trying to isolate and identify these high converting microorganisms, it is an overall positive result for the Bioscreening Project. The MixAlco™ process needs robust high converting microorganisms that can withstand not only high salt and acid concentrations but also swings in temperature, including swings below the freezing point. While interesting from a microbiology viewpoint, microorganisms that cannot withstand freezing temperatures are undesirable for the MixAlco™ process.

6.7 Conclusions

The following conclusions can be made based on the study in this chapter:

1) The CPDM method is a powerful tool to predict product concentrations and biomass conversions based on batch fermentation data.
2) Inocula A23, E08, F09, G08, H20, K49, S44, and T05 are better at converting biomass and producing carboxylic acids than Galveston (B01) inocula. They show promise for future use in industrial-scale fermentations.
3) Inocula B02, C01, H01, J04, M24, P01, Q10, R08 and S48 show no or only slight improvement over Galveston (B01) inocula.
4) Inocula B03, B04, D18, F02, G13, G23, G46, J11, J19, L10, N09, and U22 perform worse than Galveston (B01) and do not show promise for future use in industrial-scale fermentations.

CHAPTER VII
COMPARISON OF INOCULA SOURCES IN COUNTERCURRENT FERMENTATIONS

The objectives of this chapter follow:

a) Examine the long-term effects of nine inoculum sources on paper and yeast extract fermentations.
b) Apply the Continuum Particle Distribution Modeling (CPDM) method to compare the experimental with predicted acid concentration and conversion based on the experimental operational conditions.
c) Determine the community compositions of the inocula in the countercurrent cultures when using non-sterile substrates and any commonality between them.
d) Determine the effectiveness of the bioscreening selection process.

7.1 Introduction

Anaerobic fermentations are the core of the MixAlco™ process. During the fermentation, anaerobic microorganisms digest the biomass feedstock, producing carboxylic acids. Although product inhibition is always a factor with batch fermentations, it is significantly reduced with countercurrent fermentations (Holtzapple et al., 1999).

As microorganisms digest biomass, they digest the most reactive, most digestible components first, leaving the least reactive components. But, in batch fermentations, the accumulated carboxylic acids inhibit the microorganisms, making it impossible for them to digest the least reactive biomass. In a countercurrent system, the solid and liquid streams move in opposite directions. The most reactive, easily digestible (fresh) biomass encounters the highest concentration of acids whereas the least reactive biomass encounters no acid. This countercurrent flow reduces the inhibitory effect, improving the overall digestion and acid production of the fermentation.

This chapter examines the effects of different inoculum sources on the countercurrent system and on the effects the countercurrent system on the microbial community.

7.2 Materials and methods

Four-stage countercurrent fermentations were used in this chapter. Each of the fermentations was started as a batch fermentation with 90 wt% paper, 10 wt% yeast extract, and deoxygenated water. Calcium carbonate and urea were added to buffer the pH to about 6.0. The single-centrifuge procedure was used for all fermentation trains. All fermentations were operated at 55 °C. Liquid and solids were transferred at 2-day intervals. The total liquid in the fermentation train is the sum of the residual liquid in the wet solid cake and the centrifuged liquid on top of the cake. It was determined by first centrifuging each fermentor in a train and separating the solid from the liquid.

Table 7-1 shows the fermentation configurations used in this chapter. The inoculum for each train was taken from the residual liquid and solid used in the CPDM analysis in Chapter VI.

7.3 Paper and yeast extract fermentations with different inocula

A series of nine countercurrent fermentations were performed using nine different cultures of microorganisms (GA, TR, BA, PU, TI, LS, E, F, and G). All of the fermentations trains used the same fresh liquid addition (100 mL).

Table 7-1. Experimental conditions for anaerobic fermentations using different inocula sources.

Configuration		Inocula source	Fermentation temperature (°C)	Iodoform (mg/(L·day))
1	GA	Galveston marine sand, B01	55	3.0
2	TR	Terrestrial soil (Bryan, TX), B02	55	3.0
3	BA	Bahamas sand, B03	55	3.0
4	PU	Pure culture (*C. thermocellum*), B04	55	3.0
5	TI	Taiwan hot spring sand, C01	55	3.0
6	LS	La Sal del Rey, TX, A23	55	3.0
7	E	Enid, OK, E08	55	3.0
8	F	Brazoria, TX, F09	55	3.0
9	G	Roswell-Carlsbad, TX, G46	55	3.0

7.3.1 Train GA

Four batch fermentations were initiated by adding paper (36 g), yeast extract (4 g), calcium carbonate (6 g), urea (0.5 g), deoxygenated water (350 mL), Galveston inocula (B01) (50 mL), and 120 μL iodoform solution (20 g/L iodoform in ethanol). The Galveston inocula was taken from the residual liquid and solid used in the CPDM analysis from Chapter VI. On each transfer, paper (11.2 g) was added to F1. Yeast extract (0.4 g), calcium carbonate (1 g), urea (0.5 g), and iodoform (120 μL) were added to F1, F2, F3, and F4. The transfer of solids and liquid was performed as in Appendix D. Fresh deoxygenated water (100 mL) was added to F4 on each transfer. The total acid concentration profile and acetate content profile are shown in Figures 7-1 and 7-2.

7.3.2 Train TR

Four batch fermentations were initiated by adding paper (36 g), yeast extract (4 g), calcium carbonate (6 g), urea (0.5 g), deoxygenated water (350 mL), Terrestrial inocula (B02) (50 mL), and 120 μL iodoform solution (20 g/L iodoform in ethanol). The terrestrial inocula was taken from the residual liquid and solid used in CPDM analysis from Chapter VI. On each transfer, paper (11.2 g) was added to F1. Yeast extract (0.4 g), calcium carbonate (1 g), urea (0.5 g), and iodoform (120 μL) were added to F1, F2, F3, and F4. The transfer of solids and liquid was performed as in Appendix D. Fresh deoxygenated water (100 mL) was added to F4 on each transfer. The total acid concentration profile and acetate content profile are shown in Figures 7-3 and 7-4.

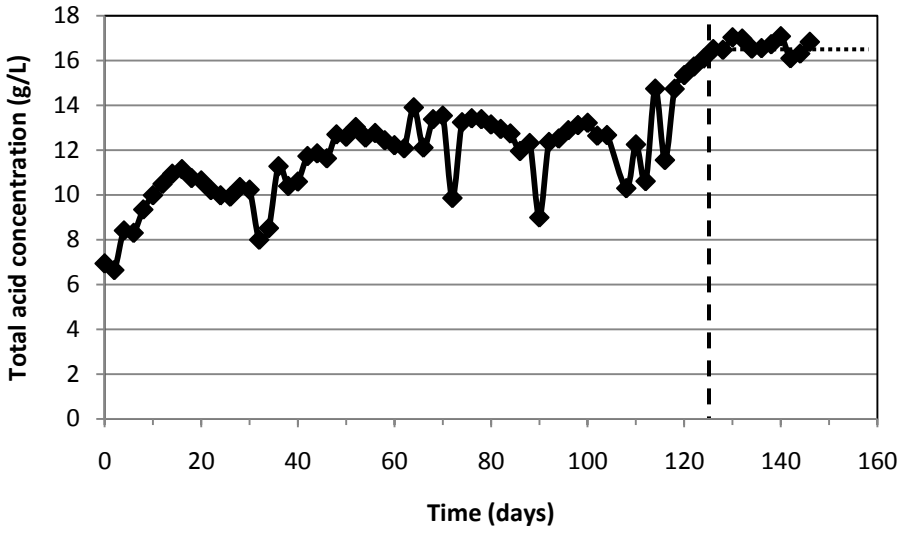

Figure 7-1. Total acid concentration for paper and yeast extract fermentation Train GA. Dash line indicates steady state (16.6 g/L).

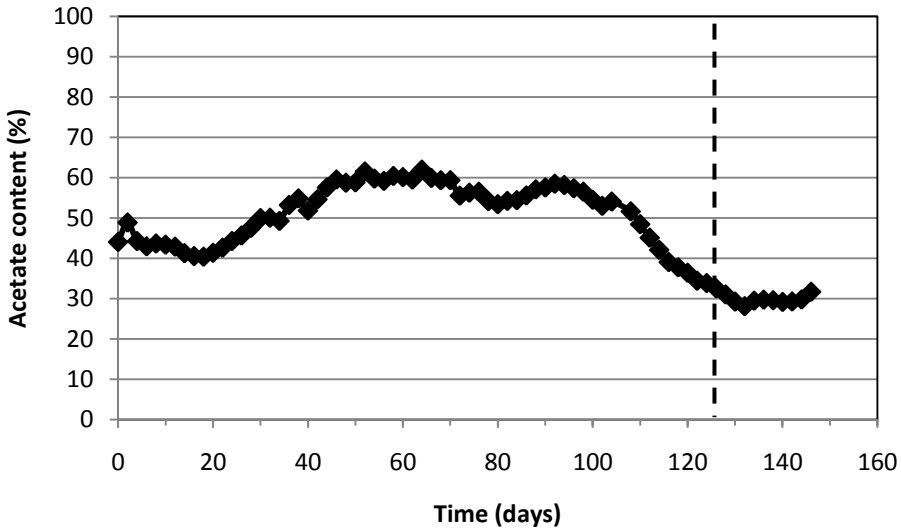

Figure 7-2. Acetate content for paper and yeast extract fermentation Train GA.

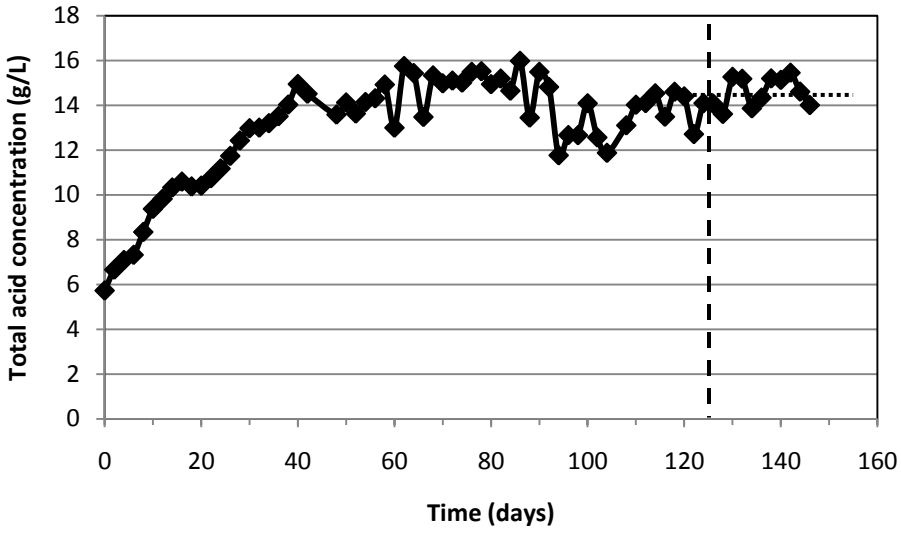

Figure 7-3. Total acid concentration for paper and yeast extract fermentation Train TR. Dash line indicates steady state (14.3 g/L).

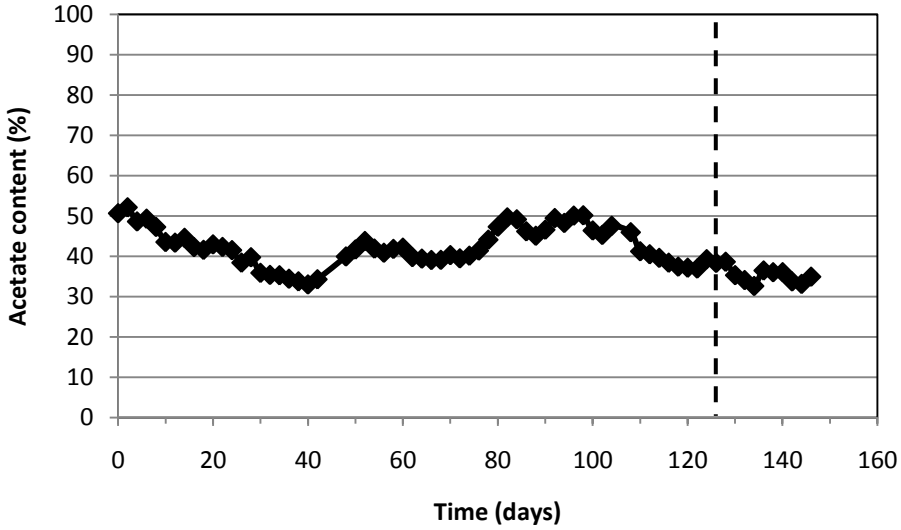

Figure 7-4. Acetate content for paper and yeast extract fermentation Train TR.

7.3.3 Train BA

Four batch fermentations were initiated by adding paper (36 g), yeast extract (4 g), calcium carbonate (6 g), urea (0.5 g), deoxygenated water (350 mL), Bahamas inocula (B03) (50 mL), and 120 μL iodoform solution (20 g/L iodoform in ethanol). The Bahamas inocula was taken from the residual liquid and solid used in CPDM analysis from Chapter VI. On each transfer, paper (11.2 g) was added to F1. Yeast extract (0.4 g), calcium carbonate (1 g), urea (0.5 g), and iodoform (120 μL) were added to F1, F2, F3, and F4. The transfer of solids and liquid was performed as in Appendix D. Fresh deoxygenated water (100 mL) was added to F4 on each transfer. The total acid concentration profile and acetate content profile are shown in Figures 7-5 and 7-6.

7.3.4 Train PU

Four batch fermentations were initiated by adding paper (36 g), yeast extract (4 g), calcium carbonate (6 g), urea (0.5 g), deoxygenated water (350 mL), pure culture inocula (B04) (50 mL), and 120 μL iodoform solution (20 g/L iodoform in ethanol). The pure culture inocula was taken from the residual liquid and solid used in CPDM analysis Chapter VI. On each transfer, paper (11.2 g) was added to F1. Yeast extract (0.4 g), calcium carbonate (1 g), urea (0.5 g), and iodoform (120 μL) were added to F1, F2, F3, and F4. The transfer of solids and liquid was performed as in Appendix D. Fresh deoxygenated water (100 mL) was added to F4 on each transfer. The total acid concentration profile and acetate content profile are shown in Figures 7-7 and 7-8.

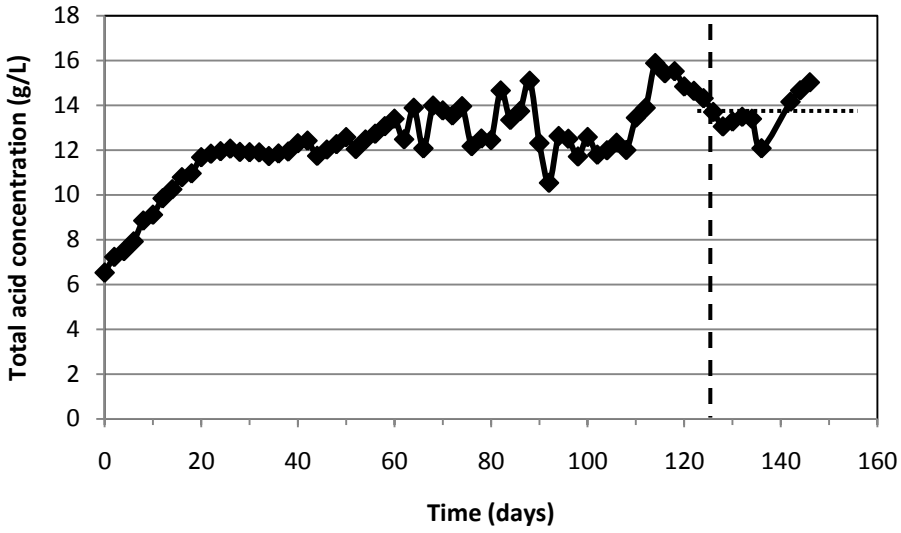

Figure 7-5. Total acid concentration for paper and yeast extract fermentation Train BA. Dash line indicates steady state (13.9 g/L).

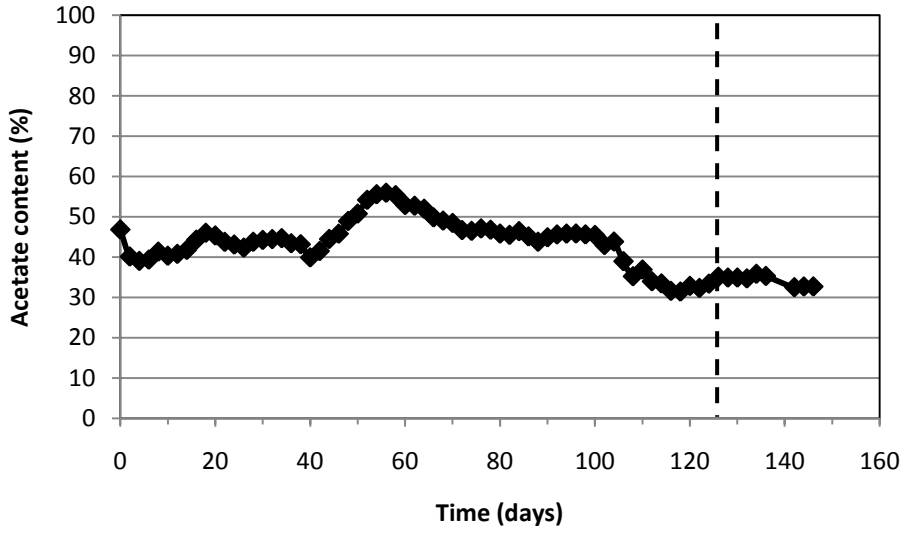

Figure 7-6. Acetate content for paper and yeast extract fermentation Train BA.

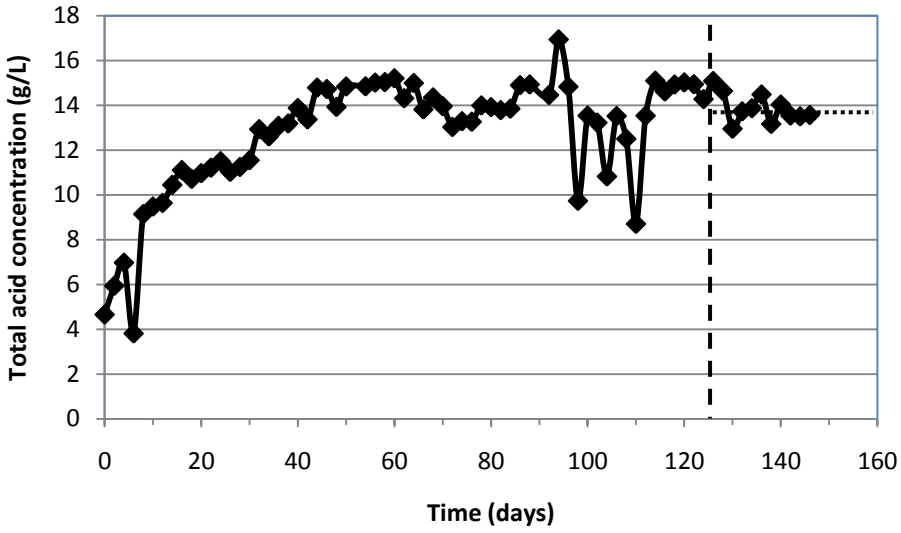

Figure 7-7. Total acid concentration for paper and yeast extract fermentation Train PU. Dash line indicates steady state (13.7 g/L).

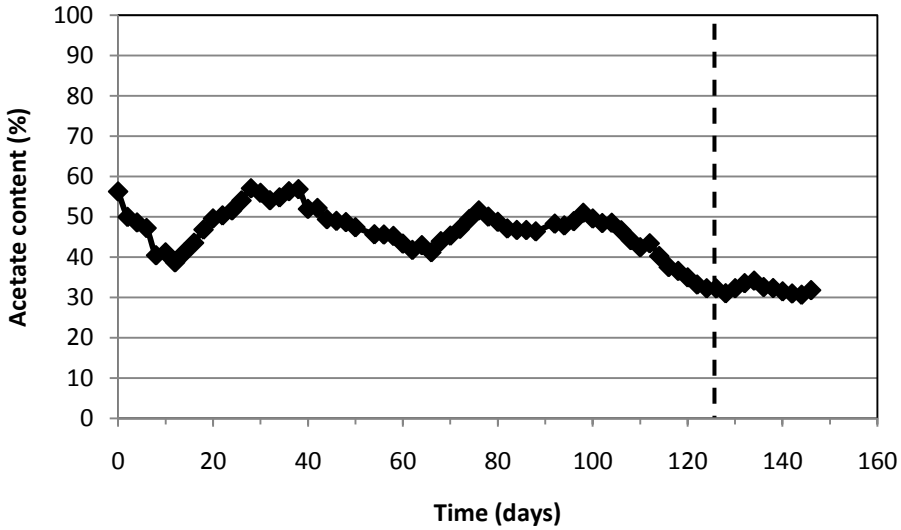

Figure 7-8. Acetate content for paper and yeast extract fermentation Train PU.

7.3.5 Train TI

Four batch fermentations were initiated by adding paper (36 g), yeast extract (4 g), calcium carbonate (6 g), urea (0.5 g), deoxygenated water (350 mL), Taiwan inocula (C01) (50 mL), and 120 μL iodoform solution (20 g/L iodoform in ethanol). The Taiwan inocula was taken from the residual liquid and solid used in CPDM analysis from Chapter VI. On each transfer, paper (11.2 g) was added to F1. Yeast extract (0.4 g), calcium carbonate (1 g), urea (0.5 g), and iodoform (120 μL) were added to F1, F2, F3, and F4. The transfer of solids and liquid was performed as in Appendix D. Fresh deoxygenated water (100 mL) was added to F4 on each transfer. The total acid concentration profile and acetate content profile are shown in Figures 7-9 and 7-10.

7.3.6 Train LS

Four batch fermentations were initiated by adding paper (36 g), yeast extract (4 g), calcium carbonate (6 g), urea (0.5 g), deoxygenated water (350 mL), La Sal del Rey inocula (A23) (50 mL), and 120 μL iodoform solution (20 g/L iodoform in ethanol). The LSDR inocula was taken from the residual liquid and solid used in Chapter VI for determination of the CPDM parameters. On each transfer, paper (11.2 g) was added to F1. Yeast extract (0.4 g), calcium carbonate (1 g), urea (0.5 g), and iodoform (120 μL) were added to F1, F2, F3, and F4. The transfer of solids and liquid was performed as in Appendix D. Fresh deoxygenated water (100 mL) was added to F4 on each transfer. The total acid concentration profile and acetate content profile are shown in Figures 7-11 and 7-12.

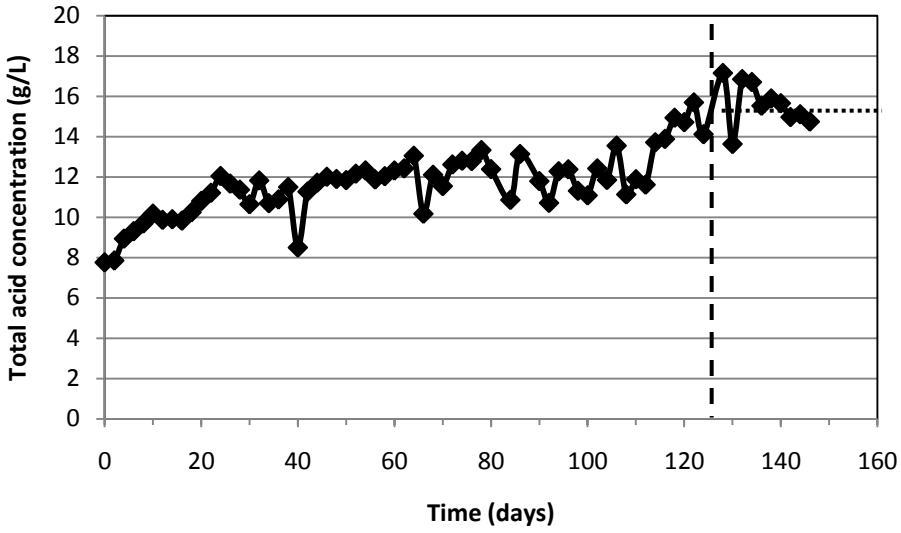

Figure 7-9. Total acid concentration for paper and yeast extract fermentation Train TI. Dash line indicates steady state (15.3 g/L).

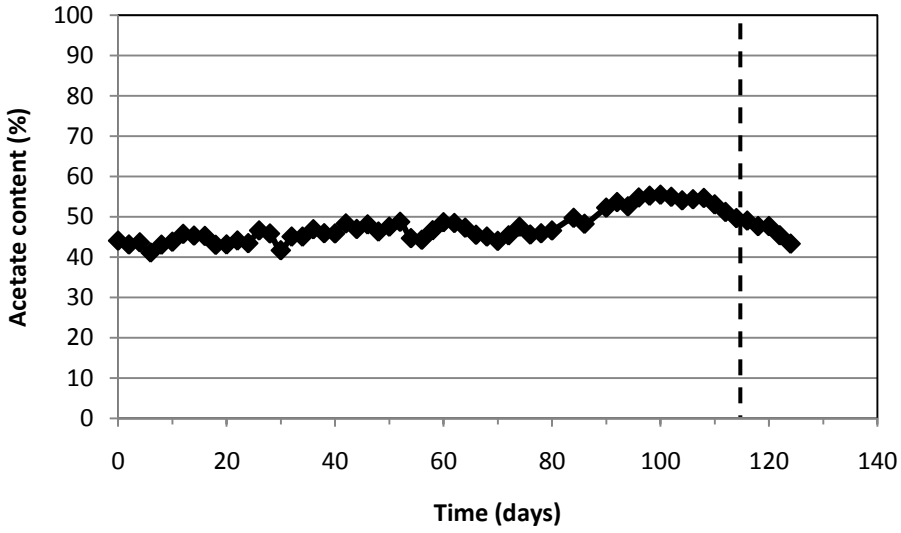

Figure 7-10. Acetate content for paper and yeast extract fermentation Train TI.

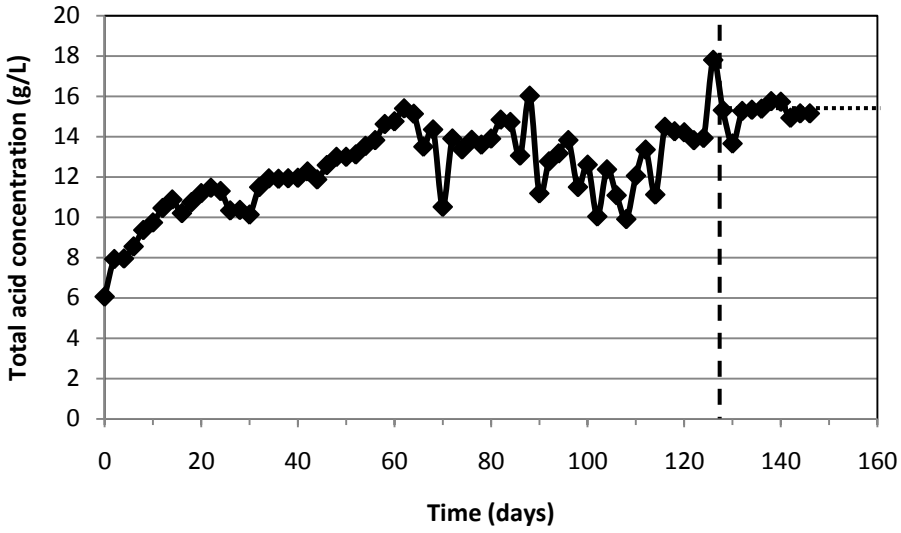

Figure 7-11. Total acid concentration for paper and yeast extract fermentation Train LS. Dash line indicates steady state (15.3 g/L).

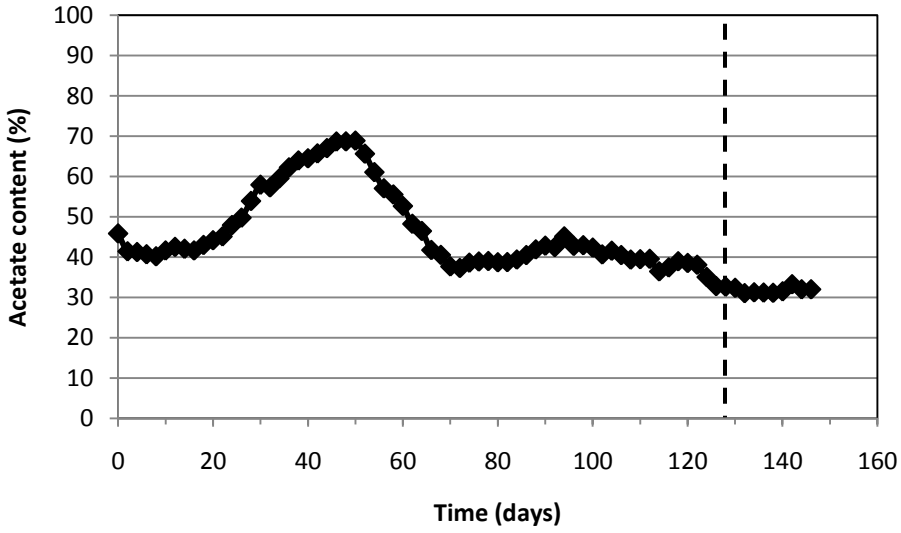

Figure 7-12. Acetate content for paper and yeast extract fermentation Train LS.

7.3.7 Train E

Four batch fermentations were initiated by adding paper (36 g), yeast extract (4 g), calcium carbonate (6 g), urea (0.5 g), deoxygenated water (350 mL), Enid, OK inocula (E08) (50 mL), and 120 μL iodoform solution (20 g/L iodoform in ethanol). The E08 inocula was taken from the residual liquid and solid used in Chapter VI for determination of the CPDM parameters. On each transfer, paper (11.2 g) was added to F1. Yeast extract (0.4 g), calcium carbonate (1 g), urea (0.5 g), and iodoform (120 μL) were added to F1, F2, F3, and F4. The transfer of solids and liquid was performed as in Appendix D. Fresh deoxygenated water (100 mL) was added to F4 on each transfer. The total acid concentration profile and acetate content profile are shown in Figures 7-13 and 7-14.

7.3.8 Train F

Four batch fermentations were initiated by adding paper (36 g), yeast extract (4 g), calcium carbonate (6 g), urea (0.5 g), deoxygenated water (350 mL), Brazoria, TX inocula (F09) (50 mL), and 120 μL iodoform solution (20 g/L iodoform in ethanol). The F09 inocula was taken from the residual liquid and solid used in Chapter VI for determination of the CPDM parameters. On each transfer, paper (11.2 g) was added to F1. Yeast extract (0.4 g), calcium carbonate (1 g), urea (0.5 g), and iodoform (120 μL) were added to F1, F2, F3, and F4. The transfer of solids and liquid was performed as in Appendix D. Fresh deoxygenated water (100 mL) was added to F4 on each transfer. The total acid concentration profile and acetate content profile are shown in Figures 7-15 and 7-16.

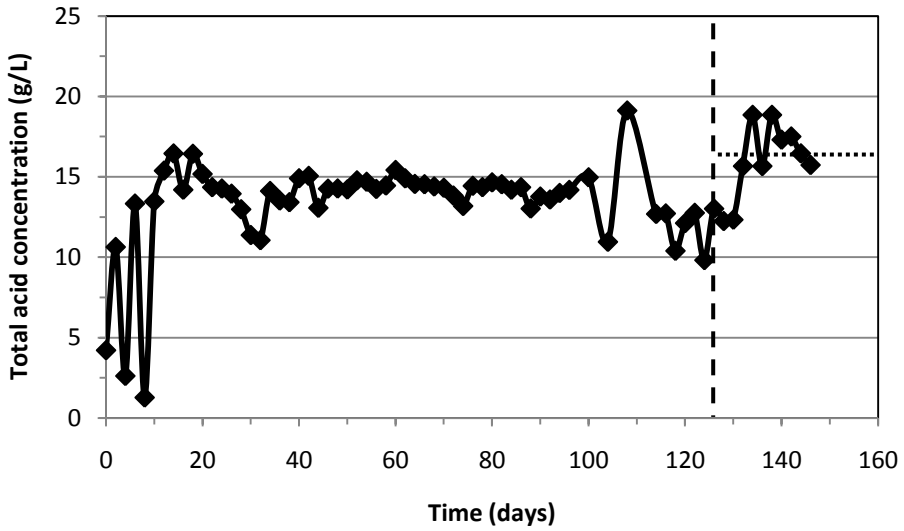

Figure 7-13. Total acid concentration for paper and yeast extract fermentation Train E. Dash line indicates steady state (16.1 g/L).

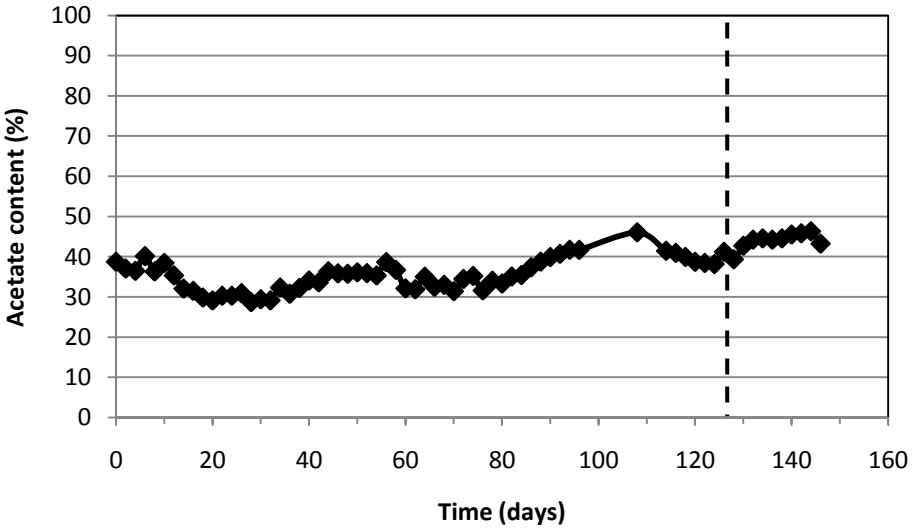

Figure 7-14. Acetate content for paper and yeast extract fermentation Train E.

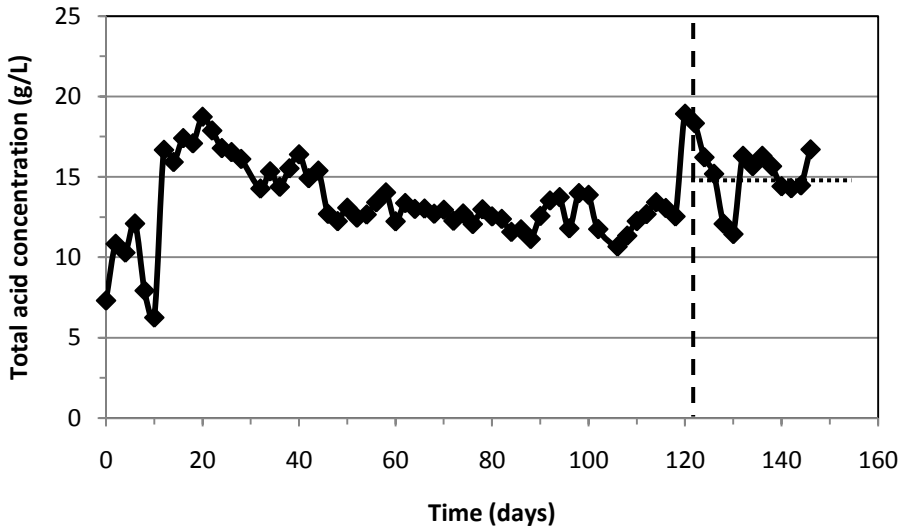

Figure 7-15. Total acid concentration for paper and yeast extract fermentation Train F. Dash line indicates steady state (14.7 g/L).

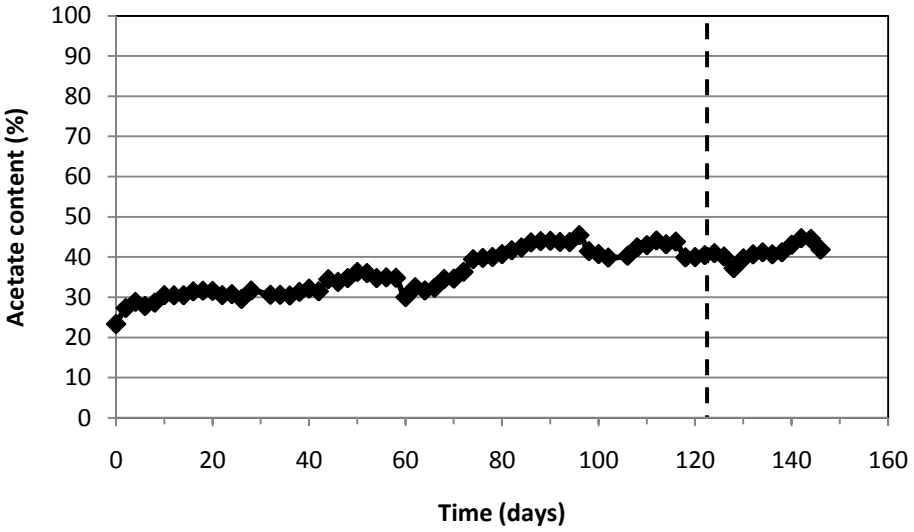

Figure 7-16. Acetate content for paper and yeast extract fermentation Train F.

7.3.9 Train G

Four batch fermentations were initiated by adding paper (36 g), yeast extract (4 g), calcium carbonate (6 g), urea (0.5 g), deoxygenated water (350 mL), Roswell-Carlsbad, NM inocula (G46) (50 mL), and 120 μL iodoform solution (20 g/L iodoform in ethanol). The G46 inocula was taken from the residual liquid and solid used in Chapter VI for determination of the CPDM parameters. On each transfer, paper (11.2 g) was added to F1. Yeast extract (0.4 g), calcium carbonate (1 g), urea (0.5 g), and iodoform (120 μL) were added to F1, F2, F3, and F4. The transfer of solids and liquid was performed as in Appendix D. Fresh deoxygenated water (100 mL) was added to F4 on each transfer. The total acid concentration profile and acetate content profile are shown in Figures 7-17 and 7-18.

7.3.10 Summary of different inocula fermentations

Table 7-2 summarizes the operating conditions for the fermentation trains using different inoculum sources. Tables 7-3 and 7-4 show the results for these countercurrent fermentations. Figures 7-19, 7-20, and 7-21 show the mass balance closures for these fermentations.

The highest acid concentration occurred at a concentration of 16.6 g/L in Train GA (LRT = 31.47 days and VSLR = 4.74 g VS/(L liq·day)) inoculated with Galveston inoculum (B01). Fermentation Train TR (LRT = 34.12 days and VSLR = 4.74 g VS/(L liq·day)) with an acid concentration of 14.3 g/L had the highest conversion (0.43 g VS digested/g VS fed). Fermentation Train F (LRT = 31.13 days and VSLR = 4.36 g VS/(L liq·day)) with an acid concentration of 14.7 g/L and conversion of 0.43 g VS digested/g VS fed had the highest productivity (0.46 g/(L liq·day)). The highest selectivity (0.27 g acid/g VS digested) was obtained from Train G (LRT = 34.37 days and VSLR = 4.44 g VS/(L liq·day)).

Overall, all nine countercurrent trains had very similar performance. The acid concentrations varied by 12% and the conversions varied by only 7%. Selectivities varied by only 10%. The similar performance could be because all nine trains had the same target VSLR and LRT, but they also should have different microbial communities. This is investigated in section 7.5.

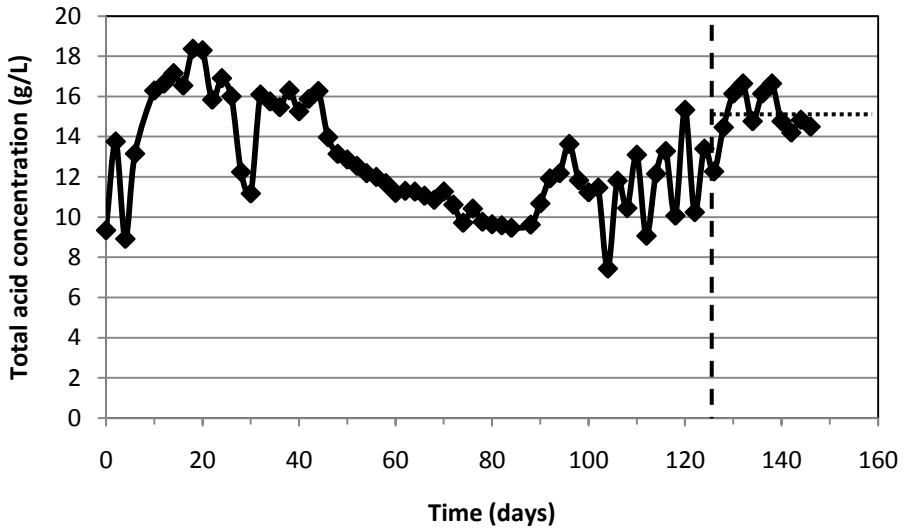

Figure 7-17. Total acid concentration for paper and yeast extract fermentation Train G. Dash line indicates steady-state (15.3 g/L).

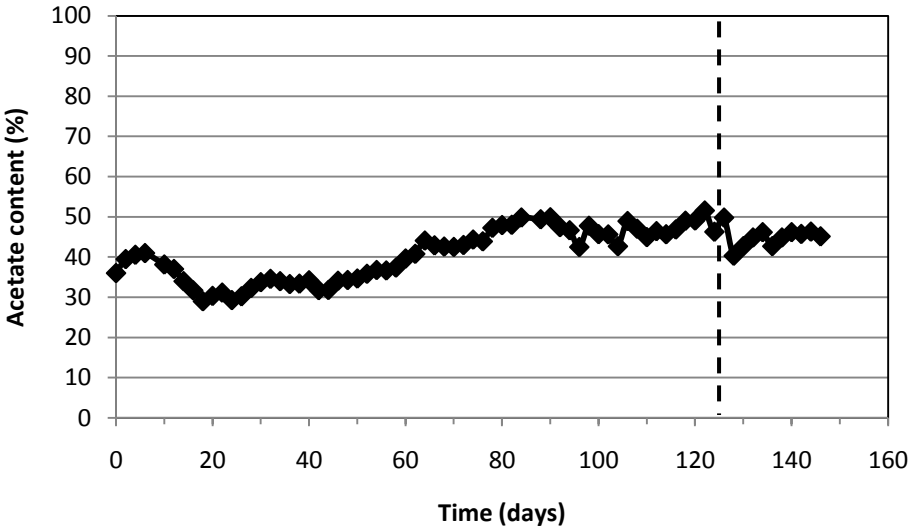

Figure 7-18. Acetate content for paper and yeast extract fermentation Train G.

Table 7-2. Operating parameters of paper and yeast extract countercurrent fermentations using different inocula.

Fermentation Trains	**GA**	**TR**	**BA**	**PU**	**TI**	**LS**	**E**	**F**	**G**
LRT (day)	31.47	34.12	39.40	33.28	32.55	36.00	31.47	31.13	34.37
VSLR (g VS/(L liq·day))	4.74	4.74	5.05	4.54	4.41	4.60	4.57	4.36	4.44
VS feed at each transfer (g VS)	10.04	10.04	10.04	10.04	10.04	10.04	10.04	10.04	10.04
Solid feed at each transfer (g)	12.4	12.4	12.4	12.4	12.4	12.4	12.4	12.4	12.4
Paper (g)	11.2	11.2	11.2	11.2	11.2	11.2	11.2	11.2	11.2
Yeast Extract (g)	1.2	1.2	1.2	1.2	1.2	1.2	1.2	1.2	1.2
Liquid fed to F4 at each transfer (L)	0.10	0.10	0.10	0.10	0.10	0.10	0.10	0.10	0.10
Liquid volume in all four fermentors (L)	1.05	1.04	1.09	1.09	1.03	1.05	1.03	1.05	1.06
Temperature (°C)	55								
Frequency of transfer	Every two days								
F1 Retained weight (wet g)	288.4	288.4	288.4	288.4	288.4	288.4	288.4	288.4	288.4
F2−F4 Retained weight (wet g)	300	300	300	300	300	300	300	300	300
Iodoform addition rate (mg/L liquid fed to F4)	96	96	96	96	96	96	96	96	96
Buffer addition rate (g $CaCO_3$/L liquid fed to F4)	40	40	40	40	40	40	40	40	40
Urea addition rate (g urea/L liquid fed to F4)	20	20	20	20	20	20	20	20	20

Table 7-3. Fermentation results for paper and yeast extract countercurrent fermentations of Trains GA, TR, BA, PU, and TI.

Fermentation Trains	GA	TR	BA	PU	TI
Total carboxylic acid concentration (g/L)	16.6 ± 0.34	14.3 ± 0.74	13.9 ± 0.87	13.7 ± 0.53	15.3 ± 0.44
Acetic acid (wt%)	30.22 ± 1.66	37.24 ± 3.17	34.33 ± 1.22	32.06 ± 1.13	37.89 ± 0.59
Propionic acid (wt %)	1.45 ± 0.08	1.67 ± 0.15	1.50 ± 0.04	1.78 ± 0.16	2.26 ± 0.28
Butyric acid (wt %)	67.64 ± 1.80	60.26 ± 3.47	63.30 ± 1.33	65.50 ± 1.16	59.29 ± 0.65
Valeric acid (wt %)	0.41 ± 0.16	0.49 ± 0.16	0.53 ± 0.19	0.48 ± 0.07	0.40 ± 0.08
Caproic acid (wt %)	0.00 ± 0.00	0.00 ± 0.00	0.00 ± 0.00	0.00 ± 0.00	0.00 ± 0.00
Heptanoic acid (wt %)	0.19 ± 0.08	0.34 ± 0.13	0.34 ± 0.03	0.19 ± 0.09	0.16 ± 0.07
Conversion (g VS digested/g VS fed)	0.38	0.43	0.38	0.41	0.42
Selectivity (g total acid/g VS digested)	0.22	0.22	0.22	0.23	0.20
Yield (g total acid/g VS fed)	0.09	0.09	0.08	0.09	0.08
Productivity (g total acid/(L liquid·day))	0.41	0.44	0.37	0.43	0.41
Mass balance closure (g VS out/g VS in)	1.069	1.037	1.001	1.043	1.008

Note: All errors are ± 1 standard deviation.

Table 7-4. Fermentation results for paper and yeast extract countercurrent fermentations for Trains LS, E, F, and G.

Fermentation Trains	LS	E	F	G
Total carboxylic acid concentration (g/L)	15.3 ± 0.28	16.0 ± 2.31	14.7 ± 1.79	15.3 ± 0.96
Acetic acid (wt %)	31.66 ± 0.74	44.0 ± 1.98	41.43 ± 2.24	44.49 ± 1.97
Propionic acid (wt %)	1.56 ± 0.21	1.75 ± 0.29	2.41 ± 0.33	1.96 ± 0.09
Butyric acid (wt %)	65.86 ± 0.90	52.59 ± 1.76	54.90 ± 2.77	51.28 ± 1.86
Valeric acid (wt %)	0.57 ± 0.03	1.66 ± 0.13	1.26 ± 0.19	2.26 ± 0.12
Caproic acid (wt %)	0.00 ± 0.00	0.00 ± 0.00	0.00 ± 0.00	0.00 ± 0.00
Heptanoic acid (wt %)	0.34 ± 0.05	0.00 ± 0.00	0.00 ± 0.00	0.00 ± 0.00
Conversion (g VS digested/g VS fed)	0.38	0.34	0.43	0.29
Selectivity (g total acid/g VS digested)	0.24	0.27	0.24	0.27
Yield (g total acid/g VS fed)	0.09	0.09	0.10	0.08
Productivity (g total acid/(L liquid·day))	0.43	0.43	0.46	0.36
Mass balance closure (g VS out/g VS in)	1.005	1.018	0.997	1.062

Note: All errors are ± 1 standard deviation.

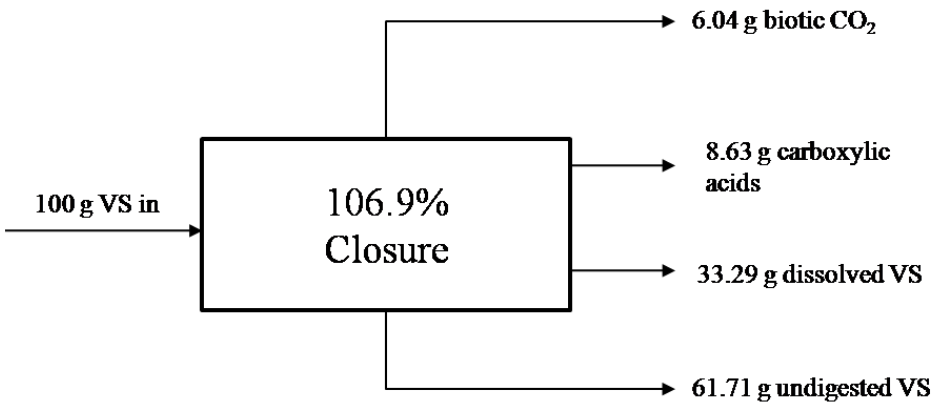

(a) For Fermentation GA.

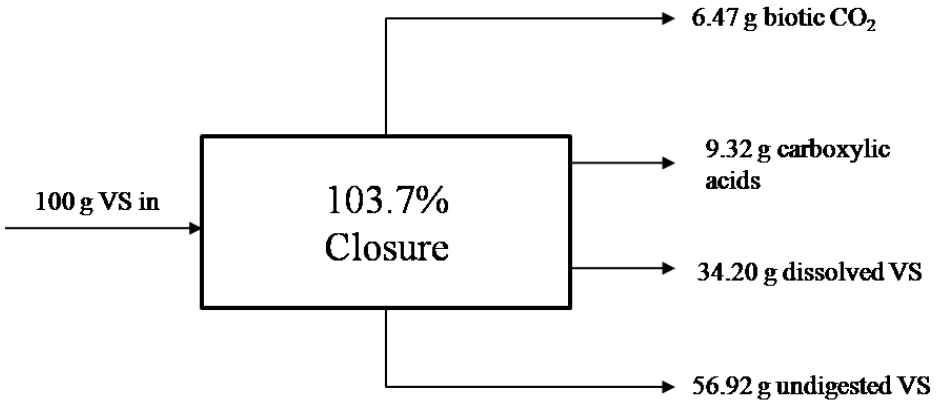

(b) For Fermentation TR.

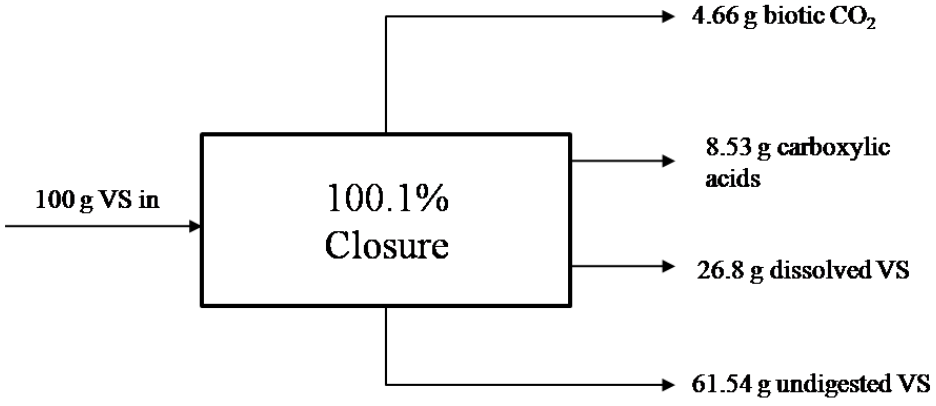

(c) For Fermentation BA.

Figure 7-19. Mass balances for paper and yeast extract fermentations GA, TR, and BA.

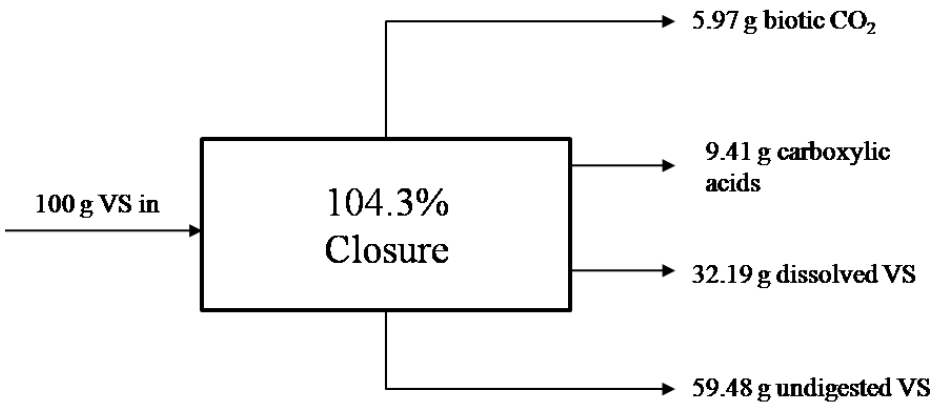

(d) For Fermentation PU.

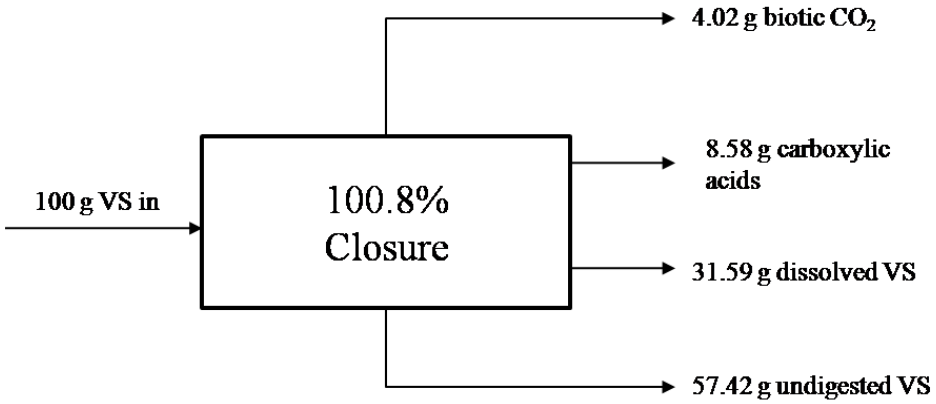

(e) For Fermentation TI.

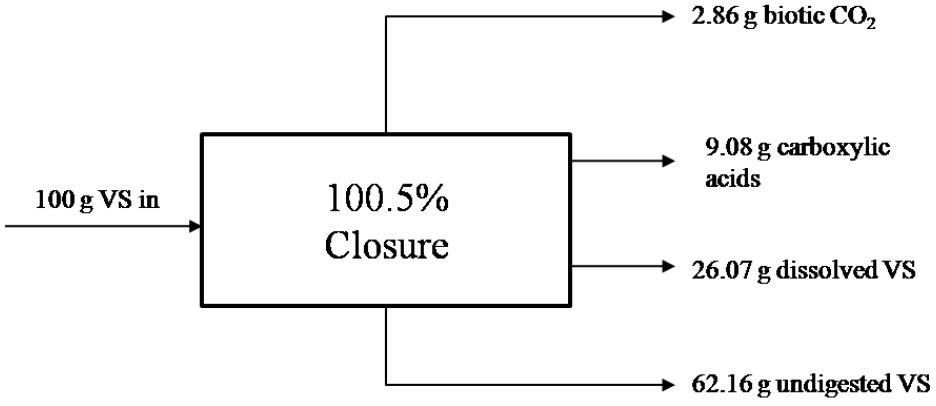

(f) For Fermentation LS.

Figure 7-20. Mass balances for paper and yeast extract fermentations PU, TI, and LS.

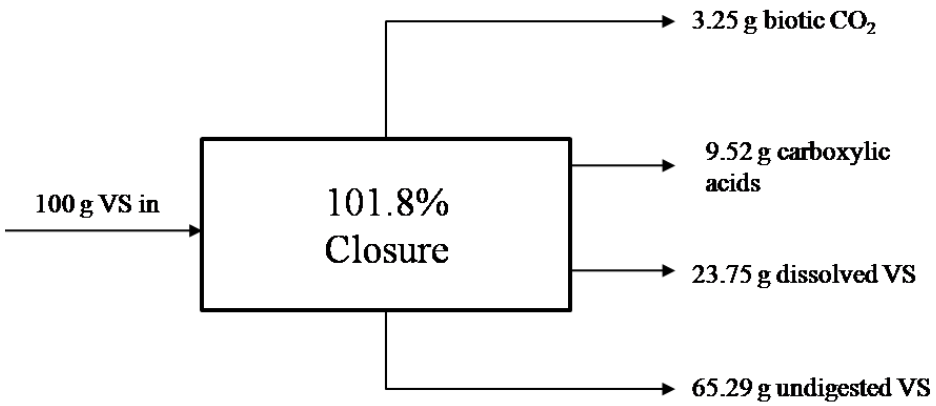

(g) For Fermentation E.

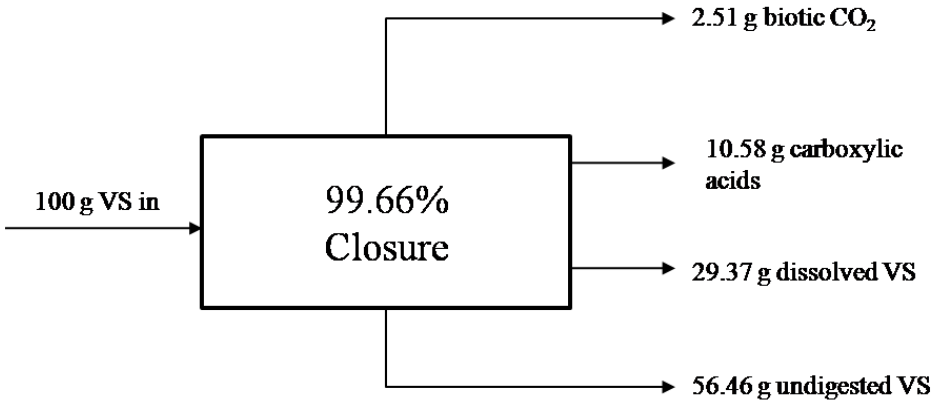

(h) For Fermentation F.

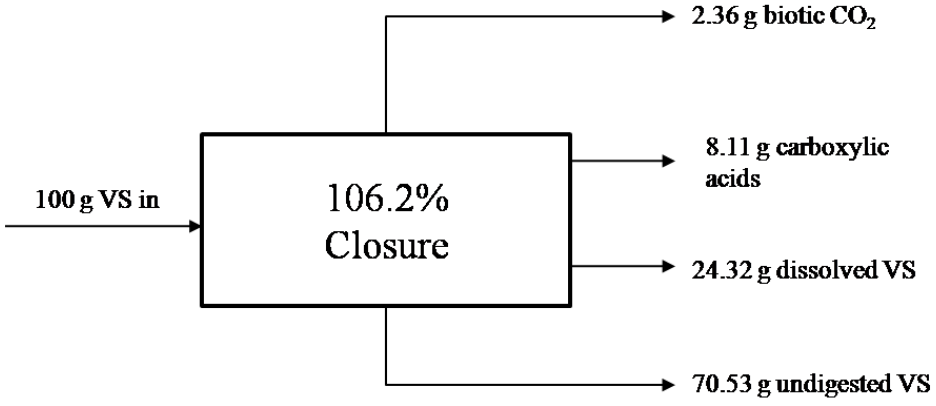

(i) For Fermentation G.

Figure 7-21. Mass balances for paper and yeast extract fermentations E, F, and G.

7.4 CPDM prediction

As mentioned in Chapter VI, countercurrent fermentations are time-consuming. It can take weeks, even months, to reach steady state. Furthermore, the long residence times require months to years to optimize for a single feedstock or inoculum. The Continuum Particle Distribution Model (CPDM) method can be used to accurately predict the biomass conversion and product concentration for these countercurrent fermentations.

Chapter VI details the parameter calculation for all nine inoculum sources. Table 7-5 lists the system-specific variables used in the CPDM prediction for each countercurrent fermentation studied in this chapter. Table 7-6 compares the experimental total carboxylic acid concentration and the conversion to the CPDM prediction. As shown, the total carboxylic acid concentrations agreed well with the CPDM predictions with an average absolute error of 7.06%. The CPDM method was even better at predicting the substrate conversions with an average absolute error of only 1.59%.

7.5 Comparison of microbial communities

For six of the fermentations detailed in this chapter (GA, TR, BA, PU, TI, and LS), community DNA sequences were taken from the CPDM and countercurrent fermentations. Emily Hollister in the Soil and Crop Sciences Department of Texas A&M University isolated and sequenced the 16S DNA. Sequences were compared against the Greengenes NAST-aligned database (DeSantis et al., 2006) and used to assign identities down to the genus level for the entire sequence data set. The quality-checked sequences were reformatted and input into the Ribosomal Database Project (RDP) pyrosequencing pipeline (Cardenas et al., 2009) and the Mothur software package (Schloss et al., 2009) to compare the bioreactor bacterial communities. RDP was used to align sequences, and Mothur was used to calculate distance matrices, assign sequences to operational taxonomic units (OTU, 97% similarity), calculate diversity indices and richness estimates, and determine the degree of overlap shared among the reactor communities. Overlap was calculated using the Yue-Clayton similarity estimator Theta YC (θ_{YC}), a metric that is scored on a scale of 0 to 1, where 0 represents complete dissimilarity and 1 represents identity (Schloss et al., 2009; Yue and Clayton, 2005). When comparing any given set of communities, θ_{YC} considers the distribution of OTUs between the communities, as well as their relative abundance.

Table 7-5. Parameter constant values in CPDM for paper and yeast extract fermentations GA, TR, BA, PU, TI, LS, E, F, and G.

Fermentation train	GA	TR	BA	PU	TI	LS	E	F	G
Holdup (g liquid/g VS cake)	4.29	4.64	5.05	4.66	4.41	4.60	4.75	4.39	4.95
Moisture (g liquid/g solid feed)	0.03	0.03	0.03	0.03	0.03	0.03	0.03	0.03	0.03
Selectivity (g Aeq/g VS digested)	0.30	0.31	0.31	0.32	0.28	0.33	0.27	0.22	0.32
F1−F4 solid concentration (g VS/L)	187	175	155	169	183	176	172	183	160
F1−F4 liquid volume (L)	0.26	0.26	0.27	0.27	0.29	0.26	0.26	0.26	0.27
Φ (g total acid/g Aeq)	0.74	0.71	0.71	0.72	0.73	0.72	0.70	0.71	0.72
e (g Aeq/(g VS·d))	0.028	0.071	0.046	0.013	0.032	0.044	0.046	0.00400	0.027
f (dimensionless)	13.3	10.8	6.80	13.00	8.10	1.00	1.02	1.63	5.56
g (L/g total acid)$^{1/h}$	0.00200	2.00	0.250	0.00400	0.0200	0.033	0.077	0.00100	0.00100
h (dimensionless)	2.30	0.26	1.40	1.50	1.50	2.50	0.97	2.23	3.36

Table 7-6. Comparison of experimental and predicted carboxylic acid concentration and conversion for paper and yeast extract fermentations with different inocula.

	GA	TR	BA	PU	TI	LS	E	F	G	Average** (%)
Experimental carboxylic acid concentration (g/L)	16.59	14.29	13.88	13.75	15.31	15.33	16.05	14.73	15.30	
Predicted (CPDM) carboxylic acid concentration (g/L)	18.70	12.73	13.28	12.44	14.23	14.80	14.61	14.88	14.43	
Error* (%)	12.68	−10.91	−4.33	−9.47	−7.01	−3.48	−8.96	1.00	−5.69	7.06
Experimental conversion	0.383	0.431	0.385	0.405	0.426	0.378	0.347	0.435	0.295	
Predicted (CPDM) conversion	0.378	0.433	0.387	0.399	0.430	0.370	0.357	0.437	0.306	
Error* (%)	−1.28	0.53	0.65	−1.34	1.08	−2.17	2.76	0.49	4.02	1.59

* Error (%) = (Predicted value – Experimental value)/Experimental value × 100

** Average errors are based on absolute value.

$$\theta_{YC} = \frac{\sum_{i=1}^{S_{12}} \frac{X_i}{n_{total}} \frac{Y_i}{m_{total}}}{\sum_{i=1}^{S_1} \left(\frac{X_i}{n_{total}}\right)^2 + \sum_{i=1}^{S_2} \left(\frac{Y_i}{m_{total}}\right)^2 - \sum_{i=1}^{S_{12}} \frac{X_i}{n_{total}} \frac{Y_i}{m_{total}}} \quad (7\text{-}1)$$

S_{12} = "species" found in both samples

X_i = The proportion of each shared "species" found in sample 1

Y_i = The proportion of each shared "species" found in sample 2

n_{total} = The total number of organisms collected in sample 1

m_{total} = The total number of organisms collected in sample 2

Within all 12 cultures, the main geni found were *Thermoanerobacterium*, *Coprothermobacter*, and *Ethanoligens*. Figures 7-22 through 7-24 show the distribution of the main genus within each culture and the change of that distribution from the CPDM culture to the countercurrent culture. By the end of the CPDM (B04) through the countercurrent fermentation (PU), the *C. thermocellum* culture from the original initial screen was no longer a pure culture. In fact, there was no *C. thermocellum* 16S DNA found in either the CPDM (B04) or the countercurrent (PU) cultures.

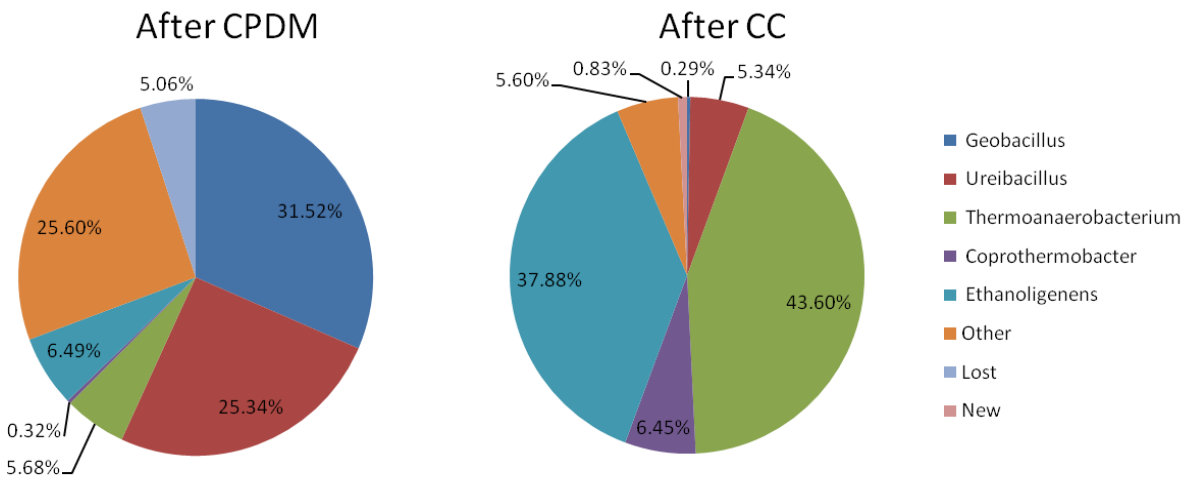

(a) Train GA

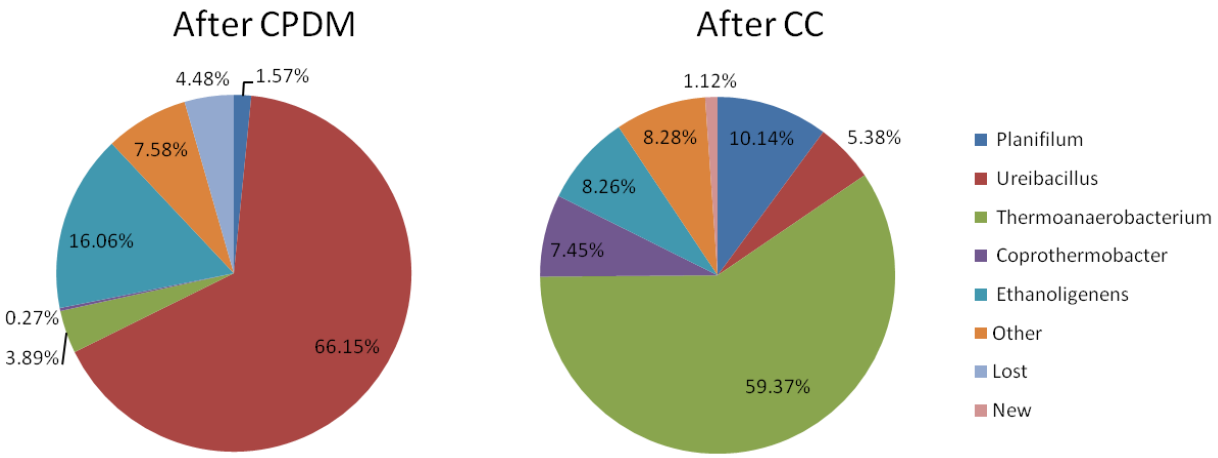

(b) Train TR

Figure 7-22. Before and after cultures from countercurrent Trains GA and TR. Only geni with more than 5% of abundance are named. 'Other' refers to the total number of species that were less than 5% individually. 'Lost' are species that were isolated in the CPDM samples but not found in the countercurrent culture. 'New' are species that were not found in the CPDM samples but were found in the countercurrent culture.

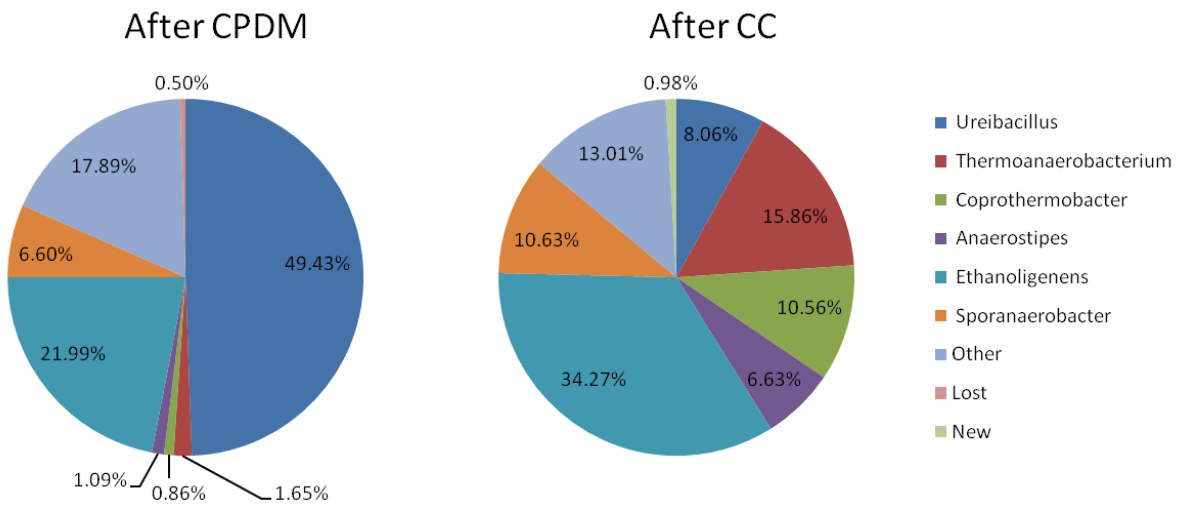

(c) Train BA

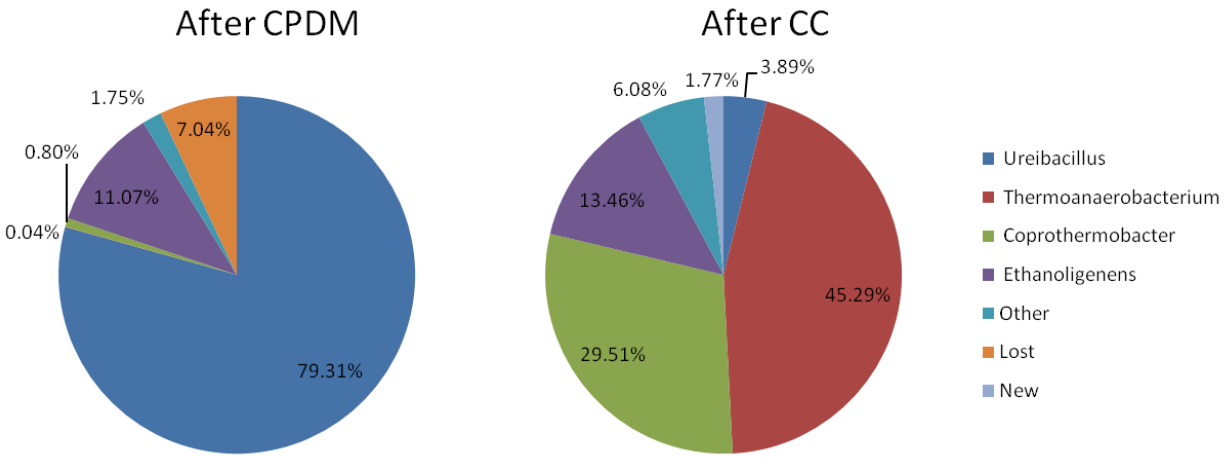

(d) Train PU

Figure 7-23. Before and after cultures from countercurrent Trains BA and PU. Only geni with more than 5% of abundance are named. 'Other' refers to the total number of species that were less than 5% individually. 'Lost' are species that were isolated in the CPDM samples but not found in the countercurrent culture. 'New' are species that were not found in the CPDM samples but were found in the countercurrent culture.

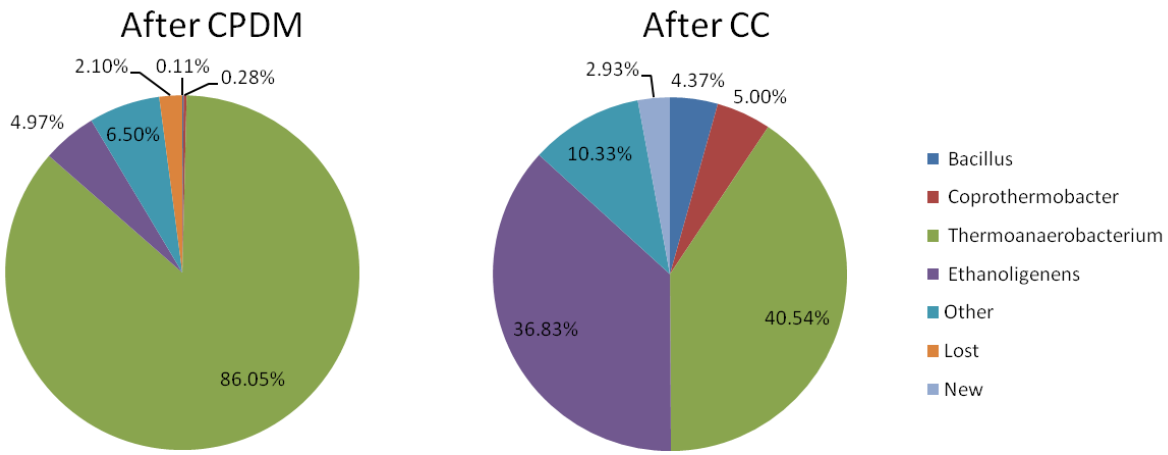

(e) Train TI

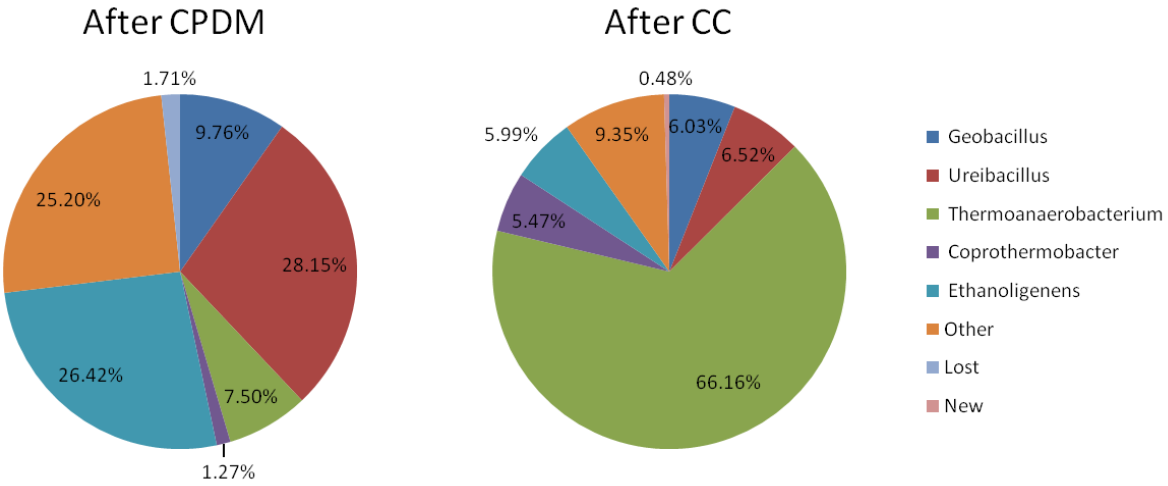

(f) Train LS

Figure 7-24. Before and after cultures from countercurrent Trains TI and LS. Only geni with more than 5% of abundance are named. 'Other' refers to the total number of species that were less than 5% individually. 'Lost' are species that were isolated in the CPDM samples but not found in the countercurrent culture. 'New' are species that were not found in the CPDM samples but were found in the countercurrent culture.

Table 7-7 shows the θ_{YC} similarity between the CPDM cultures and the final countercurrent train for each inoculum. The cultures of each inoculum changed significantly between the end of the CPDM and the end of the countercurrent fermentation. Train TI had the highest retained culture with a θ_{YC} of 0.224 whereas Train GA had the lowest at 0.015.

Table 7-7. Yue-Clayton similarity of the fermentation trains between the end of the CPDM and the end of countercurrent train. θ_{YC} is scored on a scale of 0 to 1, with a score of 0 representing complete dissimilarity and a score of 1 representing identity.

Fermentation Train	θ_{YC}
GA	0.015
TR	0.027
BA	0.169
PU	0.036
TI	0.224
LS	0.119

Table 7-8. Overlap of OTUs among the communities in paper and yeast extract fermentations, as represented by θ_{YC}, the Yue-Clayton estimator of similarity. θ_{YC} is scored on a scale of 0 to 1, with a score of 0 representing complete dissimilarity and a score of 1 representing identity.

Fermentation Train	GA	TR	BA	PU	TI	LS
GA	–					
TR	0.460	–				
BA	0.757	0.306	–			
PU	0.372	0.562	0.285	–		
TI	0.194	0.283	0.163	0.180	–	
LS	0.413	0.940	0.246	0.537	0.266	–

Table 7-8 shows the θ_{YC} similarity between the six countercurrent trains (GA, TR, BA, PU, TI, and LS). Although Train TR and Train LS had a high commonality of 0.94, all the other trains had much lower similarities. The average similarity between the six countercurrent trains was 0.40. Table 7-9 shows the percent difference in performance between the six trains in comparison to Train GA. The original inoculum source for Train GA was Galveston, TX, which is the historically used inoculum in the MixAlco™ group. The carboxylic acid production varied by 12.5% whereas the conversion varied by 6.1% between all six trains. Because the performance of the six trains was almost identical while the microbial communities were very different (average $\theta_{YC} = 0.4$), we can conclude that the performance of the continuous countercurrent fermentations does not depend on the microorganisms present, but on the conditions, i.e., the incubation temperature, the pH and buffer, and the substrate/nutrient ratios of the fermentation.

Table 7-9. Comparison of performance variables between paper and yeast extract fermentations.

Fermentation Trains	**GA**	**TR**	**BA**	**PU**	**TI**	**LS**	**Average** (%)**
Total carboxylic acid concentration (g/L)	16.59	14.29	13.88	13.75	15.31	15.33	
Change* (%)	NA	−13.86	−16.33	−17.12	−7.71	−7.59	12.52
Conversion (g VS digested/g VS fed)	0.38	0.43	0.38	0.41	0.42	0.38	
Change* (%)	NA	13.16	0.00	7.89	9.52	0.00	6.11

* Change (%) = (Value – GA value)/GA value × 100

** Average change is based on absolute value.

7.6 Effectiveness of the Bioscreening Project

The Bioscreening Project allowed the Holtzapple group, the Wilkinson group, and the Gentry group to process a wide variety of inocula sources from all across the country and beyond. It consisted of three main steps: the initial screen, CPDM, and countercurrent fermentations.

The project successfully processed the large number of samples collected, but it was not perfect. Between each fermentation step, the collected inoculum samples were frozen at −20 °C. Although this proved successful for the majority of samples, the low temperature

seems to have been detrimental to inocula collected from high temperature locations. During the initial screen of Site S – Yellowstone, samples S48 and S44, taken from thermal springs, showed promise with the highest conversions seen in the initial screen (0.46 and 0.41 g VS digested/g VS fed, respectively). But, during the CPDM step of the bioscreening process, after the inocula taken from the initial screen had been frozen and thawed, the samples showed little to no improvement over Galveston (B01) whereas other non-thermal sites (H20, K49) did show improvement over Galveston.

During the countercurrent fermentation step, it was found that the microbial communities within the fermentation trains were not only significantly different from the communities taken from the previous CPDM step, but they were significantly different from each other. It was found that the performance of the countercurrent fermentations depends on the fermentation conditions, not on the microorganisms within the fermentors.

Overall, although the Bioscreening Project isolated and identified a wide variety of microorganisms, the overall effect on fermentations was negligible. As outlined in Section 7.5, the performance of any given non-sterile fermentation system depends on the process conditions, not on the microorganisms present. For the purposes of the MixAlco™ process, the Bioscreening Project did not yield any significant improvements.

7.7 Conclusions

The following conclusions can be made based on this chapter:

1) Nine countercurrent fermentations (GA, TR, BA, PU, TI, LS, E, F, and G) of paper and yeast extract were performed with different mixed cultures. The highest acid concentration occurred at a concentration of 16.6 g/L in Train GA (LRT = 31.47 days and VSLR = 4.74 g VS/(L liq·day)) inoculated with Galveston inocula (B01). Fermentation Train TR (LRT = 34.12 days and VSLR = 4.74 g VS/(L liq·day)) − with an acid concentration of 14.3 g/L − had the highest conversion (0.43 g VS digested/g VS fed). Fermentation Train F (LRT = 31.13 days and VSLR = 4.36 g VS/(L liq·day)) − with an acid concentration of 14.7 g/L and conversion of 0.43 g VS digested/g VS fed − had the highest productivity (0.46 g/(L liq·day)). The highest selectivity (0.27 g acid/g VS digested) was obtained from Train G (LRT = 34.37 days and VSLR = 4.44 g VS/(L liq·day).
2) CPDM predictions of the nine fermentations accurately predicted the actual performance. Experimental acid concentrations and conversions agreed well with the CPDM predictions (average absolute error < 13%) in all paper and yeast extract countercurrent fermentations.
3) Microorganisms were isolated from six of the countercurrent fermentations (GA, TR, BA, PU, TI, and LS) and the CPDM cultures that were used to inoculate the countercurrent fermentations. These microbial communities changed significantly between the end of CPDM fermentations and the end of the countercurrent fermentation with an average similarity (θ_{YC}, 0 to 1 basis) of 0.10.
4) Both the performance of the countercurrent fermentations and the microbial similarity of the inocula within the fermentations were compared to each other. The six countercurrent fermentations had an average similarity (θ_{YC}) of only 0.40. All six fermentations had a very similar fermentation performance, with carboxylic acid concentrations within 12% and conversions within 7% of each other.
5) From this study, the performance of countercurrent fermentations within the MixAlco™ process is determined by the fermentation conditions, not on the specific microorganisms present within the fermentations.

6) The Bioscreening Project screened soil samples from all over the United States and beyond. The project isolated and identified a wide variety of microorganisms, but did not yield any significant improvement for the MixAlco™ process.

CHAPTER VIII
INVESTIGATION OF SEVERAL SUBSTRATES FOR VIABILITY IN THE MIXALCO™ PROCESS

The objectives of this chapter follow:

a) Evaluate the fermentation profiles of different substrates.
b) Determine the viability of different substrates in the MixAlco™ process.

8.1 Introduction

Fossil fuels are being rapidly depleted (Das and Veziroglu, 2001) and their combustion leads to global warming (Klass, 1998; Sterzinger, 1995), acid rain, and pollution. To meet our growing energy needs, renewable non-polluting energy sources will become increasingly important. Using biomass to produce liquid fuels does not cause a net increase in atmospheric carbon dioxide (Hileman, 1999; Holtzapple et al., 1999) because biomass growth removes the same amount of carbon dioxide from the atmosphere that was released during the biofuels combustion (Bungay, 1981; Sterzinger, 1995).

Another environmental problem is the accumulation of solid waste biomass. In the United States, 250 million tons of municipal solid waste was generated in 2008 (EPA, 2008). This waste contains about 63% biodegradable components, such as office paper, food scraps and yard waste (EPA, 2008). Also, millions of tons of agricultural wastes, such as pineapple residue from pineapple harvesting and wood molasses from paper processing, are discarded every year (Pandey et al., 2000), compounding the environmental problem.

Producing liquid biofuels from these waste streams is highly desirable. The objective of this study is to determine digestibility of several common waste streams using a mixed culture of marine microorganisms.

8.2 Materials and methods

A total of seven substrates were selected for this study: office paper wastes, pineapple residue, *Aloe vera* rinds, wood molasses, sugar molasses, extracted algae, and non-extracted algae. Pineapple residue was the only substrate with a lignin content greater than 12% and was treated for 1 h with hot-lime pretreatment (Appendix A). The batch fermentation procedure is detailed in Chapter II. The fermentations were conducted at 55 °C. The experimental results are presented in this chapter.

Batch fermentations were conducted in triplicate with substrate (80 wt%) and chicken manure (20 wt%) in the plastic fermentors at a concentration of 100 g dry biomass/L. The liquid volume in all fermentors was 400 mL. All fermentations were inoculated with a mixed culture of anaerobic microorganisms from a marine source (Galveston Island, TX). Ammonium bicarbonate was the only pH buffer used in this chapter. Table 8-1 lists the fermentation configurations used in this chapter. All batch fermentations were started at the same time and operated under identical conditions.

The pH in all batch fermentations was controlled near 7.0. If the measured pH fell below 7.0, ammonium bicarbonate was added to the fermentor until the pH reached the preset range (7.0−7.4). No additional ammonium bicarbonate was added if the pH was above 7.0, because the production of carboxylic acids would lower the pH.

Nutrient and methane inhibitor concentrations influence culture growth and can affect fermentation performance. Chicken manure was the nutrient source and supplied all of the nutrients required for the microorganisms. Iodoform, a methane inhibitor, was added to reduce the effect of methanogenesis. Iodoform was added to each fermentation at a rate of 2.0 mg/(L liq·day).

The total carboxylic acid concentrations, conversion, selectivity and yield were used to compare the different fermentation performance of the different pretreatment methods.

Table 8-1. Experimental conditions for anaerobic fermentations using different substrates.

Configuration		Biomass feedstock		Biomass source	Fermentation temperature (°C)	Iodoform* (mg/(L·day))
		Biomass (g)	Chicken manure (g)			
1	S01-3	32	8	Office paper wastes	55	2.0
2	S04-6	32	8	1-h hot-lime pretreated pineapple residue	55	2.0
3	S07-9	32	8	*Aloe vera* rinds	55	2.0
4	S10-12	32	8	Wood molasses	55	2.0
5	S13-15	32	8	Sugar molasses	55	2.0
6	S16-18	32	8	Extracted algae	55	2.0
7	S19-21	32	8	Non-extracted algae	55	2.0

*Iodoform added as 20 g/L ethanol solution

8.3 Results and discussion

8.3.1 Effects of substrate on fermentation profile

8.3.1.1 Effect of office paper wastes on fermentation profile

The batch fermentation performance of 80 wt% office paper wastes/20 wt% chicken manure was conducted at 55 °C. The total carboxylic acid concentration, conversion, and selectivity of the fermentations were used to evaluate the performance. Figure 8-1 shows the total carboxylic acid concentration profile. Table 8-2 summarizes the fermentation results for anaerobic fermentation of office paper wastes. Office paper waste achieved a total carboxylic acid concentration of 24.0 g/L and a conversion of 0.50 g VS digested/g VS fed. Office paper wastes obtained a selectivity of 0.53 g acid/g VS digested and a productivity of 1.00 g acid/(L liq·day).

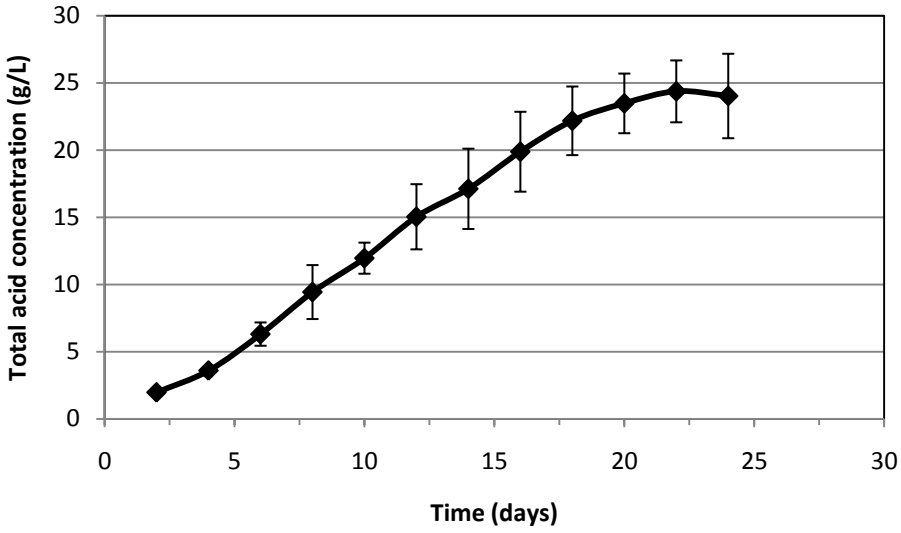

Figure 8-1. Carboxylic acid concentration for anaerobic fermentation of office paper wastes at 55 °C. Error bars are ± one standard deviation.

Table 8-2. Fermentation results for anaerobic fermentation of office paper wastes at 55 °C. Error bars are ± one standard deviation.

	Office Paper
Total carboxylic acid conc. (g/L)	24.0 ± 3.14
Acetic acid (wt %)	85.1± 0.49
Propionic acid (wt %)	2.4 ± 0.37
Butyric acid (wt %)	11.8 ± 0.92
Valeric acid (wt %)	0.7 ± 0.18
Caproic acid (wt %)	0.0
Heptanoic acid (wt %)	0.0
Conversion (g VS digested/g VS fed)	0.50 ± 0.03
Selectivity (g total acid/g VS digested)	0.53 ± 0.07
Yield (g total acid/g VS fed)	0.27 ± 0.03
Productivity (g total acid/(L liquid·day))	1.00 ± 0.13

8.3.1.2 Effect of pineapple residue on fermentation profile

Because of its high lignin content, pineapple residue was pretreated before it was fermented. The 1-h hot-lime pretreatment was used (Appendix A). Table 8.3 shows the lignin content before and after pretreatment. The batch fermentation performance of 80 wt% pretreated pineapple residue/20 wt% chicken manure was conducted at 55 °C. The total carboxylic acid concentration, conversion, and selectivity of the fermentations were used to evaluate the performance. Figure 8-2 shows the total carboxylic acid concentration profile. Table 8-4 summarizes the fermentation results for anaerobic fermentation of pineapple residue. Pineapple residue achieved a total carboxylic acid concentration of 17.2 g/L and a conversion of 0.52 g VS digested/g VS fed. This substrate obtained a selectivity of 0.33 g acid/g VS digested and a productivity of 0.65 g acid/(L liq·day).

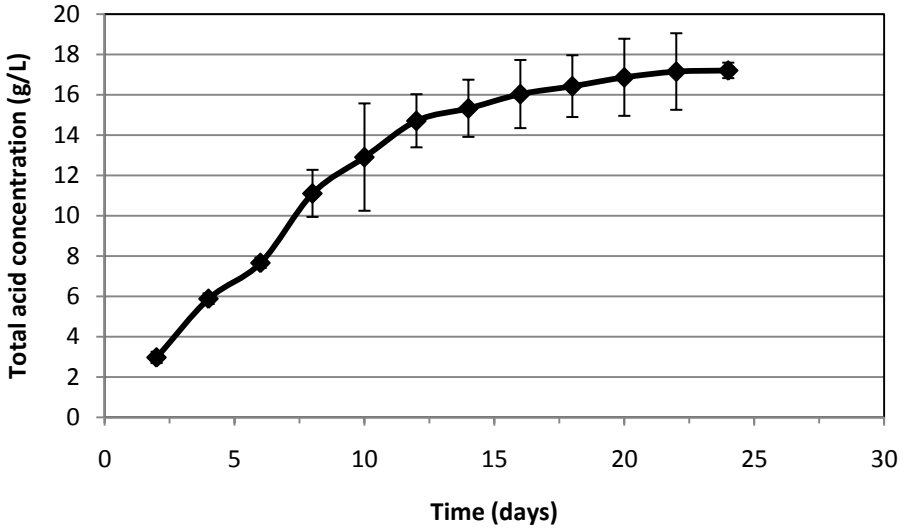

Figure 8-2. Carboxylic acid concentration for anaerobic fermentation of hot-lime pretreated pineapple residue at 55 °C. Error bars are ± one standard deviation.

Table 8-3. Sugar and lignin content of untreated and pretreated pineapple residue (g/100 g dry substrate).

	Untreated	Pretreated
Glucan	25.20	33.32
Xylan	6.32	11.57
Lignin	18.26	4.89

Table 8-4. Fermentation results for anaerobic fermentation of pretreated pineapple residue at 55 °C. Error bars are ± one standard deviation.

	Pineapple Residue
Total carboxylic acid conc. (g/L)	17.2 ± 1.89
Acetic acid (wt %)	85.3 ± 1.67
Propionic acid (wt %)	2.3 ± 0.20
Butyric acid (wt %)	11.5 ± 1.61
Valeric acid (wt %)	0.92 ± 0.26
Caproic acid (wt %)	0.0
Heptanoic acid (wt %)	0.0
Conversion (g VS digested/g VS fed)	0.52 ± 0.03
Selectivity (g total acid/g VS digested)	0.33 ± 0.01
Yield (g total acid/g VS fed)	0.17 ± 0.01
Productivity (g total acid/(L liquid·day))	0.65 ± 0.01

8.3.1.3 Effects of *Aloe vera* rinds on fermentation performance

The batch fermentation performance of 80 wt% *Aloe vera* rinds/20 wt% chicken manure was conducted at 55 °C. The total carboxylic acid concentration, conversion, and selectivity of the fermentations were used to evaluate the performance. Figure 8-3 shows the total carboxylic acid concentration profile. Table 8-5 summarizes the fermentation results for anaerobic fermentation of *Aloe vera* rinds. The rinds achieved a total carboxylic acid concentration of 25.5 g/L and a conversion of 0.59 g VS digested/g VS fed. This substrate obtained a selectivity of 0.50 g acid/g VS digested and a productivity of 1.01 g acid/(L liq·day).

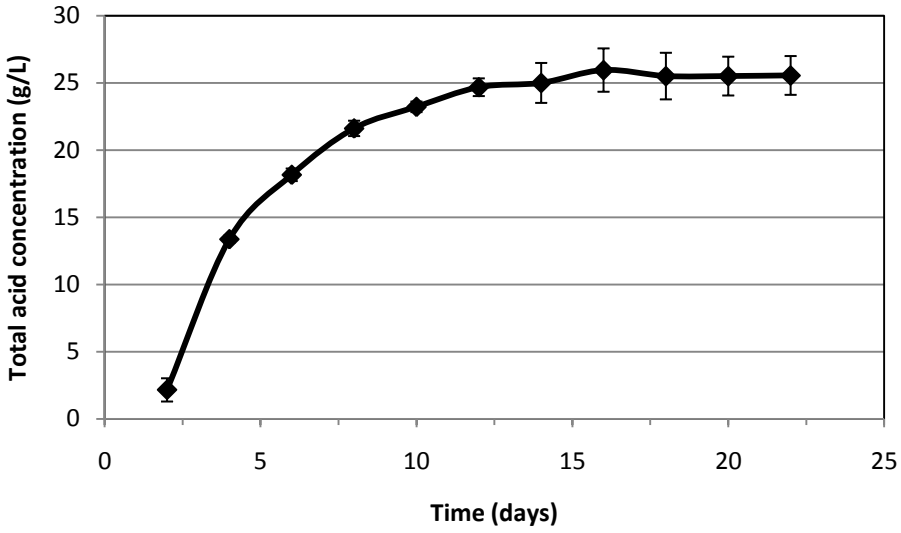

Figure 8-3. Carboxylic acid concentration for anaerobic fermentation of *Aloe vera* rinds at 55 °C. Error bars are ± one standard deviation.

Table 8-5. Fermentation results for anaerobic fermentation of *Aloe vera* rinds 55 °C. Error bars are ± one standard deviation.

	Aloe vera Rinds
Total carboxylic acid conc. (g/L)	25.5 ± 1.44
Acetic acid (wt %)	76.8 ± 0.30
Propionic acid (wt %)	5.3 ± 1.1
Butyric acid (wt %)	16.8 ± 0.99
Valeric acid (wt %)	1.2 ± 0.03
Caproic acid (wt %)	0.0
Heptanoic acid (wt %)	0.0
Conversion (g VS digested/g VS fed)	0.59 ± 0.01
Selectivity (g total acid/g VS digested)	0.50 ± 0.04
Yield (g total acid/g VS fed)	0.30 ± 0.03
Productivity (g total acid/(L liquid·day))	1.01 ± 0.03

8.3.1.4 Effect of wood molasses on fermentation performance

The batch fermentation performance of 80 wt% wood molasses/20 wt% chicken manure was conducted at 55 °C. The total carboxylic acid concentration, conversion, and selectivity of the fermentations were used to evaluate the performance. Figure 8-4 shows the total carboxylic acid concentration profile. Table 8-6 summarizes the fermentation results for anaerobic fermentation of wood molasses. The wood molasses achieved a total carboxylic acid concentration of 19.4 g/L and a conversion of 0.42 g VS digested/g VS fed. This substrate obtained a selectivity of 0.58 g acid/g VS digested and a productivity of 0.97 g acid/(L liq·day).

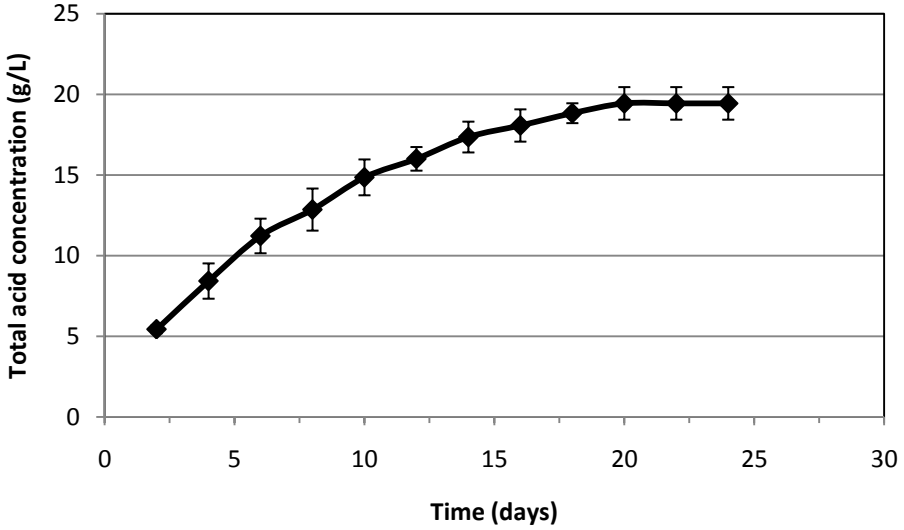

Figure 8-4. Carboxylic acid concentration for anaerobic fermentation of wood molasses at 55 °C. Error bars are ± one standard deviation.

Table 8-6. Fermentation results for anaerobic fermentation of wood molasses at 55 °C. Error bars are ± one standard deviation.

	Wood Molasses
Total carboxylic acid conc. (g/L)	19.4 ± 1.00
Acetic acid (wt %)	64.1 ± 4.33
Propionic acid (wt %)	2.2 ± 0.76
Butyric acid (wt %)	35.6 ± 2.36
Valeric acid (wt %)	0.13 ± 0.22
Caproic acid (wt %)	0.0
Heptanoic acid (wt %)	0.0
Conversion (g VS digested/g VS fed)	0.42 ± 0.16
Selectivity (g total acid/g VS digested)	0.58 ± 0.23
Yield (g total acid/g VS fed)	0.22 ± 0.01
Productivity (g total acid/(L liquid·day))	0.97 ± 0.05

8.3.1.5 Effect of sugar molasses on fermentation performance

The batch fermentation performance of 80 wt% sugar molasses/20 wt% chicken manure was conducted at 55 °C. The total carboxylic acid concentration, conversion, and selectivity of the fermentations were used to evaluate the performance. Figure 8-5 shows the total carboxylic acid concentration profile. Table 8-7 summarizes the fermentation results for anaerobic fermentation of sugar molasses. The sugar molasses achieved a total carboxylic acid concentration of 18.9 g/L and a conversion of 0.82 g VS digested/g VS fed. This substrate obtained a selectivity of 0.21 g acid/g VS digested and a productivity of 0.66 g acid/(L liq·day).

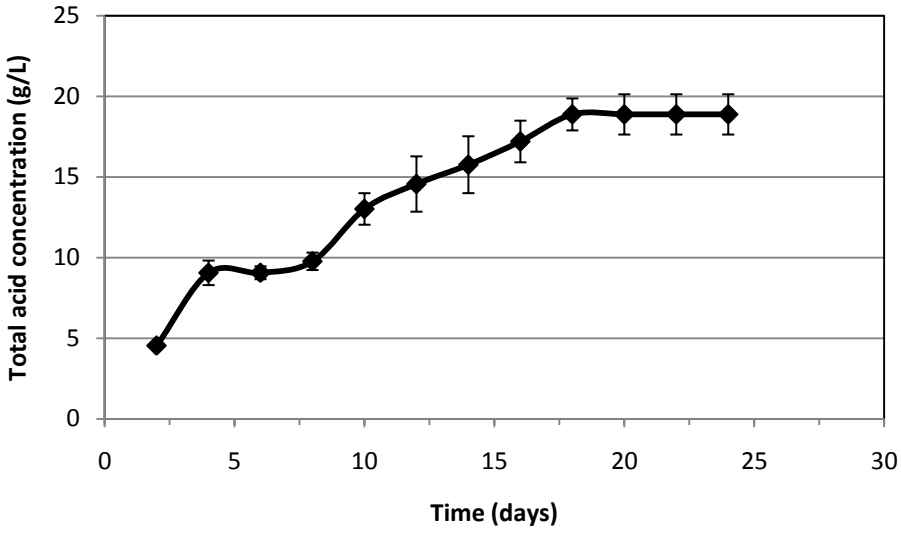

Figure 8-5. Carboxylic acid concentration for anaerobic fermentation of sugar molasses at 55 °C. Error bars are ± one standard deviation.

Table 8-7. Fermentation results for anaerobic fermentation of sugar molasses at 55 °C. Error bars are ± one standard deviation.

	Sugar Molasses
Total carboxylic acid conc. (g/L)	18.9 ± 1.25
Acetic acid (wt %)	55.0 ± 5.48
Propionic acid (wt %)	2.4 ± 0.91
Butyric acid (wt %)	42.6 ± 4.6
Valeric acid (wt %)	0.0
Caproic acid (wt %)	0.0
Heptanoic acid (wt %)	0.0
Conversion (g VS digested/g VS fed)	0.82 ± 0.07
Selectivity (g total acid/g VS digested)	0.21 ± 0.01
Yield (g total acid/g VS fed)	0.17 ± 0.02
Productivity (g total acid/(L liquid·day))	0.66 ± 0.06

8.3.1.6 Effect of extracted algae on fermentation performance

The batch fermentation performance of 80 wt% extracted algae/20 wt% chicken manure was conducted at 55 °C. The total carboxylic acid concentration, conversion, and selectivity of the fermentations were used to evaluate the performance. Figure 8-6 shows the total carboxylic acid concentration profile. Table 8-8 summarizes the fermentation results for anaerobic fermentation of extracted algae. The extracted algae achieved a total carboxylic acid concentration of 20.0 g/L and a conversion of 0.64 g VS digested/g VS fed. This substrate obtained a selectivity of 0.37 g acid/g VS digested and a productivity of 0.71 g acid/(L liq·day).

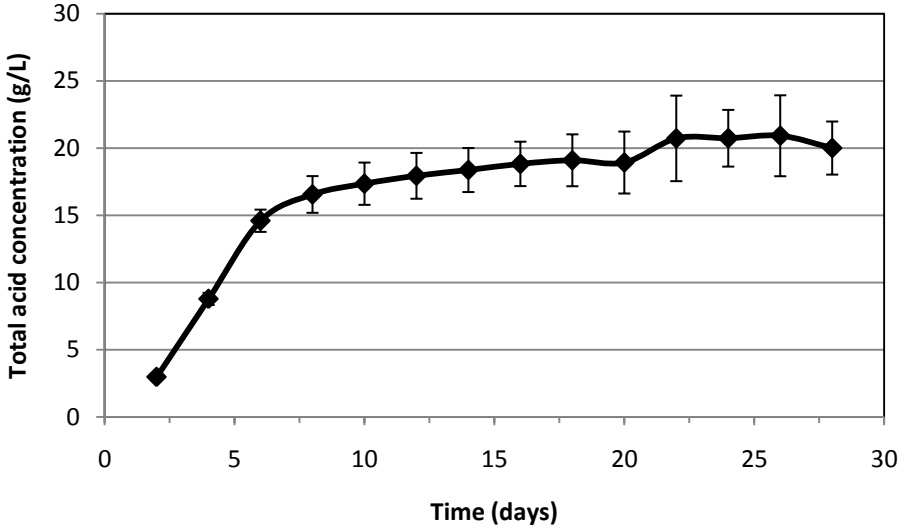

Figure 8-6. Carboxylic acid concentration for anaerobic fermentation of extracted algae at 55 °C. Error bars are ± one standard deviation.

Table 8-8. Fermentation results for anaerobic fermentation of extracted algae at 55 °C. Error bars are ± one standard deviation.

	Extracted Algae
Total carboxylic acid conc. (g/L)	20.0 ± 1.97
Acetic acid (wt %)	61.8 ± 4.16
Propionic acid (wt %)	7.3 ± 0.98
Butyric acid (wt %)	21.2 ± 2.24
Valeric acid (wt %)	9.4 ± 1.01
Caproic acid (wt %)	0.14 ± 0.08
Heptanoic acid (wt %)	0.0
Conversion (g VS digested/g VS fed)	0.64 ± 0.01
Selectivity (g total acid/g VS digested)	0.37 ± 0.03
Yield (g total acid/g VS fed)	0.24 ± 0.02
Productivity (g total acid/(L liquid·day))	0.71 ± 0.07

8.3.1.7 Effect of non-extracted algae on fermentation performance

The batch fermentation performance of 80 wt% non-extracted algae/20 wt% chicken manure was conducted at 55 °C. The total carboxylic acid concentration, conversion, and selectivity of the fermentations were used to evaluate the performance. Figure 8-7 shows the total carboxylic acid concentration profile. Table 8-9 summarizes the fermentation results for anaerobic fermentation of non-extracted algae. The non-extracted algae achieved a total carboxylic acid concentration of 21.3 g/L and a conversion of 0.63 g VS digested/g VS fed. This substrate obtained a selectivity of 0.40 g acid/g VS digested and a productivity of 0.76 g acid/(L liq·day).

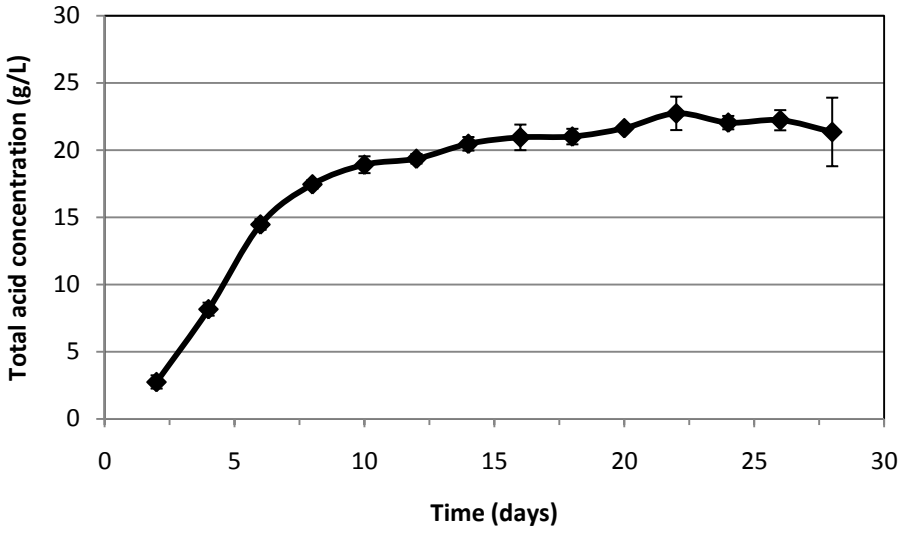

Figure 8-7. Carboxylic acid concentration for anaerobic fermentation of non-extracted algae at 55 °C. Error bars are ± one standard deviation.

Table 8-9. Fermentation results for anaerobic fermentation of non-extracted algae at 55 °C. Error bars are ± one standard deviation.

	Non-extracted Algae
Total carboxylic acid conc. (g/L)	21.3 ± 2.55
Acetic acid (wt %)	61.4 ± 1.61
Propionic acid (wt %)	7.2 ± 0.52
Butyric acid (wt %)	22.1 ± 1.38
Valeric acid (wt %)	9.2 ± 0.44
Caproic acid (wt %)	0.13 ± 0.08
Heptanoic acid (wt %)	0.0
Conversion (g VS digested/g VS fed)	0.63 ± 0.01
Selectivity (g total acid/g VS digested)	0.40 ± 0.04
Yield (g total acid/g VS fed)	0.25 ± 0.03
Productivity (g total acid/(L liquid·day))	0.76 ± 0.09

8.3.2 Comparison of substrates

Table 8-10 summarizes the fermentation results for all substrates studied in this chapter. *Aloe vera* rinds had the highest acid concentration (25.5 g/L) and highest productivity (1.01 g acid/(L liq·day)). Office paper wastes had the next highest acid concentration of 24.0 g/L followed by non-extracted algae (21.3), extracted algae (20.0), wood molasses (19.4), sugar molasses (18.9), and then pineapple residue (17.2). Sugar molasses had the highest conversion of 0.82 g VS digested/g VS fed but it also had the lowest selectivity (0.21 g acid/g VS digested).

Although the overall productivity of both extracted and non-extracted algae was only 0.7 g acid/(L liq·day), their initial productivity much higher. Like the *Aloe vera*, they produced 70% of their total acid production within the first six days of the fermentation. *Aloe vera*, extracted algae, and non-extracted algae also produced the same content of acetic acid (68%, 61%, and 61%, respectively).

It is interesting to note that the ratio of acetic to butyric acid depended on the substrate. Solid substrates with large complex macromolecules of cellulose (office paper and pineapple residue) produced nearly 80% acetic acid. Substrates with intermediate-sized lengths of cellulose (*Aloe vera*, wood molasses, extracted, and non-extracted algae) produced less acetic acid (*Aloe vera*: 68%, wood molasses: 64%, extracted algae: 61%, non-extracted algae: 61%). The substrate with the simplest chemicals (sugar molasses) produced the lowest percentage of acetic acid (55%). In fact, Figure 8-8 shows that the acetic acid percentage dropped as low as 12.5% in the first few days of the fermentation.

Bacterial cells produce carboxylic acids to gain metabolic energy for cellular processes such as enzyme production and DNA replication; however, the very products impart an osmotic stress on the cell making it more difficult for them to grow. For complex substrates (office paper, pineapple residue), the cells have an extra metabolic load because they must produce hydrolytic enzymes to break down the complex chemical structures; however, the large, insoluble substrates also impart less osmotic stress on the cell. Both these factors favor acetic acid production.

For soluble substrates, hydrolytic enzymes are not needed, so there is less energy stress; however, the soluble substrates increase the osmotic stress. By favoring butyric acid, the cells can still produce energy for the metabolic needs (as described in Chapter III), but

have less osmotic stress. The sugar molasses fermentation is a perfect example. With the high initial osmotic stress, the cells heavily favored the higher molecular weight acids. It was only as the cells used up the soluble substrate, removing that osmotic stress, that they began to produce more acetic acid, increasing the percentage from 12.5% at Day 4 to 54.7% at Day 20.

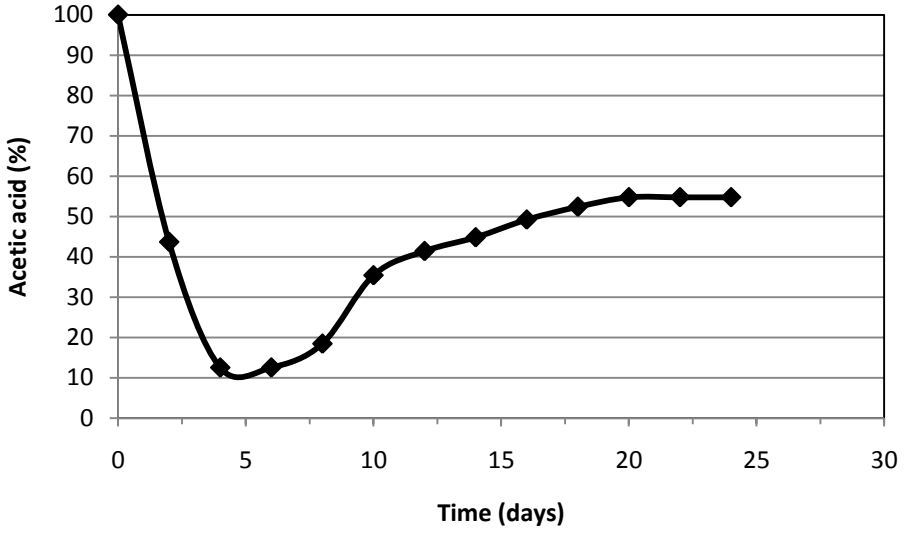

Figure 8.8. Acetic acid (C2) percentage for sugar molasses fermentation at 55 °C.

Table 8-10. Fermentation results for anaerobic fermentation of several substrates at 55 °C. Error bars are ± one standard deviation.

Substrate	Total acid conc. (g/L)	Conversion (g VS dig/g VS fed)	Selectivity (g acid/g VS dig)	Productivity (g acid/(L liq·day))
Office paper	24.0 ± 3.14	0.50 ± 0.03	0.53 ± 0.07	1.00 ± 0.13
Pineapple residue	17.2 ± 1.89	0.52 ± 0.03	0.33 ± 0.01	0.65 ± 0.01
Aloe vera rinds	25.5 ± 1.44	0.59 ± 0.01	0.50 ± 0.04	1.01 ± 0.03
Wood molasses	19.4 ± 1.00	0.42 ± 0.16	0.58 ± 0.23	0.97 ± 0.05
Sugar molasses	18.9 ± 1.25	0.82 ± 0.07	0.21 ± 0.01	0.66 ± 0.06
Extracted algae	20.0 ± 1.97	0.64 ± 0.01	0.37 ± 0.03	0.71 ± 0.07
Non-extracted algae	21.3 ± 2.55	0.63 ± 0.01	0.40 ± 0.04	0.76 ± 0.09

In summary, all substrates studied in this chapter show relatively high acid productions and substrate conversions, making them promising candidates for industrial-scale MixAlco™ fermentations. Additionally, the high initial reaction rate for *Aloe vera*, extracted algae, and non-extracted algae may reduce both the residence time and reactor size on the industrial scale, decreasing the capital costs for the fermentors. Despite the fact that it consists of soluble simple sugars, sugar molasses was probably slow to digest because of the increased osmotic stress on the microorganisms within the fermentation. A continuously fed system where small amounts of the substrate are added at a time would remove the osmotic stress and potentially produce very high concentrations of carboxylic acids.

8.4 Conclusions

The following conclusions can be made based on this study:

1) Office paper wastes, pineapple residue, *Aloe vera*, wood molasses, sugar molasses, extracted, and non-extracted algae are all highly fermentable in the MixAlco™ process, producing high carboxylic acid concentrations (24.0, 17.2, 25.5, 19.4, 18.9, 20.0, and 21.3 g/L, respectively).
2) The high lignin content of pineapple residue necessitates pretreatment before it becomes digestible but a short 1-h hot-lime pretreatment was all that was necessary to achieve an acid concentration of 17.2 g/L and a conversion of 52%.
3) *Aloe vera*, extracted algae, and non-extracted algae are highly reactive, achieving 70% of their acid production within the first 6 days of the fermentation. This could potentially reduce the residence time and the size of industrial fermentations, reducing capital costs greatly.
4) Sugar molasses and other soluble substrates increase the osmotic stress on the microorganisms which decreases the production rate and highly favors the formation of higher-molecular-weight acids until the osmotic stress is removed. Sugar molasses produced only 12.5% acetic acid on Day 4 of the fermentation and only reached a percentage of 55% by Day 20.

CHAPTER IX
FERMENTATION OF GLYCEROL FROM THE BIODIESEL PROCESS

The objectives of this chapter follow:

a) Compare the fermentation profiles of crude and distilled glycerol from the biodiesel process with refined glycerol.
b) Investigate two continuous fermentation configurations: a continuously stirred tank reactor (CSTR) and a packed-bed reactor.

9.1 Introduction

Rapidly depleting fossil fuels (Das and Veziroglu, 2001) plus increasing concerns about global warming (Klass, 1998; Sterzinger, 1995) and the environment have increased biodiesel production. It is estimated that the annual production capacity of biodiesel in the United States alone reached 700 million gallons in 2008 (NBB, 2008). Biodiesel is produced by transesterifying triglycerides in fats and vegetable oils (Figure 9-1) (NBB, 2006). To make biodiesel, methanol and an alkali catalyst (i.e., sodium hydroxide or potassium hydroxide) are mixed. This mixture is then added to the vegetable oil where the methyl esters (biodiesel) break off of the glycerol backbone of the triglyceride, resulting in a glycerol byproduct. Centrifugation or gravity settling is used to separate the biodiesel product from the glycerol. For every gallon of biodiesel produced, 1 pound of glycerol is produced (Fortenbery, 2005). This increase in glycerol production has depressed the price of refined glycerol from $1.00/lb in 1995 to less than $0.40/lb in 2005 (Heming, 2005). Unfortunately, even after methanol recovery, the crude glycerol from biodiesel processing contains about 20% water and several catalytic and waste residues that make it difficult to use. Vacuum distillation followed by carbon treatment can remove much of the impurities, but it is extremely energy intensive (NBB, 2006). As biodiesel production continues to rise, a use for crude glycerol byproduct must be found.

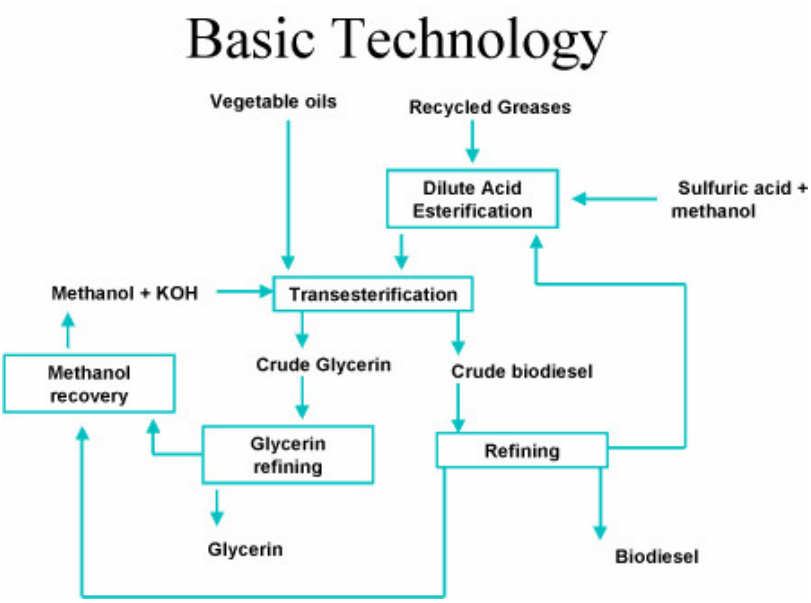

Figure 9-1. Schematic of biodiesel production. (AEN, 2009).

Through thermochemical processes, glycerol can be converted into propylene glycol (Dasari et al., 2005) and acetol (Chiu et al., 2006). Glycerol has also been used as carbon source in fermentations to produce 1,3 propanediol (Gonzalez-Pajuelo et al., 2006). Anaerobic fermentation of glycerol by *E. coli* generated the following mixture of products: ethanol, succinate, acetate, lactate, and hydrogen (Dharmadi et al., 2006). Using waste glycerol as a fermentation substrate shows great potential (Fernando et al., 2006; Saint-Amans et al., 2001; Temudo et al., 2008).

The study in this chapter was to determine the mixed-acid fermentation profiles of three types of glycerol (crude, distilled, and refined) and to investigate two possible fermentation configurations for continuous fermentations.

9.2 Materials and methods

9.2.1 Batch fermentations

Three types of glycerol were examined in this study: crude glycerol, distilled glycerol, and refined glycerol. Crude glycerol comes directly from the methanol recovery step with no other processing. The distilled glycerol has been vacuum distilled to remove the majority of the water whereas the refined glycerol is pure glycerol with no other components.

The batch fermentation procedure is detailed in Chapter II. The fermentations were conducted in triplicate at 55 °C. The experimental results are presented in this chapter.

Batch fermentations were conducted with substrate (80 wt%) and chicken manure (20 wt%) in the plastic fermentors at a concentration of 100 g dry biomass/L. The liquid volume in all fermentors was 400 mL. All fermentations were inoculated with a mixed culture of anaerobic microorganisms from a marine source (Galveston Island, TX). Ammonium bicarbonate was the only pH buffer used in this chapter. Table 9-1 lists the fermentation configurations used in this chapter. All batch fermentations were started at the same time and operated under identical conditions.

In all batch fermentations, the pH was controlled around 7.0. If the measured pH fell below 7.0, ammonium bicarbonate was added to the fermentor until the pH reached the preset range (7.0−7.4). No additional ammonium bicarbonate was added if the pH was above 7.0, because the production of carboxylic acids would lower the pH.

Nutrient and methane inhibitor concentrations influence culture growth and can effect fermentation performance. Chicken manure was the nutrient source and supplied all of the nutrients required for the microorganisms. Iodoform, a methane inhibitor, was added to reduce the effect of methanogenesis. Iodoform was added to each fermentation at a rate of 2.0 mg/(L liq·day).

The total carboxylic acid concentrations, conversion, selectivity, and yield were used to compare the different fermentation performance of the types of glycerol.

Table 9-1. Experimental conditions for anaerobic fermentations using different types of glycerol.

Configuration	Biomass feedstock		Biomass source	Fermentation temperature (°C)	Iodoform* (mg/(L liq·day))
	Biomass (g)	Chicken manure (g)			
1	32	8	Crude glycerol	55	2.0
2	32	8	Distilled glycerol	55	2.0
3	32	8	Refined glycerol	55	2.0

*Iodoform added as 20 g/L ethanol solution

9.2.2 CSTR fermentations

The CSTR fermentation procedure is detailed in Chapter II. The fermentation was conducted at 55 °C. The experimental results are presented in this chapter.

CSTR fermentations were conducted with refined glycerol (80 wt%) and chicken manure (20 wt%) in the Continuously Stirred Tank Reactor (CSTR) at a concentration of 100 g dry biomass/L. The liquid volume was 6 L. The fermentation was inoculated with a mixed culture of anaerobic microorganisms from a marine source (Galveston Island, TX). Ammonium bicarbonate was the only pH buffer used in this chapter.

The pH was controlled at 7.0. If the measured pH fell below 7.0, a 30 wt% ammonium bicarbonate solution was added to the fermentor until the pH reached the preset range (7.0−7.4). No additional ammonium bicarbonate was added if the pH was above 7.0. The production of carboxylic acids would lower the pH.

Nutrient and methane inhibitor concentrations influence culture growth and can effect fermentation performance. Chicken manure was the nutrient source and supplied all of the nutrients required for the microorganisms. Iodoform, a methane inhibitor, was added to reduce the effect of methanogenesis. Iodoform was added to each fermentation at a rate of 2.0 mg/(L liq·day).

9.2.3 Packed-bed fermentation

The packed-bed fermentation procedure is detailed in Chapter II. The fermentation was conducted at 55 °C. The experimental results are presented in this chapter.

Packed-bed (PB) fermentations were conducted with refined glycerol (80 wt%) and chicken manure (20 wt%) at a concentration of 100 g dry biomass/L. Because dried chicken manure would have plugged the packing material within the reactor, a liquefied version was used in this fermentation. For every gram of glycerol added to the fermentation, a 20/80 wt% ratio of dried chicken manure was added to the liquid media. The media was stirred for 20 minutes then the remaining solid was centrifuged out. The nutrient-rich media (Appendix C) was then used in the packed bed. The total liquid volume was 2 L. The fermentation was inoculated with a mixed culture of anaerobic microorganisms from a marine source (Galveston Island, TX). Ammonium bicarbonate was the only pH buffer used in this chapter.

The pH was controlled at 7.0. If the pH fell below 7.0, a 30 wt% ammonium bicarbonate solution was added to the fermentor until the pH reached the preset range (7.0−7.4). No additional ammonium bicarbonate was added if the pH was above 7.0. The production of carboxylic acids would lower the pH.

Nutrient and methane inhibitor concentrations influence culture growth and can effect fermentation performance. Chicken manure was the nutrient source and supplied all of the nutrients required for the microorganisms. Iodoform, a methane inhibitor, was added to reduce the effect of methanogenesis. Iodoform was added to each fermentation at a rate of 2.0 mg/(L liq·day).

9.3 Results and discussion

9.3.1 Effects of glycerol type of batch fermentation performance

At 55 °C, the batch fermentation performance of three types of glycerol: crude, distilled, and refined was evaluated. The total carboxylic acid concentration, conversion, and selectivity of the fermentations were used to evaluate the performance.

9.3.1.1 Effect on total carboxylic acid concentration

Figure 9-2 shows the total carboxylic acid concentrations from batch fermentations from each type of glycerol. All types of glycerol were highly digestible. The highest acid concentration was obtained from crude glycerol at 24.0 g/L. The distilled and refined glycerol produced 23.5 and 22.6 g/L, respectively. Although the catalytic and waste residues inhibit industrial refining and processing of glycerol, they do not inhibit the fermentation. In fact, they seem to slightly enhance acid production.

9.3.1.2 Summary of glycerol types fermentations

Table 9-2 shows the fermentation results for the different types of glycerol. The crude glycerol had the highest conversion (0.70 g VS digested/g VS fed), followed by the distilled glycerol (0.64), then refined glycerol (0.62). Selectivities for crude, distilled, and refined glycerol were 0.40, 0.38 and 0.37 g acid/g VS digested, respectively. Using a pure culture of *Clostridium butyricum*, Himmi et al. (1999) obtained a similar conversion of 0.72 g digested/g fed from a refined glycerol concentration of 123 g/L. Biebl (2001), using a

culture of *C. pasteurianum* and refined glycerol concentrations of 84 and 115 g/L, obtained conversions of 0.74 and 0.55 and selectivities of 0.42 and 0.39 g product/g glycerol digested, respectively. This study produced similar results with refined glycerol using a mixed culture of microorganisms.

Additionally, although the catalytic and waste residues inhibit industrial refining and processing of glycerol, they do not inhibit the fermentation. They actually seem to slightly enhance all aspects of the fermentation. Conversion, selectivity, yield, and productivity were all higher with crude glycerol than with refined glycerol. Also, these residues shifted the ratio of acetic to butyric acid. Crude glycerol, which has the highest concentration of these residues, also had the highest percentage of acetic acid (61.6%). The acetic acid percentage dropped slightly (59.0%) in distilled glycerol, which had some but not all of the residues removed. In the refined glycerol, the percentage of acetic acid was even lower (55.1%).

The exact composition of the residues within the crude glycerol is not known, but they do contain both organic residues and salt residues. The slightly improved performance could be caused by either or both of these residues. The salts could have acted as an additional buffer for the system, helping to maintain the pH and limiting some of the product inhibition caused by the carboxylic acids. The organic residues possibly supplied additional trace nutrients to the microorganisms, improving their performance.

Table 9-2. Effect of glycerol type on batch anaerobic fermentation at 55 °C.

Glycerol type	Crude	Distilled	Refined
Total carboxylic acids (g/L)	24.0 ± 2.03	23.5 ± 1.64	22.6 ± 0.64
Acetic (wt%)	61.66	58.99	55.07
Propionic (wt%)	1.82	0.77	0.51
Butyric (wt%)	36.52	40.23	44.42
Valeric (wt%)	0.00	0.00	0.00
Caproic (wt%)	0.00	0.00	0.00
Heptanoic (wt%)	0.00	0.00	0.00
Conversion (g VS digested/g VS fed)	0.70 ± 0.06	0.64 ± 0.02	0.62 ± 0.05
Selectivity (g acids/g VS digested	0.40 ± 0.07	0.38 ± 0.03	0.37 ± 0.04
Yield (g acids/g VS fed)	0.27 ± 0.02	0.25 ± 0.02	0.23 ± 0.01
Productivity (g acids/(L liq·day))	0.75 ± 0.06	0.74 ± 0.05	0.71 ± 0.02

Error bars are ± one standard deviation.

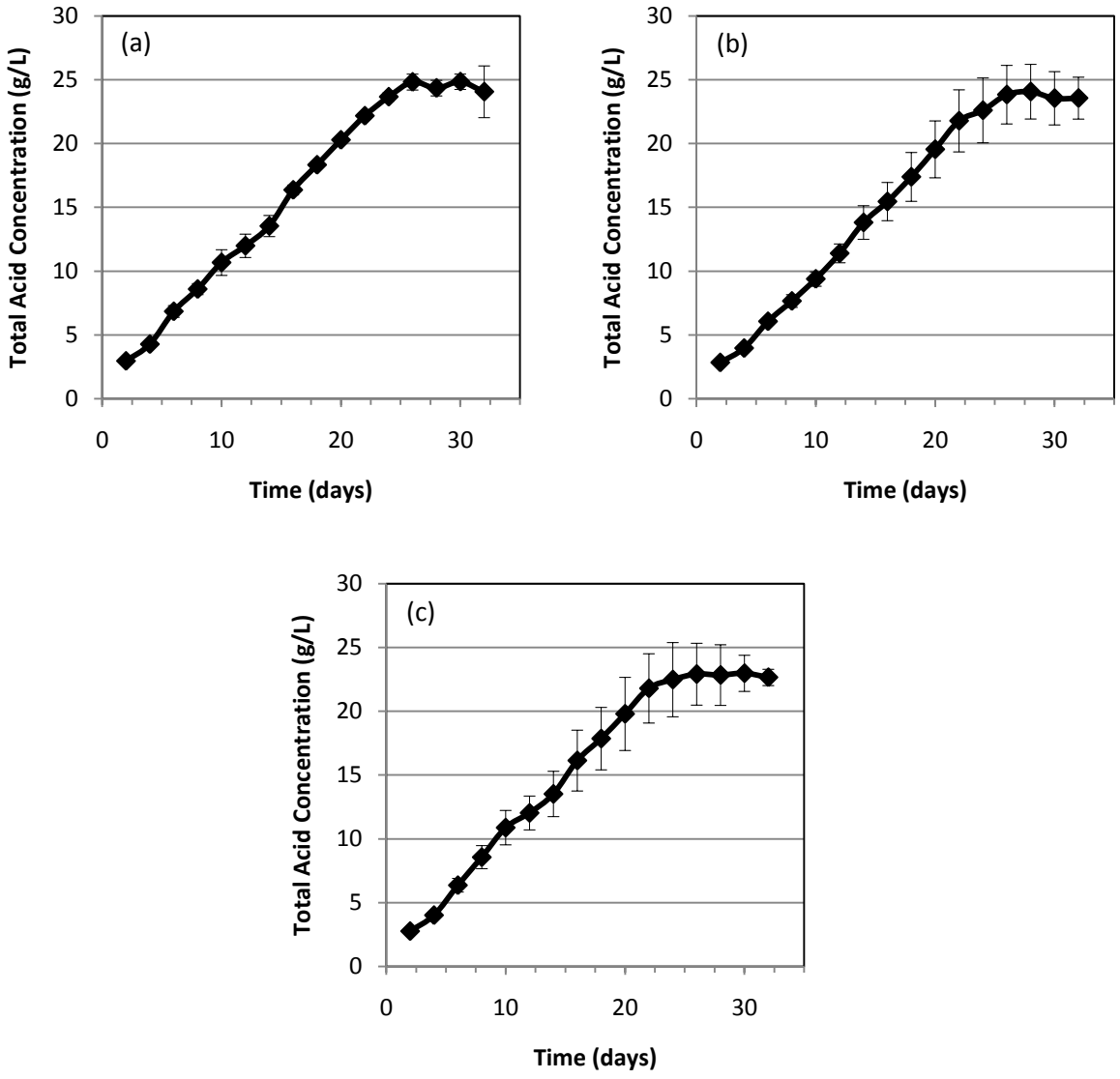

Figure 9-2. Comparison of the total acid concentration for different types of glycerol with 100 g/L of 80% substrate/20% chicken manure. (a) crude glycerol, (b) distilled glycerol, (c) refined glycerol. Error bars are ± one standard deviation.

9.3.2 Effect of fermentor configuration on continuous glycerol fermentations

Two continuous fermentor configurations were examined in this chapter: a continuously stirred tank reactor (CSTR) and a packed-bed reactor (PB).

9.3.2.1 Continuous stirred tank reactor (CSTR) fermentations

The CSTR was initiated by adding glycerol (480 g), chicken manure (120 g), anaerobic water (5420 mL), marine inoculum (200 mL), and 1.2 mL iodoform solution (20 g/L of iodoform in ethanol). The marine inoculum was fresh Galveston inoculum. Dry ammonium bicarbonate was mixed into the slurry until the pH reached 7.0. The total volume was 6 L. On each transfer, slurry volume was removed from the CSTR until total liquid volume was 5.5 L. Then, glycerol (48 g), chicken manure (12 g), and distilled water (462 mL) were added to the CSTR. The pH of the CSTR was continuously monitored and adjusted by the automatic addition of 30 wt% ammonium bicarbonate solution if the pH dropped below 7.0. The total acid concentration profile and acetate content profile are shown in Figures 9-3 and 9-4.

9.3.2.2 Packed-bed (PB) fermentations

The PB was initiated by adding glycerol (200 g), nutrient-rich water (1740 mL), marine inoculum (100 mL), and 0.4 mL iodoform solution (20 g/L of iodoform in ethanol). The marine inoculum was fresh Galveston inoculum. Dry ammonium bicarbonate was mixed into the slurry until the pH reached 7.0. Nutrient rich water (Appendix C) was distilled water that had been enriched with liquefied chicken manure. The total volume was 2 L. The fermentation broth was recirculated from the catch-basin over the packing at an approximate rate of 100 mL/min. The recirculation rate was adjusted daily to prevent the packing from flooding. As needed to prevent the basin from foaming over, a few drops of defoamer were added to the catch-basin. A fresh glycerol-nutrient solution (Appendix C) was pumped in continuously while fermentation broth was pumped out at the same rate of 0.28 mL/min. The pH of the PB was continuously monitored and adjusted by the automatic addition of 30 wt% ammonium bicarbonate solution if the pH dropped below 7.0. The total acid concentration profile and acetate content profile are shown in Figures 9-5 and 9-6.

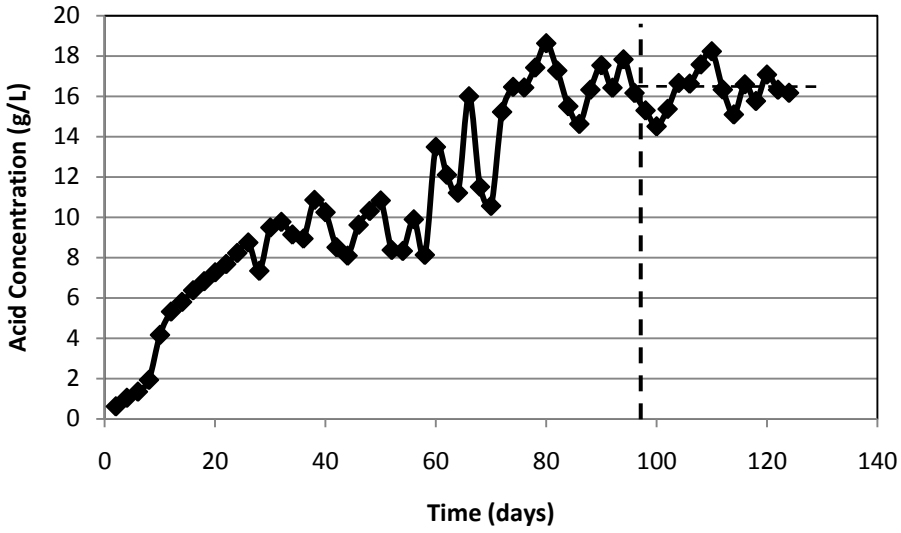

Figure 9-3. Total acid concentration for CSTR glycerol fermentation. Dash line indicates steady state (16.4 g/L).

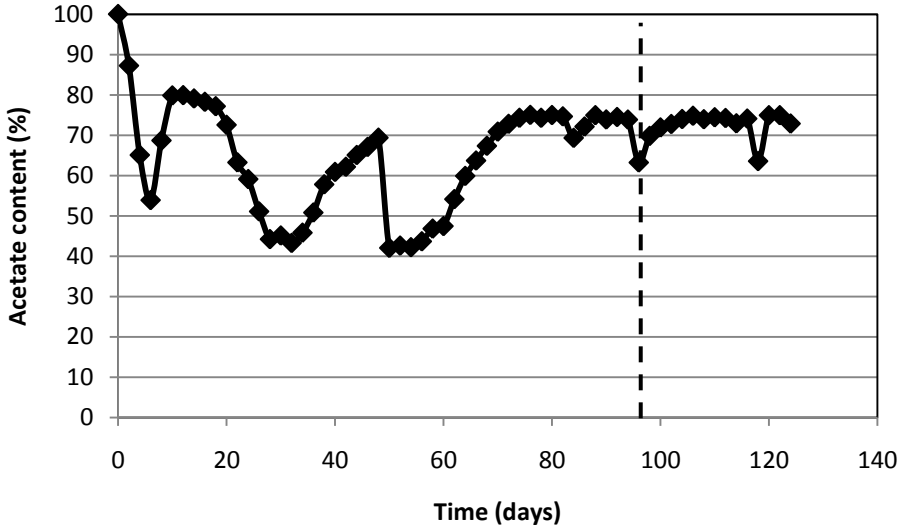

Figure 9-4. Acetate content for CSTR glycerol fermentation.

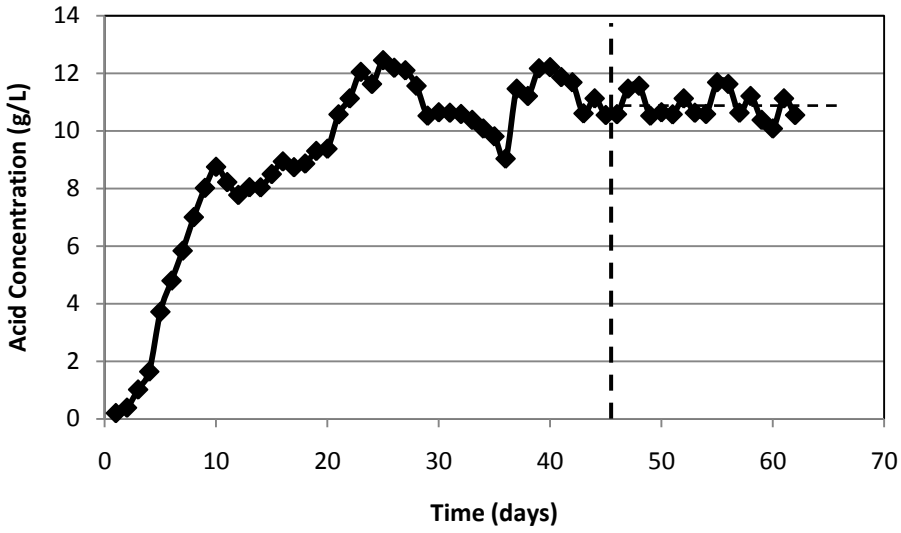

Figure 9-5. Total acid concentration for PB glycerol fermentation. Dash line indicates steady state (11.1 g/L).

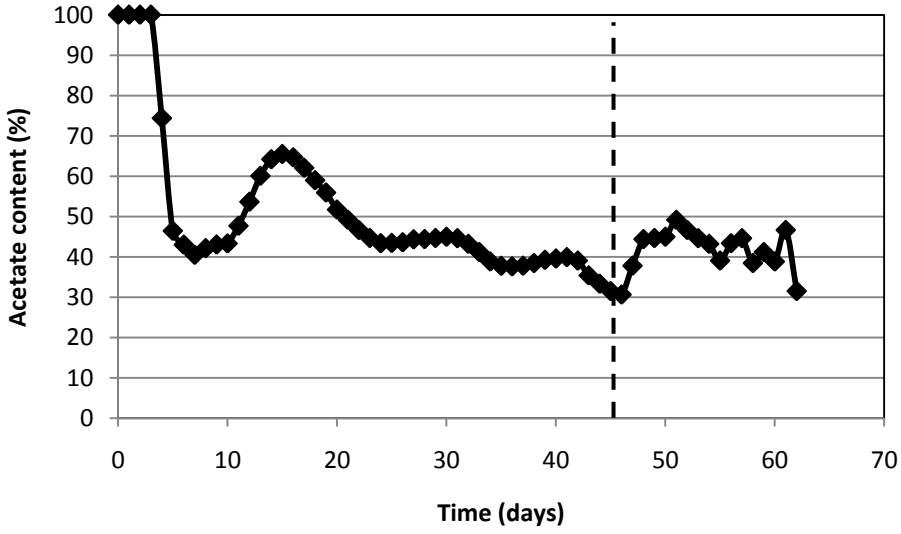

Figure 9-6. Acetate content for PB glycerol fermentation.

9.3.2.3 Summary of continuous glycerol fermentations

Table 9-3 summarizes the operating conditions for the continuous glycerol fermentations. Table 9-4 shows the results for these fermentations. Figure 9-7 lists the mass balance closures for these fermentations.

The CSTR achieved a higher acid concentration (16.4 g/L) and a higher selectivity (0.56 g acid/g VS) than the packed bed (11.1 g/L and 0.22 g acid/g VS). Both configurations achieved nearly the same yields (0.18 and 0.15 g acid/g VS fed respectfully), whereas the packed bed achieved a much higher productivity (2.28 g acid/(L liq·d)) than the CSTR did (0.72 g acid/(L liq·d)).

Table 9-3. Operating parameters for CSTR and packed-bed fermentations of refined glycerol.

	CSTR	Packed-Bed
LRT (d)	21.1	4.49
VSLR (g VS/(L·d))	4.32	15.11
VS feed (g/day)	25.90	30.23
Solid feed (g/day)	30	30.23
Glycerol (g/day)	24	30.23
Chicken manure (g/day)	6	0
H_2O feed (mL/day)	231	403.2
Total liquid volume (L)	6.08	2.04
Temperature (°C)	55	55
Frequency of transfer	2 days	Continuous

Table 9-4. Fermentation results for CSTR and packed-bed fermentation of refined glycerol.

	CSTR	Packed-Bed
Total carboxylic acid conc. (g/L)	16.42 ± 3.43	11.1 ± 0.86
Acetic acid (wt %)	74.1 ± 3.09	41.4 ± 4.58
Propionic acid (wt %)	0.9 ± 0.06	15.7 ± 2.24
Butyric acid (wt %)	26.8 ± 3.01	41.8 ± 4.39
Valeric acid (wt %)	0.32 ± 0.07	0.62 ± 0.14
Caproic acid (wt %)	0.0	0.0
Heptanoic acid (wt %)	0.0	0.0
Conversion (g VS digested/g VS fed)	0.32 ± 0.15	0.69 ± 0.03
Selectivity (g total acid/g VS digested)	0.56 ± 0.22	0.22 ± 0.04
Yield (g total acid/g VS fed)	0.18 ± 0.05	0.15 ± 0.03
Acid productivity (g total acid/(L liq·day))	0.72 ± 0.22	2.28 ± 0.29
Biomass productivity (g DW/(L liq·day))	0.89 ± 0.09	6.68 ± 0.03
Closure (g VS out/g VS in)	1.097	0.9998

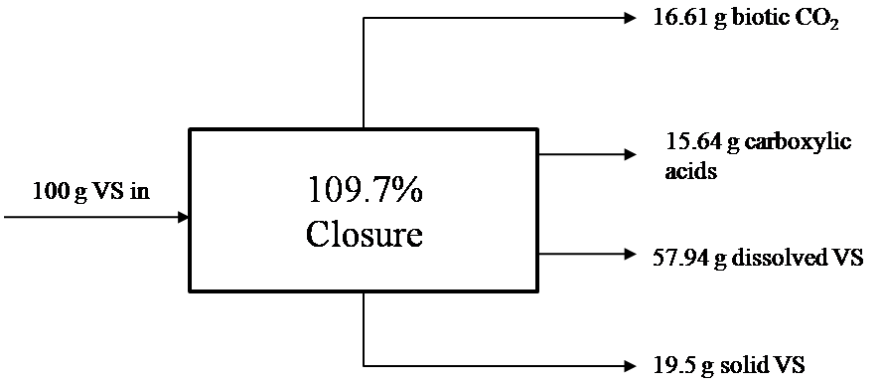

(a) For CSTR Glycerol Fermentation.

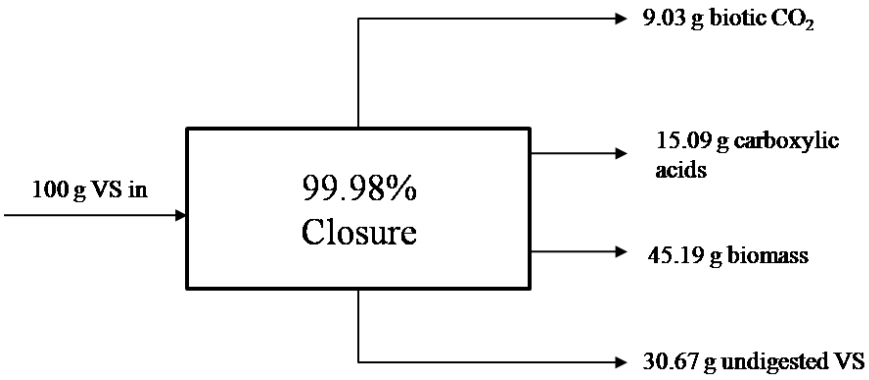

(b) For Packed-bed Glycerol Fermentation.

Figure 9-7. Mass balances for CSTR and packed-bed fermentations of refined glycerol.

9.4 Summarized comparison of the CSTR and PB for glycerol fermentations

In this study, fermentor configuration played a significant role in the performance of glycerol fermentations. Although the CSTR did not produce as high an acid concentration (16.4 g/L) as the batch glycerol fermentations (22.6 g/L refined glycerol), it did have nearly identical productivity (0.72 g acid/(L liq·d)). With a longer residence time, the CSTR should produce as high an acid concentration at the batch experiments. Additionally, the advent of continuous pH control, unlike the intermittent control of the batch experiments, removed pH swings and reduced the osmotic stress on the microorganisms, allowing them to produce more acetic acid (74.1%) and raising the selectivity to 0.56 g acid/g VS digested.

The packed-bed fermentor produced a productivity of 2.28 g acid/(L·d), three times that of either the CSTR or the batch experiments. Although longer residence times should increase the overall acid concentration above 11.1 g/L, it is unlikely that would improve the low selectivity of only 0.22 g acid/g VS digested. The greater surface area created by the packing material shifted the microorganisms to grow more biomass rather than to produce acids. Most likely, the greater surface area provided by the packing caused the microorganisms to form biofilms, facilitating the increased growth (Allison et al., 2000). The packed-bed fermentor produced 6.68 g dry weight of cell/(L liquid·day). The CSTR and batch experiments only produced 0.80 to 0.90 g dry weight of cell/(L liquid·day).

In conclusion, the CSTR configuration is better for acid production. Unfortunately, the long retention time of the CSTR (21+ days) requires a large industrial-scale fermentor. However, cell recycle could potentially speed the reaction and reduce vessel size. The packed-bed fermentation configuration could be used with other substrate/nutrient systems to produce large quantities of cells for use in cell extract products (i.e., yeast extract, cell lysing for enzyme extraction) or use as starter cultures for other fermentations.

9.5 Conclusions

The following conclusions can be made from this study:

1) Crude and distilled glycerol from the biodiesel process are just as fermentable as refined glycerol and do not need any additional processing.
2) Batch fermentations of crude, distilled, and refined glycerol achieved total acid concentrations of 24.05, 23.55, and 22.65 g/L respectively and conversions of 0.70, 0.64, and 0.62 g VS digested/g VS fed, respectively.
3) Continuously stirred tank reactor (CSTR) fermentations of refined glycerol achieved a total acid concentration of 16.4 g/L and a conversion of 0.32 g VS digested/g VS fed.
4) Packed-bed fermentations of refined glycerol achieved a total acid concentration of 11.1 g/L and a conversion of 0.62 g VS digested/g VS fed.
5) The CSTR is a better fermentor configuration for glycerol fermentation to mixed acid than the packed-bed configuration.
6) The packed-bed configuration produced a high concentration of cell mass and could be used to grow starter cultures for other fermentations.

CHAPTER X
EFFECTS OF PRETREATMENT METHODS ON WATER HYACINTH FERMENTATIONS

The objectives of this chapter follow:

a) Determine the most effective pretreatment method for lignin removal of water hyacinths.
b) Determine the most effective pretreatment method for carboxylic acid production and conversion of water hyacinths.
c) Compare the effect of thermophilic conditions (55 °C) and mesophilic conditions (40 °C) on anaerobic fermentation performance.

10.1 Introduction

An important environmental problem is the encroachment of invasive plants, such as water hyacinths, in lakes and rivers. Water hyacinth is a free-floating aquatic plant native to South America (Simpson and Sanderson, 2002). In 1884, it was introduced to North America and now chokes waterways throughout the southern United States, blocking sunlight from native plants, and starving water of oxygen thus killing fish (Schmitz et al., 1991). It is extremely prolific and can double its population in less than two weeks. A single square meter of water surface area can hold as much as 50 kg of wet water hyacinths (1 – 5 dry kg) (Wolverton and McDonald, 1979).

Because of its rapid growth rate, removing water hyacinths from clogged water ways is expensive. Water hyacinth tolerates chemical sprays, rendering them mostly ineffective. For several years, water hyacinths without pretreatment have been converted to methane for small-scale electricity production (Chanakya et al., 2009; Chynoweth et al., 1982); however, gaseous fuels do not meet the growing demand for liquid fuels caused by the rapid depletion of oil (Das and Veziroglu, 2001). Only a handful of studies have been conducted to convert water hyacinths into liquid fuels (Kahlon and Kumar, 1987; Kumar et al., 2009; Nigam, 2002).

To effectively convert water hyacinths to liquid fuels, they must be pretreated. Pretreatment is needed to break up the lignin sheath that surrounds the cellulose and hemicellulose fibers of biomass and make the carbohydrate polymers more accessible to

cellular enzymes (Figure 10-1). Pretreatment is regarded as the most expensive step in lignocellulosic biomass-to-sugars conversion with costs as high as 30 cents/gallon ethanol produced (Mosier et al., 2005; Silverstein et al., 2007; Teramoto et al., 2009).

Pretreatment can be physical, biological, or chemical. Some methods even incorporate both chemical and physical effects. Physical methods, including high temperatures and freeze/thaw cycles, are aimed at size reduction and mechanical decrystallization, but most are limited in their effectiveness. Biological methods, where living organisms are allowed to grow on the biomass, result in cellulose as well as lignin degradation and require long treatment times. Therefore, chemical methods have gained the most attention.

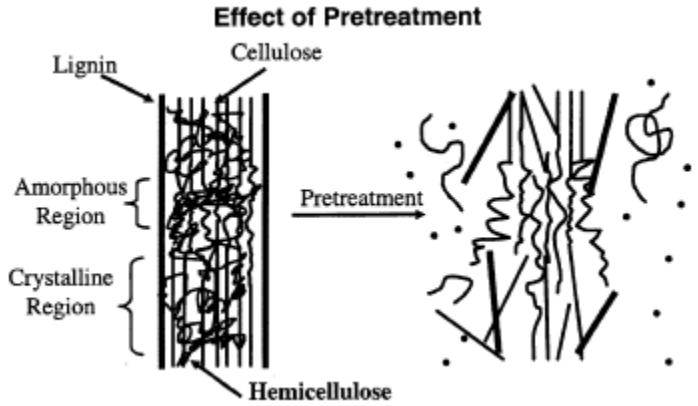

Figure 10-1. Schematic of goals of pretreatment on lignocellulosic biomass (Mosier et al., 2005).

Several chemical pretreatment methods have been proposed, including both acid and alkali pretreatments. Dilute acid pretreatments combined with steam or pressurized hot water achieve high yields of soluble sugars from the hemicelluloses fraction of the biomass. Ammonia fiber explosion (AFEX) disrupts the lignocellulose structure and reduces the cellulase requirement, but affects neither the hemicellulose nor the lignin composition. Alkali pretreatments successfully remove the lignin and can be performed at lower temperatures and pressures then other pretreatments (Mosier et al., 2005). Alkali pretreatments are also generally more effective at removing a greater fraction of lignin while leaving the hemicellulose and cellulose behind.

The focus of this study is lime pretreatment, which integrates well with the MixAlco™ process. Alkali pretreatments (0.1 – 0.3 g $Ca(OH)_2$/g dry biomass) utilize lower

temperatures and pressures then alternative pretreatments (Kim and Holtzapple, 2005; Mosier et al., 2005; Sierra et al., 2009). Additionally, the low cost reagent of calcium hydroxide is easily recovered through lime kiln technologies (Granda et al., 2009).

This chapter compares the effects of biomass pretreatments on batch water hyacinth fermentations at two fermentation temperatures.

10.2 Materials and methods

A total of four treatment methods were selected in this study: (1) hot-lime pretreatment for one hour, (2) hot-lime pretreatment for 2 hours, (3) air-lime pretreatment for 4 weeks, and (4) air-lime pretreatment for 6 weeks. Pretreatment procedures are detailed in Appendices A and B. The batch fermentation procedure is detailed in Chapter II. The fermentations were conducted at two temperatures, 40 °C and 55 °C. The experimental results are presented in this chapter.

Batch fermentations were conducted in duplicate with water hyacinths (80 wt%) and chicken manure (20 wt%) in the plastic fermentors at a concentration of 100 g dry biomass/L. The liquid volume in all fermentors was 400 mL. All fermentations were inoculated with a mixed culture of anaerobic microorganisms from a marine source (Galveston Island, TX). Ammonium bicarbonate was the only pH buffer used in this chapter. Table 10-1 lists the fermentation configurations used in this chapter. All batch fermentations were started at the same time and operated under identical conditions.

The pH in all batch fermentations was controlled around 7.0. If the measured pH fell below 7.0, ammonium bicarbonate was added to the fermentor until the pH reached the preset range (7.0−7.4). No additional ammonium bicarbonate was added if the pH was above 7.0 because the production of carboxylic acids would lower the pH.

Nutrient and methane inhibitor concentrations influence culture growth and can affect fermentation performance. Chicken manure was the nutrient source and supplied all of the nutrients required for the microorganisms. Iodoform, a methane inhibitor, was added to reduce the effect of methanogenesis. Iodoform was added to each fermentation at a rate of 2.0 mg/(L liq·day).

The total carboxylic acid concentrations, conversion, selectivity, and yield were used to compare the different fermentation performance of the different pretreatment methods.

10.3 Results and discussion

10.3.1 Pretreatment effectiveness

The temperature and duration of lime pretreatment has a significant role on the both the amount of lignin removed from the biomass and the amount of digestible cellulose and hemicellulose that are retained. Cellulose is a long-chain polymer of glucose with a molecular weight in excess of 50,000 g/mol and is the primary structural component of plant walls. Hemicellulose is a heteropolymer composed of both five-carbon sugars (xylose, arabinose) and six-carbon sugars (galactose, mannose). Hemicellulose acts as a linkage between cellulose and other components of plants, including lignin and pectin. Table 10-2 shows the compositions of fresh and each pretreatment of water hyacinths.

Neither the 1-h nor the 2-h hot-lime pretreatment made any appreciable change to the percentage of cellulose, hemicellulose, or the lignin. They only decreased the amount of extractives found in the water hyacinths. The 4-wk air-lime pretreatment did significantly decrease the amount of lignin in the water hyacinths by 50% with only a small decrease in the xylan, arabinan, and galactan. Although the 6-wk air-lime pretreatment did decrease the lignin content by 50%, the duration significantly degraded the glucan content of the cellulose by 45%.

Table 10-1. Experimental conditions for anaerobic fermentations using different pretreatments of water hyacinths.

Configuration		Biomass feedstock		Biomass source	Fermentation temperature (°C)	Iodoform* (mg/(L liq·day))
		Biomass (g)	Chicken manure (g)			
1	W401-2	32	8	Fresh untreated dried water hyacinths	40	2.0
2	W403-4	32	8	1-h Hot-lime pretreated water hyacinths	40	2.0
3	W405-6	32	8	2-h Hot-lime pretreated water hyacinths	40	2.0
4	W407-8	32	8	4-wk Air-lime pretreated water hyacinths	40	2.0
5	W409-0	32	8	6-wk Air-lime pretreated water hyacinths	40	2.0
6	W551-2	32	8	Fresh untreated dried water hyacinths	55	2.0
7	W553-4	32	8	1-h Hot-lime pretreated water hyacinths	55	2.0
8	W555-6	32	8	2-h Hot-lime pretreated water hyacinths	55	2.0
9	W557-8	32	8	4-wk Air-lime pretreated water hyacinths	55	2.0
10	W559-0	32	8	6-wk Air-lime pretreated water hyacinths	55	2.0

*Iodoform added as 20 g/L ethanol solution

Table 10-2. Compositions of fresh and four types of pretreated water hyacinths.

Components	Fresh		1-h hot-lime pretreatment		2-h hot-lime pretreatment		4-wk air-lime pretreatment		6-wk air-lime pretreatment	
	Weight (g)	Weight (%)	Weight (g)	Weight (%)	Weight (g)	Weight (%)	Weight (g)	Weight (%)	Weight (g)	Weight (%)
Glucan	24.44	24.44	26.96	28.96	22.78	28.73	20.42	32.06	12.54	23.92
Xylan	6.30	6.30	5.91	6.35	5.19	6.55	2.90	4.56	2.13	4.07
Galactan	3.88	3.88	3.17	3.40	2.92	3.68	0.83	1.31	0.62	1.19
Arabinan	8.87	8.87	7.66	8.23	7.53	9.50	2.69	4.22	2.11	4.04
Mannan	0.64	0.64	0.72	0.78	0.50	0.64	0.54	0.85	0.32	0.61
Lignin	14.55	14.55	14.54	15.63	13.12	16.54	4.48	7.04	4.62	8.83
Extractives	9.69	9.69	2.59	2.78	2.44	3.08	0.77	1.20	0.68	1.29
Ash	32.22	32.22	30.64	32.91	30.70	38.72	30.11	47.27	29.23	55.76
Total weight (g)	100.00		93.10		79.30		63.70		52.43	

10.3.2 Effects of pretreatment on fermentation performance

10.3.2.1 Effect of pretreatment condition on mesophilic fermentation (40 °C)

At 40 °C , the batch fermentation performance of four different pretreatments were compared to the fermentation performance of the fresh untreated water hyacinths. The pretreatments were 1-h hot-lime, 2-h hot-lime, 4-wk air-lime, and 6-wk air-lime. The total carboxylic acid concentration, conversion, and selectivity of the fermentations were used to evaluate the performance of each pretreatment.

10.3.2.2 Effect on total carboxylic acid concentration

Figure 10-2 shows the total carboxylic acid concentrations for each treatment of water hyacinths at mesophilic conditions (40 °C). All pretreatments increased the digestibility and produced more carboxylic acids than fresh untreated water hyacinths. The highest acid concentration was obtained from the 1-h hot lime pretreated water hyacinths at 19.9 g/L. The 2-h hot-lime pretreated water hyacinths produced 14.9 g/L compared with 19.1 g/L and 13.3 g/L of acids from the 4-wk and 6-wk air-lime pretreated water hyacinths, respectively. The fresh untreated water hyacinths only produced 7.99 g/L of acids.

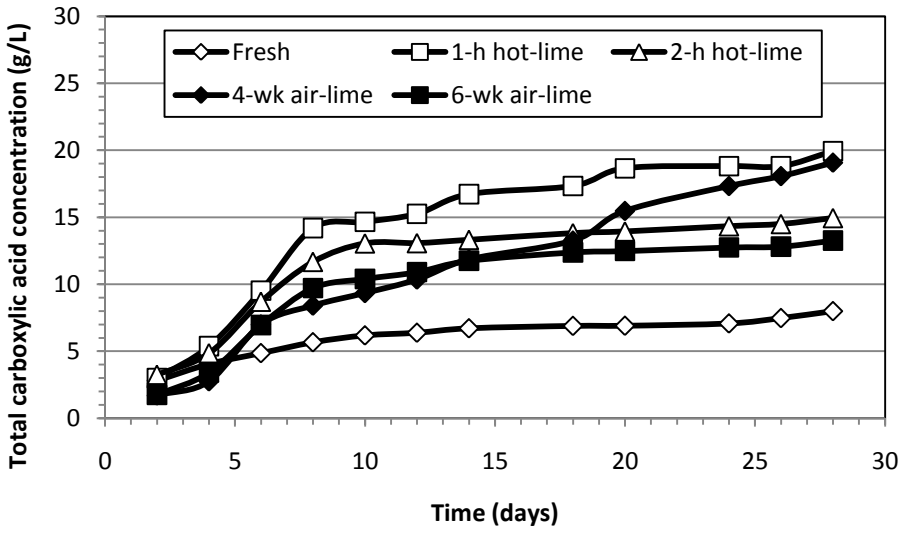

Figure 10-2. Comparison of the total acid concentrations for fresh and pretreated water hyacinth fermentations at mesophilic conditions (40 °C).

10.3.2.3 Summary of mesophilic fermentations

Table 10-3 summarizes the fermentation results for the mesophilic fermentations. All pretreated varieties of water hyacinths produced more acids and had higher conversions than the fresh untreated water hyacinths. Both the 1-h hot-lime pretreatment and the 4-wk air-lime pretreatment have high carboxylic acid concentrations (19.9 g/L and 19.1 g/L, respectively) and high conversions (0.56 and 0.62 g VS digested/g VS fed). Based on conversion, the 4-wk air-lime pretreatment did slightly better than the 1-h hot-lime pretreatment. However, based on acid production, the 1-h hot-lime pretreatment produced the most digestible biomass.

Carbohydrate compositional analysis of each pretreated biomass can be used to make additional yield calculations. Loaded carbohydrate yield ($Carb_L$ yield, g acid/g carbohydrate loaded) measures how efficiently the microorganisms convert the carbohydrate portion of the biomass into acids. $Carb_L$ yield shows the same type information as selectivity. The 4-wk air-lime pretreatment had the highest yield ($Carb_L$ yield) of 0.44 g acid/g carbohydrates loaded followed by the 1-h hot-lime pretreatment, 6-wk air-lime, and 2-h hot-lime (0.42, 0.39, 0.30, respectively). Raw carbohydrate yield ($Carb_R$ yield, g acid/g raw carbohydrate) measures how efficiently the microorganisms produce acids from the carbohydrates that were available in the biomass before pretreatment. The 1-h hot-lime pretreatment had the highest yield ($Carb_R$ yield) of 0.39 g acid/g raw carbohydrates, followed by the 4-wk air-lime, 2-h hot-lime and 6-wk air-lime (0.28, 0.24, 0.20, respectively). This clearly illustrates that the 1-h hot-lime pretreatment improved the digestion and acid production of the biomass, whereas the additional harsher pretreatments degraded the biomass resulted in overall decreased digestibility.

It also seems counter-intuitive that the 1-h hot-lime pretreatment would ferment so well. The pretreatment method left the lignin content within the water hyacinths virtually untouched so it should not have been highly digestible. Most likely, its digestibility is a result of the high temperature (100 °C) of the pretreatment. Although the 1-h time period was not long enough to cause the lignin structure to degrade, it is possible that the high temperature was sufficient to disengage the lignin sheath from the underlying hemicellulose and cellulose structure. This would allow the microorganisms to access and digest the hemicellulose and cellulose without interference from the lignin.

Table 10-3. Effect of pretreatment of water hyacinth fermentations at mesophilic conditions (40 °C).

Treatment	Fresh	1 h	2 h	4 wk	6 wk
Total carboxylic acids (g/L)	7.99	19.93	14.94	19.07	13.26
Acetic (wt%)	64.05	73.81	70.92	73.20	77.60
Propionic (wt%)	6.33	14.48	13.40	10.16	11.76
Butyric (wt%)	17.29	9.90	12.37	15.95	9.43
Valeric (wt%)	5.30	1.21	2.30	0.69	1.21
Caproic (wt%)	6.26	0.59	1.01	0.00	0.00
Heptanoic (wt%)	0.76	0.00	0.00	0.00	0.00
Conversion (g VS digested/g VS fed)	0.29	0.56	0.52	0.62	0.57
Selectivity (g acids/g VS digested	0.41	0.53	0.46	0.48	0.47
Yield (g acids/g VS fed)	0.12	0.30	0.24	0.30	0.27
$Carb_L$ yield (g acid/g carbs fed)	0.18	0.42	0.30	0.44	0.39
$Carb_R$ yield (g acid/g raw carbs)	0.18	0.39	0.24	0.28	0.20
Productivity (g acids/(L liq·day))	0.29	0.71	0.53	0.68	0.47

10.3.2.4 Effects of pretreatment on thermophilic fermentations (55 °C)

For all of four pretreatments, the batch fermentation performance was compared to the fermentation performance of the fresh untreated water hyacinths at 55 °C. The pretreatments were 1-h hot-lime, 2-h hot-lime, 4-wk air-lime, and 6-wk air-lime. The total carboxylic acid concentration, conversion, and selectivity of the fermentations were used to evaluate the performance of each pretreatment.

10.3.2.5 Effect on total carboxylic acid concentration

Figure 10-3 shows the total carboxylic acid concentrations for each treatment of water hyacinths in thermophilic fermentations (55 °C). All pretreatments increased the digestibility and produced more carboxylic acids than the fresh untreated water hyacinths. The highest acid concentration was obtained from the 1-h hot lime pretreated water hyacinths at 16.7 g/L. The 2-h hot-lime pretreated water hyacinths produced 13.4 g/L compared with 13.2 g/L and 11.6 g/L of acids from the 4-wk and 6-wk air-lime pretreated water hyacinths, respectively. The fresh untreated water hyacinths only produced 8.82 g/L of acids.

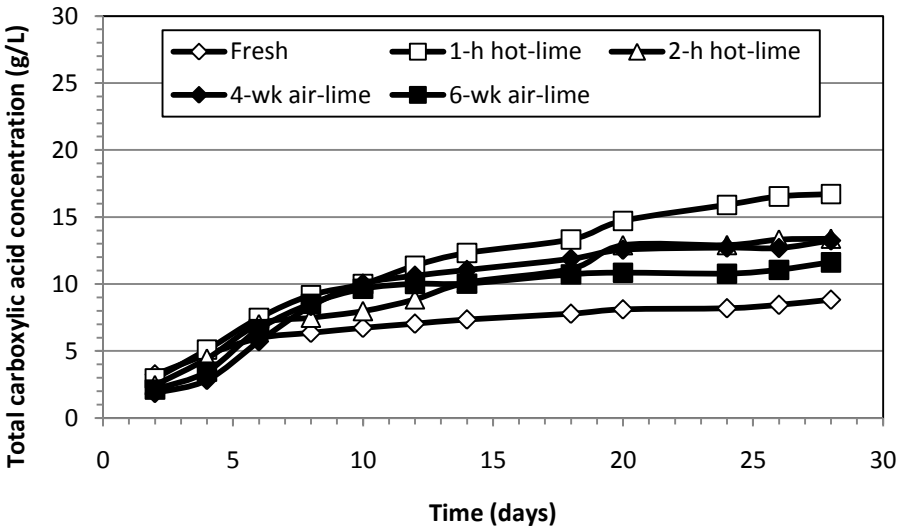

Figure 10-3. Comparison of the total acid concentrations for fresh and pretreated water hyacinth fermentations at thermophilic conditions (55 °C).

10.3.2.6 Summary of thermophilic fermentations

Table 10-4 summarizes the fermentation results for the thermophilic fermentations. All pretreated varieties of water hyacinths produced more acids and had higher conversions than the fresh untreated water hyacinths. The 1-h hot-lime pretreatment has a high carboxylic acid concentration (16.7 g/L). Both the 1-h hot-lime and the 4-wk air-lime pretreatments have high conversions (0.62 and 0.65 g VS digested/g VS fed). Based on conversion, the 4-wk air-lime pretreatment did slightly better than the 1-h hot-lime pretreatment. But, based on acid production, the 1-h hot-lime pretreatment produced the most digestible biomass.

Much like the mesophilic fermentations, all pretreatments increased the digestibility of the biomass with the 4-wk air-lime pretreatment having the highest conversion (0.65 g VS digested/g VS fed). As shown in Table 10-4, the 1-h hot-lime pretreatment had the highest selectivity (0.40 g acid/g VS digested), the highest yield ($Carb_L$ yield) of 0.35 g acid/g carbohydrates loaded, and the highest yield ($Carb_R$ yield) of 0.32 g acid/g raw carbohydrates. This clearly illustrates that the 1-h hot-lime pretreatment improved the digestion and acid production of the biomass, whereas the additional harsher pretreatments degraded the biomass and thus decreased digestibility.

Again, it seems counter-intuitive that the 1-h hot-lime pretreatment would ferment so well. The pretreatment method left the lignin content within the water hyacinths virtually unchanged so it should not have been highly digestible. Most likely, its digestibility resulted from the high pretreatment temperature (100 °C). Although the 1-h time period was not long enough to cause the lignin to degrade, the high temperature may have been sufficient to disengage the lignin sheath from the underlying hemicellulose and cellulose structure. This would allow the microorganisms to access and digest the hemicellulose and cellulose without interference from the lignin.

Table 10-4. Effect of pretreatment of water hyacinth fermentations at mesophilic conditions (55 °C).

Treatment	Fresh	1 h	2 h	4 wk	6 wk
Total carboxylic acids (g/L)	8.82	16.71	13.38	13.24	11.61
Acetic (wt%)	83.24	85.16	87.04	85.36	84.01
Propionic (wt%)	4.59	4.83	4.58	4.28	4.55
Butyric (wt%)	10.49	8.80	6.84	8.50	8.03
Valeric (wt%)	1.12	1.08	1.04	1.59	1.95
Caproic (wt%)	0.56	0.13	0.49	0.00	0.97
Heptanoic (wt%)	0.00	0.00	0.00	0.27	0.50
Conversion (g VS digested/g VS fed)	0.32	0.62	0.58	0.65	0.61
Selectivity (g acids/g VS digested	0.39	0.40	0.36	0.36	0.37
Yield (g acids/g VS fed)	0.13	0.25	0.21	0.24	0.23
$Carb_L$ yield (g acid/g carbs fed)	0.20	0.35	0.27	0.31	0.34
$Carb_R$ yield (g acid/g raw carbs)	0.20	0.32	0.21	0.20	0.18
Productivity (g acids/(L liq·day))	0.32	0.60	0.48	0.47	0.41

10.3.3 Effects of temperature on fermentation performance

Temperature is a key variable in the fermentation. The effect of temperature determines the species that exist within the mixed culture. Microorganisms produce carboxylic acid as waste metabolites from cellular processes, such as enzyme production and DNA replication. Experimental data from Section 10.2 were analyzed again in this section based on the temperature effect.

10.3.4 Effect on total acid concentration

Figure 10-4 shows the influence of temperature on the total acid concentration of each pretreatment. The four subfigures compare each pretreatment at thermophilic (55 °C) and mesophilic (40 °C). In each case, mesophilic fermentations have higher acid concentrations than the thermophilic fermentations.

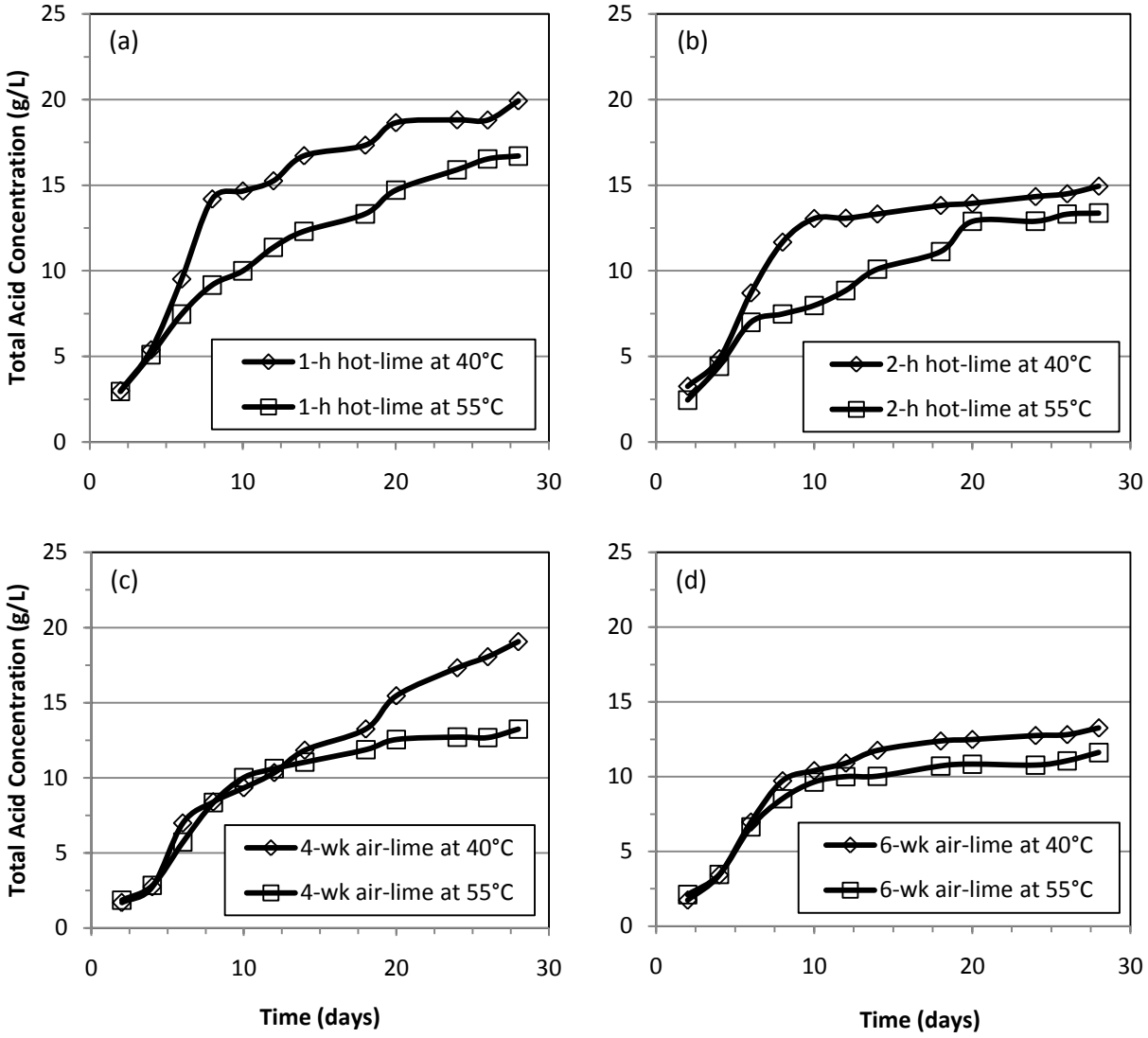

Figure 10-4. Comparison of the total acid concentration for different temperatures with 100 g/L of 80% pretreated water hyacinths/20% chicken manure. (a) 1-h hot-lime pretreatment, (b) 2-h hot-lime pretreatment, (c) 4-wk air-lime pretreatment, (d) 6-wk air-lime pretreatment.

10.3.5 Effect on acetic acid percentage

Acetic acid is the major product in the fermentation broth and reached 85% in some cases. Figure 10-5 shows the acetic acid percentages for the water hyacinth pretreatments at the two temperatures. The peak acetic acid percentage increased when the temperature increased from 40 °C to 55 °C. All 55 °C fermentations, regardless of pretreatment, maintained an acetic acid percentage of 85% or more, whereas all the 40 °C fermentations had a significantly lower percentage.

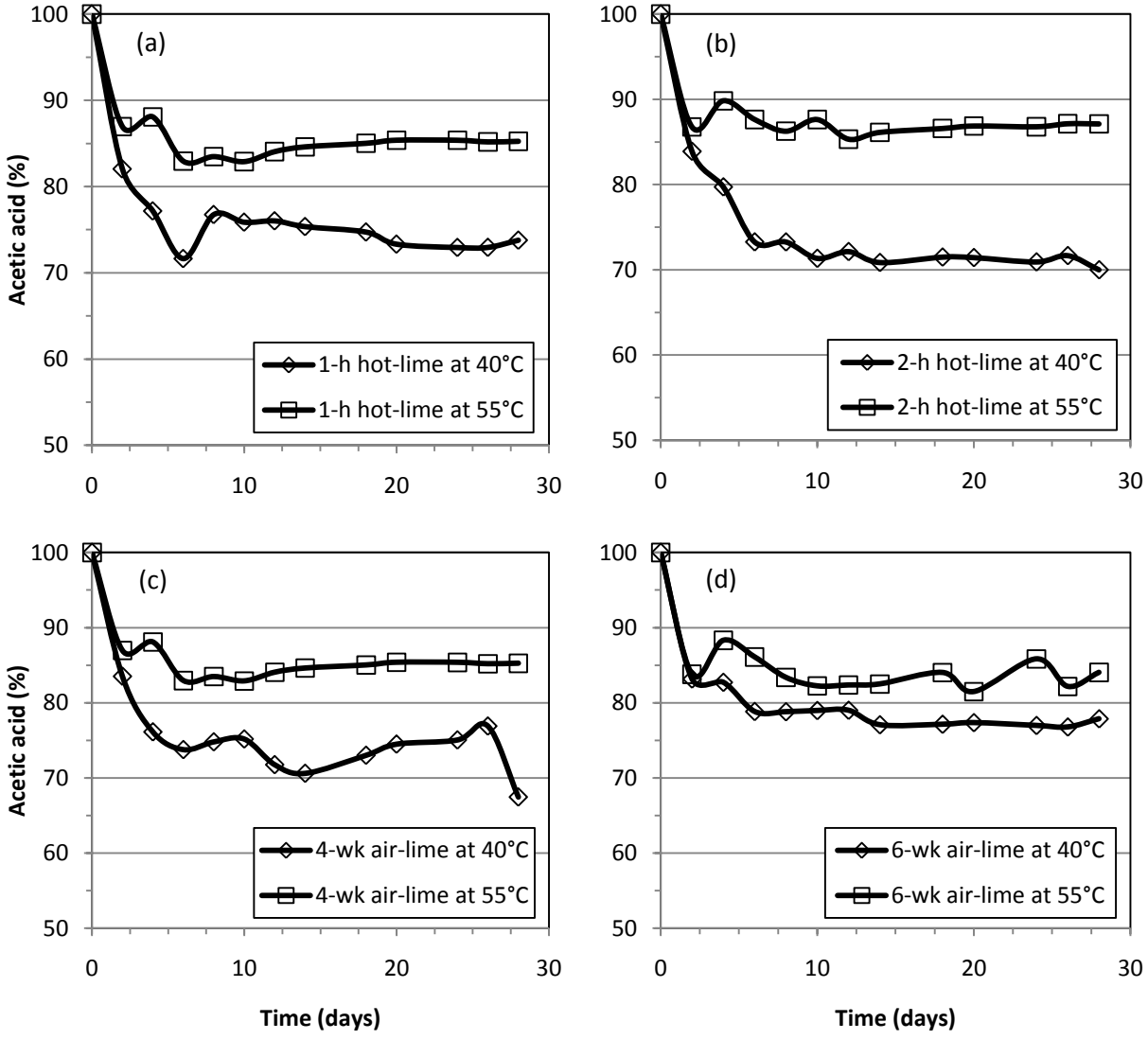

Figure 10-5. Comparison of the acetic acid percentages for different temperatures with 100 g/L of 80% pretreated water hyacinths/20% chicken manure. (a) 1-h hot-lime pretreatment, (b) 2-h hot-lime pretreatment, (c) 4-wk air-lime pretreatment, (d) 6-wk air-lime pretreatment.

10.3.6 Summary of fermentation performance

Table 10-5 summarizes the final fermentation results based on temperature effects. At 55 °C, all water hyacinth treatments achieved a higher conversion than the 40 °C fermentations, with an average increase of 8.1%. During batch fermentations of lime-pretreated bagasse at 40 and 55 °C, Fu showed a similar increase in conversions (Fu, 2007). Cokgor et al. (2009) also found increased conversion at higher temperatures during fermentations of primary sludge.

At 55 °C, water hyacinth fermentations produced as much as 30% less total acids than fermentations at 40 °C. Fermentation at 55 °C produced 20% more acetic acid than the 40 °C fermentations, which has been observed in previous experiments (Chan and Holtzapple, 2003; Fu, 2007). Although the thermophilic fermentations greatly increased the percentage of acetic acid in the fermentation broth, they did not increase the total amount of acetic acid because they produced less acids overall. If acetic acid is the desired end-product for industrial-scale fermentations, the benefit of a higher acetic acid percentage at 55 °C would be over shadowed by the decreased total acid production.

In summary, the thermophilic fermentations all had higher conversions and higher acetic acid percentages, whereas the mesophilic fermentations had higher selectivities and yields. Although the thermophilic fermentations greatly increased the percentage of acetic acid present in the fermentation broth, they did not increase the total amount of acetic acid because they produced less acids overall. If acetic acid is the desired end-product for industrial-scale fermentations, the benefit of a higher acetic acid percentage at 55 °C may be over shadowed by the increased cost to heat the fermentors to the desire incubation temperature.

Table 10-5. Effects of temperature on anaerobic fermentations of different treatments of water hyacinths.

Pretreatment	Fresh (none)		1-h hot-lime		2-h hot-lime		4-wk air-lime		6-wk air-lime	
Fermentation temperature (°C)	40	55	40	55	40	55	40	55	40	55
Total acid concentration (g/L)	7.99	8.82	19.93	16.71	14.94	13.38	19.07	13.24	13.26	11.61
Acetic (wt%)	64.05	83.24	73.81	85.16	70.92	87.04	73.20	85.36	77.60	84.01
Propionic (wt %)	6.33	4.59	14.48	4.83	13.40	4.58	10.16	4.28	11.76	4.55
Butyric (wt %)	17.29	10.49	9.90	8.80	12.37	6.84	15.95	8.50	9.43	8.03
Valeric (wt %)	5.30	1.12	1.21	1.08	2.30	1.04	0.69	1.59	1.21	1.95
Caproic (wt %)	6.26	0.56	0.59	0.13	1.01	0.49	0.00	0.00	0.00	0.97
Heptanoic (wt %)	0.76	0.00	0.00	0.00	0.00	0.00	0.00	0.27	0.00	0.50
Conversion (g VS digested/g VS fed)	0.29	0.32	0.56	0.62	0.52	0.58	0.62	0.65	0.57	0.61
Selectivity (g acid/g VS digested)	0.41	0.39	0.53	0.40	0.46	0.36	0.48	0.36	0.47	0.37
$Carb_L$ Yield (g acid/g carbs loaded)	0.18	0.20	0.42	0.35	0.30	0.27	0.44	0.31	0.39	0.34
$Carb_R$ Yield (g acid/g carbs raw)	0.18	0.20	0.39	0.32	0.24	0.21	0.28	0.20	0.20	0.18
Yield (g acid/g VS fed)	0.12	0.13	0.30	0.25	0.24	0.21	0.30	0.24	0.27	0.23
Productivity (g acid/(L liq·day))	0.29	.032	0.71	0.60	0.53	0.48	0.68	0.47	0.47	0.41

10.4 Conclusions

The following conclusions can be made from this study:

1) Water hyacinths need to be pretreated to increase their digestibility and their acid production. Although all pretreatments increased the amount of acid produced over the untreated fresh material, a short 1-hour hot-lime pretreatment is all that is needed to produce high concentrations of carboxylic acids for water hyacinth fermentations, even though it had little effect on lignin concentration within the plant,
2) Thermophilic fermentations (55 °C) increased the percentage of acetic acid by as much as 20% over mesophilic fermentations (40 °C), but decreased the total acid concentration by as much as 30%.
3) Although higher incubation temperatures produce greater percentages of acetic acid, the higher temperature also decreased the total concentration of acids because the microorganisms receive more energy per acid molecule than at lower incubation temperatures.
4) Although needing some pretreatment, water hyacinths show promise to be used as a substrate in the MixAlco™ process and provide an economic incentive to remove them from chocked waterways.

CHAPTER XI
CONCLUSIONS AND RECOMMENDATIONS

11.1 Conclusions

Mixed-acid fermentations have the potential to produce appreciable amounts of hydrogen gas. However, hydrogen is a secondary byproduct of mixed-acid fermentations and is only produced when there is both an excess of NADH within the cell and when the energy selectivity (γ) of the system has not been met. Studies of Gibbs free energy and the energy balances within the cellular environment show that microorganisms reach a specific Gibbs free energy (ΔG_C) from every gram of substrate digested. Continuous fermentations of paper and chicken manure produced 16.7 g/L of carboxylic acid and 15.7 mL/g VS digested of hydrogen with a conversion of 0.57 g VS digested/g VS fed (VSLR = 4.17 g/(L liq·d) and LRT = 31.0 days). Continuous fermentations of air-lime pretreated bagasse and chicken manure produced 17.1 g/L of carboxylic acid and 41.1 mL/g VS digested of hydrogen with a conversion of 0.53 g VS digested/g VS fed (VSLR = 3.63 g/(L liq·d) and LRT = 29.6 days). Both fermentations only produced a fraction of the theoretical amount of hydrogen (Eqn 3-33). The paper hydrogen fermentation (PHC) had a percent yield of 6.9%, whereas the bagasse hydrogen fermentation had a percent yield of 22.6%. Hydrogen production was capped at this level because the γ and the ΔG_C had been met for these two systems. The amount of hydrogen that a system will produce can be calculated if the γ has been determined for the system.

The Bioscreening Project, a joint venture between three departments, screened and analyzed a total of 505 inoculum samples from 19 sites across the United States and beyond. Initial screening fermentations with paper and yeast extract determined the best converters which were analyzed with CPDM modeling to compare them to the traditional inoculum from Galveston. A total of nine inocula were run in paper and yeast extract countercurrent fermentations. Although Train GA had the best acid production (16.6 g/L) and Train TR had the highest conversion (0.43 g VS digested/g VS fed), all trains had a similar overall performance with variation less than 13%. Analysis of the microbial cultures within both the previous CPDM fermentations and of the countercurrent trains of six of the fermentations showed that the cultures changed significantly over the course of the continuous

fermentation. Comparisons between the six countercurrent train cultures showed an average culture similarity of 0.4 (Yue-Clayton similarity). With the dissimilar microbial cultures and the very similar fermentation performance, this study supports that the performance of the MixAlco™ process depends on the conditions of the fermentation, not on the microorganisms present. The project isolated and identified a wide variety of microorganisms, but did not yield any significant improvement for the MixAlco™ process.

Several substrates were investigated during the course of this study. Batch fermentations of office paper wastes, pineapple residue, *Aloe vera* rinds, wood molasses, sugar molasses, extracted algae, and non-extracted algae produced sufficient carboxylic acids and had sufficiently high conversions to be viable substrates for the MixAlco™ process. Additionally, it was revealed that fermentation of liquid substrates favors production of higher molecular weight acids (i.e., butyric acid), presumably to relieve the osmotic stress. The solid substrates, paper, pineapple residue, and *Aloe vera* rinds, produced primarily acetic acid (80 wt% average).

Biodiesel is a growing field with concurrent increase in the production of glycerol. Biodiesel produced glycerol contains large amounts of water, waste, and catalytic residues that make it unsuitable for industrial processing. Batch fermentations of the crude glycerol revealed that it performs as well as the clean refined glycerol as a MixAlco™ substrate. Crude glycerol produced 24 g carboxylic acids/L with a conversion of 0.72 g VS fed/g VS digested, whereas the refined glycerol produced 22 g carboxylic acids/L with a conversion of 0.62 g VS fed/g VS digested. Continuous fermentations in both a CSTR (VSLR = 4.32 g/(L·d) and LRT = 21.1 days) and a packed-bed configuration (VSLR = 15.11 g/(L·d) and LRT = 4.5 days) produced 16.4 and 11.1 g/L, respectively, with conversions of 0.32 and 0.69 g VS fed/g VS digested. Additionally, the packed-bed configuration produced more cells than it did acids. It produced 6.68 g cell dry weight/(L liq·d), which is significantly greater than that produced by either the CSTR (0.89) or the batch fermentations (0.80). This suggests the packed-bed configuration may serve a role for producing cell material for enzyme extractions or inoculum sources.

Water hyacinths are fast growing aquatic plants that choke waterways and resist chemical and physical cleaning methods. These plants underwent four different pretreatments and were fermented, along with fresh untreated material, at both mesophilic

and thermophilic conditions. Although the light pretreatment (1-h hot-lime) did not reduce the amount of lignin contained within the biomass, it did improve its digestibility. At both 40 and 55 °C, the 1-h hot-lime pretreatment produced the highest acid concentration (19.9 and 16.7 g/L, respectively) and had high conversions (0.56 and 0.62 g VS fed/g VS digested). The high temperature of the pretreatment (100 °C) appears to have disengaged the lignin sheath from the underlying carbohydrates, allowing access by the microorganisms for fermentation.

11.2 Future work

Future research should focus on better understanding of the microorganisms, including their production of non-volatile carboxylic acids, and their response to varying nutrient ratios. The objective is to improve fermentation performance so that the MixAlco™ process will be cost-competitive with fossil fuels.

Mixed-acid fermentations produce more than just the C2−C7 volatile acids that are currently measured. They could potentially produce higher-molecular-weight volatile acids such as octanoic (C8) and nonanoic (C9) acids. Additionally, there are several nonvolatile carboxylic acids. Pyruvic acid is the chief product of glycolysis and the precursor of all carboxylic acids produced during mixed-acid fermentations. Succinic acid and lactic acid are nonvolatile precursors of the measured volatile propionic acid. Oxalic, malic, tartaric, and fumaric acids are nonvolatile carboxylic acids that are commonly found in nature. New analytical methods should be developed and implemented to monitor these products. These non-volatile acids can be measured through HPLC.

Current CPDM modeling gives basic predictions on the volatile acid production, conversion, and fermentation performance of the MixAlco™ system. Studies with multiple inocula to draw the CPDM maps (Chapter VI) have shown that the current model accurately functions and predicts acid concentration and conversion within a narrow range of VSLR and LRT. Additional investigations should revise the CPDM rate equation and countercurrent simulation to include recent discoveries in the biochemical pathways, Gibbs free energy demand, and carbon/nutrient ratios of the MixAlco™ process.

REFERENCES

Adjaye, J.D., Sharma, R.K., Bakhshi, N.N., 1992. Characterization and stability analysis of wood-derived bio-oil. Fuel Processing Technology, 31, 241-256.

AEN, 2009. Alternative Energy News - Biodiesel. http://www.alternativeenergy.com/. Last accessed: 9/1/10

Agbogbo, F.K., 2005. Anaerobic Fermentation of Rice Straw and Chicken Manure to Carboxylic Acids. Ph.D. Dissertation. Texas A&M University, College Station, TX.

Agbogbo, F.K., Holtzapple, M.T., 2007. Fixed-bed fermentation of rice straw and chicken manure using a mixed culture of marine mesophilic microorganisms. Bioresource Technology, 98, 1586-1595.

Aiello-Mazzarri, C., 2002. Conversion of Municipal Solid Waste to Carboxylic Acids by Anaerobic Countercurrent Fermentation. Ph.D. Dissertation. Texas A&M University, College Station, TX.

Aiello-Mazzarri, C., Agbogbo, F.K., Holtzapple, M.T., 2006. Conversion of municipal solid waste to carboxylic acids using a mixed culture of mesophilic microorganisms. Bioresource Technology, 97, 47-56.

Allison, D., Gilbert, P., Lappin-Scott, H., Wilson, M., 2000. Community Structure and Co-operation in Biofilms. Cambridge University Press, Cambridge, UK.

Alvarez, R., Lide, G., 2009. Low temperature anaerobic digestion of mixtures of llama, cow and sheep manure for improved methane production. Biomass and Bioenergy, 33, 527-533.

Amartey, S., Jeffries, T.W., 1994. Comparison of corn steep liquor with other nutrients in the fermentation of D-xylose by *Pichia stipitis* CBS 6054. Biotechnology Letters, 16, 211-214.

Angenent, L.T., Karim, K., Al-Dahhan, M.H., Wrenn, B.A., Domiguez-Espinosa, R., 2004. Production of bioenergy and biochemicals from industrial and agricultural wastewater. Trends in Biotechnology, 22, 477-485.

Antranikian, G., Vorgias, C.E., Bertoldo, C., 2005. Extreme environments as a resource for microorganisms and novel biocatalysts. Advances in Biochemical Engineering/Biotechnology, 96, 219-262.

Asada, Y., Koike, Y., Schnackenberg, J., Miyake, M., Uemura, I., Miyake, J., 2000. Heterologous expression of clostridial hydrogenase in the cyanobacterium *Synechococcus* PCC7942. Biochimica et Biophysica Acta, 1490, 269-278.

Balat, M., Balat, H., 2009. Recent trends in global production and utilization of bio-ethanol fuel. Applied Energy, 86, 2273-2282.

Bayer, E.A., Shimon, L.J.W., Shoham, Y., Lamed, R., 1998. Cellulosomes—structure and ultrastructure. Journal of Structural Biology, 124, 221-234.

Benemann, J., 1996. Hydrogen biotechnology: progress and prospects. Nature Biotechnology, 14, 1101-1106.

Bergius, F., 1932. Chemical reactions under high pressure. Nobel Lecture, pp. 245-276.

Biebl, H., 2001. Fermentation of glycerol by *Clostridium pasteurianum* — batch and continuous culture studies. Journal of Industrial Microbiology & Biotechnology, 27, 18-26.

Blasi, C.D., 2008. Modeling chemical and physical processes of wood and biomass pyrolysis. Progress in Energy and Combustion Science, 34, 47-90.

Bozbas, K., 2008. Biodiesel as an alternative motor fuel: production and policies in the European Union. Renewable and Sustainable Energy Reviews, 12, 542-552.

Bravo, V., Camacho, F., Sanchez, S., Castro, E., 1995. Influence of the concentrations of D-xylose and yeast extract on ethanol production by *Pachyiolen tannophilus*. Journal of Fermentation and Bioengineering, 79, 566-571.

Bungay, H.R., 1981. Energy, the Biomass Options. John Wiley & Sons, New York.

Cardenas, E., Cole, J.R., Tiedje, J.M., Park, J., 2009. Microbial community analysis using RDP II (Ribosomal Database Project II): methods, tools and new advances. Environmental Engineering Research, 14, 3-9.

Caspi, R., Foerster, H., Fulcher, C.A., Kaipa, P., Krummenacker, M., Latendresse, M., Paley, S., Rhee, S.Y., Shearer, A.G., Tissier, C., Walk, T.C., Zhang, P., Karp, P.D., 2008. The MetaCyc Database of metabolic pathways and enzymes and the BioCyc collection of Pathway/Genome Databases. Nucleic Acids Research, 36, D623-D631.

Castellan, G.W., 1966. Physical Chemistry. Addison-Wesley Publishing Company, Reading, MA.

Caton, T.M., Witte, L.R., Ngyuen, H.D., Buchheim, J.A., Buchheim, M.A., Schneegurt, M.A., 2004. Halotolerant aerobic heterotrophic bacteria from the Great Salt Plains of Oklahoma. Microbial Ecology, 48, 449-462.

Chan, W.N., Holtzapple, M., 2003. Conversion of Municipal Solid Wastes to Carboxylic Acids by Thermophilic Fermentation. Applied Biochemistry and Biotechnology, 11, 93-112.

Chanakya, H.N., Reddy, B.V.V., Modak, J., 2009. Biomethanation of herbaceous biomass residues using 3-zone plug flow like digesters - a case study from India. Renewable Energy, 34, 416-420.

Chase, P.A., Welch, G.C., Jurca, T., Stephan, D.W., 2007. Metal-free catalytic hydrogenation. Angewandte Chemie International Edition, 46, 8050-8053.

Chiu, C.W., Dasari, M.A., Sutterlin, W.R., Suppes, G.J., 2006. Removal of residual catalyst from simulated biodiesel's crude glycerol for glycerol hyrogenolysis to propylene glycol. Ind Eng Chem Res, 45, 791-795.

Chynoweth, D.P., Dolence, D.A., Ghosh, S., Henry, M.P., Jerger, D.E., Srivastava, V.J., 1982. Kinetics and advanced digester design for anaerobic digestion of water hyacinth and primary sludge. Biotechnology and Bioengineering Symp., 12, 381-389.

Cokgor, E.U., Oktay, S., Tas, D.O., Zengin, G.E., Orhon, D., 2009. Influence of pH and temperature on soluble substrate generation with primary sludge fermentation. Bioresource Technology, 100, 380-386.

Collins, T., Gerday, C., Feller, G., 2005. Xylanases, xylanase families and extremophilic xylanases. FEMS Microbiology Reviews, 29, 3-23.

Crabbendam, P.M., Neijssel, O.M., Tempest, D.W., 1985. Metabolic and energetic aspects of the growth of *Clostridium butyricum* on glucose in chemostat culture. Archives of Microbiology, 142, 375-382.

Das, D., Veziroglu, N., 2001. Hydrogen production by biological processes; a survey of literature. International Journal of Hydrogen Energy, 26, 13-28.

Dasari, M.A., Kiatsimkul, P.P., Sutterlin, W.R., Suppes, G.J., 2005. Low-pressure hydrogenolysis of glycerol to propylene glycol. Applied Catalysis A: General, 281, 225-231.

Datta, R., 1981. Acidogenic fermentation of corn stover. Biotechnology and Bioengineering, 23, 61-77.

DeJager, D., Blok, K., 1996. Cost-effectiveness of emission-reducing measures for methane in The Netherlands. Energy Conversion and Management, 37, 1181-1186.

Demain, A.L., Newcomb, M., Wu, J.H.D., 2005. Cellulase, clostridia, and ethanol. Microbiology and Molecular Biology Reviews, 69, 124-154.

Demirbas, A., 2009. Progress and recent trends in biodiesel fuels. Energy Conversion and Management, 50, 14-34.

Demirbas, M.F., Balat, M., 2006. Recent advances on the production and utilization trends of bio-fuels: a global perspective. Energy Conversion and Management, 47, 2371-2381.

Demirel, B., Scherer, P., Yenigun, O., Onay, T.T., 2010. Production of methane and hydrogen from biomass through conventional and high-rate anaerobic digestion processes. Critical Reviews in Environmental Science and Technology, 40, 116-146.

DeSantis, T.Z., Hugenholtz, P., Larsen, N., Rojas, M., Brodie, E.L., Keller, K., Huber, T., Dalevi, D., Hu, P., Andersen, G.L., 2006. Greengenes, a chimera-checked 16S rRNA gene database and workbench compatible with ARB. Applied and Environmental Microbiology, 72, 5069-5072.

Dharmadi, Y., Murarka, A., Gonzalez, R., 2006. Anaerobic fermentation of glycerol by *Escherichia coli*: A new platform for metabolic engineering. Biotechnology & Bioengineering, 94, 821-829.

Dowaki, K., Mori, S., Fukushima, C., Asai, N., 2005. A comprehensive economic analysis of biomass gasification systems. Electrical Engineering in Japan, 153, 1670-1679.

Dowaki, K., Ohta, T., Kasahara, Y., Kameyama, M., Sakawaki, K., Mori, S., 2007. An economic and energy analysis on bio-hydrogen fuel using a gasification process. Renewable Energy, 32, 80-94.

Dry, M.E., 2002. The Fischer–Tropsch process: 1950–2000. Catalysis Today, 71, 227-241.

EPA, 2008. Municipal solid waste generation, recycling and disposal in the United States: facts and figures for 2008. Washington DC, http://www.epa.gov/osw/nonhaz/municipal/pubs/msw2008rpt.pdf. Last accessed: 5/13/10

Evvyernie, D., Morimoto, K., Karita, S., Kimura, T., Sakka, K., Ohmiya, K., 2001. Conversion of chitinous wastes to hydrogen gas by *Clostridium paraputrificum* M-21. Journal of Bioscience and Bioengineering, 91, 339-343.

Eysmondt, J.v., Vasic-Racki, D., Wandrey, C., 1990. Acetic acid production by *Acetogenium kivui* in continuous culture - kinetic studies and computer simulations. Applied Microbiology and Biotechnology, 34, 344-349.

Fabiano, B., Perego, P., 2002. Thermodynamic study and optimization of hydrogen production by *Enterobacter aerogenes*. International Journal of Hydrogen Energy, 27, 149-156.

Fernando, S., Adhikari, S., Chandrapal, C., Murali, N., 2006. Biorefineries: current status, challenges and future direction. Energy Fuels, 20, 1727-1737.

Fortenbery, T.R., 2005. Biodiesel feasibility study: an evaluation of biodiesel feasibility in Wisconsin. Agricultural and Applied Economic Staff Paper Series. University of Wisconsin, Madison.

Freudenberg, K., Neish, A.C., 1968. Constitution and BioSynthesis of Lignin. Springer, New York.

FSEC, 2007. Hydrogen Basics - Production. Hydrogen. Florida Solar Energy Institute, University of Central Florida, Orlando, FL, http://www.fsec.ucf.edu/en/consumer/hydrogen/basics/production.htm. Last accessed: 11/25/09

Fu, Z., 2007. Conversion of Sugarcane Bagasse to Carboxylic Acids under Thermophilic Conditions. Ph.D. Dissertation. Texas A&M University, College Station, TX.

Glasstone, S., 1949. Thermodynamics for Chemists. D. Van Nostrand Company, Inc., New York, pp. 522.

Gonzalez-Pajuelo, M., Meynial-Salles, I., Mendes, F., Soucaille, P., Vasconcelos, I., 2006. Microcial conversion of glycerol to 1,3-propanediol: physiological comparison of a natural producer, *Clostridium butyricum* VPI 3266, and an engineered strain, *Clostridium acetobutylicum* DG1(pSPD5). Applied and Environmental Microbiology, 72, 96-101.

Granda, C.B., Holtzapple, M.T., Luce, G., Searcy, K., Mamrosh, D.L., 2009. Carboxylate platform: the Mixalco process part 2: process economics. Applied Biochemistry and Biotechnology, 156, 107-124.

Hahn-Hagerdal, B., Galbe, M., Gorwa-Grauslund, M.F., Liden, G., Zacchi, G., 2006. Bio-ethanol – the fuel of tomorrow from the residues of today. Trends in Biotechnology, 24, 549-556.

Han, H., Long, J., Li, S., Qian, G., 2010. Comparison of green-house gas emission reductions and landfill gas utilization between a landfill system and an incineration system. Waste Management and Research, 28, 315-321.

Hansen, T.L., Sommer, S.G., Gabriel, S., Christensen, T.H., 2006. Methane production during storage of anaerobically digested municipal organic waste. Journal of Environmental Quality, 35, 830-836.

Heijnen, S.J., 1994. Thermodynamics of microbial growth and its implications for process design. Trends in Biotechnology, 12, 483-492.

Heming, M., 2005. Oleolone Glycerine Market Report No 71., http://www.oleoline.com/admin/oleoftp/marketreport/samples/Q_glycerine_sample.pdf. Last accessed: 8/1/10

Henry, C.S., Jankowski, M.D., Broadbelt, L.J., Hatzimanikatis, V., 2006. Genome-scale thermodynamic analysis of *Escherichia coli* metabolism. Biophysical Journal, 90, 1453-1461.

Hespell, R.B., Whitehead, T.R., 1990. Physiology and genetics by gastrointestinal tract of xylan degradation bacteria. Journal of Dairy Science, 73, 7013-3022.

Hileman, B., 1999. Case grows for climate change. Chemical Engineering News, 77, 16-23.

Himmi, E.H., Bories, A., Barbirato, F., 1999. Nutrient requirements for glycerol conversion to 1,3-propanediol by *Clostridium butyricum*. Bioresource Technology, 67, 123-128.

Hollister, E.B., Engledow, A.S., Hammett, A.M., Provin, T.L., Wilkinson, H.H., Gentry, T.J., 2010. Shifts in microbial community structure along an ecological gradient of hypersaline soils and sediments. ISME Journal, 4, 829-838.

Holtzapple, M.T., Davidson, R.R., Ross, M.K., Aldrett-Lee, S., Nagawani, M., Lee, C.-M., Lee, C., Adelson, S., Karr, W., Gaskin, D., Shiraga, H., Chang, N.-S., Chang, V.S., Loescher, M.E., 1999. Biomass conversion to mixed alcohol fuels using the MixAlco process. Applied Biochemistry and Biotechnology, 77-79, 609-631.

Holtzapple, M.T., Granda, C.B., 2009. Carboxylate platform: the MixAlco process part 1: comparison of three biomass conversion platforms. Applied Biochemistry and Biotechnology, 156, 525-536.

Homann, P.H., 2003. Hydrogen metabolism of green algae: discovery and early research – a tribute to Hans Gaffron and his coworkers. Photosynthesis Research, 76, 93-103.

Humayoun, S.B., Bano, N., Hollibaugh, J.T., 2003. Depth distribution of microbial diversity in mono lake, a meromictic soda lake in California. Applied and Environmental Microbiology, 69, 1030-1042.

Jessop, P.G., Ikariya, T., Noyori, R., 1995. Homogeneous hydrogenation of carbon dioxide. Chemical Reviews, 95, 259-272.

Joback, K.G., Reid, R.C., 1987. Estimation of pure-component properties from group-contributions. Chemical Engineering Communications, 157, 233-243.

Johnson, E.A., Madia, A., Demain, A.L., 1981. Chemically defined minimal medium for growth of the anaerobic cellulolytic thermophile *Clostridium thermocellum*. Applied and Environmental Microbiology, 41, 1060-1062.

Kahlon, S.S., Kumar, P., 1987. Simulation of fermentation conditions for ethanol production from water hyacinths. Indian Journal of Economics, 14, 213-217.

Kayali, H.A., Tarhan, L., Soran, H., 2005. Variations of alcohol dehydrogenase activity and fermentative pyruvate, ethanol production of *F. equiseti* and *F. acuminatum* depend on the yeast extract and urea concentrations. Enzyme and Microbial Technology, 36, 706-711.

Kim, S., Holtzapple, M.T., 2005. Lime pretreatment and enzymatic hydrolysis of corn stover. Bioresource Technology, 96, 1994–2006.

Klass, D.L., 1998. Biomass for Renewable Energy, Fuels and Chemicals. California Academic Press, San Diego.

Kleerebezem, R., van Loosdrecht, M.C.M., 2007. Mixed culture biotechnology for bioenergy production. Current Opinions in Biotechnology, 18, 207-212.

Kumar, A., Bhattacharya, S.C., Pham, H.L., 2003. Greenhouse gas mitigation potential of biomass energy technologies in Vietnam using the long range energy alternative planning system model. Energy, 28, 627-654.

Kumar, A., Singh, L.K., Ghosh, S., 2009. Bioconversion of lignocellulosic fraction of water hyacinth (*Eichhornia crassipes*) hemicelluloses acid hydrolysate to ethanol by *Pichia stipitis*. Bioresource Technology, 100, 3293-3297.

Lay, J.-J., Lee, Y.-J., Noike, T., 1999. Feasibility of biological hydrogen production from the organic fraction of municipal solid waste. Water Resource, 33, 2579-2586.

Lee, P.C., Lee, W.G., Lee, S.Y., Chang, H.N., Chang, Y.K., 2000. Fermentative production of succinic acid from glucose and corn steep liquor by *Anaerobiospirillum succiniciproducens*. Biotechnology and Bioprocess Engineering, 5, 379-381.

Ley, R.E., Harris, J.K., Wilcox, J., Spear, J.R., Miller, S.R., Bebout, B.M., Maresca, J.A., Bryant, D.A., Sogin, M.L., Pace, N.R., 2006. Unexpected diversity and complexity of the Guerrero Negro hypersaline microbial mat. Applied and Environmental Microbiology, 72, 3685-3695.

Lide, D.R., 2009. CRC Handbook of Chemistry and Physics, 90th Edition (Internet Version 2010). CRC Press/Taylor and Francis, Boca Raton, FL.

Lin, Y., Tanaka, S., 2006. Ethanol fermentation from biomass resources: current state and prospects. Applied Microbiology and Biotechnology, 69, 627-642.

Loescher, M.E., 1996. Volatile Fatty Acid Fermentation of Biomass and Kinetic Modeling using the CPDM Method. Ph.D. Dissertation. Texas A&M University, College Station, TX.

Lou, J., Dawson, K.A., Strobel, H.J., 1996. Role of phosphorolytic cleavage in cellobiose and cellodextrin metabolism by the ruminal bacterium *Prevotella ruminicola*. Applied and Environmental Microbiology, 26, 1770-1773.

Lou, J., Dawson, K.A., Strobel, H.J., 1997. Cellobiose and cellodextrin metabolism by the ruminal bacterium *Ruminococcus albus*. Current Microbiology, 35, 221-227.

Lynd, L.R., Wyman, C.E., Gerngross, T.U., 1999. Biocommodity engineering. Biotechnology Progress, 15, 777-793.

Ma, F., Hanna, M.A., 1999. Biodiesel production: a review. Bioresource Technology, 70, 1-15.

Melis, A., Happe, T., 2001. Hydrogen production: green algae as a source of energy. Plant Physiology, 127, 740-748.

Mesbah, N.M., Abou-El-Ela, S.H., Wiegel, J., 2007. Novel and unexpected prokaryotic diversity in water and sediments of the alkaline, hypersaline lakes of the Wadi An Natrun, Egypt. Microbial Ecology, 54, 598-617.

Miao, X., Wu, Q., 2004. High yield bio-oil production from fast pyrolysis by metabolic controlling of *Chlorella protothecoides*. Journal of Biotechnology, 110, 85-93.

Mitchell, W.J., 1998. Physiology of carbohydrate to solvent conversion by clostridia. Advances in Microbial Physiology, 39, 31-130.

Mizuno, O., Dibsdale, R., Hawkes, F.R., Hawkes, D.R., Noike, T., 2000. Enhancement of hydrogen production from glucose by nitrogen gas sparging. Bioresource Technology, 73, 59-65.

Mizuno, O., Ohara, T., Shinya, M., Noike, T., 2000. Characteristics of hydrogen production from bean curd manufacturing waste by anaerobic microflora. Water Science and Technology, 42, 345-350.

Mosier, N., Wyman, C., Dale, B., Elander, R., Lee, Y.Y., Holtzapple, M.T., Ladisch, M., 2005. Features of promising technologies for pretreatment of lignocellulosic biomass. Bioresource Technology, 96, 673-686.

Nandi, R., Sengupta, S., 1998. Microbial production of hydrogen: an overview. Critical Rev Microbiology, 24, 61-84.

NBB, 2006. The Official Site of the National Biodiesel Board. National Biodiesel Board, http://www.biodiesel.org/resources/biodiesel_basics/default.shtm. Last accessed: 5/13/10

NBB, 2008. U.S. Biodiesel Production Capac [Online]. National Biodiesel Board, http://www.biodiesel.org/pdf_files/fuelfactsheets/Production_Capacity.pdf. Last accessed: 5/13/10

Nguyen, P.H.L., Kuruparan, P., Visvanathan, C., 2007. Anaerobic digestion of municipal solid waste as a treatment prior to landfill. Bioresource Technology, 98, 380-387.

Nicholson, C.A., Fathepure, B.Z., 2005. Aerobic biodegradation of benzene and toluene under hypersaline conditions at the Great Salt Plains, Oklahoma. FEMS Microbiology Reviews, 245, 257-262.

Nigam, J.N., 2002. Bioconversion of water-hyacinth (*Eichhornia crassipes*) hemiculluloses acid hydrolysate to motor fuel ethanol by xylose fermenting yeast. Journal of Biotechnology, 97, 107-116.

NREL, 2004. Biomass analysis technology team laboratory analytical procedure. National Renewable Energy Laboratory, Golden, CO.

Oren, A., 2002. Halophilic Microorganisms and Their Environment. Kluwer Academic, Boston.

Pandey, A., Soccol, C.R., Nigam, P., Soccol, V.T., 2000. Biotechnological potential of agro-industrial residues. I: sugarcane bagasse. Bioresource Technology, 74, 69-80.

Parry, I.W.H., Darmstadter, J., 2003. The Costs of U.S. Oil Dependency. RFF Discussion Paper 03-59. Resources of the Future, Washington, D.C.

Perlack, R.D., Wright, L.L., Turhollow, A.F., Graham, R.L., Stokes, B.J., Erbach, D.C., 2005. Biomass as Feedstock for A Bioenergy and Bioproducts Industry: The Technical Feasibility of a Billion-Ton Annual Supply. Oak Ridge National Laboratory, Oak Ridge, TN.

Prins, R.A., 1977. Biochemical activities of gut microorganisms. in: R.T.J. Clarke, T. Bauchop (Eds.), Microbial Ecology of the Gut. Academic Press, New York, pp. 73-184.

Qin, W., Egolfopoulos, F.N., Tsotsis, T.T., 2001. Fundamental and environmental aspects of landfill gas utilization for power generation. Chemical Engineering Journal, 82, 157-172.

Rokem, J.S., Goldberg, I., Mateles, R.I., 1980. Growth of mixed cultures of bacteria on methanol. Journal of General Microbiology, 116, 225-232.

Ross, M.K., 1998. Production of Acetic Acid from Waste Biomass. Ph.D. Dissertation. Texas A&M University, College Station, TX.

Saint-Amans, S., Girbal, L., Andrade, J., Ahrens, K., Soucaille, P., 2001. Regulation of carbon and electron flow in *Clostridium butyricum* VPI 3266 grown on glucose-glycerol mixtures. Journal of Bacteriology, 183, 1748-1754.

Schloss, P.D., Westcott, S.L., Ryabin, T., Hall, J.R., Hartmann, M., Hollister, E.B., Lesniewski, R.A., Oakley, B.B., Parks, D.H., Robinson, C.J., Sahl, J.W., Stres, B., Thallinger, G.G., Horn, D.J.V., Weber, C.F., 2009. Introducing mothur: open-source, platform-independent, community-supported software for describing and comparing microbial communities. Applied and Environmental Microbiology, 75, 7537-7541.

Schmitz, D.C., Schardt, J.D., Leslie, A.G., Dray, F.A., Osborne, J.A., Nelson, B.V., 1991. The ecological impact and management history of three invasive alien aquatic plants in Florida. in: B.N. McKnight (Ed.) Biological Pollution - the Control and Impact of Invasive Exotic Species. Indiana Academy of Science, Indianapolis, pp. 173-194.

Sierra, R., Granda, C., Holtzapple, M.T., 2009. Short-term lime pretreatment of poplar wood. Bioresource Technology, 25, 323-332.

Silverstein, R.A., Chen, Y., Sharma-Shivappa, R.R., Boyette, M.D., Osborne, J., 2007. A comparison of chemical pretreatment methods for improving saccharification of cotton stalks. Bioresource Technology, 98, 3000-3011.

Simpson, D., Sanderson, H., 2002. *Eichhornia crassipes*. Curtis's Botanical Magazine, 19, 28-34.

South, C.R., Hogsett, D.A.L., Lynd, L.R., 1995. Modeling simultaneous saccharification and fermentation of lignocellulose to ethanol in batch and continous reactors. Enzyme and Microbial Technology, 17, 797-803.

Sparling, R., Risbey, D., Poggi-Varaldo, H.M., 1997. Hydrogen production from inhibited anaerobic composters. International Journal of Hydrogen Energy, 22, 563-566.

Sterzinger, G., 1995. Making biomass energy a contender. Technology Review, 98, 34-40.

Stockar, U.v., Maskow, T., Liu, J., Marison, I.W., Patino, R., 2006. Thermodynamics of microbial growth and metabolism: an analysis of the current situation. Journal of Biotechnology, 121, 517-533.

Streekstra, H., Buurman, E.T., Hoitink, C.W.G., Teixeira de Mattos, M.J., Neijssel, O.M., Tempest, D.W., 1987. Fermentation shifts and metabolic reactivity during anaerobic carbon-limited growth of *Klebsiella aerogenes* NCTC 418 on fructose, gluconate, mannitol and pyruvate. Archives of Microbiology, 148, 137-143.

Streekstra, H., Teixeira de Mattos, M.J., Neijssel, O.M., Tempest, D.W., 1987. Overflow metabolism during anaerobic growth of *Klebsiella aerogenes* NCTC 418 on glycerol and dihydroxyacetone in chemostat culture. Archives of Microbiology, 147, 268-275.

Strobel, H.J., Caldwell, F.C., Dawson, K.A., 1995. Carbohydrate transport by the anaerobic thermophile *Clostridium thermocellum* LQRI. Applied and Environmental Microbiology, 61, 4012-4015.

Temudo, M.F., Muyzer, G., Kleerebezem, R., van Loosdrecht, M.C., 2008. Diversity of microbial communities in open mixed culture fermentations: impact of pH and carbon source. Applied Microbiology and Biotechnology, 80, 1121-1130.

Teramoto, Y., Lee, S.H., Endo, T., 2009. Cost reduction and feedstock diversity for sulfuric acid-free ethanol cooking of lignocellulosic biomass as a pretreatment to enzymatic saccharification. Bioresource Technology, 100, 4783-4789.

Thanakoses, P., 2002. Conversion of Bagasse and Corn Stover to Mixed Carboxylic Acids using a Mixed Culture of Mesophilic Microorganisms. Ph.D. Dissertation. Texas A&M University, College Station, TX.

Tijhuis, L., van Loosdrecht, M.C.M., Heijnen, J.J., 1993. A thermodynamically based correlation for maintenance Gibbs energy requirements in aerobic and anaerobic chemotrophic growth. Biotechnology and Bioengineering, 42, 509-519.

Veziroglu, T.N., Barbir, F., 1992. Hydrogen: the wonder fuel. International Journal of Hydrogen Energy, 17, 391-404.

Wolverton, B.C., McDonald, R.C., 1979. Water hyacinth (*Eichhornia crassipes*) productivity and harvesting studies. Economic Botany, 33, 1-10.

Woodward, J., Orr, M., Cordray, K., Greenbaum, E., 2000. Enzymatic production of biohydrogen. Nature, 405, 1014-1015.

Wu, K.-T., Lee, H.T., Juch, C.I., Wan, H.P., Shim, H.S., Adams, B.R., Chenc, S.L., 2004. Study of syngas co-firing and reburning in a coal fired boiler. Fuel, 83, 1991-2000.

Yue, J.C., Clayton, M.K., 2005. A similarity measure based on species proportions. Communications in Statistics—Theory and Methods, 34, 2123-2131.

Zhang, Y.-H.P., Lynd, L.R., 2004. Kinetics and relative importance of phosphorolytic and hydrolytic cleavage of cellodextrins and cellobiose in cell extracts of *Clostridium thermocellum*. Applied and Environmental Microbiology, 70, 1563-1569.

Zhu, L., 2005. Fundamental Study of Structural Feactures Affecting Enzymatic Hydrolysis of Lignocellulosic Biomass. Ph.D. Dissertation. Texas A&M University, College Station, TX.

APPENDIX A
HOT-LIME-WATER PRETREATMENT PROCEDURE

Lignocellulosic biomass (e.g., sugarcane bagasse) was treated with calcium hydroxide in the presence of water in a metal tray. The biomass and calcium hydroxide (0.3 g/g dry biomass) was placed in the metal tray and thoroughly mixed. Enough distilled water was added to cover the material. The tray was then covered with aluminum foil and the mixture was brought to a boil with Bunsen burners. After the mixture had boiled for the designated time, it was allowed to cool to room temperature then neutralized with bubbled CO_2 until the pH was 7.0.

1. In a stainless steel pan, place the preweighed biomass, lime, and distilled water using a loading of 0.3 g $Ca(OH)_2$/g dry biomass. It is helpful to add the distilled water in two or three batches and knead the liquid into the biomass to prevent the biomass from floating on the top of the liquid.
2. Mix the three components very thoroughly to ensure even distribution of the lime.
3. Place the pan over two Bunsen burners and heat to boiling. Boil the mixture for 1 – 2 h, stirring occasionally. Add additional distilled water if it evaporates.
4. Allow the mixture to cool to room temperature (this takes several hours).
5. Add more distilled water to the mixture to completely cover the biomass (only if needed). Add a few drops of Dow Corning silicone antifoam solution to prevent foaming.
6. Bubble CO_2 through the mixture using diffusing stones to neutralize the lime and the pH drops below 7.0. This step may take several hours.
7. Spread the mixture onto aluminum foil and allow to air dry (5 – 7 days). Store the dried biomass in a labeled container.

APPENDIX B
AIR-LIME PRETREATMENT PROCEDURE

A pile of biomass (e.g., sugarcane bagasse) was lime pretreated for a maximum of 8 weeks according to the desired conditions (Holtzapple et al. 1999). Approximately 2 kg dry weight of biomass was mixed with weighed calcium hydroxide (0.3 g $Ca(OH)_2$/g dry biomass) and placed in a large jacketed steel vessel (L × W × H = 36 L). The vessel was then filled with distilled water until it covered the biomass. A heat exchanger circulated hot water through the jacket and maintained the biomass treatment system at a constant temperature of 50 °C. Air was scrubbed through a lime slurry container and then bubbled through the pile via an air diffusers in the bottom of the vessel. At the end of the designated pretreatment time, the biomass was removed and allowed to cool to room temperature then neutralized with bubbled CO_2 until the pH was 7.0.

1. Mix a large amount of raw biomass (e.g., 2 kg) with excess lime (0.3 $Ca(OH)_2$/g dry biomass). Mix well to ensure a complete contact between the lime and the biomass.
2. Fill the steel vessel with the lime/biomass mixture. Add distilled water to the vessel until the biomass mixture is covered.
3. Fill the heat exchanger with water and start the circulation pump.
4. Set the temperature controller to 50 °C.
5. Adjust the air valve connected to the diffusers until the air gently bubbles up through the mixture.
6. Add more water to the heat exchanger every day so it does not evaporate dry.
7. Add more distilled water to the vessel to maintain full coverage of the biomass.
8. Check the system daily for leaks and monitor the circulation pump to ensure it retains prime.
9. Monitor the pH of the lime slurry to ensure basic conditions are maintained (e.g., desired pH > 9).
10. Maintain conditions for 4 – 8 weeks. At the end of the time period, turn off the temperature controller, the circulation pump and the air valve.
11. Remove the biomass slurry from the vessel and allow to cool to room temperature.

12. Add more distilled water to the mixture to completely cover the biomass (only if needed). Add a few drops of Dow Corning silicone antifoam solution to prevent foaming.
13. Bubble CO_2 through the mixture using diffusing stones to neutralize the lime and the pH drops below 7.0. This step may take several hours.
14. Spread the mixture onto aluminum foil and allow to air dry (5 – 7 days). Store the dried biomass in a labeled container.
15. Clean the interior of the steel vessel and flush with distilled water.

APPENDIX C
LIQUID MEDIA PREPARATION

C.1 DEOXYDIZED LIQUID MEDIA PREPARATION

The liquid media used in all fermentation experiments was deoxygenated water with cysteine hydrochloride and sodium sulfide.

1. Fill a large glass container (4 L+) with distilled water. Place the container over a Bunsen burner to boil.
2. Boil the distilled water under a nitrogen purge for 10 min.
3. Seal the top of the container and cool to room temperature.
4. Add 0.275 g cysteine hydrochloride and 0.275 g sodium sulfide per liter of boiled water.
5. Stir the solution until both chemicals are completely dissolved and pour into storage bottles.

C.2 NUTRIENT RICH MEDIA PREPARATION

The nutrient-rich media was used in the packed-bed glycerol fermentations because the solid chicken manure would have plugged the packing material.

1. Place 37.5 g of dried chicken manure in a 2-L beaker.
2. Fill with 1500 mL of distilled water and stir for 10 min.
3. Centrifuge slurry at 4000 rpm (3200 × g) for 10 min.
4. Dilute supernatant to 2 L with distilled water.
5. Store in sealed container in 4 °C for no more than a week.

APPENDIX D
COUNTERCURRENT TRANSFER PROCEDURE

Liquid and solid flow in opposite directions in the countercurrent fermentations. A typical countercurrent train has four fermentors. For a laboratory-scale countercurrent transfer, the transfer of liquid and solids is made every 1, 2, or 3 days, operating in a semi-continuous manner. Countercurrent fermentations are initiated as batch fermentations. The experiments were performed in batch mode until the culture is established in the fermentor (7−10 days). After the culture developed, the countercurrent operation was started, and the liquid and solids were transferred using the single-centrifuge method (Figure D-1). To maintain anaerobic conditions in the fermentors, solid caps were placed on the bottles at any time solid and liquid was not actively being moved and a nitrogen purge was utilized to remove all oxygen before the fermentors were returned to the incubator.

1. Remove the fermentors from the incubator and allow to cool for 10 min at room temperature.
2. Release and record the gas production using the device illustrated in Figure 2-10.
3. Remove the fermentor caps and using a nitrogen purge line, remove the residual solids adhered to the stopper and metal bars.
4. Measure and record the pH for each fermentor.
5. Cap the fermentor with a regular solid centrifuge cap.
6. Balance each pair of fermentors using some additional weight supplements. Pay attention to balance the centrifuge bottles before placing them in the centrifuge.
7. Centrifuge the fermentors to separate the solid and liquid. Centrifuge for 25 min at 4000 rpm and a brake level of 5.
8. After centrifuging, carefully move the bottles to ensure that the solid and liquid do not remix.
9. Place the liquid from Fermentor 1 (F1 in Figure) into a previously weighed plastic graduated cylinder. Record the weight and volume of liquid.

10. Take a 3 mL liquid sample for carboxylic acids analysis. Decant the remaining liquid from F1 into a liquid collection bottle for further VS analysis. Store the sample and collection bottle in a freezer for future analysis.
11. Weigh the fermentor bottle with the remained solids and compare against the goal weight. Remember that the regular centrifuge cap is not included in this weight. To achieve steady state, a constant wet cake weight must be maintained in each fermentor. If the fermentor weight (wet solids + centrifuge bottle) weighs more than the goal weight, remove the difference and the solids will be added to the next fermentor (F2 in Figure). To simplify the transfer calculation, the goal weight includes the desired wet cake plus the weight of fresh biomass to be added to F1.
12. Add fresh biomass to F1.
13. Pour the liquid from F2 into a preweighed graduated cylinder. Record the weight and volume.
14. Pour the liquid into F1.
15. Weigh F2. Remove the solids resulting of: Solid removed = (F2 wet solids + solids from F1) – the goal weight.
16. Add the solids from F1 to F2.
17. Repeat Steps 13−16 from Fermentors 3 and 4 (F3 and F4 in Figure D-1).
18. Add fresh liquid medium (Appendix C) to F4 according to the predetermined volume.
19. Place the solids removed from F4 in a solid collection bottle and store it in the freezer until the VS analysis is performed.
20. Add buffer, urea (if desired), and methane inhibitor to each fermentor.
21. Mix content well and measure and record the pH.
22. Purge each fermentor with nitrogen and replace fermentor caps.
23. Return fermentors to the incubator.

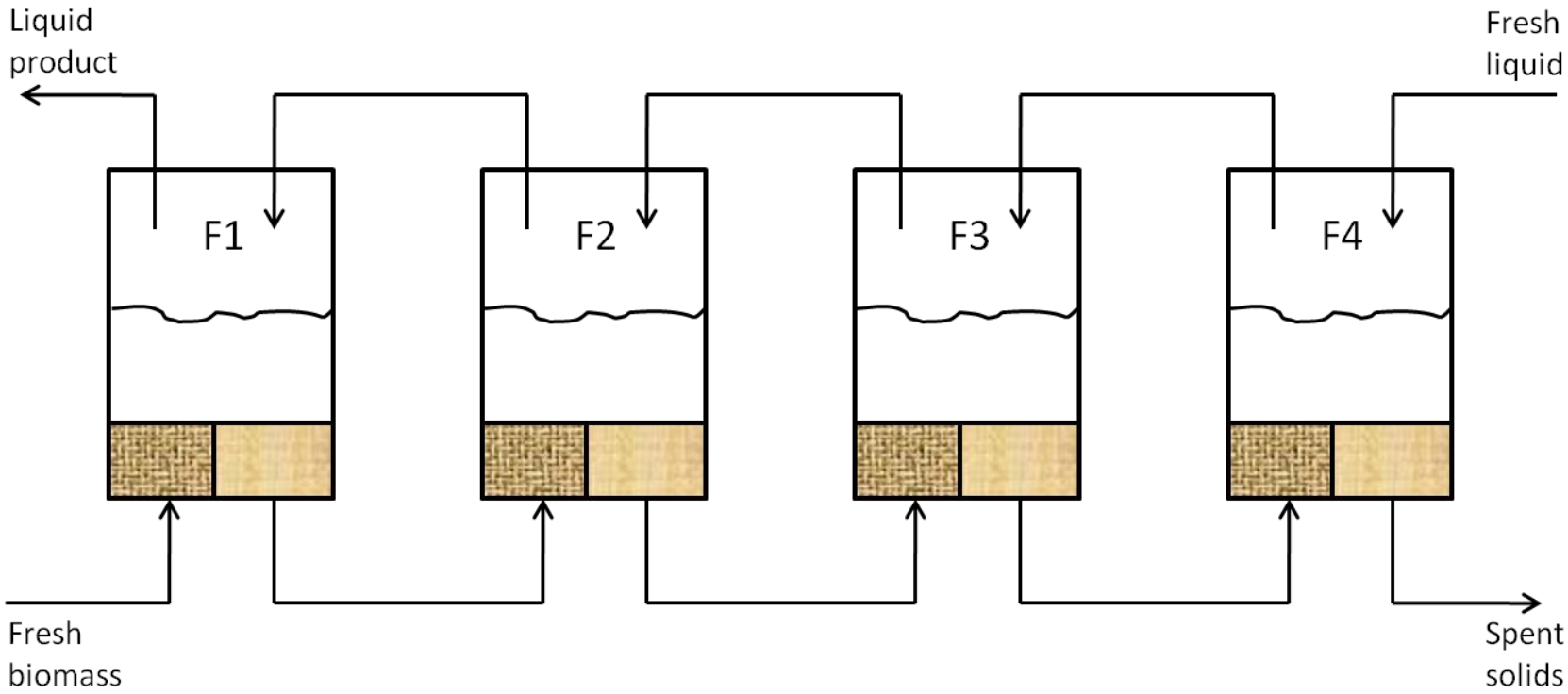

Figure D-1. Single-centrifuge countercurrent procedure.

APPENDIX E
CARBOXYLIC ACID ANALYSIS

For carboxylic acids analysis, at least 3 mL of liquid should be withdrawn from the fermentor and placed in a 15-mL conical centrifuge tube. If samples were not immediately analyzed, they were stored in the freezer. At the moment of analysis, for frozen samples, the samples were defrosted and vortexed before beginning the procedure. If the acid concentration is high, they may require further dilution (e.g., 50 vol% sample/50 vol% water) before the standard method mentioned in the following.

GC LIQUID SAMPLE PREPARATION

1. Centrifuge the liquid sample for 5 min at 4000 rpm.
2. Pipette 1 mL of clear liquid broth into a round bottom ultracentrifuge tube.
3. Add 1 mL of internal standard 4-methyl-valeric acid (1.162 g/L internal standard, ISTD).
4. Add 1 mL of 3-M phosphoric acid to acidify the sample and allow the carboxylic acids to be released in the GC injection port.
5. Cap the tube.
6. Centrifuge the mixture at 15,000 rpm in the IEC B-20A centrifuge machine (Industrial Equipment Co., Needham Hts, MA). Accelerate the centrifuge to 15,000 rpm then immediately turn to 0 rpm.
7. Remove the ultracentrifuge tube and pipette 1 mL of the mixture into a glass GC vial and cap the GC vial. The centrifuged sample in the vial is ready to be analyzed now.
8. If the prepared sample will not be analyzed immediately, it can be stored in the freezer. If frozen, care should be taken to thaw and vortex the sample before GC analysis.

GC OPERATION

1. Before starting the GC, check the gas supply cylinders (compressed hydrogen, compressed helium and compressed air from Praxair Co., Bryan, TX) to insure at least 200 psig pressure in each gas cylinder. If there is not enough gas, switch cylinders and place an order for new ones.
2. Check the solvent and waste bottles on the injection tower. Fill up the solvent bottles with methanol. Empty the waste bottles.

3. Replace the septum beneath the injection tower before starting the GC.
4. Up to 100 samples can be loaded in the autosampler plate in one analysis batch. Place the samples in the autosampler racks, not leaving empty spaces between samples. Place a volatile acid standard mix (Matreya Inc., Catalog # 1075) solution at the beginning of the sequence.
5. Check the setting conditions in the method:
    1. Inlet Conditions:
        a. Temperature: 230 °C
        b. Pressure: 15 psig
        c. Flowrate: 185 mL/min (179 mL split)
    2. Detector conditions:
        a. Temperature: 230 °C
        b. Air flow rate: 400 mL/min
        c. H2 flow rate: 40 mL/min
        d. He (makeup) flow rate: 45 mL/min
    3. Oven conditions:
        a. Initial temperature: 40 °C
        b. Initial hold time: 2 min
        c. Ramp rate: 20 °C/min
        d. Final temperature: 200 °C
        e. Final hold time: 1 min
        f. Total run time per vial: 11 min
6. Start the GC on the computer by selecting the method with the setting conditions mentioned above. Set and load the sequence of sample to run.
7. Be sure to rerun the standard mix every 25 samples. At the end of the sequence table, instruct the computer to return the GC into standby.
8. Once the conditions are reached and the green start signal is on the screen, start the sequence. Details about operation, setting sequence, and calibration are in the Agilent 6890 instrument manual.
9. Periodically check to ensure that the equipment is working properly.

APPENDIX F
MOISTURE AND VOLATILE SOLID ANALYSIS

This procedure follows NREL Standard Procedures (2004)

1. Record the label and weight of a clean, dry crucible (W1).
2. Place a representative sample of the material (liquid or solid) into the crucible and record the weight (W2).
3. Dry the crucible at 105 °C for 1 day in the drying oven. Allow to cool to room temperature before weighing. Record the dry weight (W3).
4. Ash the crucible at 550 °C for at least 4 h. Remove and allow to cool to room temperature. Record the ash weight (W4).

The moisture content (MC) of the sample is calculated as

$$\mathrm{MC}(\%) = \frac{\mathrm{W2} - \mathrm{W3}}{\mathrm{W2} - \mathrm{W1}} \times 100$$

The volatile solids content (VS) of the sample is calculated as

$$\mathrm{VS}(\%) = \frac{\mathrm{W3} - \mathrm{W4}}{\mathrm{W3} - \mathrm{W1}} \times 100$$

APPENDIX G
DETERMINATION OF CARBOHYDRATES AND LIGNIN IN BIOMASS

This method used a two-step acid hydrolysis to fractionate biomass into forms that are more easily quantified. The biomass sample was taken through a primary 72% (w/w) sulfuric acid hydrolysis at 30 ºC for 1 h, followed by a secondary dilute acid hydrolysis at 121 ºC for 1 h. The resulting sugar monomers and acetyl content were analyzed using HPLC. The acid-soluble lignin was measured by UV-Vis spectroscopy. This method is based on the NREL standard procedure No. 002 (2004).

PREPARATION OF SAMPLE FOR HYDROLYSIS AND ANALYSIS

1. Determine the moisture content of the biomass following NREL standard procedure N.001 (2004). Total solid content is determined as T_f.
2. Weigh 0.3 ± 0.01 g of biomass to the nearest 0.1 mg and place in a glass test tube. (W_i).
3. Add 3.00 ± 0.01 mL of 72% H_2SO_4 to each tube and mix with a glass stirring rod to wet biomass thoroughly.
4. Place the test tubes in a water bath at 30 ± 3 ºC and incubate for 1 h. Using the stir rod, stir the sample every 5 to 10 min without removing the test tube from the bath.
5. After 1-h hydrolysis reaction, transfer each sample to its own septum bottle and dilute to a 4% acid concentration by adding 84 mL of deionized water. Carefully transfer all residual solids along with the liquid. The total volume of solution (V_f) is 87.0 mL.
6. Prepare a set of sugar recovery standards (SRS). Place a small amount of glucose and xylose in a septum bottle. Transfer 84.0 mL of deionized water to the bottle, dissolving the sugars. Add 3.0 mL of 72% H_2SO_4 to the bottle.
7. Mix well and transfer approximately 15 mL of the SRS to a small flask and neutralize with $CaCO_3$.
8. Stopper each bottle and crimp aluminum seals in place.
9. Autoclave samples and SRS for 1 h at 121 ± 3 ºC.
10. After autoclaving, allow bottles to cool to room temperature before removing seals and stoppers.

11. These autoclaved sample can be used to determine the acid insoluble/acid soluble lignin, carbohydrates, and/or acetyl content.

ANALYSIS OF ACID INSOLUBLE LIGNIN

1. Place filtering crucibles into 105 °C oven for a minimum of 4 h. Remove the crucibles from the oven and place directly into a desiccators and cool for 1 h. Weigh the crucibles to the nearest 0.1 mg (W_1).
2. Vacuum filter the autoclaved hydrolysis solution through the filtering crucibles. Capture the filtrate in a vacuum flask.
3. Transfer 50 mL of filtrate into a small flask to determine acid-soluble lignin and carbohydrates.
4. Used deionized water to transfer all remaining solids out of the septum bottle into the filtering crucible.
5. Dry the crucibles at 105 °C until a constant weight is achieved, usually a minimum of 4 h.
6. Remove the crucibles from the oven and cool in a desiccator. Record the weight of the crucibles and the dry residue to the nearest 0.1 mg (W_2).
7. Place the crucibles in a muffle furnace at 575 °C for 24 h.
8. Remove the crucibles from the furnace and cool in a desiccator. Weigh the crucibles and ash to the nearest 0.1 mg (W_3).

ANALYSIS OF ACID SOLUBLE LIGNIN

1. Measure the absorbance of the filtrate at 320 nm on a UV-Visible spectrophotometer.
2. Dilute the sample as necessary to bring the absorbance into the range of 0.7 to 1.0. Deionized water may be used to dilute the sample and must be used as a blank. Record the absorbance to three decimal places.
3. The absorbance must be measured within 6 h of hydrolysis. If the liquid must be stored, it should be stored in the refrigerator for a maximum of 2 weeks.

ANALYSIS OF CARBOHYDRATES

1. Transfer 20 mL of filtrate of each sample to a 50-mL flask.

2. Use calcium carbonate to neutralize all samples, including the SRS before and after autoclaving, to pH 5−6. Avoid neutralizing to a pH greater than 6 by monitoring with pH paper.
3. After neutralizing, allow the sample to settle.
4. Using a syringe, filter the supernatant through a 0.2-µm filter into autosampler vials.
5. Prepare a series of sugar calibration standards containing the compounds to be quantified; the suggested range is 0.1 to 4.0 g/L for each component. Use a four-point calibration curve.
6. Analyze the calibration standard and sample using a Biorad Aminex HPX-87P column equipped with the deashing guard column.

HPLC conditions:

Injection volume: 20 µL

Mobile phase: 0.2-µm filtered and degassed, deionized water

Flow rate: 0.6 mL/min

Column temperature: 85 °C

Detector: refractive index

Run time: 20 min data collection plus a 15-min post-run

CALCULATION

1. Calculate the oven dry weight (W_o) of the sample.

$$W_o = \frac{W_i \times \%T_f}{100}$$

2. Calculate acid-insoluble lignin (AIL) content.

$$\%\text{AIL} = \frac{W_2 - W_3}{W_o} \times 100$$

3. Calculate acid-soluble lignin (ASL) content.

$$\%\text{ASL} = \frac{\text{Abs} \times \text{V}_\text{f} \times \text{Dil}}{\varepsilon \times \text{W}_\text{o}}$$

Abs = the average UV-Vis absorbance for the sample at 320 nm

V_f = the volume of the filtrate, 87 mL

Dil = the dilution factor

ε = the absorptivity of the biomass[i]

4. Calculate total lignin content.

$$\%\ \text{Lignin} = \%\text{AIL} + \%\text{ASL}$$

5. Calculate carbohydrate content.
   a. Create calibration curves by linear regression analysis from each sugar to be quantified. From these curves, determine the concentration in g/L of the sugars present in the sample.
   b. Calculate the amount of sugar recovered in the SRS after acid hydrolysis.

$$\%\text{RSRS} = \frac{\text{C}_2}{\text{C}_1} \times 100$$

where

%RSRS = the percent recovery of the sugar recovery standard (SRS)

C_2 = the concentration of the SRS after hydrolysis

C_1 = the concentration of the SRS before hydrolysis

   c. Correct the sugar concentration obtained by the HPLC in the sample by using %RSRS.

$$\text{C}_\text{corr} = \text{C}_\text{HPLC} \times \frac{100}{\%\text{RSRS}}$$

d. Calculate the percentage of each sugar in the samples as follows.

$$\% \text{ Sugar} = \frac{C_{corr} \times A \times \mathrm{V_f} \times \frac{1\ \mathrm{L}}{1000\ \mathrm{mL}}}{\mathrm{W_o}}$$

where *A* is the anhydro correction of 0.9 (or 162/180) for C-6 sugars and 0.88 (or 132/150) for C-5 sugars. The hydrolysis reaction causes each glucan monomer of the cellulose and each xylan monomer of hemicellulose to gain one molecule of water.

i. Absorptivity (ε) measures how strongly a given substance absorbs light at a given wavelength. It varies depending on the specific substrate, but is 15 L/(g·cm) for rice straw, bagasse, and poplar wood (Zhu, 2005) and 15 was the number used for all calculations in this dissertation.

APPENDIX H

GS2 NUTRIENT MIXTURE FOR *C. THERMOCELLUM* GROWTH

This mixture is taken from Johnson et al. (1981) and used for the growth of *Clostridium thermocellum* used in all bioscreening experiments. Solution was autoclaved and stored in sealed containers until use.

Table H-1. Composition of GS-2 media (per liter).

Ingredient	
KH_2PO_4	1.5 g
K_2HPO_4	2.9 g
Urea	2.1 g
$MgCl_2 \cdot 6H_2O$	1.0 g
$CaCl_2 \cdot 2H_2O$	150 mg
$FeSO_4 \cdot 6H_2O$	1.25 mg
Cysteine hydrochloride	1.0 g
Resazurin	2.0 mg
Cellobiose	5.0 g
Morpholinopropane sulfonic acid	10.0 g
Yeast extract	6.0 g
Sodium citrate$\cdot 2H_2O$	3.0 g

Cellobiose and the mixture of Mg, Ca, and Fe salts were autoclaved separately as 10-fold-concentrated solutions. The media had a pH of 7.4.

APPENDIX I

GIBBS FREE ENERGY TABLE AND CALCULATIONS

Table I-1. List of Standard Gibbs Free Energies of Formation and Standard Enthalpies of Formation. (All values are for P = 1 atm, T = 298.15 K, pH = 0*.)

Chemical	Gibbs, ΔG_F° (kJ/mol)	Enthalpy, ΔH_F° (kJ/mol)
ADP	−1906.13	−2626.54
ATP	−2768.1	−3619.21
Acetate	−369.31	−486.01
Butyrate	−352.63	−535.55
Caproate	−341.599	−580.182
CO_2 (aq)	−527.81	−677.14
CO_2 (g)	−394.36	−393.5
D-Glucose	−915.9	−1262.19
D-Xylose	−750.49	−1045.94
Glucose-1P	−1756.87	−2276.44
Glucose-6P	−1763.94	−2276.44
Glucan	−610.94	−975.17
H+	0	0
H_2 (aq)	17.6	−4.2
H_2 (g)	0	0
H_2O	−237.19	−285.83
Heptanoate	−333.245	−603.325
Lactate	−516.72	−686.64
NAD+	0	0
NADH	22.65	−31.94
Phosphate	−1096.1	−1299
Propionate	−360	−511.08
Pyruvate	−472.27	−596.22
Valerate	−368.4	−556.8
Xylan	−398.973	−710.599

Values taken from CRC Handbook of Chemistry and Physics (Lide, 2009) or calculated by the Joback Method (Joback and Reid, 1987).

* pH = 0 is used in the notation to refer to NO pH or ionic activity.

Gibbs free energy of reaction

The standard Gibbs free energy of reaction ΔG_R° can be calculated from the Standard Gibbs free energy of formation ΔG_F°.

$$\Delta G_R^\circ = \sum v_i \, \Delta G_F^\circ$$

where *v* is the stoichiometric number of reactant *i*. *v* is positive for reactants on the right side of the equation and negative for reactants on the left side of the equation. For example, the conversion of pyruvate to propionate:

$$\text{Pyruvate} + 2\ \text{NADH} + 2\ \text{H}^+ \rightarrow \text{Propionate} + 2\ \text{NAD}^+ + \text{H}_2\text{O}$$

Taking the standard Gibbs free energies from Table I-1, the Gibbs free energy of reaction is

$$\Delta G_R^\circ = [(1) \times -360 + (2) \times 0 + (1) \times -237.19] + [(-1) \times -472.27 + (-2) \times 22.65 + (-2) \times 0]$$

$$\Delta G_R^\circ = -170.22 \text{ kJ/mol}$$

Enthalpy of reaction

The standard enthalpy of reaction ΔH_R° is calculated in the same way. The enthalpy of reaction for pyruvate to propionate is

$$\Delta H_R^\circ = -136.81 \text{ kJ/mol}$$

Temperature calculation

As described in Chapter III, the Van't Hoff equation describes the effect of temperature changes on the equilibrium and therefore to the Gibbs free energy.

$$\Delta G_R = \frac{T_2}{T_1} \times \left[\Delta G_R^\circ - \frac{(T_2 - T_1)}{T_2} \times \Delta H_R^\circ \right]$$

Substituting in for ΔG_R° and ΔH_R° and using $T_1 = 298.15$ K and $T_2 = 328.15$ K (55 °C), which is the fermentation temperature used for the majority of the experiments in this study, the Gibbs free energy of reaction of pyruvate to propionate at 55 °C and pH = 0 is

$$\Delta G_R = -173.58 \text{ kJ/mol}$$

pH calculation

The affect that the pH of the solution has on a given reaction depends on the number of hydrogen ions that are either absorbed or released in the reaction.

$$\Delta G_R = \frac{T_2}{T_1} \times \left[\Delta G_R^\circ - \frac{(T_2 - T_1)}{T_2} \times \Delta H_R^\circ \right] - nRT\ln(10) \times \text{pH}$$

where *n* is the stoichiometric value of the hydrogen ions in the reaction of interest. For the reaction of pyruvate to propionate, 2 hydrogen ions are absorbed resulting in $n = -2$. At pH = 7.0, with $T = 328.15$ K and $R = 8.314$ J/(mol·K), the Gibbs free energy of reaction actually experienced at cellular conditions is

$$\Delta G_R = -85.63 \text{ kJ/mol}$$

APPENDIX J

CPDM MATLAB PROGRAM FOR SIMULATION OF A FOUR BOTTLE COUNTERCURRENT FERMENTATION

```
%MATLAB Code for CPDM Prediction
%This code is for a standard four-stage countercurrent fermentation
%Program predicts acid concentrations and conversion at varying VSLR and LRT.
%Code by Andrea Forrest 09/28/2009
%Department of Chemical Engineering, Texas A&M University, College St, TX

clear all
close all
global so taus a1 b1 e1 f1 g1 h1
global holdup moist ratio stages loading tauloverall
global ratio acid nnot factr1
global x_1 nhat_1 x_2 nhat_2 x_3 nhat_3 x_4 nhat_4

%Start Simulation
disp(['Program starts at: ', datestr(now)]);
tic;

VSLR_data=[4,6,8,10,12]';
LRT_data=[10,15,20,25,30]';
ACID = [];
CONVERSION = [];
VSLR_loop=4; %loop is for varying VSLR.
%To make map, set to lowest VSLR, otherwise, set to specific VSLR
while VSLR_loop<12.1 % if want loop, set to highest VSLR
   LRT_loop=10;   %loop is for varying LRT.
   %To make map, set to lowest LRT, otherwise set to specific LRT
   while LRT_loop<30.01 %if want loop, set to highest VSLR

      %%Basic parameters for Fermentation
      stages=4; %Fermentor stages
      so=0.21; %Aeq selectivity (gAEQ/g VS digested)  Please note that in older versions of the code (i.e.
      %Please note that in older versions of the code (i.e. Loescher's)
      %this term referred to a VS selectivity of g VS/g total solids and
      %was carried over in the differiental equations in Ross and Fu.
      holdup =2.0; %ratio of liq to solid in wet cake (g liq/gVS cake)
      %Note: holdup is the liq in the solid cake NOT the lig of the total slurry
      moist =.06; %ratio of liquid to solid in feed (g liq/gVS cake)
      SQ =1.0;
      ratio=0.79; %phi ratio of g total acid to g AEQ
      loading = VSLR_loop;
      tauloverall = LRT_loop;
      vol=[.48,.28,.28,.28]'; %Liquid volime in each fermentor
      totvol=sum(vol);
      liquidfeed = totvol/tauloverall;
      nnotreal = [169,214,214,214]'; %VS concentration (gVS/L) in each fermentor
      solidfeed = loading*totvol; %Solid Feed (g dry weight)
      Convrsn = [.1,.2,.3,.4]'; %Initial value for conversion
      nnot = nnotreal./(1-Convrsn);
```

```
taus = nnot.*vol/solidfeed;
L =0.1*ones(stages+1,1); %L initial value for liquid flow rate in every reactor
taul = tauloverall/stages*ones(stages,1);

e1=0.027; f1=5.56; g1=.001; h1=3.36; %CPDM parameters
rmodel = @(x1,acid) e1.*(1-x1).^f1./(1+g1.*(acid.*ratio).^h1);
syms x1 acid
drmodel_1 = diff(e1.*(1-x1).^f1./(1+g1.*(acid.*ratio).^h1),x1);
drmodel = @(x2,acd2) subs(drmodel_1,{x1,acd},{x2,acd2});

done = 0; %The index used to trace whether the condition is satisfied
liqtoler = 0.05; %tolerance for Liquid flowrate
acidtoler = 0.1; %tolerance for acid concentration
nnottoler = 1; %tolerance for nnot

%Initial values for acid, acidold
ans=ones(stages,1);
acid=[30,20,15,5]';
acidold=ones(stages,1);
taulnew = 1000*ones(stages,1);  %column vector
nhatzero =100*ones(stages,1);  %CP concentration
creation = ones(stages,1);
destruction = ones(stages,1);
tauloverallnew = 20;

disp('Calculation is in progress.....');

while done < 0.50
   taulnew = 1000*ones(stages,1);  %Obtain Flowrate for each fermentor
   taulover_error = 0.001;
   while abs(tauloverall-tauloverallnew) > taulover_error
      liquidfeed = liquidfeed*(1+(tauloverallnew-tauloverall)/tauloverall*0.5);
      L(5) = liquidfeed;
      L(4) = L(5) + solidfeed/1000*holdup*(Convrsn(4)-Convrsn(3));
      L(3) = L(4) + solidfeed/1000*holdup*(Convrsn(3)-Convrsn(2));
      L(2) = L(3) + solidfeed/1000*holdup*(Convrsn(2)-Convrsn(1));
      L(1) = moist*solidfeed/1000 + L(2) - solidfeed/1000*holdup*(1.0-Convrsn(1));
      tauloverallnew = totvol/L(1);
   end

   taul = vol./L(1:stages);
   nnot = nnotreal./(1-Convrsn);
   taus = nnot.*vol/solidfeed;
   scale = ones(stages,1);

   disp([' nnot= ',num2str(nnot','%15.5f')]);

   %parameters for ODE45
   options = odeset('RelTol',1e-3,'AbsTol', 1e-3);
   x_low=0; x_high=0.99;

%Reactor 1

   i=1;
```

```
        while abs(taulnew(i) - taul(i))> liqtoler
           nhat0 =nhatzero(i);
           [x,nhat]= ode15s(@Chan1,[x_low,x_high],nhat0,options);
           x_1=x;  nhat_1 = nhat;
           F_1 = @(x_1)interp1(x,nhat,x_1);
           factr1 = nnot(i)/quad(F_1,x_low,x_high);  %calculate factor
           F_11 = @(x_1) factr1*interp1(x,nhat,x_1).*rmodel(x_1,acid(i));
           robs = quad(F_11,x_low,x_high);
           F_12 = @(x_1) interp1(x,nhat,x_1).*x_1;
           Convrsn(i) = quad(F_12,x_low,x_high)/nnot(i)*factr1;
           taulnew(i) = (L(i)*acid(i) + solidfeed/1000*(1-Convrsn(i))*holdup*acid(i)-
L(i+1)*acid(i+1))/(L(i)*robs);
           acid(i) = acid(i) + (taul(i)*robs-(L(i)*acid(i)+solidfeed/1000*(1-Convrsn(i))*holdup*acid(i)-
L(i+1)*acid(i+1))/L(i))*.4;
        end
        disp([' acid(',num2str(i),')=',num2str(acid(i),'%15.5f'),'
taulnew(',num2str(i),')=',num2str(taulnew(i),'%15.5f'),'  robs=', num2str( robs, '%15.5f')]);

        %Reactor 2

        i=2;
        nnottoler = nnot(i)/500;
        while abs(taulnew(i)-taul(i))>liqtoler;
           ndone = 0;
           while ndone <0.50
              nhat0=nhatzero(i);
              options = odeset('RelTol',1e-3,'AbsTol',1e-3);
              [x,nhat] = ode15s(@Chan2,[x_low,x_high],nhat0,options);
              x_2=x;  nhat_2=nhat;
              F_2 = @(x_2)interp1(x,nhat,x_2);
              nhattot=quad(F_2,x_low,x_high);
              disp([' nhatzero= ',num2str(nhatzero(i), '%15.5f'),';  nhattot= ',num2str(nhattot, '%15.5f'),';
nnot(',num2str(i),')= ',num2str(nnot(i), '%15.5f')]);
              if abs(nhattot - nnot(i))<nnottoler;
                 ndone = 1;
              end
              if (nhatzero(i) + (nnot(i) - nhattot)*1.0)>0
                 nhatzero(i)= nhatzero(i) + (nnot(i) - nhattot)*0.7;
              else
                 nhatzero(i)= nhatzero(i) + (nnot(i) - nhattot)*0.7;
              end
           end

           F_22 = @(x_2)interp1(x,nhat,x_2).*x_2;
           Convrsn(i)= quad(F_22,x_low,x_high)/nnot(i);
           robs = solidfeed*so/vol(i)*(Convrsn(i)-Convrsn(i-1));

           taulnew(i) = (L(i)*acid(i) + solidfeed/1000*(1-Convrsn(i))*holdup*acid(i)-
L(i+1)*acid(i+1))/(L(i)*robs);
           acid(i) = acid(i) + (taul(i)*robs-(L(i)*acid(i)+solidfeed/1000*(1-Convrsn(i))*holdup*acid(i)-
L(i+1)*acid(i+1))/L(i))*.5;
           disp([' taulnew(',num2str(i),')=',num2str(taulnew(i), '%15.5f'),'
taul(',num2str(i),')=',num2str(taul(i),'%15.5f'),]);
        end
```

```
        disp([' acid(',num2str(i),')=',num2str(acid(i),'%15.5f'),'
taulnew(',num2str(i),')=',num2str(taulnew(i),'%15.5f'),' robs=', num2str( robs, '%15.5f')]);

        %Reactor 3

        i=3;
        nnottoler = nnot(i)/500;
        while abs(taulnew(i)-taul(i))>liqtoler;
           ndone = 0;
           while ndone <0.50
              nhat0 =nhatzero(i);
              options = odeset('RelTol',1e-3,'AbsTol',1e-3);
              [x,nhat] = ode15s(@Chan3,[x_low,x_high],nhat0,options); %was chan3
              x_3=x;  nhat_3=nhat;
              F_3 = @(x_3)interp1(x,nhat,x_3);
              nhattot=quad(F_3,x_low,x_high);
              disp([' nhatzero= ',num2str(nhatzero(i), '%15.5f'),';  nhattot= ',num2str(nhattot, '%15.5f'),';
nnot(',num2str(i),')= ',num2str(nnot(i), '%15.5f')]);
              if abs(nhattot - nnot(i))<nnottoler;
                 ndone = 1;
              end
              if (nhatzero(i) + (nnot(i) - nhattot)*1.0)>0
                 nhatzero(i)= nhatzero(i) + (nnot(i) - nhattot)*0.7;
              else
                 nhatzero(i)= nhatzero(i) + (nnot(i) - nhattot)*0.7;
              end
           end

           F_32 = @(x_3)interp1(x,nhat,x_3).*x_3;
           Convrsn(i)= quad(F_32,x_low,x_high)/nnot(i);
           robs = solidfeed*so/vol(i)*(Convrsn(i)-Convrsn(i-1));
           taulnew(i) = (L(i)*acid(i) + solidfeed/1000*(1-Convrsn(i))*holdup*acid(i)-
L(i+1)*acid(i+1))/(L(i)*robs);
           acid(i) = acid(i) + (taul(i)*robs-(L(i)*acid(i)+solidfeed/1000*(1-Convrsn(i))*holdup*acid(i)-
L(i+1)*acid(i+1))/L(i))*.5;
           disp([' taulnew(',num2str(i),')=',num2str(taulnew(i), '%15.5f'),'
taul(',num2str(i),')=',num2str(taul(i),'%15.5f'),]);
        end
        disp([' acid(',num2str(i),')=',num2str(acid(i),'%15.5f'),'
taulnew(',num2str(i),')=',num2str(taulnew(i),'%15.5f'),' robs=', num2str( robs, '%15.5f')]);



        %Reactor 4

        i=4;
        nnottoler = nnot(i)/500;
        while abs(taulnew(i)-taul(i))>liqtoler;
           ndone = 0;
           while ndone <0.50
              nhat0 =nhatzero(i);
              options = odeset('RelTol',1e-3,'AbsTol',1e-3);
              [x,nhat] = ode15s(@Chan4,[x_low,x_high],nhat0,options);
              x_4=x;  nhat_4=nhat;
              F_4 = @(x_4)interp1(x,nhat,x_4);
              nhattot=quad(F_4,x_low,x_high);
```

```
            disp([' nhatzero= ',num2str(nhatzero(i), '%15.5f'),';  nhattot= ',num2str(nhattot, '%15.5f'),';
nnot(',num2str(i),')= ',num2str(nnot(i), '%15.5f')]);
            if abs(nhattot - nnot(i))<1;%nnottoler;
               ndone = 1;
            end
            if (nhatzero(i) + (nnot(i) - nhattot)*1.0)>0
               nhatzero(i)= nhatzero(i) + (nnot(i) - nhattot)*0.7; %25/nnot(i);
            else
               nhatzero(i)= nhatzero(i) + (nnot(i) - nhattot)*0.7;
            end
         end

         F_42 = @(x_4)interp1(x,nhat,x_4).*x_4;
         Convrsn(i)= quad(F_42,x_low,x_high)/nnot(i);
         robs = solidfeed*so/vol(i)*(Convrsn(i)-Convrsn(i-1));

         taulnew(i) = (L(i)*acid(i) + solidfeed/1000*(1-Convrsn(i))*holdup*acid(i)-solidfeed/1000*(1-
Convrsn(i-1))*holdup*acid(i-1))/(L(i)*robs);
         acid(i) = acid(i) + (taul(i)*robs-(L(i)*acid(i)+solidfeed/1000*(1-Convrsn(i))*holdup*acid(i)-
solidfeed/1000*(1-Convrsn(i-1))*holdup*acid(i-1))/L(i))*0.5;
         disp([' taulnew(',num2str(i),')=',num2str(taulnew(i), '%15.5f'),'
taul(',num2str(i),')=',num2str(taul(i),'%15.5f'),]);
      end
      disp([' acid(',num2str(i),')=',num2str(acid(i),'%15.5f'),'
taulnew(',num2str(i),')=',num2str(taulnew(i),'%15.5f'),' robs=', num2str( robs, '%15.5f')]);
      disp([' Conversion in each stage (from nhat):  ',num2str(Convrsn','%13.5f')]);

      if max(abs(acid-acidold))<acidtoler
         done=1;
      end
      acidold = acid;
   end

   %Output results section

   disp('Congratulations!  The simulation is successfully finished!')
   toc  %toc is used to check the whole time of the process

   for i3 = 1:(stages+1);
      disp([' L(',int2str(i3),')= ',num2str(L(i3))]);
   end

   creation(1) = L(1)*acid(1) + solidfeed/1000*(1-Convrsn(1))*holdup*acid(2)-L(2)*acid(2);
   creation(2) = L(2)/acid(2) + solidfeed/1000*(1-Convrsn(2))*holdup*acid(3)-L(3)*acid(3)-
solidfeed/1000*(1-Convrsn(1))*holdup*acid(2);
   creation(3) = L(3)*acid(3) + solidfeed/1000*(1-Convrsn(3))*holdup*acid(4)-L(4)*acid(4)-
solidfeed/1000*(1-Convrsn(2))*holdup*acid(3);
   creation(4) = L(4)*acid(4) - solidfeed/1000*(1-Convrsn(3))*holdup*acid(4);

   %Calculation of Destruction

   destruction(1) = solidfeed/1000*(Convrsn(1)-0);
   for i3=2:stages;
      destruction(i3)=solidfeed/1000*(Convrsn(i3)-Convrsn(i3-1));
```

```
        end
        selectivi = creation./destruction;
        selec = L(1)*acid(1)/(solidfeed*Convrsn(4));

        %output the results
        disp([' Selectivity = ',num2str(selectivi','%15.5f')]);
        disp([' Creation = ',num2str(creation','%15.5f')]);
        disp([' Destruction = ',num2str(destruction','%15.5f')]);
        disp([' selectivity = ',num2str(selec','%15.5f')]);
        disp([' tauloverall = ',num2str(tauloverall,'%15.5f')]);
        disp([' taus = ',num2str(sum(taus),'%15.5f')]);
        disp([' acid levels = ',num2str(acid','%13.5f')]);

        disp([' VSLR_LOOP = ',num2str(VSLR_loop),' LRT_loop = ',num2str(LRT_loop)]);

        %Collect data for CPDM map
        ACID = [ACID;acid(1)];
        CONVERSION = [CONVERSION;Convrsn(4)];
        LRT_loop = LRT_loop + 5;
    end
    VSLR_loop = VSLR_loop + 2;
end

disp([' acid levels = ',num2str(acid','%13.5f')]);  %shows acids levels for the last simulation run
disp([' convrsn levels = ',num2str(Convrsn','%13.5f')]);  %shows conversion levels for the last sim run
 disp([' VSLR = ',num2str(VSLR_data','%13.5f')]);
 disp([' LRT = ',num2str(LRT_data','%13.5f')]);
 disp([' Acid levels = ',num2str(ACID','%13.5f')]);  %output final acid conc for each VSLR and LRT loop
 disp([' Conversions = ',num2str(CONVERSION','%13.5f')]);  %output final conversion for each VSLR and
LRT
```

******End of the MATLAB code**

******The following are the four function files used in the main source code.

***Chan1.m

```
function dnhat = nhateq1(x,nhat1)
global so taus a1 b1 e1 f1 g1 h1 i x1
global ratio acid

rmodel = @(x1,acid)e1.*(1-x1).^f1./(1+g1.*(acid.*ratio).^h1);
drmodel = @(x1,acid)-28341/100000.*(1-
x1)^(101/100)./(1+517/500*3^(273/1000)*5^(727/1000).*acid^(273/1000));

i=1;
dnhatdt = -nhat1*(drmodel(x,acid(i))+1/taus(i))/rmodel(x,acid(i));
dnhat = [dnhatdt];
```

***Chan2.m

```
function dnhat = nhateq1(x,nhat1)
global so taus a1 b1 e1 f1 g1 h1 i RN x1
global ratio acid nnot factr1
global x_1 nhat_1 x_2 nhat_2 x_3 nhat_3 x_4 nhat_4

rmodel = @(x1,acid) e1.*(1-x1).^f1./(1+g1.*(acid.*ratio).^h1);
drmodel = @(x1,acid) -28341/100000.*(1-
x1)^(101/100)./(1+517/500*3^(273/1000)*5^(727/1000).*acid^(273/1000));

F_1m = @(x_m)interp1(x_1,nhat_1,x_m);

i=2;
dnhatdt = -nhat1*(drmodel(x,acid(i))+1/taus(i))/rmodel(x,acid(i)) + F_1m(x).*nnot(i)./nnot(i-
1)*factr1*1/taus(i)/rmodel(x,acid(i));
 dnhat = [dnhatdt];
```

***Chan3.m

```
function dnhat = nhateq1(x,nhat1)
global so taus a1 b1 e1 f1 g1 h1 i RN x1
global ratio acid nnot factr1
global x_1 nhat_1 x_2 nhat_2 x_3 nhat_3 x_4 nhat_4

rmodel = @(x1,acid) e1.*(1-x1).^f1./(1+g1.*(acid.*ratio).^h1);
drmodel = @(x1,acid) -2247/5000*(1-
x1)^(271/50)/(1+6741/31250*21^(33/100)*25^(67/100)*acid^(133/100));

F_2m = @(x_m)interp1(x_2,nhat_2,x_m);

i=3;
dnhatdt = -nhat1*(drmodel(x,acid(i))+1/taus(i))/rmodel(x,acid(i)) + F_2m(x).*nnot(i)./nnot(i-
1)*1/taus(i)/rmodel(x,acid(i));
 dnhat = [dnhatdt];
```

***Chan4.m

```
function dnhat = nhateq1(x,nhat1)
global so taus a1 b1 e1 f1 g1 h1 i RN x1
global ratio acid nnot factr1
global x_1 nhat_1 x_2 nhat_2 x_3 nhat_3 x_4 nhat_4

rmodel = @(x1,acid) e1.*(1-x1).^f1./(1+g1.*(acid.*ratio).^h1);
drmodel = @(x1,acid) -28341/100000.*(1-
x1)^(101/100)./(1+517/500*3^(273/1000)*5^(727/1000).*acid^(273/1000));

F_3m = @(x_m)interp1(x_3,nhat_3,x_m);

i=4;
dnhatdt = -nhat1*(drmodel(x,acid(i))+1/taus(i))/rmodel(x,acid(i)) + F_3m(x).*nnot(i)./nnot(i-
1)*1/taus(i)/rmodel(x,acid(i));
dnhat = [dnhatdt];
```

APPENDIX K

MATLAB CODE FOR CPDM PREDICTION MAP

```
VSLR=[12;12;12;12;12;10;10;10;10;10;8;8;8;8;8;6;6;6;6;6;4;4;4;4;4];
LRT=[10;15;20;25;30;10;15;20;25;30;10;15;20;25;30;10;15;20;25;30;10;15;20;25;30];
CONVERSION=[0.14;0.135;0.134;0.13;0.127;0.16;0.15;0.149;0.143;0.14;0.184;0.18;0.17;0.163;0.16;0.24;0.2
2;0.218;0.2;0.19;0.45;0.4;0.39;0.32;0.3];
ACID=[9.1;10.8;11.9;15.4;16.5;9.2;10.9;11.9;15.5;16.8;9.4;10.9;12;15.7;17;9.5;10.9;12.1;15.7;17.2;10.9;12.3;1
3.3;16.6;17.9];
%Enter collected Conversion and Acid data into the two above matrices that correspond to the VSLR and LRT
mapdata=[VSLR,LRT,CONVERSION,ACID];
VSLR_sorted=sortrows(mapdata,1);
LRT_sorted=sortrows(mapdata,2); %sort
[map_num,map_1]=size(mapdata);
VSLR_sort = sort(mapdata(:,1));
uniqueM = [diff(VSLR_sort);1] > 0;
VSLR_sort1 = VSLR_sort(uniqueM);
VSLR_number = diff(find([1;uniqueM]));
LRT_sort = sort(mapdata(:,2));
uniqueM = [diff(LRT_sort);1] > 0;
LRT_sort1 = LRT_sort(uniqueM);  %Unique LRT
LRT_number = diff(find([1;uniqueM]));
%plot for VSLR part
temp1=zeros(length(VSLR_sort1)+1,1);
for j1=1:length(VSLR_sort1)
temp1(j1+1)=temp1(j1)+VSLR_number(j1);
mapdata_1=VSLR_sorted(temp1(j1)+1:temp1(j1+1),:) ;

%for VSLR(j1)
F = @(x)interp1(mapdata_1(:,3),mapdata_1(:,4),x,'spline');
hold on;
plot(mapdata_1(:,3),F(mapdata_1(:,3)),'k');
%notes of formatting the plots:
%default is a solid line '-'
%a dashed line is '--'
%a dotted line is ':'
%a dash and dotted line is '-.'
% colors are r = red, g = green, b = blue, c = cyan
% m = magenta, y = yellow, k = black, w = white
%note remember to do both the VSLR lines and the LRT lines
if j1==1
for j3=1:length(mapdata_1(:,3))
text(mapdata_1(j3,3)-0.01,mapdata_1(j3,4)+0.5, ['  ', num2str(mapdata_1(j3,2))] ,'HorizontalAlignment','left');
end
text(mapdata_1(1,3)-0.3,mapdata_1(1,4)-5.5, 'VSLR (g/(L.d))' ,'HorizontalAlignment','left');
end
end

%plot for LRT part
temp1=zeros(length(LRT_sort1)+1,1);
for j1=1:length(LRT_sort1)
temp1(j1+1)=temp1(j1)+LRT_number(j1);
mapdata_2=LRT_sorted(temp1(j1)+1:temp1(j1+1),:) ;
%for LRT(j1)
F2 = @(x)interp1(mapdata_2(:,3),mapdata_2(:,4),x,'spline');
```

```
hold on;
plot(mapdata_2(:,3),F2(mapdata_2(:,3)),'k');
if j1==1
for j3=1:length(mapdata_2(:,3))
text(mapdata_2(j3,3)+0.02,mapdata_2(j3,4)-1.5, ['  ',num2str(mapdata_2(j3,1))] ,
'HorizontalAlignment','right');
end
text(mapdata_2(1,3)+0.31,mapdata_2(1,4)+5, ' LRT (day)' ,'HorizontalAlignment','left');
end
end
legend('Galveston',1) %adjust as necessary, number is the legend position
hold off;
xlabel('Conversion');
ylabel('Total carboxylic acid concentration (g/L)');
axis([0 1 0 25]); %adjust as necessary for size of map
```

APPENDIX L

CPDM COMPARISON MAPS OF BIOSCREENING INOCULA VS GALVESTON.

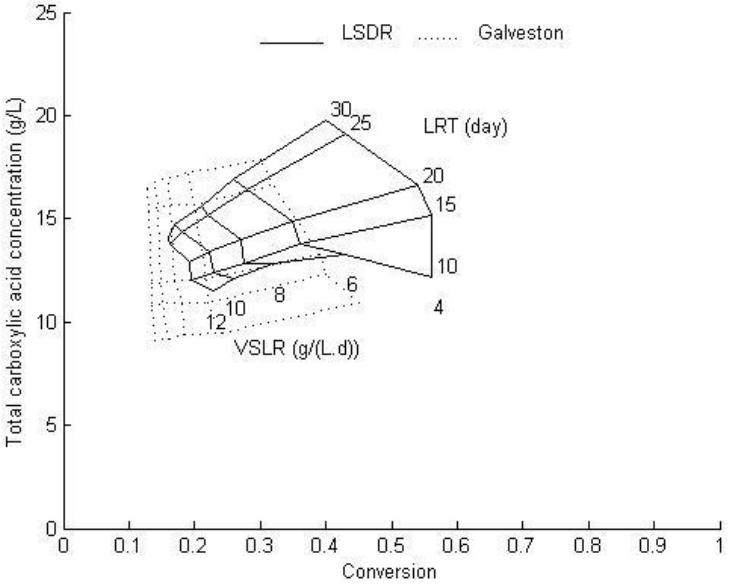

Figure L-1. Comparison map of Site A – La Sal del Rey, TX (LSDR) Sample A23 and B01 – Galveston.

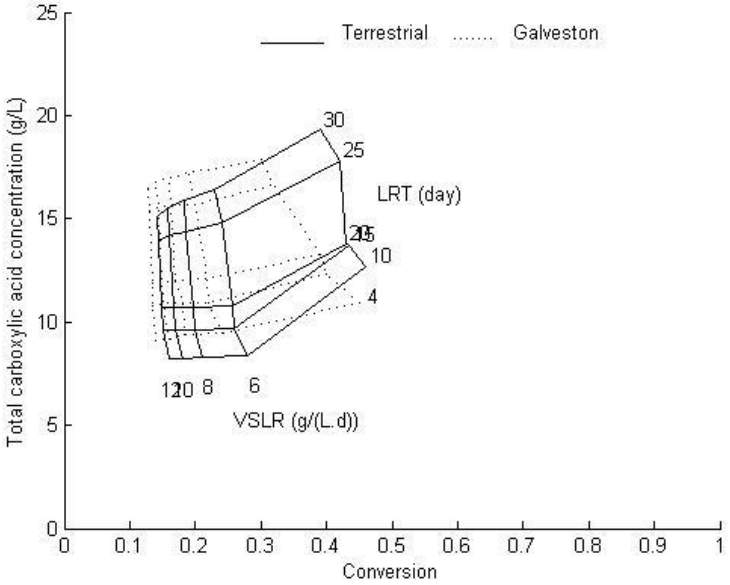

Figure L-2. Comparison map of Site B –Sample B02 (Bryan, TX) and B01 – Galveston.

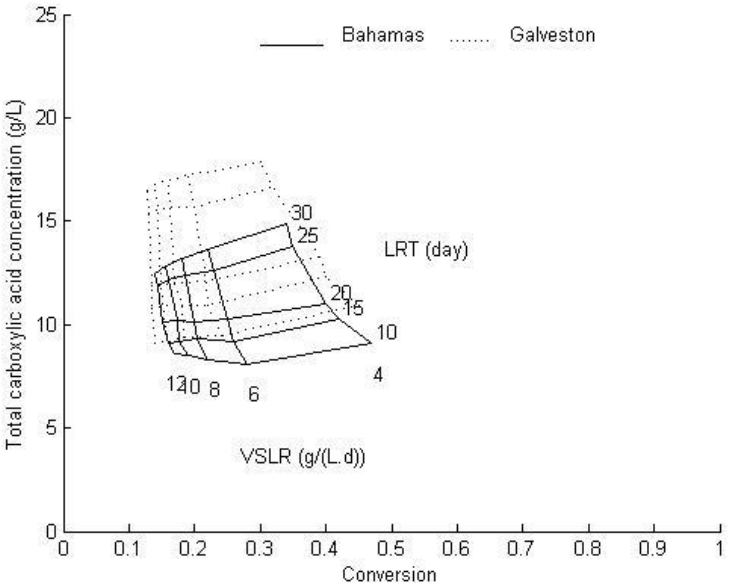

Figure L-3. Comparison map of Site B Sample B03 (Bahamas) and B01 – Galveston.

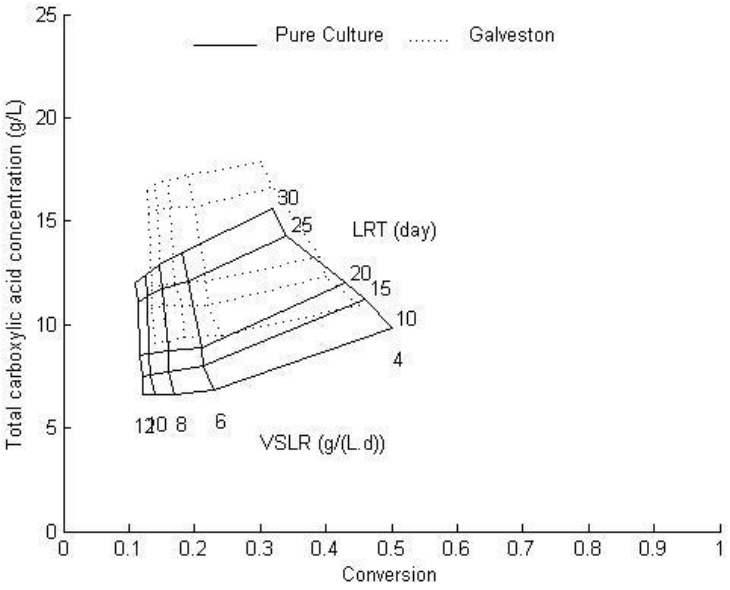

Figure L-4. Comparison map of Site B Sample B04 – Pure culture of *C. thermocellum* and B01 – Galveston.

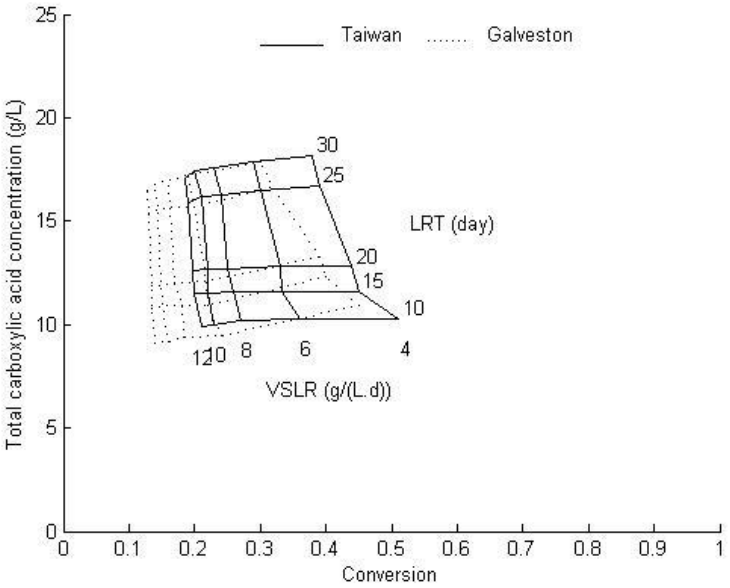

Figure L-5. Comparison map of Site C Sample C01 – Taiwan and B01 – Galveston.

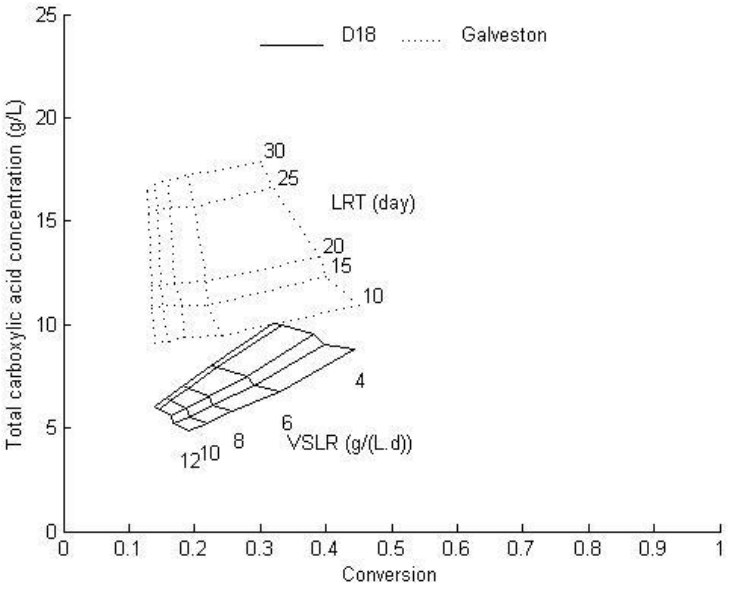

Figure L-6. Comparison map of Site D Sample D18 and B01 – Galveston.

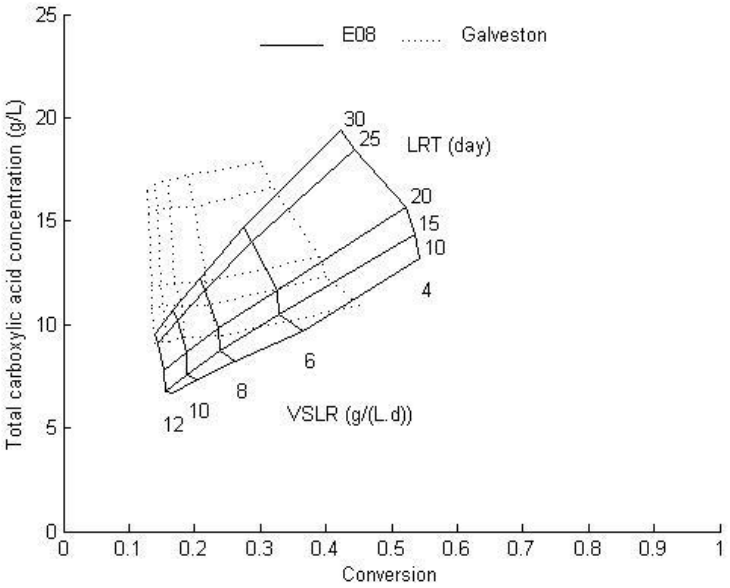

Figure L-7. Comparison map of Site E Sample E08 and B01 – Galveston.

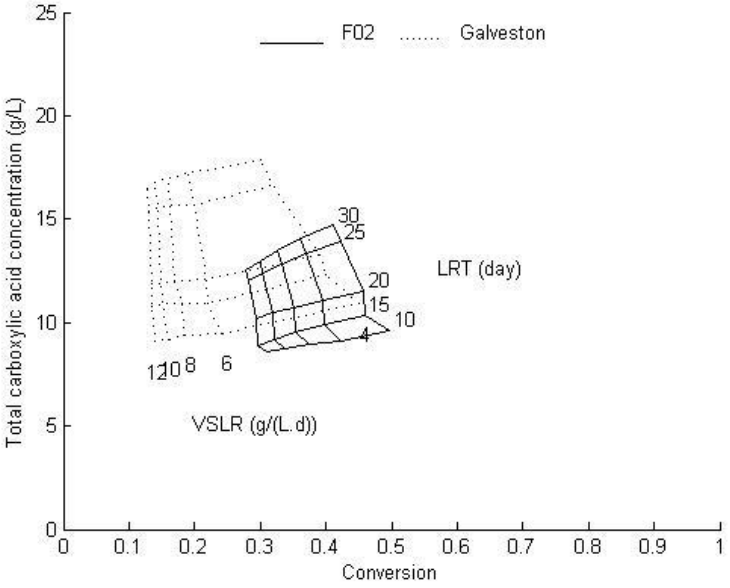

Figure L-8. Comparison map of Site F Sample F02 and B01 – Galveston.

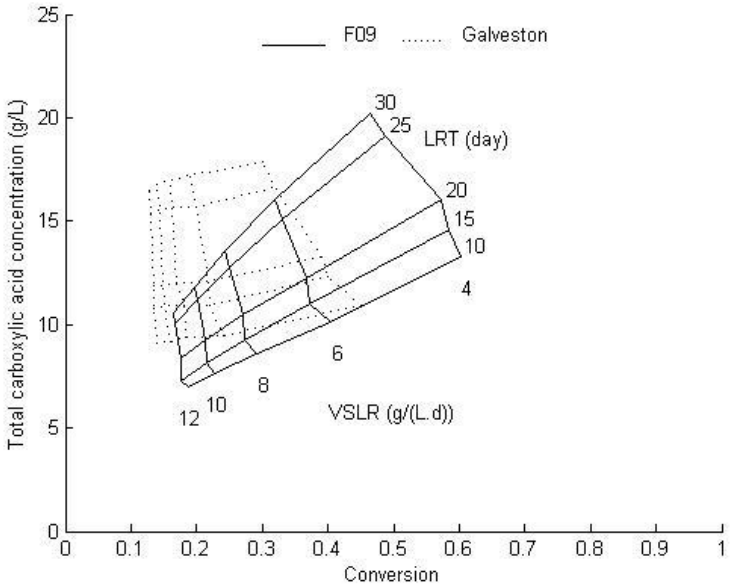

Figure L-9. Comparison map of Site F Sample F09 and B01 – Galveston.

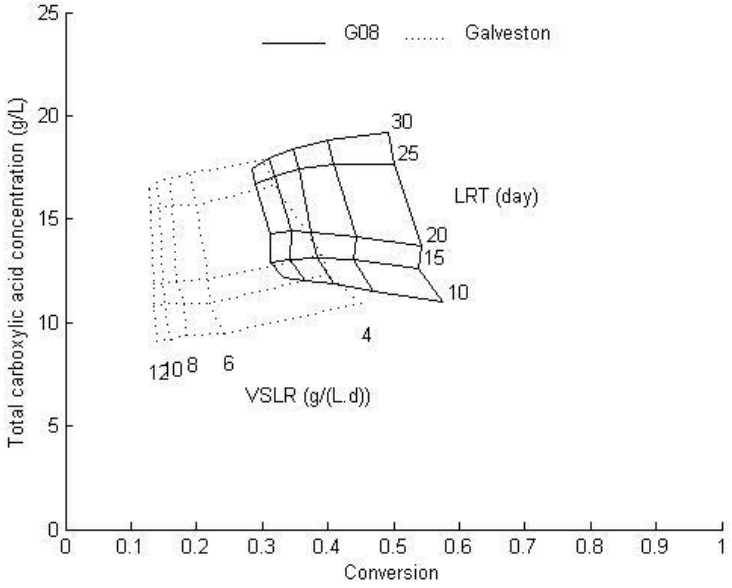

Figure L-10. Comparison map of Site G Sample G08 and B01 – Galveston.

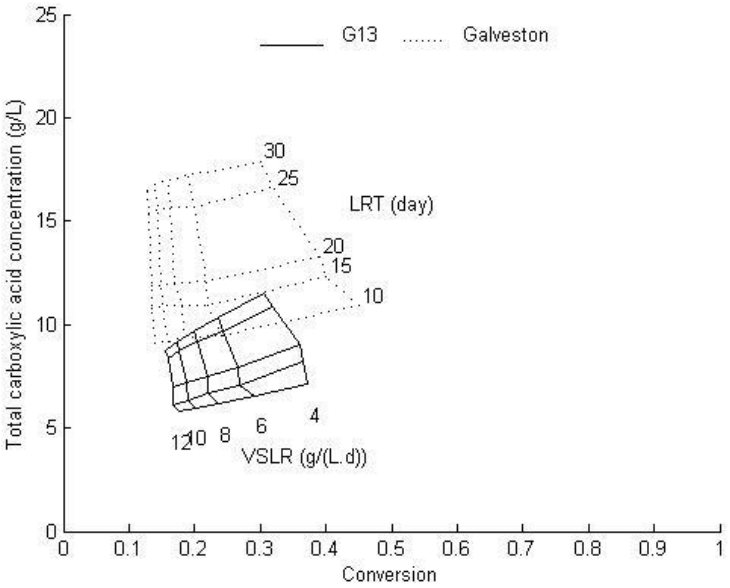

Figure L-11. Comparison map of Site G Sample G13 and B01 – Galveston.

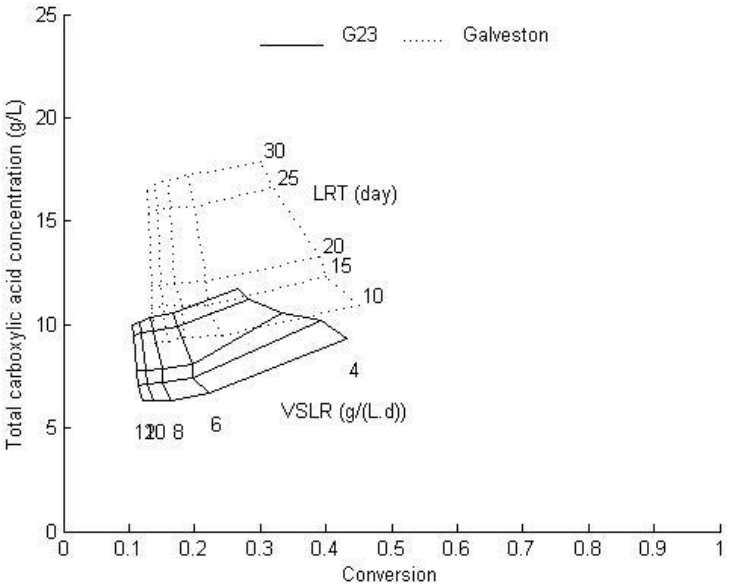

Figure L-12. Comparison map of Site G Sample G23 and B01 – Galveston.

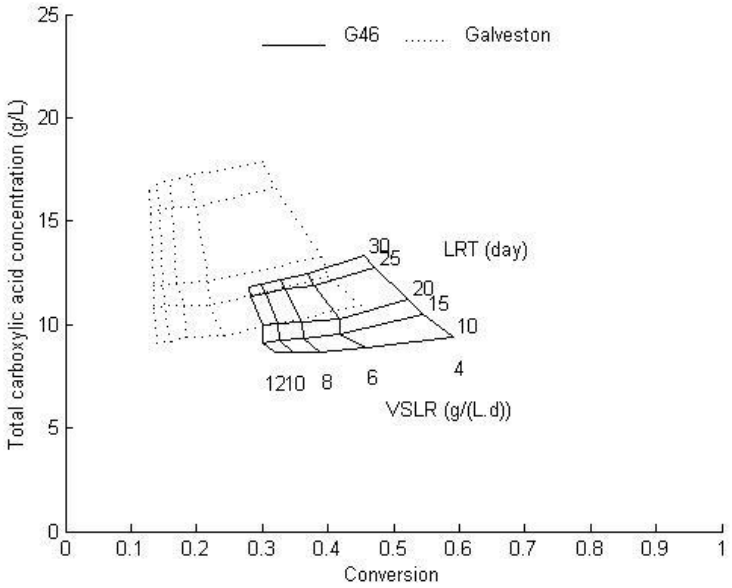

Figure L-13. Comparison map of Site G Sample G46 and B01 – Galveston.

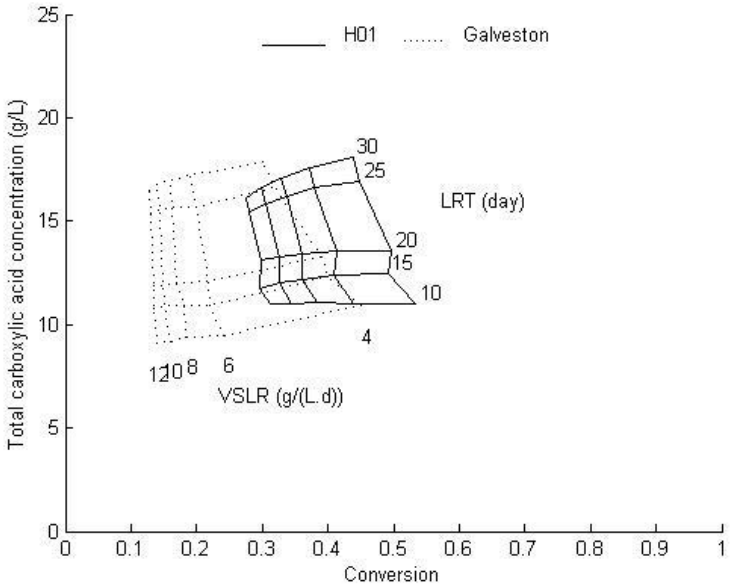

Figure L-14. Comparison map of Site H Sample H01 and B01 – Galveston.

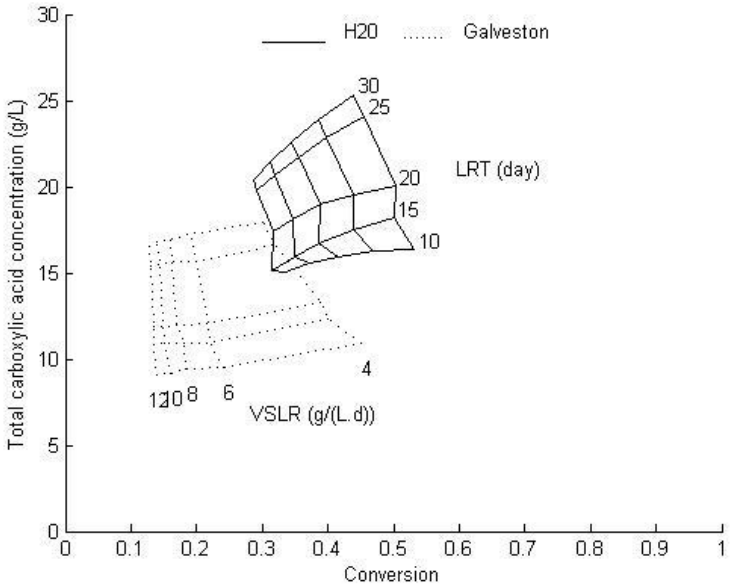

Figure L-15. Comparison map of Site H Sample H20 and B01 – Galveston.

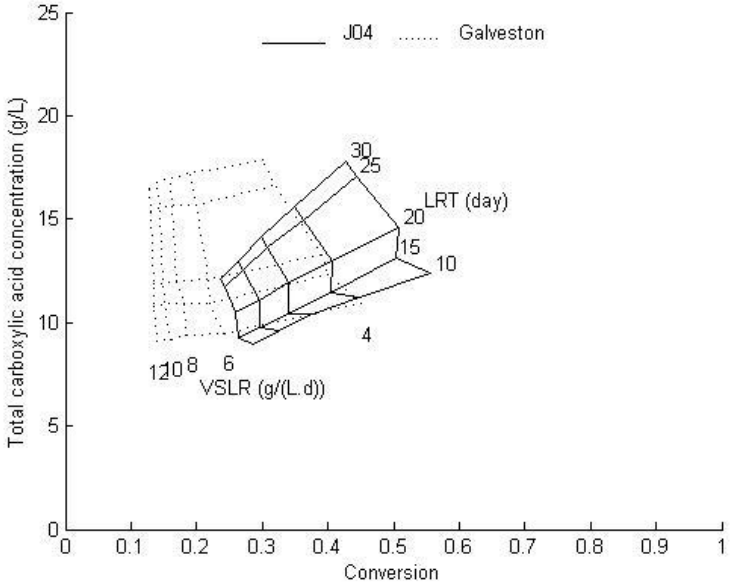

Figure L-16. Comparison map of Site J Sample J04 and B01 – Galveston.

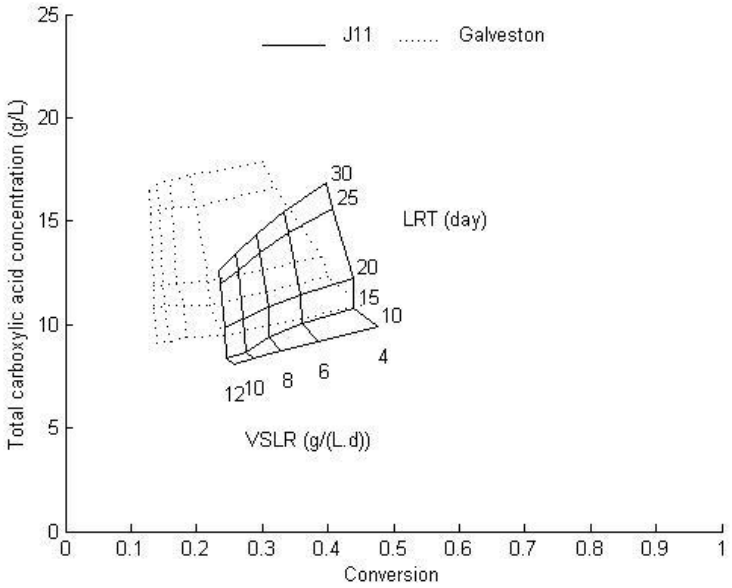

Figure L-17. Comparison map of Site J Sample J11 and B01 – Galveston.

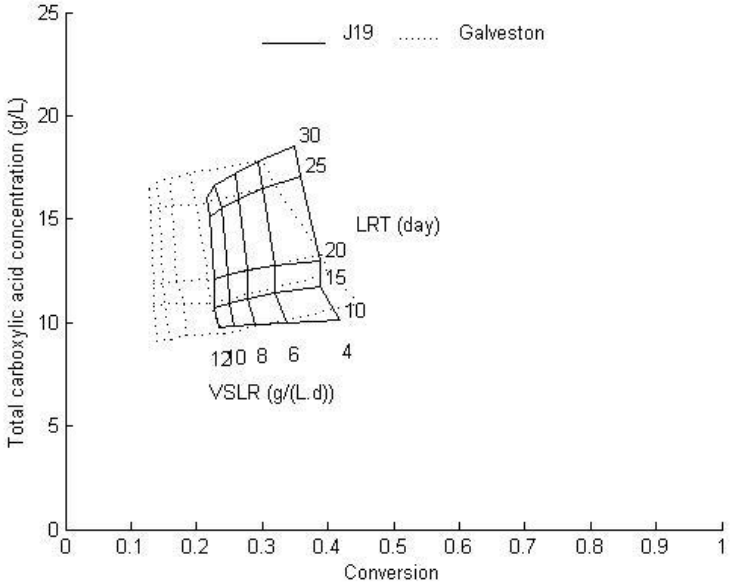

Figure L-18. Comparison map of Site J Sample J19 and B01 – Galveston.

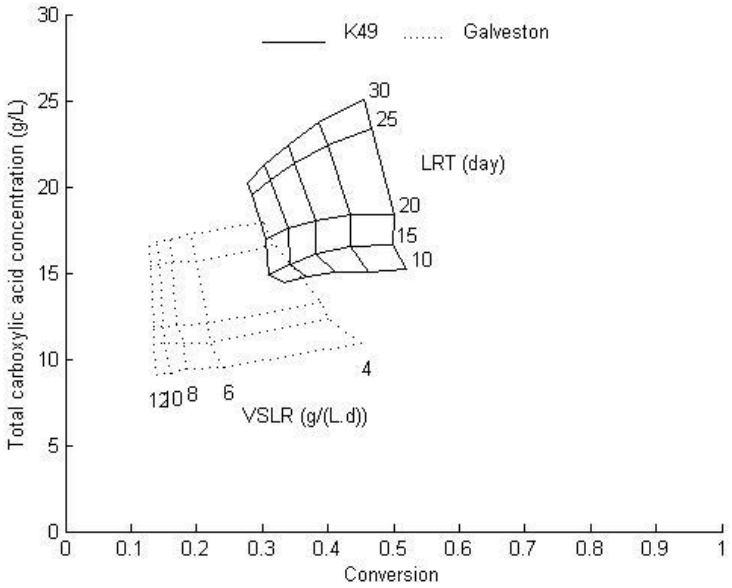

Figure L-19. Comparison map of Site K Sample K49 and B01 – Galveston.

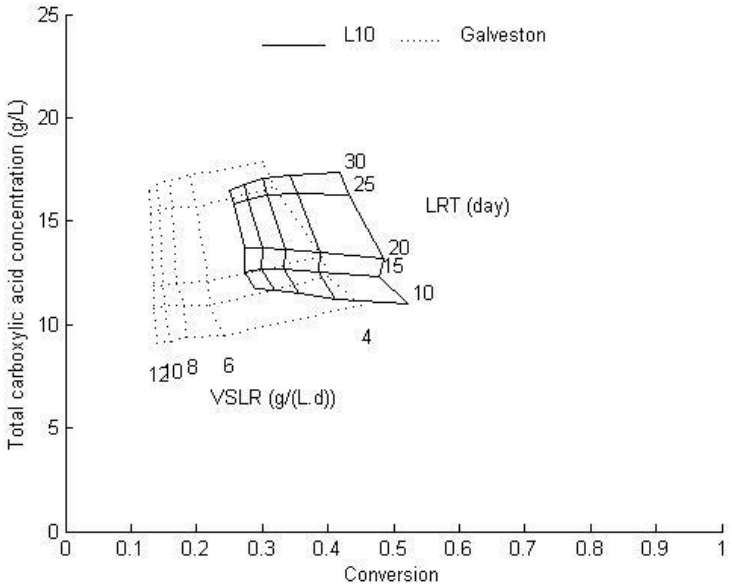

Figure L-20. Comparison map of Site L Sample L10 and B01 – Galveston.

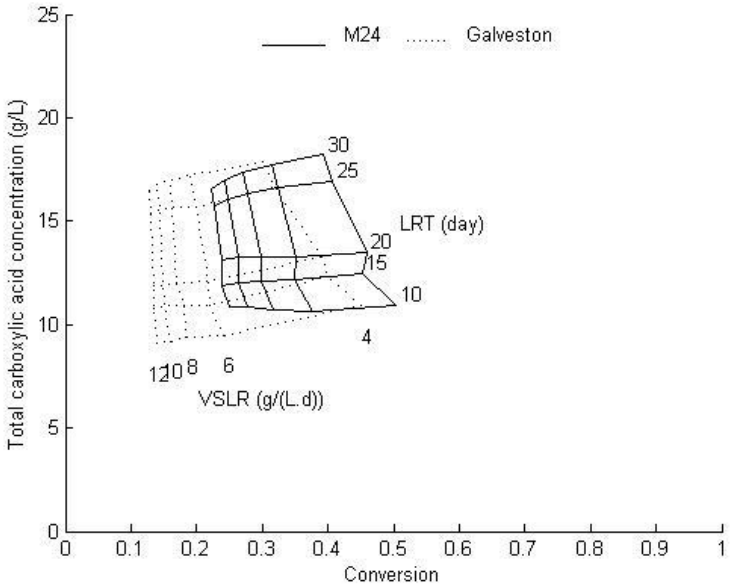

Figure L-21. Comparison map of Site M Sample M24 and B01 – Galveston.

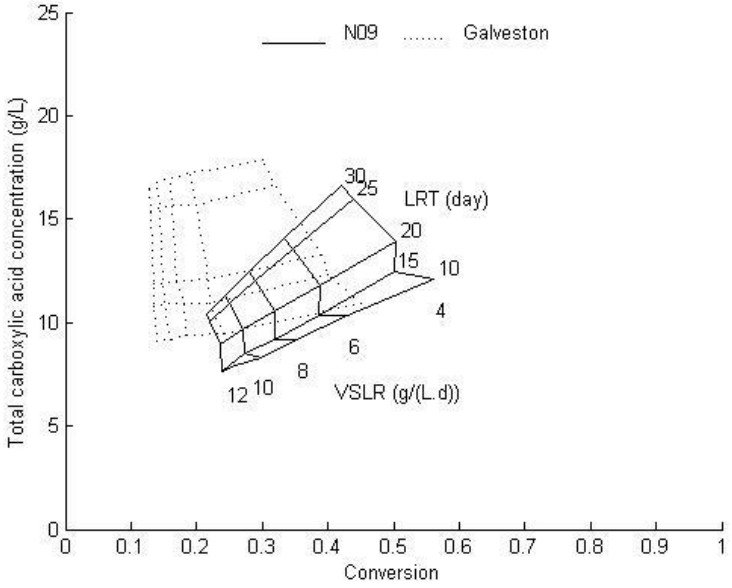

Figure L-22. Comparison map of Site N Sample N09 and B01 – Galveston.

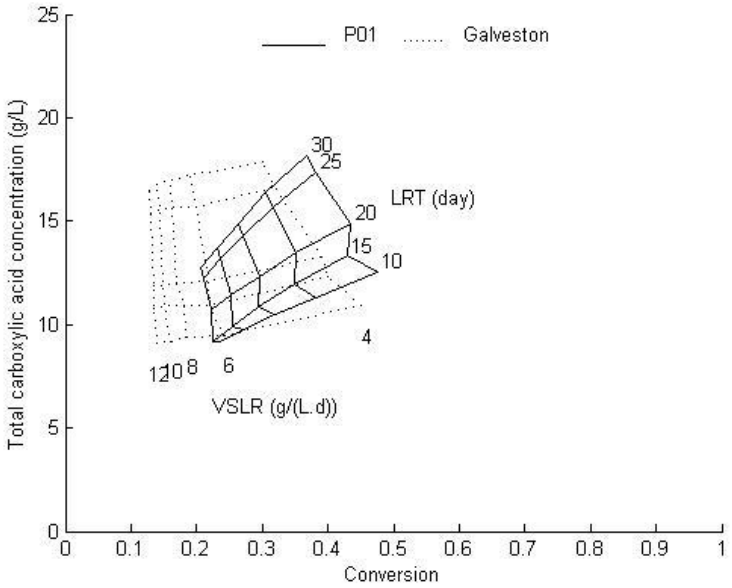

Figure L-23. Comparison map of Site P Sample P01 and B01 – Galveston.

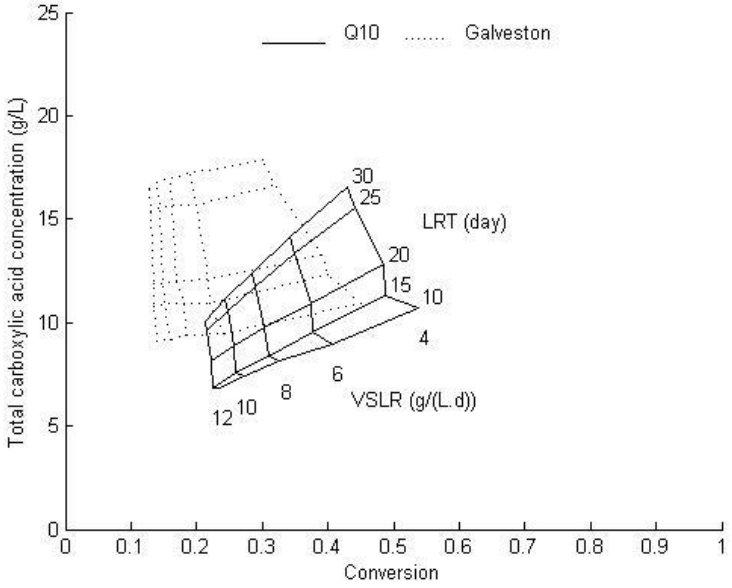

Figure L-24. Comparison map of Site Q Sample Q10 and B01 – Galveston.

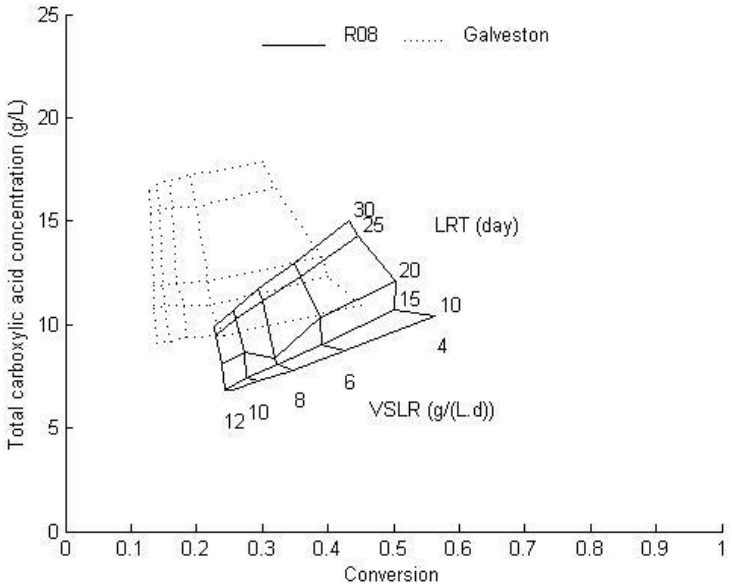

Figure L-25. Comparison map of Site R Sample R08 and B01 – Galveston.

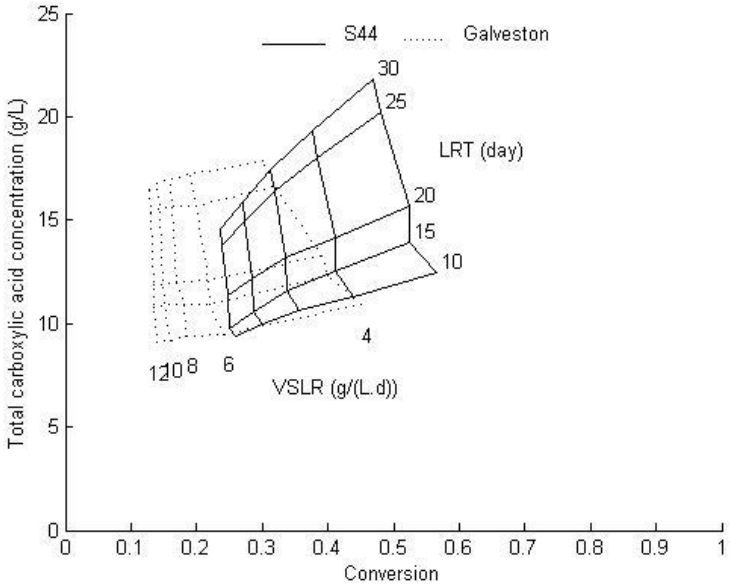

Figure L-26. Comparison map of Site S Sample S44 and B01 – Galveston.

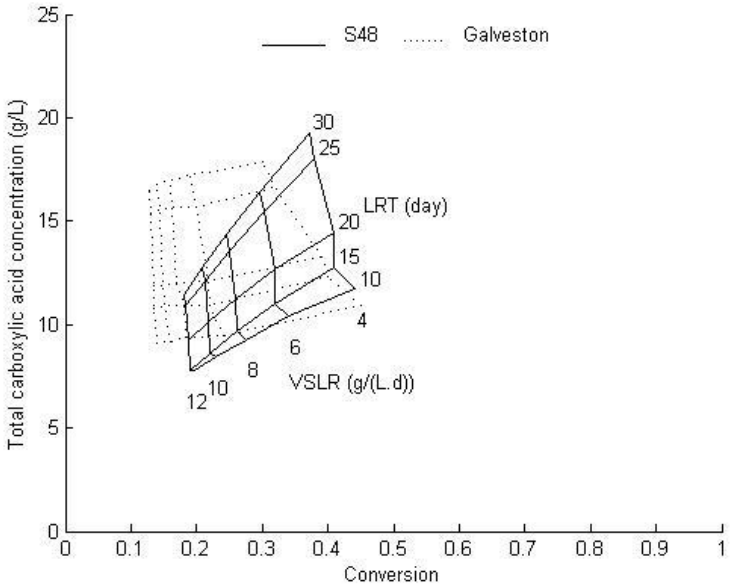

Figure L-27. Comparison map of Site S Sample S48 and B01 – Galveston.

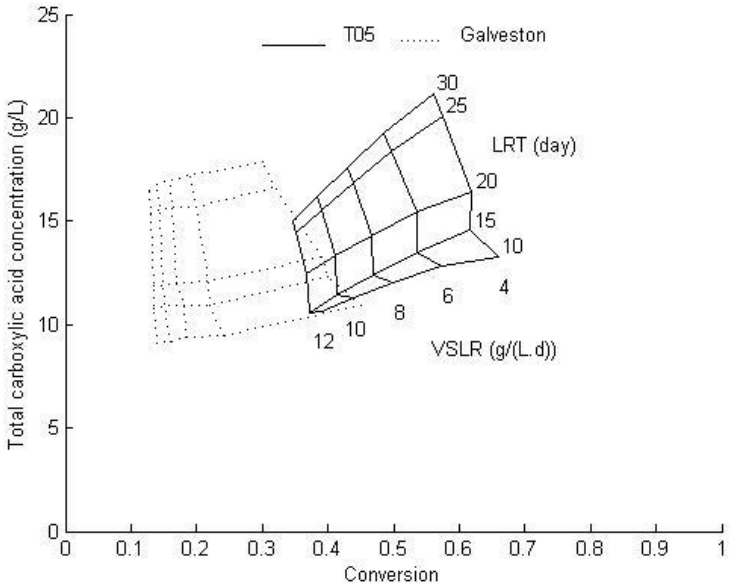

Figure L-28. Comparison map of Site T Sample T05 and B01 – Galveston.

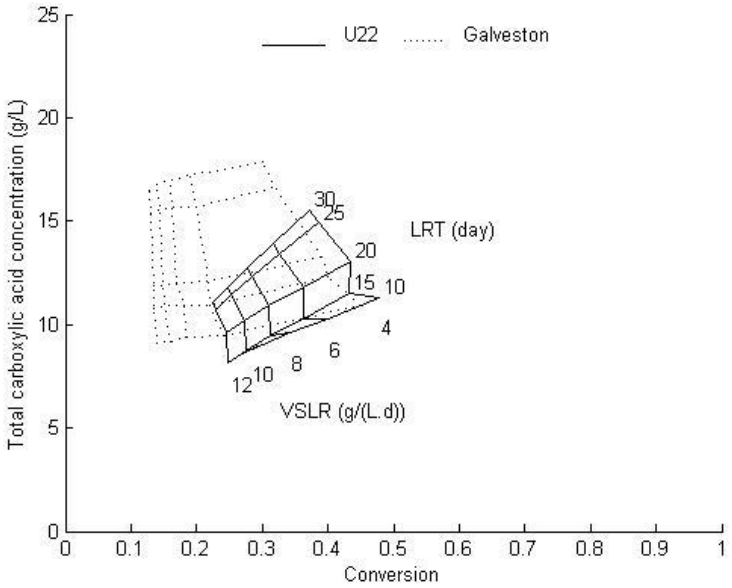

Figure L-29. Comparison map of Site U Sample U22 and B01 – Galveston.

APPENDIX M

GPS COORDINATES FOR BIOSCREENING SAMPLES

Table M-1. GPS coordinates for Bioscreening Site A – La Sal del Rey, TX.

Reactor ID	Latitude	Longitude	Reactor ID	Latitude	Longitude
A02	26.54056	-98.04939	A15	26.5395	-98.06161
A03	26.54056	-98.04939	A16	26.53944	-98.06142
A04	26.54054	-98.04958	A17	26.53935	-98.06124
A05	26.5405	-98.0498	A18	26.53928	-98.06106
A06	26.54047	-98.05001	A19	26.53919	-98.06088
A07	26.54046	-98.05018	A20	26.53002	-98.06296
A08	26.54042	-98.05038	A21	26.53019	-98.06296
A09	26.5404	-98.05057	A22	26.5304	-98.06291
A10	26.54037	-98.05081	A23	26.53055	-98.06289
A11	26.54034	-98.05097	A24	26.53075	-98.06286
A12	26.53975	-98.06214	A25	26.53092	-98.06284
A13	26.53966	-98.06198	A26	26.53111	-98.06279
A14	26.53958	-98.06178	A27	26.53127	-98.06274

Table M-2. GPS coordinates for Bioscreening Site B and Site C.

Reactor ID	Location	Latitude	Longitude
B01	Galveston, TX	29.23488	-94.88295
B02	Bryan, TX	30.6469	-96.37812
B03	Bahamas	24.041451	-74.49295
B04	Pure (*C. thermocellum*)	N/A	N/A
C01	Taiwan	25.138073	121.5119

Table M-3. GPS coordinates for Bioscreening Site D – Gruella, NM and Muleshoe, TX.

Reactor ID	Latitude	Longitude	Reactor ID	Latitude	Longitude
D01	34.0974281	-103.054633	D16	33.9837719	-102.718886
D02	34.0966506	-103.056786	D17	33.9835875	-102.719151
D03	34.0963092	-103.057997	D18	33.98	-102.72
D04	34.09624	-103.058183	D19	33.9833878	-102.719081
D05	34.0961811	-103.058455	D20	33.9842019	-102.718258
D06	34.0961125	-103.058684	D21	33.9845414	-102.718086
D07	34.0960536	-103.058945	D22	33.9477722	-102.771161
D08	34.0959761	-103.059186	D23	33.9478575	-102.770889
D09	34.0959256	-103.059404	D24	33.9477306	-102.77086
D10	34.0958303	-103.059655	D25	33.9479831	-102.770853
D11	34.0973492	-103.050798	D26	33.9572517	-102.749544
D12	34.09688	-103.05135	D27	33.9571886	-102.749546
D13	33.9841147	-102.718412	D28	33.9569503	-102.747367
D14	33.9840619	-102.718489	D29	33.9571911	-102.747231
D15	33.9838933	-102.718634	D30	33.9559233	-102.752836

Table M-4. GPS coordinates for Bioscreening Site E – Enid, OK (Great Salt Plain).

Reactor ID	Latitude	Longitude	Reactor ID	Latitude	Longitude
E01	36.711556	-98.269889	E07	36.79925	-98.249667
E02	36.712861	-98.270667	E08	36.8	-98.2495
E03	36.712861	-98.270694	E09	36.81125	-98.192694
E04	36.801389	-98.251472	E10	36.811167	-98.192722
E05	36.800722	-98.250861	E11	36.811139	-98.192778
E06	36.799222	-98.249667			

Table M-5. GPS coordinates for Bioscreening Site F – Brazoria, TX.

Reactor ID	Latitude	Longitude
F01	29.06031	-95.26809
F02	29.06071	-95.26022
F03	29.06099	-95.24221
F04	29.06111	-95.24221
F05	29.06083	-95.24095
F06	29.06145	-95.23797
F07	29.05743	-95.22941
F08	29.03794	-95.26758
F09	29.03791	-95.26693

Table M-6. GPS coordinates for Bioscreening Site G – Rosewell and Carlsbad, NM.

Reactor ID	Latitude	Longitude	Reactor ID	Latitude	Longitude
G01	33.4767	-104.41093	G28	32.57158	-103.81595
G02	33.47678	-104.41092	G29	32.5719	-103.81592
G03	33.47675	-104.41093	G30	32.57116	-103.81534
G04	33.47675	-104.41083	G31	32.55714	-103.78246
G05	33.47679	-104.41089	G32	32.55712	-103.7825
G06	29.23488	-94.88295	G33	32.55491	-103.78332
G07	33.47637	-104.41084	G34	32.5549	-103.78331
G08	33.47665	-104.4106	G35	32.58537	-103.75041
G09	33.47645	-104.41027	G36	32.58555	-103.75049
G10	33.47616	-104.41001	G37	32.58678	-103.75097
G11	33.47608	-104.41015	G38	32.58637	-103.75103
G12	33.47748	-104.41156	G39	32.58636	-103.75123
G13	33.48433	-104.41254	G40	32.5869	-103.75131
G14	33.48438	-104.41253	G41	32.58716	-103.75141
G15	33.4749	-104.41996	G42	32.58058	-103.74753
G16	33.47498	-104.41896	G43	32.61189	-103.67965
G17	33.47568	-104.41901	G44	32.6119	-103.67954
G18	33.4753	-104.41959	G45	32.6119	-103.67956
G19	33.47541	-104.42092	G46	32.61194	-103.67937
G20	33.47548	-104.4208	G47	32.56469	-103.69756
G21	33.47504	-104.42078	G48	32.56522	-103.69743
G22	33.35378	-104.34125	G49	32.56545	-103.6974
G23	33.25377	-104.34126	G50	32.34662	-103.96127
G24	33.35347	-104.34136	G51	32.34661	-103.96135
G25	33.35347	-104.34139	G52	32.33785	-103.98898
G26	33.31957	-104.33134	G53	32.37233	-103.94394
G27	33.31943	-104.33158			

Table M-7. GPS coordinates for Bioscreening Site H – San Francisco Bay, CA.

Reactor ID	Latitude	Longitude	Reactor ID	Latitude	Longitude
H01	37.49897	-122.12807	H18	37.53267	-122.08501
H02	37.4915	-122.13855	H19	37.53268	-122.085
H03	37.49164	-122.13852	H20	37.53262	-122.08481
H04	37.49031	-122.14211	H21	37.48841	-122.97262
H05	37.49032	-122.14176	H22	37.48462	-121.96939
H06	37.47631	-122.12467	H23	37.48465	-121.96942
H07	37.47625	-122.12459	H24	37.4844	-121.96524
H08	37.47487	-122.12618	H25	37.48201	-121.96414
H09	37.46878	-122.12448	H26	37.48185	-121.96413
H10	37.46862	-122.12439	H27	37.48187	-121.9644
H11	37.46872	-122.11977	H28	37.48145	-121.96882
H12	37.48298	-122.15121	H29	37.48022	-121.96863
H13	37.48682	-122.17701	H30	37.4805	-121.96908
H14	37.4869	-122.17385	H31	37.44041	-121.96094
H15	37.48697	-122.17388	H32	37.44037	-121.96169
H16	37.49905	-122.12796	H33	37.43904	-121.96181
H17	37.52921	-122.06172	H34	37.43905	-121.96183

Table M-8. GPS coordinates for Bioscreening Site J – Big Bend National Park, TX.

Reactor ID	Latitude	Longitude	Reactor ID	Latitude	Longitude
J01	29.19979	-102.91743	J12	29.18213	-102.99237
J02	29.20088	-102.91495	J13	29.18215	-102.99232
J03	29.17961	-102.99555	J14	29.18216	-102.99236
J04	29.17961	-102.99555	J15	29.18218	-102.99226
J05	29.17961	-102.99555	J16	29.18218	-102.9922
J06	29.17961	-102.99555	J17	29.17718	-103.00127
J07	29.17961	-102.99555	J18	29.14979	-103.00346
J08	29.18208	-102.9924	J19	29.14979	-103.00346
J09	29.18208	-102.9924	J20	29.14979	-103.00346
J10	29.18208	-102.9924	J21	29.14979	-103.00346
J11	29.18209	-102.99237	J22	29.14986	-103.00404

Table M-9. GPS coordinates for Bioscreening Site K – Utah1.

Reactor ID	Latitude	Longitude	Reactor ID	Latitude	Longitude
K01	41.23589	-111.924	K29	39.85957	-113.37751
K02	41.23575	-111.92481	K30	39.8594	-113.3778
K03	41.23499	-111.92708	K31	39.85908	-113.37823
K04	41.23466	-111.92745	K32	39.84984	-113.39555
K05	39.90848	-113.42739	K33	39.81984	-113.39522
K06	39.90848	-113.42734	K34	39.83228	-113.39167
K07	39.90848	-113.42734	K35	39.83407	-113.3907
K08	39.90782	-113.42729	K36	39.83421	-113.38833
K09	39.90784	-113.42738	K37	39.8342	-113.38831
K10	39.90754	-113.42929	K38	39.84161	-113.39196
K11	39.9074	-113.42937	K39	39.4564	-112.79061
K12	39.90698	-113.43097	K40	39.61189	-112.72747
K13	39.90676	-113.43084	K41	39.61205	-112.72751
K14	39.90662	-113.43079	K42	39.61255	-112.72929
K15	39.9065	-113.43108	K43	39.61255	-112.7293
K16	39.90622	-113.43146	K44	39.61255	-112.7293
K17	39.90591	-113.432	K45	39.61139	-112.72996
K18	39.90432	-113.43264	K46	39.61136	-112.72992
K19	39.88738	-113.41326	K47	39.61113	-112.72962
K20	39.88738	-113.41319	K48	39.6111	-112.72944
K21	39.88726	-113.4127	K49	39.6111	-112.72943
K22	39.8872	-113.41269	K50	39.61107	-112.72939
K23	39.88767	-113.41215	K51	39.6111	-112.72944
K24	39.88186	-113.37465	K52	39.61097	-112.72937
K25	39.88233	-113.38259	K53	39.61104	-112.7293
K26	39.88233	-113.38259	K54	39.61104	-112.7293
K27	39.88338	-113.38981	K55	39.61066	-112.73028
K28	39.88343	-113.38999			

Table M-10. GPS coordinates for Bioscreening Site L – Utah2.

Reactor ID	Latitude	Longitude	Reactor ID	Latitude	Longitude
L01	40.2627	-111.66437	L14	41.4815	-112.28072
L02	40.13836	-111.80196	L15	41.48371	-112.30993
L03	40.13743	-111.93693	L16	41.48128	-112.31256
L04	40.35265	-111.89934	L17	41.63346	-112.25749
L05	40.35278	-111.89959	L18	41.57959	-112.2342
L06	40.79135	-111.90076	L19	41.57601	-112.23415
L07	40.79131	-111.90077	L20	41.57602	-112.23391
L08	40.79122	-111.90089	L21	41.57622	-112.23376
L09	40.79089	-111.90062	L22	41.05686	-112.25206
L10	40.69574	-111.9491	L23	41.057	-112.25059
L11	40.73554	-112.21073	L24	41.07565	-112.22187
L12	40.74851	-112.18609	L25	41.07493	-122.22114
L13	40.70045	-112.28488			

Table M-11. GPS coordinates for Bioscreening Site M – Georgia1.

Reactor ID	Latitude	Longitude	Reactor ID	Latitude	Longitude
M01	32.16222	-81.11403	M22	32.90959	-79.58672
M02	32.16226	-81.11399	M23	32.90419	-79.59888
M03	32.92027	-79.59494	M24	32.90656	-79.61488
M04	32.92033	-79.59494	M25	32.91298	-79.61333
M05	32.92037	-79.59493	M26	32.9399	-79.65724
M06	32.92635	-79.58544	M27	32.93987	-79.65714
M07	32.92639	-79.58557	M28	32.26295	-80.76013
M08	32.9279	-79.58293	M29	32.26214	-80.76319
M09	32.92791	-79.58291	M30	32.26215	-80.76318
M10	32.92938	-79.57901	M31	32.25858	-80.76606
M11	32.92678	-79.57674	M32	32.25779	-80.76542
M12	32.9181	-79.57662	M33	32.25779	-80.76543
M13	32.91934	-79.57753	M34	32.25421	-80.75639
M14	32.91778	-79.57793	M35	32.25432	-80.75631
M15	32.91788	-79.5779	M36	32.24395	-80.77541
M16	32.91233	-79.58088	M37	32.24204	-80.77625
M17	32.90959	-79.58036	M38	32.24071	-80.77653
M18	32.90615	-79.58254	M39	32.24076	-80.77678
M19	32.90621	-79.58259	M40	32.2384	-80.77825
M20	32.90634	-79.58264	M41	32.23866	-80.77831
M21	32.91014	-79.58323			

Table M-12. GPS coordinates for Bioscreening Site N – Georgia2.

Reactor ID	Latitude	Longitude	Reactor ID	Latitude	Longitude
N01	31.39024	-81.26427	N12	31.45966	-81.27784
N02	31.39024	-81.26427	N13	31.45947	-81.277683
N03	31.39187	-81.26329	N14	31.45947	-81.277683
N04	31.38953	-81.2841	N15	31.45947	-81.277683
N05	31.39017	-81.28489	N16	31.45947	-81.277683
N06	31.3902	-81.27746	N17	31.45951	-81.277707
N07	31.39273	-81.27266	N18	31.43195	-81.23861
N08	31.43136	-81.28293	N19	31.43261	-81.23948
N09	31.43978	-81.2778	N20	31.43471	-81.23911
N10	31.43978	-81.2778	N21	31.39784	-81.27876
N11	31.43978	-81.2778	N22	32.1616	-81.11426

Table M-13. GPS coordinates for Bioscreening Site P – Puerto Rico.

Reactor ID	Latitude	Longitude	Reactor ID	Latitude	Longitude
P01	18.00959019	-67.1709251	P19	17.95211656	-67.1964169
P02	18.00959019	-67.1709251	P20	17.95211656	-67.1964169
P03	18.00959019	-67.1709251	P21	17.95211656	-67.1964169
P04	18.00959019	-67.1709251	P22	17.94501269	-66.2393188
P05	18.00959019	-67.1709251	P23	17.94501269	-66.2393188
P06	18.00959019	-67.1709251	P24	17.94501269	-66.2393188
P07	18.00959019	-67.1709251	P25	17.94501269	-66.2393188
P08	18.012365	-67.101681	P26	17.93390723	-66.2528801
P09	18.012365	-67.101681	P27	17.93390723	-66.2528801
P10	18.012365	-67.101681	P28	17.93390723	-66.2528801
P11	18.012365	-67.101681	P29	17.93390723	-66.2528801
P12	17.96150628	-67.2061157	P30	17.95342298	-66.2212944
P13	17.96150628	-67.2061157	P31	17.95342298	-66.2212944
P14	17.96150628	-67.2061157	P32	17.95342298	-66.2212944
P15	17.96150628	-67.2061157	P33	17.95342298	-66.2212944
P16	17.96150628	-67.2061157	P34	17.95342298	-66.2212944
P17	17.95211656	-67.1964169	P35	17.95342298	-66.2212944
P18	17.95211656	-67.1964169			

Table M-14. GPS coordinates for Bioscreening Site Q – Florida.

Reactor ID	Latitude	Longitude	Reactor ID	Latitude	Longitude
Q01	28.03691	-82.819287	Q15	26.84609	-82.23879
Q02	28.033671	-82.818246	Q16	26.84939	-82.23745
Q03	28.035404	-82.819051	Q17	26.8494	-82.23743
Q04	28.03571	-82.82124	Q18	25.93208	-81.65522
Q05	28.03563	-82.82116	Q19	25.93091	-81.67734
Q06	28.03563	-82.82116	Q20	25.93185	-81.6774
Q07	28.03563	-82.82116	Q21	25.98402	-81.72775
Q08	28.06157	-82.88411	Q22	26.02539	-81.7289
Q09	28.07613	-82.83224	Q23	26.02746	-81.72796
Q10	28.07841	-82.83236	Q24	26.02759	-81.72767
Q11	28.07801	-82.83236	Q25	26.02368	-81.70964
Q12	27.02194	-82.04329	Q26	26.05067	-81.70126
Q13	26.73842	-82.06823	Q27	25.98796	-81.59447
Q14	26.72683	-82.26221	Q28	25.97143	-81.55548

Table M-15. GPS coordinates for Bioscreening Site R – Santa Fe, NM.

Reactor ID	Latitude	Longitude	Reactor ID	Latitude	Longitude
R01	35.77254043	-106.691052	R09	35.90733705	-106.616149
R02	35.7719972	-106.691217	R10	35.90733869	-106.616028
R03	35.77184227	-106.691336	R11	35.90770188	-106.615836
R04	35.7720289	-106.690886	R12	35.9080203	-106.61562
R05	35.77214778	-106.690767	R13	35.80861	-106.17806
R06	35.90685924	-106.616151	R14	35.97094201	-106.562084
R07	35.90685097	-106.616095	R15	35.91730972	-106.594442
R08	35.90719888	-106.616368			

Table M-16. GPS coordinates for Bioscreening Site S – Yellowstone National Park, WY.

Reactor ID	Latitude	Longitude	Reactor ID	Latitude	Longitude
S01	44.72662	-110.70906	S25	44.56191	-110.83729
S02	44.72662	-110.70913	S26	44.65135	-110.48046
S03	44.72283	-110.71014	S27	44.65135	-110.48046
S04	44.72792	-110.71026	S28	44.65138	-110.4805
S05	44.72792	-110.71026	S29	44.6513	-110.48065
S06	44.72854	-110.71005	S30	44.65266	-110.47659
S07	44.72896	-110.71194	S31	44.65281	-110.48209
S08	44.72866	-110.71198	S32	44.65284	-110.48273
S09	44.72866	-110.71198	S33	44.65284	-110.48273
S10	44.72964	-110.71204	S34	44.65278	-110.48329
S11	44.72973	-110.71176	S35	44.65329	-110.48474
S12	44.73168	-110.71133	S36	44.65329	-110.48474
S13	44.73204	-110.71116	S37	44.65381	-110.47796
S14	44.73254	-110.7098	S38	44.5359	-110.82634
S15	44.73162	-110.71006	S39	44.53521	-110.82498
S16	44.73326	-110.70973	S40	44.5467	-110.81074
S17	44.73434	-110.70752	S41	44.53413	-110.7978
S18	44.73494	-110.70747	S42	44.53406	-110.79783
S19	44.73506	-110.70774	S43	44.53282	-110.79742
S20	44.56115	-110.83535	S44	44.53279	-110.79746
S21	44.56111	-110.83546	S45	44.53346	-110.79766
S22	44.56145	-110.8362	S46	44.80024	-110.72825
S23	44.56166	-110.83635	S47	44.79937	-110.72836
S24	44.56174	-110.83642	S48	44.79937	-110.72836

Table M-17. GPS coordinates for Bioscreening Site T – Nevada.

Reactor ID	Latitude	Longitude	Reactor ID	Latitude	Longitude
T01	39.59249	-118.41799	T10	40.66174	-119.36606
T02	39.602	-118.40915	T11	40.66288	-119.36649
T03	39.60254	-118.39923	T12	40.66284	-119.36681
T04	40.666261	-119.36647	T13	40.86139	-119.33281
T05	40.66254	-119.36644	T14	40.86139	-119.33281
T06	40.66244	-119.36645	T15	40.8592	-119.33195
T07	40.66136	-119.36629	T16	40.85928	-119.3318
T08	40.66134	-119.36628	T17	40.85906	-119.3337
T09	40.66146	-119.36621			

Table M-18. GPS coordinates for Bioscreening Site U – Nevada – California.

Reactor ID	Latitude	Longitude	Reactor ID	Latitude	Longitude
U01	38.23951	-119.32615	U13	37.99391	-119.02356
U02	38.23949	-119.3262	U14	37.99387	-119.02359
U03	38.2391	-119.32531	U15	37.98822	-119.02663
U04	38.2391	-119.32531	U16	37.95632	-119.05291
U05	37.941	-119.02295	U17	37.66052	-118.82903
U06	37.941	-119.02295	U18	37.66096	-118.82895
U07	37.941	-119.02295	U19	37.6613	-118.82877
U08	37.94112	-119.02205	U20	37.6613	-118.82876
U09	37.94109	-119.02017	U21	37.66139	-118.8286
U10	37.9937	-119.02366	U22	36.40028	-117.95216
U11	37.99368	-119.02367	U23	36.37568	-117.97728
U12	37.99395	-119.02338	U24	36.35583	-117.98262

APPENDIX N

CARBOXYLIC ACID PRODUCTION DATA FOR HYDROGEN FERMENTATIONS

Table N-1. Carboxylic acid concentration (g/L) and cumulative gas production (mL) for PH batch paper fermentation (fresh Galveston inocula, ammonium bicarbonate buffer, 55 °C).

Days	C2	C3	IC4	C4	IC5	C5	C6	C7	Total	H_2	CO_2
2	1.284	0.124	0.000	0.385	0.000	0.000	0.000	0.000	1.794	19.2	166.1
4	1.895	0.172	0.000	0.410	0.000	0.000	0.000	0.000	2.478	31.8	287.0
6	2.651	0.210	0.000	1.080	0.021	0.000	0.000	0.000	3.962	61.0	575.4
8	4.140	0.266	0.000	2.057	0.000	0.000	0.000	0.000	6.463	415.4	1461.6
10	5.368	0.354	0.058	4.094	0.048	0.000	0.000	0.000	9.921	891.3	2645.0
12	7.371	0.423	0.042	4.222	0.072	0.000	0.000	0.000	12.131	1043.1	3189.8
14	8.696	0.454	0.051	4.113	0.088	0.000	0.000	0.000	13.402	1065.5	3397.1
16	10.569	0.494	0.031	4.308	0.110	0.000	0.000	0.000	15.512	1088.7	3611.9
18	11.508	0.488	0.042	4.413	0.145	0.000	0.000	0.000	16.595	1093.3	3741.3
20	13.574	0.517	0.209	4.804	0.169	0.000	0.027	0.000	19.300	1100.1	3804.8
22	14.418	0.504	0.220	4.842	0.148	0.000	0.028	0.000	20.160	1104.1	3882.5
24	14.705	0.481	0.225	4.800	0.193	0.000	0.026	0.000	20.430	1105.3	3960.4
26	15.216	0.493	0.235	4.878	0.205	0.000	0.028	0.000	21.055	1107.2	3999.9
28	15.437	0.487	0.241	4.920	0.212	0.000	0.050	0.000	21.346	1110.0	4031.2
30	15.609	0.481	0.246	5.013	0.220	0.000	0.050	0.000	21.619	1110.9	4060.8
32	15.705	0.475	0.251	5.129	0.231	0.000	0.053	0.000	21.844	1111.5	4080.6
34	15.763	0.456	0.173	5.226	0.232	0.000	0.049	0.000	21.899	1113.6	4101.2
36	15.637	0.434	0.194	5.300	0.236	0.000	0.055	0.000	21.855	1114.9	4119.7

Table N-2. Carboxylic acid concentration (g/L) and cumulative gas production (mL) for BH batch bagasse fermentation (fresh Galveston inocula, ammonium bicarbonate buffer, 55 °C).

Days	C2	C3	IC4	C4	IC5	C5	C6	C7	Total	H_2	CO_2
2	1.589	0.128	0.000	0.568	0.000	0.000	0.000	0.000	2.284	37.4	118.4
4	2.608	0.183	0.000	0.647	0.000	0.000	0.000	0.000	3.438	135.7	494.5
6	3.899	0.227	0.000	0.792	0.019	0.000	0.000	0.000	4.937	173.1	881.7
8	5.607	0.264	0.021	0.910	0.025	0.000	0.000	0.000	6.827	335.9	1238.9
10	7.312	0.292	0.027	0.974	0.047	0.000	0.000	0.000	8.651	500.5	1667.8
12	8.900	0.308	0.086	1.053	0.074	0.000	0.000	0.000	10.420	602.8	1979.0
14	10.276	0.314	0.109	1.151	0.084	0.000	0.000	0.000	11.933	648.8	2212.7
16	11.481	0.322	0.135	1.387	0.094	0.000	0.000	0.000	13.420	691.0	2444.4
18	12.388	0.318	0.108	1.527	0.109	0.000	0.000	0.000	14.450	726.0	2653.3
20	14.091	0.336	0.199	1.836	0.135	0.000	0.029	0.000	16.628	788.8	2862.5
22	14.954	0.336	0.222	2.028	0.153	0.000	0.030	0.000	17.722	815.3	3032.9
24	15.679	0.338	0.171	2.194	0.167	0.000	0.000	0.000	18.548	817.3	3179.9
26	16.144	0.337	0.181	2.365	0.176	0.000	0.000	0.000	19.203	836.5	3273.2
28	16.554	0.337	0.266	2.488	0.184	0.000	0.000	0.000	19.829	852.4	3360.8
30	16.929	0.335	0.273	2.576	0.190	0.000	0.000	0.000	20.303	854.9	3422.4
32	17.166	0.330	0.091	2.617	0.192	0.000	0.000	0.000	20.396	863.9	3471.8
34	17.491	0.323	0.202	2.678	0.196	0.000	0.000	0.000	20.889	873.1	3520.7
36	17.610	0.312	0.205	2.742	0.198	0.000	0.000	0.000	21.067	876.5	3555.5

Table N-3. Carboxylic acid concentration (g/L) and gas production (mL) for PHC countercurrent paper fermentations (PH inocula, ammonium bicarbonate buffer, 55 °C).

Days	C2	C3	IC4	C4	IC5	C5	C6	C7	Total	H_2	CO_2
2	3.067	0.224	0.012	2.214	0.067	0.000	0.000	0.000	5.583		
4	3.824	0.305	0.074	2.252	0.098	0.000	0.000	0.000	6.552		
6	4.607	0.336	0.104	2.253	0.116	0.000	0.000	0.000	7.416		
8	5.344	0.365	0.114	2.255	0.125	0.000	0.000	0.000	8.203		
10	7.047	0.543	0.130	2.608	0.106	0.000	0.000	0.000	10.435		
12	7.823	0.644	0.146	2.788	0.152	0.000	0.039	0.000	11.592		
14	9.570	0.812	0.177	3.189	0.178	0.044	0.000	0.000	13.970		
16	11.339	1.017	0.209	3.607	0.208	0.052	0.043	0.040	16.516	73.5	383.7
18	14.387	1.326	0.249	4.189	0.245	0.064	0.046	0.000	20.506	41.9	504.9
20	15.016	1.523	0.248	4.305	0.249	0.064	0.061	0.000	21.467	68.6	715.4
22	17.770	1.781	0.266	4.418	0.261	0.066	0.046	0.000	24.608	95.2	593.2
24	18.999	1.991	0.267	4.378	0.249	0.066	0.042	0.037	26.028	58.2	454.2
26	19.977	2.034	0.263	4.350	0.239	0.060	0.047	0.000	26.971	107.2	858.3
28	19.976	2.146	0.246	4.302	0.218	0.058	0.044	0.000	26.990	71.7	555.4
30	20.799	2.272	0.252	4.758	0.225	0.059	0.057	0.000	28.422	79.3	465.0
32	21.201	2.345	0.249	4.753	0.222	0.058	0.062	0.000	28.889	83.7	626.5
34	21.635	2.351	0.240	4.702	0.221	0.055	0.051	0.046	29.300	53.5	415.4
36	20.619	2.255	0.221	4.915	0.202	0.056	0.062	0.000	28.330	59.0	455.1
38	19.740	2.091	0.200	4.891	0.184	0.056	0.077	0.000	27.239	77.5	602.9
40	19.353	2.119	0.188	4.878	0.174	0.062	0.096	0.000	26.871	63.2	471.4
42	19.689	2.151	0.184	4.670	0.172	0.068	0.106	0.000	27.039	73.7	382.5
44	19.148	2.196	0.159	4.716	0.138	0.072	0.114	0.040	26.582	74.6	500.2
46	18.829	2.214	0.149	4.695	0.133	0.074	0.117	0.042	26.254	67.8	518.5
48	18.846	2.290	0.141	4.790	0.127	0.078	0.116	0.000	26.388	77.5	479.5
50	18.330	2.313	0.135	5.298	0.128	0.082	0.125	0.000	26.411	67.8	427.5
52	17.639	2.264	0.127	5.562	0.118	0.082	0.121	0.000	25.913	52.3	310.3
54	15.932	2.040	0.114	5.600	0.107	0.080	0.130	0.000	24.003	59.0	353.0
56	15.296	1.978	0.112	5.840	0.106	0.081	0.122	0.000	23.534	53.1	294.4
58	13.292	1.680	0.096	5.057	0.087	0.073	0.098	0.000	20.383	68.6	411.4
60	12.528	1.588	0.090	5.441	0.091	0.073	0.089	0.000	19.900	68.7	438.2
62	11.359	1.595	0.092	5.117	0.092	0.070	0.088	0.000	18.413	39.6	245.5
64	10.864	1.569	0.094	5.300	0.096	0.076	0.115	0.000	18.114	53.8	323.3
66	10.419	1.563	0.095	5.224	0.100	0.089	0.165	0.000	17.655	40.6	216.1
68	9.287	1.703	0.086	4.538	0.090	0.075	0.122	0.000	15.902	74.8	421.9
70	9.942	1.855	0.103	5.094	0.109	0.078	0.112	0.000	17.292	36.5	200.1
72	9.433	1.766	0.103	4.956	0.106	0.077	0.105	0.000	16.546	60.0	338.8
74	9.641	1.907	0.106	4.925	0.112	0.075	0.101	0.000	16.867	69.7	424.3
76	9.537	1.985	0.105	5.129	0.110	0.077	0.107	0.000	17.049	81.9	506.5
78	10.333	2.229	0.115	5.061	0.117	0.076	0.090	0.000	18.021	93.8	577.4
80	10.321	2.244	0.114	4.636	0.113	0.068	0.073	0.000	17.569	69.8	422.2
82	10.129	2.298	0.114	4.452	0.116	0.064	0.063	0.000	17.236	83.2	496.1
84	10.539	2.420	0.120	4.819	0.119	0.067	0.058	0.000	18.142	96.8	587.8
86	10.379	2.463	0.120	4.909	0.114	0.068	0.055	0.000	18.108	93.9	572.0
88	10.816	2.588	0.126	4.655	0.115	0.064	0.052	0.000	18.415	75.0	435.5
90	11.167	2.695	0.126	4.577	0.113	0.062	0.058	0.000	18.798	87.8	517.6
92	10.591	2.620	0.119	4.452	0.103	0.064	0.046	0.000	17.994	93.7	554.2
94	10.924	2.684	0.123	4.857	0.110	0.069	0.050	0.000	18.815	80.4	471.9

Table N-3. Continued.

Days	C2	C3	IC4	C4	IC5	C5	C6	C7	Total	H_2	CO_2
96	11.122	2.836	0.124	5.098	0.119	0.069	0.048	0.000	19.415	81.7	455.0
98	11.040	2.788	0.121	5.139	0.116	0.070	0.074	0.000	19.348	92.5	555.8
100	11.032	2.781	0.122	5.158	0.119	0.067	0.059	0.000	19.338	90.5	533.2
102	11.276	2.745	0.125	5.337	0.125	0.069	0.041	0.000	19.718	88.6	551.2
104	11.886	2.767	0.130	4.995	0.134	0.062	0.038	0.000	20.012	80.3	480.5
106	12.280	2.796	0.135	4.701	0.135	0.063	0.000	0.000	20.110	81.3	484.7
108	11.839	2.656	0.126	4.290	0.132	0.059	0.000	0.000	19.102	76.7	462.4
110	12.038	2.703	0.129	4.255	0.122	0.057	0.000	0.000	19.304	74.8	459.5
112	12.604	2.818	0.145	4.261	0.141	0.061	0.050	0.000	20.079	71.8	444.0
114	12.664	2.826	0.142	4.007	0.136	0.054	0.000	0.000	19.829	76.4	464.4
116	12.845	2.880	0.139	4.048	0.137	0.055	0.000	0.000	20.103	70.9	438.4
118	12.179	2.723	0.138	3.806	0.129	0.051	0.000	0.000	19.024	68.2	413.1
120	12.280	2.765	0.142	3.895	0.134	0.054	0.000	0.000	19.269	68.7	423.9
122	12.301	2.756	0.147	3.773	0.134	0.052	0.000	0.000	19.164	78.1	468.2
124	12.251	2.809	0.149	3.606	0.134	0.054	0.000	0.000	19.003	69.5	426.8
126	12.732	2.888	0.156	3.601	0.138	0.053	0.000	0.000	19.568	86.5	524.0
128	12.712	2.891	0.153	3.399	0.133	0.052	0.000	0.000	19.339	73.1	427.1
130	13.537	3.032	0.167	3.477	0.139	0.052	0.000	0.000	20.404	77.0	475.8
132	11.879	2.625	0.147	3.017	0.120	0.046	0.000	0.000	17.834	71.5	437.0
134	11.131	2.390	0.142	2.831	0.112	0.000	0.000	0.000	16.605	72.7	442.4
136	10.599	2.232	0.138	2.719	0.107	0.039	0.000	0.000	15.834	74.7	438.6
138	11.680	2.362	0.149	3.026	0.118	0.041	0.000	0.000	17.376	69.6	467.7
140	11.696	2.315	0.147	3.156	0.120	0.043	0.000	0.000	17.476	73.6	474.4
142	11.027	2.076	0.137	2.940	0.110	0.040	0.000	0.000	16.330	79.0	515.6
144	12.480	2.206	0.153	3.317	0.117	0.043	0.000	0.000	18.315	79.5	479.7
146	12.379	2.107	0.148	3.276	0.107	0.044	0.049	0.000	18.111	91.1	563.5
148	12.476	2.073	0.142	3.226	0.100	0.041	0.000	0.000	18.057	71.8	432.9
150	13.271	2.132	0.147	3.529	0.104	0.043	0.042	0.000	19.268	76.2	449.5
152	12.965	2.020	0.143	3.285	0.101	0.041	0.047	0.000	18.602	98.0	614.4
154	15.089	2.210	0.157	4.047	0.107	0.000	0.044	0.000	21.655	70.7	426.5
156	15.906	2.446	0.162	3.968	0.109	0.045	0.000	0.000	22.635	74.3	450.3
158	15.289	2.341	0.155	3.726	0.112	0.045	0.045	0.000	21.714	77.6	450.0
160	14.771	2.107	0.153	4.094	0.106	0.043	0.000	0.000	21.274	73.0	456.5
162	14.685	2.063	0.159	4.175	0.113	0.045	0.043	0.000	21.283	107.7	592.8
164	15.451	2.071	0.169	4.358	0.118	0.045	0.000	0.000	22.211	92.8	494.3
166	15.386	1.993	0.170	4.453	0.120	0.044	0.000	0.000	22.166	59.9	357.6
168	13.904	1.717	0.151	4.042	0.114	0.043	0.000	0.000	19.971	82.7	517.5
170	16.115	1.822	0.158	3.901	0.136	0.044	0.000	0.038	22.214	88.3	538.9
172	15.797	1.699	0.156	4.663	0.148	0.048	0.000	0.047	22.559	88.5	547.0
174	15.389	1.544	0.157	4.566	0.149	0.046	0.039	0.059	21.949	77.8	463.4
176	15.795	1.440	0.149	3.927	0.142	0.046	0.000	0.000	21.498	78.5	468.1
178	14.508	0.719	0.090	2.288	0.121	0.000	0.000	0.040	17.767	89.3	541.1
180	13.987	0.745	0.103	2.441	0.137	0.000	0.044	0.040	17.497	77.6	470.2
182	10.707	0.647	0.086	1.987	0.112	0.000	0.000	0.042	13.581	53.2	316.2
184	12.621	0.820	0.095	2.301	0.128	0.000	0.000	0.047	16.011	50.5	316.0
186	10.734	0.706	0.076	1.709	0.101	0.000	0.039	0.040	13.404	40.8	254.4
188	12.036	0.848	0.078	1.689	0.117	0.000	0.000	0.050	14.818	31.0	197.8
190	15.579	1.150	0.108	2.257	0.154	0.000	0.000	0.041	19.290	33.1	200.9
192	16.045	1.187	0.112	1.997	0.158	0.000	0.000	0.046	19.546	58.3	292.6

Table N-3. Continued.

Days	C2	C3	IC4	C4	IC5	C5	C6	C7	Total	H_2	CO_2
194	15.126	1.188	0.116	2.315	0.150	0.000	0.000	0.055	18.949	101.6	554.0
196	14.340	1.158	0.119	2.665	0.138	0.000	0.044	0.056	18.521	120.7	623.3
198	13.452	1.126	0.115	2.977	0.118	0.000	0.000	0.050	17.838	88.0	562.6
200	14.605	0.724	0.086	2.334	0.143	0.000	0.045	0.000	17.937	105.3	765.6
202	16.499	0.726	0.081	2.031	0.133	0.000	0.000	0.000	19.470	89.0	507.0
204	17.339	0.696	0.079	2.174	0.136	0.000	0.000	0.070	20.493	62.9	338.1
206	15.581	0.587	0.061	1.914	0.121	0.000	0.000	0.065	18.330	82.3	473.2
208	13.474	0.485	0.049	1.612	0.085	0.000	0.000	0.063	15.768	82.5	471.1
210	17.036	0.626	0.058	2.062	0.102	0.000	0.000	0.063	19.948	44.8	358.2
212	16.263	0.604	0.055	2.177	0.102	0.000	0.000	0.058	19.259	49.4	408.3
214	16.260	0.584	0.052	2.201	0.097	0.000	0.000	0.063	19.257	47.8	218.0
216	15.937	0.583	0.054	2.169	0.099	0.000	0.000	0.061	18.902	58.5	289.7
218	15.243	0.569	0.051	2.162	0.091	0.000	0.000	0.000	18.116	45.2	341.4
220	15.148	0.600	0.058	2.323	0.099	0.000	0.000	0.000	18.228	64.3	324.6
222	14.366	0.563	0.059	2.317	0.097	0.000	0.000	0.000	17.402	96.8	542.4
224	14.634	0.557	0.069	2.408	0.105	0.000	0.000	0.000	17.772	61.5	291.8
226	14.439	0.543	0.073	2.328	0.111	0.000	0.000	0.000	17.494	56.1	309.6
228	14.753	0.545	0.080	2.339	0.116	0.000	0.000	0.000	17.833	56.1	291.6
230	14.326	0.512	0.078	2.210	0.113	0.000	0.000	0.037	17.276	75.4	479.6
232	14.454	0.520	0.077	2.209	0.109	0.000	0.000	0.000	17.370	37.3	262.1
234	14.200	0.506	0.070	2.047	0.099	0.000	0.000	0.039	16.962	41.5	205.4
236	14.073	0.507	0.066	2.103	0.094	0.000	0.000	0.039	16.882	54.1	288.0
238	12.342	0.427	0.058	1.893	0.079	0.000	0.000	0.038	14.837	46.6	353.1
240	12.982	0.426	0.059	2.055	0.082	0.000	0.000	0.038	15.643	45.4	217.6
242	12.851	0.432	0.058	2.012	0.075	0.000	0.000	0.000	15.428	51.9	290.0
244	10.065	0.368	0.048	1.788	0.067	0.000	0.000	0.000	12.335	49.4	370.4
246	12.870	0.387	0.062	2.191	0.084	0.000	0.000	0.000	15.593	28.9	96.8
248	12.947	0.409	0.065	2.195	0.083	0.000	0.000	0.000	15.699	51.1	276.3
250	14.196	0.461	0.081	2.208	0.097	0.000	0.000	0.000	17.044	32.7	206.2
252	13.710	0.433	0.065	2.003	0.083	0.000	0.000	0.037	16.331	26.4	203.6

Table N-4. Carboxylic acid concentration (g/L) and gas production (mL) for BHC countercurrent bagasse fermentation (BH inocula, ammonium bicarbonate buffer, 55 °C).

Days	C2	C3	IC4	C4	IC5	C5	C6	C7	Total	H_2	CO_2
2	3.813	0.219	0.036	1.427	0.056	0.000	0.000	0.000	5.551		
4	4.835	0.268	0.060	1.509	0.066	0.000	0.000	0.000	6.739		
6	6.538	0.332	0.094	1.795	0.089	0.000	0.000	0.000	8.849		
8	6.820	0.300	0.158	1.910	0.111	0.000	0.000	0.040	9.339		
10	9.477	0.626	0.212	4.733	0.165	0.059	0.000	0.045	15.318		
12	11.597	0.714	0.236	5.147	0.183	0.065	0.043	0.042	18.026		
14	13.584	0.756	0.257	5.663	0.192	0.069	0.050	0.049	20.619	160.6	285.2
16	14.447	0.725	0.261	5.772	0.190	0.069	0.057	0.041	21.562	244.8	570.5
18	15.677	0.819	0.272	5.826	0.206	0.069	0.058	0.042	22.968	371.2	812.1
20	16.383	0.879	0.274	5.542	0.208	0.066	0.055	0.041	23.448	161.6	353.3
22	16.977	0.879	0.267	5.851	0.209	0.066	0.054	0.041	24.344	252.6	650.5
24	17.020	0.841	0.258	5.606	0.202	0.061	0.049	0.041	24.078	141.3	260.8
26	16.848	0.843	0.240	5.476	0.192	0.057	0.044	0.046	23.744	207.7	545.2
28	16.138	0.797	0.217	5.444	0.179	0.054	0.040	0.041	22.910	131.7	288.6
30	15.488	0.779	0.201	5.406	0.172	0.049	0.000	0.000	22.095	197.6	528.3
32	15.308	0.779	0.195	5.683	0.162	0.047	0.000	0.000	22.174	241.2	596.7
34	15.472	0.836	0.193	5.810	0.158	0.047	0.038	0.000	22.554	174.3	464.4
36	14.386	0.829	0.172	5.581	0.132	0.044	0.000	0.000	21.144	223.0	583.0
38	14.170	0.932	0.161	5.540	0.120	0.044	0.000	0.000	20.966	187.0	514.9
40	13.730	0.934	0.157	5.455	0.108	0.000	0.000	0.000	20.384	173.6	402.5
42	13.371	0.914	0.148	5.569	0.101	0.000	0.000	0.000	20.104	196.6	480.7
44	13.628	1.005	0.148	5.819	0.099	0.043	0.000	0.000	20.742	198.7	514.2
46	12.734	0.954	0.134	5.384	0.089	0.000	0.000	0.000	19.296	166.0	446.8
48	13.159	1.038	0.138	5.400	0.093	0.000	0.000	0.000	19.828	205.5	517.1
50	13.025	1.027	0.125	5.448	0.096	0.000	0.000	0.000	19.721	210.6	544.8
52	12.688	1.035	0.132	5.531	0.095	0.000	0.000	0.000	19.481	195.8	495.4
54	11.958	1.013	0.126	5.218	0.088	0.000	0.000	0.000	18.403	203.1	543.0
56	11.462	0.985	0.115	4.953	0.088	0.000	0.000	0.000	17.603	225.2	577.5
58	11.880	1.038	0.121	5.117	0.085	0.000	0.000	0.000	18.240	217.1	554.7
60	11.830	1.050	0.113	5.107	0.085	0.000	0.000	0.000	18.185	226.7	571.1
62	12.501	1.106	0.118	5.277	0.083	0.000	0.000	0.000	19.086	248.8	597.1
64	11.539	1.008	0.106	4.786	0.080	0.000	0.000	0.000	17.520	224.0	548.9
66	12.625	1.089	0.115	5.224	0.085	0.000	0.000	0.000	19.138	232.1	575.0
68	13.401	1.138	0.122	5.560	0.088	0.000	0.000	0.000	20.309	229.2	510.5
70	12.421	1.092	0.112	5.018	0.089	0.000	0.000	0.000	18.732	196.3	483.2
72	13.499	1.215	0.126	5.443	0.092	0.000	0.000	0.000	20.375	218.1	524.9
74	14.041	1.240	0.129	5.522	0.100	0.000	0.000	0.039	21.071	211.0	498.7
76	13.449	1.171	0.126	5.242	0.095	0.000	0.000	0.000	20.084	228.1	520.6
78	13.740	1.177	0.127	5.210	0.100	0.000	0.000	0.000	20.354	222.0	521.3
80	14.126	1.184	0.130	5.227	0.100	0.000	0.040	0.040	20.846	239.1	564.4
82	13.676	1.139	0.125	4.950	0.093	0.000	0.000	0.039	20.021	199.9	491.2
84	14.428	1.173	0.127	5.124	0.097	0.000	0.040	0.040	21.028	225.8	565.7
86	14.396	1.121	0.130	5.088	0.094	0.000	0.000	0.038	20.867	247.5	607.6
88	13.924	1.086	0.122	4.816	0.093	0.000	0.000	0.000	20.041	219.2	546.9
90	14.826	1.163	0.131	5.121	0.094	0.000	0.000	0.000	21.335	242.4	594.7
92	14.844	1.171	0.130	5.002	0.093	0.000	0.000	0.000	21.240	216.8	547.4
94	13.612	1.068	0.121	4.620	0.082	0.000	0.000	0.000	19.502	218.2	560.0

Table N-4. Continued.

Days	C2	C3	IC4	C4	IC5	C5	C6	C7	Total	H_2	CO_2
96	15.038	1.215	0.133	5.284	0.085	0.000	0.000	0.000	21.756	222.2	548.5
98	17.318	1.435	0.149	6.297	0.102	0.000	0.000	0.000	25.301	234.0	591.8
100	14.528	1.205	0.112	5.453	0.077	0.000	0.000	0.000	21.374	216.5	541.5
102	13.989	1.179	0.113	5.400	0.078	0.000	0.000	0.039	20.797	209.5	545.8
104	14.168	1.197	0.113	5.476	0.069	0.000	0.000	0.000	21.025	201.2	562.9
106	14.540	1.228	0.113	5.591	0.073	0.000	0.000	0.000	21.546	111.7	272.8
108	14.095	1.193	0.111	5.474	0.071	0.000	0.000	0.000	20.944	226.1	570.5
110	13.510	1.143	0.107	5.300	0.071	0.000	0.000	0.000	20.131	216.6	562.8
112	13.753	1.181	0.111	5.264	0.067	0.000	0.000	0.000	20.376	174.2	438.5
114	13.276	1.100	0.111	4.953	0.078	0.000	0.044	0.037	19.598	171.8	430.3
116	9.462	0.724	0.083	3.485	0.059	0.000	0.053	0.031	13.897	159.8	405.7
118	10.416	0.790	0.093	3.848	0.074	0.038	0.081	0.035	15.375	138.0	349.2
120	10.710	0.829	0.098	3.993	0.077	0.044	0.121	0.036	15.909	165.0	401.5
122	10.605	0.846	0.098	3.834	0.081	0.047	0.147	0.040	15.698	165.4	415.2
124	9.898	0.788	0.095	3.627	0.079	0.045	0.154	0.037	14.723	157.9	404.9
126	9.818	0.841	0.096	3.525	0.079	0.047	0.158	0.040	14.604	113.9	274.1
128	9.694	0.913	0.096	3.313	0.082	0.047	0.159	0.041	14.344	141.0	379.8
130	10.291	0.796	0.092	2.889	0.085	0.044	0.126	0.041	14.365	172.8	388.6
132	10.451	0.760	0.082	2.591	0.078	0.041	0.106	0.046	14.155	145.1	353.2
134	10.777	0.768	0.077	2.368	0.077	0.039	0.090	0.047	14.243	158.6	378.5
136	10.796	0.984	0.073	1.991	0.073	0.000	0.072	0.050	14.037	158.8	381.4
138	11.485	0.937	0.066	1.840	0.072	0.000	0.064	0.056	14.521	137.6	365.4
140	12.287	0.940	0.062	1.759	0.077	0.000	0.062	0.057	15.244	124.9	316.8
142	11.328	0.881	0.048	1.428	0.072	0.000	0.057	0.000	13.814	101.2	254.3
144	9.995	0.704	0.000	1.091	0.060	0.000	0.048	0.000	11.898	89.7	237.9
148	12.154	0.784	0.050	1.546	0.072	0.000	0.060	0.041	14.706	57.4	160.4
150	11.492	0.667	0.000	1.406	0.059	0.000	0.063	0.000	13.687	135.5	371.5
152	11.438	0.616	0.051	1.528	0.051	0.000	0.000	0.000	13.684	221.8	583.9
154	11.301	0.585	0.000	1.866	0.000	0.000	0.042	0.038	13.833	191.7	510.1
156	12.083	0.509	0.000	1.641	0.000	0.000	0.000	0.038	14.270	272.9	595.8
158	12.774	0.494	0.000	1.657	0.000	0.000	0.040	0.042	15.006	176.1	417.5
160	13.172	0.498	0.000	1.556	0.000	0.000	0.000	0.000	15.226	205.0	493.5
162	13.605	0.499	0.000	1.493	0.000	0.000	0.061	0.000	15.658	108.1	275.6
164	14.382	0.535	0.000	1.460	0.000	0.000	0.000	0.000	16.376	96.0	144.7
166	14.819	0.588	0.000	1.547	0.000	0.000	0.042	0.038	17.034	173.5	345.5
168	15.454	0.662	0.000	1.431	0.000	0.000	0.000	0.039	17.585	165.3	406.0
170	15.672	0.654	0.000	1.680	0.000	0.000	0.051	0.044	18.101	171.4	347.4
172	15.882	0.633	0.000	1.775	0.000	0.000	0.000	0.042	18.332	151.4	378.6
174	16.539	0.661	0.000	1.490	0.000	0.000	0.000	0.042	18.733	86.1	300.8
176	16.882	0.696	0.000	1.261	0.000	0.000	0.049	0.042	18.929	141.3	362.0
178	17.170	0.661	0.000	1.452	0.000	0.000	0.000	0.042	19.326	136.0	285.7
180	16.392	0.638	0.000	1.814	0.043	0.000	0.049	0.042	18.977	126.1	275.6
182	16.704	0.622	0.000	1.947	0.046	0.000	0.040	0.043	19.403	115.7	281.0
184	17.079	0.583	0.000	1.939	0.044	0.000	0.000	0.044	19.689	90.7	230.4
186	16.660	0.544	0.000	2.039	0.047	0.000	0.000	0.042	19.332	139.6	340.1
188	16.523	0.534	0.000	2.024	0.000	0.000	0.000	0.040	19.121	86.7	297.6
190	16.160	0.530	0.000	2.086	0.000	0.000	0.000	0.043	18.818	108.6	282.2
192	15.086	0.492	0.000	1.547	0.000	0.000	0.055	0.037	17.217	83.2	182.5
194	14.523	0.484	0.000	1.854	0.000	0.000	0.000	0.045	16.906	99.9	368.6

Table N-4. Continued.

Days	C2	C3	IC4	C4	IC5	C5	C6	C7	Total	H_2	CO_2
196	15.635	0.484	0.000	1.695	0.000	0.000	0.000	0.088	17.901	86.3	219.7
198	13.556	0.439	0.000	1.541	0.000	0.000	0.000	0.000	15.536	111.4	379.7
200	13.319	0.434	0.000	1.566	0.000	0.000	0.000	0.000	15.320	79.9	284.8
202	14.679	0.521	0.000	1.746	0.000	0.000	0.000	0.044	16.990	92.8	237.1
204	15.149	0.481	0.000	1.733	0.000	0.000	0.000	0.040	17.403	109.5	246.5
206	14.787	0.488	0.000	1.990	0.000	0.000	0.000	0.000	17.265	173.3	432.6
208	14.372	0.476	0.000	2.098	0.000	0.000	0.000	0.000	16.946	161.3	428.8
210	14.784	0.490	0.000	2.116	0.000	0.000	0.000	0.039	17.429	76.7	183.5

APPENDIX O

CARBOXYLIC ACID PRODUCTION DATA FOR BIOSCREENING NUTRIENT DETERMINATION

Table O-1. Carboxylic acid concentration (g/L) for YE01 99 wt% paper, 1 wt% yeast extract (fresh Galveston inocula, ammonium bicarbonate buffer, 55 °C).

Days	C2	C3	IC4	C4	IC5	C5	C6	C7	Total
2	0.788	0.000	0.000	0.162	0.000	0.000	0.000	0.000	0.949
4	1.706	0.000	0.000	0.192	0.000	0.000	0.000	0.000	1.897
6	3.575	0.000	0.000	0.254	0.000	0.000	0.000	0.000	3.828
8	4.706	0.085	0.062	0.278	0.000	0.000	0.000	0.000	5.131
10	5.561	0.096	0.000	0.285	0.049	0.000	0.000	0.000	5.992
12	5.862	0.108	0.000	0.304	0.052	0.000	0.000	0.000	6.327
14	5.756	0.092	0.000	0.298	0.054	0.000	0.000	0.000	6.200
18	5.927	0.088	0.083	0.297	0.059	0.000	0.000	0.000	6.455
20	6.423	0.096	0.000	0.326	0.068	0.000	0.000	0.000	6.913
24	6.402	0.090	0.000	0.324	0.069	0.000	0.000	0.000	6.884
26	6.266	0.076	0.000	0.321	0.069	0.000	0.000	0.000	6.732
28	5.925	0.000	0.000	0.323	0.069	0.000	0.000	0.000	6.318

Table O-2. Carboxylic acid concentration (g/L) for YE05 95 wt% paper 5 wt% yeast extract fermentation (fresh Galveston inocula, ammonium bicarbonate buffer, 55 °C).

Days	C2	C3	IC4	C4	IC5	C5	C6	C7	Total
2	1.382	0.097	0.000	1.083	0.085	0.000	0.000	0.000	2.647
4	2.272	0.281	0.075	1.277	0.178	0.000	0.000	0.000	4.082
6	4.145	0.358	0.128	1.354	0.234	0.000	0.000	0.000	6.220
8	6.537	0.433	0.136	1.628	0.202	0.000	0.000	0.000	8.936
10	8.163	0.437	0.150	1.768	0.213	0.000	0.000	0.000	10.732
12	10.830	0.481	0.192	2.052	0.260	0.000	0.000	0.000	13.815
14	12.932	0.515	0.233	2.474	0.308	0.000	0.000	0.000	16.462
18	14.416	0.536	0.243	2.508	0.316	0.000	0.000	0.000	18.019
20	15.582	0.553	0.247	2.644	0.305	0.000	0.000	0.000	19.330
24	15.850	0.544	0.254	3.001	0.326	0.000	0.000	0.000	19.976
26	15.813	0.528	0.259	3.263	0.332	0.000	0.000	0.000	20.195
28	16.070	0.527	0.268	3.552	0.346	0.000	0.000	0.000	20.763

Table O-3. Carboxylic acid concentration (g/L) for YE10 90 wt% paper, 10 wt% yeast extract fermentations (fresh Galveston inocula, ammonium bicarbonate buffer, 55 °C).

Days	C2	C3	IC4	C4	IC5	C5	C6	C7	Total
2	1.511	0.088	0.000	0.743	0.000	0.000	0.000	0.000	2.341
4	2.959	0.300	0.137	1.291	0.395	0.000	0.000	0.000	5.082
6	4.922	0.484	0.247	1.407	0.491	0.000	0.000	0.000	7.551
8	7.511	0.572	0.295	1.503	0.508	0.000	0.000	0.000	10.389
10	10.212	0.730	0.439	2.406	0.576	0.000	0.000	0.000	14.363
12	12.473	0.806	0.500	2.653	0.566	0.000	0.000	0.000	16.998
14	13.814	0.795	0.509	2.744	0.549	0.000	0.000	0.000	18.411
18	15.425	0.809	0.541	2.941	0.564	0.000	0.000	0.000	20.279
20	16.045	0.776	0.531	3.024	0.543	0.000	0.000	0.000	20.919
24	17.534	0.824	0.594	3.619	0.576	0.000	0.000	0.000	23.146
26	18.386	0.827	0.624	3.990	0.598	0.000	0.000	0.000	24.424
28	17.805	0.817	0.626	4.565	0.601	0.000	0.000	0.000	24.415

Table O-4. Carboxylic acid concentration (g/L) for YE20 80 wt% paper, 20 wt% yeast extract fermentation (fresh Galveston inocula, ammonium bicarbonate buffer, 55 °C).

Days	C2	C3	IC4	C4	IC5	C5	C6	C7	Total
2	2.014	0.288	0.088	1.780	0.316	0.000	0.000	0.000	4.486
4	3.771	0.906	0.251	2.490	0.712	0.000	0.000	0.000	8.130
6	6.135	1.045	0.393	2.683	0.969	0.000	0.000	0.000	11.225
8	7.350	1.139	0.511	2.771	1.063	0.000	0.000	0.000	12.834
10	7.859	1.148	0.543	2.771	1.058	0.000	0.000	0.000	13.378
12	8.529	1.183	0.560	2.846	1.078	0.000	0.000	0.000	14.196
14	8.815	1.163	0.551	2.818	1.050	0.000	0.000	0.000	14.396
18	9.228	1.148	0.554	2.901	1.053	0.000	0.000	0.000	14.884
20	9.878	1.160	0.555	3.070	1.054	0.000	0.000	0.000	15.717
24	10.231	1.149	0.561	3.330	1.070	0.000	0.000	0.000	16.342
26	10.385	1.109	0.558	3.537	1.070	0.000	0.000	0.000	16.659
28	10.365	1.058	0.551	3.693	1.055	0.000	0.000	0.000	16.722

Table O-5. Carboxylic acid concentration (g/L) for CS01 99 wt% paper, 1 wt% corn steep liquor (CSL) fermentation (fresh Galveston inocula, ammonium bicarbonate buffer, 55 °C).

Days	C2	C3	IC4	C4	IC5	C5	C6	C7	Total
2	1.012	0.000	0.000	0.554	0.000	0.000	0.000	0.000	1.566
4	1.576	0.068	0.000	0.676	0.000	0.000	0.000	0.000	2.319
6	2.819	0.089	0.000	0.730	0.000	0.000	0.000	0.000	3.639
8	4.000	0.116	0.000	0.756	0.000	0.000	0.000	0.000	4.872
10	4.933	0.144	0.000	0.758	0.053	0.000	0.000	0.000	5.887
12	5.776	0.156	0.000	0.778	0.058	0.000	0.000	0.000	6.769
14	6.319	0.158	0.000	0.775	0.057	0.000	0.000	0.000	7.309
18	7.197	0.168	0.058	1.088	0.000	0.000	0.000	0.000	8.511
20	8.079	0.195	0.059	1.391	0.000	0.000	0.000	0.000	9.723
24	9.018	0.198	0.055	1.716	0.000	0.000	0.000	0.000	10.986
26	9.093	0.180	0.000	1.891	0.000	0.000	0.000	0.000	11.165
28	9.418	0.183	0.000	2.120	0.000	0.000	0.000	0.000	11.721

Table O-6. Carboxylic acid concentration (g/L) for CS05 95 wt% paper 5 wt % CSL fermentation (fresh Galveston inocula, ammonium bicarbonate buffer, 55 °C).

Days	C2	C3	IC4	C4	IC5	C5	C6	C7	Total
2	0.393	0.000	0.000	1.817	0.000	0.000	0.000	0.000	2.211
4	2.031	0.000	0.000	1.948	0.000	0.000	0.000	0.000	3.979
6	4.845	0.098	0.127	2.168	0.066	0.000	0.000	0.000	7.305
8	6.914	0.113	0.150	2.171	0.071	0.000	0.000	0.000	9.418
10	8.511	0.130	0.153	2.232	0.074	0.000	0.000	0.000	11.099
12	10.033	0.155	0.165	2.329	0.095	0.000	0.000	0.000	12.778
14	11.165	0.181	0.170	2.437	0.106	0.000	0.000	0.000	14.058
18	11.625	0.208	0.173	2.460	0.114	0.000	0.000	0.000	14.580
20	12.065	0.224	0.173	2.542	0.117	0.000	0.000	0.000	15.122
24	12.698	0.246	0.188	2.650	0.133	0.000	0.000	0.000	15.915
26	13.106	0.246	0.196	2.815	0.143	0.000	0.000	0.000	16.507
28	13.012	0.238	0.197	2.858	0.148	0.000	0.000	0.000	16.453

Table O-7. Carboxylic acid concentration (g/L) for CS10 90 wt% paper 10 wt% CSL fermentation (fresh Galveston inocula, ammonium bicarbonate buffer, 55 °C).

Days	C2	C3	IC4	C4	IC5	C5	C6	C7	Total
2	0.221	0.000	0.000	2.377	0.000	0.000	0.000	0.000	2.598
4	2.001	0.082	0.000	2.535	0.000	0.000	0.000	0.000	4.619
6	5.629	0.192	0.079	3.020	0.062	0.000	0.000	0.000	8.982
8	8.755	0.223	0.142	3.143	0.093	0.000	0.000	0.000	12.356
10	10.362	0.236	0.157	3.266	0.104	0.000	0.000	0.000	14.125
12	11.543	0.347	0.223	3.494	0.129	0.000	0.000	0.000	15.737
14	12.623	0.398	0.256	3.647	0.149	0.000	0.000	0.000	17.074
18	13.282	0.449	0.273	3.775	0.160	0.000	0.000	0.000	17.940
20	13.637	0.470	0.275	3.817	0.160	0.000	0.000	0.000	18.357
24	13.609	0.564	0.279	3.998	0.167	0.000	0.000	0.000	18.617
26	14.386	0.598	0.291	4.077	0.172	0.000	0.000	0.000	19.524
28	14.610	0.683	0.155	5.038	0.098	0.000	0.000	0.000	20.585

Table O-8. Carboxylic acid concentration (g/L) for CS20 80 wt% paper 20 wt% CSL fermentation (fresh Galveston inocula, ammonium bicarbonate buffer, 55 °C).

Days	C2	C3	IC4	C4	IC5	C5	C6	C7	Total
2	1.798	0.000	0.000	0.000	0.000	0.000	0.000	0.000	1.798
4	2.120	0.090	0.000	3.308	0.073	0.000	0.000	0.000	5.592
6	5.479	0.266	0.062	3.595	0.092	0.000	0.000	0.000	9.493
8	6.647	0.320	0.079	3.562	0.123	0.000	0.000	0.000	10.731
10	8.034	0.378	0.094	3.712	0.143	0.000	0.000	0.000	12.362
12	8.587	0.398	0.101	3.660	0.158	0.000	0.000	0.000	12.904
14	8.804	0.578	0.107	3.591	0.167	0.000	0.000	0.000	13.247
18	8.680	0.548	0.110	3.499	0.171	0.000	0.000	0.000	13.008
20	9.010	0.542	0.113	3.547	0.177	0.000	0.000	0.000	13.388
24	10.923	0.586	0.118	3.525	0.107	0.000	0.000	0.000	15.259
26	13.074	0.670	0.137	4.618	0.092	0.000	0.000	0.000	18.591
28	14.150	0.571	0.295	4.272	0.180	0.000	0.000	0.000	19.468

Table O-9. Carboxylic acid concentration (g/L) for R1 80 wt% paper 20 wt% chicken manure fermentation (fresh Galveston inocula, ammonium bicarbonate buffer, 55 °C).

Days	C2	C3	IC4	C4	IC5	C5	C6	C7	Total
2	1.213	0.209	0.000	0.656	0.044	0.000	0.000	0.000	2.123
4	3.179	0.244	0.000	0.804	0.000	0.000	0.000	0.000	4.227
6	2.903	0.193	0.000	4.044	0.000	0.000	0.000	0.000	7.139
8	4.768	0.221	0.000	5.181	0.053	0.000	0.000	0.000	10.222
10	7.000	0.264	0.000	5.389	0.058	0.000	0.000	0.000	12.710
12	8.647	0.302	0.059	5.845	0.067	0.000	0.000	0.000	14.919
14	10.300	0.325	0.073	5.974	0.088	0.000	0.000	0.000	16.761
18	11.059	0.346	0.086	6.080	0.102	0.000	0.000	0.000	17.673
20	11.749	0.391	0.096	6.096	0.116	0.000	0.000	0.000	18.448
24	12.298	0.424	0.106	6.131	0.121	0.000	0.000	0.000	19.079
26	12.497	0.417	0.109	6.069	0.107	0.000	0.000	0.000	19.200
28	12.787	0.426	0.113	5.997	0.101	0.000	0.000	0.000	19.426

APPENDIX P

CARBOXYLIC ACID PRODUCTION DATA FOR BIOSCREENING COUNTERCURRENT FERMENTATIONS

Table P-1. Carboxylic acid concentration (g/L) for GA paper countercurrent fermentation (Galveston inocula, calcium carbonate buffer, 55 °C).

Days	C2	C3	IC4	C4	IC5	C5	C6	C7	Total
2	3.243	0.126	0.000	3.208	0.065	0.000	0.000	0.000	6.642
4	3.716	0.149	0.000	4.470	0.071	0.000	0.000	0.000	8.406
6	3.563	0.146	0.000	4.516	0.076	0.000	0.000	0.000	8.301
8	4.076	0.154	0.000	5.033	0.082	0.000	0.000	0.000	9.344
10	4.324	0.169	0.000	5.387	0.101	0.000	0.000	0.000	9.981
12	4.492	0.194	0.000	5.679	0.122	0.000	0.000	0.000	10.487
14	4.509	0.220	0.000	6.149	0.063	0.000	0.000	0.000	10.942
16	4.514	0.226	0.000	6.260	0.145	0.000	0.000	0.000	11.145
18	4.336	0.224	0.000	6.082	0.064	0.000	0.000	0.041	10.747
20	4.395	0.319	0.000	5.729	0.155	0.000	0.000	0.043	10.642
22	4.346	0.359	0.000	5.308	0.155	0.000	0.000	0.042	10.211
24	4.413	0.380	0.000	4.974	0.163	0.000	0.000	0.045	9.975
26	4.522	0.407	0.050	4.704	0.184	0.000	0.000	0.049	9.916
28	4.914	0.511	0.057	4.593	0.205	0.000	0.000	0.064	10.345
30	5.108	0.587	0.060	4.254	0.221	0.000	0.000	0.000	10.229
32	3.997	0.385	0.000	3.373	0.176	0.000	0.000	0.062	7.994
34	4.192	0.468	0.058	3.515	0.213	0.000	0.000	0.070	8.515
36	5.996	0.655	0.093	4.139	0.339	0.000	0.000	0.054	11.275
38	5.696	0.505	0.083	3.726	0.306	0.000	0.000	0.076	10.392
40	5.486	0.490	0.086	4.109	0.314	0.000	0.000	0.107	10.591
42	6.402	0.616	0.105	4.135	0.373	0.000	0.000	0.097	11.729
44	6.817	0.598	0.116	3.836	0.405	0.000	0.000	0.076	11.850
46	6.919	0.607	0.120	3.456	0.410	0.000	0.000	0.116	11.628
48	7.453	0.595	0.123	4.000	0.423	0.000	0.000	0.103	12.697
50	7.402	0.671	0.127	3.861	0.429	0.000	0.000	0.101	12.589
52	8.009	0.625	0.131	3.711	0.440	0.000	0.000	0.107	13.024
54	7.496	0.587	0.128	3.811	0.421	0.000	0.000	0.110	12.552
56	7.547	0.571	0.134	4.011	0.433	0.000	0.000	0.063	12.759
58	7.507	0.564	0.130	3.727	0.415	0.000	0.000	0.090	12.432
60	7.339	0.506	0.123	3.732	0.394	0.000	0.000	0.119	12.214
62	7.181	0.556	0.129	3.683	0.404	0.000	0.000	0.120	12.073
64	8.613	0.607	0.139	4.001	0.438	0.000	0.000	0.105	13.904
66	7.250	0.498	0.114	3.777	0.359	0.000	0.000	0.110	12.107
68	7.932	0.601	0.123	4.207	0.387	0.000	0.000	0.121	13.372
70	8.029	0.509	0.116	4.405	0.370	0.000	0.000	0.105	13.534
72	5.471	0.368	0.081	3.574	0.259	0.000	0.000	0.106	9.858
74	7.443	0.591	0.113	4.620	0.362	0.000	0.000	0.109	13.239
76	7.576	0.545	0.106	4.762	0.350	0.000	0.000	0.076	13.416

Table P-1. Continued.

Days	C2	C3	IC4	C4	IC5	C5	C6	C7	Total
78	7.242	0.539	0.101	5.056	0.332	0.000	0.000	0.106	13.376
80	7.013	0.498	0.102	5.087	0.335	0.000	0.000	0.104	13.139
82	7.011	0.441	0.099	5.022	0.313	0.000	0.000	0.053	12.939
84	6.925	0.467	0.097	4.936	0.312	0.000	0.000	0.000	12.737
86	6.638	0.416	0.096	4.411	0.304	0.000	0.000	0.087	11.952
88	7.025	0.418	0.100	4.353	0.319	0.000	0.000	0.097	12.311
90	5.172	0.315	0.074	3.094	0.238	0.000	0.000	0.097	8.990
92	7.222	0.438	0.102	4.172	0.324	0.000	0.000	0.098	12.356
94	7.272	0.417	0.103	4.334	0.313	0.000	0.000	0.070	12.510
96	7.386	0.453	0.100	4.534	0.318	0.000	0.000	0.093	12.884
98	7.407	0.408	0.098	4.902	0.296	0.000	0.000	0.000	13.111
100	7.196	0.359	0.090	5.296	0.272	0.000	0.000	0.000	13.213
102	6.693	0.347	0.087	5.159	0.263	0.000	0.000	0.087	12.637
104	6.843	0.412	0.087	5.052	0.273	0.000	0.000	0.000	12.667
108	5.311	0.292	0.066	4.343	0.204	0.000	0.000	0.079	10.294
110	5.930	0.336	0.070	5.693	0.221	0.000	0.000	0.000	12.250
112	4.780	0.253	0.054	5.289	0.172	0.000	0.000	0.060	10.609
114	6.196	0.323	0.070	8.067	0.084	0.000	0.000	0.000	14.740
116	4.507	0.239	0.000	6.653	0.154	0.000	0.000	0.000	11.553
118	5.555	0.301	0.057	8.685	0.079	0.000	0.000	0.050	14.728
120	5.576	0.279	0.054	9.312	0.071	0.000	0.000	0.050	15.342
122	5.403	0.275	0.000	9.925	0.072	0.000	0.000	0.048	15.723
124	5.435	0.272	0.000	10.237	0.090	0.000	0.000	0.046	16.079
126	5.363	0.258	0.000	10.754	0.082	0.000	0.000	0.047	16.504
128	5.100	0.252	0.000	11.001	0.073	0.000	0.000	0.046	16.472
130	4.970	0.249	0.000	11.691	0.076	0.000	0.000	0.044	17.030
132	4.762	0.251	0.000	11.812	0.070	0.000	0.000	0.079	16.974
134	4.861	0.239	0.000	11.221	0.074	0.052	0.000	0.075	16.522
136	4.910	0.243	0.000	11.249	0.057	0.046	0.000	0.041	16.546
138	4.937	0.244	0.000	11.478	0.059	0.000	0.000	0.000	16.719
140	4.972	0.240	0.000	11.805	0.061	0.000	0.000	0.000	17.078
142	4.704	0.224	0.000	11.168	0.000	0.000	0.000	0.000	16.096
144	4.846	0.232	0.000	11.109	0.117	0.000	0.000	0.000	16.304
146	5.324	0.261	0.000	11.176	0.066	0.000	0.000	0.000	16.827

Table P-2. Carboxylic acid concentration (g/L) for TR paper countercurrent fermentation (Terrestrial inocula, calcium carbonate buffer, 55 °C).

Days	C2	C3	IC4	C4	IC5	C5	C6	C7	Total
2	3.472	0.132	0.000	2.953	0.054	0.000	0.000	0.051	6.662
4	3.446	0.111	0.000	3.469	0.064	0.000	0.000	0.000	7.090
6	3.609	0.116	0.000	3.537	0.060	0.000	0.000	0.000	7.322
8	3.941	0.123	0.000	4.213	0.067	0.000	0.000	0.000	8.344
10	4.078	0.134	0.000	5.085	0.077	0.000	0.000	0.000	9.375
12	4.256	0.135	0.000	5.354	0.079	0.000	0.000	0.000	9.824
14	4.600	0.144	0.000	5.495	0.089	0.000	0.000	0.000	10.328
16	4.472	0.142	0.000	5.877	0.099	0.000	0.000	0.000	10.590
18	4.310	0.143	0.000	5.871	0.049	0.000	0.000	0.000	10.374
20	4.465	0.130	0.000	5.694	0.119	0.000	0.000	0.000	10.409
22	4.541	0.132	0.000	6.020	0.051	0.000	0.000	0.000	10.744
24	4.635	0.128	0.000	6.360	0.052	0.000	0.000	0.000	11.176
26	4.503	0.127	0.000	7.018	0.053	0.000	0.000	0.037	11.738
28	4.934	0.122	0.000	7.214	0.050	0.000	0.000	0.108	12.427
30	4.648	0.122	0.000	8.047	0.051	0.000	0.000	0.105	12.973
32	4.591	0.125	0.000	8.199	0.086	0.000	0.000	0.000	13.000
34	4.649	0.123	0.000	8.377	0.048	0.000	0.000	0.000	13.197
36	4.641	0.119	0.000	8.671	0.078	0.000	0.000	0.000	13.510
38	4.729	0.120	0.000	9.113	0.064	0.000	0.000	0.000	14.027
40	4.923	0.120	0.000	9.827	0.076	0.000	0.000	0.000	14.946
42	4.967	0.128	0.000	9.345	0.074	0.000	0.000	0.000	14.514
48	5.420	0.188	0.000	7.914	0.064	0.000	0.000	0.000	13.585
50	5.879	0.237	0.000	7.929	0.080	0.000	0.000	0.000	14.125
52	5.962	0.264	0.000	7.281	0.083	0.000	0.000	0.039	13.630
54	5.921	0.293	0.050	7.787	0.094	0.000	0.000	0.000	14.144
56	5.841	0.345	0.056	7.880	0.089	0.000	0.000	0.098	14.309
58	6.235	0.377	0.064	8.037	0.110	0.000	0.000	0.100	14.923
60	5.470	0.260	0.049	7.091	0.077	0.000	0.000	0.052	12.998
62	6.258	0.308	0.058	8.962	0.105	0.000	0.000	0.059	15.749
64	6.074	0.280	0.052	8.879	0.099	0.000	0.000	0.050	15.435
66	5.258	0.243	0.000	7.848	0.076	0.000	0.000	0.051	13.477
68	5.987	0.287	0.051	8.866	0.095	0.000	0.000	0.045	15.331
70	6.024	0.261	0.000	8.605	0.085	0.000	0.000	0.000	14.975
72	5.953	0.259	0.000	8.753	0.085	0.000	0.000	0.050	15.101
74	6.016	0.269	0.000	8.590	0.087	0.000	0.000	0.046	15.009
76	6.406	0.258	0.000	8.684	0.087	0.000	0.000	0.055	15.489
78	6.839	0.246	0.000	8.298	0.086	0.000	0.000	0.050	15.518
80	7.066	0.237	0.000	7.508	0.076	0.000	0.000	0.054	14.941
82	7.537	0.253	0.000	7.240	0.066	0.000	0.000	0.095	15.190
84	7.197	0.232	0.000	7.061	0.064	0.000	0.000	0.095	14.648
86	7.375	0.240	0.000	8.241	0.073	0.000	0.000	0.052	15.981
88	6.057	0.317	0.061	6.761	0.197	0.000	0.000	0.054	13.448
90	7.213	0.342	0.059	7.734	0.093	0.000	0.000	0.049	15.491

Table P-2. Continued.

Days	C2	C3	IC4	C4	IC5	C5	C6	C7	Total
92	7.326	0.434	0.068	6.834	0.089	0.000	0.000	0.064	14.815
94	5.675	0.314	0.053	5.490	0.170	0.000	0.000	0.063	11.766
96	6.340	0.280	0.057	5.749	0.173	0.000	0.000	0.069	12.667
98	6.348	0.263	0.056	5.758	0.171	0.000	0.000	0.066	12.663
100	6.530	0.275	0.061	7.084	0.077	0.000	0.000	0.059	14.086
102	5.686	0.233	0.053	6.383	0.156	0.000	0.000	0.053	12.564
104	5.644	0.205	0.049	5.776	0.145	0.000	0.000	0.055	11.875
106	9.770	0.355	0.085	10.235	0.134	0.000	0.000	0.061	20.641
108	6.017	0.228	0.000	6.655	0.151	0.000	0.000	0.053	13.103
110	5.775	0.232	0.052	7.810	0.075	0.000	0.000	0.078	14.022
112	5.701	0.243	0.052	7.974	0.075	0.000	0.000	0.049	14.094
114	5.747	0.255	0.055	8.367	0.067	0.000	0.000	0.041	14.533
116	5.172	0.243	0.052	7.924	0.055	0.000	0.000	0.041	13.488
118	5.456	0.251	0.054	8.717	0.065	0.000	0.000	0.058	14.601
120	5.341	0.263	0.054	8.614	0.068	0.000	0.000	0.055	14.394
122	4.689	0.257	0.000	7.661	0.049	0.000	0.000	0.055	12.712
124	5.528	0.269	0.055	8.117	0.071	0.000	0.000	0.055	14.094
126	5.389	0.243	0.051	8.266	0.072	0.000	0.000	0.049	14.070
128	5.251	0.225	0.000	8.016	0.062	0.000	0.000	0.057	13.611
130	5.382	0.240	0.000	9.515	0.075	0.000	0.000	0.055	15.266
132	5.166	0.232	0.000	9.654	0.078	0.000	0.000	0.052	15.182
134	4.514	0.215	0.000	9.013	0.065	0.000	0.000	0.056	13.862
136	5.221	0.211	0.000	8.785	0.069	0.000	0.000	0.053	14.338
138	5.467	0.225	0.000	9.445	0.060	0.000	0.000	0.000	15.197
140	5.445	0.218	0.000	9.411	0.057	0.000	0.000	0.000	15.131
142	5.205	0.230	0.000	9.892	0.062	0.000	0.000	0.063	15.453
144	4.830	0.236	0.000	9.421	0.062	0.000	0.000	0.057	14.606
146	4.884	0.234	0.000	8.785	0.054	0.000	0.000	0.051	14.008

Table P-3. Carboxylic acid concentration (g/L) for BA paper countercurrent fermentations (Bahamas inocula, calcium carbonate buffer, 55 °C).

Days	C2	C3	IC4	C4	IC5	C5	C6	C7	Total
2	2.896	0.117	0.000	4.140	0.072	0.000	0.000	0.000	7.225
4	2.918	0.114	0.000	4.376	0.075	0.000	0.000	0.000	7.484
6	3.113	0.118	0.000	4.607	0.078	0.000	0.000	0.000	7.916
8	3.654	0.119	0.000	4.987	0.086	0.000	0.000	0.000	8.846
10	3.669	0.131	0.000	5.210	0.099	0.000	0.000	0.000	9.108
12	4.010	0.179	0.000	5.527	0.124	0.000	0.000	0.000	9.841
14	4.275	0.252	0.049	5.510	0.158	0.000	0.000	0.000	10.245
16	4.773	0.320	0.062	5.383	0.202	0.000	0.000	0.042	10.782
18	5.037	0.361	0.068	5.216	0.219	0.000	0.000	0.053	10.955
20	5.291	0.359	0.070	5.659	0.229	0.000	0.000	0.069	11.677
22	5.173	0.345	0.068	5.956	0.218	0.000	0.000	0.071	11.831
24	5.143	0.322	0.065	6.126	0.219	0.000	0.000	0.069	11.945
26	5.100	0.359	0.064	6.257	0.208	0.000	0.000	0.070	12.058
28	5.211	0.388	0.062	5.998	0.198	0.000	0.000	0.054	11.911
30	5.260	0.358	0.060	5.979	0.191	0.000	0.000	0.051	11.899
32	5.282	0.327	0.058	5.968	0.191	0.000	0.000	0.065	11.891
34	5.235	0.276	0.056	5.916	0.184	0.000	0.000	0.059	11.727
36	5.137	0.264	0.056	6.245	0.079	0.000	0.000	0.061	11.842
38	5.145	0.234	0.054	6.249	0.187	0.000	0.000	0.059	11.928
40	4.904	0.244	0.054	6.952	0.088	0.000	0.000	0.057	12.299
42	5.148	0.365	0.058	6.693	0.096	0.000	0.000	0.055	12.416
44	5.216	0.381	0.059	5.938	0.089	0.000	0.000	0.054	11.737
46	5.499	0.483	0.070	5.800	0.107	0.000	0.000	0.058	12.016
48	5.997	0.582	0.079	5.261	0.285	0.000	0.000	0.057	12.260
50	6.379	0.570	0.092	5.135	0.332	0.000	0.000	0.065	12.573
52	6.521	0.556	0.095	4.458	0.334	0.000	0.000	0.077	12.041
54	6.925	0.543	0.100	4.455	0.350	0.000	0.000	0.094	12.467
56	7.114	0.622	0.105	4.466	0.350	0.000	0.000	0.066	12.723
58	7.225	0.647	0.097	4.705	0.327	0.000	0.000	0.059	13.060
60	7.083	0.639	0.094	5.163	0.314	0.000	0.000	0.102	13.394
62	6.574	0.582	0.085	4.849	0.286	0.000	0.000	0.100	12.476
64	7.212	0.594	0.092	5.575	0.309	0.000	0.000	0.099	13.882
66	6.012	0.453	0.076	5.189	0.252	0.000	0.000	0.091	12.073
68	6.850	0.491	0.087	6.161	0.287	0.000	0.000	0.103	13.980
70	6.665	0.417	0.081	6.248	0.271	0.000	0.000	0.082	13.765
72	6.317	0.372	0.074	6.434	0.252	0.000	0.000	0.092	13.541
74	6.482	0.387	0.075	6.662	0.256	0.000	0.000	0.092	13.954
76	5.726	0.351	0.065	5.727	0.220	0.000	0.000	0.080	12.169
78	5.846	0.343	0.066	5.951	0.220	0.000	0.000	0.083	12.508
80	5.694	0.316	0.064	6.073	0.217	0.000	0.000	0.076	12.440
82	6.662	0.345	0.073	7.282	0.235	0.000	0.000	0.057	14.655
84	6.189	0.295	0.064	6.534	0.201	0.000	0.000	0.058	13.342
86	6.193	0.305	0.064	7.024	0.071	0.000	0.000	0.080	13.737

Table P-3. Continued.

Days	C2	C3	IC4	C4	IC5	C5	C6	C7	Total
88	6.602	0.232	0.000	8.106	0.075	0.000	0.000	0.075	15.090
90	5.521	0.266	0.057	6.215	0.177	0.000	0.000	0.071	12.307
92	4.799	0.236	0.000	5.290	0.151	0.000	0.000	0.056	10.533
94	5.777	0.254	0.061	6.277	0.188	0.000	0.000	0.063	12.621
96	5.725	0.249	0.061	6.219	0.195	0.000	0.000	0.050	12.499
98	5.336	0.243	0.060	5.833	0.180	0.000	0.000	0.056	11.707
100	5.715	0.246	0.060	6.313	0.184	0.000	0.000	0.060	12.578
102	5.062	0.214	0.054	6.241	0.156	0.000	0.000	0.061	11.788
104	5.248	0.210	0.000	6.314	0.145	0.000	0.000	0.066	11.983
106	4.798	0.201	0.000	7.215	0.051	0.000	0.000	0.058	12.323
108	4.222	0.183	0.000	7.421	0.117	0.000	0.000	0.054	11.997
110	4.953	0.182	0.000	8.194	0.052	0.000	0.000	0.060	13.441
112	4.712	0.184	0.000	8.876	0.060	0.000	0.000	0.051	13.883
114	5.304	0.198	0.000	10.261	0.061	0.000	0.000	0.053	15.878
116	4.867	0.198	0.000	10.295	0.062	0.000	0.000	0.000	15.423
118	4.871	0.220	0.000	10.313	0.067	0.000	0.000	0.046	15.516
120	4.866	0.214	0.000	9.647	0.066	0.000	0.000	0.044	14.835
122	4.725	0.214	0.000	9.586	0.070	0.000	0.000	0.044	14.639
124	4.772	0.213	0.000	9.209	0.070	0.000	0.000	0.046	14.310
126	4.804	0.205	0.000	8.569	0.071	0.000	0.000	0.047	13.696
128	4.550	0.202	0.000	8.192	0.058	0.000	0.000	0.048	13.049
130	4.627	0.195	0.000	8.337	0.065	0.000	0.000	0.045	13.269
132	4.671	0.209	0.000	8.494	0.061	0.000	0.000	0.045	13.481
134	4.794	0.207	0.000	8.285	0.056	0.000	0.000	0.049	13.391
136	4.258	0.183	0.000	7.462	0.123	0.000	0.000	0.049	12.075
138	2.860	0.122	0.000	5.267	0.083	0.000	0.000	0.043	8.375
140	3.933	0.163	0.000	7.486	0.089	0.000	0.000	0.000	11.672
142	4.595	0.183	0.000	9.300	0.073	0.000	0.000	0.000	14.151
144	4.786	0.194	0.059	9.527	0.093	0.000	0.000	0.000	14.660
146	4.904	0.207	0.059	9.704	0.095	0.000	0.000	0.050	15.020

Table P-4. Carboxylic acid concentration (g/L) for PU paper countercurrent fermentation (pure culture inocula, calcium carbonate buffer, 55 °C).

Days	C2	C3	IC4	C4	IC5	C5	C6	C7	Total
2	2.964	0.131	0.000	2.771	0.069	0.000	0.000	0.000	5.935
4	3.384	0.128	0.000	3.377	0.078	0.000	0.000	0.000	6.968
6	1.797	0.063	0.000	1.948	0.000	0.000	0.000	0.000	3.808
8	3.695	0.130	0.000	5.229	0.085	0.000	0.000	0.000	9.139
10	3.899	0.123	0.000	5.351	0.103	0.000	0.000	0.000	9.475
12	3.725	0.138	0.000	5.638	0.135	0.000	0.000	0.000	9.636
14	4.300	0.248	0.053	5.604	0.185	0.000	0.000	0.054	10.444
16	4.833	0.332	0.072	5.548	0.255	0.000	0.000	0.065	11.104
18	5.014	0.374	0.083	4.858	0.294	0.000	0.000	0.088	10.710
20	5.436	0.404	0.094	4.592	0.328	0.000	0.000	0.114	10.968
22	5.640	0.420	0.095	4.597	0.333	0.000	0.000	0.124	11.208
24	5.927	0.449	0.102	4.564	0.357	0.000	0.000	0.100	11.499
26	5.955	0.500	0.114	3.950	0.397	0.000	0.000	0.106	11.023
28	6.412	0.508	0.117	3.713	0.397	0.000	0.000	0.093	11.241
30	6.455	0.495	0.114	3.999	0.383	0.000	0.000	0.100	11.545
32	6.992	0.528	0.119	4.759	0.398	0.000	0.000	0.136	12.932
34	6.907	0.579	0.118	4.471	0.397	0.000	0.000	0.134	12.607
36	7.365	0.658	0.125	4.370	0.419	0.000	0.000	0.141	13.078
38	7.492	0.603	0.119	4.427	0.405	0.000	0.000	0.138	13.185
40	7.206	0.581	0.113	5.442	0.385	0.000	0.000	0.148	13.875
42	6.973	0.553	0.109	5.219	0.371	0.000	0.000	0.144	13.369
44	7.301	0.579	0.116	6.267	0.393	0.000	0.000	0.132	14.788
46	7.208	0.594	0.115	6.482	0.198	0.000	0.000	0.125	14.722
48	6.776	0.595	0.109	6.270	0.176	0.000	0.000	0.000	13.926
50	7.030	0.596	0.109	6.597	0.379	0.000	0.000	0.124	14.835
54	6.773	0.514	0.096	7.222	0.167	0.000	0.000	0.069	14.843
56	6.839	0.461	0.089	7.386	0.162	0.000	0.000	0.073	15.010
58	6.799	0.395	0.079	7.494	0.146	0.000	0.000	0.120	15.032
60	6.584	0.366	0.081	7.926	0.152	0.000	0.000	0.095	15.203
62	5.976	0.392	0.084	7.711	0.149	0.000	0.000	0.000	14.313
64	6.437	0.436	0.093	7.762	0.165	0.000	0.000	0.100	14.993
66	5.689	0.427	0.088	7.364	0.148	0.000	0.000	0.099	13.815
68	6.302	0.487	0.103	7.198	0.162	0.000	0.000	0.097	14.348
70	6.322	0.497	0.107	6.776	0.163	0.000	0.000	0.093	13.957
72	6.119	0.536	0.114	5.774	0.380	0.000	0.000	0.105	13.028
74	6.569	0.703	0.135	5.342	0.434	0.000	0.000	0.104	13.287
76	6.838	0.687	0.134	5.072	0.424	0.000	0.000	0.108	13.263
78	6.996	0.643	0.133	5.681	0.414	0.000	0.000	0.125	13.991
80	6.779	0.527	0.121	5.987	0.379	0.000	0.000	0.122	13.914
82	6.488	0.449	0.113	6.306	0.348	0.000	0.000	0.078	13.783
84	6.467	0.370	0.111	6.557	0.343	0.000	0.000	0.000	13.847
86	6.954	0.397	0.122	7.178	0.149	0.000	0.000	0.095	14.896
88	6.920	0.449	0.130	6.931	0.405	0.000	0.000	0.094	14.929

Table P-4. Continued.

Days	C2	C3	IC4	C4	IC5	C5	C6	C7	Total
92	6.979	0.472	0.138	6.707	0.162	0.000	0.000	0.000	14.457
94	8.102	0.541	0.163	7.899	0.235	0.000	0.000	0.000	16.940
96	7.248	0.538	0.156	6.308	0.466	0.000	0.000	0.114	14.830
98	4.959	0.356	0.104	3.962	0.301	0.000	0.000	0.050	9.731
100	6.707	0.504	0.139	5.733	0.407	0.000	0.000	0.046	13.536
102	6.402	0.477	0.131	5.719	0.384	0.000	0.000	0.109	13.222
104	5.247	0.426	0.106	4.726	0.315	0.000	0.000	0.000	10.821
106	6.302	0.526	0.126	6.080	0.380	0.000	0.000	0.103	13.516
108	5.524	0.447	0.111	5.995	0.335	0.000	0.000	0.090	12.501
110	3.691	0.277	0.068	4.368	0.211	0.000	0.000	0.087	8.701
112	5.874	0.413	0.095	6.950	0.116	0.000	0.000	0.087	13.534
114	6.076	0.429	0.091	8.323	0.128	0.000	0.000	0.051	15.098
116	5.482	0.390	0.076	8.509	0.113	0.000	0.000	0.045	14.615
118	5.454	0.360	0.069	8.853	0.103	0.000	0.000	0.087	14.925
120	5.248	0.317	0.061	9.224	0.096	0.000	0.000	0.073	15.019
122	4.954	0.293	0.057	9.478	0.093	0.000	0.000	0.064	14.938
124	4.603	0.264	0.053	9.214	0.082	0.000	0.000	0.059	14.275
126	4.858	0.261	0.053	9.759	0.092	0.000	0.000	0.058	15.081
128	4.539	0.237	0.000	9.726	0.085	0.000	0.000	0.053	14.640
130	4.178	0.214	0.000	8.438	0.067	0.000	0.000	0.054	12.950
132	4.600	0.229	0.000	8.778	0.069	0.000	0.000	0.051	13.726
134	4.732	0.234	0.000	8.787	0.067	0.000	0.000	0.046	13.866
136	4.713	0.246	0.000	9.406	0.067	0.000	0.000	0.050	14.482
138	4.250	0.222	0.000	8.619	0.071	0.000	0.000	0.000	13.163
140	4.417	0.256	0.000	9.308	0.051	0.000	0.000	0.000	14.031
142	4.189	0.272	0.000	9.027	0.048	0.000	0.000	0.000	13.537
144	4.137	0.275	0.000	9.023	0.068	0.000	0.000	0.000	13.503
146	4.310	0.261	0.000	8.923	0.069	0.000	0.000	0.000	13.563

Table P-5. Carboxylic acid concentration (g/L) for TI paper countercurrent fermentation (Taiwan inocula, calcium carbonate buffer, 55 °C).

Days	C2	C3	IC4	C4	IC5	C5	C6	C7	Total
2	3.380	0.194	0.000	4.071	0.076	0.000	0.000	0.123	7.844
4	3.894	0.191	0.000	4.769	0.073	0.000	0.000	0.000	8.927
6	3.823	0.183	0.000	5.217	0.074	0.000	0.000	0.000	9.297
8	4.166	0.182	0.000	5.250	0.080	0.000	0.000	0.000	9.677
10	4.452	0.175	0.000	5.462	0.081	0.000	0.000	0.000	10.170
12	4.508	0.169	0.000	5.102	0.082	0.000	0.000	0.000	9.861
14	4.478	0.164	0.000	5.164	0.084	0.000	0.000	0.000	9.890
16	4.439	0.154	0.000	5.140	0.086	0.000	0.000	0.000	9.820
18	4.404	0.143	0.000	5.596	0.099	0.000	0.000	0.000	10.241
20	4.654	0.139	0.000	5.953	0.050	0.000	0.000	0.000	10.796
22	4.939	0.132	0.000	6.083	0.050	0.000	0.000	0.000	11.204
24	5.227	0.134	0.000	6.624	0.052	0.000	0.000	0.000	12.038
26	5.428	0.109	0.000	5.901	0.092	0.000	0.000	0.125	11.657
28	5.202	0.117	0.000	5.877	0.045	0.000	0.000	0.115	11.356
30	4.431	0.114	0.000	5.925	0.051	0.000	0.000	0.114	10.635
32	5.322	0.113	0.000	6.327	0.053	0.000	0.000	0.000	11.816
34	4.813	0.106	0.000	5.679	0.052	0.000	0.000	0.036	10.686
36	5.097	0.113	0.000	5.574	0.054	0.000	0.000	0.038	10.875
38	5.271	0.129	0.000	5.921	0.129	0.000	0.000	0.040	11.489
40	3.890	0.109	0.000	4.350	0.097	0.000	0.000	0.045	8.490
42	5.441	0.145	0.000	5.490	0.143	0.000	0.000	0.045	11.264
44	5.492	0.155	0.000	5.909	0.147	0.000	0.000	0.000	11.703
46	5.766	0.167	0.000	5.856	0.157	0.000	0.000	0.052	11.998
48	5.503	0.171	0.048	5.954	0.159	0.000	0.000	0.052	11.888
50	5.620	0.225	0.055	5.683	0.194	0.000	0.000	0.055	11.831
52	5.917	0.191	0.052	5.753	0.181	0.000	0.000	0.057	12.151
54	5.500	0.176	0.058	6.379	0.202	0.000	0.000	0.000	12.315
56	5.251	0.149	0.052	6.186	0.186	0.000	0.000	0.041	11.865
58	5.606	0.127	0.052	5.993	0.179	0.000	0.000	0.071	12.028
60	5.982	0.117	0.049	5.929	0.169	0.000	0.000	0.063	12.309
62	6.009	0.109	0.050	6.018	0.172	0.000	0.000	0.056	12.414
64	6.162	0.111	0.052	6.578	0.078	0.000	0.000	0.062	13.043
66	4.624	0.090	0.000	5.315	0.136	0.000	0.000	0.000	10.164
68	5.450	0.122	0.054	6.226	0.185	0.000	0.000	0.060	12.097
70	5.074	0.131	0.053	6.056	0.177	0.000	0.000	0.047	11.537
72	5.717	0.164	0.062	6.517	0.086	0.000	0.000	0.061	12.608
74	6.074	0.174	0.062	6.210	0.210	0.000	0.000	0.063	12.793
76	5.821	0.186	0.064	6.425	0.216	0.000	0.000	0.068	12.779
78	6.110	0.241	0.071	6.591	0.236	0.000	0.000	0.073	13.323
80	5.761	0.258	0.066	6.014	0.209	0.000	0.000	0.069	12.377
84	5.391	0.194	0.062	4.893	0.181	0.000	0.000	0.130	10.851
86	6.329	0.306	0.078	6.039	0.246	0.000	0.000	0.129	13.128
90	6.151	0.391	0.087	4.821	0.269	0.000	0.000	0.064	11.784

Table P-5. Continued.

Days	C2	C3	IC4	C4	IC5	C5	C6	C7	Total
92	5.734	0.319	0.083	4.235	0.253	0.000	0.000	0.080	10.703
94	6.445	0.358	0.096	4.993	0.299	0.000	0.000	0.082	12.272
96	6.766	0.415	0.106	4.668	0.330	0.000	0.000	0.082	12.367
98	6.233	0.415	0.103	4.166	0.319	0.000	0.000	0.065	11.302
100	6.135	0.401	0.103	4.022	0.318	0.000	0.000	0.096	11.075
102	6.812	0.458	0.117	4.572	0.366	0.000	0.000	0.089	12.414
104	6.394	0.447	0.112	4.439	0.358	0.000	0.000	0.092	11.841
106	7.351	0.575	0.126	4.988	0.405	0.000	0.000	0.099	13.543
108	6.074	0.413	0.097	4.141	0.311	0.000	0.000	0.090	11.124
110	6.295	0.406	0.093	4.672	0.308	0.000	0.000	0.103	11.876
112	5.936	0.405	0.081	4.827	0.271	0.000	0.000	0.088	11.609
114	6.801	0.438	0.091	6.025	0.305	0.000	0.000	0.048	13.708
116	6.799	0.404	0.085	6.302	0.287	0.000	0.000	0.000	13.876
118	7.112	0.418	0.075	7.146	0.088	0.000	0.000	0.089	14.928
120	7.008	0.359	0.063	7.114	0.083	0.000	0.000	0.082	14.709
122	7.117	0.349	0.058	8.008	0.085	0.000	0.000	0.073	15.690
124	6.109	0.294	0.000	7.582	0.061	0.000	0.000	0.066	14.111
126	9.086	0.403	0.065	12.293	0.134	0.000	0.000	0.062	22.042
128	7.239	0.297	0.000	9.473	0.088	0.000	0.000	0.052	17.148
130	5.471	0.225	0.000	7.789	0.070	0.000	0.000	0.073	13.627
132	6.522	0.266	0.000	9.934	0.070	0.000	0.000	0.053	16.844
134	6.510	0.285	0.000	9.839	0.066	0.000	0.000	0.000	16.700
136	5.941	0.292	0.000	9.193	0.059	0.000	0.000	0.041	15.526
138	5.976	0.317	0.000	9.481	0.050	0.000	0.000	0.063	15.886
140	5.895	0.342	0.000	9.362	0.048	0.000	0.000	0.000	15.648
142	5.595	0.360	0.000	8.898	0.067	0.000	0.000	0.043	14.962
144	5.661	0.387	0.000	8.987	0.067	0.000	0.000	0.000	15.101
146	5.736	0.373	0.000	8.553	0.075	0.000	0.000	0.000	14.737

Table P-6. Carboxylic acid concentration (g/L) for LS paper countercurrent fermentation (La Sal del Rey (LSDR) inocula, calcium carbonate buffer, 55 °C).

Days	C2	C3	IC4	C4	IC5	C5	C6	C7	Total
2	3.279	0.148	0.000	4.407	0.088	0.000	0.000	0.000	7.922
4	3.276	0.141	0.000	4.446	0.085	0.000	0.000	0.000	7.948
6	3.475	0.157	0.000	4.815	0.099	0.000	0.000	0.000	8.546
8	3.759	0.162	0.000	5.338	0.102	0.000	0.000	0.000	9.360
10	4.050	0.159	0.000	5.425	0.101	0.000	0.000	0.000	9.734
12	4.441	0.164	0.000	5.799	0.049	0.000	0.000	0.000	10.453
14	4.570	0.165	0.000	6.086	0.054	0.000	0.000	0.000	10.875
16	4.243	0.148	0.000	5.758	0.051	0.000	0.000	0.000	10.200
18	4.617	0.144	0.000	5.924	0.060	0.000	0.000	0.000	10.746
20	4.938	0.158	0.000	5.935	0.158	0.000	0.000	0.000	11.190
22	5.167	0.188	0.055	5.820	0.187	0.000	0.000	0.040	11.457
24	5.410	0.215	0.064	5.336	0.224	0.000	0.000	0.047	11.295
26	5.138	0.275	0.074	4.528	0.260	0.000	0.000	0.058	10.332
28	5.580	0.311	0.085	4.024	0.296	0.000	0.000	0.062	10.358
30	5.862	0.351	0.093	3.443	0.319	0.000	0.000	0.060	10.127
32	6.575	0.425	0.108	3.908	0.371	0.000	0.000	0.104	11.490
34	7.093	0.506	0.118	3.687	0.405	0.000	0.000	0.114	11.922
36	7.402	0.567	0.119	3.269	0.414	0.000	0.000	0.132	11.903
38	7.621	0.550	0.116	3.091	0.408	0.000	0.000	0.141	11.927
40	7.700	0.539	0.117	3.033	0.416	0.000	0.000	0.146	11.951
42	8.054	0.571	0.122	2.937	0.436	0.000	0.000	0.148	12.268
44	7.947	0.582	0.123	2.630	0.440	0.000	0.000	0.148	11.870
46	8.630	0.589	0.130	2.620	0.462	0.000	0.000	0.151	12.582
48	8.914	0.614	0.136	2.694	0.483	0.000	0.000	0.150	12.990
50	8.940	0.616	0.135	2.669	0.475	0.000	0.000	0.157	12.992
52	8.597	0.545	0.121	3.267	0.417	0.000	0.000	0.162	13.110
54	8.256	0.466	0.118	4.219	0.404	0.000	0.000	0.069	13.533
56	7.876	0.392	0.100	5.043	0.341	0.000	0.000	0.068	13.819
58	8.109	0.356	0.091	5.612	0.308	0.000	0.000	0.144	14.619
60	7.764	0.306	0.078	6.218	0.259	0.000	0.000	0.129	14.754
62	7.422	0.276	0.076	7.377	0.128	0.000	0.000	0.116	15.395
64	7.025	0.238	0.069	7.587	0.108	0.000	0.000	0.101	15.128
66	5.631	0.197	0.060	7.417	0.102	0.000	0.000	0.089	13.495
68	5.812	0.190	0.061	8.093	0.110	0.000	0.000	0.083	14.348
70	3.959	0.137	0.000	6.281	0.059	0.000	0.000	0.077	10.513
72	5.181	0.193	0.056	8.292	0.104	0.000	0.000	0.076	13.902
74	5.153	0.194	0.056	7.800	0.102	0.000	0.000	0.051	13.356
76	5.377	0.205	0.072	7.984	0.123	0.000	0.000	0.073	13.834
78	5.301	0.174	0.073	7.855	0.121	0.000	0.000	0.073	13.596
80	5.375	0.176	0.065	8.082	0.109	0.000	0.000	0.090	13.897
82	5.745	0.198	0.067	8.617	0.116	0.000	0.000	0.091	14.835
84	5.793	0.188	0.066	8.464	0.117	0.000	0.000	0.091	14.719
86	5.281	0.184	0.062	7.361	0.089	0.000	0.000	0.074	13.051

Table P-6. Continued.

Days	C2	C3	IC4	C4	IC5	C5	C6	C7	Total
88	6.709	0.221	0.077	8.815	0.128	0.000	0.000	0.073	16.023
90	4.784	0.153	0.051	5.966	0.167	0.000	0.000	0.061	11.181
92	5.418	0.230	0.064	6.889	0.087	0.000	0.000	0.078	12.766
94	5.935	0.233	0.065	6.661	0.210	0.000	0.000	0.057	13.162
96	5.906	0.203	0.073	7.460	0.100	0.000	0.000	0.078	13.821
98	4.932	0.167	0.065	6.032	0.215	0.000	0.000	0.083	11.494
100	5.332	0.183	0.070	6.856	0.087	0.000	0.000	0.075	12.603
102	4.077	0.140	0.058	5.500	0.194	0.000	0.000	0.066	10.035
104	5.138	0.172	0.077	6.821	0.103	0.000	0.000	0.060	12.370
106	4.485	0.150	0.069	6.096	0.237	0.000	0.000	0.048	11.085
108	3.897	0.129	0.063	5.539	0.213	0.000	0.000	0.063	9.904
110	4.755	0.149	0.076	6.915	0.094	0.000	0.000	0.067	12.056
112	5.277	0.160	0.078	7.667	0.115	0.000	0.000	0.053	13.351
114	4.052	0.124	0.061	6.637	0.207	0.000	0.000	0.041	11.121
116	5.416	0.163	0.075	8.664	0.119	0.000	0.000	0.042	14.479
118	5.551	0.162	0.068	8.325	0.102	0.000	0.000	0.050	14.259
120	5.471	0.158	0.062	8.356	0.097	0.000	0.000	0.064	14.209
122	5.257	0.158	0.057	8.199	0.083	0.000	0.000	0.060	13.815
124	4.882	0.162	0.056	8.684	0.084	0.000	0.000	0.060	13.928
126	5.834	0.202	0.064	11.514	0.130	0.000	0.000	0.056	17.800
128	4.995	0.164	0.056	9.938	0.099	0.000	0.000	0.055	15.307
130	4.417	0.154	0.000	8.940	0.076	0.000	0.000	0.067	13.653
132	4.738	0.190	0.000	10.198	0.087	0.000	0.000	0.053	15.267
134	4.788	0.196	0.053	10.147	0.095	0.000	0.000	0.048	15.327
136	4.793	0.238	0.000	10.202	0.089	0.000	0.000	0.054	15.376
138	4.901	0.245	0.054	10.413	0.092	0.000	0.000	0.046	15.752
140	4.950	0.253	0.054	10.334	0.088	0.000	0.000	0.043	15.723
142	4.963	0.249	0.000	9.577	0.080	0.000	0.000	0.060	14.929
144	4.845	0.274	0.056	9.829	0.084	0.000	0.000	0.059	15.146
146	4.845	0.274	0.056	9.829	0.084	0.000	0.000	0.059	15.146

Table P-7. Carboxylic acid concentration (g/L) for E paper countercurrent fermentation (E08 inocula, calcium carbonate buffer, 55 °C).

Days	C2	C3	IC4	C4	IC5	C5	C6	C7	Total
2	3.932	0.421	0.057	6.133	0.084	0.000	0.000	0.000	10.628
4	0.951	0.065	0.000	1.560	0.035	0.000	0.000	0.000	2.611
6	5.344	0.318	0.051	7.469	0.090	0.000	0.000	0.053	13.325
8	0.461	0.000	0.000	0.810	0.000	0.000	0.000	0.000	1.271
10	5.169	0.195	0.038	7.955	0.071	0.000	0.000	0.035	13.463
12	5.426	0.176	0.037	9.607	0.076	0.049	0.000	0.000	15.370
14	5.264	0.195	0.040	10.779	0.077	0.045	0.000	0.041	16.442
16	4.465	0.165	0.000	9.416	0.060	0.000	0.049	0.033	14.187
18	4.889	0.180	0.000	11.249	0.070	0.000	0.000	0.031	16.419
20	4.408	0.177	0.000	10.454	0.067	0.032	0.000	0.029	15.168
22	4.337	0.187	0.005	9.719	0.063	0.010	0.006	0.017	14.344
24	4.311	0.189	0.000	9.707	0.052	0.000	0.000	0.000	14.259
26	4.305	0.196	0.000	9.380	0.058	0.000	0.000	0.000	13.939
28	3.716	0.206	0.000	8.997	0.051	0.000	0.000	0.000	12.970
30	3.339	0.191	0.000	7.768	0.070	0.000	0.000	0.000	11.368
32	3.215	0.197	0.000	7.560	0.076	0.000	0.000	0.000	11.049
34	4.555	0.277	0.000	9.202	0.075	0.000	0.000	0.000	14.110
36	4.153	0.276	0.000	9.024	0.061	0.000	0.000	0.000	13.513
38	4.315	0.299	0.000	8.738	0.059	0.000	0.000	0.000	13.411
40	5.067	0.351	0.000	9.354	0.069	0.055	0.000	0.000	14.897
42	5.051	0.382	0.000	9.497	0.058	0.059	0.000	0.000	15.046
44	4.745	0.352	0.000	7.835	0.072	0.058	0.000	0.000	13.061
46	5.101	0.409	0.000	8.618	0.058	0.063	0.000	0.000	14.250
48	5.091	0.410	0.000	8.636	0.062	0.063	0.000	0.000	14.263
50	5.121	0.419	0.000	8.499	0.058	0.060	0.000	0.044	14.201
52	5.296	0.424	0.000	8.874	0.068	0.062	0.000	0.043	14.767
54	5.180	0.424	0.000	8.897	0.072	0.062	0.000	0.045	14.679
56	5.496	0.406	0.000	8.158	0.068	0.058	0.000	0.047	14.233
58	5.297	0.391	0.000	8.586	0.070	0.055	0.000	0.048	14.447
60	4.941	0.366	0.000	9.924	0.083	0.057	0.000	0.042	15.413
62	4.744	0.346	0.056	9.552	0.094	0.053	0.000	0.045	14.891
64	5.088	0.322	0.000	8.952	0.083	0.055	0.000	0.046	14.545
66	4.715	0.306	0.000	9.326	0.078	0.051	0.000	0.050	14.526
68	4.740	0.305	0.007	9.190	0.079	0.033	0.000	0.034	14.388
70	4.489	0.289	0.000	9.351	0.083	0.048	0.000	0.047	14.307
72	4.757	0.277	0.000	8.669	0.074	0.000	0.000	0.044	13.821
74	4.633	0.264	0.000	8.217	0.061	0.000	0.000	0.000	13.175
76	4.556	0.272	0.000	9.526	0.074	0.000	0.000	0.000	14.428
78	4.875	0.259	0.000	9.140	0.073	0.000	0.000	0.000	14.347
80	4.873	0.259	0.000	9.431	0.078	0.000	0.000	0.000	14.642
82	5.088	0.258	0.000	9.106	0.076	0.000	0.000	0.000	14.528
84	5.019	0.248	0.053	8.786	0.077	0.000	0.000	0.000	14.183
86	5.351	0.252	0.059	8.595	0.086	0.000	0.000	0.000	14.342

Table P-7. Continued.

Days	C2	C3	IC4	C4	IC5	C5	C6	C7	Total
88	5.040	0.214	0.000	7.698	0.065	0.000	0.000	0.000	13.017
90	5.485	0.220	0.057	7.925	0.074	0.000	0.000	0.000	13.761
92	5.520	0.211	0.065	7.699	0.082	0.000	0.000	0.000	13.577
94	5.827	0.215	0.068	7.788	0.087	0.000	0.000	0.000	13.985
96	5.902	0.000	0.067	8.117	0.087	0.000	0.000	0.000	14.173
100	3.183	1.368	0.057	5.614	0.268	0.448	3.777	0.243	14.958
104	3.353	1.006	0.206	2.394	0.403	0.474	2.672	0.438	10.947
108	8.792	0.866	0.112	9.194	0.075	0.071	0.000	0.000	19.109
114	5.252	0.370	0.083	6.751	0.225	0.000	0.000	0.000	12.682
116	5.198	0.360	0.087	6.835	0.232	0.000	0.000	0.000	12.713
118	4.142	0.237	0.063	5.740	0.162	0.000	0.000	0.044	10.388
120	4.684	0.255	0.073	6.914	0.187	0.000	0.000	0.000	12.112
122	4.894	0.242	0.079	7.340	0.194	0.000	0.000	0.000	12.749
124	3.740	0.186	0.058	5.687	0.139	0.000	0.000	0.000	9.810
126	5.354	0.253	0.084	7.113	0.200	0.006	0.000	0.000	13.010
128	4.811	0.302	0.085	6.836	0.205	0.000	0.000	0.000	12.239
130	5.260	0.251	0.098	6.497	0.221	0.000	0.000	0.000	12.326
132	6.917	0.247	0.098	8.170	0.225	0.000	0.000	0.000	15.657
134	8.384	0.306	0.119	9.715	0.271	0.044	0.000	0.000	18.841
136	6.917	0.247	0.098	8.170	0.225	0.000	0.000	0.000	15.657
138	8.384	0.306	0.119	9.715	0.271	0.044	0.000	0.000	18.841
140	7.862	0.304	0.111	8.721	0.253	0.046	0.000	0.000	17.298
142	8.008	0.295	0.112	8.777	0.257	0.047	0.000	0.000	17.495
144	7.609	0.259	0.108	8.170	0.253	0.045	0.000	0.000	16.445
146	6.794	0.241	0.105	8.332	0.255	0.000	0.000	0.000	15.726

Table P-8. Carboxylic acid concentration (g/L) for F paper countercurrent fermentation (F09 inocula, calcium carbonate buffer, 55 °C).

Days	C2	C3	IC4	C4	IC5	C5	C6	C7	Total
2	2.955	0.295	0.000	7.459	0.044	0.039	0.000	0.042	10.834
4	2.962	0.179	0.000	7.110	0.035	0.000	0.000	0.000	10.286
6	3.360	0.352	0.000	8.248	0.060	0.042	0.000	0.034	12.097
8	2.265	0.228	0.000	5.383	0.047	0.000	0.000	0.000	7.922
10	1.903	0.124	0.000	4.139	0.035	0.000	0.000	0.045	6.246
12	5.076	0.332	0.000	11.118	0.066	0.054	0.000	0.033	16.681
14	4.852	0.318	0.000	10.602	0.057	0.067	0.000	0.029	15.925
16	5.471	0.304	0.000	11.454	0.056	0.077	0.000	0.049	17.410
18	5.397	0.263	0.000	11.290	0.049	0.047	0.000	0.041	17.087
20	5.909	0.254	0.000	12.390	0.051	0.057	0.033	0.044	18.738
22	5.452	0.222	0.000	12.075	0.047	0.047	0.000	0.038	17.882
24	5.161	0.187	0.000	11.442	0.000	0.000	0.000	0.000	16.790
26	4.882	0.171	0.000	11.489	0.000	0.000	0.000	0.000	16.542
28	5.095	0.155	0.000	10.863	0.000	0.000	0.000	0.000	16.113
30	2.207	0.084	0.000	4.770	0.000	0.000	0.000	0.000	7.061
32	4.362	0.122	0.000	9.787	0.000	0.000	0.000	0.000	14.272
34	4.689	0.123	0.000	10.481	0.000	0.000	0.050	0.000	15.343
36	4.370	0.128	0.000	9.881	0.000	0.000	0.000	0.000	14.379
38	4.858	0.143	0.000	10.529	0.000	0.000	0.000	0.000	15.530
40	5.267	0.138	0.000	10.996	0.000	0.000	0.000	0.000	16.401
42	4.688	0.123	0.000	10.104	0.000	0.000	0.000	0.000	14.915
44	5.302	0.123	0.000	9.963	0.000	0.000	0.000	0.000	15.389
46	4.287	0.110	0.000	8.298	0.000	0.000	0.000	0.000	12.695
48	4.251	0.103	0.000	7.888	0.000	0.000	0.000	0.000	12.241
50	4.741	0.107	0.000	8.232	0.000	0.000	0.000	0.000	13.079
52	4.483	0.106	0.000	7.870	0.000	0.000	0.000	0.000	12.458
54	4.396	0.110	0.000	8.150	0.000	0.000	0.000	0.000	12.656
56	4.685	0.116	0.000	8.618	0.000	0.000	0.000	0.000	13.419
58	4.883	0.119	0.000	9.030	0.000	0.000	0.000	0.000	14.032
60	3.670	0.097	0.000	8.466	0.000	0.000	0.000	0.000	12.233
62	4.341	0.107	0.000	8.925	0.000	0.000	0.000	0.000	13.372
64	4.115	0.105	0.000	8.784	0.000	0.000	0.000	0.000	13.004
66	4.207	0.109	0.000	8.711	0.000	0.000	0.000	0.000	13.027
68	4.384	0.124	0.000	8.176	0.021	0.000	0.000	0.000	12.704
70	4.478	0.125	0.000	8.348	0.000	0.000	0.000	0.000	12.951
72	4.449	0.143	0.000	7.609	0.063	0.000	0.000	0.000	12.264
74	5.016	0.147	0.000	7.508	0.050	0.000	0.000	0.000	12.721
76	4.794	0.157	0.000	7.061	0.050	0.000	0.000	0.000	12.063
78	5.188	0.160	0.000	7.581	0.051	0.000	0.000	0.000	12.980
80	5.103	0.150	0.000	7.217	0.068	0.000	0.000	0.000	12.537
82	5.157	0.152	0.000	7.002	0.071	0.000	0.000	0.000	12.382
84	4.899	0.159	0.000	6.439	0.075	0.000	0.000	0.000	11.572
86	5.117	0.150	0.000	6.388	0.076	0.000	0.000	0.000	11.731

Table P-8. Continued.

Days	C2	C3	IC4	C4	IC5	C5	C6	C7	Total
88	4.891	0.146	0.000	6.024	0.073	0.000	0.000	0.000	11.134
90	5.529	0.160	0.000	6.827	0.048	0.000	0.000	0.000	12.564
92	5.914	0.164	0.000	7.392	0.055	0.000	0.000	0.000	13.526
94	6.002	0.177	0.000	7.505	0.055	0.000	0.000	0.000	13.738
96	5.359	0.000	0.119	5.973	0.347	0.000	0.000	0.000	11.797
98	5.796	0.207	0.000	7.891	0.095	0.000	0.000	0.000	13.989
100	5.651	0.206	0.000	7.931	0.091	0.000	0.000	0.000	13.878
102	4.680	0.171	0.000	6.815	0.083	0.000	0.000	0.000	11.749
104	3.011	0.110	0.000	4.325	0.059	0.000	0.000	0.000	7.506
106	4.296	0.182	0.000	6.093	0.097	0.000	0.000	0.000	10.667
108	4.807	0.380	0.050	5.954	0.149	0.000	0.000	0.000	11.339
110	5.257	0.413	0.063	6.327	0.187	0.000	0.000	0.000	12.246
112	5.592	0.327	0.055	6.549	0.159	0.000	0.000	0.000	12.682
114	5.793	0.313	0.063	7.082	0.174	0.000	0.000	0.000	13.425
116	5.722	0.264	0.062	6.848	0.165	0.000	0.000	0.000	13.061
118	5.002	0.260	0.056	7.080	0.143	0.000	0.000	0.000	12.540
120	7.563	0.339	0.077	10.752	0.195	0.000	0.000	0.000	18.926
122	7.417	0.301	0.071	10.370	0.180	0.000	0.000	0.000	18.339
124	6.639	0.305	0.066	9.044	0.163	0.000	0.000	0.000	16.217
126	6.090	0.301	0.050	8.581	0.153	0.014	0.000	0.000	15.189
128	4.491	0.237	0.000	7.236	0.116	0.000	0.000	0.000	12.080
130	4.535	0.207	0.000	6.591	0.108	0.000	0.000	0.000	11.441
132	6.627	0.366	0.067	9.033	0.162	0.052	0.000	0.000	16.307
134	6.446	0.397	0.066	8.540	0.158	0.059	0.000	0.000	15.665
136	6.627	0.366	0.067	9.033	0.162	0.052	0.000	0.000	16.307
138	6.446	0.397	0.066	8.540	0.158	0.059	0.000	0.000	15.665
140	6.198	0.398	0.060	7.554	0.145	0.059	0.000	0.000	14.414
142	6.382	0.400	0.059	7.306	0.145	0.000	0.000	0.000	14.292
144	6.436	0.393	0.060	7.371	0.145	0.061	0.000	0.000	14.466
146	6.986	0.415	0.070	8.995	0.169	0.071	0.000	0.000	16.708

Table P-9. Carboxylic acid concentration (g/L) for G paper countercurrent fermentation (G46 inocula, calcium carbonate buffer, 55 °C).

Days	C2	C3	IC4	C4	IC5	C5	C6	C7	Total
2	5.430	0.454	0.055	7.641	0.104	0.036	0.000	0.029	13.750
4	3.612	0.325	0.043	4.875	0.049	0.000	0.000	0.000	8.905
6	5.389	0.451	0.064	7.080	0.107	0.000	0.000	0.058	13.149
8	1.562	0.095	0.000	2.405	0.048	0.000	0.000	0.042	4.153
10	6.212	0.376	0.058	9.424	0.118	0.035	0.000	0.063	16.286
12	6.158	0.338	0.054	9.928	0.106	0.047	0.000	0.000	16.630
14	5.832	0.283	0.046	10.780	0.090	0.059	0.000	0.062	17.153
16	5.244	0.257	0.039	10.825	0.075	0.046	0.000	0.051	16.537
18	5.327	0.270	0.037	12.553	0.080	0.042	0.000	0.057	18.365
20	5.549	0.267	0.039	12.278	0.080	0.040	0.000	0.039	18.291
22	4.933	0.285	0.020	10.471	0.073	0.023	0.000	0.026	15.831
24	4.951	0.296	0.000	11.593	0.064	0.000	0.000	0.000	16.904
26	4.837	0.319	0.000	10.780	0.064	0.000	0.000	0.000	15.999
28	3.954	0.294	0.000	7.921	0.066	0.000	0.000	0.000	12.235
30	3.768	0.296	0.000	7.035	0.066	0.000	0.000	0.000	11.164
32	5.563	0.489	0.000	9.969	0.071	0.000	0.000	0.000	16.091
34	5.351	0.524	0.000	9.797	0.070	0.000	0.000	0.000	15.743
36	5.143	0.518	0.000	9.679	0.064	0.051	0.000	0.000	15.456
38	5.438	0.548	0.000	10.131	0.071	0.058	0.000	0.046	16.292
40	5.218	0.497	0.000	9.415	0.062	0.058	0.000	0.000	15.250
42	5.042	0.497	0.000	10.166	0.066	0.055	0.000	0.046	15.873
44	5.175	0.496	0.000	10.461	0.075	0.061	0.000	0.000	16.268
46	4.762	0.428	0.000	8.655	0.064	0.055	0.000	0.000	13.965
48	4.503	0.388	0.000	8.133	0.060	0.052	0.000	0.000	13.136
50	4.455	0.374	0.000	7.914	0.060	0.052	0.000	0.000	12.854
52	4.491	0.345	0.000	7.594	0.056	0.049	0.000	0.000	12.537
54	4.476	0.323	0.000	7.321	0.053	0.000	0.000	0.000	12.173
56	4.394	0.314	0.000	7.220	0.059	0.000	0.000	0.000	11.987
58	4.364	0.303	0.000	6.947	0.063	0.000	0.000	0.000	11.677
60	4.436	0.315	0.056	6.335	0.052	0.000	0.000	0.000	11.194
62	4.607	0.317	0.069	6.073	0.228	0.000	0.000	0.000	11.293
64	4.964	0.296	0.068	5.717	0.213	0.000	0.000	0.000	11.258
66	4.741	0.270	0.064	5.773	0.202	0.000	0.000	0.000	11.051
68	4.621	0.295	0.066	5.683	0.183	0.000	0.000	0.000	10.847
70	4.787	0.268	0.068	5.937	0.202	0.000	0.000	0.000	11.261
72	4.558	0.270	0.070	5.503	0.203	0.000	0.000	0.000	10.605
74	4.303	0.306	0.063	4.856	0.177	0.000	0.000	0.000	9.706
76	4.570	0.319	0.067	5.268	0.187	0.000	0.000	0.000	10.411
78	4.610	0.000	0.075	4.859	0.212	0.000	0.000	0.000	9.755
80	4.616	0.000	0.074	4.729	0.210	0.000	0.000	0.000	9.629
82	4.596	0.000	0.076	4.686	0.217	0.000	0.000	0.000	9.575
84	4.709	0.000	0.078	4.439	0.227	0.000	0.000	0.000	9.453
86	1.536	0.000	0.215	1.537	0.101	0.000	0.000	0.000	3.390

Table P-9. Continued.

Days	C2	C3	IC4	C4	IC5	C5	C6	C7	Total
88	4.746	0.000	0.086	4.520	0.258	0.000	0.000	0.000	9.611
90	5.321	0.000	0.122	4.873	0.352	0.000	0.000	0.000	10.668
92	5.649	0.000	0.127	5.769	0.369	0.000	0.000	0.000	11.914
94	5.678	0.000	0.118	6.032	0.343	0.000	0.000	0.000	12.170
96	5.790	0.000	0.000	7.788	0.049	0.000	0.000	0.000	13.627
98	5.645	0.320	0.133	5.339	0.381	0.000	0.000	0.000	11.818
100	5.125	0.300	0.129	5.300	0.366	0.000	0.000	0.000	11.220
102	5.226	0.392	0.151	5.280	0.407	0.000	0.000	0.000	11.455
104	3.170	0.203	0.077	3.766	0.211	0.000	0.000	0.000	7.426
106	5.775	0.400	0.161	5.047	0.417	0.000	0.000	0.000	11.800
108	4.906	0.386	0.134	4.655	0.354	0.000	0.000	0.000	10.435
110	5.884	0.504	0.184	6.048	0.473	0.000	0.000	0.000	13.093
112	4.206	0.330	0.134	4.051	0.339	0.000	0.000	0.000	9.058
114	5.546	0.419	0.183	5.545	0.454	0.000	0.000	0.000	12.147
116	6.218	0.450	0.209	5.894	0.505	0.000	0.000	0.000	13.276
118	4.932	0.301	0.143	4.334	0.350	0.000	0.000	0.000	10.060
120	7.522	0.422	0.225	6.632	0.529	0.000	0.000	0.000	15.330
122	5.276	0.251	0.162	4.188	0.355	0.000	0.000	0.000	10.233
124	6.198	0.342	0.175	6.271	0.408	0.000	0.000	0.000	13.393
126	6.105	0.296	0.174	5.300	0.384	0.000	0.000	0.000	12.260
128	5.829	0.266	0.156	7.862	0.347	0.000	0.000	0.000	14.459
130	6.889	0.331	0.165	8.369	0.379	0.000	0.000	0.000	16.134
132	7.464	0.338	0.157	8.317	0.365	0.000	0.000	0.000	16.641
134	6.816	0.290	0.132	7.215	0.309	0.000	0.000	0.000	14.762
136	6.889	0.331	0.165	8.369	0.379	0.000	0.000	0.000	16.134
138	7.464	0.338	0.157	8.317	0.365	0.000	0.000	0.000	16.641
140	6.816	0.290	0.132	7.215	0.309	0.000	0.000	0.000	14.762
142	6.493	0.274	0.134	6.977	0.318	0.000	0.000	0.000	14.196
144	6.870	0.289	0.147	7.175	0.352	0.000	0.000	0.000	14.833
146	6.540	0.259	0.143	7.199	0.347	0.000	0.000	0.000	14.489

APPENDIX Q

CARBOXYLIC ACID PRODUCTION DATA FOR BATCH FERMENTATIONS OF SEVERAL SUBSTRATES

Table Q-1. Carboxylic acid concentration (g/L) for S01-3 80 wt% office paper wastes, 20 wt% chicken manure (fresh Galveston inocula, ammonium bicarbonate buffer, 55 °C).

Days	C2	C3	IC4	C4	IC5	C5	C6	C7	Total
2	1.065	0.000	0.000	0.908	0.000	0.000	0.000	0.000	1.973
4	2.449	0.182	0.000	0.964	0.000	0.000	0.000	0.000	3.594
6	4.962	0.255	0.000	1.039	0.047	0.000	0.000	0.000	6.303
8	7.664	0.335	0.137	1.197	0.099	0.000	0.000	0.000	9.432
10	10.103	0.387	0.096	1.246	0.122	0.000	0.000	0.000	11.952
12	12.763	0.462	0.184	1.496	0.128	0.000	0.000	0.000	15.033
14	14.659	0.523	0.135	1.646	0.149	0.000	0.000	0.000	17.112
16	17.011	0.585	0.258	1.884	0.135	0.000	0.000	0.000	19.873
18	19.001	0.624	0.192	2.221	0.134	0.000	0.000	0.000	22.172
20	20.015	0.622	0.292	2.383	0.156	0.000	0.000	0.000	23.468
22	20.679	0.613	0.303	2.575	0.175	0.000	0.000	0.017	24.363
24	20.425	0.569	0.202	2.631	0.170	0.000	0.000	0.021	24.019

Table Q-2. Carboxylic acid concentration (g/L) for S04-6 80 wt% hot-lime treated pineapple residue 20 wt% chicken manure fermentation (fresh Galveston inocula, ammonium bicarbonate buffer, 55 °C).

Days	C2	C3	IC4	C4	IC5	C5	C6	C7	Total
2	4.468	0.324	0.000	1.047	0.038	0.000	0.000	0.000	5.878
4	6.073	0.379	0.000	1.149	0.055	0.000	0.000	0.000	7.656
6	9.215	0.457	0.090	1.267	0.072	0.000	0.000	0.000	11.100
8	9.695	0.427	0.078	1.121	0.061	0.000	0.000	0.000	11.382
10	12.489	0.516	0.141	1.441	0.115	0.000	0.000	0.000	14.702
12	13.070	0.505	0.098	1.521	0.126	0.000	0.000	0.000	15.321
14	13.676	0.495	0.119	1.601	0.136	0.000	0.000	0.000	16.027
16	14.087	0.478	0.055	1.653	0.147	0.000	0.000	0.000	16.419
18	14.361	0.457	0.188	1.700	0.153	0.000	0.000	0.000	16.859
20	14.620	0.432	0.191	1.745	0.155	0.000	0.000	0.000	17.144
22	14.677	0.397	0.193	1.776	0.158	0.000	0.000	0.000	17.200

Table Q-3. Carboxylic acid concentration (g/L) for S07-9 80 wt% *Aloe vera* rinds, 20 wt% chicken manure fermentations (fresh Galveston inocula, ammonium bicarbonate buffer, 55 °C).

Days	C2	C3	IC4	C4	IC5	C5	C6	C7	Total
2	1.277	0.132	0.000	0.185	0.000	0.559	0.000	0.000	2.152
4	6.902	0.235	0.000	6.114	0.110	0.000	0.000	0.000	13.361
6	10.900	0.607	0.115	6.370	0.164	0.000	0.000	0.000	18.156
8	13.519	0.764	0.175	6.916	0.234	0.000	0.000	0.000	21.608
10	14.774	0.883	0.209	7.060	0.287	0.000	0.000	0.000	23.212
12	16.031	0.967	0.000	7.288	0.321	0.000	0.000	0.066	24.671
14	16.343	0.970	0.238	7.114	0.326	0.000	0.000	0.000	24.992
16	17.139	0.996	0.245	7.226	0.341	0.000	0.000	0.000	25.947
18	16.974	0.970	0.242	6.892	0.332	0.000	0.000	0.090	25.500
20	17.137	0.976	0.241	6.701	0.313	0.000	0.000	0.088	25.456
22	17.528	0.994	0.236	6.416	0.276	0.000	0.000	0.097	25.547

Table Q-4. Carboxylic acid concentration (g/L) for S10-12 80 wt% wood molasses, 20 wt% chicken manure fermentation (fresh Galveston inocula, ammonium bicarbonate buffer, 55 °C).

Days	C2	C3	IC4	C4	IC5	C5	C6	C7	Total
2	5.035	0.258	0.000	0.129	0.000	0.000	0.000	0.000	5.422
4	5.609	0.242	0.000	2.564	0.000	0.000	0.000	0.000	8.415
6	6.513	0.241	0.000	4.455	0.000	0.000	0.000	0.000	11.210
8	7.876	0.241	0.000	4.730	0.000	0.000	0.000	0.000	12.847
10	8.830	0.246	0.000	5.768	0.000	0.000	0.000	0.000	14.844
12	9.717	0.270	0.000	6.006	0.000	0.000	0.000	0.000	15.993
14	10.786	0.299	0.000	6.238	0.020	0.000	0.000	0.000	17.344
16	11.445	0.321	0.000	6.270	0.023	0.000	0.000	0.000	18.060
18	12.101	0.368	0.021	6.307	0.025	0.000	0.000	0.000	18.822
20	12.425	0.429	0.043	6.507	0.025	0.000	0.000	0.000	19.430

Table Q-5. Carboxylic acid concentration (g/L) for S13-15 80 wt% sugar molasses, 20 wt% chicken manure fermentation (fresh Galveston inocula, ammonium bicarbonate buffer, 55 °C).

Days	C2	C3	IC4	C4	IC5	C5	C6	C7	Total
2	1.983	0.121	0.000	2.157	0.000	0.260	0.021	0.000	4.541
4	1.133	0.107	0.000	7.551	0.000	0.262	0.000	0.000	9.053
6	1.134	0.099	0.000	7.575	0.000	0.246	0.000	0.000	9.054
8	1.800	0.095	0.000	7.660	0.000	0.210	0.000	0.000	9.765
10	4.605	0.132	0.000	8.220	0.000	0.056	0.000	0.000	13.013
12	6.027	0.248	0.000	8.261	0.000	0.022	0.000	0.000	14.558
14	7.060	0.362	0.000	8.332	0.000	0.000	0.000	0.000	15.755
16	8.460	0.432	0.000	8.303	0.000	0.000	0.000	0.000	17.195
18	9.887	0.474	0.000	8.512	0.000	0.000	0.000	0.000	18.873
20	10.331	0.456	0.000	8.083	0.000	0.000	0.000	0.000	18.870

Table Q-6. Carboxylic acid concentration (g/L) for S16-18 80 wt% extracted algae 20 wt % chicken manure fermentation (fresh Galveston inocula, ammonium bicarbonate buffer, 55 °C).

Days	C2	C3	IC4	C4	IC5	C5	C6	C7	Total
2	1.222	0.377	0.000	1.279	0.025	0.000	0.059	0.000	2.963
4	4.970	0.666	0.271	2.133	0.650	0.000	0.080	0.000	8.770
6	8.456	1.029	0.675	3.056	1.296	0.000	0.072	0.000	14.585
8	9.935	1.170	0.755	3.197	1.460	0.000	0.024	0.000	16.540
10	10.321	1.252	0.822	3.294	1.609	0.000	0.044	0.000	17.341
12	10.753	1.288	0.854	3.318	1.678	0.000	0.037	0.000	17.928
14	11.060	1.315	0.877	3.316	1.728	0.000	0.061	0.000	18.358
16	11.409	1.352	0.902	3.335	1.782	0.000	0.034	0.000	18.815
18	11.590	1.379	0.919	3.321	1.818	0.000	0.055	0.000	19.082
20	11.505	1.384	0.928	3.275	1.804	0.000	0.021	0.000	18.917
22	12.609	1.530	1.017	3.537	1.966	0.000	0.052	0.000	20.712
24	12.683	1.515	1.020	3.466	1.970	0.000	0.069	0.000	20.723
26	12.853	1.550	1.034	3.481	1.989	0.000	0.000	0.000	20.908
28	12.313	1.482	0.992	3.285	1.902	0.000	0.019	0.000	19.993

Table Q-7. Carboxylic acid concentration (g/L) for S19-21 80 wt% non-extracted algae 20 wt% chicken manure fermentation (fresh Galveston inocula, ammonium bicarbonate buffer, 55 °C).

Days	C2	C3	IC4	C4	IC5	C5	C6	C7	Total
2	0.792	0.353	0.000	1.539	0.000	0.000	0.060	0.000	2.744
4	4.414	0.557	0.282	2.275	0.611	0.000	0.019	0.000	8.160
6	8.755	0.909	0.602	3.091	1.062	0.000	0.044	0.000	14.463
8	10.703	1.145	0.755	3.455	1.370	0.000	0.022	0.000	17.450
10	11.474	1.291	0.864	3.669	1.590	0.000	0.018	0.000	18.906
12	11.734	1.330	0.895	3.652	1.675	0.020	0.045	0.000	19.351
14	12.505	1.424	0.958	3.769	1.806	0.000	0.000	0.000	20.462
16	12.784	1.466	0.981	3.839	1.852	0.000	0.018	0.000	20.939
18	12.817	1.471	0.994	3.770	1.893	0.018	0.036	0.000	20.999
20	13.186	1.530	1.039	3.859	1.947	0.000	0.065	0.000	21.626
22	14.015	1.657	1.037	4.073	1.872	0.032	0.041	0.000	22.727
24	13.546	1.578	1.069	3.846	1.998	0.000	0.000	0.000	22.037
26	13.643	1.594	1.084	3.846	2.032	0.000	0.019	0.000	22.216
28	13.071	1.541	1.051	3.695	1.968	0.000	0.017	0.000	21.343

APPENDIX R

CARBOXYLIC ACID PRODUCTION DATA FOR GLYCEROL FERMENTATIONS

Table R-1. Carboxylic acid concentration (g/L) for crude glycerol fermentation (fresh Galveston inocula, ammonium bicarbonate buffer, 55 °C).

Days	C2	C3	IC4	C4	IC5	C5	C6	C7	Total
2	1.346	0.117	0.000	1.500	0.000	0.000	0.000	0.000	2.962
4	1.187	0.157	0.000	2.934	0.000	0.000	0.000	0.000	4.277
6	3.061	0.193	0.000	3.592	0.000	0.000	0.000	0.000	6.846
8	4.091	0.216	0.000	4.285	0.000	0.000	0.000	0.000	8.592
10	5.668	0.243	0.000	4.760	0.000	0.000	0.000	0.000	10.671
12	6.332	0.269	0.000	5.383	0.000	0.000	0.000	0.000	11.985
14	7.103	0.295	0.017	6.116	0.000	0.000	0.000	0.000	13.531
16	8.101	0.345	0.000	7.912	0.000	0.000	0.000	0.000	16.358
18	9.015	0.369	0.036	8.902	0.000	0.000	0.000	0.000	18.321
20	10.403	0.393	0.019	9.462	0.000	0.000	0.000	0.000	20.278
22	11.309	0.416	0.042	10.367	0.030	0.000	0.000	0.000	22.164
24	12.123	0.443	0.022	11.034	0.032	0.000	0.000	0.000	23.654
26	13.019	0.474	0.047	11.225	0.033	0.016	0.000	0.000	24.814
28	13.573	0.502	0.068	10.180	0.000	0.000	0.018	0.000	24.341
30	13.982	0.533	0.070	10.250	0.000	0.000	0.000	0.000	24.835
32	14.843	0.434	0.000	8.775	0.000	0.000	0.000	0.000	24.052

Table R-2. Carboxylic acid concentration (g/L) for distilled glycerol fermentation (fresh Galveston inocula, ammonium bicarbonate buffer, 55 °C).

Days	C2	C3	IC4	C4	IC5	C5	C6	C7	Total
2	1.260	0.102	0.000	1.474	0.000	0.000	0.000	0.000	2.837
4	1.168	0.130	0.000	2.666	0.000	0.000	0.000	0.000	3.964
6	2.511	0.152	0.000	3.382	0.015	0.000	0.000	0.000	6.060
8	3.499	0.163	0.000	3.976	0.015	0.000	0.000	0.000	7.654
10	4.796	0.176	0.000	4.412	0.000	0.000	0.000	0.000	9.385
12	5.806	0.193	0.017	5.377	0.000	0.000	0.000	0.000	11.392
14	7.144	0.204	0.036	6.408	0.014	0.000	0.000	0.000	13.806
16	7.504	0.207	0.020	7.717	0.000	0.000	0.000	0.000	15.449
18	8.463	0.211	0.040	8.622	0.046	0.000	0.000	0.000	17.382
20	9.433	0.212	0.000	9.840	0.054	0.000	0.000	0.000	19.540
22	10.688	0.213	0.072	10.744	0.056	0.000	0.000	0.000	21.773
24	11.002	0.208	0.025	11.297	0.062	0.000	0.000	0.000	22.594
26	12.721	0.210	0.053	11.766	0.060	0.000	0.015	0.000	24.825
28	12.049	0.208	0.054	11.733	0.000	0.000	0.017	0.000	24.060
30	12.439	0.218	0.076	10.813	0.000	0.000	0.000	0.000	23.545
32	13.909	0.184	0.021	9.438	0.000	0.000	0.000	0.000	23.552

Table R-3. Carboxylic acid concentration (g/L) for refined glycerol fermentations (fresh Galveston inocula, ammonium bicarbonate buffer, 55 °C).

Days	C2	C3	IC4	C4	IC5	C5	C6	C7	Total
2	1.256	0.094	0.000	1.430	0.000	0.000	0.000	0.000	2.780
4	0.901	0.135	0.000	2.992	0.000	0.000	0.000	0.000	4.027
6	2.090	0.149	0.000	4.133	0.000	0.000	0.000	0.000	6.372
8	3.495	0.165	0.000	4.908	0.000	0.000	0.000	0.000	8.568
10	4.793	0.181	0.017	5.890	0.000	0.000	0.000	0.000	10.882
12	5.322	0.178	0.018	6.516	0.000	0.000	0.000	0.000	12.034
14	6.116	0.173	0.000	7.229	0.000	0.000	0.000	0.000	13.519
16	7.023	0.179	0.000	8.936	0.000	0.000	0.000	0.000	16.138
18	7.973	0.170	0.035	9.676	0.000	0.000	0.000	0.000	17.855
20	9.163	0.167	0.019	10.443	0.000	0.000	0.000	0.000	19.791
22	10.124	0.168	0.046	11.436	0.015	0.000	0.000	0.000	21.790
24	10.301	0.161	0.072	11.875	0.049	0.016	0.000	0.000	22.474
26	10.341	0.155	0.074	12.264	0.054	0.016	0.000	0.000	22.903
28	10.745	0.159	0.078	11.849	0.000	0.000	0.000	0.000	22.831
30	10.891	0.149	0.079	11.851	0.000	0.000	0.000	0.000	22.971
32	11.522	0.116	0.000	11.015	0.000	0.000	0.000	0.000	22.653

Table R-4. Carboxylic acid concentration (g/L) for refined glycerol CSTR fermentation (fresh Galveston inocula, ammonium bicarbonate buffer, 55 °C).

Days	C2	C3	IC4	C4	IC5	C5	C6	C7	Total
2	0.530	0.078	0.000	0.000	0.000	0.000	0.000	0.000	0.608
4	0.672	0.106	0.000	0.254	0.000	0.000	0.000	0.000	1.033
6	0.721	0.116	0.000	0.501	0.000	0.000	0.000	0.000	1.338
8	1.320	0.104	0.000	0.498	0.000	0.000	0.000	0.000	1.922
10	3.318	0.104	0.075	0.593	0.066	0.000	0.000	0.000	4.156
12	4.243	0.095	0.088	0.801	0.084	0.000	0.000	0.000	5.311
14	4.580	0.082	0.095	0.937	0.097	0.000	0.000	0.000	5.791
16	4.983	0.072	0.102	1.105	0.106	0.000	0.000	0.000	6.369
18	5.260	0.064	0.106	1.272	0.115	0.000	0.000	0.000	6.818
20	5.267	0.065	0.110	1.698	0.121	0.000	0.000	0.000	7.261
22	4.853	0.068	0.113	2.508	0.132	0.000	0.000	0.000	7.674
24	4.859	0.067	0.115	3.045	0.136	0.000	0.000	0.000	8.222
26	4.466	0.068	0.117	3.951	0.139	0.000	0.000	0.000	8.742
28	3.244	0.064	0.000	3.916	0.112	0.000	0.000	0.000	7.337
30	4.280	0.078	0.114	4.877	0.138	0.000	0.000	0.000	9.487
32	4.225	0.091	0.106	5.212	0.130	0.000	0.000	0.000	9.765
34	4.186	0.085	0.000	4.755	0.111	0.000	0.000	0.000	9.138
36	4.541	0.078	0.081	4.141	0.097	0.000	0.000	0.000	8.938
38	6.274	0.090	0.000	4.388	0.104	0.000	0.000	0.000	10.856
40	6.235	0.085	0.000	3.830	0.093	0.000	0.000	0.000	10.243
42	5.285	0.072	0.062	3.013	0.073	0.000	0.000	0.000	8.505
44	5.261	0.068	0.056	2.637	0.064	0.000	0.000	0.000	8.087
46	6.451	0.087	0.065	2.940	0.076	0.000	0.000	0.000	9.619
48	7.149	0.098	0.000	2.979	0.081	0.000	0.000	0.000	10.307
50	4.553	0.115	0.000	6.084	0.075	0.000	0.000	0.000	10.827
52	3.566	0.102	0.000	4.646	0.056	0.000	0.000	0.000	8.371
54	3.513	0.111	0.000	4.645	0.053	0.000	0.000	0.000	8.322
56	4.319	0.144	0.052	5.314	0.062	0.000	0.000	0.000	9.891
58	3.805	0.124	0.000	4.148	0.050	0.000	0.000	0.000	8.128
60	6.400	0.198	0.064	6.748	0.077	0.000	0.000	0.000	13.487
62	6.550	0.152	0.051	5.287	0.059	0.000	0.000	0.000	12.100
64	6.711	0.127	0.000	4.320	0.049	0.000	0.000	0.000	11.208
66	10.190	0.169	0.059	5.514	0.066	0.000	0.000	0.000	15.998
68	7.748	0.117	0.000	3.596	0.045	0.000	0.000	0.000	11.506
70	7.480	0.101	0.000	2.977	0.000	0.000	0.000	0.000	10.558
72	11.081	0.140	0.000	3.949	0.055	0.000	0.000	0.000	15.225
74	12.231	0.147	0.000	4.030	0.058	0.000	0.000	0.000	16.465
76	12.324	0.145	0.000	3.907	0.057	0.000	0.000	0.000	16.433
78	12.943	0.148	0.056	4.221	0.056	0.000	0.000	0.000	17.424
80	13.967	0.150	0.059	4.400	0.056	0.000	0.000	0.000	18.632
82	12.894	0.148	0.056	4.122	0.056	0.000	0.000	0.000	17.276
84	10.748	0.117	0.000	4.596	0.045	0.000	0.000	0.000	15.506

Table R-4. Continued.

Days	C2	C3	IC4	C4	IC5	C5	C6	C7	Total
86	10.548	0.101	0.000	3.977	0.000	0.000	0.000	0.000	14.626
88	12.232	0.145	0.000	3.891	0.057	0.000	0.000	0.000	16.325
90	12.954	0.148	0.056	4.322	0.056	0.000	0.000	0.000	17.536
92	12.232	0.145	0.000	3.991	0.057	0.000	0.000	0.000	16.425
94	13.167	0.150	0.059	4.400	0.056	0.000	0.000	0.000	17.832
96	10.219	0.169	0.059	5.651	0.066	0.000	0.000	0.000	16.165
98	10.675	0.117	0.000	4.460	0.045	0.000	0.000	0.000	15.297
100	10.430	0.101	0.000	3.977	0.000	0.000	0.000	0.000	14.508
102	11.181	0.140	0.000	3.995	0.055	0.000	0.000	0.000	15.371
104	12.323	0.147	0.000	4.130	0.058	0.000	0.000	0.000	16.658
106	12.432	0.145	0.000	3.991	0.057	0.000	0.000	0.000	16.625
108	12.994	0.148	0.056	4.322	0.056	0.000	0.000	0.000	17.576
110	13.567	0.150	0.059	4.400	0.056	0.000	0.000	0.000	18.232
112	12.123	0.147	0.000	4.003	0.058	0.000	0.000	0.000	16.331
114	11.008	0.140	0.000	3.895	0.055	0.000	0.000	0.000	15.097
116	12.293	0.147	0.000	4.093	0.058	0.000	0.000	0.000	16.591
118	10.019	0.169	0.059	5.451	0.066	0.000	0.000	0.000	15.765
120	12.794	0.148	0.056	4.022	0.056	0.000	0.000	0.000	17.076
122	12.232	0.145	0.000	3.891	0.057	0.000	0.000	0.000	16.325
124	11.781	0.140	0.000	4.195	0.055	0.000	0.000	0.000	16.171

Table R-5. Carboxylic acid concentration (g/L) for refined glycerol Packed-bed fermentation (fresh Galveston inocula, ammonium bicarbonate buffer, 55 °C).

Days	C2	C3	IC4	C4	IC5	C5	C6	C7	Total
1	0.198	0.000	0.000	0.000	0.000	0.000	0.000	0.000	0.198
2	0.386	0.000	0.000	0.000	0.000	0.000	0.000	0.000	0.386
3	1.016	0.000	0.000	0.000	0.000	0.000	0.000	0.000	1.016
4	1.219	0.112	0.000	0.308	0.000	0.000	0.000	0.000	1.639
5	1.725	0.816	0.000	1.125	0.050	0.000	0.000	0.000	3.716
6	2.062	1.122	0.000	1.538	0.073	0.000	0.000	0.000	4.794
7	2.362	1.748	0.051	1.595	0.078	0.000	0.000	0.000	5.834
8	2.949	2.429	0.054	1.489	0.079	0.000	0.000	0.000	7.001
9	3.449	3.332	0.000	1.175	0.058	0.000	0.000	0.000	8.014
10	3.788	3.743	0.000	1.163	0.053	0.000	0.000	0.000	8.747
11	3.918	3.209	0.000	1.090	0.000	0.000	0.000	0.000	8.216
12	4.167	2.414	0.000	1.189	0.000	0.000	0.000	0.000	7.770
13	4.827	1.892	0.000	1.318	0.000	0.000	0.000	0.000	8.038
14	5.156	1.443	0.000	1.435	0.000	0.000	0.000	0.000	8.034
15	5.562	1.232	0.000	1.702	0.000	0.000	0.000	0.000	8.495
16	5.775	0.990	0.000	2.168	0.000	0.000	0.000	0.000	8.934
17	5.419	0.777	0.000	2.538	0.000	0.000	0.000	0.000	8.734
18	5.224	0.642	0.000	2.994	0.000	0.000	0.000	0.000	8.860
19	5.199	0.566	0.000	3.533	0.000	0.000	0.000	0.000	9.298

Table R-5. Continued.

Days	C2	C3	IC4	C4	IC5	C5	C6	C7	Total
20	4.846	0.649	0.000	3.879	0.000	0.000	0.000	0.000	9.375
21	5.196	1.067	0.000	4.254	0.052	0.000	0.000	0.000	10.568
22	5.188	1.561	0.000	4.314	0.060	0.000	0.000	0.000	11.123
23	5.377	2.136	0.000	4.470	0.060	0.000	0.000	0.000	12.042
24	5.039	2.358	0.000	4.147	0.078	0.000	0.000	0.000	11.622
25	5.406	2.658	0.000	4.304	0.079	0.000	0.000	0.000	12.447
26	5.311	2.656	0.000	4.100	0.068	0.049	0.000	0.000	12.184
27	5.363	2.531	0.000	4.091	0.062	0.051	0.000	0.000	12.097
28	5.129	2.190	0.000	4.102	0.076	0.060	0.000	0.000	11.557
29	4.697	1.759	0.000	3.932	0.076	0.056	0.000	0.000	10.520
30	4.783	1.485	0.000	4.237	0.074	0.060	0.000	0.000	10.639
31	4.739	1.282	0.000	4.476	0.073	0.052	0.000	0.000	10.623
32	4.571	1.105	0.000	4.768	0.086	0.050	0.000	0.000	10.580
33	4.272	1.032	0.000	5.004	0.067	0.000	0.000	0.000	10.376
34	3.912	1.087	0.000	4.984	0.093	0.000	0.000	0.000	10.075
35	3.701	1.279	0.000	4.751	0.073	0.000	0.000	0.000	9.804
36	3.398	1.493	0.000	4.073	0.067	0.000	0.000	0.000	9.031
37	4.330	2.090	0.000	4.902	0.076	0.062	0.000	0.000	11.459
38	4.308	2.182	0.000	4.573	0.076	0.066	0.000	0.000	11.205
39	4.773	2.450	0.000	4.786	0.076	0.080	0.000	0.000	12.166
40	4.830	2.445	0.000	4.777	0.063	0.089	0.000	0.000	12.205
41	4.735	2.265	0.000	4.706	0.059	0.098	0.000	0.000	11.862
42	4.562	2.090	0.000	4.862	0.059	0.107	0.000	0.000	11.681
43	3.751	1.556	0.000	5.174	0.000	0.121	0.000	0.000	10.602
44	3.706	1.512	0.000	5.709	0.063	0.133	0.000	0.000	11.123
45	3.322	1.419	0.000	5.610	0.061	0.132	0.000	0.000	10.545
46	3.239	1.525	0.000	5.611	0.062	0.136	0.000	0.000	10.573
47	4.330	2.090	0.000	4.902	0.076	0.062	0.000	0.000	11.459
48	5.129	2.190	0.000	4.102	0.076	0.060	0.000	0.000	11.557
49	4.697	1.759	0.000	3.932	0.076	0.056	0.000	0.000	10.520
50	4.783	1.485	0.000	4.237	0.074	0.060	0.000	0.000	10.639
51	5.196	1.067	0.000	4.254	0.052	0.000	0.000	0.000	10.568
52	5.188	1.561	0.000	4.314	0.060	0.000	0.000	0.000	11.123
53	4.739	1.282	0.000	4.476	0.073	0.052	0.000	0.000	10.623
54	4.571	1.105	0.000	4.768	0.086	0.050	0.000	0.000	10.580
55	4.562	2.090	0.000	4.862	0.059	0.107	0.000	0.000	11.681
56	5.039	2.358	0.000	4.147	0.078	0.000	0.000	0.000	11.622
57	4.739	1.282	0.000	4.476	0.073	0.052	0.000	0.000	10.623
58	4.308	2.182	0.000	4.573	0.076	0.066	0.000	0.000	11.205
59	4.272	1.032	0.000	5.004	0.067	0.000	0.000	0.000	10.376
60	3.912	1.087	0.000	4.984	0.093	0.000	0.000	0.000	10.075
61	5.188	1.561	0.000	4.314	0.060	0.000	0.000	0.000	11.123
62	3.322	1.419	0.000	5.610	0.061	0.132	0.000	0.000	10.545

APPENDIX S

CARBOXYLIC ACID PRODUCTION DATA FOR WATER HYACINTH FERMENTATIONS

Table S-1. Carboxylic acid concentration (g/L) for W401-2 fresh water hyacinth fermentation (fresh Galveston inocula, ammonium bicarbonate buffer, 40 °C).

Days	C2	C3	IC4	C4	IC5	C5	C6	C7	Total
2	1.965	0.372	0.000	0.451	0.000	0.000	0.023	0.000	2.811
4	2.616	0.569	0.000	0.638	0.064	0.068	0.092	0.000	4.047
6	3.210	0.629	0.000	0.656	0.047	0.130	0.185	0.000	4.857
8	3.739	0.637	0.050	0.695	0.059	0.177	0.261	0.049	5.666
10	3.971	0.607	0.060	0.857	0.069	0.230	0.329	0.055	6.179
12	4.092	0.475	0.076	0.940	0.076	0.273	0.392	0.055	6.379
14	4.299	0.439	0.078	1.059	0.039	0.298	0.439	0.058	6.708
18	4.632	0.500	0.081	0.835	0.087	0.262	0.420	0.070	6.888
20	4.486	0.262	0.093	1.069	0.094	0.326	0.505	0.062	6.900
24	4.537	0.471	0.083	1.067	0.088	0.303	0.461	0.062	7.071
26	4.787	0.458	0.081	1.203	0.087	0.321	0.477	0.061	7.473
28	5.119	0.506	0.085	1.298	0.091	0.333	0.500	0.061	7.992

Table S-2. Carboxylic acid concentration (g/L) for W403-4 1 h hot-lime treated water hyacinth fermentation (fresh Galveston inocula, ammonium bicarbonate buffer, 40 °C).

Days	C2	C3	IC4	C4	IC5	C5	C6	C7	Total
2	2.453	0.142	0.000	0.368	0.000	0.000	0.027	0.000	2.990
4	4.153	0.632	0.000	0.563	0.000	0.000	0.033	0.000	5.381
6	6.820	1.725	0.000	0.843	0.000	0.062	0.068	0.000	9.518
8	10.894	1.965	0.000	1.083	0.000	0.131	0.120	0.000	14.192
10	11.123	2.015	0.032	1.216	0.031	0.133	0.109	0.000	14.660
12	11.598	2.029	0.038	1.300	0.056	0.130	0.103	0.000	15.255
14	12.603	2.364	0.072	1.413	0.027	0.132	0.111	0.000	16.722
18	12.955	2.550	0.083	1.432	0.053	0.131	0.131	0.000	17.335
20	13.677	2.714	0.105	1.793	0.078	0.136	0.148	0.000	18.651
24	13.724	2.737	0.114	1.869	0.094	0.136	0.141	0.000	18.815
26	13.719	2.736	0.119	1.871	0.103	0.134	0.123	0.000	18.805
28	14.705	2.887	0.119	1.856	0.101	0.141	0.119	0.000	19.928

Table S-3. Carboxylic acid concentration (g/L) for W405-6 2 h hot-lime treated water hyacinth fermentations (fresh Galveston inocula, ammonium bicarbonate buffer, 40 °C).

Days	C2	C3	IC4	C4	IC5	C5	C6	C7	Total
2	2.726	0.178	0.000	0.346	0.000	0.000	0.000	0.000	3.249
4	3.872	0.499	0.000	0.486	0.000	0.000	0.000	0.000	4.858
6	6.374	1.410	0.000	0.800	0.000	0.079	0.036	0.000	8.699
8	8.549	1.497	0.000	1.258	0.000	0.214	0.150	0.000	11.668
10	9.308	1.871	0.029	1.398	0.061	0.224	0.156	0.000	13.047
12	9.426	1.775	0.040	1.365	0.079	0.215	0.146	0.020	13.067
14	9.432	2.051	0.000	1.418	0.022	0.227	0.161	0.000	13.311
18	9.873	2.005	0.068	1.410	0.079	0.221	0.154	0.000	13.810
20	9.955	2.048	0.066	1.419	0.076	0.220	0.153	0.000	13.936
24	10.161	1.968	0.086	1.636	0.103	0.217	0.156	0.000	14.328
26	10.252	1.947	0.091	1.722	0.113	0.215	0.151	0.000	14.492
28	10.588	2.005	0.096	1.753	0.124	0.219	0.151	0.000	14.936

Table S-4. Carboxylic acid concentration (g/L) for W407-8 4 wk air-lime treated water hyacinth fermentation (fresh Galveston inocula, ammonium bicarbonate buffer, 40 °C).

Days	C2	C3	IC4	C4	IC5	C5	C6	C7	Total
2	1.422	0.130	0.000	0.150	0.000	0.000	0.000	0.000	1.703
4	2.096	0.307	0.000	0.331	0.000	0.000	0.020	0.000	2.755
6	5.159	1.399	0.000	0.437	0.000	0.000	0.000	0.000	6.996
8	6.283	1.576	0.000	0.523	0.000	0.000	0.020	0.000	8.402
10	7.020	1.678	0.000	0.594	0.028	0.000	0.000	0.020	9.340
12	7.424	1.802	0.000	1.071	0.028	0.000	0.000	0.022	10.348
14	8.360	1.879	0.026	1.519	0.058	0.000	0.000	0.000	11.843
18	9.676	1.644	0.062	1.799	0.074	0.000	0.000	0.000	13.256
20	11.519	1.677	0.072	2.083	0.093	0.022	0.000	0.000	15.466
24	12.704	1.744	0.087	2.679	0.107	0.000	0.000	0.000	17.322
26	13.154	1.772	0.096	2.889	0.128	0.024	0.000	0.000	18.063
28	13.887	1.931	0.103	3.015	0.133	0.000	0.000	0.000	19.069

Table S-5. Carboxylic acid concentration (g/L) for W409-0 6 wk air-lime treated water hyacinth fermentation (fresh Galveston inocula, ammonium bicarbonate buffer, 40 °C).

Days	C2	C3	IC4	C4	IC5	C5	C6	C7	Total
2	1.443	0.125	0.000	0.167	0.000	0.000	0.000	0.000	1.735
4	2.825	0.291	0.000	0.299	0.000	0.000	0.000	0.000	3.415
6	5.482	1.102	0.000	0.370	0.000	0.000	0.000	0.000	6.954
8	7.658	1.418	0.000	0.573	0.023	0.024	0.022	0.000	9.718
10	8.209	1.481	0.027	0.629	0.024	0.026	0.000	0.000	10.396
12	8.611	1.522	0.031	0.663	0.047	0.026	0.000	0.000	10.900
14	9.058	1.628	0.032	0.953	0.055	0.028	0.000	0.000	11.753
18	9.548	1.565	0.076	1.079	0.082	0.028	0.000	0.000	12.378
20	9.652	1.413	0.096	1.173	0.117	0.027	0.000	0.000	12.477
24	9.810	1.575	0.085	1.146	0.099	0.029	0.000	0.000	12.745
26	9.832	1.618	0.084	1.149	0.095	0.027	0.000	0.000	12.806
28	10.322	1.500	0.103	1.181	0.121	0.029	0.000	0.000	13.256

Table S-6. Carboxylic acid concentration (g/L) for W551-2 fresh water hyacinth fermentation (fresh Galveston inocula, ammonium bicarbonate buffer, 55 °C).

Days	C2	C3	IC4	C4	IC5	C5	C6	C7	Total
2	2.136	0.405	0.000	0.659	0.051	0.000	0.000	0.000	3.250
4	3.428	0.473	0.052	0.730	0.056	0.000	0.000	0.000	4.738
6	4.600	0.507	0.058	0.738	0.062	0.000	0.000	0.000	5.966
8	4.947	0.390	0.092	0.800	0.100	0.000	0.026	0.000	6.356
10	5.234	0.460	0.098	0.802	0.110	0.000	0.025	0.000	6.727
12	5.507	0.337	0.129	0.877	0.136	0.000	0.053	0.000	7.038
14	5.831	0.552	0.075	0.777	0.073	0.000	0.022	0.019	7.348
18	6.122	0.497	0.118	0.843	0.132	0.000	0.049	0.019	7.780
20	6.560	0.436	0.102	0.838	0.099	0.000	0.048	0.020	8.103
24	6.720	0.399	0.095	0.804	0.090	0.000	0.053	0.023	8.185
26	6.796	0.590	0.088	0.836	0.084	0.000	0.045	0.000	8.440
28	7.345	0.408	0.099	0.825	0.099	0.000	0.049	0.000	8.824

Table S-7. Carboxylic acid concentration (g/L) for W553-4 1 h hot-lime treated water hyacinth fermentation (fresh Galveston inocula, ammonium bicarbonate buffer, 55 °C).

Days	C2	C3	IC4	C4	IC5	C5	C6	C7	Total
2	2.570	0.222	0.000	0.143	0.000	0.022	0.000	0.000	2.956
4	4.492	0.332	0.000	0.204	0.022	0.050	0.000	0.000	5.100
6	6.197	0.455	0.076	0.648	0.047	0.047	0.000	0.000	7.471
8	7.656	0.529	0.095	0.756	0.087	0.024	0.024	0.000	9.171
10	8.288	0.601	0.115	0.875	0.118	0.000	0.000	0.000	9.997
12	9.556	0.642	0.127	0.930	0.114	0.000	0.000	0.000	11.369
14	10.417	0.670	0.135	0.968	0.122	0.000	0.000	0.000	12.312
18	11.330	0.695	0.146	1.017	0.137	0.000	0.000	0.000	13.326
20	12.560	0.744	0.158	1.102	0.146	0.000	0.000	0.000	14.710
24	13.578	0.776	0.170	1.218	0.161	0.000	0.000	0.000	15.904
26	14.082	0.801	0.178	1.275	0.174	0.000	0.021	0.000	16.531
28	14.242	0.806	0.183	1.273	0.181	0.000	0.021	0.000	16.706

Table S-8. Carboxylic acid concentration (g/L) for W555-6 2 h hot-lime treated water hyacinth fermentation (fresh Galveston inocula, ammonium bicarbonate buffer, 55 °C).

Days	C2	C3	IC4	C4	IC5	C5	C6	C7	Total
2	2.124	0.196	0.000	0.129	0.000	0.000	0.000	0.000	2.449
4	3.980	0.263	0.000	0.145	0.000	0.021	0.022	0.000	4.430
6	6.130	0.407	0.038	0.398	0.021	0.000	0.000	0.000	6.995
8	6.877	0.449	0.078	0.510	0.060	0.000	0.000	0.000	7.973
10	6.554	0.466	0.089	0.303	0.067	0.000	0.000	0.000	7.480
12	7.551	0.504	0.095	0.609	0.036	0.000	0.055	0.000	8.850
14	8.696	0.539	0.096	0.638	0.072	0.000	0.057	0.000	10.097
18	9.633	0.570	0.102	0.681	0.077	0.000	0.064	0.000	11.127
20	11.198	0.627	0.121	0.778	0.099	0.000	0.068	0.000	12.891
24	11.194	0.618	0.122	0.773	0.101	0.023	0.068	0.000	12.899
26	11.600	0.638	0.125	0.779	0.103	0.000	0.069	0.000	13.313
28	11.653	0.613	0.131	0.774	0.117	0.023	0.066	0.000	13.377

Table S-9. Carboxylic acid concentration (g/L) for W557-8 4 wk air-lime treated water hyacinth fermentation (fresh Galveston inocula, ammonium bicarbonate buffer, 55 °C).

Days	C2	C3	IC4	C4	IC5	C5	C6	C7	Total
2	1.612	0.125	0.000	0.122	0.000	0.000	0.000	0.000	1.860
4	2.560	0.162	0.000	0.114	0.000	0.000	0.000	0.000	2.837
6	5.167	0.282	0.000	0.270	0.000	0.000	0.000	0.000	5.719
8	7.427	0.365	0.086	0.415	0.060	0.000	0.000	0.000	8.353
10	8.773	0.448	0.149	0.526	0.096	0.000	0.000	0.027	10.018
12	9.245	0.475	0.164	0.615	0.112	0.000	0.000	0.000	10.611
14	9.587	0.495	0.178	0.655	0.126	0.000	0.000	0.000	11.041
18	10.211	0.520	0.194	0.795	0.154	0.000	0.000	0.000	11.874
20	10.761	0.544	0.209	0.870	0.164	0.000	0.000	0.000	12.548
24	10.885	0.536	0.232	0.838	0.195	0.000	0.000	0.023	12.708
26	10.828	0.529	0.237	0.830	0.202	0.000	0.000	0.050	12.678
28	11.320	0.564	0.248	0.867	0.207	0.000	0.000	0.034	13.240

Table S-10. Carboxylic acid concentration (g/L) for W559-0 6 wk air-lime treated water hyacinth fermentation (fresh Galveston inocula, ammonium bicarbonate buffer, 55 °C).

Days	C2	C3	IC4	C4	IC5	C5	C6	C7	Total
2	1.771	0.168	0.000	0.137	0.000	0.000	0.038	0.000	2.113
4	3.058	0.217	0.000	0.147	0.000	0.000	0.041	0.000	3.463
6	5.711	0.372	0.000	0.481	0.031	0.000	0.038	0.000	6.633
8	7.109	0.492	0.078	0.651	0.111	0.026	0.060	0.000	8.527
10	8.225	0.593	0.101	0.764	0.146	0.030	0.076	0.066	10.001
12	7.938	0.570	0.099	0.723	0.143	0.027	0.072	0.066	9.639
14	8.273	0.595	0.107	0.749	0.158	0.030	0.085	0.032	10.028
18	8.867	0.596	0.122	0.774	0.177	0.029	0.092	0.056	10.712
20	8.962	0.616	0.123	0.782	0.180	0.030	0.091	0.051	10.835
24	9.037	0.505	0.126	0.737	0.177	0.029	0.098	0.060	10.769
26	9.298	0.499	0.131	0.753	0.185	0.029	0.103	0.059	11.056
28	9.752	0.527	0.138	0.796	0.196	0.032	0.116	0.058	11.613

APPENDIX T
BIOCHEMICAL PATHWAYS

This appendix highlights the major steps on the hydrolysis of cellulose, the glycolysis process, and the production of acetate, propionate, and fatty acids in general. All pathways were taken from the Metacyc Encyclopedia of Metabolic Pathways website (Caspi et al., 2008).

Degradation of cellulose

Step 1.

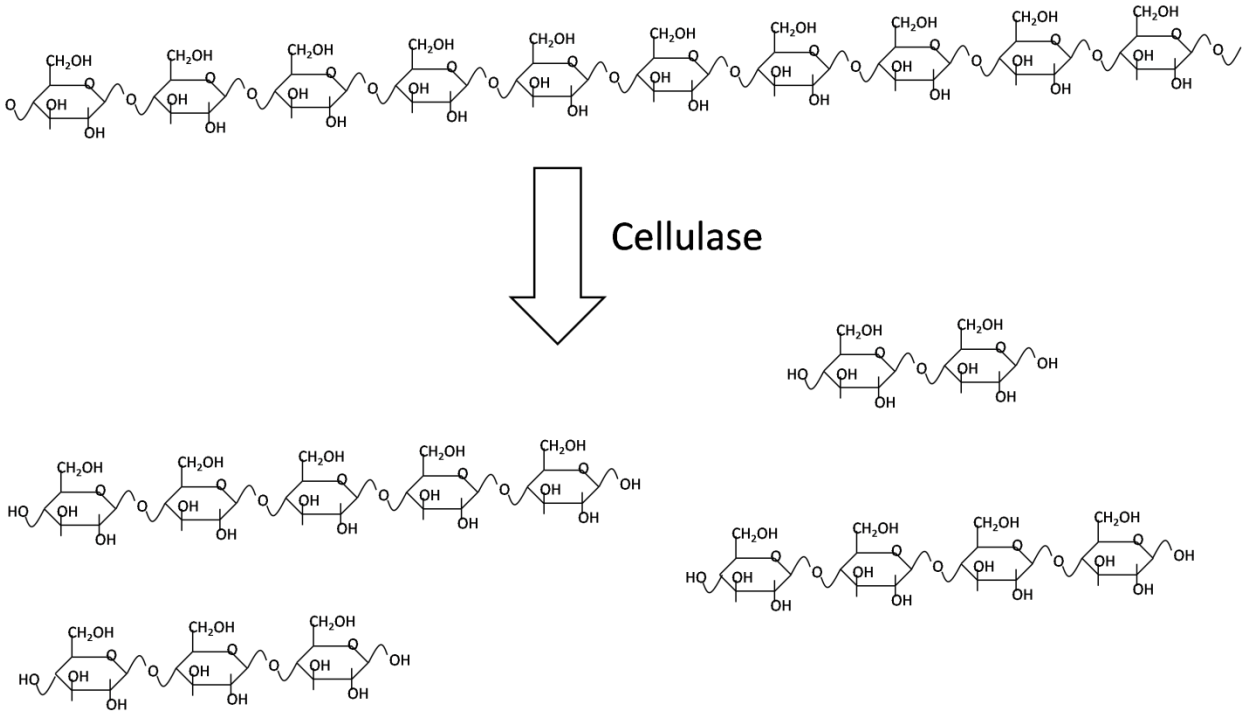

Figure T-1. Hydrolysis of cellulose. Long chains of cellulose are broken down by large cellulosomes containing multiple cellulase units into shorter chains of between two and six glucans in length and then passed through the cellular membrane.

Degradation of cellulose

Step 2a.

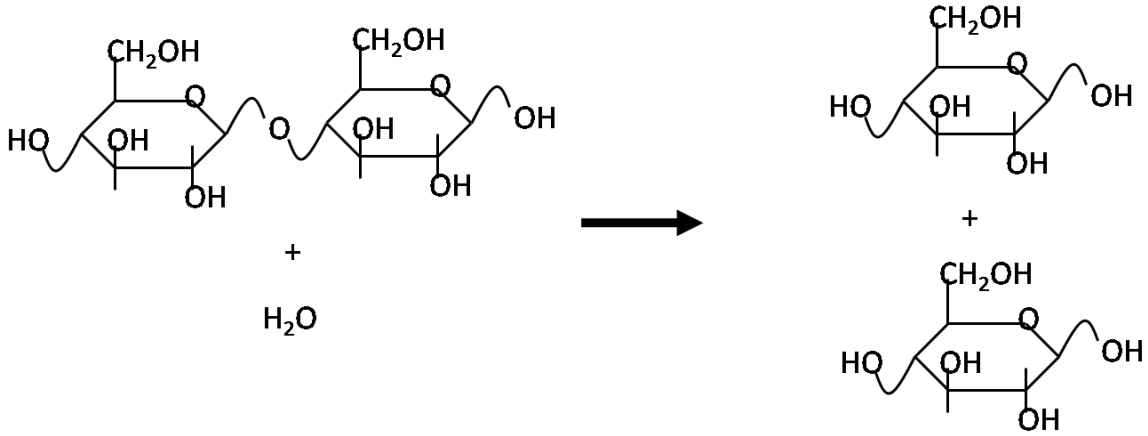

Figure T-2. Hydrolytic cleavage of cellulose. Once inside the cell, the short-chain celluloses can be broken hydrolyzed by glucosidases into glucose, thus incorporating water.

Step 2b.

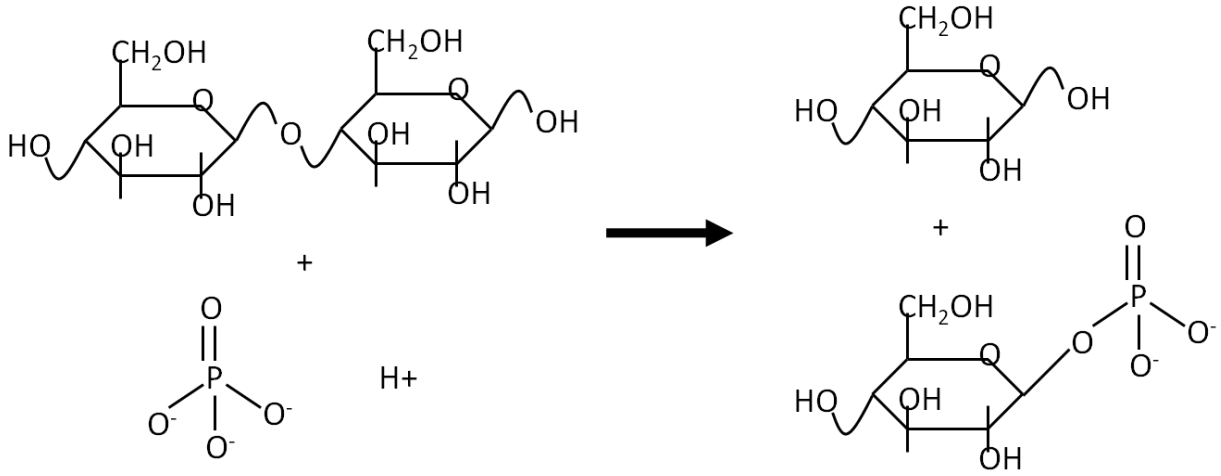

Figure T-3. Phosphorilytic cleavage of cellulose. The short-chain celluloses can also be broken down phosphorilytically by phosphorylases into glucose-1-phosphate.

Glycolysis

Step 1a.

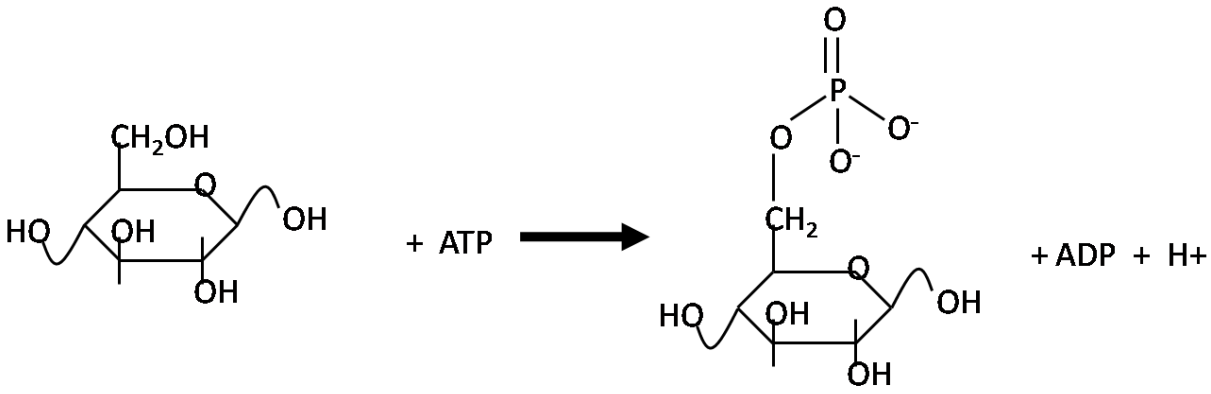

Figure T-4. Conversion of glucose to glucose-6-phosphate.

Step 1b.

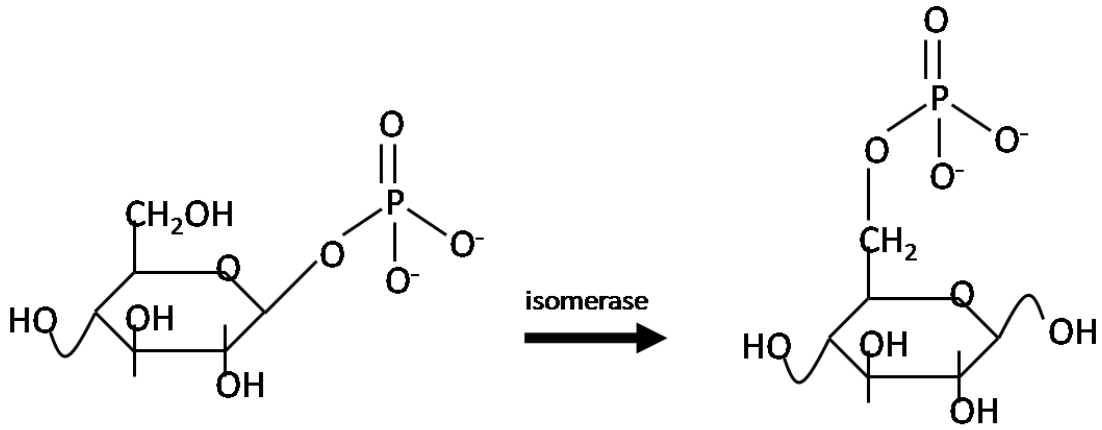

Figure T-5. Conversion of glucose-1-phosphate to glucose-6-phosphate.

Glycolysis

Step 2.

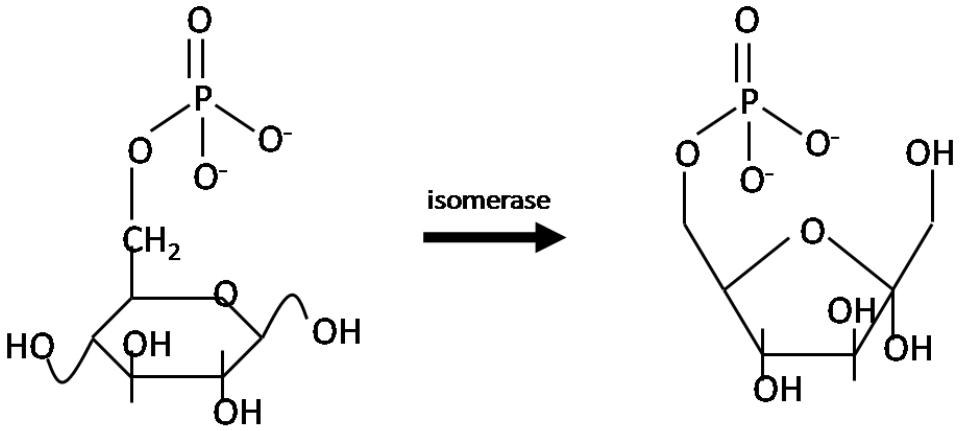

Figure T-6. Conversion of glucose-6-phosphate to fructose-6-phosphate.

Step 3.

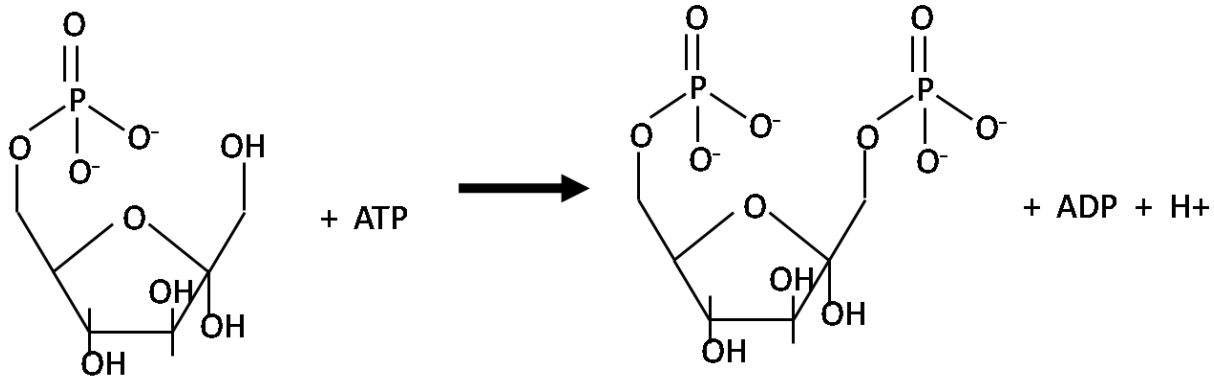

Figure T-7. Conversion of fructose-6-phosphate to fructose-1-6-phosphate.

Glycolysis

Step 4.

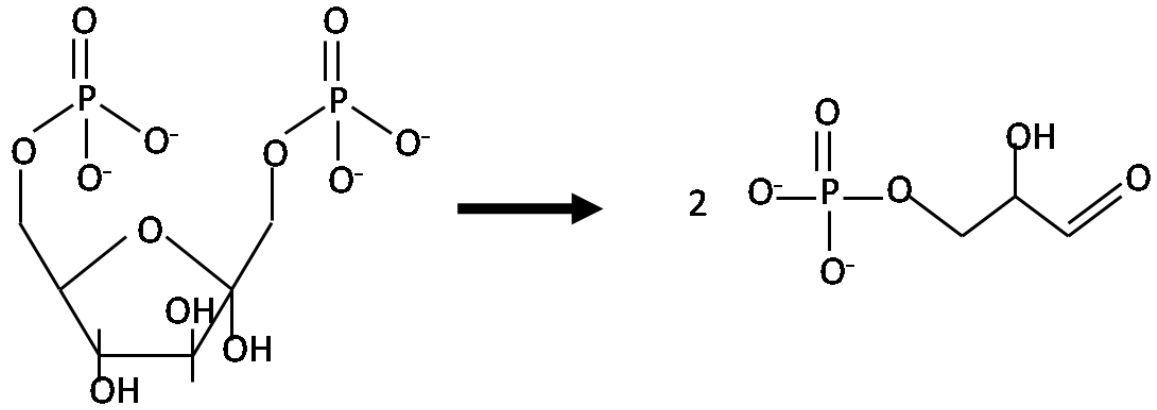

Figure T-8. Conversion of fructose-1-6-phosphate to two glyceraldhyde-3-phosphates. Each fructose-1-6-phosphate reacts to produce one glyceraldhyde-3-phosphate (GADP) and one dihydroxyacetone phosphate (DHAP). The DHAP is then converted by an isomerase into a GADP, resulting in two GADPs.

Step 5.

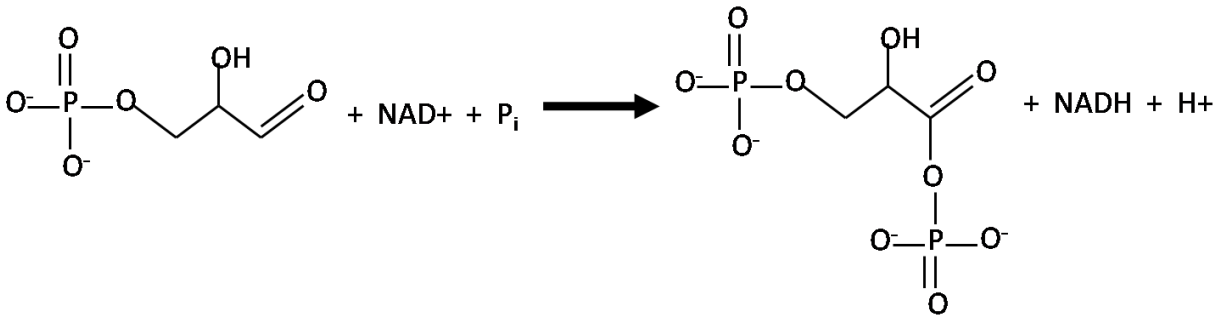

Figure T-9. Conversion of glyceraldhyde-3-phosphate to 1,3 bisphosphoglycerate.

Glycolysis

Step 6.

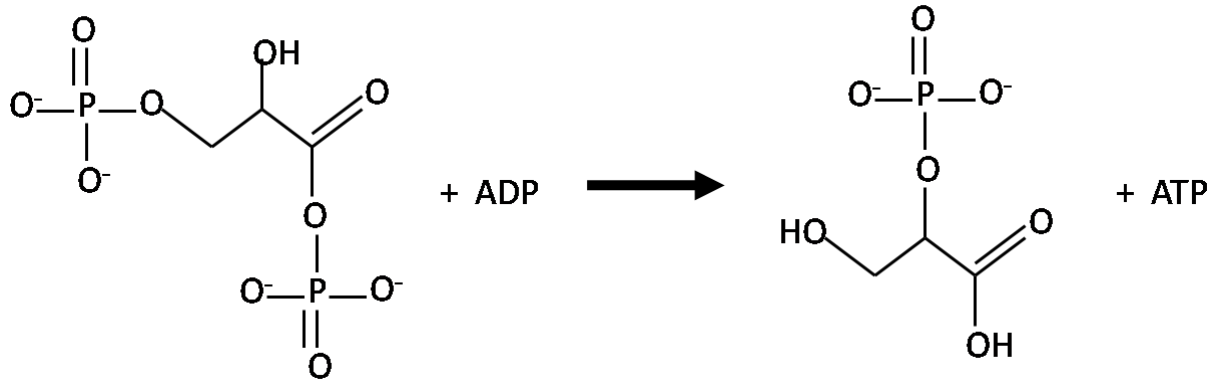

Figure T-10. Conversion of 1,3 bisphosphoglycerate into 2-phosphoglycerate. One of the phosphate groups is pulled from the 1,3 bisphosphoglycerate by a ADP, making 3-phosphoglycerate and a ATP. The 3-phosphoglycerate is then converted into a 2-phosphoglycerate by an isomerace.

Step 7.

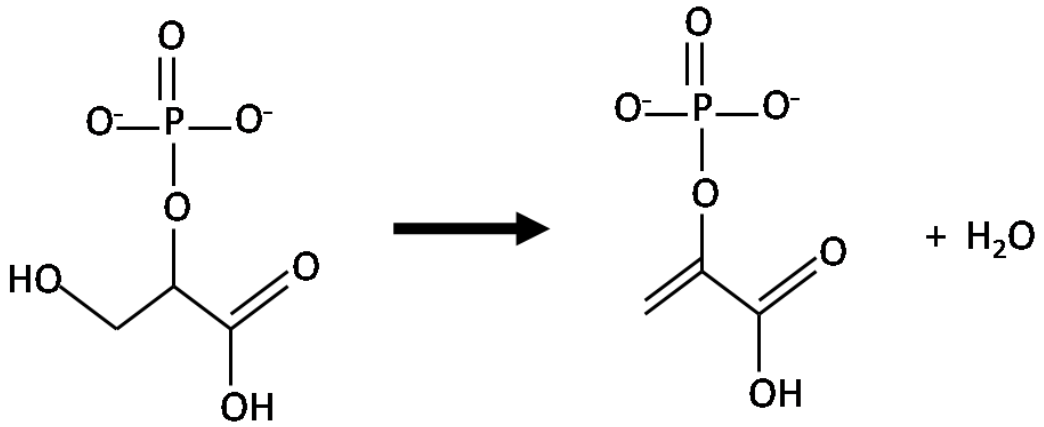

Figure T-11. Conversion of 2 phosphoglycerate into phosphoenolpyruvate.

Glycolysis

Step 8.

Figure T-12. Conversion of phosphoenolpyruvate into pyruvate.

Acetate synthesis

Step 1.

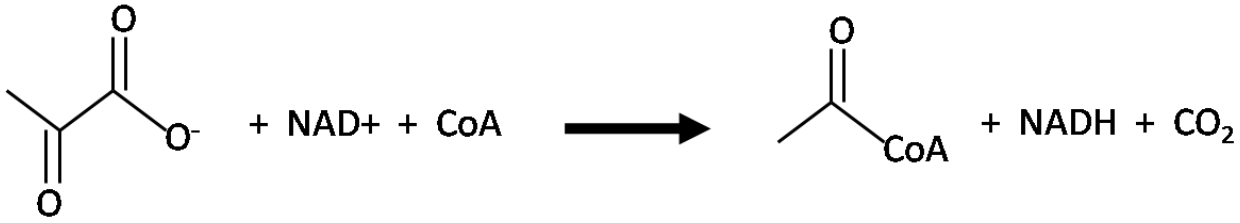

Figure T-13. Conversion of pyruvate to acetyl-CoA.

Step 2.

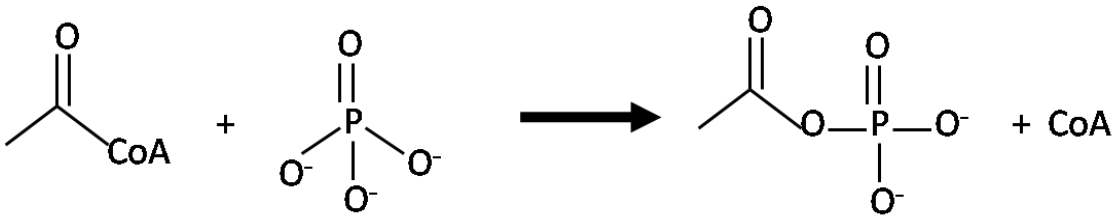

Figure T-14. Conversion of acetyl-CoA to acetyl-phosphate.

Acetate synthesis

Step 3.

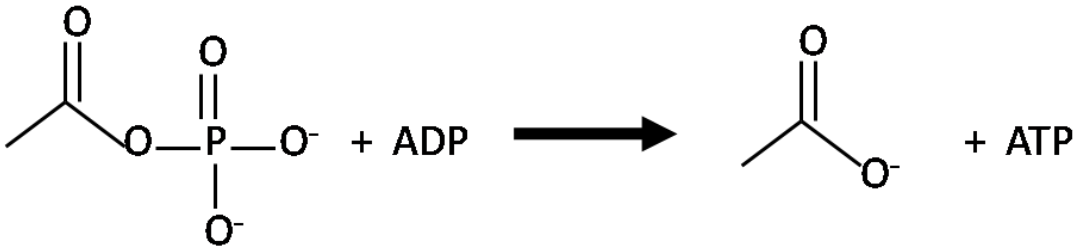

Figure T-15. Conversion of acetyl-phosphate to acetate.

Propionate synthesis

Step 1.

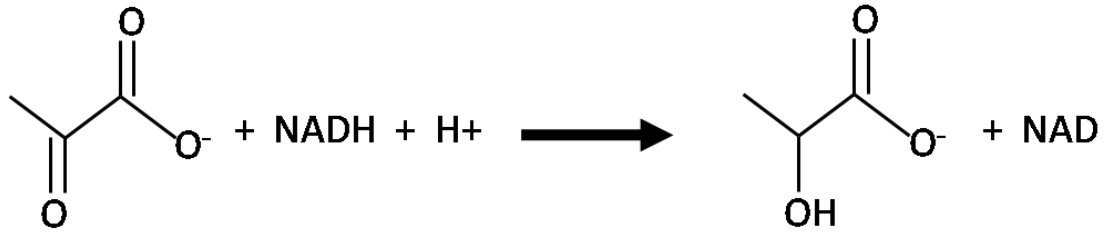

Figure T-16. Conversion of pyruvate to lactate.

Step 2.

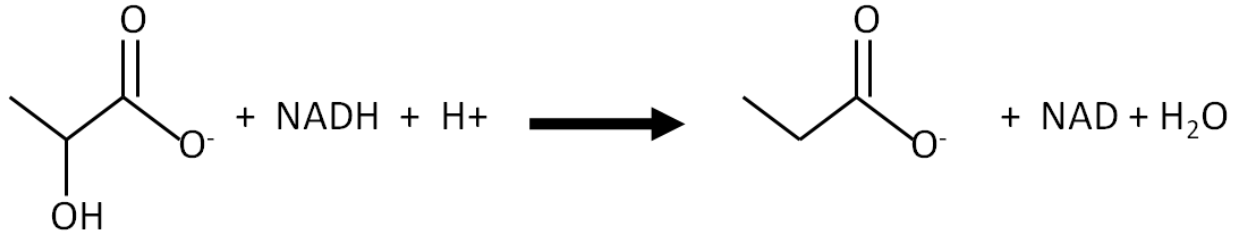

Figure T-17. Conversion of lactate to propionate.

Fatty Acid synthesis
All higher acids are made from the building blocks of both propionate and acetate.

Step 1. Initiation

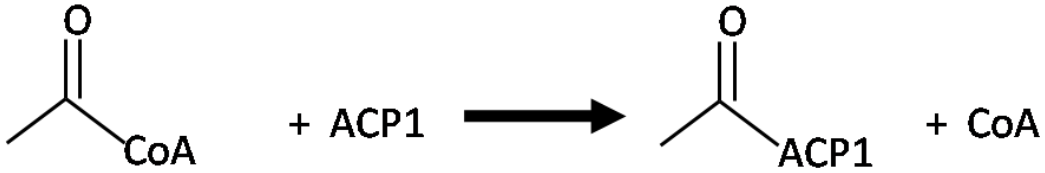

Figure T-18. Fatty acid synthesis initiation. Either an acetyl-CoA (shown) or a propionyl-CoA attaches to the first acyl-carrier protein (ACP1) site in the enzyme.

Step 2a. Elongation

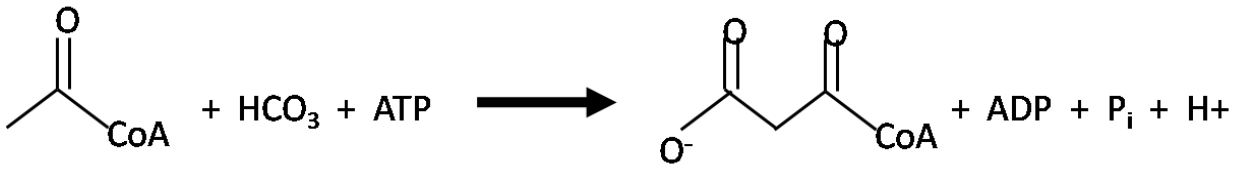

Figure T-19. Conversion of acetyl-CoA to malonyl-CoA.

Step 2b.

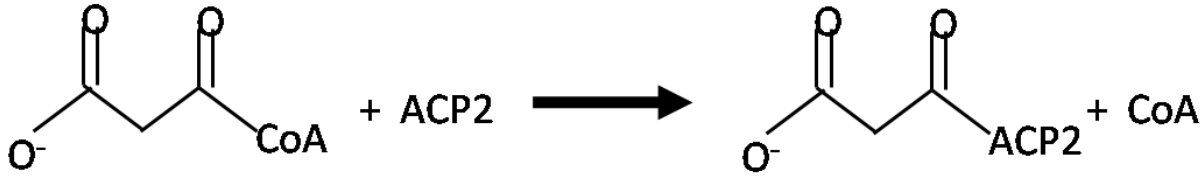

Figure T-20. Malonyl-CoA attachment to ACP2. A malonyl-CoA attaches to the second acyl-carrier protein (ACP2) in the protein. Because this site can only accept a malonyl-CoA, the elongation of a fatty acid will always progress in steps of two-carbon chain lengths.

Fatty Acid synthesis

Step 3.

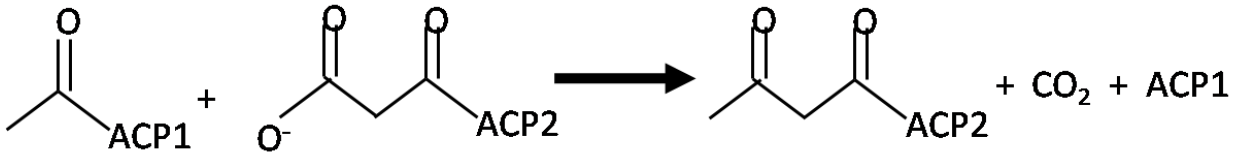

Figure T-21. Elongation. The acetyl group from ACP1 is added to the end of the malonyl group of the ACP2, releasing a CO_2.

Step 4.

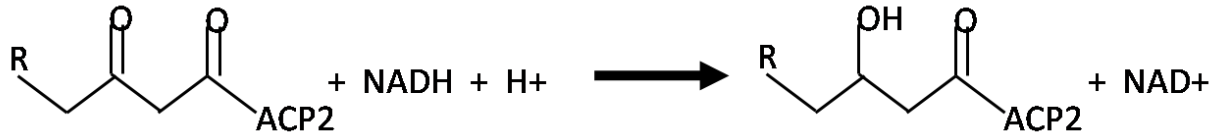

Figure T-22. Oxygen double bond removal.

Step 5.

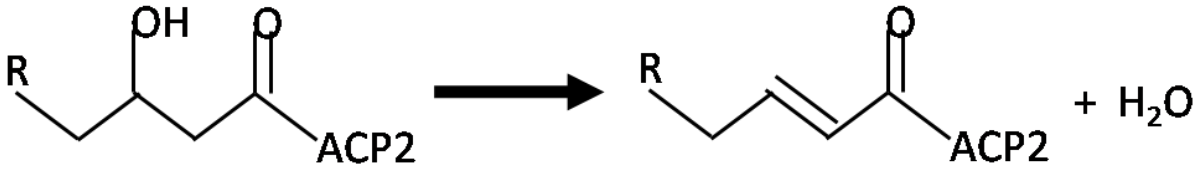

Figure T-23. Water release.

Fatty Acid synthesis

Step 6.

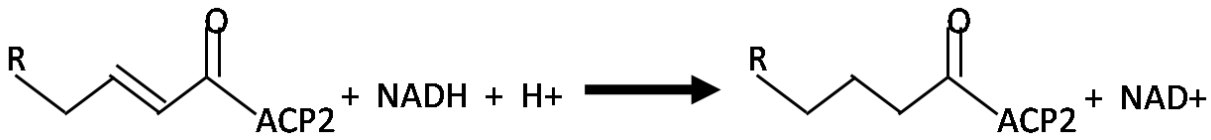

Figure T-24. Hydrocarbon double bond removal.

Step 7.

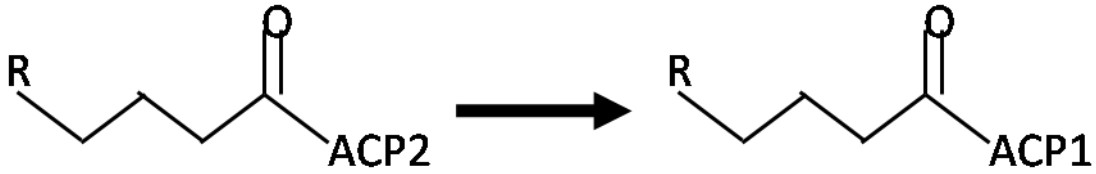

Figure T-25. ACP transfer. Once the extra oxygen has been released, the lengthening chain is moved back to the first acyl-carrier protein (ACP1) to begin the cycle over again. Steps 2 through 7 are repeated again and again until the fatty acid is of the desired length.

Step 8. Termination

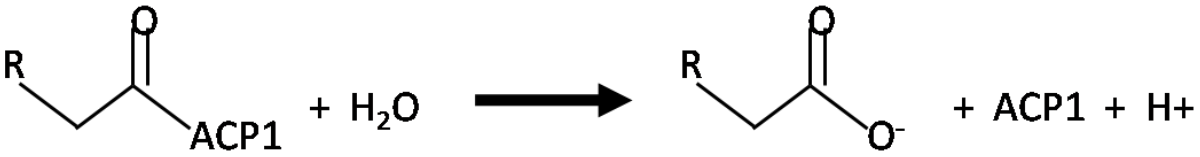

Figure T-26. Fatty acid termination. Once the fatty acid has reached the desired chain length, the acid is released from the ACP1 site as a carboxylate acid salt.

VITA

Andrea Kelly Forrest was born and raised in Beaumont, TX. She attended Louisiana Tech University where she received a Bachelor of Science in chemical engineering in 2001. She worked for four years as a Process Engineer I and II with Georgia-Pacific Corporation at their pulp and paper facility in Monticello, MS. She joined the graduate program in the Department of Chemical Engineering at Texas A&M University where she studied under Dr. Mark T. Holtzapple for five years in the pursuit of her Ph.D., and graduated in December 2010. Her field of study was the biological conversion of biomass into carboxylic acids by anaerobic fermentation.

Andrea Kelly Forrest
C/O Dr. Mark T. Holtzapple
Department of Chemical Engineering
Texas A&M University
College Station, TX 77843-3122